THE PHARMACOLOGY AND FUNCTION OF CENTRAL VPAC/PAC RECEPTORS

by

LOUISE DICKSON

Submitted in accordance with the requirements for the degree of Doctor of Philosophy

The University of Edinburgh

School of Biomedical and Clinical Laboratory Sciences

2007

The candidate confirms that the work submitted is her own and that appropriate credit has been given where reference has been made to the work of others.

Signed:

Date:

Abstract

The physiological actions of the neuropeptides VIP, PACAP-27 and PACAP-38 are mediated by $VPAC_1$, $VPAC_2$ and PAC_1 receptors which preferentially couple to G-proteins that stimulate adenylate cyclase and hence increase the concentration of intracellular cAMP ($[cAMP]_i$), although stimulation of calcium ($[Ca^{2+}]_i$) and phospholipase D levels have also been reported. The activation of these receptors has been implicated in a plethora of physiological processes (e.g. control of circadian rhythms) and clinical conditions (e.g. Alzheimer's disease), although the availability and paucity of selective, non-peptide ligands has hindered advances in this field. Moreover, as new peptide ligands have been developed, their intracellular signalling properties have not been systematically evaluated, with the use of different expression systems and assay methodologies resulting in inconsistencies in the literature. To address these issues, chapter one of this thesis describes the thorough and systematic characterisation of human (h) VPAC/PAC receptor pharmacology using non-radioactive, high-throughput (HT) amenable, whole cell, $[cAMP]_i$ and $[Ca^{2+}]_i$ assays. Chapter two describes HT-screening studies that were performed through an industrial collaboration, in an attempt to identify receptor selective, non-peptide ligands and finally, in chapter three the potential roles for VPAC/PAC receptors in the brain were explored using both *in vitro* and *in vivo* techniques.

Standardised $[cAMP]_i$ and $[Ca^{2+}]_i$ assays (96-well plate) were used to directly compare hVPAC/PAC receptor pharmacology in CHO-K1 cells stably expressing the receptors, with additional studies evaluating cell lines with endogenous receptor expression. A range of peptide agonists were utilised in these studies, including non-selective (e.g. PACAP-27) and classical ligands (e.g. VIP), as well as recently described (e.g. R3P65) and highly selective compounds (e.g. maxadilan). The agonist rank order of potencies were identical between assays for each receptor in all of the cell lines examined, with EC_{50} values consistently ~ 100 fold lower in the $[Ca^{2+}]_i$ assay. The pharmacology of the reportedly selective peptide antagonists PG7-269 ($VPAC_1$), PG99-465 ($VPAC_2$) and M65 (PAC_1) was also examined, with these studies identifying complexities in the pharmacology of PG99-465.

The standardised assay conditions and the excellent correlation between the $[cAMP]_i$ and $[Ca^{2+}]_i$ data, underpinned the establishment of an HT $[Ca^{2+}]_i$ assay (384-well plate) which was used to identify hVPAC receptor selective ligands from the compound libraries of the Fujisawa Pharmaceutical Company. Approximately

100,000 compounds were tested, with several non-peptides identified as potential ligands. The potency and selectivity of these compounds were subsequently fully characterised using the 96- and 384-well $[Ca^{2+}]_i$ assay formats, although none were as potent as the peptides examined in chapter one.

In the final section of this thesis, putative roles for VPAC/PAC receptors in the brain were investigated. Firstly, as VIP and PACAP are thought to stimulate the release of cytokines from astrocytes in the brain, VPAC/PAC receptor pharmacology was examined in primary cultures of rat cortical astrocytes (RCA). Receptor characterisation studies ($[cAMP]_i$ and $[Ca^{2+}]_i$ assays) established that the PAC_1 was the predominant VPAC/PAC receptor subtype in RCA, with preliminary studies also showing that VIP and PACAP-27 stimulated the release of the cytokines IL-1β and TNF-α from these cells. In addition, behavioural studies using mice further examined the role of the $VPAC_2$ receptor in the maintenance of circadian activity rhythms, as previous collaborative studies have highlighted an important role for this receptor. Temporarily moving the mice from their home cages was found to be as disruptive to their activity cycles as anaesthesia/surgery, a finding which has implications for all work of this nature. Finally, PG99-465 was administered to mice and wheel running activity in response to an advance in the light/dark cycle monitored, however no significant alterations in response to the phase advance were found.

The findings described in this thesis clearly demonstrate the importance of systematically characterising VPAC/PAC receptor pharmacology, with these studies highlighting that there remains a paucity of receptor selective, non-peptide ligands. Moreover, identifying or designing such non-peptide ligands thus remains an important task, with the success of such studies critical to delineating the physiological roles for VPAC/PAC receptors in normal and disease states.

Publications arising from the thesis

Papers:

Dickson L., Aramori I., Sharkey J. & Finlayson K. (2006). VIP and PACAP receptor pharmacology: a comparison of intracellular signaling pathways. *Ann. N. Y. Acad. Sci.*, 1070: 239-42.

Dickson L., Aramori I., McCulloch J., Sharkey J. & Finlayson K. (2006). A systematic comparison of intracellular cyclic AMP and calcium signalling highlights complexities in human VPAC/PAC receptor pharmacology. *Neuropharmacology*, 51(6): 1086-98.

Published abstracts:

Dickson L., Aramori I., Sharkey J. & Finlayson K. (2005). VIP and PACAP receptor pharmacology, a systematic study comparing $[cAMP]_i$ and $[Ca^{2+}]_i$ signalling. *Regul. Pept.*, 130:161.

Dickson L., Aramori I., Sharkey J. & Finlayson K. (2005). $hVPAC_2$ receptor pharmacology; a systematic study comparing $[cAMP]_i$ and $[Ca^{2+}]_i$ signalling. P015 - Abstracts of the British Pharmacological Society 4th Focused Meeting of Cell Signalling, Leicester, UK.

Dickson L., Sharkey J., McCulloch J. & Finlayson K. (2005). Maxadilan may discriminate between PAC_1 receptor splice variants. 726.21/D59 - Abstracts of the Society for Neuroscience 36th Annual Meeting, Atlanta, USA.

Acknowledgements

The studies reported in this thesis were carried out in the Astellas CNS Research group in Edinburgh, University of Edinburgh and in Astellas Pharma Inc. Japan. This thesis, in whole or in part, has not been submitted to any other University.

I would like to thank a number of people who have helped and supported me throughout these studies:

- Astellas Pharma Inc. (formerly the Fujisawa Pharmaceutical Company) for providing the funding and resources necessary to carry out this research.

- All of my colleagues, past and present, from the Astellas CNS group in Edinburgh (formerly Fujisawa Institute of Neuroscience in Edinburgh) for their advice and support over the past few years. In particular, I would like to thank Jill Fowler and Chris Spratt for their technical help and advice in the behavioural studies, and also Jonathan Rhodes for performing the immunohistochemical staining of primary cortical cultures. I would also like to thank Joyce McCluckie for her invaluable help and technical advice at the beginning of these studies. I would like to extend special thanks to Paul Jones, Ian Heron, Jui-Lee Birse-Archbold, Jared Young, Sally Williamson and David Macdonald for their friendship and support throughout these studies.

- Jim McCulloch, John Sharkey and Adriano Rossi, for their interest in my studies and their advice over the past few years.

- My colleagues in Astellas Pharma Inc. in Tsukuba, Japan for welcoming me into their group and helping me to experience and enjoy life in Japan.

- Keith Finlayson for being the best supervisor I could have ever hoped to have. The encouragement, advice and friendship you have given me over the last few years were invaluable and I sincerely appreciate everything you have done for me.

- Finally, I would like to thank my family who have always provided me with immense support and encouragement. Thank you for everything.

Contents

GENERAL INTRODUCTION

A. General introduction

The VIP and PACAP peptides have been intensively studied over the past thirty years and alongside their associated G-protein coupled receptors (GPCRs) have been implicated in a plethora of physiological processes, with new and exciting roles continuing to be described in the literature. The physiological properties of the peptides/receptors have been investigated using a range of *in vitro* and *in vivo* technologies, including cell-based functional approaches, transgenic animals and rodent models of various diseases. As a consequence of the many interesting functions reported for these peptides and their cognate receptors in recent years, they remain attractive drug targets, with the ultimate goal being to develop selective, potent, non-peptide ligands as potential therapeutic tools for a variety of diseases and disorders. In this introduction I shall describe the discovery of the VIP and PACAP peptides, the cloning of their cognate receptors, the pharmacology and distribution of these receptors and finally, I shall discuss some of the many physiological roles associated with the peptides and receptors.

A.1. VIP and PACAP peptides

A.1.1. Discovery of VIP

The isolation and purification of 'vasoactive intestinal peptide' (VIP) was reported some 36 years ago by Said and Mutt (1970), who at the time were investigating the high incidence of systemic hypotension in patients with severe lung injuries (Said & Mutt, 1970). Whilst looking for the vasoactive substance responsible for the reduction in blood pressure, a 28 amino acid vasoactive peptide (VIP) was isolated from pig small intestine, an organ which originates from the same embryonic bud as the lung. Initial experiments showed the peptide to have a diverse range of effects including: increasing vasodilatation and lowering arterial blood pressure (Said & Mutt, 1970), causing smooth muscle relaxation in respiratory and intestinal tissues (Piper *et al.*, 1970), as well as stimulating electrolyte secretion in the gut (Barbezat & Grossman, 1971). Details regarding the mechanisms by which VIP mediated these effects began to emerge a few years later and appeared to primarily depend upon the stimulation of adenylate cyclase (AC) and the resulting production of cyclic adenosine monophosphate (cAMP) production. The first association between VIP and AC was reported in 1973, when VIP was shown to increase the activity of this enzyme in liver tissue (Desbuguois *et al.*, 1973). Around

the same time, it was also reported that patients who had tumours expressing high concentrations of VIP or elevated plasma VIP levels were often found to have diarrhoea (Bloom *et al.*, 1973; Said & Faloona, 1975). These secretory effects of VIP on the gut were likened to that of cholera endotoxin (which was thought to stimulate AC) and were subsequently shown to occur through stimulation of AC and cAMP (Schwartz *et al.*, 1974; Swift *et al.*, 1975). Since these early studies, many other investigations have verified that VIP activity is generally synonymous with an increase in AC activity and cAMP levels. As a consequence of the isolation of VIP from the gut and its effect on electrolyte secretion, it was initially defined as a gut hormone. However, further investigation of VIP distribution and function demonstrated that this peptide had a much more widespread distribution, and through immunohistochemical and radioimmuno assays, this peptide was shown to be mainly localised in neurons throughout the CNS and PNS in several species (Larsson *et al.*, 1976a; Larsson *et al.*, 1976b). This lead to the suggestion that VIP may also have a role as a neurotransmitter, in addition to being a gut hormone, with findings from many subsequent studies continuing to support a putative neurotransmitter role for this peptide (Bryant *et al.*, 1976; Duckles & Said, 1982; Fahrenkrug & Hannibal, 2004; Van Geldre & Lefebvre, 2004).

A.1.2. VIP gene products

The human VIP gene was cloned in 1985 and was subsequently mapped to chromosome 6, region q25 [Entrez GeneID: 7432; http://www.ncbi.nlm.nih.gov] (Tsukada *et al.*, 1985; Gozes *et al.*, 1987). The rat and mouse VIP genes were both cloned in 1991 and have chromosomal locations 1p11 [rat: Entrez GeneID: 117064] and 10A1 [Entrez GeneID: 22353] (Lamperti et al., 1991).

Translation of the mRNA sequence produced from transcription of the human VIP gene yields a 170 amino acid precursor named prepro-VIP. Post-translational processing of this precursor yields the 28 amino acid VIP, in addition to the 27 amino acid peptide histidine methionine (PHM) in humans or peptide histidine isoleucine (PHI) in rodents (Figure A.1; Itoh *et al.*, 1983). Two alternatively processed forms of the latter peptide have been isolated, namely PHV-42 and PHI-GLY (Yiangou *et al.*, 1986; Cauvin *et al.*, 1990b). VIP and PHM/PHI are located on two adjacent exons and share 44 % amino acid sequence identity (Tatemoto & Mutt, 1981; Bodner *et al.*, 1985).

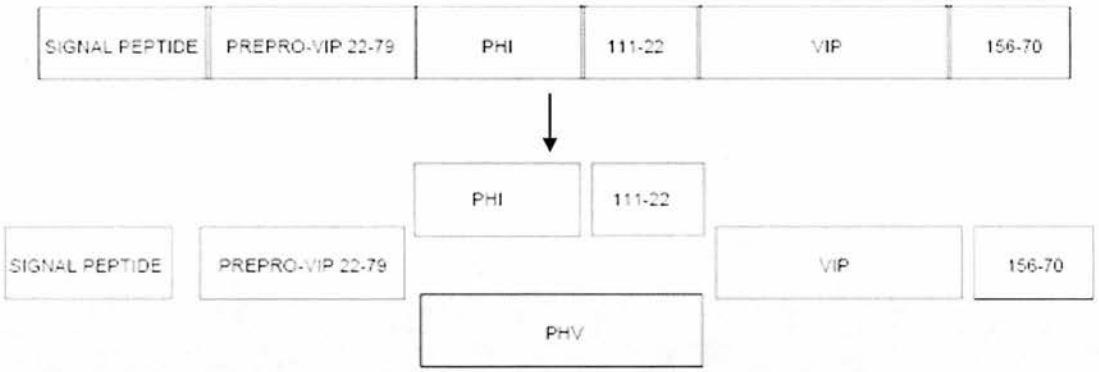

Figure A.1 Schematic illustration of the peptide products produced from processing of the VIP precursor (Fahrenkrug & Hannibal, 2004).

The rate of transcription of the VIP gene can be regulated by many factors. One of the first reported regulators of this gene was cAMP, which was shown to act via a 17 base pair cAMP response element (CRE) in the VIP gene sequence (Hayakawa *et al.*, 1984; Ohsawa *et al.*, 1985; Tsukada *et al.*, 1987). Transcription of the VIP gene has also been shown to be enhanced by the activation of protein kinase C (PKC), an effect which has been suggested to be mediated in part by the CRE, although there is some debate over this issue (Ohsawa *et al.*, 1985; Hahm & Eiden, 1996). In addition, the VIP gene is reported to contain a cytokine-responsive area that is sensitive to factors such as ciliary neurotrophic factor and leukaemia inhibitory factor (Symes *et al.*, 1994). GPCRs can also mediate VIP gene expression, with the cholinergic agonist carbachol shown to increase VIP mRNA expression in neuroblastoma cell lines via specific muscarinic receptors (Kristensen *et al.*, 1997). Furthermore, even at nanomolar concentrations pituitary adenylate cyclase activating polypeptide (PACAP) has been shown to increase the rate of VIP gene transcription in NB-OK-1 cells, leading to a rapid increase in intracellular VIP levels, which is suggested to be cAMP independent (Georg & Fahrenkrug, 2000). Indeed, Adler and Fink (1993) have shown that VIP mRNA levels in SHSY-5Y cells are increased by calcium and cAMP independently, with only the calcium mediated pathway involving new protein synthesis.

A.1.3. Discovery of PACAP

While attempting to isolate hypothalamic hypophysiotropic hormones, characterised by their ability to stimulate AC in ovine pituitary extracts, Arimura and colleagues discovered a novel, 38 amino acid peptide (Miyata *et al.*, 1989). When

tested in similar tissue extracts prepared from rats, this peptide was again observed to potently activate AC and as a consequence was named PACAP-38 (pituitary adenylate cyclase activating polypeptide; Miyata *et al.*, 1989). Less than a year later a second peptide, produced as a side product during PACAP-38 purification from hypothalamic extracts, was shown to produce an identical level of AC stimulation in terms of potency (EC_{50} for both: 0.3 nM) and maximal stimulation (Miyata *et al.*, 1990). Following sequence analysis, this second peptide was demonstrated to be a C-terminally truncated form of PACAP-38 that was 27 amino acids in length and was therefore named PACAP-27. The PACAP peptides were suggested to be closely related to VIP as a result of the high level of amino acid homology that was evident between their sequences (68 %; Table A.1; Miyata *et al.*, 1990). Early studies in which the physiological actions of the three peptides were directly compared in cultured rat pituitary cells, revealed that both PACAP peptides were 1000 times more potent than VIP in their ability to active AC (Miyata *et al.*, 1990).

A.1.4. The PACAP gene

The human PACAP gene was cloned in 1992 and mapped to the P11 region of chromosome 18 [Entrez GeneID: 116] (Hosoya *et al.*, 1992). The rat PACAP gene has been mapped to 9q37 [Entrez GeneID: 24166], with the mouse gene also cloned and mapped to chromosome 17 [Entrez GeneID: 11516] (Cai *et al.*, 1995; Okazaki *et al.*, 1995; Yamamoto *et al.*, 1998).

Transcription of the human PACAP gene and subsequent translation of the mRNA product yields a 176 amino acid precursor called prepro-PACAP (Hosoya *et al.*, 1992). This precursor can be cleaved and modified (Figure A.2) to produce

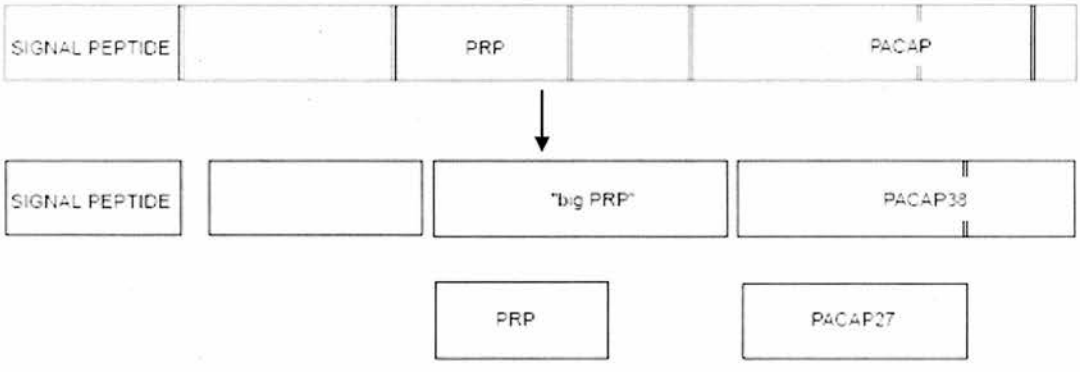

Figure A.2 The basic structure of the PACAP precursor and the resulting mature peptide products (Fahrenkrug & Hannibal, 2004).

Table A.1 Amino acid sequences for peptides of the VIP/PACAP/secretin family

	1				5					10					15					20					25					30					35					40					
GHRF	Y	A	D	A	I	F	T	N	S	Y	R	K	V	L	G	Q	L	S	A	R	K	L	L	Q	D	I	M	S	R	Q	Q	G	E	S	N	Q	E	R	G	A	R	A	R	L
GIP	Y	A	E	G	T	F	I	S	D	Y	S	I	A	M	D	K	I	H	Q	Q	D	F	V	N	W	L	L	A	Q	K	G	K	K	N	D	W	K	H	N	I	T	Q		
GLP-1	H	D	E	F	E	R	H	A	E	G	T	F	T	S	D	V	S	S	Y	L	E	G	Q	A	A	Q	G	F	I	A	W	L	V	K	G	R	G							
Glucagon	H	S	Q	G	T	F	T	S	D	Y	S	K	Y	L	D	S	R	R	A	Q	D	F	V	Q	W	L	M	N	T																
PACAP-27	H	S	D	G	I	F	T	D	S	Y	S	R	Y	R	K	Q	M	A	V	K	K	Y	L	A	A	V	L																			
PACAP-38	H	S	D	G	I	F	T	D	S	Y	S	R	Y	R	K	Q	M	A	V	K	K	Y	L	A	A	V	L	G	K	R	Y	K	Q	R	V	K	N	K						
PHM	H	A	D	G	V	F	T	S	D	F	S	K	L	L	G	Q	L	S	A	K	K	Y	L	E	S	L	M																		
PrP	D	V	A	H	G	I	L	N	E	A	Y	R	K	V	L	G	Q	L	S	A	G	K	H	L	Q	S	L	V	A																
Secretin	H	S	D	G	T	F	T	S	E	L	S	R	L	R	E	G	A	R	L	Q	R	L	L	Q	G	L	V																		
VIP	H	S	D	A	V	F	T	D	N	Y	T	R	L	R	K	Q	M	A	V	K	K	Y	L	N	S	I	L	N																	

PACAP-27 and PACAP-38, in addition to a third peptide named PACAP-related peptide (PRP; 29 amino acids), with which the PACAP peptides share just over 20 % amino acid homology (Okazaki *et al.*, 1992). The PACAP and VIP precursor peptides are relatively similar in terms of general structure and processing, as can be seen in Figure A.3 (Vaudry *et al.*, 2000). As for VIP, multiple factors are known to stimulate PACAP gene expression, including PACAP-38, phorbol esters and cAMP analogues (Suzuki *et al.*, 1994; Yamamoto *et al.*, 1998).

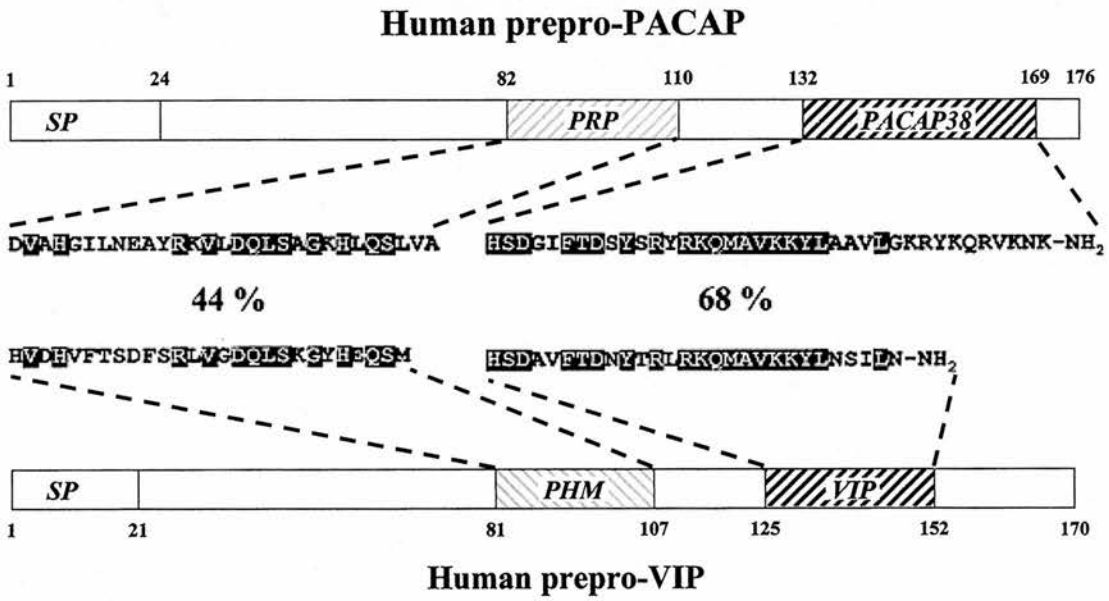

Figure A.3 **The general organisation of the human VIP and PACAP precursors.** The sequence homologies between mature peptide products are shown, with conserved amino acids highlighted in black (Vaudry *et al.*, 2000).

A.1.5. Distribution of VIP and PACAP

Many studies have investigated the distribution of VIP and PACAP in a variety of species. In general, these peptides are found throughout the body, including in the brain and in nerves innervating peripheral organs, as well as in non-neuronal cells and tissues in the periphery. There is a generally distinct pattern of distribution for VIP and PACAP in the CNS, however the locations of the peptides appear more similar in the periphery (Fahrenkrug & Hannibal, 2004). The distribution of the peptides shall be discussed here in brief, however more detailed reviews can be found elsewhere (Besson *et al.*, 1979; Arimura *et al.*, 1991; Masuo *et al.*, 1993; Vaudry *et al.*, 2000).

A.1.5.1. VIP/PACAP distribution in the nervous system

In the CNS, VIP and PACAP are generally found in different layers or cells of particular structures, with few reports describing their co-localisation (Fahrenkrug & Hannibal, 2004). VIP has a widespread distribution throughout the brain, with high expression found in the cerebral cortex, hippocampus, amygdala suprachiasmatic nucleus (SCN) and hypothalamus (Roberts *et al.*, 1980; Card *et al.*, 1981; Said, 1984; Fahrenkrug & Hannibal, 2004). The majority of investigations into PACAP expression in the CNS have focussed on PACAP-38, as this is the predominant form found in the brain, with some reports suggesting that PACAP-27 expression accounts for only 10 % of the total PACAP content in the brain (Arimura *et al.*, 1991). In the CNS, the highest levels of PACAP-38 expression have been reported to be in the hypothalamus, particularly in the SCN and the paraventricular and periventricular nuclei (Arimura *et al.*, 1991; Masuo *et al.*, 1993). Other brain areas in which a high expression of this peptide has been detected include multiple brainstem nuclei, the arcuate nucleus, the amygdala, thalamic nuclei, the cerebral cortex, the medulla oblongata and the posterior pituitary (Arimura *et al.*, 1991; Ghatei *et al.*, 1993; Masuo *et al.*, 1993; Fukuhara *et al.*, 1997). Although PACAP expression in neurons has been well documented, the peptide has also been shown to be expressed in primary cultures of cortical astrocytes derived from newborn rat cortices (Jaworski, 2000). In addition, both VIP and PACAP have been localised to nerve fibres that innervate cerebral blood vessels (Edvinsson & Ekman, 1984; Uddman *et al.*, 1993).

A.1.5.2. Peripheral distribution of VIP/PACAP

Co-expression of the VIP and PACAP peptides has been well documented in many peripheral tissues, although it is not always clear from these studies whether the peptides are found within the innervating nerves or within non-neuronal cells of particular organs. However, expression of both peptides has been documented throughout the digestive tract, in the genito-urinary tract, and in multiple exocrine glands (Alm *et al.*, 1980; Ghatei *et al.*, 1993; Vaudry *et al.*, 2000). As for the CNS, PACAP-38 has been shown to be the predominant form of PACAP expressed in peripheral tissues and organs (Arimura *et al.*, 1991). A particularly high concentration of this peptide was detected in germ cells of rat testis, with the total

concentration of PACAP-38 shown to be higher than that found in the entire rat brain (Arimura *et al.*, 1991).

A.1.5.3. Distribution of VIP and PACAP in the immune system

In contrast to the distinct localisation of VIP and PACAP in the CNS, the distribution of these peptides is actually very similar in cells and tissues of the immune system. Both VIP and PACAP have been detected in the thymus, spleen and lymph nodes (Gaytan *et al.*, 1994; Leceta *et al.*, 1994; Abad *et al.*, 2002). In addition, the peptides are also expressed in lymphocytes and thymocytes (Delgado *et al.*, 1996b; Gomariz *et al.*, 2001; Abad *et al.*, 2002). In agreement with the general distribution of these peptides in the body, PACAP-38 was again reported to be the predominant form of PACAP expressed in the immune system (Gaytan *et al.*, 1994).

A.1.6. Conservation of VIP and PACAP

The sequences of VIP and the PACAP peptides are highly conserved between species. The VIP amino acid sequence is identical in humans (Bunnett *et al.*, 1984), rats (Dimaline *et al.*, 1984), cows (Carlquist *et al.*, 1979), rabbits (Gossen *et al.*, 1990), pigs (Mutt & Said, 1974), dogs (Wang *et al.*, 1985) and goats (Eng *et al.*, 1986). Both guinea pig and chicken VIP deviate from the conserved sequence by four amino acids (Du *et al.*, 1985; McFarlin *et al.*, 1995). The PACAPs are similar to VIP, with their amino acid sequences identical in human (Kimura *et al.*, 1990), sheep (Miyata *et al.*, 1990; Miyata *et al.*, 1989), rat (Ogi *et al.*, 1990), and mouse (Okazaki *et al.*, 1995), with the chicken (McRory *et al.*, 1997) and frog (Chartrel *et al.*, 1991) sequences differing by only a single amino acid residue. Interestingly, PACAP has also been identified in a group of ancient protochordates – the tunicates or sea squirts (a group that is suggested to have given rise to the vertebrates), and has been shown to differ by only one residue when compared to the human form, suggesting a strong evolutionary pressure to maintain the PACAP sequence (McRory & Sherwood, 1997). The finding that PACAP has been so well conserved over 700 million years of evolution, has lead to the suggestion that it is the 'most likely ancestral molecule for the superfamily' to which it belongs (Figure A.4; Sherwood *et al.*, 2000). This superfamily of peptides will be discussed in the following section.

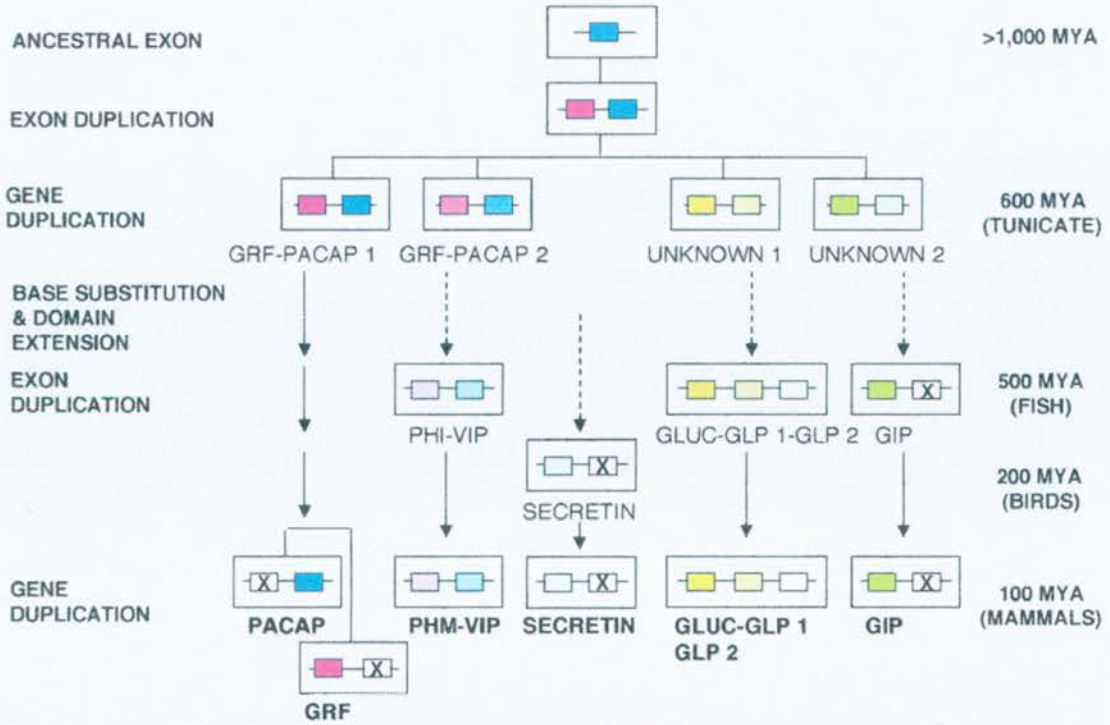

Figure A.4 **Proposed evolution of the VIP/PACAP/secretin family of peptides (Sherwood *et al.*, 2000).**

A.1.7. The VIP/PACAP peptide family

Due to the degree of sequence similarity with peptides such as secretin and glucagon, VIP and the PACAP peptides have been classed as members of the secretin peptide family, which was named after the first member of the family to be discovered (Bayliss & Starling, 1902). As shown for VIP and PACAP (Figures A.1 - A.3), the precursor peptides of this family characteristically have a signal peptide, an N-terminal peptide, 1 - 3 bioactive peptides and a C-terminal peptide (Sherwood *et al.*, 2000). The superfamily contains mature, linear peptides of between approximately 25 - 50 amino acids in length (Table A.1). In addition to sequence homology, the majority of peptides in this family also share certain primary (C-terminal amide) and secondary structural similarities, with disordered random coil structures at the N-termini and extended α-helical regions at the C-termini (Clore *et al.*, 1986; Gronenborn *et al.*, 1987; Theriault *et al.*, 1991; Wray *et al.*, 1998). There is evidence to suggest that the structures of both the N- and C- terminal regions are important for the biological activity of the peptides and for specific receptor recognition (Onoue *et al.*, 2001, 2004). For example, the NMR structure of PACAP-27, published recently by Inooka and colleagues (2001), was shown to contain a disordered N-terminal sequence (residues: 1 - 4) and an adjoining C-terminal α-helix

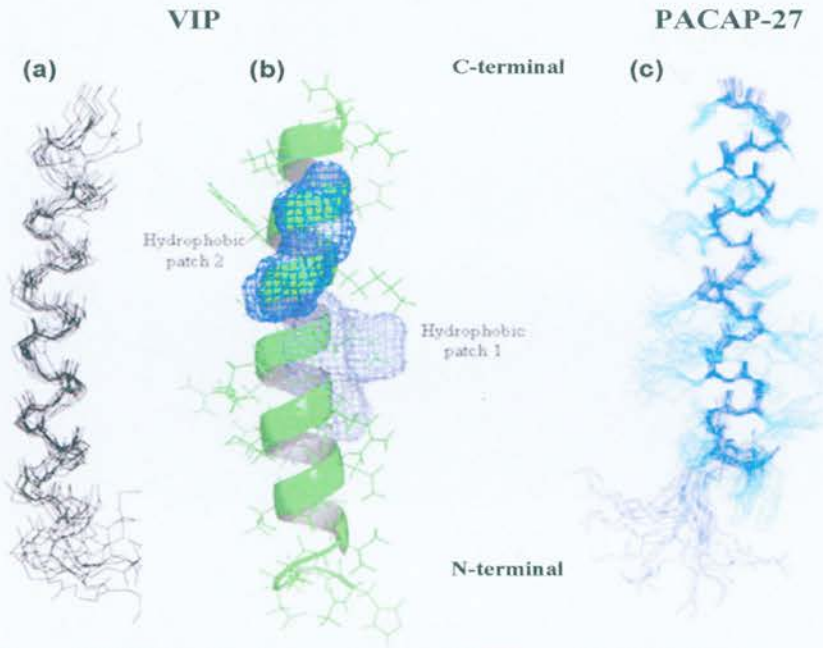

Figure A.5 **NMR derived structures of VIP and PACAP**. A superposition of the 10 lowest energy structures (**a**) and the average conformation (**b**) are shown for VIP, as derived from NMR studies (Tan *et al.*, 2006). For PACAP-27 (**c**), 25 NMR derived structures of the peptide are shown superposed (Inooka *et al.*, 2001).

(residues: 5 – 27; Figure A.5). The structure of VIP, as determined by NMR (Figure A.5), also contains an N-terminal disordered region (residues: 1 - 6) and an α-helix (residues: 7 - 24), with the remaining residues in the C-terminal appearing to form a helical shape (Tan *et al.*, 2006). For PACAP-27, the C-terminal region has been show to be important for receptor binding, however it is not sufficient for agonist activity as N-terminally truncated PACAPs such as PACAP(6-27), are competitive antagonists of PACAP receptors (Gourlet *et al.*, 1991; Robberecht *et al.*, 1992). It has been suggested that a hydrophobic β-coil may form in the N-terminal region (for which His^1, Phe^6 and Thr^7 may be involved) and that this structure may be important for receptor binding affinity (Inooka *et al.*, 2001).

The peptides in this family have wide range of functions, with the majority of these physiological actions mediated by GPCRs, as discussed below.

A.2. VIP and PACAP receptors

A.2.1. VIP and PACAP interactions with GPCR

Prior to cloning, the VIP and PACAP receptors were postulated to stimulate AC by interacting with GTP binding proteins (G-proteins), as GTP, Gpp(nNH)p and

GDP were all shown to inhibit VIP binding to rat prostate epithelial membranes and rat liver plasma membranes (Ramirez-Cardenas *et al.*, 1981; Carmena & Prieto, 1985). In addition, Couvineau *et al.* (1986) reported the solubilisation of a VIP receptor complex from rat liver membranes that was associated with a GTP regulatory protein. Using cholera toxin to induce [^{32}P]ADP ribosylation of liver membranes, this group suggested that the G-protein associated with the VIP receptors was $G\alpha_s$ (Couvineau *et al.*, 1986). At that time, more detailed studies were emerging regarding the control of AC activity by guanine nucleotides, with the isolation of these proteins and the development of specific antisera allowing further investigations of the precise mechanisms involved (Mumby *et al.*, 1986). In 1992, by using cross-liking methods and antisera for different G-protein subunits, Kermode and colleagues reported a direct physical interaction between VIP, VIP receptors and $G\alpha_s$ subunits (Kermode *et al.*, 1992). It is now well established that VIP and PACAP interact with GPCRs to stimulate intracellular signalling cascades.

For VIP and PACAP, along with many other peptides and neurotransmitters, it was not until advances in molecular biology were achieved, that the cloning of their cognate GPCRs was reported. In the following section I will give a general view of GPCRs, prior to specifically addressing the group B GPCR subfamily which contains the receptors for VIP and PACAP.

A.2.2. GPCR stoichiometry and families

G-protein coupled receptors (GPCRs) are heptahelical membrane proteins that have been described as the 'most important set of targets for research aimed at the design of new medicines' (Horn *et al.*, 1998), and account for 30 - 45 % of today's drugs targets (Drews, 2000; Hopkins & Groom, 2002). The human genome has been estimated to contain ~ 950 GPCRs (Takeda *et al.*, 2002), which is approximately 5 % of the total estimated protein encoding gene repertoire in the genome (International Human Genome Sequencing Consortium, 2004; http://ensembl.lcb.uu.se:8080/Homo_sapiens/). All of the receptors in the heptahelical family contain 7 transmembrane (TM) hydrophobic regions, linked by intracellular (IC) and extracellular (EC) loops, with an EC N-terminal and IC C-terminal. 7-TM receptors are generally assigned into one of 5 - 6 families (depending on the classification system) based on protein sequence similarities, with the receptors in each family generally sharing over 25 % sequence identity in the 7-TM region (Fredriksson *et al.*, 2003b; Jacoby *et al.*, 2006). The three main GPCR

families (A, B and C) encompass the mammalian GPCRs and schematic illustrations of the general structures of receptors in these families are shown in Figure A.6. Group A or the 'rhodopsin receptor family' includes amine, chemokine and purinergic receptors amongst others (Foord *et al.*, 2005). This group is the largest within the GPCR superfamily and the IUPHAR receptor database currently recognises 282 members of this family (http://www.iuphar-db.org). The smaller group B or 'secretin receptor family' mostly consists of peptide hormone and neuropeptide receptors such as secretin, calcitonin, VIP and PACAP receptors, with 55 members of this group currently represented on the IUPHAR GPCR database. The group C family is the 'metabotropic glutamate receptor family' which in addition to mGluR, counts the $GABA_B$, calcium-sensing receptors and some taste receptors amongst its members. There are 19 members of this group reported in the IUPHAR database, with all members having distinct, long N-terminal domains of approximately 500 - 600 amino acids (Takahashi *et al.*, 1993). Another group of GPCRs found in mammals is the small 'frizzled' receptor family, of which 11 members are currently described in the IUPHAR database. These receptors bind 'Wnt' secreted glycoprotein ligands and are suggested to be most closely related to receptors of the group B family, as a result of certain sequence similarities observed between the groups (Barnes *et al.*, 1998; Harmar, 2001). The other smaller families of GPCRs which have been identified are generally considered to contain pheromone and cAMP receptors that are found only in fungi and moulds (Gether, 2000; Harmar, 2001; Fredriksson *et al.*, 2003b). Among the three main mammalian GPCR groups there are few similarities other than the gross structural features of 7-TM domains and a disulphide bridge between EC loops 1 and 2 (Figure A.6). As VIP/PACAP receptors are members of the group B GPCR family, I will focus on this sub-family, however for excellent reviews on all GPCRs please see Gether (2000), Pierce *et al.* (2002) and Kristiansen (2004).

A.2.3. Group B GPCR family

The G-protein coupled receptor for the brain/gut peptide secretin was cloned in 1991 and subsequent sequence analysis found it had virtually no homology to any of the other GPCRs identified at that time (Ishihara *et al.*, 1991). Hence, the secretin receptor became the first member of a new GPCR family, later designated as group B. Many members of this family are activated by peptides and have the same general structural features described in the preceding section, having ~ 30 %

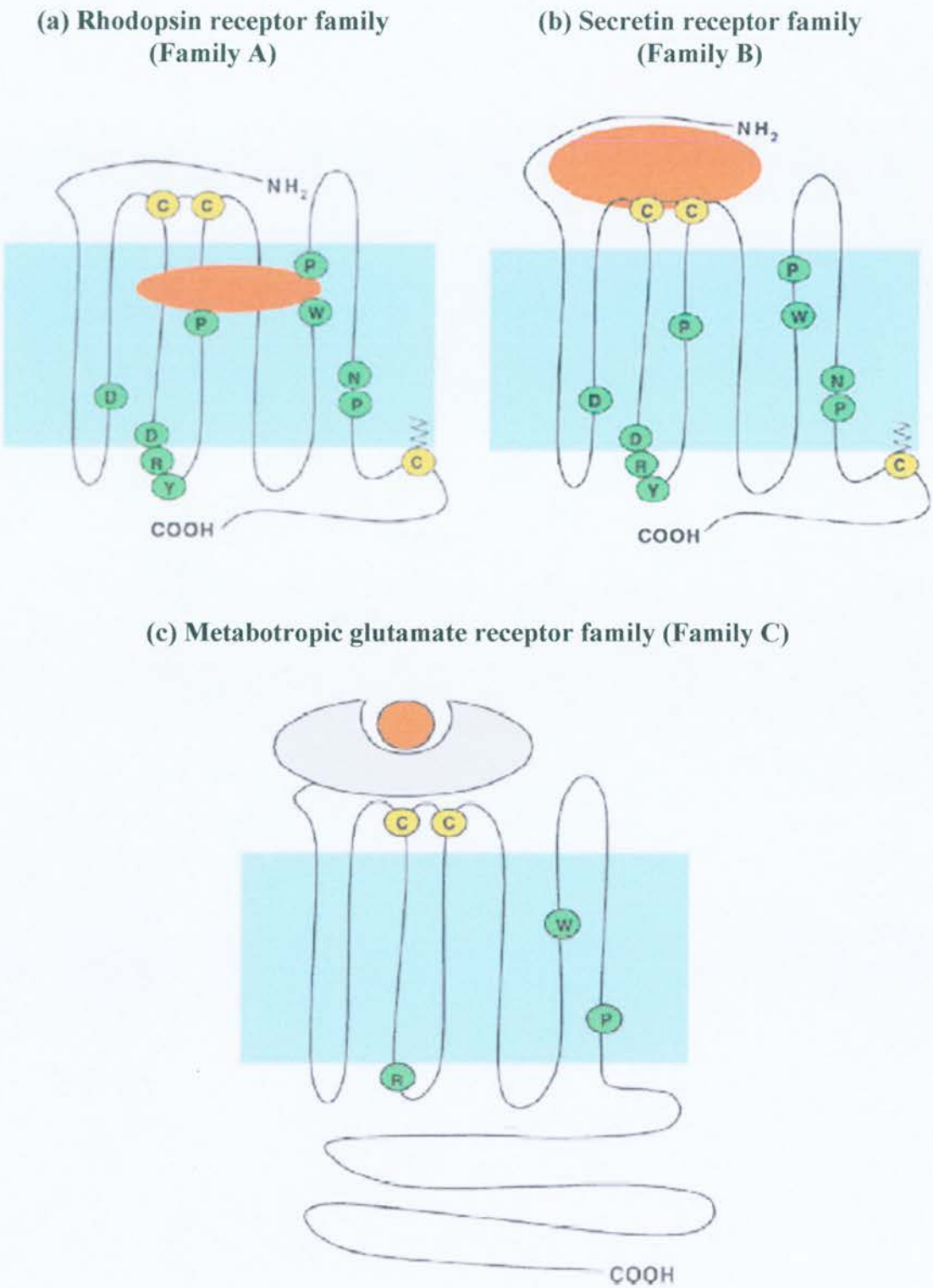

Figure A.6 **Schematic illustrations of the general structural features of the three main GPCR families.** Endogenous hormone ligands are shown in orange, with conserved amino acid residues and disulphide bridges for each family highlighted in green and yellow respectivley. Figure taken from Jacoby *et al.* (2006).

homology within the 7-TM region (McKnight & Gordon, 1998; Stacey *et al.*, 2000). The majority of the group B receptors also have a hydrophobic N-terminal signal peptide, as well as an N-terminal domain of > 120 residues (Figure A.7), which has been designated the 'hormone binding domain' and contains numerous conserved amino acids, including several cysteines residues (Harmar, 2001; Laburthe & Couvineau, 2002). The receptors' N-termini alone are not sufficient for ligand binding and the binding domain is discontinuous, with contact points on both the N-terminus and the EC loops (Unson, 2002; Lins *et al.*, 2001). The family B GPCRs have been further categorised into three sub-families: B1, B2 and B3 (Harmar, 2001). The 'B1' sub-family contains the classical peptide hormone receptors such as those for GLP, VIP, PACAP and GHRH, i.e. the secretin family of peptides described earlier. All members of the subfamily signal through $G\alpha_s$ and AC to increase the production of intracellular cAMP, although coupling to additional pathways, for example those leading to increased calcium levels, has been reported for some receptors (Aiyar *et al.*, 1999; McCulloch *et al.*, 2002). The 'B2' sub-family is the largest of the group and encompasses several sets of receptors, including the orphan receptors that have been described as the LN-TM7 (Zendman *et al.*, 1999) or LNB-TM7 family (Stacey *et al.*, 2000). The members of this group have very long N-terminal domains, which can be up to 2000 - 3000 residues in length (Fredriksson *et*

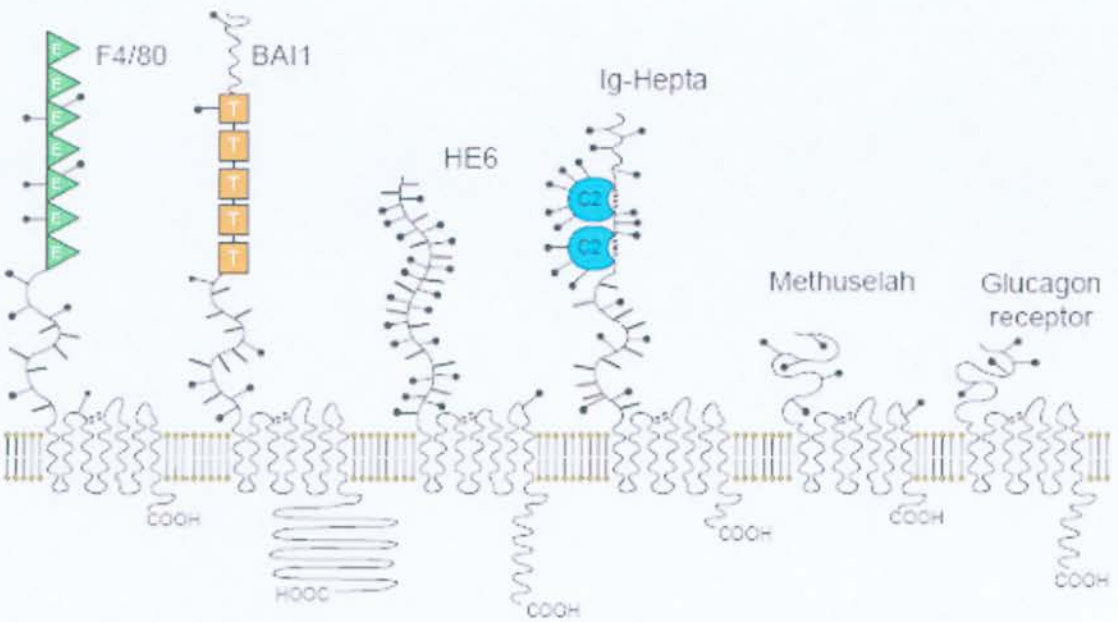

Figure A.7 **Schematic illustration of the structures of selected group B GPCRs.** The diagram shows the general structural features of six group B receptors, with 'E' representing EGF domains, 'T' representing thrombospondin type-1 repeats and C2 representing C2-set IgSF domains (Stacey *et al.*, 2000).

al., 2003a) and a 7-TM region that is typical of the other members of the group B GPCR family. Additional characteristics of receptors in this family include a region consisting of ~ 20 % SER/THR residues and a CYS-box, both of which are found on the EC terminal just before the start of the first TM domain (Stacey *et al.*, 2000). The B2 family also includes the EGF-TM7 group, which are almost exclusively found on immune cells and have distinct long N-terminal domains which contain variable numbers of tandemly repeated endothelial growth factor (EGF) domains (McKnight & Gordon, 1998; Kwakkenbos *et al.*, 2004). Despite showing significant homology to other group B GPCRs in the 7-TM region, evidence for G-protein coupling and transduction mechanisms for B2 receptors, akin to the B1 receptors is scarce. Only four members of the B2 family have been reported to couple to specific G-proteins (Lelianova *et al.*, 1997; Foord *et al.*, 2002). The third sub-family is the 'B3' or 'Methuselah-like' GPCRs, aptly named after the P-element insertion gene mutation in drosophila which generates mutant 7-TM receptors that are associated with an extended life-span (Lin *et al.*, 1998). Methuselah receptors have some homology to the other group B receptors in the 7-TM region, however they do not have a SER/THR rich region or CYS-box (Stacey *et al.*, 2000).

Over the last few years a generally accepted model of ligand binding to, and activation of group B GPCRs has emerged. This model proposes that the C-terminus of the activating peptide binds to the long EC N-terminal domain of the receptor, after which the N-terminus of the ligand docks to the body of the receptor or the 'J' domain (i.e. juxtamembrane region consisting of transmembrane regions and intervening loops), causing a conformational change that allows intracellular loops to trigger signal transduction cascades (Figure A.8; Laburthe & Couvineau, 2002;

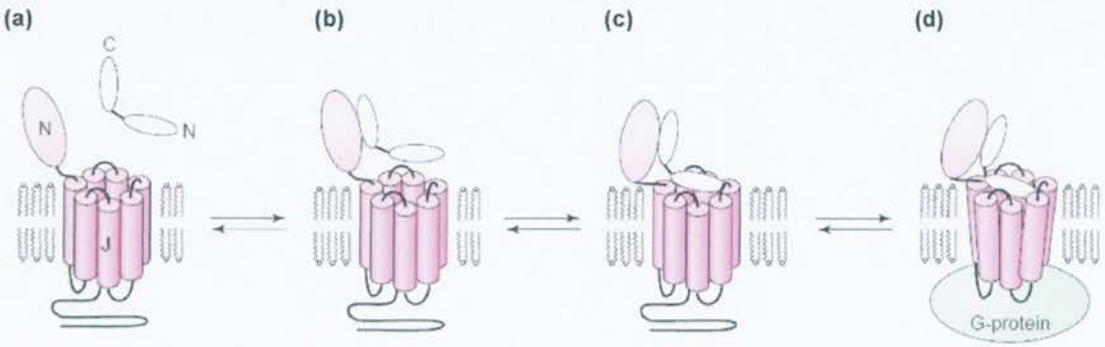

Figure A.8 **Suggested mechanism for peptide binding to, and activation of the group B GPCR.** In this model, the C-terminal region of the peptide binds to the EC N-terminal of the receptor (**a, b**), after which the N-terminal of the peptide binds to the TM bundle (**c**). A conformational change then occurs in the receptor, leading to G-protein activation (**d**). Figure modified from Hoare *et al.* (2005).

Hoare, 2005). An interesting alternative model has recently been proposed by Dong and colleagues (Dong *et al.*, 2006), who suggested that the hormone (secretin in this case) may expose a hidden, built-in agonist epitope in the amino terminus of the GPCR which interacts with specific regions in the body of the receptor (TM6 for secretin) causing activation. However, it remains to be seen whether this mechanism will apply to other members of this receptor family.

A.2.4. Classification of VIP and PACAP receptors

Initial pharmacological studies of putative VIP receptors generally involved either cAMP stimulation assays or binding studies using iodinated VIP, with these approaches existing long before modern advances in molecular biological techniques, such as receptor cloning. Such studies identified generic 'VIP receptors' in a variety of tissues and cells, including guinea pig pancreatic acinar cells (Christophe *et al.*, 1976; Robberecht *et al.*, 1976), various preparations of rat brain membranes (Taylor & Pert, 1979), peripheral blood lymphocytes (Guerrero *et al.*, 1981a; O'Dorisio *et al.*, 1981), rat liver membranes (Guerrero *et al.*, 1981b), human lymphoblasts (Beed *et al.*, 1983), epithelial cells from human gallbladder (Dupont *et al.*, 1981), neonatal astrocytes (Magistretti *et al.*, 1983), multiple areas of the adult CNS (Staun-Olsen *et al.*, 1985) and human colonic epithelial cells (Broyart *et al.*, 1981). 'VIP receptors' were also identified in various human carcinoma cell lines, including those derived from the gut (Laburthe *et al.*, 1978), the cervix (Prieto *et al.*, 1981), the lung (Laburthe *et al.*, 1981), the breast (Gespach *et al.*, 1988) and from the pancreas (Estival *et al.*, 1983). During the same period many autoradiographic studies were published, in which iodinated VIP was used to identify the anatomical distribution of non-specific VIP receptors in a variety of central and peripheral tissues, from a range of species (Besson *et al.*, 1984; Farmery *et al.*, 1984; Leroux *et al.*, 1984; Carstairs & Barnes, 1986; Shaffer & Moody, 1986; Power *et al.*, 1988). The specific distribution of each receptor subtype shall be discussed further in section A.2.9. (p 33).

The VIP receptors characterised in these tissues using VIP and the VIP-like peptides available at the time, showed variations in pharmacology due, in part, to the presence of multiple receptors and because of the lack of suitable ligands. It was not until more selective ligands were identified and generated that the receptors could be more clearly identified and characterised. In 1982, Raufman and colleagues identified a bioactive peptide from the venom of the Gila monster (*Heloderma*

suspectum) that was able to stimulate AC and cAMP in guinea-pig acinar cells, in a manner similar to VIP and secretin; hence the action of the venom was attributed to secretin/VIP receptor activation (Raufman *et al.*, 1982). In further studies on intestinal epithelial cells (which are devoid of secretin receptors), new data indicated that the action of the venom was specific for VIP receptors, interacting equally well with both rat and human receptors (Amiranoff *et al.*, 1983). This distinguished the pharmacology of this ligand from other VIP like peptides, such as PHI and secretin, which showed differences in affinity for the VIP receptors of the two species (Laburthe *et al.*, 1983). The active peptide in the venom, helodermin, was subsequently isolated and purified (Vandermeers *et al.*, 1984), which led to more extensive analysis of its specific properties and the resultant identification of many VIP-like physiological effects (Blank *et al.*, 1986; Naruse *et al.*, 1986; Koshiyama *et al.*, 1987). However, differences between these peptides were beginning to emerge in terms of potency/binding characteristics, with a study by Robberecht and colleagues (1984) clearly showing variations between helodermin, VIP and secretin in their ability to stimulate cAMP production in membranes from several rat and human organs. These researchers tentatively suggested that the distinct actions of helodermin (from both secretin and VIP) may be a result of the activation of specific helodermin receptors (Robberecht *et al.*, 1984). Four years later, the same group used iodinated helodermin and SUP-T1 cells, to provide further evidence for a single population of helodermin–preferring VIP receptors in this human T-cell lymphoma cell line (Robberecht *et al.*, 1988). In this study, the rank order of potency (ROP) of the various VIP-like peptides examined was distinct from that of all other VIP receptors previously described, with helodermin shown to have an even higher affinity than VIP (5 - 7 times higher) in the radioligand binding studies. In parallel cAMP studies, the same ROP was produced, with helodermin being ~ 3 fold more potent than VIP (Robberecht *et al.*, 1988). Around the same time, Turner and colleagues (1986) reported that rat basophilic leukaemia (RBL) cells produced a VIP fragment, N-terminally truncated VIP(10-28), that was functionally distinct from normal VIP (Turner *et al.*, 1986). This peptide was shown to inhibit VIP binding and VIP induced AC activity in HT-29 cells, having no effect alone on AC activity and was therefore suggested to be a VIP receptor antagonist. More interestingly, this peptide had no affinity for, or effect on, agonist stimulated responses from VIP receptors in SUP-T1 cells (Robberecht *et al.*, 1989), in contrast to its antagonist effects in HT-29 cells. These data again suggested a degree of diversity in the VIP receptor population.

The gradual accumulation of the pharmacological evidence which led to the eventual identification of distinct VIP receptors contrasts with the rapid identification of a selective PACAP receptor, following the isolation of PACAP-27 and PACAP-38. Soon after the isolation of both peptides (Miyata *et al.*, 1989, 1990), high affinity, selective PACAP receptors were identified in the rat AR4-2J pancreatic cancer acinar cell line (Buscail *et al.*, 1990). Initially, PACAP was tested in this cell line as the cells were known to express VIP receptors, and as a consequence of the sequence similarities between the peptides, it was proposed that PACAP may interact with the VIP receptors (Svoboda *et al.*, 1988; Buscail *et al.*, 1990). However, PACAP-27 and PACAP-38 were shown to have an equally high affinity for PACAP binding sites in these cells, with both VIP and helodermin being of much lower (~ 1000 fold) affinity (Buscail *et al.*, 1990). Similarly, these studies showed that the PACAPs potently stimulated adenylate cyclase (EC_{50}: 0.2 nM for both peptides) in AR4-2J cells, with VIP and helodermin again being much less potent. In contrast to PACAP-27 and PACAP-38, VIP and helodermin actually appeared to be partial agonists in the adenylate cyclase assay (Buscail *et al.*, 1990). In the same year, similar high affinity PACAP-preferring binding sites were also identified in primary cultures of rat cortical astrocytes (Tatsuno *et al.*, 1990), bovine brain membranes (Ohtaki *et al.*, 1990), rat hypothalamus, brain stem, cerebellum and lung (Lam *et al.*, 1990) and in the NB-OK-1 human neuroblastoma cell line (Cauvin *et al.*, 1990a).

Around this time, data from many studies using a combination of VIP, PACAP-27, PACAP-38 and helodermin amongst others (e.g. secretin and PHI) began to draw out differences in pharmacology that could clearly distinguish distinct receptor subtypes. For example, PACAP and helodermin were found to bind with equal affinity to the VIP-helodermin preferring receptors in SUP-T1 cells (Gourlet *et al.*, 1991). Autoradiography studies clearly identified two PACAP binding sites, one of which was PACAP preferring, whereas VIP and PACAP had equal affinity at other sites (Shivers *et al.*, 1991). PACAP and VIP also bound equally well to receptors in jejunal epithelial plasma membranes, with helodermin being less potent (Salomon *et al.*, 1993). The emerging pattern suggested there were two classes of VIP receptors, both of which PACAP bound to with high affinity, however the two subtypes could be distinguished by examining the potency of other ligands, such as helodermin. In addition, a third receptor class was more easily recognisable by its clear preference for PACAP compared to VIP. These three receptor subtypes were later classified by IUPHAR into 'VPAC receptors' for VIP and PACAP, and 'PAC_1 receptors' which were the PACAP-preferring subtype (Harmar *et al.*, 1998). The

VPAC receptors were further distinguished into $VPAC_1R$ and $VPAC_2R$ subtypes, based upon helodermin binding/potency ($VPAC_2R$ being helodermin preferring).

A.2.5. Cloning of VPAC/PAC receptors

The $VPAC_1R$ was initially cloned from a rat lung cDNA library by Ishihara and colleagues (1991) and soon after, the human homologue was cloned from the HT-29 colon carcinoma cell line (Sreedharan *et al.*, 1993). The mouse sequence was then cloned three years later from mouse lymphoid cells (Johnson *et al.*, 1996). When examined in stably transfected cell lines, the general agonist ROP at this receptor (in cAMP studies) was VIP = PACAP-27 = PACAP-38 = PHM > secretin, with the EC_{50} values for the former four agonists being approximately 0.01 - 0.1 nM (Ishihara *et al.*, 1992; Sreedharan *et al.*, 1993). A small number of studies have examined endogenous $VPAC_1R$ function in the HT-29 cell line and have similarly shown the VIP and PACAP peptides to be equipotent and of low nanomolar potency at this receptor in stimulating cAMP production, with secretin being considerably less potent (Laburthe *et al.*, 1978; Mangeat *et al.*, 1981; Lelievre *et al.*, 1998; Summers *et al.*, 2003). Additional human cell lines in which endogenous $VPAC_1R$ function has been studied include the LoVo (colon adenocarcinoma: Yu *et al.*, 1992; Gourlet *et al.*, 1997b) and HeLa (cervical carcinoma: Laburthe *et al.*, 1980; Prieto *et al.*, 1981) cell lines.

The $VPAC_2R$ was first cloned by Lutz and co-workers from a rat pituitary cDNA library (Lutz *et al.*, 1993). This was quickly followed by a report on the cloning of the human receptor from SUP-T1 cells (Svoboda *et al.*, 1994) and then the mouse transcript from the MIN-6 insulin secreting β-cell line (Inagaki *et al.*, 1994). When these groups expressed the transcripts in COS-7 and CHO cells, the general ROP from cAMP studies was VIP = PACAP-27 = PACAP-38 = helodermin > PHI/PHM, with very little response to secretin observed even at micromolar peptide concentrations. The majority of cell based studies examining endogenously expressed $hVPAC_2R$ receptors have focussed on the SUP-T1 cell line, however some have also used human Molt-4b lymphoblastic leukaemia cells (Summers *et al.*, 2003) and THP-1 monocytic leukaemia cells (Chedeville *et al.*, 1993). From the SUP-T1 studies, the generally observed ROP was helodermin > VIP = PACAP = PHI >> secretin, although a degree of variability is evident between studies (Robberecht *et al.*, 1988, 1989; Xia *et al.*, 1996; Gourlet *et al.*, 1997b; Igarashi *et al.*, 2002b).

Average EC_{50} values reported in these studies from the examination of cAMP stimulations, were ~ 0.3 nM for helodermin and ~ 10 nM for VIP and the PACAPs.

Finally, the rat PAC_1R was simultaneously cloned by several groups within just a few weeks of each other (Hashimoto *et al.*, 1993; Hosoya *et al.*, 1993; Morrow *et al.*, 1993; Pisegna & Wank, 1993; Spengler *et al.*, 1993; Svoboda *et al.*, 1993), either from rat brain cDNA libraries or the rat AR4-2J cell line. The human transcript was cloned in the same year, whereas the mouse variant was cloned three years later (Ogi *et al.*, 1993; Hashimoto *et al.*, 1996b). Several of these groups also expressed the transcripts in various host cell lines for functional assessment of receptor activity, with the clear ROP from all such studies being PACAP-27 = PACAP-38 > VIP. In terms of endogenous cell lines, PAC_1R pharmacology has been examined using AR4-2J cells and the human neuroblastoma cell line NB-OK-1, with many studies also performed using the rat phaeochromocytoma PC12 cell line (Buscail *et al.*, 1990; Cauvin *et al.*, 1990a; Deutsch & Sun, 1992). In general, the data from human cell lines expressing PAC_1R (in cAMP assays) has shown the PACAPs and VIP to have EC_{50} values of ~ 0.2 nM and ~ 40 nM respectively (Cauvin *et al.*, 1990a; Buscail *et al.*, 1990).

From the sequences of the cloned receptors, hydropathy plots of the individual amino acid residues were suggestive of a heptahelical transmembrane receptor structure (Lutz *et al.*, 1993; Morrow *et al.*, 1993). As mentioned previously, these receptors have since been classified by IUPHAR as GPCRs and are regarded to be members of the group B1 GPCR family, due to the presence of characteristic structural features as described earlier (Harmar *et al.*, 1998).

A.2.6. VPAC/PAC receptor pharmacology

A.2.6.1. Generic ligands

Prior to cloning of the individual VPAC/PAC receptors, multiple non-specific VIP receptor ligands were reported, in addition to the endogenous ones already described (VIP, PACAP, PHM etc.). Several of these ligands are VIP receptor antagonists which have proven to be useful in defining receptor function, although the majority of these ligands are modified analogues of existing agonists. These analogues, discussed further below, fall into three main categories: C-terminal fragments of VIP/PACAP, chimeric or hybrid peptides and finally, D enantiomer substituted peptides. Some of the better characterised receptor antagonists of VIP/PACAP action are (N-Ac-Tyr^1, D-Phe^2)-GRF(1-29)-NH_2 (Waelbroeck *et al.*,

1985), [4Cl-D-Phe^{6}, Leu^{17}]VIP (Pandol *et al.*, 1986), VIP(10-28) (Turner *et al.*, 1986), PACAP(6-27) (Robberecht *et al.*, 1991) and PACAP(6-38) (Robberecht *et al.*, 1992). Most of these antagonists had relatively low affinity (μM) for VIP receptors and over the next few years, as the individual VPAC/PAC receptors were cloned and peptide design studies improved, these generic peptides were superseded by novel ligands of higher potency and selectivity. Some of these ligands have proven to be useful tools in defining the physiological functions of the VPAC/PAC receptors, with the use of BAY 55-9837 for example, highlighting important roles for the $VPAC_2R$ in glucose homeostasis (Tsutsumi *et al.*, 2002). However, to date all of the ligands reported are peptides and are mostly modified versions of VIP and the PACAPs (sequences provided in Table A.2), with no non-peptide agonists or antagonists described. A summary of the most potent and selective of these ligands will be discussed briefly below, with further discussion of selected ligands in chapter one.

A.2.6.2. $VPAC_1R$ selective peptides

A highly potent and selective agonist and antagonist have been described for the $VPAC_1R$. In 1997, Gourlet and colleagues described a modified hybrid peptide of VIP and GRF which was reported to be a $VPAC_1R$ antagonist (Gourlet *et al.*, 1997a). This peptide, PG97-269, inhibited agonist induced cAMP responses in rat and human $VPAC_1R$ expressing cell lines with IC_{50} values of 15 nM and 2 nM respectively (Gourlet *et al.*, 1997a; Juarranz *et al.*, 1999). When tested up to 0.3 μM, PG97-269 had no effect alone, or on any agonist induced response in $VPAC_2$ (human and rat) or PAC_1 (rat) receptor expressing cell lines (Gourlet *et al.*, 1997a).

Three years later in 2000, the generation of a $VPAC_1R$ selective agonist [Ala^{11,22,28}]VIP was reported (Nicole *et al.*, 2000), from structure-function studies of VIP binding to VPAC receptors. In AC stimulation studies, this modified VIP analogue was observed to have low nanomolar potency at $hVPAC_1R$ (EC_{50}: 0.4 nM) and was more than 3000 fold selective for $VPAC_1R$ over $VPAC_2R$. To date, no studies have examined the effect of this agonist at PAC_1R.

A.2.6.3. $VPAC_2R$ selective peptides

The first of the more selective and potent $VPAC_2R$ agonists were developed by Roche in the mid 1990s, as potential bronchodilators (Bolin *et al.*, 1995). Two

Table A.2. **Amino acid sequences of putatively selective agonisrs and antagonists of VPAC/PAC receptors, with the sequences of VIP and the PACAPs shown for comparison.**

	1		5	10	15	20	25	30	35	40	45	50	55	60
VIP	H	S	D A V F T D N Y T R L R K Q M A V K K Y L N S I L N											
PACAP-27	H	S	D G I F T D S Y S R Y R K Q M A V K K Y L A A V L											
PACAP-38	H	S	D G I F T D S Y S R Y R K Q M A V K K Y L A A V L G K R Y K Q R V K N K											
[Ala^{11,22,28}]VIP	H	S	D A V F T D N Y A R L R K Q M A V K K A L N S I L A											
Ro25-1553	AcH	S	D A V F T E N Y T K L R K Q L A A K K Y L N D L K K G G T											
Ro25-1392	AcH	S	D A V F T E N Y T K L R K Q L A A K K Y L N D L K K											
BAY55-9837	H	S	D A V F T D N Y T R L R K Q V A A K K Y L Q S I K N K R Y											
R3P65	H	S	D A V F T D N Y T R L R K Q M A A K K Y L N S I K N K R											
Maxadilan	C	D	A T C Q F R K A I D D C Q K Q A H H S N V L Q T S V Q T T A T F T S M D T S Q L P G N S V F K E C M K Q K K K E F K A G K											
PG97-269	AcH	D-Phe	D A V F T N S Y R K V L K R L S A R K L L Q D I L											
PG99-465	MyrH	S	D A V F T D N Y T K L R K Q M A V K K Y L N S I K K G G T											
Max.d.4.	C	D	A T C Q F R K A I D D C Q K Q A H H S N V - P G N S V F K E C M K Q K K K E F K A G K											
M65	C	D	A T C Q F R K A I D D C Q K Q A H H S N V L - - - - - - - - - - - - - - - - - L P G N S V F K E C M K Q K K K E F K A G K											

cyclic peptide analogues of VIP, Ro25-1553 and Ro25-1392 were described, both of which stimulated cAMP production in CHO cells expressing the $VPAC_2R$, with EC_{50} values of ~ 1 nM (O'Donnell *et al.*, 1994; Xia *et al.*, 1997). These peptides were 300 - 1000 fold selective for the $VPAC_2R$, however both compounds also showed clear agonist activity at $VPAC_1R$, when applied at micromolar concentrations (Gourlet *et al.*, 1997b; Xia *et al.*, 1997). A number of $VPAC_2R$ agonists have been developed by Bayer in an attempt to determine whether they could be potential therapeutic agents for type II diabetes, with the most potent ligands being BAY 55-9837 and R3P65 (Tsutsumi *et al.*, 2002; Yung *et al.*, 2003). Both peptides were produced following site directed mutagenesis studies of VIP, PACAP and Ro25-1553 and were found to be potent $VPAC_2R$ agonists (cAMP stimulation, EC_{50}: ~ 0.3 nM). BAY 55-9837 was shown to be 100 fold selective for $VPAC_2R$ over $VPAC_1R$ (EC_{50}: 30 nM; Tsutsumi *et al.*, 2002). R3P65, which differs from VIP by only 4 amino acids, was slightly more selective (~ 200 fold) for $VPAC_2R$ than BAY 55-9837, however at higher concentrations R3P65 stimulated both $VPAC_1$ (EC_{50}: 90 nM) and PAC_1 receptors (partial agonist at micromolar concentrations; Yung *et al.*, 2003).

In attempts to develop $VPAC_2R$ selective antagonists, Moreno and co-workers (2000) investigated how modifications of $VPAC_2R$ agonists, such as Ro25-1553, affected peptide potency and binding to the receptor. Following acylation of the amino-terminus of the extended VIP(1–26)KKGGT peptide by myristic acid (C14 fatty acid), the resulting peptide, named PG99-465 was reported as the first selective $VPAC_2R$ antagonist (Moreno *et al.*, 2000). In AC stimulation studies, these authors showed that the peptide was a potent $VPAC_2R$ antagonist (IC_{50}: 2 nM), however partial agonism at $VPAC_1R$ was also observed (EC_{50}: 200 nM), giving this peptide a 100 fold selectivity (Moreno *et al.*, 2000). Again, to date, the effect of PG99-465 at the PAC_1R has not been reported.

A.2.6.4. PAC_1R selective peptides

In contrast to that described above for the VPAC receptors, the peptides which have been reported to be PAC_1R selective ligands have no significant sequence homology to VIP, PACAP or any other member of this peptide family. Maxadilan, the first truly selective PAC_1R agonist, was extracted from the salivary gland of sand flies (*Lutzomyia longipalpis*) and was found to be a potent vasodilator (Lerner *et al.*, 1991). Upon cloning, maxadilan was shown to be a 63 amino acid peptide (Figure A.9), which is processed by C-terminal amidation to give a mature

61 amino acid peptide. This peptide was found to have similar biological effects to calcitonin gene-related peptide (CGRP) and was therefore evaluated for binding site interactions on rat and rabbit brain membranes, with other members of the peptide family, including VIP, PACAP, glucagon and secretin (Moro & Lerner, 1997). In addition, these authors also examined functional responses induced by maxadilan in COS cell lines transfected with the three individual VPAC/PAC receptor subtypes. Maxadilan was shown to specifically bind to the PAC_1R and was equipotent with PACAP-38 in stimulating cAMP production (EC_{50}: 1 nM). No interactions in the binding or functional studies were observed with maxadilan at either of the VPAC receptor subtypes (Moro & Lerner, 1997).

From structure function studies using maxadilan, two deletion variants have been identified as PAC_1R selective antagonists (Figure A.9). The first, M65, was described by Tajima and colleagues following the deletion of amino acids 25 – 41 of the maxadilan sequence (Uchida *et al.*, 1998). These authors reported that M65 inhibited PACAP responses mediated by the PAC_1R in a concentration dependent manner, however no IC_{50} values or graphical data was presented for the functional

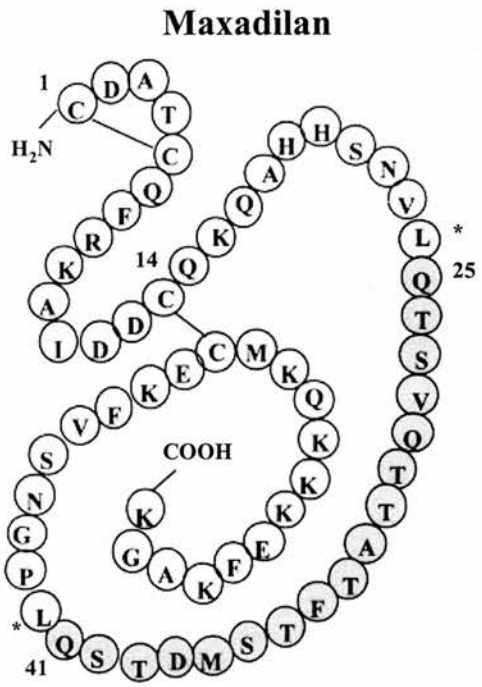

Figure A.9 **The amino acid sequence of the PAC_1R agonist maxadilan.** The full length maxadilan sequence is shown, prior to C-terminal amidation to a 61 residue peptide. Deletion of the residues highlighted in grey (25 – 41) produces M65, a PAC_1R antagonist. The additional removal of two leucine resides (*) results in a peptide named max.d.4, which is also reported to be a PAC_1R antagonist. The figure shown has been modifed from Tatsuno *et al.* (2001).

studies discussed (cAMP) in that report. In a more recent set of studies examining the effect of agonists on pigment dispersion in *Xenopus* melanophores expressing the PAC_1 receptors, M65 was shown to inhibit PAC_1R agonist responses with an IC_{50} of 4 nM (Reddy *et al.*, 2006). Tajima's group also reported a second deletion variant of maxadilan, max.d.4., with residues 24 - 42 omitted from the parent peptide, which inhibited PACAP-38 simulated cAMP production in PAC_1R expressing stable cell lines with an IC_{50} of ~ 0.3 nM (Moro *et al.*, 1999).

In summary, despite intensive investigation in the last 20 years only a limited number of selective VPAC/PACR ligands have been reported in the literature, including PG97-269, maxadilan and M65. However the majority of compounds identified as agonists or antagonists at these receptors show some interaction with more than one subtype (at least at higher concentrations) and additionally, some of these ligands have not been fully characterised with all three receptor subtypes. To date, all of the VPAC/PACR agonists and antagonists are peptides, the majority of which are derived from the structures of the endogenous peptides VIP and PACAP.

A.2.7. VPAC/PAC receptor signalling

In addition to the classical stimulation of $G\alpha_s$ proteins which activate AC and increase cAMP levels, the VPAC/PAC receptors have been observed to stimulate the production of additional second messengers. This coupling to multiple G-proteins has also been observed for other members of the group B1 GPCR family, e.g. calcitonin receptors (Aiyar *et al.*, 1999). Prior to VPAC/PAC receptor cloning, many groups reported elevated levels of calcium in a variety of cells types upon exposure to VIP and PACAP. These include rat superior cervical ganglion cells (Audigier *et al.*, 1986), adrenal medulla cells (Malhotra *et al.*, 1988), PC12 cells (Deutsch & Sun, 1992), hippocampal neurons (Tatsuno *et al.*, 1992), pituitary cells (Canny *et al.*, 1992) and the SK-N-SH human neuroblastoma cell line (Oettling *et al.*, 1990). The specific interaction of VPAC/PAC receptors with G-proteins that couple to pathways stimulating intracellular calcium was reported soon after the cloning of each receptor subtype ($VPAC_1R$: Sreedharan *et al.*, 1994; $VPAC_2R$: Xia *et al.*, 1996; PAC_1R: Spengler *et al.*, 1993). The receptors also couple to additional signalling pathways, including those modulating phospholipase D (Morisset *et al.*, 1995; McCulloch *et al.*, 2000), tyrosine kinases (Morisset *et al.*, 1995) and L-type calcium channels (Chatterjee *et al.*, 1996). The signalling pathways mediated by the

receptors, particularly those modulating cAMP and calcium, will be discussed more extensively in chapter one.

A.2.8. Receptor splice variants

Although many of the mammalian genes encoding GPCRs are intronless, the VPAC/PAC receptors are one exception, along with other group B receptors including the calcitonin and GHRH receptors (Gentles & Karlin, 1999). The presence of introns introduces the possibility that the genes may be processed differently (alternative splicing, exon skipping and intron retention), thereby generating receptor splice variants, which may lead to alterations in the pharmacology and signal transduction of those receptors (Kilpatrick *et al.*, 1999). Until recently VPAC receptors splice variants were not thought to occur, which contrasts with the multiple PAC_1R variants which have been identified, all of which shall be discussed below.

A.2.8.1. VPACR splice variants

A recent report using human peripheral blood mononuclear cells and SUP-T1 cells, described putative 5-TM variants of both the $VPAC_1R$ (88 amino acid deletion) and $VPAC_2R$ (74 amino acid deletion; Bokaei *et al.*, 2006). Both of these variants were postulated to lack sections of the third intracellular loop, the third extracellular loop and the TM domains 6 – 7, as illustrated in Figure A.10 (Bokaei *et*

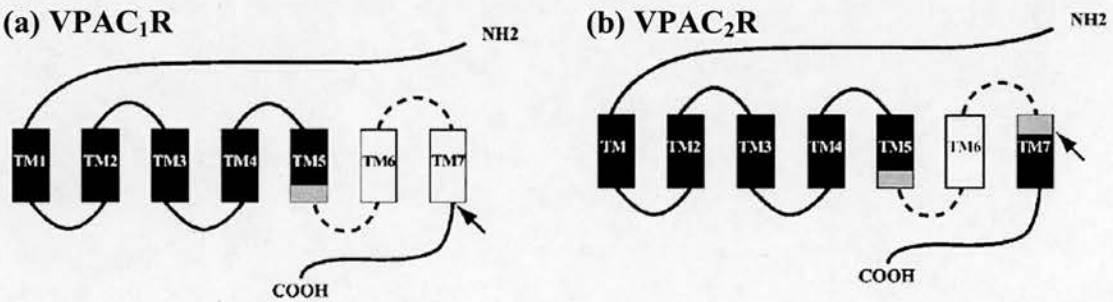

Figure A.10 **Schematic illustration comparing the structures of the wild type VPAC receptors and the postulated 5-TM splice variants.** Sections of the wild-type receptors (**a**: $VPAC_1$; **b**: $VPAC_2$) which are thought to be deleted in the splice variants are indicated by lighter shading, with arrows showing the suggested connection point of TM-5 to the C-terminus. Figure taken from Bokai *et al.* (2006).

al., 2006). These authors examined the functionality of the truncated $VPAC_1R$ variant only and found that when expressed in CHO cells, this receptor demonstrated poor coupling to cAMP pathways in response to agonist stimulation, however stimulation of protein tyrosine kinase activity was observed. As this is first report of a functional $VPAC_1R$ variant, and the first report of 5-TM VPAC/PAC variants, clearly further studies will be required to determine the distribution and physiological roles of such receptors. In addition, two naturally occurring deletion variants of the $VPAC_2R$ have been identified in recent years by the Goetzl laboratory. The first, $VPAC_2$de367-380, was identified from mouse thymus and spleen and has a 42 base pair deletion in exon 12, resulting in a 14 amino acid omission (367 - 380) at the C-terminal of the seventh TM domain (Grinninger *et al.*, 2004). It has been postulated that this variant may be a 6-TM receptor with an extracellular C-terminal, however as to how this variant arises is unknown, with its distribution and physiological function remaining unclear (Huang *et al.*, 2006). When transfected into Jurkat T cells, VIP bound to the mutant receptor with the same affinity as the standard $VPAC_2$ receptor, however modulation of intracellular signalling molecules, including cAMP and IL-2, was not observed, in contrast to the wild type receptor (Grinninger *et al.*, 2004). In addition, T-cells transfected with the mutant receptor have been shown to secrete less IL-4 upon VIP stimulation than cells transfected with the standard $VPAC_2R$ receptor (Huang *et al.*, 2006). The second $VPAC_2R$ variant was identified from both a human malignant T-cell line and activated normal T-cells, and was produced as a consequence of the deletion of exon 11, resulting in the loss of 114 amino acids from 325 – 438, with 10 new amino acids in positions 325 – 334 (Miller *et al.*, 2006). This created a frame shift and introduced a premature stop codon, with the resulting $VPAC_2$ variant ($VPAC_2$de325-438(i325-334)), suggested to be a 5-TM receptor. In preliminary studies these authors found that VIP had a lower affinity for the mutant variant compared to the wild type $VPAC_2R$ and that the mutant receptor was less sensitive to agonist-induced down regulation and showed a weaker coupling to intracellular signalling pathways (Miller *et al.*, 2006).

In 2001, Murthy and co-workers reported the presence of a VIP receptor in guinea-pig smooth muscle cells that was VIP specific and for which PACAP had very low affinity (Teng *et al.*, 2001). The same authors have just reported the cloning of this 'VIPs' receptor from the same cell type, and through binding and functional studies have confirmed that PACAP has a much lower affinity (radioligand binding) and efficacy (cAMP studies) than VIP for this receptor when expressed in COS-1 cells (Zhou *et al.*, 2006). The sequence of 'VIPs' was shown to differ from the $VPAC_2R$ by only two residues, located in the N-terminal ligand

binding domain (Zhou *et al.*, 2006). The existence of a putative VIP selective receptor has been previously suggested by other groups. For example Gressens and colleagues suggested that a VIP selective receptor was responsible for mediating the neuroprotective effects of VIP against ibotenate induced excitotoxic brain lesions in newborn mice (Gressens *et al.*, 1999; Rangon *et al.*, 2006). In this model, VIP was a potent neuroprotectant, as were other $VPAC_2R$ agonists and PHI, however $VPAC_1R$ agonists and the PACAP peptides were without effect (Rangon *et al.*, 2006). The presence of a 'VIPs' receptor was also described by Ekblad and colleagues when investigating the properties of VPAC/PAC receptors in the mouse intestine (Ekblad & Sundler, 1997; Ekblad *et al.*, 2000). The recent cloning of the 'VIPs' receptor may facilitate more extensive studies into the distribution and function of such a receptor and may confirm whether it is the same VIP selective receptor described by other groups.

A.2.8.2. PAC_1R splice variants

The PAC_1R has been described as 'one of the most extensively spliced GPCRs known', with variants carrying changes in the intracellular loops, transmembrane domains, and N-terminal regions (Dautzenberg *et al.*, 1999). Although the presence of potential splice sites in such a range of regions is not common, a similar pattern has been reported for the calcitonin and GHRH receptors (Kilpatrick *et al.*, 1999). In contrast to the VPAC receptors, the first PAC_1R variants were identified at the time of the initial receptor cloning by Spengler and co-workers (1993). These authors reported the cloning of five distinct PAC_1 receptor variants from a newborn rat colliculi cDNA library, which were named null, hip, hop1, hop2 and hiphop1, according to the presence of two 28 amino acid cassettes (hip and hop) in the third intracellular loop (Figure A.11). The PAC_1-hop1 (28 residue insertion) and hop2 (27 residue insertion) variants were suggested to originate from the alternative use of splice acceptor sites in the hop cassette. The null and hop1 variants were shown to be the predominant PAC_1R variants found in several rat brain regions (Spengler *et al.*, 1993). Using the same techniques, these authors subsequently reported the cloning of the sixth and final combination of these cassettes, the PAC_1-hiphop2 receptor (Journot *et al.*, 1995). When expressed in a porcine kidney cell line (LLC PK1), the presence of the hip cassette was generally shown to reduce agonist induced AC stimulation and abolish calcium responses, whereas the hop cassette appeared to have no influence on the ability of the receptor to increase cAMP or

calcium following agonist stimulation (Spengler *et al.*, 1993; Journot *et al.*, 1995). The receptors which contained both cassettes were shown to have an intermediate phenotype, with agonists stimulating cAMP and calcium pathways through the PAC_1-hiphop1 receptor with marginally reduced potency and producing a smaller peak calcium response (compared to PAC_1-null; Journot *et al.*, 1995).

One year later, the same group identified an N-terminal PAC_1R variant from a mouse genomic library, with the corresponding human sequence isolated from a fetal brain cDNA library (Pantaloni *et al.*, 1996). They suggested this variant was produced from alternative splicing of exons, resulting in a 21 amino acid deletion in the N-terminal region (Figure A.11; residues 89 - 109). At the time, this variant was called the 'very short' (vs) PAC_1R and the only apparent functional consequence was a marginal increase in the potency with which PACAP-27 activated phospholipase C (PLC; VIP was not tested). In a subsequent study, VIP and PACAP induced stimulations of cAMP were compared in HEK-293 cells expressing this variant, and in contrast to the PACAP preferring null receptors, these peptides were shown to be equipotent (Dautzenberg *et al.*, 1999). In later studies, a PAC_1R mutant equivalent to the 21 amino acid deletion variant described above combined with the hop1 cassette, was shown to be the predominantly expressed PAC_1R variant in rat superior cervical ganglion (SCG) neurons (Braas & May, 1999). In accompanying pharmacological studies (cAMP and inositol phosphate assays) using the cultured SCG neurons, the PACAPs had similar potencies in both assays and were over 1000 fold more potent than VIP. In both of these assays, the maximum PACAP-27 induced responses were slightly larger than those of PACAP-38.

Following on from the cloning of the rat hip and hop splice variants, Pisegna and Wank identified four human homologues from a frontal cortex cDNA library (Pisegna & Wank, 1996). As for the rat receptors, the human variants were distinguished by the presence of two exons, SV-1 and SV-2 (corresponding to two 28 amino acid insertions), which were suggested to be equivalent to the hip and hop cassettes respectively. In addition to the human PAC_1-null, the SV-1, SV-2 (two variants potentially from alternative splice acceptor sites) and SV-3 variants were found and when stably expressed in a mouse embryonic fibroblast cell line (NIH/3T3), all four were shown to couple to pathways increasing cAMP and calcium following agonist activation (Pisegna & Wank, 1996). In these studies, the PACAP peptides were equipotent at all four variants, with an approximate 50 fold reduction in potency observed in the calcium assay. Maximal cAMP responses were similar for all four variants, however maximum calcium responses varied (Pisegna & Wank, 1996). The PACAP-38 calcium response from the SV-2 variant was approximately 8

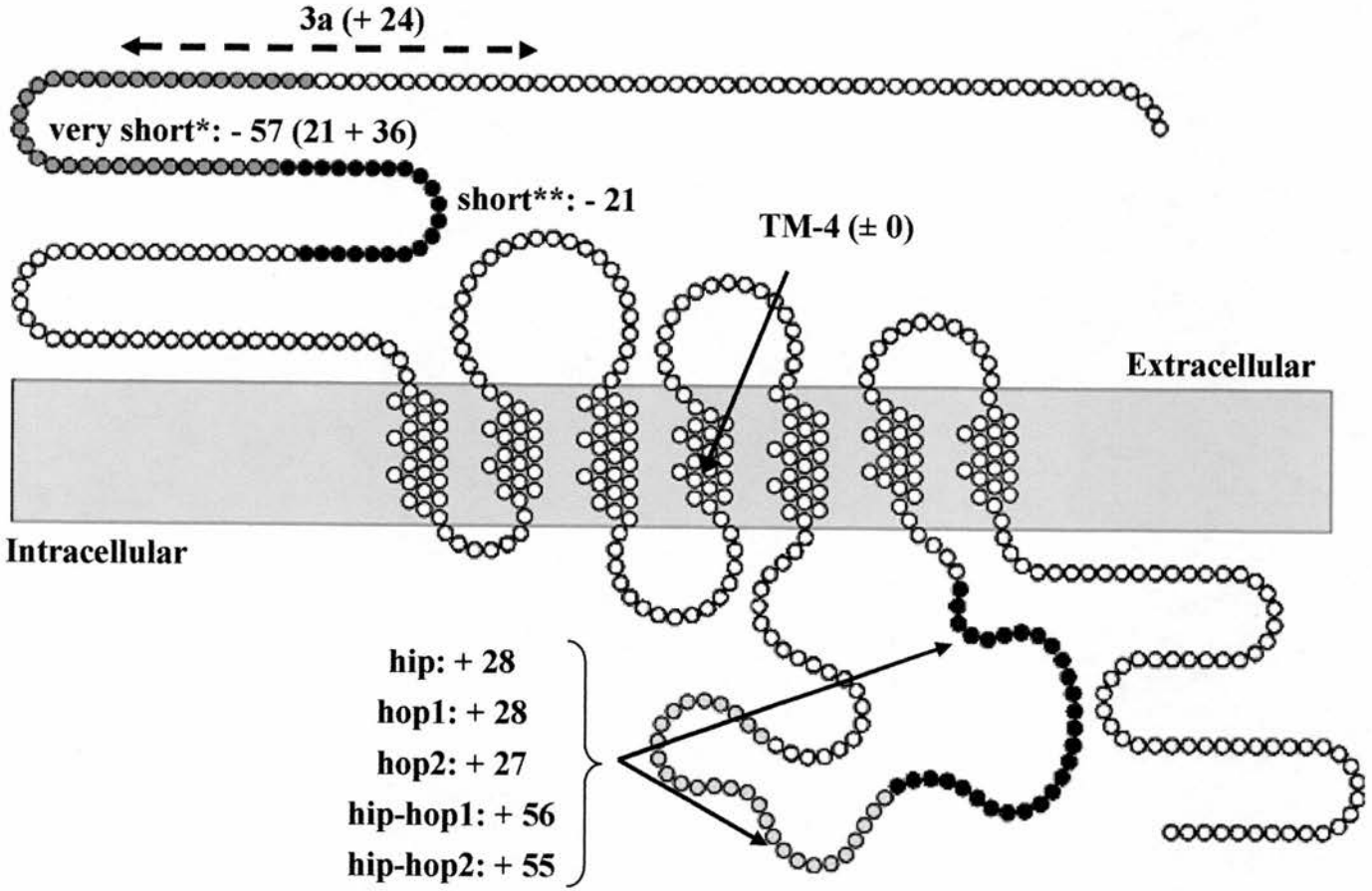

Figure A.11 **Splice variants of the PAC_1R.** The figure illustrates the sites in the PAC_1R sequence which can be alternatively processed to produce different types of PAC_1R splice variants. For each variant highlighted, the number of deleted (-) or inserted (+) residues (as compared to PAC_1-null) is shown in parenthesis. For the 'very short' variant*, the deleted residues include those also omitted from the 'short' variant** in addition to the preceding 36 residues. The figure shown has been modified from Arimura (1998) and Braas & May (1999).

fold higher than the null or SV-1 responses, with the SV-3 variant showing intermediate level of calcium stimulation (measured from total inositol phosphate accumulation/receptor). The null variant was found to be the predominant form expressed in a human frontal cortex cDNA library, with the rank order of expression being: null > SV-2 > SV-1 > SV-3 (Pisegna & Wank, 1996). Similar to the larger calcium responses observed for the SV-2 receptor, further studies demonstrated that this variant also produced a greater stimulation of immediate early gene expression (c-fos and c-myc) compared to the other splice variants (Pisegna *et al.*, 1996).

The final PAC_1R variant reported that year was cloned from rat cerebellar cDNA and was shown to differ from the null at several residues, primarily in the fourth TM domain and was consequently called PACAP-TM4 (Chatterjee *et al.*, 1996). The substitution and deletion of two amino acids in the fourth TM region (CVTV to SA--; residues 279 – 283), was in addition to the D136N (N-terminal) and N190D substitutions (second TM domain). When expressed in BHK-21 cells (a hamster kidney cell line) this receptor did not mediate any effect on cAMP or inositol phosphate levels following PACAP stimulation, although interestingly a clear calcium influx through L-type calcium channels was observed (Chatterjee *et al.*, 1996).

Three years later, Dautzenberg and colleagues (1999) identified a PAC_1R variant in which 57 amino acids were deleted from the N-terminus. The deleted sequence was comprised of the 21 amino acids from the 'very short' variant described by Pantaloni (1996), in addition to the preceding 36 residues (i.e. a deletion of residues 53 – 109; Figure A.11). This variant was subsequently isolated from human cerebellar tissue and Y-79 retinoblastoma cells and was described as the 'vs' variant, with these authors referring to the receptor described by Pantaloni *et al.* (1996) as the short or 's' variant (Dautzenberg *et al.*, 1999). From RT-PCR analysis, appropriate mRNA bands for the null, short and very short variants were identified in human cerebellar and cortical tissues, and in Y-79 retinoblastoma cells (Dautzenberg *et al.*, 1999). The PACAP peptides were shown to be less potent at the 'vs' receptor (~ 40 fold; cAMP assay) compared to the null or short variants, although the 'vs' variant remained a PACAP selective receptor with only a small VIP induced response detected at micromolar concentrations. In fact, the maximum VIP induced cAMP responses from both the null and 'vs' expressing cells, were reported to be two thirds smaller than those from the short variant (in which the VIP and PACAP-38 responses were equivalent; Dautzenberg *et al.*, 1999).

In 2001, Daniel and colleagues described a splice variant identified from rat testis, which had an additional 24 amino acids between exons 3 and 4 (EC ligand

binding domain), and was consequently called PAC_1R(3a). The exact location of the insert in the PAC_1R sequence has not been described, but it lies in the N-terminal region, near the deletion site for the 'vs' and 's' variants. In functional studies (cAMP and IP_3) using transfected HEK-293 cells, both PACAPs were slightly less potent at the (3a) variant compared to the null receptor. More recently the (3a) variant has also identified in newborn rat cortical astrocytes (Pilzer & Gozes, 2006a).

The range of PAC_1R variants was recently extended by Lutz and co-workers, who identified fourteen different human PAC_1R splice variants from the SHSY-5Y neuroblastoma cell line (Lutz *et al.*, 2006). The most abundant variants detected were the 'short' (Pantaloni *et al.*, 1996; referred to as δ5, 6 + null), the short-hop1 (Braas & May, 1999; δ5, 6 + hop) and the 'very short' variants (Dautzenberg *et al.*, 1999; δ4, 5, 6 + null). These authors also compared the ability of the variants to couple to cAMP and calcium signalling pathways when expressed in COS7 cells. In cAMP and inositol phosphate studies, PACAP-38 was shown to be ~ 30 fold more potent than VIP in activating the δ5, 6 + null variant, which is in contrast to the previous data (cAMP) showing these peptides to be equipotent (Dautzenberg *et al.*, 1999). Although the agonist ROP for this variant was similar in both assays, there was a shift to lower agonist potency (~ 140 fold) in the calcium studies. For the δ5, 6 + hop variant, VIP was less potent than PACAP-38 in both assays as reported by Braas & May (1999), although the reduction in potency was only about 50 fold, in contrast to the 1000 fold shift described previously. In addition, there was a small shift to lower agonist potency in the calcium assay (~ 25 fold on average) which was not reported in the original studies. Finally, in cAMP studies the δ4, 5, 6 + null variant was confirmed to be a PACAP preferring receptor, and as reported previously, agonists were less potent at this variant when compared to the PAC_1-null receptor (Dautzenberg *et al.*, 1999). The implications of these studies shall be discussed further in chapter one.

A.2.9. VPAC/PAC receptor distribution

The distribution of VPAC/PAC receptors has now been thoroughly investigated in several species, using a range of techniques (e.g. autoradiography, *in-situ* hybridisation studies) and in varying degrees of detail. The following discussion is a brief summary of VPAC/PAC receptor distribution, with more extensive descriptions of the distribution available elsewhere (Usdin *et al.*, 1994; Sheward *et al.*, 1995; Vertongen *et al.*, 1998; Vaudry *et al.*, 2000; Harmar *et al.*, 2004).

A.2.9.1. $VPAC_1R$ distribution

Following the cloning of the $VPAC_1R$, initial studies indicated expression of this receptor in brain, heart, lung, kidney, small intestine, hippocampus and cerebral cortex (Ishihara *et al.*, 1991; Sreedharan *et al.*, 1993). More detailed studies in the CNS have described expression of the $VPAC_1R$ in the pyrifom cortex, cerebral cortex, dentate gyrus, lateral amygdaloid nucleus, caudate putamen, supraoptic nucleus, choroid plexus, dentate gyrus and the pineal gland (Usdin *et al.*, 1994; Vertongen *et al.*, 1998; Vaudry *et al.*, 2000). In peripheral tissues, the $VPAC_1R$ has been shown to be expressed in the mucosa of the gastro-intestinal tract, liver, spleen and also on lymphocytes in lymph nodes (Reubi, 2000). $VPAC_1$ receptors have been shown to be expressed in almost all human epithelial tissues (Reubi, 2000).

A.2.9.2. $VPAC_2R$ distribution

Upon cloning, initial studies demonstrated that the $VPAC_2R$ was expressed in the hippocampus, thalamus, SCN, olfactory bulb, lung and colon (Lutz *et al.*, 1993; Inagaki *et al.*, 1994). Further studies of $VPAC_2R$ distribution in the CNS revealed a high expression in the cerebral cortex, periventricular nucleus, SCN, thalamus, hypothalamus and amygdala (Sheward *et al.*, 1995; Vertongen *et al.*, 1998; Vaudry *et al.*, 2000). Although both VPACR subtypes are reported to be co-expressed in many areas of the CNS, several reports suggest that in the majority of cases where this occurs, the two subtypes have a complementary distribution, being found in different areas or layers of cells, e.g. in the olfactory bulb and cerebral cortex (Usdin *et al.*, 1994; Vaudry *et al.*, 2000). In 2004, Harmar and co-workers performed an extensive study of $VPAC_2R$ distribution in peripheral tissues of the mouse, reporting a predominant expression in the smooth muscle layers of organs and blood vessels. In addition, the receptor was also expressed in colonic mucosal epithelia, pancreatic acinar cells, thyroid follicular cells, adrenal medulla, the retina, in lung alveoli and in blood vessels from many tissues (Harmar *et al.*, 2004).

A.2.9.3. PAC_1R distribution

In 1993 when the PAC_1R was first cloned, abundant receptor expression was observed in the brain (Ogi *et al.*, 1993; Hashimoto *et al.*, 1993), with a lower

expression detected in lung and liver (Hosoya *et al.*, 1993). Several detailed studies of PAC_1R distribution have since been reported, most of which have investigated the expression of generic PAC_1R, with limited studies investigating the distribution of specific splice variants. In the CNS, PAC_1R expression has been reported in the olfactory bulb, dentate gyrus, cerebral cortex, hippocampus, cerebellar cortex, hypothalamic nuclei, cingulate and entorhinal cortices, amygdaloid nucleus, thalamic nuclei, hypothalamus, raphe nuclei, SCN and the area postrema (Hashimoto *et al.*, 1996a; Vaudry *et al.*, 2000; Joo *et al.*, 2004; Kalamatianos *et al.*, 2004). In peripheral tissues expression of this receptor has been reported in the pituitary, adrenal medulla, uterus, lymphoid tissue of the gut, testes and epididymis (Shivers *et al.*, 1991; Reubi *et al.*, 2000; Vaudry *et al.*, 2000).

From the few studies in which localisation of specific PAC_1R variants has been investigated, the PAC_1-null and hop variants were shown be the predominant variants detected in brain tissue, with a specific and high expression of PAC_1-hop in the testes, olfactory bulb and adrenal glands (Spengler *et al.*, 1993; Zhou *et al.*, 2000). These studies showed the PAC_1-hip variant was also expressed in the olfactory bulb and hippocampus, but at lower levels than the null or hop variants. The PAC_1-TM4 mRNA transcript was detected in the cerebral cortex, cerebellum, brainstem, vas deferens, lung and pancreatic β cells (Chatterjee *et al.*, 1996). Expression of the 21 amino acid 'short' deletion variant, reported by Pantaloni and colleagues (1996), was shown to be restricted to the pituitary, adrenal gland, hypothalamus and thalamus. The combined short and hop1 variant described by Braas & May (1999), is the predominant variant expressed in SCG neurons, however the expression of this receptor in other tissues has not been examined. Finally, the PAC_1(3a) variant was originally identified in the testes by Daniel *et al.* (2001), but has very recently been detected in cultured newborn rat cortical astrocytes (Pilzer & Gozes, 2006).

A.2.9.4. VPAC/PACR distribution in cells of the CNS

Soon after the PACAP peptides were identified and before any of the VPAC/PAC receptors were cloned, PACAP binding sites were identified on rat astrocytes (Tatsuno *et al.*, 1990). Since then, several studies (RT-PCR, ISH) have described the expression of $VPAC_1R$, $VPAC_2R$ and PAC_1R (null, hop-1, hop-2, and (3a) splice variants) in cultured rat astrocytes (Ashur-Fabian *et al.*, 1997; Grimaldi & Cavallaro, 1999; Jaworski, 2000; Pilzer & Gozes, 2006b). Cultured rat neurons have

also been investigated for VPAC/PAC receptor expression and have been shown to express $VPAC_2$ and PAC_1-hop1 receptors (Grimaldi & Cavallaro, 1999). In addition, microglia are reported to express $VPAC_1R$ and PAC_1R, although the presence of specific PAC_1R splice variants has not yet been investigated (Kim *et al.*, 2000; Delgado *et al.*, 2002). Finally, Joo and colleagues (2004) have described the expression of PAC_1R in oligodendrocytes, although this is the only study to date where expression in this cell type has been investigated.

A.2.9.5. VPAC/PACR distribution in cancerous cells

As described in previous sections, a high expression of VPAC/PAC receptors has been identified in a number of cancerous cell lines ($VPAC_1R$: HT-29, LoVo, HeLa cells; $VPAC_1R$: SUP-T1, Molt-4b, THP-1; PAC_1R: AR4-2J, NB-OK-1, PC12). In addition, epithelial neoplasms originating from many organs express VIP/PACAP binding sites (Vaudry *et al.*, 2000), with the $VPAC_1R$ being the most commonly expressed VPAC/PACR in several cancers, including those found in the lung, GI tract, breast, pancreas and liver (Reubi, 2000; Busto *et al.*, 2003; Moody & Jensen, 2006). In contrast, $VPAC_2R$ expression only predominates in a few tumours, for example in leiomyomas (benign smooth muscle tumours; Reubi, 2000). The PAC_1R has been shown to be predominantly expressed in several neuronal and endocrine tumours including glial tumours, neuroblastoma, pituitary adenomas, phaeochromocytomas and prostate tumours (Vertongen *et al.*, 1996; Reubi, 2000; Lieu *et al.*, 2006; Mammi *et al.*, 2006; Muller *et al.*, 2006). Several studies have investigated VPAC/PACR expression in neuroblastoma biopsy samples, where a high expression of PAC_1R variants are generally found (Vertongen *et al.*, 1996; Jaworski, 2000; Lutz *et al.*, 2006), however there appears to be a degree of variability in such samples. A recent study from Isobe and colleagues (2004), described a high level of $VPAC_1R$ expression in all of the neuroblastoma biopsy specimens tested, with lower frequency of expression of $VPAC_2R$ (~ 30 %) and PAC_1R (~ 40 %). In immortalised cell lines derived from neuroblastomas, e.g. the SHSY-5Y cell line, the PAC_1R is predominantly expressed (Vertongen *et al.*, 1996; Lutz *et al.*, 2006). In the recent study by Lutz and co-workers (2006) which identified several new PAC_1R splice variants from the SHSY-5Y cell line, these authors reported that the PAC_1R δ5, 6-null variant (21 residue deletion variant originally identified by Pantaloni) was the predominant isoform expressed.

A.2.9.6. VPAC/PACR distribution in cells of the immune system

As discussed earlier, prior to receptor cloning, generic VIP receptors were identified on several types of immune cells, including lymphocytes and lymphoblasts (A.2.4., p 17). The identity of the specific receptors present on such cell types has since been clarified, with extensive studies performed by Delgado and colleagues (reviewed by Gomariz *et al.*, 2001), and shall be described here in brief. Specific and constitutive expression of $VPAC_1R$ has been described on thymocytes (CD4+, CD8+), peripheral lymphocytes and macrophages (Delgado *et al.*, 1996b, 1996c). In studies by the same authors, the $VPAC_2R$ was shown only to be expressed on lymphocytes or macrophages following bacterial or viral exposure (Delgado *et al.*, 1996a; Lara-Marquez *et al.*, 2000). In addition, some of the cell types described have been used to identify splice variants of the $VPAC_2R$, as discussed previously (A.2.8.1., p 27). Finally, the expression of the PAC_1R in the immune system appears to be very specific, with macrophages being the only cells shown to constitutively express these receptors (Pozo *et al.*, 1997).

A.3. Functions and roles of VIP/PACAP and VPAC/PAC receptors

Given the widespread distribution of VIP, PACAP and their cognate receptors, it is not surprising to find that the range of physiological effects produced by these peptides is extensive. Early reports suggested that VIP and PACAP exerted a multitude of effects on cardiovascular, circulatory and respiratory systems and on metabolic function (Said & Mutt, 1970; McCulloch & Edvinsson, 1980; Miyata *et al.,* 1989, 1990), whereas a number of more recent studies have pointed to a plethora of putative roles in the nervous (Dickinson & Fleetwood-Walker, 1999; Harmar *et al.*, 2002) and immune systems (Gomariz *et al.*, 2001; Pozo & Delgado, 2004). Investigations into the roles of these peptides and receptors have been driven by an extensive range of research interests. However, a large proportion of the published work in recent years has focused upon a limited number of areas, including the roles of the peptides/receptors in circadian function, glucose homeostasis, neuroprotection and in modulation of the immune system. The intensive interest in these particular areas has proven fruitful, with many exciting roles proposed for VIP/PACAP and their receptors. These roles, amongst others, shall be discussed here with regard to studies using transgenic animals, and in addition the roles of the peptides and

receptors in circadian function and in neuroprotection/inflammation shall be examined more extensively in chapter three.

A.3.1. Transgenic mice

As for many peptides and receptors, clear insights into the physiological roles of VIP/PACAP and their cognate receptors can be gained from the creation and study of transgenic animals. This approach has proven particularly important for the study of VPAC/PACR function in the absence of low molecular weight, selective, non-peptide ligands. To date, transgenic mice have been developed with altered gene expression for VIP, PACAP, $VPAC_2R$ and PAC_1R. The impact of the transgenes for each type of mutant strain will be discussed below.

A.3.1.1. VIP transgenics

Several different types of VIP transgenic mice have been reported, ranging from mice over-expressing (OE) the peptides to mice with reduced VIP expression and finally to complete knock-out (KO) animals (Gozes *et al.*, 1993; Kato *et al.*, 1994; Colwell *et al.*, 2003). These studies have focussed primarily on the impact on glucose-insulin balance and on circadian cycles, of which the major findings shall be briefly discussed below.

To study the role of VIP in the control of secretory functions of pancreatic islet cells, mice over-expressing the human VIP gene specifically directed to pancreatic β cells (by linking the VIP gene to an insulin promoter which is active in these cells) were created (Kato *et al.*, 1994). The over-expression of these peptides was found to enhance glucose-induced insulin secretion, leading to a significant reduction in blood glucose levels. In addition, VIP over-expression abolished glucose intolerance in mice that had a reduced functional pancreatic islet cell mass (70 % of pancreatic tissue had been removed). From these findings, the authors suggested that VIP-like peptides may be of therapeutic value in enhancing insulin secretion in diabetes (Kato *et al.*, 1994).

The first of the VIP transgenic mouse lines with a reduced peptide expression was reported by Gozes and colleagues (1993). These mice harboured disrupted VIP genes, leading to reduced expression of the peptide. In a line of mice with a 20 % reduction in VIP expression in the brain, these animals were shown to

have learning impairments, retardation in memory acquisition and additionally, male mice showed reduced sexual activity (Gozes *et al.*, 1993). The first line of VIP knock-out mice was reported in 2003 by Colwell and colleagues, with these mice produced through targeted homologous recombination in embryonic stem (ES) cells, leading to the complete disruption of the VIP gene. The resulting mice appeared healthy and fertile and were used in subsequent circadian function studies to address the impact of VIP gene disruption on the sleep/wake cycle. The intrinsic circadian rhythms of the KO mice (determined under constant darkness) were found to be weaker and in some cases completely arrhythmic when compared to WT littermates (Colwell *et al.*, 2003). In addition, the knockout mice displayed altered entrainment patterns to light cues, with these animals appearing to show no phase shift in response to light pulses. These studies highlight the critical involvement of VIP in the mammalian circadian system. Some recently published data using the VIP KO mice described by Colwell (2003), reported that the transgenic mice were more prone to display symptoms of bronchial asthma, to develop pulmonary hypertension and were more susceptible to die from experimentally induced endotoxemia than WT littermates (Hamidi *et al.*, 2006).

A.3.1.2. PACAP transgenics

Studies using PACAP transgenic mice have focussed primarily on PACAP knock-out mice, with several groups independently generating KO mice lines through targeted disruption of the PACAP gene in ES cells. One of the first lines of PACAP knock-out animals was described by Gray and colleagues (2001). These authors reported that PACAP KO mice appeared normal at birth, however the majority of pups died in the second postnatal week (Gray *et al.*, 2001). In most of these cases, the death of the pups was coincident with a difficulty in gaining weight and eventual weight loss. In addition, a role for PACAP in lipid metabolism was suggested given the finding that there was an accumulation of lipids in the heart, skeletal muscle and liver of the KO mice (Gray *et al.*, 2001).

In agreement with the findings of Gray *et al.* (2001), pups from a similar KO line generated by Baba and colleagues were also reported to have a high mortality rate, with ~ 50 % dying before weaning (Hashimoto *et al.*, 2001). Surviving adult mice demonstrated several hyperactive behaviours, including increased locomotor activity, novelty related exploration and explosive jumping behaviour, leading the authors to propose a role for PACAP in the regulation of

psychomotor behaviours. In addition, homozygous matings of KO mice generally resulted in fewer successful pregnancies. A specific role for PACAP in the female reproductive cycle was further delineated when these authors proceeded to examine the reduced mating success of their PACAP -/- mice. These studies showed that the female mice were less fertile, mated less frequently and showed reduced crouching behaviour (Shintani *et al.*, 2002). The same group also examined circadian function in their PACAP null mice (Kawaguchi *et al.*, 2003). The mice were shown to have an intact SCN, no developmental complications and in addition, had a similar free running period to their WT littermates. These findings suggested that PACAP was unlikely to be necessary for the generation of endogenous circadian rhythms. However, further studies highlighted an important role for PACAP in the light induced phase advance mechanism of the circadian clock (Kawaguchi *et al.*, 2003). This group has also investigated the role that PACAP plays in neuroprotection, by examining the extent of damage in WT, heterozygous and homozygous PACAP mice following permanent middle cerebral artery occlusion (pMCAO; Ohtaki *et al.*, 2006). The infarct volume and neurological damage observed following pMCAO was significantly higher in the null mice, suggesting a role for endogenous PACAP in the prevention of neuronal damage. Further studies indicated that the neuroprotective effect of PACAP may result from modulation of cytochrome C release through the regulation of mitochondrial bcl-2 expression, via a mechanism involving IL-6 (Ohtaki *et al.*, 2006). Baba's group also examined the role of PACAP in pancreatic function by generating another PACAP transgenic mouse line which over-expressed the peptide specifically in the β-cells of the pancreas, akin to the transgenic VIP mice described earlier (Kato *et al.*, 1994; Yamamoto *et al.*, 2003). In contrast to the VIP over-expressing mice, glucose levels were normal in these PACAP mutants, suggesting a differential role for the peptides in pancreatic function. In further extensive analyses of these mice, this group have suggested roles for PACAP in stimulating feeding and energy homeostasis (Nakata *et al.*, 2004) and in the processes leading to inflammatory and neuropathic pain states (Mabuchi *et al.*, 2004).

In a third line of PACAP null mice, Hamelink and colleagues (2002) investigated the function of the adrenal glands, in which PACAP had been proposed to act as co-transmitter with acetylcholine. This group found that despite basal adrenaline secretions appearing normal, the mice were unable to survive following exposure to a metabolic stress (insulin induced hypoglycaemia) that should stimulate a prolonged adrenaline secretion (Hamelink *et al.*, 2002). The authors suggested that the mice were unable to recover from the initial hypoglycaemia and proposed a role

for PACAP as an emergency response hormone during prolonged episodes of metabolic stress (Hamelink *et al.*, 2002).

Following on from their studies of circadian cycles in VIP null mice (2003), Colwell and colleagues examined circadian function in another PACAP null mouse strain (Colwell *et al.*, 2004). These mice were observed to show less robust phase shifts (approximately 50 % reduction compared to WT) in response to light pulses. These studies highlighted a specific role for the peptide in modulating advances and delays in the sleep/wake cycle in response to light, in agreement with the findings described earlier by Baba and colleagues (Kawaguchi *et al.*, 2003).

In summary, multiple studies using PACAP transgenic mice have shown that these mice display hyperactive psychomotor behaviours, high early mortality rates, abnormalities in lipid and glucose homeostasis, impaired reproductive function, a reduced ability to resynchronise sleep/wake cycles in response to light cues and reduced neuroprotective mechanisms in response to pMCAO. These studies suggest important and complex roles for this peptide in a multitude of physiological processes.

A.3.1.3. $VPAC_2R$ transgenics

The first $VPAC_2R$ transgenic animals were described in 2000 by Harmar and colleagues, who generated transgenic mice over-expressing the human $VPAC_2R$ (Shen *et al.*, 2000). The pattern of receptor expression was reported to be similar to that in WT mice, with the highest levels of expression detected in the SCN. In circadian function studies, a role for the receptor in controlling circadian cycles was suggested, with these mice observed to adjust more rapidly than their WT littermates to an 8 h phase advance in the light/dark cycle (OE: 3.86 days; WT: 5.4 days). Additionally, these mice displayed a shorter circadian free running period (OE: 23.36 h; WT 23.59 h) when assessed under conditions of constant darkness (Shen *et al.*, 2000).

The following year, Voice and colleagues (2001) reported the generation of another $hVPAC_2R$ transgenic mouse line, in which the T-cells of the mice constitutively expressed $hVPAC_2R$. This expression is in contrast to WT mice, in which $VPAC_2R$ are normally only detected upon T-cell stimulation (see section A.2.9.6, p 37; Lara-Marquez *et al.*, 2000). The highest levels of $hVPAC_2R$ expression were detected in the spleen and thymus, with splenic T-cells showing a higher expression than B-lymphocytes or macrophages (Voice *et al.*, 2001).

Elevated serum levels of IgE, IgG1 and eosinophils were detected in these mice and were attributed to an increase in the effective ratio of functional Th2 and Th1 T-cells and the associated cytokines which these cells express. These authors showed that this altered balance in cytokine production resulted in a depression of delayed hypersensitive reactions (Voice *et al.*, 2001).

The first $VPAC_2R$ null animals were described by Harmar and colleagues in 2001, with the initial studies involving these mice reporting altered immune responses (Goetzl *et al.*, 2001). The mice were described as appearing normal in general health, social behaviour and in breeding patterns. However, when delayed type hypersensitive responses were induced in these mice (through subcutaneous administration of the hapten NP OSu), enhanced reactions were observed, in contrast to the $VPAC_2R$ transgenics described above (Voice *et al.*, 2001). This observation was suggested to result from an inability of VIP to increase the level of Th2 cells and associated cytokines (relative to Th1) in these mice. From these studies and those described by Voice and colleagues, the $VPAC_2R$ clearly has an important role in hypersensitive immune responses.

Further studies of this particular mouse line examined their circadian characteristics and identified critical roles for the $VPAC_2R$ in the maintenance and expression of normal circadian activity patterns (Harmar *et al.*, 2002). Under a 12 h light/dark cycle, these null mice were shown to have a similar pattern of activity to WT mice, despite their overall activity levels being lower. When exposed to a phase advance in the light/dark cycle the null mice entrained to the new cycle much faster than WT animals (KO: 2.4 days; WT: 6.7 days). In addition, when exposed to brief periods of darkness during the daytime, the KO mice were active, in contrast to WT littermates. This demonstrated that masking by light was the principal factor governing the activity cycles of these mice. This finding was emphasised by the observation that under constant darkness the null mice expressed only very weak endogenous rhythms and lacked coordinated clock gene expression. Subsequent *in vitro* electrophysiological studies using these mice indicated that there was a loss of electrical activity rhythms, an observation that could be mimicked in WT mice upon application of the putative $VPAC_2R$ antagonist PG99-465 (Cutler *et al.*, 2003). Further support for disruption to the normal function of the SCN at the cellular level in these null mice has also been gained from immunohistochemical studies in which the null mice were shown to have no rhythmic expression of p-ERK or c-fos in SCN cells, in contrast to WT animals (Hughes *et al.*, 2004).

Following the original description in 2001 of $VPAC_2R$ null mice (Goetzl *et al.*, 2001), a second line of receptor null mice were independently generated by

Asnicar and colleagues (2002). These authors investigated the role of the $VPAC_2$ receptor in energy balance and glucose homeostasis using their transgenic mice. The KO animals described were deletion mutants, in which multiple sections of the receptor were predicted to be deleted, thus disrupting normal receptor function. These mice were shown to have reduced levels of body fat and became significantly leaner than WT littermates as they became older. These authors also report reduced fertility rates in older male mice, due to a degeneration of the seminiferous tubules. In contrast, these effects have not been reported for the original colony of $VPAC_2R$ null mice (Goetzl *et al.*, 2001).

A.3.1.4. PAC_1R transgenics

The first colony of PAC_1R null mice reported, were created by Jamen and colleagues in 2000, following targeted homologous recombination in embryonic stem cells. In this initial report the authors examined insulin secretion and glucose homeostasis, and found that the KO mice had impaired glucose-induced insulin secretion responses and increased glucose intolerance. The null mice were also shown to weigh significantly less (~ 10 %) than their WT littermates, with these studies highlighting the importance of PAC_1R mediated responses in glucose homeostasis. Interestingly, although the null mice appeared normal at birth, ~ 60 % died at around one month old from unknown causes (Jamen *et al.*, 2000). The same line of null mice were also examined in various behavioural tasks to determine any effect of null PAC_1R expression in the hippocampus (Sauvage *et al.*, 2000). In these studies, the null mice displayed no deficits in accuracy during water maze tasks, with the authors suggesting that PAC_1R in the hippocampus do not have a critical or major role in memory formation. However, a more subtle role for this receptor was identified, with minor differences observed in contextual fear conditioning studies. The circadian activity cycles of these mice have also been examined (Hannibal *et al.*, 2001). In a 12 h light/dark cycle, the circadian pattern of activity in the null mice was similar to WT, however in constant darkness, the null mice showed a significantly shorter period length (KO: 23.3 ± 0.1 h; WT: 23.7 ± 0.1 h). In response to light pulses in the early night, the null mice demonstrated large phase delays, which were twice as pronounced than in WT mice, suggesting that the SCN of the null mice was more sensitive to light stimulation. Additionally, the normal increase in clock genes (e.g. c-fos, mPer2) in response to light was not observed following light stimulated phase shifts in the null mice, indicating that altered cycles of clock

gene expression are not always observed in response to phase shifts in the sleep/wake cycle (Hannibal *et al.*, 2001).

In 2001, Otto and co-workers also reported the generation of two PAC_1R transgenic mouse lines to study the involvement of the receptor in synaptic plasticity. The first was a fully receptor null mutant and the second was a novel mutant in which only the PAC_1R receptors in the forebrain/hippocampus were inactive (under the control of the Cre/loxP recombination system). In hippocampal slices prepared from the null and WT mice, post tetanic stimulation was observed in the mossy fibre pathway, although interestingly sustained stimulation i.e. long term potentiation (LTP), was only observed in slices from WT mice (Otto *et al.*, 2001). These findings suggest an essential role for the PAC_1R in the expression of LTP in this neural pathway. In addition, both lines of transgenic mice showed impairments in contextual fear conditioning paradigms, but no deficits in spatial learning were observed, consistent with the earlier findings of Sauvage and co-workers (2000). These authors also reported differences in body weight between the receptor null mice and WT littermates, with most of the transgenic animals dying within the second postnatal week (Otto *et al.*, 2004). These observations are similar to those originally described by Jamen *et al.* (2000). Furthermore, the cause of death in these mice was suggested to be selective right heart failure, as these animals were shown to have a high incidence of cardiac hypertrophy, with a particularly pronounced dilatation of the right ventricle observed (Otto *et al.*, 2004).

The most recent studies of PAC_1R transgenic animals have pointed to a putative involvement of the receptors in the development of hydrocephalus (Lang *et al.*, 2006). In three lines of transgenic mice over-expressing the receptor to different degrees, an enlargement of the ventricles and reduced cerebral cortex mass was observed, the severity of which was proportional to the degree of receptor over-expression. PAC_1R over-expression was associated with a decrease in neuronal proliferation and an increase in apoptosis in the developing embryo. The presence of abnormal cilia (shorter and more disorganised than in WT) in the ventricular ependyma were also observed and were suggested by these authors to be partially responsible for the hydrocephalus-like effects seen in the transgenic mice. Interestingly, the PAC_1R OE mice demonstrated growth retardation and high pre-weaning death rates, two observations which were also reported for the PAC_1R null mice (Jamen *et al.*, 2000; Otto *et al.*, 2004).

The creation and investigation of the VIP/PACAP and VPAC/PACR transgenic mice described in this section has proven to be extremely useful in delineating some of the physiological roles for the peptides and receptors. Further

examination of the behaviour and physiology of these transgenic mice may yet provide more extensive insights into VIP/PACAP and VPAC/PACR function.

A.4. Summary

As discussed in this introduction, a large field of research has developed since the discovery of VIP and PACAP. Cloning of specific receptors for the peptides in the early 1990's has greatly advanced our knowledge regarding the functions of the peptides, with the development of useful peptide ligands and transgenic mouse models. These advances have led to the identification of many important roles for the peptides/receptors under normal physiological conditions, and consequently the modulation of the activity of these peptides and receptors has emerged as an attractive prospect in the treatment of many disease states. However, a key limiting factor to research in this field is the paucity of truly receptor selective ligands, particularly non-peptides.

To address some of these issues, this thesis will begin by describing an extensive and systematic characterisation of human VPAC/PAC receptor pharmacology using two standardised, high-throughput (HT) amenable, cell-based assays (chapter one). In these studies several peptide ligands were examined, ranging form the classical endogenous peptides (VIP and PACAP) to more recently described and less well studied peptides (e.g. R3P65, PG99-465, M65). Following on from these characterisation studies I will report the development of an HT-assay to detect potential VPAC/PAC receptor selective ligands from the compound collections of Astellas Pharma Inc., formerly the Fujisawa Pharmaceutical Company (chapter two). The use of this assay in subsequent screening studies as well as a full evaluation of hit compounds will be presented. Finally (chapter three), I shall describe the establishment and outcomes of studies performed to explore particular roles and functions of central VPAC/PAC receptors, using both *in vivo* (circadian activity studies) and *in vitro* (primary cortical cultures) techniques.

MATERIALS AND METHODS

B.1. General molecular biology and stable cell line production

In order to perform a systematic characterisation of human VPAC/PAC receptor pharmacology using cell-based functional assays, it was necessary to generate mammalian cell lines stably expressing the individual hVPAC/PAC receptors. The production of such cell lines first requires the preparation of suitable DNA constructs containing the receptor DNA sequences and the identification of an appropriate host cell line. The procedures involved in this process are described below for the specific generation of CHO-K1 cells stably expressing the $hVPAC_2$ receptor.

B.1.1. Sub-cloning of the $hVPAC_2R$

The Invitrogen Ultimate human $VPAC_2R$ ORF (IOH9624) is a sequence verified clone that includes the open reading frame (ORF) of the $hVPAC_2R$ (NM 003382, 1317 nucleotides), supplied in the Gateway® pENTR™221 vector (2546 nucleotides; kanamycin resistance). The Gateway® entry vector is not suitable for expression in mammalian cell lines, therefore the insert was sub-cloned into the standard mammalian expression vector, pcDNA3.1™(+) (5428 nucleotides; ampicillin resistance). Restriction enzyme sites were identified on both plasmids that could be used to excise the insert from the Gateway® vector and ligate the sequence into pcDNA3.1™(+). The clone was supplied transformed into DH10B™ *E. coli* as a frozen culture in LB media (-80 °C; 8 % glycerol), consequently it was necessary to isolate colonies and purify plasmid DNA before manipulation of sequences.

B.1.1.1. Isolation and purification of plasmid DNA

Prior to DNA manipulation, agar plates were prepared containing appropriate antibiotics to allow the selection of different plasmids. The plates were prepared (in a laminar flow hood) from sterile LB agar (35 g/l in distilled water; autoclaved), which was heated until molten, with antibiotics added during cooling and finally poured into sterile Petri dishes (10 cm diameter).

In order to isolate single colonies from the DH10B™ *E. coli* glycerol stock, an innoculum of the bacteria was removed from the frozen sample using a sterile plastic loop and streaked out over an agar plate (kanamycin: 50 µg/ml) which was

then sealed, inverted and kept overnight at 37 °C. After the overnight incubation, three distinct colonies were picked and used to inoculate aliquots (10 ml) of LB media (20 g/l in distilled water; autoclaved) containing kanamycin (50 μg/ml). The cultures were then left overnight at 37 °C and continuously shaken (200 rpm), prior to plasmid DNA purification using the Promega Wizard® *Plus* SV Minipreps DNA kit. Briefly, 3 ml of each sample was centrifuged in a Micro Centaur MSE centrifuge (5 min, 13,000 g), after which the supernatant was decanted, with excess media removed from the top of the eppendorf by blotting on a paper towel. The bacterial pellets were then re-suspended in cell re-suspension solution (250 μl; 50 mM Tris-HCl (pH 7.5), 10 mM EDTA, 100 μg/ml RNase A), followed by the addition of a cell lysis solution (250 μl; 0.2 M sodium hydroxide, 1 % SDS), prior to mixing (4x) by inverting the eppendorfs. The bacterial suspensions were then left for 3 - 5 min at room temperature (RT) whilst the lysates cleared and then an alkaline protease solution was added (10 μl, ~ 250 μg) to inactivate endonucleases and other proteins released during lysis; the suspensions were again mixed by inverting and were incubated for 5 min at RT. A neutralisation solution (350 μl; 4.09 M guanidine hydrochloride, 0.759 M potassium acetate, 2.12 M glacial acetic acid; final pH 4.2) was then added to the samples and each tube mixed by inverting, prior to centrifugation (10 min, 13,000 g). The cleared lysates were decanted into spin columns (placed in 2 ml collection tubes) and centrifuged (1 min, 13,000 g), trapping the DNA on the column membranes and allowing the flow through to be discarded. A wash solution (750 μl; 60 mM potassium acetate, 8.3 mM Tris-HCl (pH 7.5), 0.04 mM EDTA (pH 8.0), 60 % ethanol) was then added to each column, the samples centrifuged (1 min, 13,000 g) and again the flow through disposed of. This step was repeated with a further 250 μl of column wash solution and the empty columns were then spun for an extra 2 min (13,000 g) before being transferred to new eppendorfs. Plasmid DNA was eluted from the membranes by the addition of nuclease free water (100 μl), followed by centrifugation (1 min, 13,000 g) and stored at -20 °C. The DNA content of the samples (10 μl diluted to 0.5 ml with nuclease free water) was determined by measuring the absorption at 260 nM (A_{260}), using a spectrophotometer (DU 800, Beckman Coulter). DNA concentrations (μg/ml) were calculated by multiplying the A_{260} by 50 (dilution factor) and then by 50 again, to account for the fact that an A_{260} of 1 corresponds to the presence of 50 μg/ml of double stranded DNA (Qiagen Bench Guide, p 16; http://www.qiagen.com).

From a limited stock of pcDNA3.1™(+) plasmid DNA, 5 μl was transformed into chemically competent One Shot® TOP10 *E. coli* (50 μl), for which the full procedure is described in a later section (B.1.1.5., p 52). Between 50 - 150 μl

of the transformation reaction was spread onto pre-warmed (37 °C) agar plates (ampicillin; 100 μg/ml), which were then inverted and incubated overnight (37 °C). The following day selected colonies (six in total) were chosen to inoculate LB media cultures, from which DNA was extracted and quantified as described in the above paragraph. The DNA content of all six DNA preparations was very similar, at approximately 320 μg/ml (mean: 324 ± 11 μg/ml). These were the pcDNA3.1™(+) samples that were used in all subsequent studies.

B.1.1.2. Restriction enzyme digests

To remove the hVPAC$_2$R insert from the pENTR™221 plasmid, two pairs of restriction enzyme sites (AflII and EcoRV; NheI and EcoRV) were identified that could be used to excise the entire insert from the plasmid (Figure B.1). These enzymes were selected as they should facilitate ligation of the insert directly into pcDNA3.1™(+) (also digested with the enzymes to linearise the plasmid and generate compatible ends; Figure B.1). Double enzyme digests of purified DNA were generally performed in a total volume of 20 μl, incorporating the restriction enzymes (1 μl each; 8 - 20 units depending on the enzyme), bovine serum albumin (BSA; 0.1 mg/ml), purified DNA (volume dependent on concentration utilised) and nuclease free water (to make up the total volume). Digests were typically conducted for 1 h, with samples incubated in a water bath at 37 °C. The resulting DNA fragments were then visualised on 1 % agarose gels, which is an optimal concentration for visualising DNA fragments in the 0.5 to 10 kb range (Qiagen Bench Guide, p 12; http://www.qiagen.com). To prepare gels, solid agarose was added to Tris-acetate-EDTA (TAE) buffer (1x) and the mixture heated until the agarose had fully dissolved. After the solution had cooled, ethidium bromide was added (0.3 μg/ml), the solution gently mixed and poured into gel moulds to set. Prior to use, gels were placed in the electrophoresis chambers and submerged in TAE buffer (1x). Samples of DNA digests (2 – 20 μl, depending on gel size) were mixed with blue/orange loading dye (2 μl/sample, 6x dye) and, along with a KiloBase DNA marker (1 μl/well), added to the wells of a gel and exposed to an electric current (100 v) for approximately 20 min. DNA bands were then visualised under a UV light (Fluorochem, Alpha Innotech).

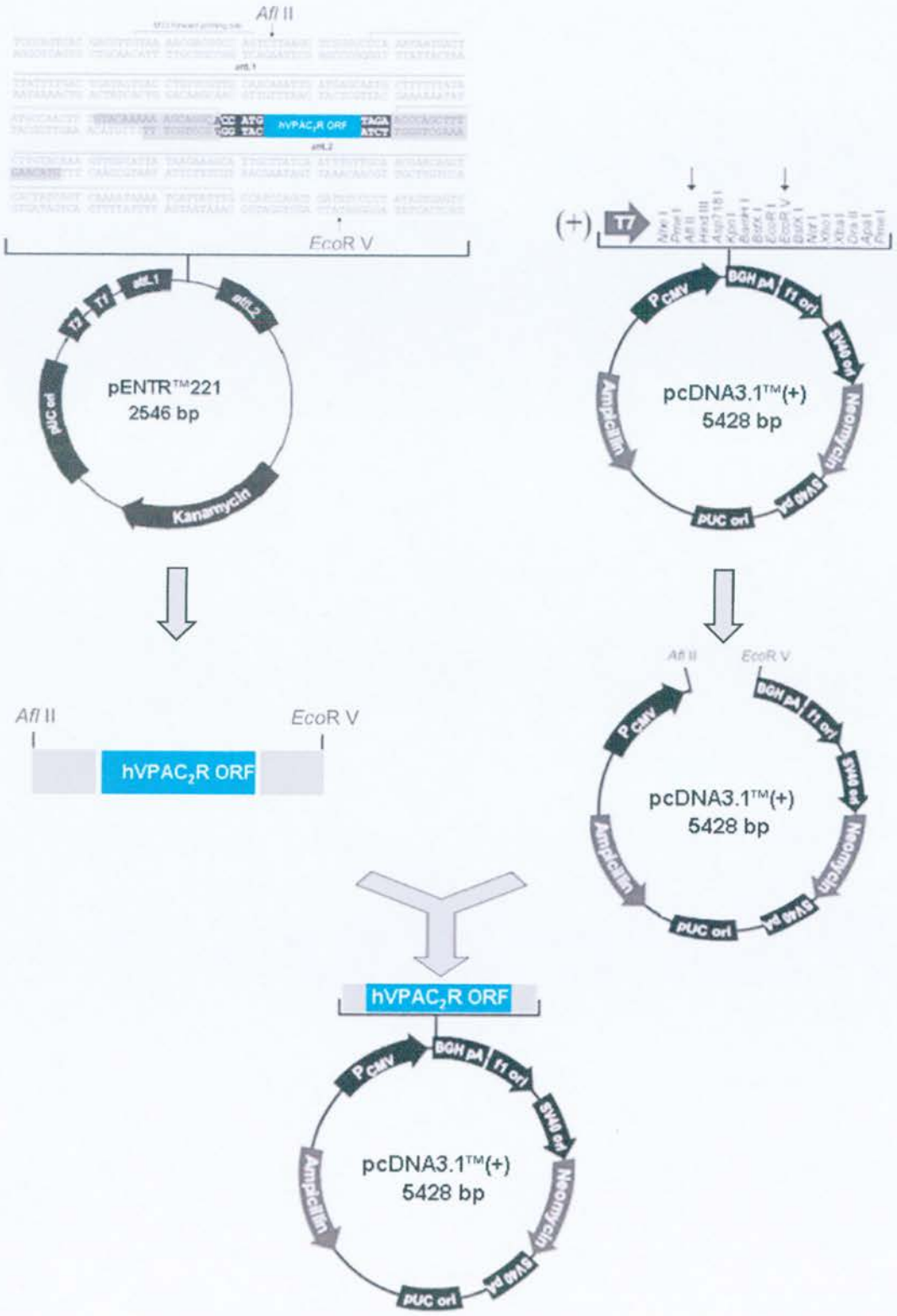

Figure B.1 **Schematic of the initial cloning strategy.** The initial cloning strategy attempted to excise the $hVPAC_2R$ insert from the pENTR™221 vector (with AflII and EcoRV) and directly ligate it with the compatible ends following double digestion of pDNA3.1™(+).

B.1.1.3. Gel purification of DNA fragments

To isolate the digested DNA fragments, gel purification was performed using the QIAquick Gel Extraction Kit. Briefly, using a UV light box to visualise the bands, the DNA fragment of interest was cut from the gel with a sterile scalpel blade and placed in a sterile, pre-weighed eppendorf. The mass of the sample was calculated and 3 'gel volumes' of buffer QG added to solubilise the gel; the 'gel volume' was calculated using the assumption that 100 μg ≡ 100 μl. The gel solutions (pH ≤ 7.5) were placed in a heating block (50 °C, 10 min) to ensure the agarose gel was dissolved, after which isopropanol (1 gel volume) was added to precipitate the DNA. The sample was then mixed and decanted into a QIAquick spin column (held in a 2 ml collection tube) and centrifuged to bind the DNA to the membrane of the column (1 min; 13,000 g). To remove all traces of agarose, buffer QG was added to the column (0.5 ml), and the sample again centrifuged (1 min; 13,000 g). The flow through was disposed of and the process repeated with an ethanol containing buffer (PE; 0.75 ml) to wash the bound sample. The flow through was discarded once more and the column centrifuged for a further 1 min (13,000 g), to remove any residual buffer. Spin columns were placed in fresh, sterile eppendorf tubes and the DNA was eluted from the membrane by the addition of nuclease free water (50 μl), followed by centrifugation (1 min, 13,000g). All DNA samples were stored at -20 °C as described previously.

B.1.1.4. DNA Ligation reactions

To ligate the compatible ends of the digested hVPAC$_2$R insert and pcDNA3.1™(+) plasmid (Figure B.1), reactions were performed using *E. coli* bacteriophage T4 DNA ligase. Standard ligations were performed in a total volume of 10 μl, containing T4 DNA ligase enzyme (1 μl; 1 - 3 units), T4 DNA ligase 10x buffer (1 μl) and DNA from the insert and vector, with the volumes of the latter two being dependent on both the abundance of DNA in the solutions and the vector to insert ratio required (8 μl total volume). Nuclease free water was added, as necessary, to bring the final reaction volume to 10 μl, with the reactions gently mixed and incubated overnight in a water bath (16 °C), prior to storage at -20 °C.

B.1.1.5. Transformation of DNA into competent *E. coli*

The ligation reactions were transformed using chemically competent One Shot® TOP10 or DH5α™ *E. coli* strains, in accordance with the manufacturer's protocol. Briefly, the ligation reactions were gently mixed and kept on ice, whilst one vial of One Shot® TOP10 *E. coli* (50 µl) was thawed for each ligation. The ligation mix (5 µl) was added to the *E. coli* and the suspension mixed by gentle tapping. This was followed by a 30 min incubation on ice, prior to a 30 s heat-shock in a 42 °C water bath. The reactions were then returned immediately to ice and 250 µl of SOC medium (RT) was added to each tube. The vials were then secured into an eppendorf rack, which was then shaken (on its side) at 225 rpm for 1 h (37 °C). Between 50 - 150 µl of the ligation reactions were spread onto pre-warmed (37 °C) agar plates (ampicillin; 100 µg/ml), which were then inverted and incubated overnight (37 °C). Colony growth was examined the next day and selected colonies were chosen, as previously described (B.1.1.1., p 47), to inoculate LB media cultures from which DNA was extracted and subsequently analysed to determine whether transfer of the insert had been successful. For transformations using DH5α™ competent *E. coli*, one vial of cells was thawed and 100 µl aliquots were apportioned into eppendorfs (one aliquot per transformation reaction). Ligation mixes were added (5 µl per reaction) and the reactions incubated for 30 min on ice, before a 20 s heat-shock in a 37 °C water bath. The eppendorfs were then returned to the ice for 2 min, followed by the addition of SOC medium to each reaction (0.9 ml/eppendorf; RT). The DH5α™ transformations were shaken, spread onto agar plates, colonies selected and DNA extracted and analysed as described above for the One Shot® TOP10 cells.

B.1.1.6. TOPO-TA cloning®

As the direct transfer of the hVPAC$_2$R insert from the pENTR™221 vector to the pcDNA3.1™(+) vector proved challenging, a second PCR-based strategy was adopted which utilised the TOPO-TA cloning® system. Using this system, the hVPAC$_2$R insert was transferred into an intermediate TOPO® vector before finally being sub-cloning into pcDNA3.1™(+) (Figure B.2). The procedure involved PCR amplification of the insert to produce abundant copies of the sequence that were modified (by *Taq* DNA polymerase) by the addition of single deoxyadenosine tails to the 3' ends of the sequences (Figure B.2). These PCR products were then ligated

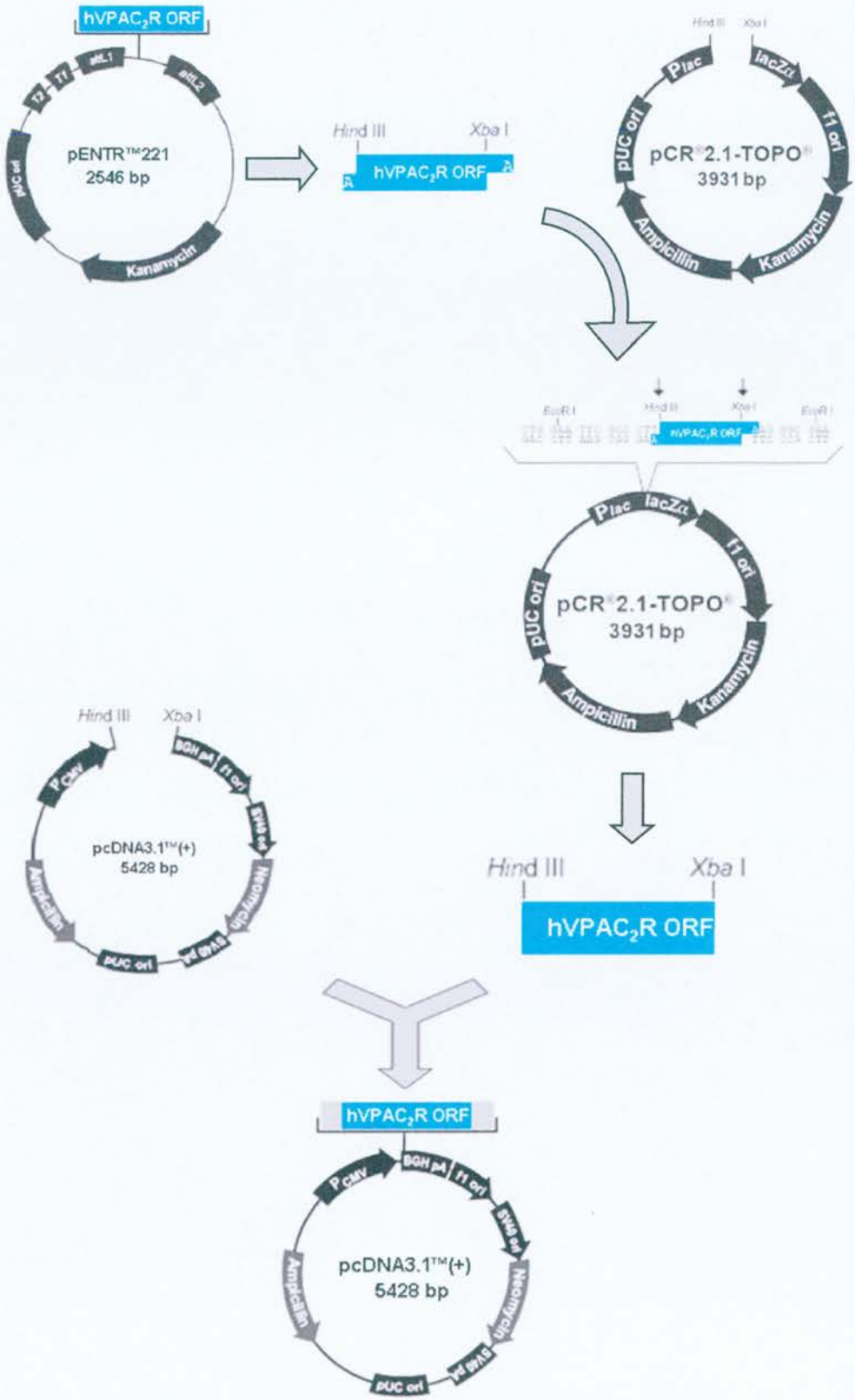

Figure B.2 **TOPO TA cloning® strategy.** The cloning procedure involved PCR amplification of the hVPAC$_2$R insert and sub-cloning into pCR2.1®-TOPO®. The insert was then excised by enzymatic digestion and ligated into pcDNA3.1™(+).

into a linearised TOPO® plasmid which had single thymidine overhangs to aid ligation. The forward (F1: AAGCTTGGCACCATGCGGACG) and reverse (R1: GGGTCTAGATGACCGAGGT) primers were designed to amplify the full hVPAC$_2$R ORF insert from the pENTR™221 plasmid, and included two restriction enzyme sites (HindIII and XbaI). Additional forward (F2: TACAGCAAAGCAGGAAACATAA) and reverse (R2: CAGGAGGGTGTGGAGGTAG) primers were designed to amplify short sequence fragments. Primers were reconstituted in nuclease free water to generate master stocks (50 µM) from which working solutions of 5 µM were prepared (stored at -20 C). PCR reactions were carried out using the Expand High Fidelity PCR system (Roche). Reaction mixes were prepared containing PCR buffer with magnesium chloride (5 µl; 10x buffer), PCR nucleotide mix (0.25 mM), forward and reverse primers (0.5 µM each), High Fidelity polymerase enzyme mix (0.75 µl) and PCR water to generate a total volume of 49 µl. Finally, the DNA to be amplified (pENTR™221 plus hVPAC$_2$R insert) was added (1 µl) and the complete 50 µl reaction was mixed. The reactions were placed in a thermocycler (Thermo Hybaid PCR express) and the following protocol utilised: 94 °C (5 min), 30 cycles of 94 °C (30 s), 60 °C (1 min), 72 °C (1 min) and finally 72 °C for 7 min. Samples of the resulting PCR products were loaded onto agarose gels (1 %) and the DNA bands visualised. The band produced from the amplification of the full length insert sequence (using F1/R1 primers) was excised from the gel and purified as described previously (B.1.1.3., p 51). Ligation reactions (5 µl total volume) between the pCR®2.1-TOPO® vector (1 µl) and the gel purified insert (1 - 4 µl) were set up (Figure B.2), with PCR water added as required to achieve a final reaction volume of 5 µl. The solutions were mixed gently and left for 5 min at RT, followed by the addition of 6x TOPO cloning® Stop Solution (1 µl). Samples of the ligation reactions (2 µl) were transformed into One Shot® TOP10 *E. coli* as described previously (B.1.1.5., p 52), with 20 and 50 µl of each transformation reaction spread onto ampicillin-containing agar plates. Following an overnight incubation at 37 °C, selected colonies were picked and used to inoculate aliquots of LB broth, prior to DNA extraction the following day. Restriction digests were performed on the DNA using enzymes (HindIII and XbaI) that should excise the insert (if present), with the digest products visualised on an agarose gel (1 %). Bands corresponding to the appropriate insert size were gel purified, the DNA extracted and used in a ligation reaction with double digested vector (pcDNA3.1™(+)), using T4 DNA ligase (B.1.1.4., p 51). The ligation reactions were transformed into One Shot® TOP10 *E. coli*, individual colonies isolated and propagated and DNA prepared using the

standard protocols previously described (B.1.1.1., p 47; B1.1.5., p 52). Finally, restriction digests (HindIII and XbaI) were used to determine whether the pcDNA3.1™(+) plasmid contained the $hVPAC_2R$ insert.

B.1.2. Stable cell lines expressing human VPAC/PAC receptors

Whilst producing a plasmid containing the $hVPAC_2R$ insert for the generation of stable cell lines, I was fortunate to find that Astellas Pharma Inc. (formerly the Fujisawa Pharmaceutical Company) had previously generated stable cell lines expressing the human $VPAC_1$, $VPAC_2$ and PAC_1 receptors. These cell lines were kindly transferred to our laboratory and have been used in the studies described. The generation of CHO cell lines stably expressing the VPAC/PACR was performed by Dr I. Aramori (Astellas, Japan) and will be described here in brief. Following the design of sequence specific primers, cDNA clones encoding the $hVPAC_1R$, $hVPAC_2R$, and $hPAC_1R$ were obtained by PCR, from a Clontech human brain cDNA template. The resultant PCR products were individually sub-cloned into pBluescript SK(-), with the identities of the resultant clones confirmed by nucleotide sequence analysis, using an automated sequence analyser. CHO cell lines expressing the hVPAC/PAC receptors were established in a manner similar to that described previously (Aramori & Nakanishi, 1992). Briefly, individual hVPAC/PAC receptor cDNAs were sub-cloned into a eukaryotic expression vector (pMH009) containing the simian virus 40 early promoter and the mouse dihydrofolate reductase (dhfr) gene as a selective marker, with the resultant plasmids transfected into CHO(dhfr-) cells using calcium phosphate precipitation (Aramori *et al.*, 1997). CHO cells were chosen as it is known that phospholipase C/$[Ca^{2+}]_i$ stimulation can occur via either $G\alpha_q$ or $G\alpha_i$ proteins in this cell line and that these cells do not constitutively express VPAC or PAC receptors (Ciccarelli *et al.*, 1994; Van Rampelbergh *et al.*, 1997). Cell lines expressing hVPAC/PAC receptors together with dihydrofolate reductase were selected in α-MEM lacking ribonucleosides and deoxyribonucleosides, but supplemented with 10 % dialysed FBS. From the selected cell populations, clonal lines were isolated by single cell cloning, and the resultant CHO cell lines expressing $hVPAC_1R$, $hVPAC_2R$, and $hPAC_1R$ were maintained in culture as described below. The $hPAC_1$ cell line generated was the $hPAC_1$-null variant described by Pisegna & Wank (1996). The three stable cell lines examined produced equivalent maximum responses in the $[cAMP]_i$ (~ 60 nM, ~ 25x basal) and $[Ca^{2+}]_i$ (~ 7x basal) assays, following stimulation with a saturating concentration of ligand (VIP or PACAP).

Vertongen *et al.* (2004) have shown that this level of cAMP correlates with a receptor density of approximately 1 pmol/mg and moreover, that cAMP and $[Ca^{2+}]_i$ levels are linearly correlated with a receptor density up to 5 pmol/mg (Langer & Robberecht, 2005).

B.2. Cell culture

B.2.1 Cell stock storage and resuscitation

Aliquots of all immortalised cell lines were stored in liquid nitrogen (-170 °C) and resuscitated, as required, by loosening the vial cap slightly and warming the vial, in a water bath (37 °C), for 1 - 2 min. The cell suspension was then added drop wise, into a flask of appropriate, pre-warmed media. All cell lines underwent at least two passages after resuscitation before use in the assays and with the exception of the SHSY-5Y cell line, were sub-cultured for an additional 20 passages before a new aliquot of cells was resuscitated. SHSY-5Y cells were only used over a 5 passage period (P13 - 18) as there is an obvious change in morphology after this point.

B.2.2. Maintenance of immortalised cell lines

CHO-K1 host cells (Figure B.3a) were maintained in culture in Ham's F-12 media, containing FBS (10 %) and gentamicin (1 %). The CHO-K1 cell lines stably expressing the $hVPAC_1R$, $hVPAC_2R$ and $hPAC_1R$ were grown in α-MEM supplemented with dialysed FBS (10%), L-glutamine (2 mM), penicillin (100 U/ml) and streptomycin (100 µg/ml). HEK-293 cells (Figure B.3b) were cultured in MEM, with the addition of FBS (10 %), L-glutamine (2 mM) and non-essential amino acids (1 %). HT-29 cells (Figure B.3c) were grown in McCoy's 5A media supplemented with FBS (10 %), and L-glutamine (2 mM). SUP-T1 cells were maintained in RPMI 1640 supplemented with FBS (10 %), L-glutamine (2 mM), sodium pyruvate (1 mM), HEPES (10 mM; filter sterilised, 0.2 µm filters) and 1.25 g glucose (dissolved in 10 ml of the RPMI 1640 and filter sterilised (0.2 µm filters) before addition to the complete media). SHSY-5Y cells (Figure B.3d) were cultured in DMEM containing FBS (10 %), L-glutamine (2 mM), penicillin (100 U/ml) and streptomycin (100 µg/ml). All of the cells described are adherent cell lines (except SUP-T1) and were generally sub-cultured when observed to be ~ 90 % confluent. To sub-culture these cells, the media was first removed from the flasks and the cells rinsed with pre-

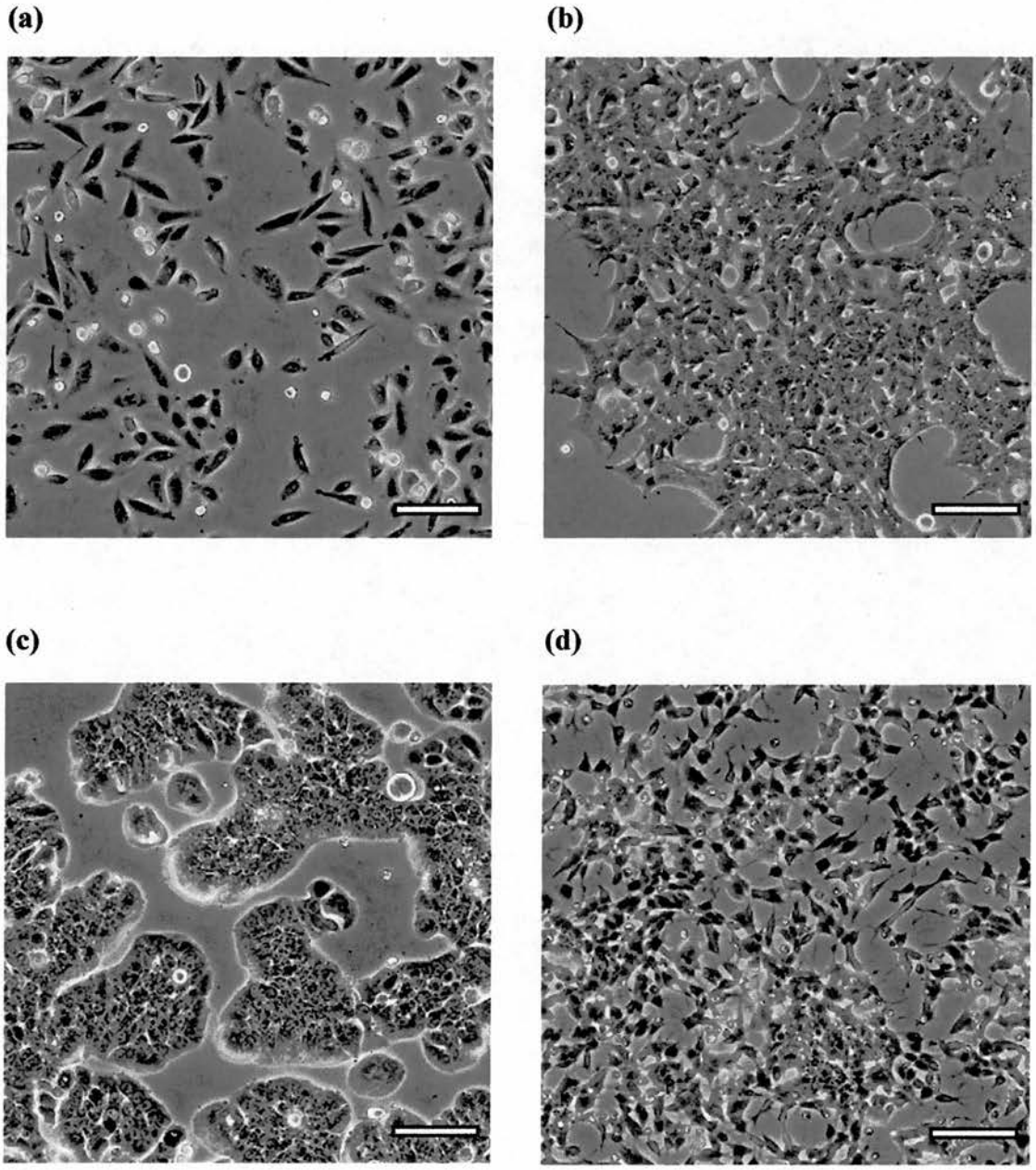

Figure B.3 **Morphology of the adherent immortalised cell lines.** The photographs illustrate the different morphologies of the following adherent cell lines: CHO-K1 (**a**), HEK-293 (**b**), HT-29 (**c**) and SHSY-5Y (**d**). The cells are shown at a high density, with the scale bar representing 100 μm. The images are modified from the ATCC website (http://www.lgcpromochem.com/atcc).

warmed HBSS. Trypsin–EDTA solution (0.25 %, pre-warmed) was then added to the cells and the flasks returned to the incubator for 3 - 5 min. After the majority of cells had detached from the surface of the flask, an equivalent volume of the appropriate media (pre-warmed) was added to neutralise the trypsin-EDTA, and the resulting cell suspension was centrifuged in a Thermo IEC centrifuge (5 min, 850 rpm). The supernatant (media and trypsin-EDTA) was removed by pipette and the remaining cell pellet re-suspended in 5 ml of media (1 ml initially, followed by a further 4 ml). Cells were then seeded into new flasks containing media, at a 1:5, 1:10 or 1:20 dilution (depending on cell usage requirements) and the media changed twice weekly. For the SUP-T1 cell line, sub-culturing was performed once per week. Cell suspensions were removed from culture flasks and pelleted by centrifugation (5 min, 850 rpm). As described for the adherent cell lines, the supernatant was gently removed and the cell pellet re-suspended in media before dilution into fresh media in new culture flasks. An equivalent volume of fresh media was added to each flask 3 - 4 days after seeding.

B.2.3. Rat primary cultures

B.2.3.1. Generation and maintenance of rat primary cultures

In order to isolate primary astrocytes, a mixed cell culture was initially prepared from the cortices of rat pups, following the procedures outlined by McCarthy and colleagues (McCarthy & de Vellis, 1980; Kuhlow *et al.*, 2003). Prior to the preparation of the cortical cultures, all necessary instruments and glass Petri dishes were wrapped in tin foil, sealed and sterilised overnight at 200 °C, with the required media and DNase solutions prepared on the day. Complete media for the primary cultures consisted of BME supplemented with FBS (10 %; heat inactivated at 48 °C for 35 min), dextrose (0.5 % w/v; added from a 30 % w/v stock prepared in water and filter sterilised, 0.2 μm filters), L-glutamine (2 mM), penicillin (100 U/ml) and streptomycin (100 μg/ml). DNase solutions were prepared by dissolving the contents of a 10,000 unit bottle of DNase in 3 ml of HBSS, of which 2 ml was subsequently added to 8 ml of media and the remaining 1 ml was added to 4 ml of trypsin solution (12.5 mg trypsin dissolved in 4 ml of HBSS). The media/DNase and typsin/DNase solutions were both filter sterilised (0.2 μm filters) immediately and pre-warmed before use. The primary cultures were prepared from the cortices of Sprague-Dawley rat pups (P0 - P2), which were decapitated and the heads immediately submerged in 50 ml of HBSS (on ice). Using sterile scissors, a midline

cut was made through the skin on the dorsal surface of the head (caudal → rostral), with the skin peeled back to expose the skull. Using a second pair of sterile scissors, a caudal-rostral incision was gently made along the midline of the skull, directing the points of the scissors away from the surface of the brain. To expose the entire brain, both sides of the skull were peeled away from the midline using sterile curved tweezers (with the tips submerged in 70 % ethanol between dissections). The cerebellum was detached using tweezers and discarded, whilst the rest of the brain was gently removed from the skull and placed directly into a sterile Petri dish containing HBSS (on ice). For dissection, each individual brain was moved to a second sterile glass Petri dish, containing HBSS. Using sterile curved and straight tweezers, the olfactory bulbs were removed (if present), as was the inner brain, meninges and associated surface blood vessels. The remaining cortex was transferred to a universal tube, containing 5 ml of HBSS (on ice). When all of the dissections were complete, the HBSS containing the cortices was transferred into a third sterile glass Petri dish and the tissue finely chopped with a sterile scalpel blade. The chopped cortex/HBSS preparation was taken up into a 15 ml pipette, the tissue allowed to settle in the tip and then only the tissue (not the excess HBSS) was added to a universal tube containing the trypsin/DNase combination (5 ml) and placed in a water bath (37 °C). After 30 min, 5 ml of the media/DNase mixture was added and the solution was gently mixed with a 15 ml pipette. The remaining volume of media/DNase mixture (5 ml) was added and the solution was centrifuged (10 min, 850 rpm). The majority of the supernatant was gently removed (taking care not to disturb the cells as the pellet is very fluid) and the pellet re-suspended in approximately 4 ml of media, using a 15 ml pipette. The cell suspension was then filtered through sterile nylon gauze (125 μm mesh opening) to remove any remaining clumps of tissue. The appropriate volume of media was added to the cells to allow 1 ml of cell suspension per two cortices and the suspension gently mixed with a 15 ml pipette. The cells were then aliquoted into culture flasks (80 cm^2) containing 11 ml of media (1 ml of cell suspension per flask). The flasks containing the primary cultures were kept in a separate incubator from the immortalised cell lines (to reduce any risk of contamination) and were maintained at 37 °C in a humidified atmosphere (with 5 % CO_2), with the media changed every 2 - 3 days. To isolate the astrocytes used in the assays, the flasks were left for 14 - 18 days in culture, removed from the incubator, the lids covered with parafilm and the flasks wrapped in tin foil. The flasks were then shaken (90 min, 300 rpm), after which the media containing mostly microglia was removed. The remaining adherent cells (predominantly astrocytes) were washed with HBSS, trypsinised (0.25 % trypsin-EDTA solution) and

centrifuged (5 min, 850 rpm,). The astrocyte pellet was re-suspended in media and the cells counted and prepared for seeding into the appropriate assay plates (section B.2.4, p 61). To determine the purity of the cultures (see below) samples of microglia were retained and used in immunohistochemical studies alongside the astrocytes. Following removal of the microglia from the shaken flasks, the cell suspension was centrifuged (10 min, 850 rpm), the media removed from the microglia pellet and the cells were then re-suspended in 2 - 3 ml of the same media (conditioned media). The microglia were then counted and seeded into wells of the microscope slide as described in the following section.

B.2.3.2. Immunohistochemistry of rat primary cultures

To confirm the purity of the primary cultures, microglia and astrocytes were isolated as described above, counted and seeded into separate chambers of a multi-welled glass microscope slide (microglia: 1 x 10^4 cells/well; astrocytes: 2 x 10^4 cells/well). Following an overnight incubation (37 °C), the media was aspirated and the cells rinsed in phosphate buffered saline (PBS; 3x 3 min washes). The cells were then fixed in cold 4 % paraformaldehyde (10 min), rinsed in PBS as before, permeabilised in 0.1 % Triton X (5 min) and rinsed again (PBS). The slides were then incubated in 3 % hydrogen peroxide (prepared in methanol; 5 min), to block endogenous peroxidase activity. The cells were then rinsed (PBS) and blocked for 1 h with normal horse serum (2 % in PBS), prior to incubation (overnight; 4 °C) with appropriate primary antibodies. For microglia and astrocyte identification, the primary antibodies used were mouse anti-rat CD11b (1:100 dilution in blocking solution) and mouse anti-pig glial fibrillary acid protein (GFAP; 1:200 dilution in blocking solution), respectively. Following the incubation with primary antibodies, the cells were rinsed with PBS and incubated with a biotinylated anti-mouse antibody (30 min to 1 h) from an anti-mouse Vectastain ABC kit. The cells were then rinsed in PBS, the kit avidin/biotinylated peroxidase enzyme complex (ABC) added (30 min) and following another rinse with PBS, antigen staining was visualised with the Vector stain VIP substrate. The proportion of astrocytes and microglia present in the samples was then assessed in order to determine the purity of the isolated cells.

B.2.4. Cell plating for assorted assays

B.2.4.1. FlexStation® assays

In the $[Ca^{2+}]_i$ assay, fluorescence readings are measured by scanning the bottom of the assay plates; as a result it is recommended that cells in the 96-well assay plates are seeded at an appropriate density to form an adherent monolayer. An excess or insufficient number of cells or the presence of poorly adhered cells could lead to a number of artefacts and inconsistencies in the data generated. Following cell density studies using the CHO-hVPAC/PACR lines (chapter one, section 1.2.2.2, p 96), 1 x 10^5 cells per well was selected as the optimum overnight seeding density for both the FlexStation® $[Ca^{2+}]_i$ and $[cAMP]_i$ assays. This density was also used for all of the other adherent cell lines (including astrocytes from the primary cultures) in these two assays, with the exception of SHSY-5Y cells which were seeded overnight at 1.25 x 10^5 cells per well to obtain an adherent monolayer. In general, flasks of cells were washed with pre-warmed HBSS, trypsinised (0.25 %) and centrifuged at 850 rpm for 5 min. The cell pellets were then re-suspended in the appropriate media, the cell number determined using a haemocytometer, and if required, additional media was added to obtain the desired cell density. The cell lines were seeded overnight (0.1 ml per well) into 96-well flat clear bottom, black ($[Ca^{2+}]_i$ assay) or clear plates ($[cAMP]_i$ assay). The assay plates had been pre-treated for 2 h (minimum) with poly-D-lysine, (20 μg/ml in H_2O; 0.1 ml/well) in order to aid cell adhesion. Previous work in our laboratory has shown that SHSY-5Y cells adhere sufficiently well to untreated plates. As SUP-T1 cells grow in suspension, cell seeding procedures were modified accordingly and performed on the assay day. For the $[Ca^{2+}]_i$ assay, cells were pelleted as described (section B.2.2., p 56), re-suspended in calcium assay cell buffer (5 ml) and counted. The volume of the cell suspension was adjusted to achieve the correct density and cells were seeded into poly-D-lysine treated, black-walled plates (1 x 10^5 cells, 0.1 ml). The cell plates, were then centrifuged (4 min, 1000 rpm) to ensure the cells settled on the bottom of the wells, with the rest of the assay performed as described for adherent cells (section B.3.1.2., p 64). For the $[cAMP]_i$ assay, SUP-T1 cells were pelleted as before (section B.2.2., p 56) on the assay day, re-suspended in PBS (pre-warmed) and counted. The cell suspension was centrifuged again and the pellet re-suspended in pre-warmed $[cAMP]_i$ assay stimulation buffer to generate the required cell density. The cells were then seeded into the 96-well plate (0.1 ml; 1 x 10^5 cells/well) and the assay started immediately.

B.2.4.2. FLIPR® assays

For the FLIPR® $[Ca^{2+}]_i$ assay, flasks of CHO-hVPAC$_2$R cells were rinsed with pre-warmed PBS, detached by trypsinisation (0.25 %) and pelleted by centrifugation (4 min, 1000 rpm). Pelleted cells were re-suspended in media (5 ml total) and counted, with further media added to generate the required cell density (3 x 10^5 cells/ml). Cells were seeded into flat clear bottom, black 384-well plates (1.5 x 10^4 cells/well; 50 µl) and left overnight to adhere. In contrast to the FlexStation® assays, plates were not pre-treated with poly-D-lysine, with the degree of cell adhesion deemed satisfactory for this 384-well plate assay.

B.2.4.3. Cytokine ELISAs

RCA were isolated and counted as previously described (section B.2.3.1., p 58), and the volume of the suspension was adjusted with media to provide the desired density. Cells were seeded into 24-well plates (5 x 10^5 cells/well, 0.5 ml) overnight. The following day the media was aspirated from the cells and the wells were gently washed (3x) with HBSS. After the final wash step, 200 µl of HBSS was added to the cells followed by the addition of 50 µl of peptide solution (5x final assay concentration; FAC). Following peptide treatment for 1 h, the supernatants were removed to eppendorfs, centrifuged to remove any cell debris (5 min, 10,000 g) and finally transferred to fresh eppendorfs which were stored at -20 °C until use.

B.3. *In vitro* assay procedures

B.3.1. FlexStation® assays

The FlexStation® is a bench top scanning fluorometer with an integrated fluid transfer system (Figure B.4a). For the studies described, the FlexStation® was used in the 96-well plate format with the integrated 8-channel pipettor able to transfer drugs from 8 wells of a compound plate to an assay plate (containing cells), whilst continuously monitoring the fluorescence levels in those 8 wells. In addition, the FlexStation® was also used to perform endpoint reads of fluorescence levels across an entire 96-well plate.

B.3.1.1. Intracellular cAMP assay

$[cAMP]_i$ was quantified using an ELISA kit (CatchPoint® Cyclic-AMP, MD). Cell seeding for the individual cell lines was performed as described previously (section B.2.4.1., p 61). On the assay day, media was aspirated from wells containing adherent cells, and the wells rinsed with 0.25 ml of pre-warmed Krebs-Ringer bicarbonate buffer with glucose (KRBG). KRBG (pH 7.4) was composed of D-glucose (9.1 mM), anhydrous magnesium chloride (0.49 mM), potassium chloride (4.56 mM), sodium chloride (0.12 M), anhydrous sodium phosphate dibasic (0.70 mM), anhydrous sodium phosphate monobasic (1.5 mM) and sodium bicarbonate (15 mM). Following removal of the KRBG, 0.1 ml of pre-warmed stimulation buffer was added and the plates incubated for 10 min in the FlexStation® at 37 °C. Stimulation buffer consisted of KRBG (10 ml per plate) containing 9.4 µl of 800 mM 3-isobutyl-1-methylxanthine (IBMX) in 100 % dimethyl sulfoxide (DMSO), bringing the final IBMX and DMSO concentrations to 0.75 mM and 0.094 % respectively. For the SUP-T1 cell line, cells re-suspended in stimulation buffer were seeded into wells as described (section B.2.4.1., p 61), and the 10 min incubation period started immediately. To evaluate agonist potencies (or antagonists alone), 50 µl of peptide solutions (3x FAC in PBS, containing 1 mg/ml BSA) were added to the 96-well plate (using the FlexStation®), which was gently mixed and then incubated at 37 °C for 15 min. The reaction was terminated by addition of pre-warmed lysis buffer (50 µl) to individual wells and the plate shaken (10 min, 450 rpm). Lysates (40 µl; a maximum of 84 per plate) were then transferred to wells in columns 3 - 12 of a second 96-well flat clear bottom, black plate, pre-coated with Goat anti-Rabbit IgG (excess lysates were stored at -20 °C). cAMP standards were prepared from the serial dilution a 30 µM stock (diluted in 3 parts assay buffer: 1 part lysis buffer), producing final in-well concentrations of 3300, 33, 11, 3.7, 1.2, 0.41 and 0.14 mM, which (in addition to a zero standard) were added to duplicate wells in columns 1 and 2 of the plate (40 µl/well). Rabbit anti-cAMP antibody (40 µl) was added to all wells and the plate shaken for 5 min, prior to the addition of HRP-cAMP conjugate (40 µl) to each well. The plate was mixed for a further 5 min and left for 2 h at RT, protected from light. Individual wells were then rinsed (4x with 250 µl wash buffer) before addition of Stoplight Red Substrate (0.1 ml per well; 15 ml of substrate buffer containing 0.15 ml Stoplight Red Substrate and 1 mM hydrogen peroxide). The plate was again protected from light and left at RT (10 min), prior to the measurement of fluorescence levels (excitation, 530 nm; emission, 590 nm; cut-off, 570 nm). For inhibition studies, the KRBG was replaced

with 75 µl of stimulation buffer and the plate incubated at 37 °C for 5 min prior to addition of antagonist (25 µl; 6x FAC in PBS with 1 mg/ml BSA). The cells were then pre-incubated with antagonist for a further 10 min prior to agonist (50 µl) addition in the FlexStation® and the procedure followed as above.

B.3.1.2. Intracellular calcium assay

$[Ca^{2+}]_i$ responses were monitored fluorometrically using the Calcium Plus Kit and FlexStation®. The day after cell seeding (section B.2.4.1., p 61), the media was aspirated from the black-walled cell plates, followed by the addition of freshly prepared cell buffer (0.1 ml per well, pH 7.4). The cell buffer was composed of HBSS (with Ca^{2+} and Mg^{2+}) containing 20 mM HEPES and 0.25 mM sulfinpyrazone (diluted 1 in 100 from a freshly prepared 25 mM solution, dissolved in 1 M sodium hydroxide). Calcium Plus dye, prepared from lyophilised dye reconstituted in cell buffer (10 ml/vial), was added to each well (0.1 ml), the plates were protected from light and left for 1 h at 37 °C, followed by 30 min at RT. Before drug addition, all wells of the assay plates were scanned simultaneously for baseline fluorescence levels (to monitor dye loading) using the endpoint read option on the FlexStation®. To determine compound potencies, peptides were added (50 µl/well; 5x FAC in cell

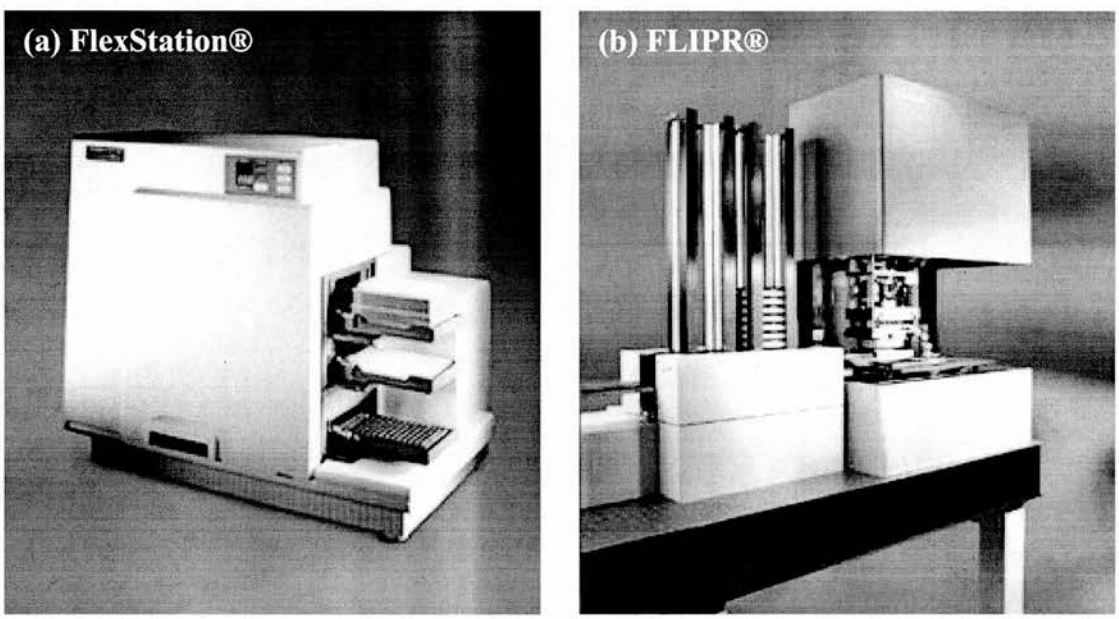

Figure B.4 **The FlexStation® and FLIPR® workstations (Molecular Devices).** Both of these workstations are fluorometric imaging plate readers with liquid transfer capabilities. Pictures are taken from http:www.moleculardevices.com.

buffer containing 1 mg/ml BSA) and fluorescence levels measured (for 90 s unless otherwise stated) by the FlexStation®, with excitation, emission and cut-off wavelengths set at 485, 525 and 515 nM respectively. For inhibition studies, the procedure was followed as above, except the volume of cell buffer initially added to wells was reduced to 50 µl, with the addition of 50 µl of antagonist (5x FAC in cell buffer, plus 1 mg/ml BSA) to appropriate wells, 10 min before the end of the RT incubation period. Agonist addition (approximately EC_{50} concentration) and fluorescence measurements were then performed by the FlexStation®, as previously described. For intracellular calcium assays performed in calcium free conditions, HBSS without Ca^{2+} and Mg^{2+} was used to prepare the cell buffer (dye and drug buffer).

B.3.2. FLIPR® assays

The FLIPR® workstation (Figure B.4b) is similar in principle to the FlexStation®, with both machines being fluorometric imaging plate readers with integrated liquid handling systems. However, and in contrast to the FlexStation®, the FLIPR® has the added capability of measuring fluorescence levels and transferring compounds to all wells of a 96- or 384-well plate simultaneously. This allows for a much higher assay throughput, making the FLIPR® ideally suited for use in HT-screening studies.

B.3.2.1. Intracellular calcium assay for HTS

The calcium assay procedure using the FLIPR® is very similar to that of the FlexStation®, but is constructed to be ultra HT-compatible by allowing simultaneous drug transfer and fluorescence measurement over all wells of either 96- or 384-well plates. In this case, the assay was miniaturised to a 384-well plate format (total volume: 80 µl) with the cell and agonist plates prepared as before, but in the FLIPR® assay the addition of pre-incubated compounds was performed by the fluidics module of the machine. Instead of performing two additions to the cell plate of cell buffer and calcium dye (see FlexStation® calcium assay, B.3.1.2., p 64), the FLIPR® assay was simplified to a single step addition of Calcium 3 dye assay solution, composed of cell buffer and calcium dye. This step was taken to reduce the risk of dislodging the cells with multiple additions to the wells and to reduce the time

taken when preparing the cell plates. For each 384-well assay plate, 20 ml of Calcium 3 dye assay solution was prepared using a sterile inorganic salts buffer (ISB; supplemented with 0.175 g sodium bicarbonate per 500 ml), containing 2 ml of Calcium 3 dye concentrate (2x recommended concentration) and 0.11 ml of 500 mM probenecid/sodium hydroxide (2.75 mM). Calcium 3 dye concentrate was prepared from lyophilised stock, reconstituted in 10 ml of inorganic salts buffer (ISB) per vial and stored at -20 °C (1 ml aliquots). On the day following cell seeding (section B.2.4.2., p 62), the media was removed from the wells by gently tapping the plates onto a paper towel. The Calcium 3 dye assay solution was added to each well (50 µl/well) and the plates incubated for 1 h at 37 °C, followed by 45 min at RT. 384-well compound plates containing samples (2 µl/well) from the 4-mix Fujisawa 'F' and 'M' compound libraries were prepared and kept at -70 °C until use. Library stocks were stored at -70 °C in 96 deep-well plates with four compounds per well, each of which was present at a concentration of 0.25 mg/ml, in 100 % DMSO. Each 384-well compound plate (clear bottom, clear plate) was designed to contain 160 4-mix samples, resulting in 640 individual compounds being tested per plate (in duplicate). From preliminary studies (chapter two, section 2.2.2.5, p 166), the maximum strength of DMSO that could be added to cells was 2 % (FAC: 0.5 % after in-well dilution), so the library compounds (2 µl/well, 100 % DMSO) were diluted in ISB on the day of assay (1 in 50 dilution to 100 µl/well, 2 % DMSO, 5 µg/ml/compound). To stimulate the receptor of choice an agonist plate was freshly prepared on each assay day, containing VIP (800 nM; 8x FAC) diluted in ISB with BSA (1 mg/ml). A single agonist plate could be used sequentially for up to 10 assay plates (10 µl added per plate, 125 µl well capacity). The additions of library compounds, VIP and the simultaneous measurement of fluorescence levels was performed by the FLIPR® in accordance with the manufacturer's instructions. As for the FlexStation® calcium assay, the excitation and emission wavelengths used in the FLIPR® were 485 and 525 nm respectively (cut-off 515 nM). The FLIPR® was programmed to provide a 2 min pre-incubation with library compounds, prior to the addition of VIP, with fluorescence levels recorded for a total of 5 min. The size of the VIP response from each well was calculated (max - min analysis), averaged for duplicate wells and expressed as a percentage of the control VIP response. The four compounds contained in each 'hit' well were then tested separately, using concentrated samples (1 mg/ml in 100 % DMSO) from the 'F' and 'M' libraries in which compounds are stored individually. Samples from selected compounds were transferred to eppendorfs (1.5 µl/tube) and stored at -20 °C until use. On the day of testing, each sample was diluted in ISB (1 in 200 dilution to 300 µl, 0.5 % DMSO, 5

μg/ml) and added to 384-well plates (5 wells per compound). If appropriate, additional studies of hit compounds were performed using powder samples, which were dissolved in DMSO (to 10 mM), diluted in buffer and tested in both the FLIPR® and FlexStation® assays.

In a number of assays performed during screening (section 2.2.3.2., p 168), FLIPR® tips were trialled which had been coated with silicon. Using a 16-channel multi-pipette, 30 μl of the silicon solution (Sigmacote) was taken up into the tips and held for 10 s. The silicon solution was then removed from the tips and replaced with 30 μl of distilled water to remove any excess silicon. The tips were rinsed in this way 3x before being left either in an oven or at RT to dry. These tips were used in the standard FLIPR® calcium assays.

B.3.3. Quantikine® cytokine ELISAs

The Quantikine® cytokine assays (IL-1β, TNF-α, IL-6, RANTES) were enzyme immunoassays in a 96-well plate format. The kit assay plates were supplied pre-coated with an immobilised monoclonal antibody that specifically bound to the cytokine of interest. All controls and standards were prepared in accordance with the protocols supplied. Briefly, assay diluent (50 μl; RD1-40) was added to wells of a 96-well assay plate, followed by the addition of standards, controls or samples. The plate was mixed gently (1 min) by tapping the frame, covered with an adhesive plate sealer and incubated for 2 h (RT). The supernatant and hence any unbound substances were removed by aspiration and the wells rinsed (5x) with wash buffer (400 μl/well), with the plate blotted on a paper towel after each step to remove excess buffer. The kit conjugate solution, which contains an enzyme-linked polyclonal antibody specific for the cytokine, was then added to each well (100 μl) and the plate covered and left at RT for a further 2 h. As before, any unbound substances were then removed by aspiration and the wells washed (5x). A substrate solution was then added to each well (100 μl), after which the plate was protected from light and left at RT (30 min). Finally, a Stop Solution (100 μl) was added to each well and the plate gently tapped to ensure mixing. The binding of the enzyme-antibody reagent produced a blue product, which in the presence of Stop Solution turned yellow. The intensity of this colour was determined from optical density (OD) readings at 450 nm (measured using a microplate reader; Dynex Technologies) and was proportional to the amount of bound cytokine.

B.3.4. Data analysis (*in vitro* studies)

Data collection and analysis were performed using SoftMax Pro 4.7 and SigmaPlot 8.0. For the $[cAMP]_i$ assay, standard curve and regression analysis were performed using a four parameter logistic equation to determine intracellular cAMP concentrations (nM) and ligand potencies (EC_{50} values). In the $[Ca^{2+}]_i$ assay the minimum fluorescence level was subtracted from the maximum response and compound potencies determined as above; the concentration of $[Ca^{2+}]_i$ produced following agonist stimulation could not be determined with the chosen calcium kit. The data from both functional assays are presented in the form of representative concentration effect curves. Agonist EC_{50} values and antagonist IC_{50} values are expressed as mean ± S.E.M, for a minimum of 3 separate experiments (unless otherwise stated), with each data point representing the mean value obtained from duplicate wells. Where appropriate, data was analysed using one-way ANOVA, with significant results interpreted after post-hoc analysis with the Holm-Sidak test (SigmaStat 3.0).

B.4. *In vivo* studies

B.4.1. General

C57BL/6J adult male mice (~ 8 weeks of age, ~ 25 g) were individually housed in clear polycarbonate cages (length: 425 mm, width: 266 mm, height: 185 mm), given *ad libitum* access to food and water, and subjected to a strictly controlled 12 h light/dark cycle (lights off: 1900 to 0700 h). During the dark phase of the cycle, a dim red light was permanently on, to aid animal husbandry procedures. Animals were inspected daily, in accordance with UK Home Office regulations, following a randomized entry time schedule. Each cage was equipped with a running wheel (240 x 80 mm) which had four small magnets fitted to the outside, at 90° intervals. Upon wheel rotation, the magnets passed a reed relay switch on the cage lid, causing the switch to close transiently, with the frequency of closures or counts per minute recorded using Dataquest ART software. Each count was equivalent to a horizontal distance of 189 mm. From analysis of the activity patterns, the mice were demonstrably habituated to their environment and stably entrained to the 12 h light/dark cycle before any further studies ensued.

B.4.2. Effects of displacement and surgery on activity patterns

As drug studies were to involve the central administration (i.c.v.) of test compounds under anaesthesia, the effects of physically displacing the mice from their home cages and anaesthesia/surgery were examined. In this study, sixteen mice were randomly divided into three groups; moved (6 mice), sham surgery (6 mice) and the not moved group (4 mice). The twelve mice in the former two groups were removed from their home cages and transferred to a well-lit procedure room during the 12 h 'lights on' period when the mice were typically inactive (1030 to 1400 h). Six mice were left in an incubator (the moved group) and the other six (the sham surgery group) were individually subjected to halothane anaesthesia (3 % halothane in 30 % oxygen/70 % nitrous oxide) for 2 - 3 min in a Perspex box, prior to surgery. Under anaesthesia, the mice were transferred to a Kopf stereotaxic frame, with anaesthesia (1.5 % halothane) maintained through a snout mask. Throughout the surgical procedure, rectal temperature was monitored and body temperature maintained at 37 °C by means of heating pads. A small midline incision was made in the scalp to expose the surface of the skull, after which a small burr hole was drilled in the skull (stereotaxic co-ordinates: - 0.22 mm posterior to bregma, 0.9 mm lateral

from the midline (AP - 0.22 and L 0.9); from the mouse brain atlas of Paxinos and Franklin, 2001). An empty, blunt-ended needle attached to a 2 µl Hamilton syringe was slowly lowered into the lateral ventricle to a depth of 1.8 mm from the dural surface. The lateral ventricle was selected as the location for drug administration in these studies as it was hypothesised that once injected into the ventricle, the compound would diffuse through the CSF to the fourth ventricle and be taken up into the suprachiasmatic nucleus (SCN; Figure B.5). After 10 min, the needle was slowly withdrawn and the skin was sutured. The anaesthesia was then withdrawn and all of the mice (moved and surgery groups) were placed back into their home cages within 4 h and their sleep/wake cycles were monitored as before.

Figure B.5 **Coronal section of a C57BL/6J mouse brain.** The coronal section shown was taken from the Mouse Brain Library (http://www.mbl.org) and represents a slice taken - 0.82 mm from Bregma. For the *in vivo* studies described, the approximate location of the needle tip is indicated in the ventricles by the asterisk. The location of the SCN are also highlighted by the dashed circle.

B.4.3. Phase shifts

A second group of mice (16 adult C57BL/6J males, as before) were entrained to a 12 h light/dark cycle (lights off: 1900 to 0700 h) as described above. The effects on activity of introducing an 8 h phase advance, i.e. lights off: 1100 to 2300 h, were determined. The re-entrainment period was defined as the number of 24 h cycles that the animals took to entrain to the new light/dark cycle. The presence

of activity bursts within the first 2 h of the novel dark cycle was also assessed. The mice were subsequently re-entrained to the original light dark cycle (lights off: 1900 to 0700 h), following which the ability of the mice to adapt to a slightly shorter phase advance (6 h; lights off: 1300 to 0100 h) was determined, with performance measured as before. A 6 h phase advance was evaluated as its use would facilitate the planned surgical intervention in the following study. This protocol would allow for a 4 h treatment period during the animals inactive cycle, followed by a minimum of 1 h in the home cage before the proposed phase-advanced lights off period began. Following successful demonstration of stable entrainment to this shorter phase advance, mice were re-entrained to a third light/dark cycle (lights on: 2000 - 0800 h), in preparation for surgery.

B.4.4. Effect of PG99-465 on responses to phase shifts

Surgery was limited to 7 - 8 animals within the 4 h period. Therefore, on the first treatment day, 7 mice were transferred from the holding room to the surgery room, 1 h into their inactive cycle. The remaining subjects (9 mice) were maintained on the pre-surgery light/dark cycle in a separate holding room. Surgery was performed with administration of anaesthetic and insertion of a Hamilton syringe/needle into the ventricle as described previously (section B.4.2., p 69). Prior to insertion of the needle, the barrel of the syringe was filled with PG99-465 (0.1 mM; 8 mice) or vehicle (saline; 8 mice). During surgery, 1 µl of drug/vehicle was injected into the lateral ventricle at a rate of 0.1 µl/min. Mice were returned to their home cages at least 1 h before the onset of the dark phase of the new light/dark cycle (lights off: 1400 - 0200 h). A three day gap was enforced between the two surgery sessions (7 and 9 animals on day 1 and 2 respectively) to allow the initial group of animals to respond to treatment with minimal disturbance.

B.4.5. Data analysis (*in vivo* studies)

The data output from the running wheels, i.e. number of magnet passes per minute, was collected using Dataquest ART software. The data was subsequently exported into MS Excel for analysis, where the intensity and timing of activity patterns was analysed. Where appropriate, data were analysed using two-way

ANOVA, with significant results interpreted after post hoc analysis with Tukey's test (SigmaStat 3.0).

B.5. Materials

The following lists detail all of the chemicals and reagents used in the studies described in this thesis, with the supplier of each chemical, in addition to its reference number (where applicable) shown in parenthesis. Additional laboratory resources (plasticware, cell lines etc.) and specific computer software utilised are also described.

B.5.1. General chemicals and reagents

α-MEM	Sigma-Aldrich (M5426)
ATP	Sigma-Aldrich (A7699)
Ampicillin	Sigma-Aldrich (A9518)
[Ala^{11,22,28}]VIP	Tocris, UK (1386)
Anti-mouse Vectastain ABC kit	Vector Laboratories (PK - 4002)
BME	Sigma-Aldrich (B1522)
BSA	Sigma-Aldrich (A7906)
CD11b antibody (mouse anti-rat)	Serotec, UK (MCA 275G)
DMEM	Sigma-Aldrich (D5671)
DMSO	Sigma-Aldrich (D2650)
DNase (10, 000 U/bottle)	Sigma-Aldrich (D4527)
F12 Hams media	Sigma-Aldrich (N6658)
Fetal bovine serum	Invitrogen (10106-169)
Fetal bovine serum (dialysed)	Invitrogen (26400-044)
Forskolin	Sigma-Aldrich (F3917)
Gentamicin	Invitrogen (15710-049)
GFAP antibody (mouse anti-pig)	Abcam, UK (Ab 8136)
Glucose (dextrose)	Sigma-Aldrich (G5146)
HBSS (without Ca^{2+} or Mg^{2+})	Sigma-Aldrich (H6648)
HBSS (10x; with Ca^{2+} and Mg^{2+})	Invitrogen (14065-049)
HEPES	Sigma-Aldrich (H4034)
Horse serum	Vector Laboratories (S - 2000)
Human brain cDNA template	Clontech, USA
Hydrogen peroxide (30 %)	Sigma-Aldrich (H1009)
IBMX	Sigma-Aldrich (I7018)
Inorganic salts buffer (10x)	Sigma-Aldrich (H1641)

Isopropanol	Sigma-Aldrich (I9516)
Kanamycin	Sigma-Aldrich (K1377)
KiloBase DNA marker	Amersham (27-4004-01)
Krebs-Ringer bicarbonate buffer	Sigma-Aldrich (K4002)
LB agar	Sigma-Aldrich (L2897)
LB broth	Sigma-Aldrich (L3022)
L-glutamine	Sigma-Aldrich (G7513)
MEM	Sigma-Aldrich (M2279)
Methanol	Sigma-Aldrich (M1775)
McCoy's 5A media	Sigma-Aldrich (M8403)
Mouse anti-rat CD11b	Serotec, UK (MCA 275G)
Mouse anti-pig GFAP	Abcam, UK (Ab 8136)
Non-essential amino acids	Sigma-Aldrich (M7145)
PACAP-27	Synpep, USA or NeoMPS France
PACAP-38	Synpep, USA or NeoMPS, France
Paraformaldehyde	Sigma-Aldrich (HT153020)
PG99-465	Albachem, UK (custom synthesized)
PG97-269	Phoenix Pharmaceuticals, USA (064-25)
pBluescript SK(-)	Stratagene, USA
pcDNA3.1™(+)	Invitrogen (V790-20)
Penicillin/streptomycin	Sigma-Aldrich (P0781)
Phosphate buffered saline	Invitrogen (20012019)
Poly-D-lysine	Sigma-Aldrich (P6407)
Primers for PCR	Invitrogen (custom synthesized)
Probenecid	Sigma-Aldrich (P8761)
R3P65	Albachem, UK (custom synthesized)
RPMI 1640	Sigma-Aldrich (R0883)
Restriction enzymes	Promega or New England Biolabs
Saline	Ivex Pharmaceuticals
Sigmacote silicone solution	Sigma-Aldrich (SL2)
Sodium bicarbonate	Sigma-Aldrich (S6297)
Sodium hydroxide pellets	Sigma-Aldrich (S8405)
Sodium pyruvate	Sigma-Aldrich (S8638)
T4 DNA ligase	Promega (M1801)
Triton X-100	Sigma-Aldrich (X100)
Trypsin–EDTA solution	Sigma-Aldrich (T4049)
Trypsin powder	Sigma-Aldrich (T4665)

Sulfinpyrazone	Sigma-Aldrich (S9509)
Vector stain VIP substrate	Vector Laboratories (SK - 4600)
VIP (for screening)	Sigma-Aldrich (V3628)
VIP	Synpep, USA or NeoMPS, France

B.5.2. Additional equipment and resources

24-well flat clear bottom clear plates	Nunc (142475)
96-well flat clear bottom black plates	Costar (3595)
96-well flat clear bottom clear plates	Costar (3603)
384-well flat clear bottom clear plates	Corning (3675)
384-well flat clear bottom black plates	Corning (3680)
Running wheels, cages and magnets	Tecniplast
Sprague-Dawley rat pups (from an in-house breeding colony)	Charles River UK, UK
C57BL/6J adult male mice	Charles River UK, UK
Nylon gauze (125 µm mesh opening)	Lockertex (Clarcor), UK
FlexStation® tips (96/box; clear)	Molecular Devices (X9000-0623)
FLIPR® tips (384/box; clear)	Molecular Devices (X9000-0512)
FLIPR® Calcium Plus Kit	Molecular Devices (R8041)
FLIPR® Calcium 3 kit	Molecular Devices (R8091)
Multi-welled glass microscope slides	Nalgene, Nunc, USA (154534)
CatchPoint® Cyclic-AMP Kit	Molecular Devices (R8088)
Expand High Fidelity PCR Kit	Roche (11732641001)
Quantikine® ELISAs kits	R & D Systems, UK
TOPO TA Cloning® kit	Invitrogen (K4500)
Wizard® *Plus* Minipreps DNA Purification System	Promega (A7100)
CHO-K1 cells	ECACC (85050302)
HEK-293 cells	ECACC (85120602)
HT-29 cells	ECACC (91072201)
SHSY-5Y cells	ECACC (94030304)
SUP-T1 cells	ATCC (CRL-1942)
Maxadilan and M65	Gift from Dr. E. Lerner, Massachusetts General Hospital, MA, USA

B.5.3. Computer software

Dataquest ART software	Data Sciences International
SigmaStat 3.0	SPSS Limited
SoftMax Pro 4.7	Molecular Devices
MS Excel	Microsoft Corporation

CHAPTER ONE
PHARMACOLOGY OF hVPAC/PAC RECEPTORS

1.1. Introduction

1.1.1. VPAC/PACR coupling to signal transduction pathways

As described in the general introduction, one of the main characteristics of GPCRs in the group B family, including VPAC/PAC receptors, is a ligand induced, $G\alpha_s$ dependent increase in intracellular cAMP ($[cAMP]_i$; Figure 1.1.1; Harmar, 2001). However, as is common for many GPCRs, including β_2 adrenoceptors and calcitonin receptors amongst others (Zhu *et al.*, 1994; Aiyar *et al.*, 1999; Xiao *et al.*, 1999), no exclusive signalling pathway exists. In addition to pathways that modulate cAMP levels, VPAC/PAC receptor activation has also been observed to stimulate phospholipase D (PLD) activity and intracellular calcium ($[Ca^{2+}]_i$; Figure 1.1.1) production in both human and rat stable cell lines (Spengler *et al.*, 1993; Sreedharan *et al.*, 1994; Pisegna & Wank, 1996; Xia *et al.*, 1996; McCulloch *et al.*, 2000). Only a limited number of studies have described VPAC receptor mediated increases in $[Ca^{2+}]_i$ in cells endogenously expressing hVPAC receptors (HT-29, Sreedharan *et al.*, 1994; SUP-T1, Xia *et al.*, 1996) and in transfected cell lines (HEK-293, Sreedharan

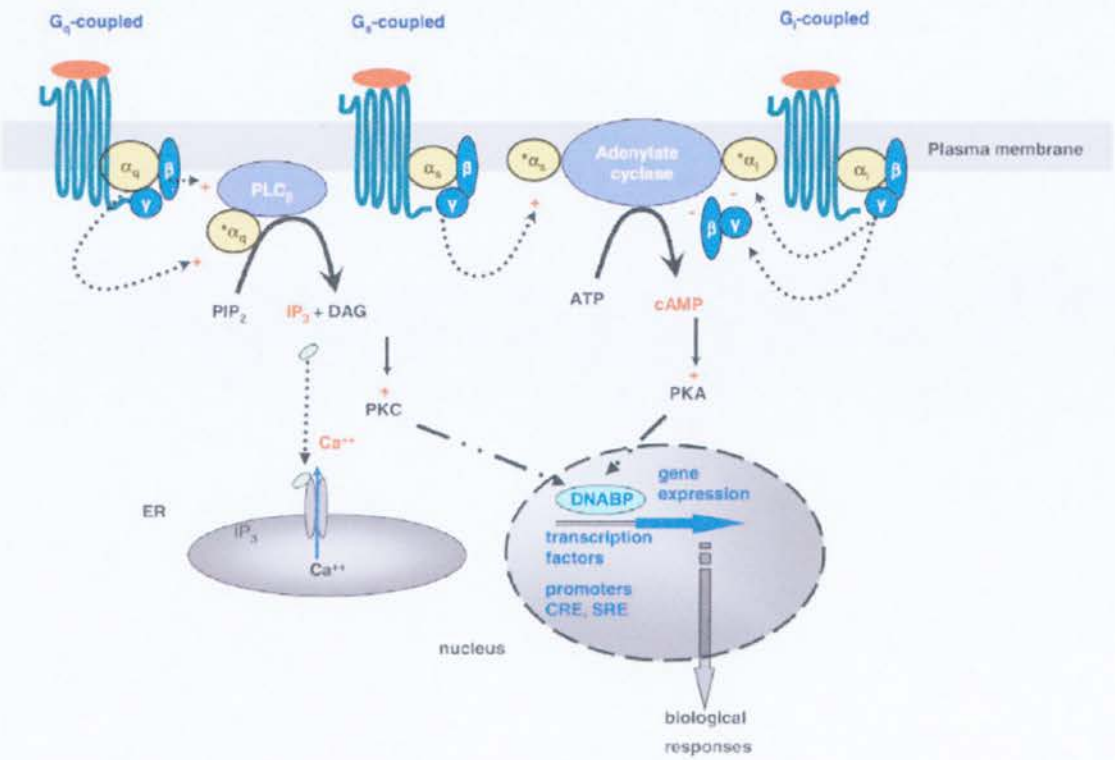

Figure 1.1.1 **Schematic of the main intracellular transduction pathways stimulated by G-protein coupled receptors.** The figure illustrates the principal signalling pathways activated by 7-TM receptors coupled to heterotrimeric G-proteins containing $G\alpha_q$, $G\alpha_s$ and $G\alpha_i$ subunits (Jacoby *et al.*, 2006).

et al., 1994; CHO, Xia *et al.*, 1997; Langer *et al.*, 2002a). The transduction mechanisms which contribute to the rise in $[Ca^{2+}]_i$ reportedly include both $G\alpha_i$ and $G\alpha_q$ coupled pathways, with the $G\alpha_i$ pathway reported to account for ~ 40 % of the total $[Ca^{2+}]_i$ response in VPAC receptor expressing stable cell lines (for human and rat receptors; MacKenzie *et al.*, 1996; Langer & Robberecht, 2005). In contrast, although $hPAC_1R$ mediated stimulation of $[Ca^{2+}]_i$ has also been reported in native (SHSY-5Y: Eggenberger *et al.*, 1999; NB-OK-1: Delporte *et al.*, 1993) and recombinant cell lines (CHO: McCulloch *et al.*, 2000), this calcium transduction pathway appears to be exclusively mediated via $G\alpha_q$ (MacKenzie *et al.*, 1996; Van Rampelbergh *et al.*, 1997). The complex and differential coupling of VPAC/PACR to pathways stimulating $[Ca^{2+}]_i$ is paralleled in the mechanisms involved in VPAC/PACR stimulation of PLD activity. VPAC and PAC_1-hop1 receptor mediated elevations in PLD activity have been shown to be dependent on the small G-protein ARF (ADP-ribosylation factor; McCulloch *et al.*, 2000). In contrast, PLD stimulation resulting from PAC_1-null receptor activation was shown to be entirely independent of ARF, with a component of the response identified as PLC dependent (McCulloch *et al.*, 2000).

1.1.2. VPAC/PACR ligand potencies in activating transduction pathways

In general, although cAMP, calcium and PLD can all be modulated by VIP/PACAP stimulation of CHO cells over-expressing VPAC/PAC receptors, production of the former second messenger occurs more readily than the latter two. In the few studies in which PLD responses have been examined, VPAC/PAC receptor agonists were on average ~ 70 fold less potent in stimulating PLD activity than cAMP production in CHO cells expressing the rat $VPAC_1$, $VPAC_2$ and PAC_1 receptors (McCulloch *et al.*, 2000, 2001). However, for VPAC receptors even in the presence of a considerable agonist induced cAMP response, sometimes no alteration in calcium is observed (McCulloch *et al.*, 2000; McCulloch *et al.*, 2001). Moreover, when an VPAC receptor mediated calcium signal can be detected, the EC_{50} concentration of agonist required to elicit this response varies considerably, ranging from at least one to two orders of magnitude greater than that required for cAMP (Sreedharan *et al.*, 1994; Xia *et al.*, 1996; Langer *et al.*, 2001; MacKenzie *et al.*, 2001). This difference in agonist potency in stimulating cAMP and calcium responses can also be seen for PAC_1 receptors (Deutsch & Sun, 1992; Spengler *et al.*, 1993; McCulloch *et al.*, 2001). As discussed below, assay methodologies and

receptor expression levels have varied considerably in studies of VPAC/PAC receptor pharmacology and it is therefore difficult to conclude exactly what underlies the different agonist potencies for the various VPAC/PAC receptor transduction pathways (Ciccarelli *et al.*, 1994; Laburthe & Couvineau, 2002). Finally, species differences for the individual receptor subtypes further complicates the interpretation of published studies, when comparing different transduction pathways and receptor pharmacology (Deutsch & Sun, 1992; Spengler *et al.*, 1993; Gourlet *et al.*, 1997; Laburthe & Couvineau, 2002).

1.1.3. Functional studies characterising VPAC/PACR pharmacology

A diverse range of assay methodologies has been used to examine VPAC/PACR pharmacology, particular in studies examining cAMP and calcium production. Coupling of VPAC/PACR to $G\alpha_s$ pathways has generally been investigated using radioactive and non-radioactive assays to measure either AC activity or $[cAMP]_i$ production (Xia *et al.*, 1997; Langer *et al.*, 2003). In addition, the varying use of whole cells or membranes adds a further complexity to the methodologies adopted, with the majority of studies to date utilising membrane-based approaches. Importantly, in recent years it has been shown that the potency of VIP to induce cAMP production can vary as much as 30-fold between assays, on switching from membranes to whole cells (Langer *et al.*, 2002a). A range of techniques can also be found upon examination of the methods used to measure VPAC/PACR coupling to signaling pathways which stimulate calcium production. In addition to directly monitoring calcium levels with fluorescent indicators such as fura-2 and fluo-4 (Delporte *et al.*, 1995; Masmoudi *et al.*, 2003), luminescence based approaches have been utilized (aequorin/coelenterazine assay; Langer *et al.*, 2002a), as have more indirect measures, such as the accumulation of inositol phosphate which is often associated with calcium stimulation (MacKenzie *et al.*, 2001). In contrast, the assays that have been reported for investigating PLD activity show very little variation (quantification of radiolabelled phosphatidylalcohol), perhaps because only three groups have examined VPAC/PACR modulation of PLD (Morisset *et al.*, 1995; McCulloch *et al.*, 2000; Dejda *et al.*, 2006). Further variation emerges in VPAC/PAC receptor cell based studies with regard to the specific characteristics of the expression system utilised. Whether in cell lines in which the receptors are endogenously expressed or in cells in which the receptors are stably transfected, changing levels of receptor expression may influence the characteristics of the

responses observed (Langer *et al.*, 2002b; Langer & Robberecht, 2005). Furthermore, in transfected cell lines, the nature of the host cell line may alter the repertoire of agonist induced responses observed following VPAC/PAC receptor activation. For example, $hVPAC_1R$ have been shown to mediate calcium responses via coupling to $G\alpha_q$ and $G\alpha_i$ (pertussis toxin sensitive) proteins in stably transfected CHO cells (Langer & Robberecht, 2005), however in HEK-293 cells expressing the $hVPAC_1R$, no coupling to pertussis toxin sensitive G-proteins ($G\alpha_i$) was observed (Shreeve *et al.*, 2000). This was despite the demonstration of agonist induced calcium responses in that cell line (Sreedharan *et al.*, 1994). These findings indicate that the G-protein and second messenger complement of the cell line being examined may introduce a further source of variation into the transduction pathways/pharmacology observed for VPAC/PAC receptors (Laburthe & Couvineau, 2002; Langer *et al.*, 2002b). Further variability in VPAC/PAC pharmacology of different cell types may also involve the interesting interactions between these receptors and receptor activity-modifying proteins (RAMPs). The RAMPs are single transmembrane proteins which are reported to alter the trafficking, pharmacology, and signalling characteristics of GPCRs (Hay *et al.*, 2006). Sexton and colleagues have shown that the $VPAC_1R$ strongly interacts with RAMPs, with the specific interaction with RAMP2 shown to augment VIP induced phosphatidylinositol (PI) hydrolysis with no effect on cAMP responses (Figure 1.1.2; Christopoulos *et al.*, 2003; Sexton *et al.*, 2006). In contrast, these authors showed no significant

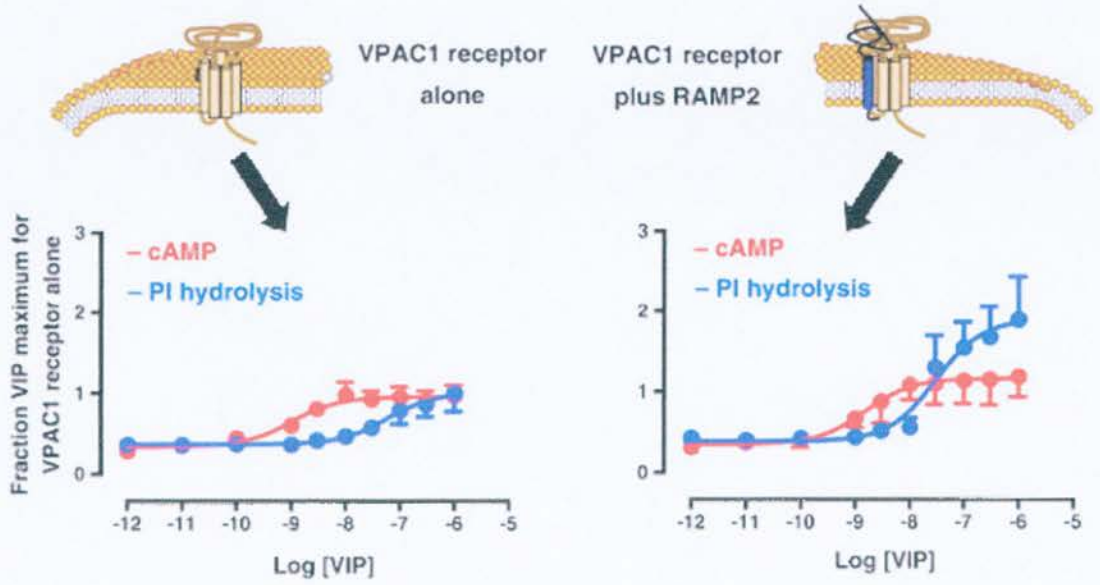

Figure 1.1.2. The modulation of $VPAC_1R$ signalling by RAMP2. Co-expression of $hVPAC_1R$ and RAMP2 in COS cells enhances the agonist induced hydrolysis of PI with no change in the cAMP stimulation. This figure was modified from Sexton *et al.* (2006).

interaction of $VPAC_2R$ with RAMPs (Sexton *et al.*, 2006) and no examination of the PAC_1R was reported. With the RAMPs shown to have a widespread distribution throughout the nervous system and peripheral tissues, their potential influence on VPAC/PACR pharmacology and signalling merits future consideration (Hay *et al.*, 2006). In addition, several studies of VPAC/PAC receptor pharmacology and signaling mechanisms have only utilised rat receptors (McCulloch *et al.*, 2001). With differences in compound potencies observed in studies in which human and rat receptors have been compared (Laburthe *et al.*, 1983; Gourlet *et al.*, 1998), it is clearly not appropriate to extrapolate ROPs determined using rat VPAC/PAC receptors to the human homologues. For this reason, caution must be applied when comparing data from studies of multiple species, which adds further difficulty to the complex task of clearly defining human VPAC/PAC receptor pharmacology from published studies. Finally, even between reports from the same group, in which the same cell line and assay methodology have been followed, potency differences arise. For example in a membrane AC stimulation assay, VIP induced responses from the same CHO-$hVPAC_2R$ cell line were 6 fold different between published studies from the Robberecht group (Vertongen *et al.*, 2001; Nachtergael *et al.*, 2003).

1.1.4. Systematic characterisation of VPAC/PACR pharmacology

To date, there is still no single study that systematically investigates functional responses at all three human VPAC/PAC receptor subtypes, using a broad range of agonists and antagonists. To provide a comprehensive characterisation of human VPAC/PAC receptor pharmacology and eliminate variability arising from the use of different assay and expression systems, CHO-K1 cell lines stably expressing the three individual human receptor subtypes were generated, and standardised whole cell, non-radioactive, HT-amenable, fluorescence based assays established to measure $[cAMP]_i$ and $[Ca^{2+}]_i$. Agonist profiles for the transfected cell lines were generated using the endogenous peptides VIP, PACAP-27 and PACAP-38, in addition to the putatively $VPAC_1$ ($[Ala^{11,22,28}]$VIP; Nicole *et al.*, 2000), $VPAC_2$ (R3P65; Yung *et al.*, 2003) and PAC_1 (maxadilan; Moro & Lerner, 1997) receptor selective agonists. The potency and selectivity of the reportedly receptor specific antagonists, PG97-269 ($VPAC_1$; Gourlet *et al.*, 1997a), PG99-465 ($VPAC_2$; Moreno *et al.*, 2000), and M65 (PAC_1; Uchida *et al.*, 1998) were also thoroughly examined. Furthermore, using the same repertoire of peptide ligands, the pharmacology of the hVPAC/PAC receptors were evaluated in cell lines which endogenously express the

individual receptors ($VPAC_1R$: HT-29 cells; $VPAC_2R$: SUP-T1 cells; PAC_1R: SHSY-5Y cells).

1.2. Results

1.2.1. Sub-cloning of hVPAC/PACR

In order to generate mammalian cell lines stably expressing the three hVPAC/PAC receptors, it was necessary to incorporate the receptor DNA sequences into an appropriate mammalian expression vector prior to transfection. This process was attempted first for the $hVPAC_2R$, as a commercially available, sequence verified clone was identified, which encompassed the entire ORF (IOH9624 Invitrogen; 1317 nucleotides). The $hVPAC_2R$ ORF was supplied in the pENTR™221 vector (2546 nucleotides), with the DNA construct provided already expressed in Dh10B™ *E. coli*. As pENTR™221 has no promoter for mammalian expression, the $hVPAC_2R$ was sub-cloned into pcDNA3.1™(+) vector (5428 nucleotides), which has the CMV promoter.

1.2.1.1. Preparation of hVPAC/PACR cDNA for stable cell line generation

The initial cloning strategy involved the direct transfer of the insert into the pcDNA3.1™(+) vector and a schematic of this procedure is illustrated in Figure B.1 (methods section, p 50). To prepare plasmid DNA, an innoculum of Dh10B™ *E. coli*, expressing the pENTR™221-$hVPAC_2R$ clone, was streaked out onto agar plates (overnight; 37 °C; kanamycin: 50 μg/ml) and three individual colonies were picked to innoculate LB media. Plasmid DNA (MP1-3) was then extracted and purified using the Promega Wizard® *Plus* SV Minipreps DNA kit and eluted in nuclease free water (100 μl). Using spectrophotometric analysis (A_{260}), the concentration of DNA in the minipreps MP1, MP2 and MP3 was calculated to be 157, 155 and 153 μg/ml, respectively. Restriction enzyme sites (for AflII and EcoRV) were identified on the pENTR™221 plasmid, which flanked either side of the $hVPAC_2R$ insert, with compatible recognition sequences also present in the multiple cloning site of the pcDNA3.1™(+) plasmid. Digests with these enzymes would therefore produce an $hVPAC_2R$ insert and pcDNA3.1™(+) expression vector sequences with compatible DNA ends for subsequent ligations. Single and double enzyme digests with AflII and EcoRV were performed (~ 2 μg DNA, 1 h, 37 °C) using the three minipreps and pcDNA3.1™(+), with the digest products run on agarose gels (1 %) and the DNA bands visualised under UV light (Figure 1.2.1). Single digests of MP1-3 produced DNA band sizes of just under 4 kb, consistent with the expected size of linearised plasmid and insert (3863 nucleotides), with two

bands clearly visible following the double digest. The first band corresponded to the excised insert (~1.5 kb) and the second, to linearised pENTR™221 plasmid sequence (~2.3 kb; Figure 1.2.1). The single digests of pcDNA3.1™(+) generated bands on the gel between 5 - 6 kb, consistent with the presence of linearised plasmid (5428 nucleotides), with the products from double digests being of a similar size, which was as expected, given the proximity of the enzymes' recognition sequences within the multiple cloning site (AflII – 909 and EcoRV – 965). The bands corresponding to the hVPAC$_2$R insert and linearised pcDNA3.1™(+) vector produced from the double digests, were excised from the gel and the DNA extracted and purified. Following extraction, the DNA was again visualised on a gel (Figure 1.2.2), with fragments of the expected size present. Ligation reactions (T4 DNA ligase; 10 µl reaction volume) were performed using the double digested, gel purified hVPAC$_2$R insert and pcDNA3.1™(+) vector (ligated overnight; 16 °C). The ligation reaction was then transformed into One Shot® TOP10 *E. coli* and the bacteria were cultured overnight on agar plates (ampicillin; 100 µg/ml). Individual colonies were used to inoculate samples of LB media and following an overnight incubation (37 °C), the DNA was extracted and double digested using AflII and EcoRV. Digest products from 6 of the cultures (1.1 - 1.6) are shown in Figure 1.2.3, where the absence of a DNA band at approximately 1.5 kb indicated that none of these colonies contained the ligated DNA. Despite several attempts to directly transfer the insert from pENTR™221 into pcDNA3.1™(+), which included using other *E. coli* strains (DH5α™) and different restriction enzymes (NheI and EcoRV), none were successful despite almost 50 colonies being examined. Throughout the process, bacterial colonies grew as expected and all control reactions were successful, suggesting that the transformation step had worked efficiently and leaving the ligation reaction as the most likely point of failure in the process.

1.2.1.2. TOPO-TA cloning®

Due to the failure of the standard sub-cloning procedures, a TOPO-TA cloning® strategy was adopted. This involved PCR amplification of the hVPAC$_2$R fragment and its insertion into a TOPO-TA cloning® vector (pCR®2.1-TOPO®), before finally sub-cloning into pcDNA3.1™(+) (Figure B.2, p 53). Two primer pairs were designed for PCR amplification of the hVPAC$_2$R insert; F1/R1 and F2/R2 (see methods for sequences, p 54). F1 and R1 were designed to amplify the entire length of the hVPAC$_2$R insert and also contained restriction enzyme sites (F1 - XbaI; R1 -

HindIII), to facilitate the sub-cloning into pcDNA3.1™ (+). F2 and R2 were internal primers and were used to check the integrity of the insert. PCR reactions were performed using purified DNA from MP3 as described in the methods section (p 54). PCR products were visualised on an agarose gel (Figure 1.2.4), with the full length primers F1/R1 producing an intense band of approximately 1.3 kb, correlating well with the expected insert size; all other bands were as expected. The PCR product containing the full length $hVPAC_2R$ insert was gel purified and ligated with the pCR®2.1-TOPO® vector (TOPO-TA cloning®). As PCR amplification of DNA using Taq polymerase generates a product with single deoxyadenosine overhangs at the 3' ends, the pCR®2.1-TOPO® vector is supplied linearised with single thymidine residue overhangs and is ideal for ligation. The ligation products were then transformed using One Shot® TOP10 *E. coli*, with colonies selected and propagated and the DNA extracted as described previously. Restriction digests were then performed with EcoRI, as it was expected to cut twice (residues 284 and 302), on either side of the pCR®2.1-TOPO® cloning site (Figure B.2, p 53). Almost two thirds of the colonies selected for analysis contained the PCR amplified $hVPAC_2R$ insert (1.3 kb; Figure 1.2.5). Five were selected for digestion with the restriction enzymes XbaI and HindIII, and the digest products visualised on an agarose gel. This resulted in digest products which contained the full length insert sequence (~1.3 kb) and the remaining empty pCR®2.1-TOPO® plasmid (~3.9 kb; Figure 1.2.6a). Parallel restriction digests were run with samples of pcDNA3.1™(+), to linearise the plasmid and generate compatible ends for ligation with the $hVPAC_2R$ insert (Figure 1.2.6b). Three of the bands containing the $hVPAC_2R$ insert were gel purified, as was the linearised pcDNA3.1™(+) vector, with the recovered, gel purified products visualised on a gel (Figure 1.2.7). Finally, samples of the gel purified, double digested $hVPAC_2R$ insert and pcDNA3.1™(+) vector were ligated, transformed (One Shot® TOP10 *E. coli*) and the DNA extracted as described previously. Restriction digests (XbaI and HindIII) were then carried out to determine if the ligation had been successful. In the majority (13/15) of DNA samples examined (Figure 1.2.8) it appeared that the $hVPAC_2R$ insert (~ 1.3 kb) had been successfully sub-cloned into the pcDNA3.1™(+) expression vector (~ 5.4 kb). Therefore, a construct was created that was suitable for transfection into an appropriate host cell, to generate cells stably expressing $hVPAC_2R$.

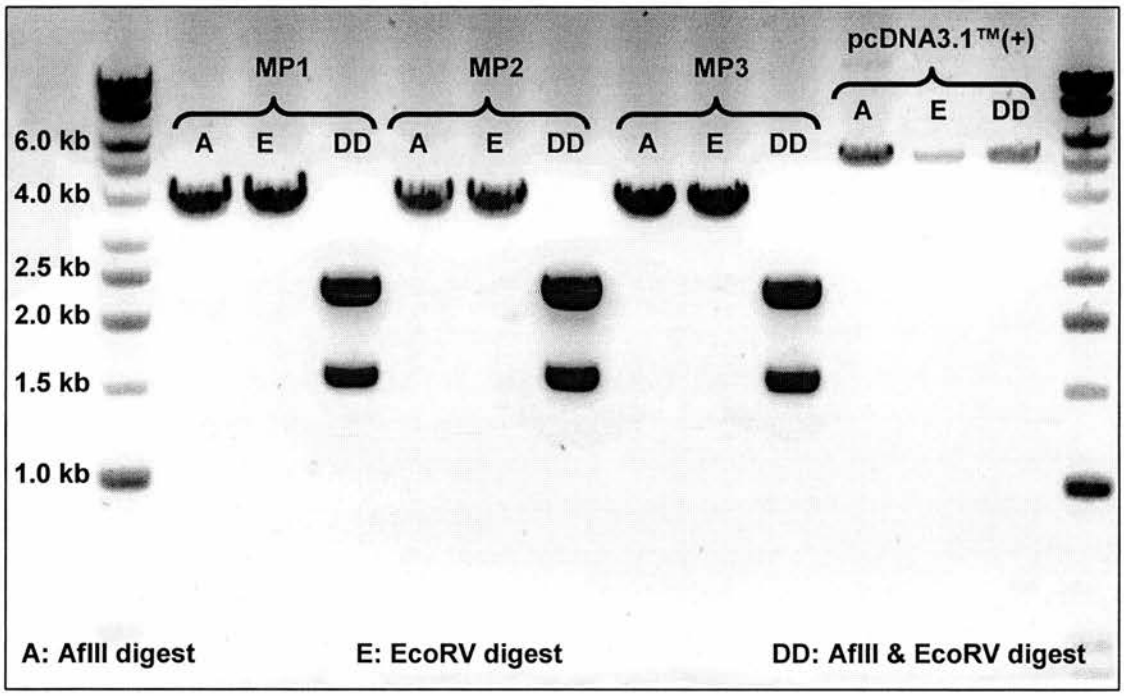

Figure 1.2.1 **Restriction enzyme digests of the pENTR™221 vector containing the hVPAC$_2$R insert and the pcDNA3.1™(+) plasmid.** DNA from MP1-3 (hVPAC$_2$R-pENTR™221 construct) was digested with AflII and EcoRV to excise the hVPAC$_2$R insert from the entry vector. In addition, products are shown from single digests with each enzyme, with the equivalent digests of the pcDNA3.1™(+) vector also presented.

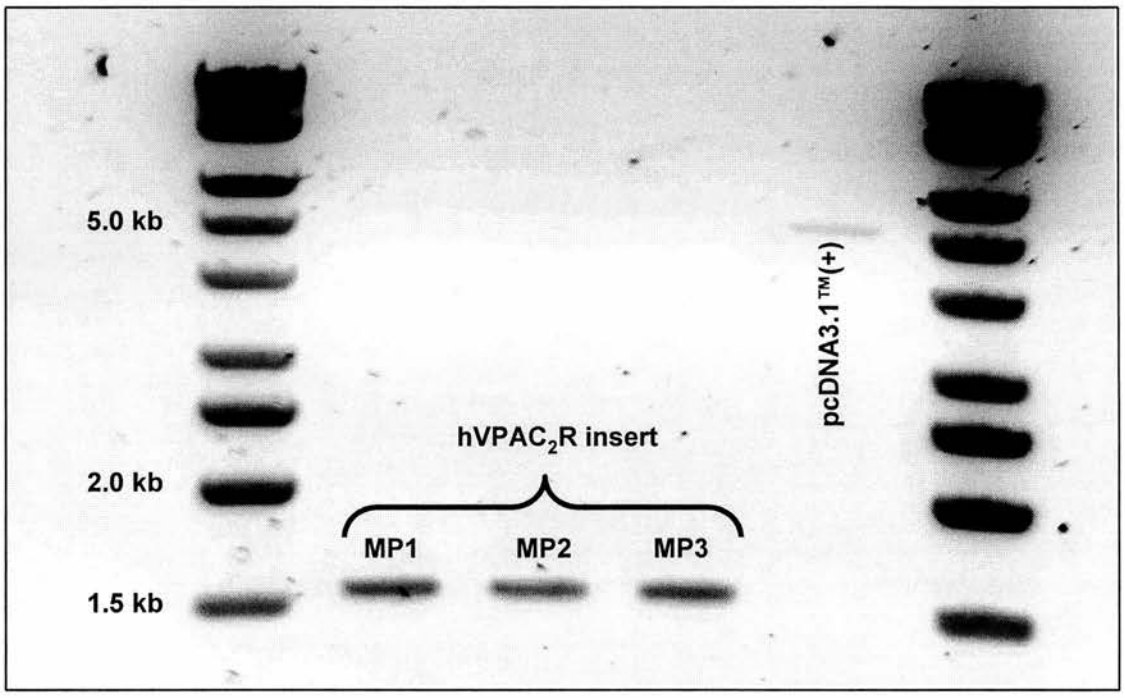

Figure 1.2.2 **Gel purified $hVPAC_2R$ inserts and linearised pcDNA3.1™(+) plasmid.** The inserts and plasmid (previously digested with AflII and EcoRV) were extracted from the gel in Figure 1.2.1 and run on a second gel, confirming successful purification of the resultant DNA.

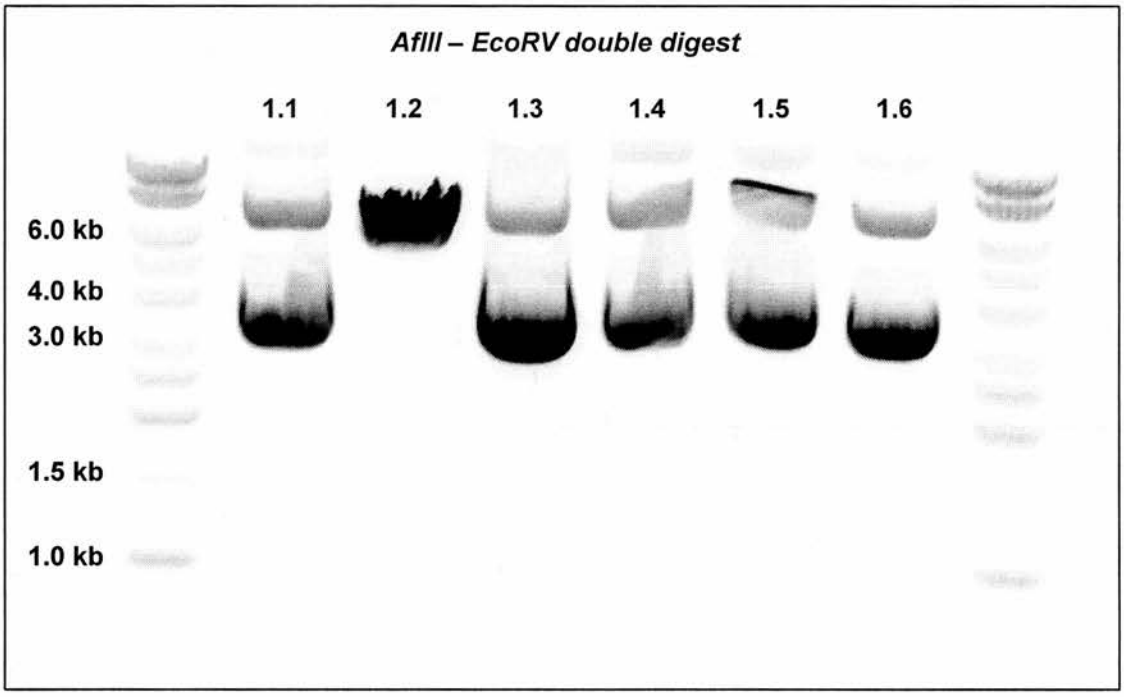

Figure 1.2.3 **Double digests of DNA extracted from bacterial colonies transformed with hVPAC$_2$R-pcDNA3.1™(+) ligation reactions.** Products from the ligation of the hVPAC$_2$R insert and pcDNA3.1™(+) vector were transformed into One Shot® Top10 *E. coli* and bacterial cultures were prepared from the resulting colonies (1.1 - 1.6). DNA was extracted from the cultures, enzyme digested (with AflII and EcoRV) and the DNA bands visualised on a gel to determine the whether the insert (~1.3 kb) was present.

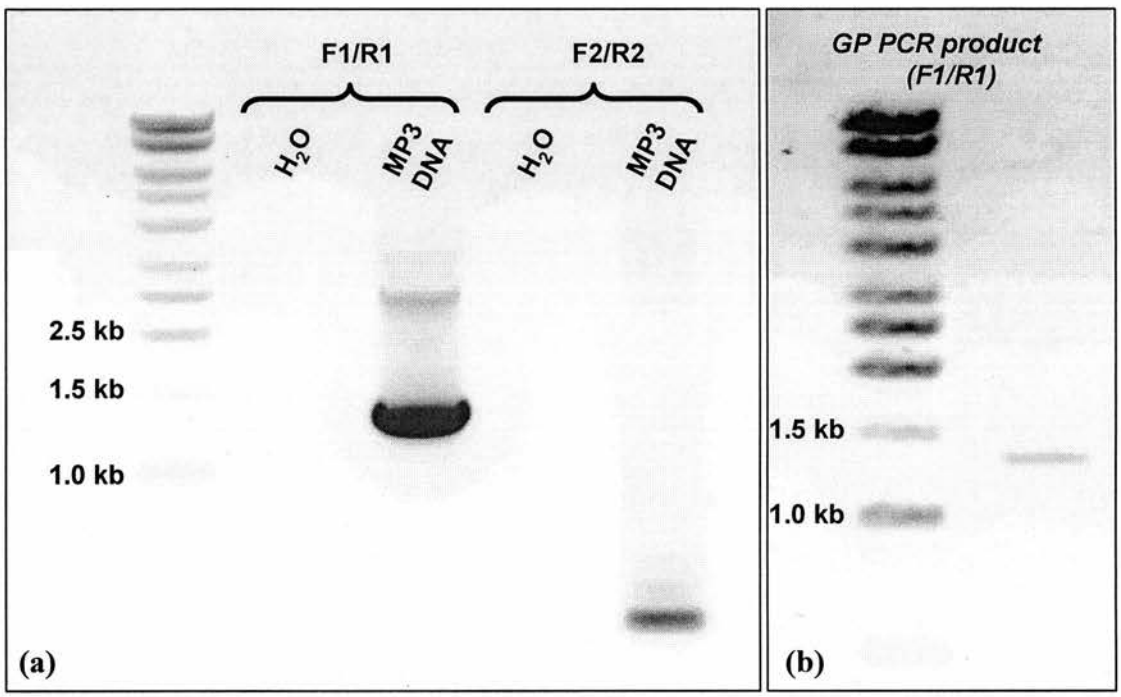

Figure 1.2.4 **PCR amplification of the hVPAC$_2$R insert from the pENTR™221 vector.** Primers F1 and R1 were designed to amplify the full length hVPAC$_2$R sequence (~1.3 kb), whereas F2 and R2 were designed to amplify a short section (0.5 kb) within the sequence (**a**). The amplified insert was then gel purified and the successful extraction of DNA confirmed on a second gel (**b**).

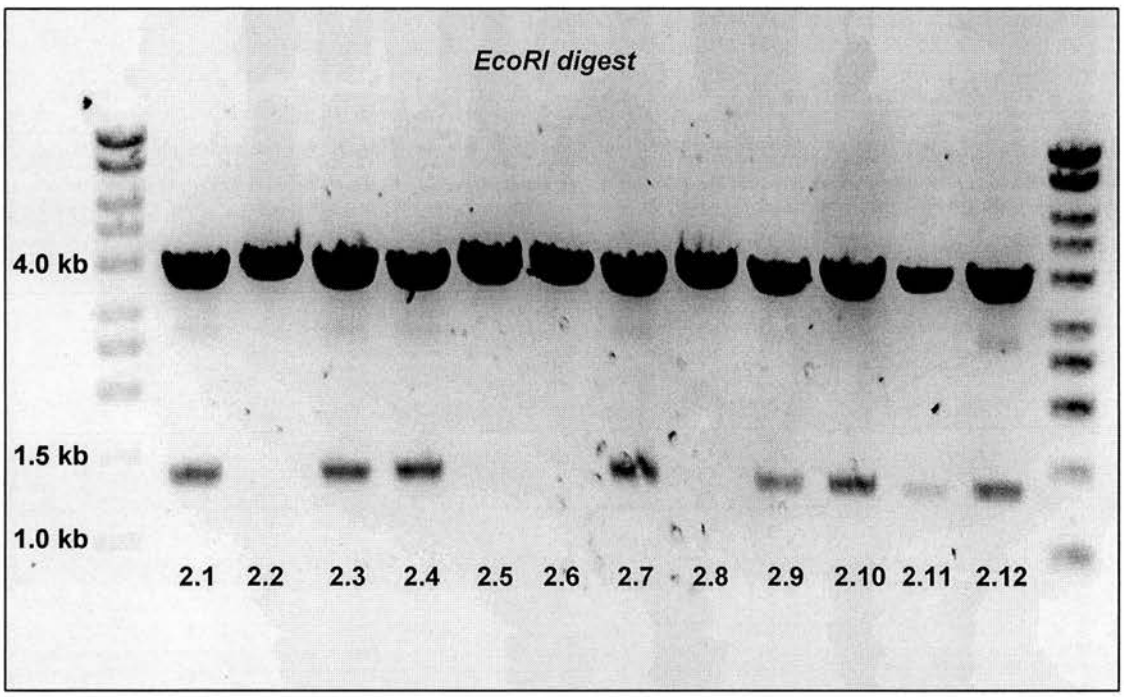

Figure 1.2.5 **Restriction enzyme digests of DNA extracted from One Shot® TOP10 *E. coli* colonies, transformed with the TOPO-TA cloning® reaction.** DNA from the ligation reaction of the pCR®2.1-TOPO® vector and the PCR amplified hVPAC$_2$R insert was transformed into One Shot® TOP10 *E. coli*, cultured on agar plates and selected colonies used to innoculate LB media cultures (2.1 - 2.12). The DNA was extracted and purified from the cultures and digested with EcoRI to evaluate the presence of the hVPAC$_2$R insert (~1.3 kb), which was apparent in 8 of the DNA preparations.

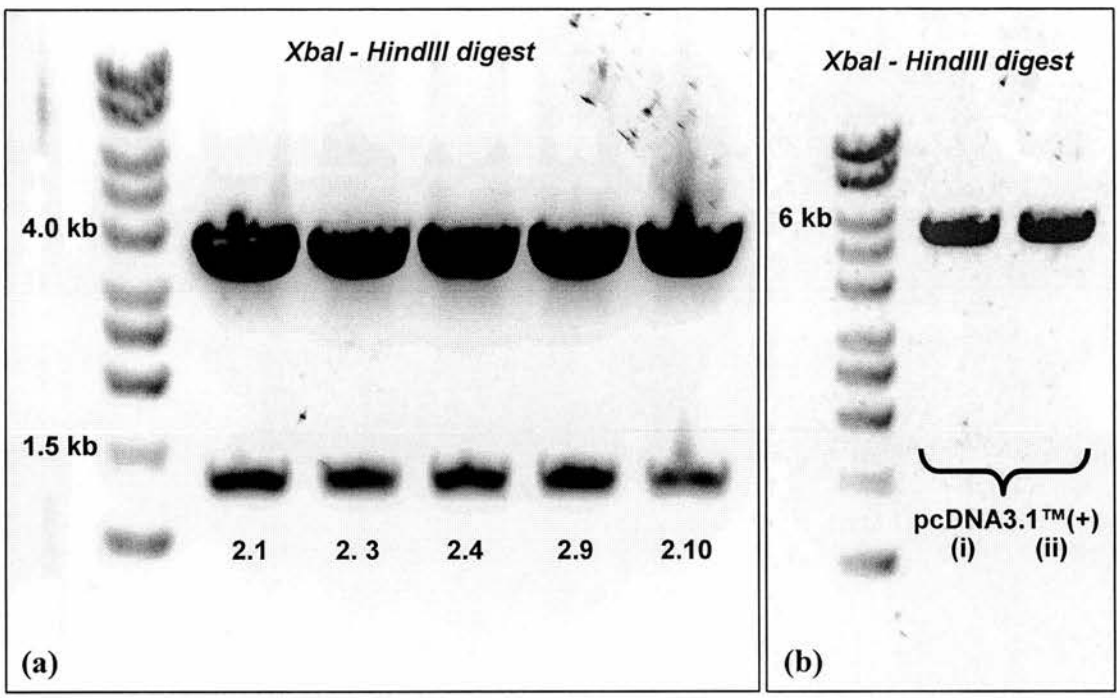

Figure 1.2.6 **Enzyme digests of hVPAC$_2$R-pCR®2.1-TOPO® and pcDNA3.1™(+).** Utilising the restriction sites incorporated into the F1/R1 primer sequences, hVPAC$_2$R-pCR®2.1-TOPO® construct samples were digested with XbaI and HindIII to isolate the insert (**a**). Parallel digests were run using pcDNA3.1™(+), in order to linearise the plasmid and create compatible ends for the subsequent ligations (**b**).

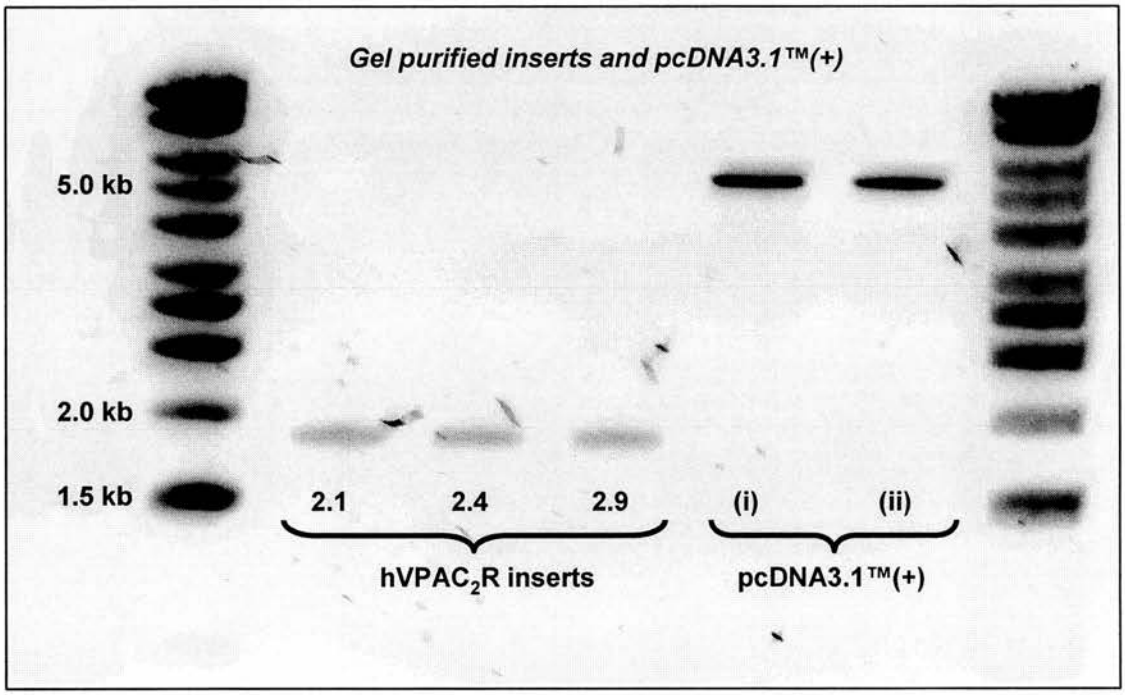

Figure 1.2.7 **Products from gel purification of hVPAC$_2$R insert and linearised pcDNA3.1™(+) vector.** XbaI and HindIII double digested hVPAC$_2$R insert and pcDNA3.1™(+) plasmid DNA were extracted from the agarose gel shown in Figure 1.2.6. Purified DNA samples are shown above, confirming successful extraction from the agarose.

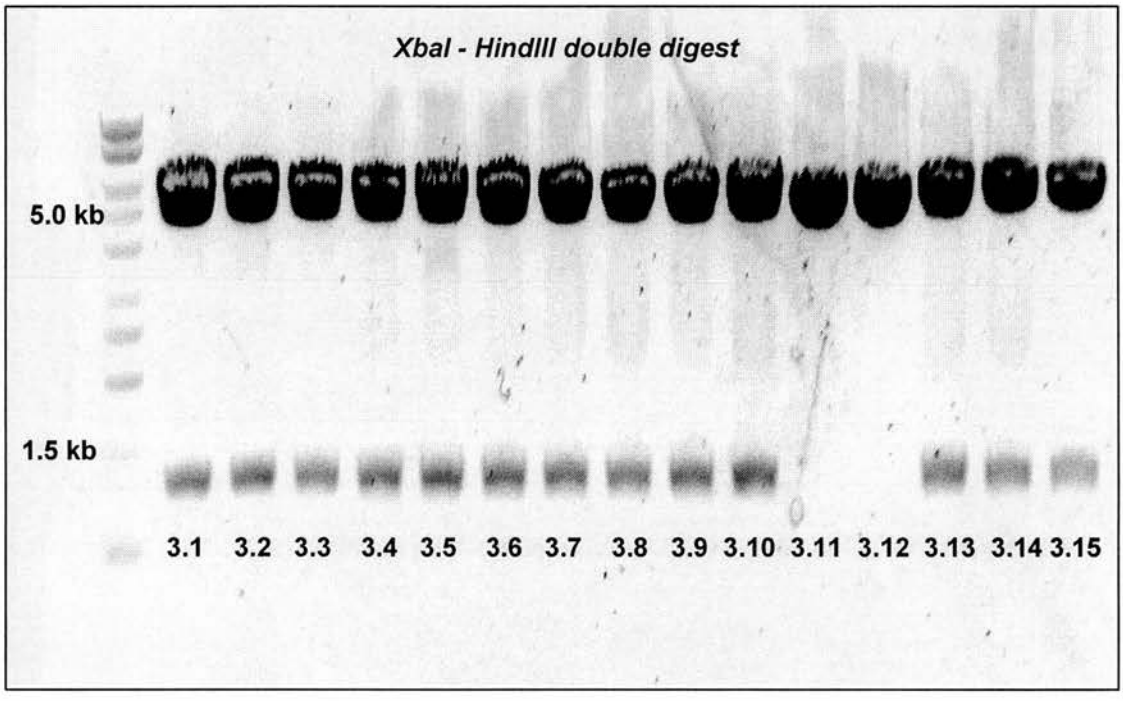

Figure 1.2.8 **Successful production of DNA constructs consisting of the hVPAC$_2$R insert in the pcDNA3.1™(+) mammalian expression vector.** DNA from the ligation reaction of the hVPAC$_2$R insert and pcDNA3.1™(+) vector was transformed into One Shot® TOP10 *E. coli* and cultured on agar plates. Selected colonies were used to innoculate LB media cultures (3.1 – 3.15), and following an overnight incubation (37 °C), the DNA was extracted and purified from the cultures and enzyme digests were performed (Xba1 and HindIII). The hVPAC$_2$R insert (~1.3 kb) was present in 13/15 colonies examined.

1.2.1.3. Identification of a suitable host cell line

On examination of the literature, it appeared that CHO-K1 or HEK-293 cells were suitable host cell lines in which to stably express VPAC/PACR, as the G-protein complement of these cell lines included those subunits to which VPAC/PACR couple (G_s, G_i, G_q; Van Rampelbergh *et al.*, 1997; Wietfeld *et al.*, 2004). To ensure that these cell lines were appropriate host cells for transfection with the hVPAC$_2$R-pcDNA3.1™(+) construct, the presence of endogenous VPAC/PACR was examined by stimulating the cells with an excess concentration of PACAP-27 and monitoring both $[cAMP]_i$ and $[Ca^{2+}]_i$ levels, with forskolin and ATP respectively used as positive controls (Figure 1.2.9). The responses were compared with those from SHSY-5Y cells, a human neuroblastoma cell line that is known to express native VPAC/PACR (Vertongen *et al.*, 1996). In the CHO-K1 cells, PACAP-27 (1 μM) had no stimulatory effect in either assay, suggesting that these cells do not express endogenous VPAC/PACR. In contrast, PACAP-27 (1 μM) induced small responses in HEK-293 and SHSY-5Y cells, indicating the presence of native VPAC/PAC receptors in these cell lines. These results indicated that CHO-K1 cells were the most suitable host cell line in which to stably express the hVPAC$_2$R construct. However, at this stage it was identified that three CHO-K1 cell lines stably expressing human VPAC$_1$R, VPAC$_2$R and PAC$_1$R had been generated previously by Fujisawa (Japan) and were kindly gifted to our laboratory by Dr I. Aramori. These three cell lines are the stable hVPAC/PACR cell lines described in all the subsequent pharmacological studies, with the hPAC$_1$R being the PAC$_1$-null variant described by Pisegna & Wank (1996).

1.2.2. Establishment and characterisation of $[cAMP]_i$ and $[Ca^{2+}]_i$ assays for the examination of human VPAC/PAC receptor pharmacology

The FlexStation® (Molecular Devices) is a bench-top fluorimeter with an integrated system of optics, fluidics and temperature control. It is capable of running 96-well plates and is suitable for rapid characterisation of receptor pharmacology. Although routinely used for measuring $[Ca^{2+}]_i$ and membrane potential, at the outset of these studies a 96 well plate, FlexStation® compatible $[cAMP]_i$ kit became available from MD. As the $[cAMP]_i$ assay for the FlexStation® was new and we were one of the first laboratories in the UK to use it, the protocol was optimised before embarking on the hVPAC/PACR characterisation studies.

1.2.2.1. Optimisation of $[cAMP]_i$ assay incubation period

The initial assay protocol recommended that cells be exposed to test compounds for 15 min prior to cell lysis and measurement of $[cAMP]_i$. To establish whether 15 min was the optimal assay time, the time-course of agonist induced $[cAMP]_i$ production was investigated using VIP (100 nM) and the CHO-hVPAC$_2$R cell line (1 x 10^5 per well), with the assay then conducted as described in the methods section (p 63). $[cAMP]_i$ concentrations in the cell lysates increased in a time-dependent manner, peaking at 15 min of agonist exposure (Figure 1.2.10a), confirming that this time-point was optimal. The second parameter verified was the time at which fluorescence levels could be measured on the final assay plate. The assay protocol stated that the final reading could be taken at any point between 10 min and 24 h following the addition of the substrate solution. In order to verify this, a cAMP standard curve was generated and fluorescence levels compared over a range of time points (Figure 1.2.10b). Fluorescence levels appeared to increase in a time dependent manner up to 18 h following substrate addition, reaching a plateau thereafter. Although the signal size increased, the shape of the standard curves remained consistent with only a minimal increase in the EC_{50} for the standard curve over the course of the experiment (t = 0, EC_{50}: 5.23 nM; t = 48 h, EC_{50}: 8.7 nM). This result verified that fluorescence measurements to determine $[cAMP]_i$ could be made up to 48 h.

1.2.2.2. Optimisation of cell densities for the $[cAMP]_i$ and $[Ca^{2+}]_i$ assays

The protocols for the $[cAMP]_i$ and $[Ca^{2+}]_i$ assays suggested that the optimum cell density for a 96-well plate, was likely to fall between 0.2 and 1 x 10^5 cells per well, with the optimum number ultimately being dependent on the size and growth characteristics of the cell line being tested. To establish optimal assay conditions for the hVPAC/PAC stable cell lines, cells were seeded overnight at a range of densities (0.5 - 1.5 x 10^5 cells per well) and agonist responses in the $[cAMP]_i$ and $[Ca^{2+}]_i$ assays measured using the FlexStation®. In the $[Ca^{2+}]_i$ assay, the response to a saturating concentration of agonist for each of the cell lines increased with cell density, plateauing around 1 x 10^5 cells per well (Figure 1.2.11a-c). Similarly in the $[cAMP]_i$ assay, the increasing cell density corresponded with a rise in $[cAMP]_i$, reaching a maximum at around 1.25 - 1.5 x 10^5 cells per well (Figure 1.2.11d-f). For direct comparability, the cell number utilised in all

subsequent experiments was set at 1 x 10^5 cells per well, as this density produced consistent and near maximal responses in both assays.

1.2.2.3. Analysis of calcium traces

The final parameter to be established was the generation of a standardised method for data analysis. For the $[cAMP]_i$ assay, this was straightforward, with the standard curve used to define $[cAMP]_i$ in test wells using endpoint fluorescence readings from those wells. The $[cAMP]_i$ levels measured were then plotted against drug concentrations, giving concentration-response curves from which EC_{50}/IC_{50} values could be determined. However, in the calcium assay the options for data analysis are more numerous, and include maximum to minimum (max-min), area under the curve (AUC), peak, slope and time to maximum. An example of the traces produced following agonist stimulation of the CHO-hVPAC/PACR cell lines is shown in Figure 1.2.12. Although the raw data sets associated with the individual measures cannot be directly compared, processing the raw values into concentration-response curves allowed a comparison of EC_{50} values to be calculated and provided a parameter with which the different methods of analysis could be compared. Agonist concentration-response curves in the calcium assay were compared with the three most common measures (max-min, AUC and peak), for each of the hVPAC/PACR cell lines (Figure 1.2.13: a - $hVPAC_1R$ with VIP; b - $hVPAC_2R$ with PACAP-27; c - $hPAC_1R$ with PACAP-38). When the EC_{50} values for VIP, PACAP-27 and PACAP-

Table 1.2.1 Agonist potencies (EC_{50} values) from concentration response curves produced from analysing calcium assay traces with max-min, AUC and peak analyses.

	$hVPAC_1R$ with VIP EC_{50} (nM)	$hVPAC_2R$ with PACAP-27 EC_{50} (nM)	$hPAC_1R$ with PACAP-38 EC_{50} (nM)
Max-min	16.5	23.1	5.7
Peak	18.9	24.2	5.9
AUC	26.1	33.5	7.5

Values shown were produced from the concentration response curves shown in Figure 1.2.13, for the agonist stimulation of CHO-$hVPAC_1R$, -$hVPAC_2R$ and -$hPAC_1R$ cell lines, with VIP, PACAP-27 and PACAP-38 respectively.

(a)

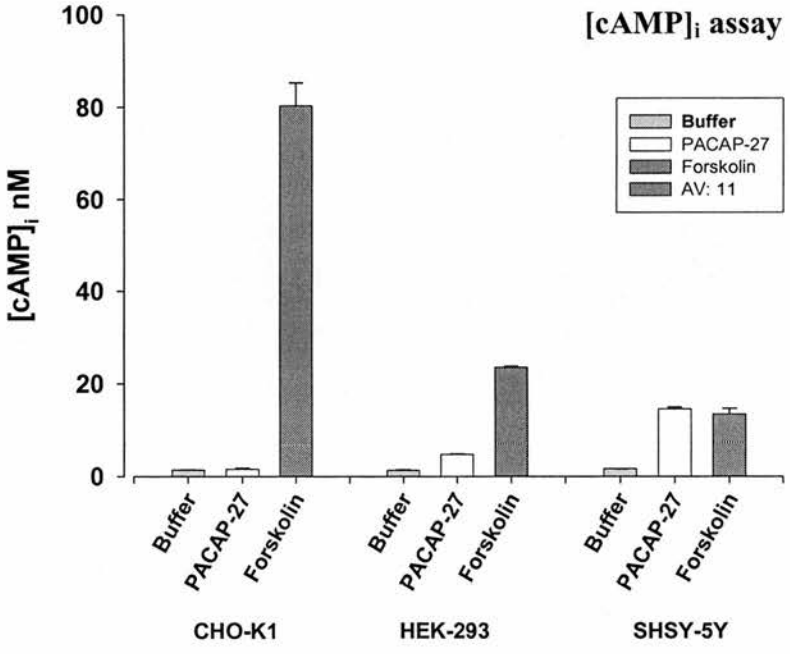

(b)

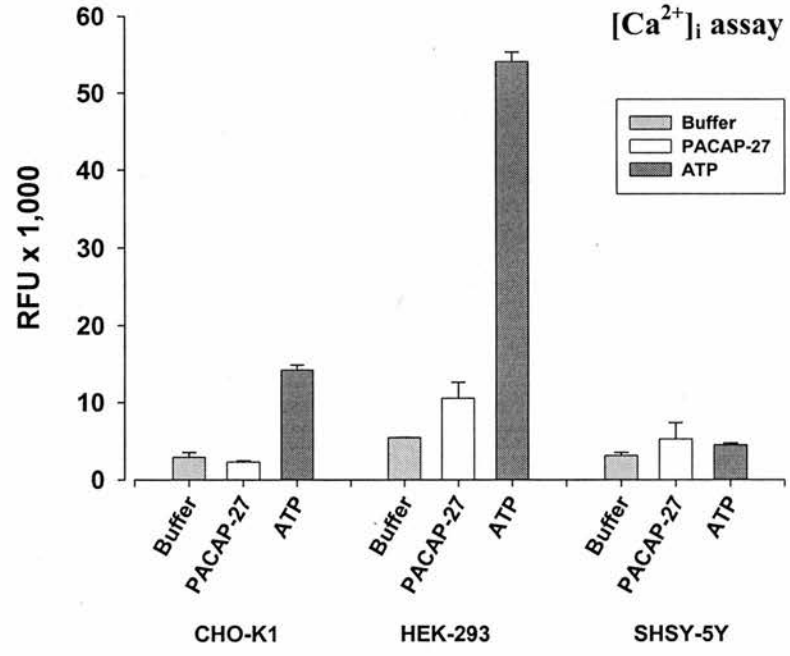

Figure 1.2.9 **$[cAMP]_i$ and $[Ca^{2+}]_i$ responses following PACAP-27 application to CHO-K1, HEK-293 and SHSY-5Y cells.** The three cell lines (cells per well: CHO-K1, HEK-293 - 1 x 10^5; SHSY-5Y - 1.25 x 10^5) were stimulated with buffer, PACAP-27 (1 μM) and either forskolin (10 μM; $[cAMP]_i$ assay) or ATP (10 μM; $[Ca^{2+}]_i$ assay), which served as positive controls. The responses shown are representative (**a,** $[cAMP]_i$: n = 2; **b**, $[Ca^{2+}]_i$: n = 3).

(a)

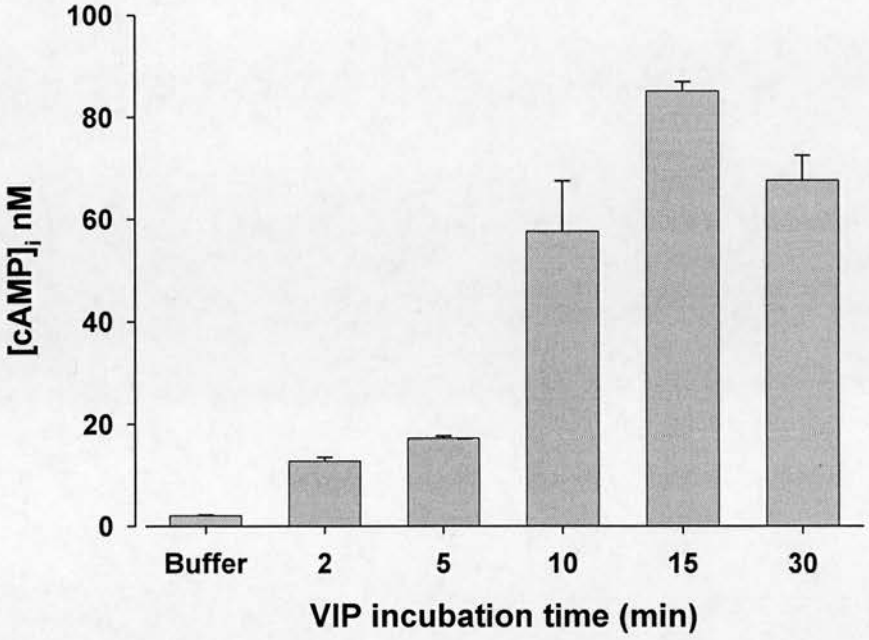

(b)

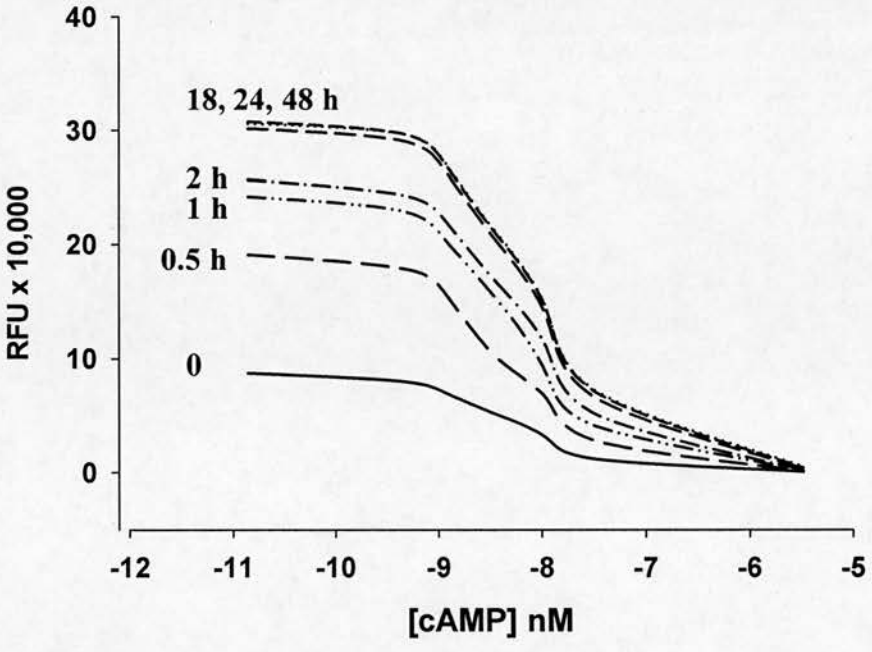

Figure 1.2.10 Effect of altering the agonist exposure period and the final plate read time on levels of cAMP detected. The concentration of cAMP released from CHO-hVPAC$_2$R cells after VIP stimulation (100 nM) increased with time and peaked at 15 min (**a**; n = 1). Increasing the time prior to the final reading of the assay plate produced a rise in fluorescence for all samples, although the overall shape of the standard curve remained constant (**b**; n = 1).

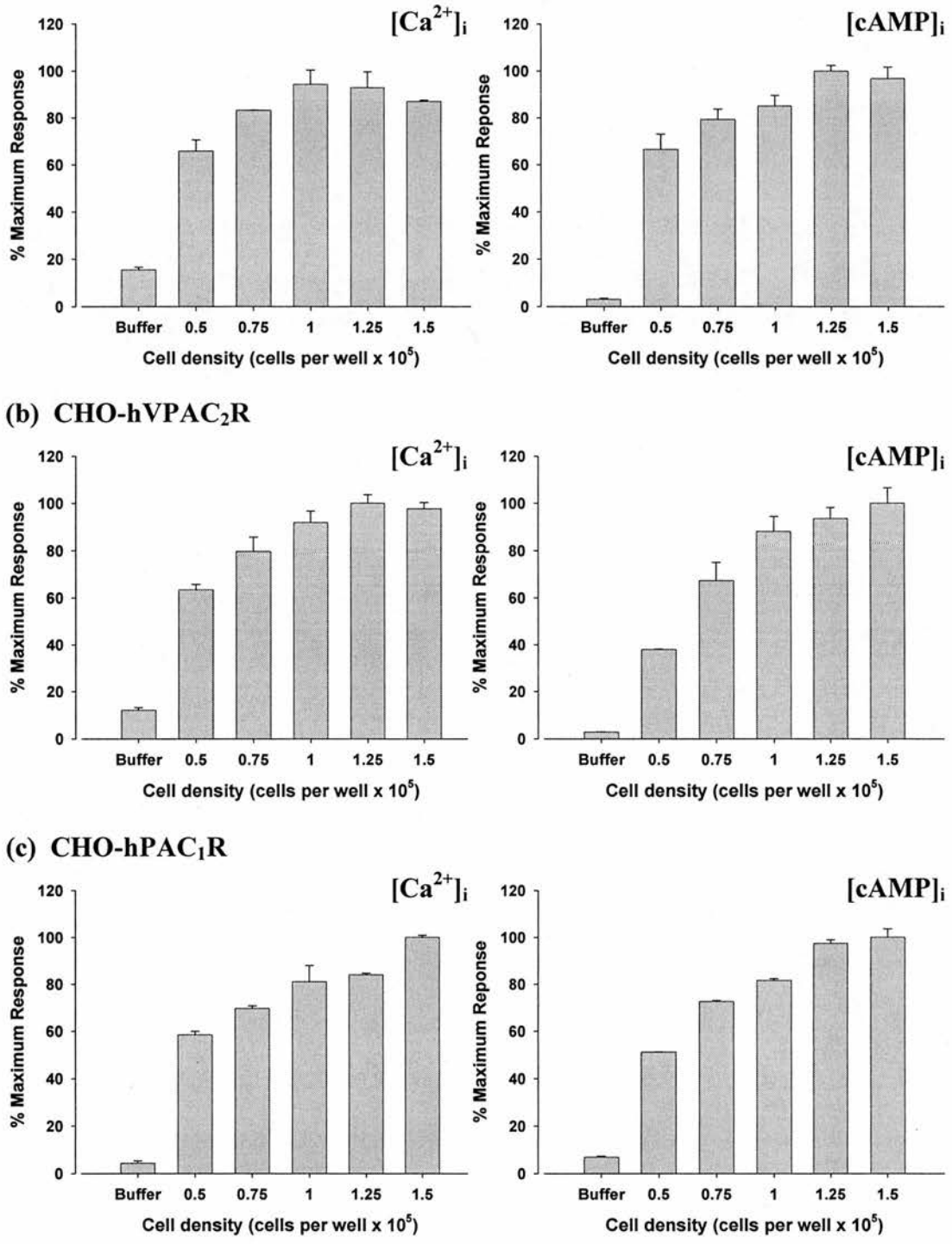

Figure 1.2.11 Effect of hVPAC/PACR seeding density upon response size to agonist. The hVPAC/PACR stable cell lines were seeded into 96-well plates (0.5 - 1.5 x 10^5 per well) and stimulated with saturating concentrations of agonists (hVPACR: VIP - 1 μM; $hPAC_1R$: PACAP-27 – 1 μM) in the $[cAMP]_i$ and $[Ca^{2+}]_i$ assays. The figures shown are representative of three independent experiments.

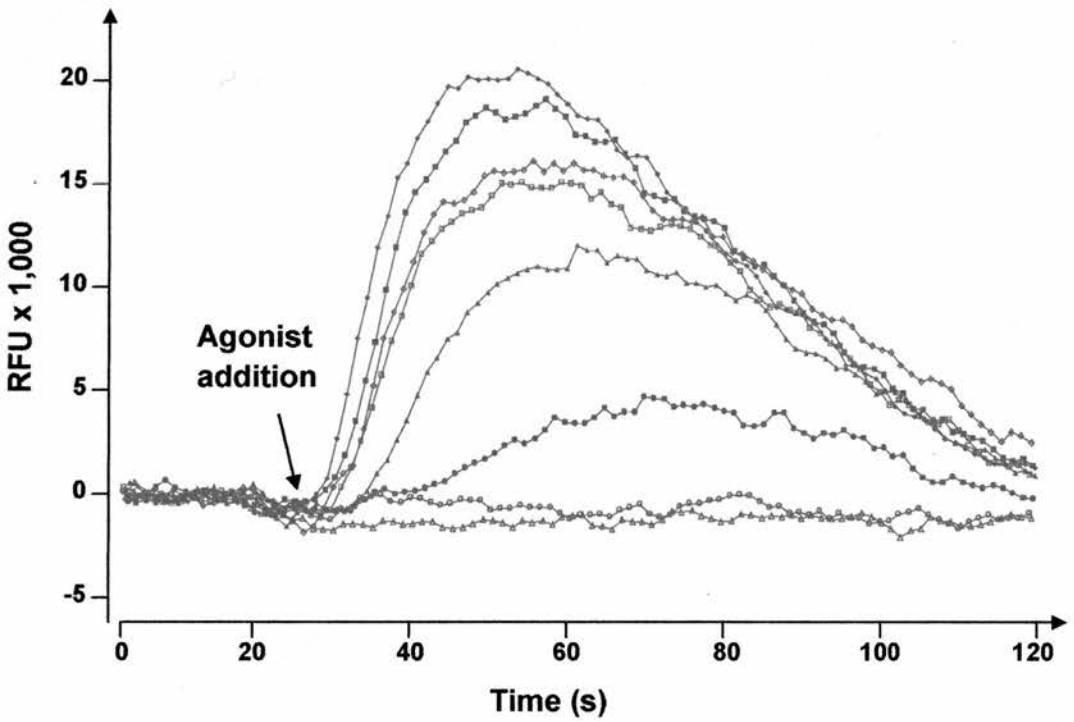

Figure 1.2.12 An example of the data traces produced in the calcium assay following addition of increasing agonist concentrations to CHO-hVPAC/PACR cells. CHO-hVPAC$_2$R cells (1 x 10^5 per well) were seeded overnight and stimulated with PACAP-38 (as indicated by the arrow) over a range of concentrations (0.1 nM to 3 μM).

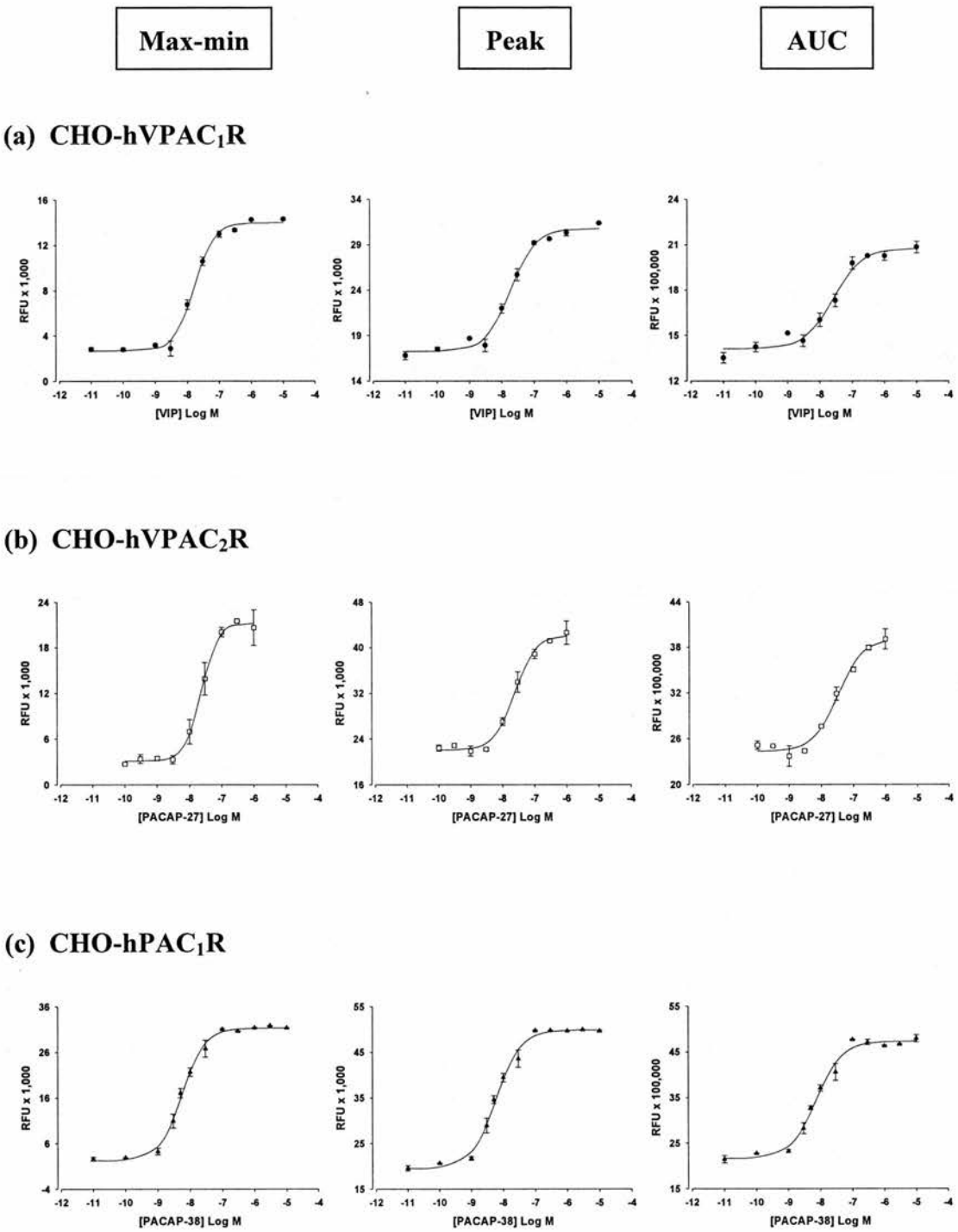

Figure 1.2.13 Agonist concentration response curves for the calcium assay generated using different data analysis methods. $hVPAC_1R$ **(a)**, $hVPAC_2R$ (**b**) and $hPAC_1R$ (**c**) stable cell lines were stimulated with VIP, PACAP-27 and PACAP-38 respectively. The resultant fluorescence responses were measured using max-min, peak and AUC analyses, and concentration response curves generated from the data produced (n = 1). The EC_{50} value from each curve is presented in Table 1.2.1.

38 were compared for each receptor, it was evident that the different methods of analysis did not greatly alter EC_{50} values in all three stable cell lines (Table 1.2.1). As the different methods of analysis did not obviously affect the agonist potencies calculated from the concentration response curves, additional factors were considered when selecting the most appropriate measure to use for data analysis in the $[Ca^{2+}]_i$ assay. In these preliminary studies, baseline fluorescence levels in wells were similar for individual cell lines, however well to well variation was observed between baselines when different cell lines were used. The measurement of peak values from such traces cannot accommodate this variation and may have reduced the accuracy of the data, hence this measure was deemed unsuitable for data analysis. In addition, as trace shape changed on progression from low to high agonist concentrations (Figure 1.2.12) and between cell lines (section 1.2.3.3., p 106), the use of AUC analysis may not have provided a fair comparison between data sets. Therefore, max-min appeared to be the most accurate and reproducible measure with which to process the data for comparison between different compounds and cell types.

1.2.3. Pharmacology of hVPAC/PACR expressing stable cell lines

The pharmacology of human VPAC/PACR was systematically characterised using the CHO-K1 stable cell lines and the optimised $[cAMP]_i$ and $[Ca^{2+}]_i$ assays described above. The potency of the classical agonists VIP, PACAP-27 and PACAP-38 was determined, in addition to three reportedly receptor selective agonists $[Ala^{11,22,28}]$VIP ($VPAC_1R$; Nicole *et al.*, 2000), R3P65 ($VPAC_2R$; Yung *et al.*, 2003) and maxadilan (PAC_1R; Moro & Lerner, 1997). The pharmacological properties of the putatively receptor selective antagonists PG97-269 ($VPAC_1R$; Gourlet *et al.*, 1997a), PG99-465 ($VPAC_2R$; Moreno *et al.*, 2000) and M65 (PAC_1R; Uchida *et al.*, 1998) were also thoroughly investigated.

1.2.3.1. hVPAC/PACR agonist pharmacology – $[cAMP]_i$ assay

The three endogenous agonists VIP, PACAP-27 and PACAP-38 increased $[cAMP]_i$ in all three stable cell lines in a concentration dependent manner (Figures 1.2.14a, 1.2.15a and 1.2.16a). These peptides were approximately equipotent at the $hVPAC_1R$ (Figure 1.2.14a; EC_{50} values: VIP = 0.109 ± 0.026 (7) nM; PACAP-27 =

0.127 ± 0.018 (3); PACAP-38 = 0.218 ± 0.039 (4) nM) and at the hVPAC$_2$R (Figure 1.2.15a; EC_{50} values: VIP = 0.628 ± 0.187 (6) nM; PACAP-27 = 0.383 ± 0.094 (3); PACAP-38 = 0.528 ± 0.136 (4) nM), with all three marginally less potent at the latter receptor (Table 1.2.2). At the hPAC$_1$R (Figure 1.2.16a), both PACAP-27 and PACAP-38 exhibited picomolar potencies with EC_{50} values of 0.026 ± 0.003 (7) nM and 0.049 ± 11 (3) nM respectively, resulting in these peptides being ~ 4 and ~ 10 fold more potent than at the hVPAC$_1$R and hVPAC$_2$R. VIP however was ~ 40 times less potent than the PACAP peptides, with an EC_{50} of 15.1 ± 2.76 (4) nM (Table 1.2.2). The reportedly VPAC$_1$R selective agonist [Ala^{11,22,28}]VIP was confirmed as a potent sub-nanomolar peptide agonist at that receptor (EC_{50}: 0.057 ± 0.015 (4) nM). In addition, this peptide was also a full agonist at the hPAC$_1$R, albeit at micromolar concentrations (EC_{50}: 1.49 ± 0.208 (3) μM), with a negligible effect at the hVPAC$_2$R. R3P65 (putatively VPAC$_2$R selective) was a full agonist at the hVPAC$_2$R, demonstrating a similar potency (EC_{50}: 1.75 ± 0.4 (4) nM) to the endogenous agonists at this receptor (Table 1.2.2). However, in our hands R3P65 was not selective, eliciting full agonist responses at both hVPAC$_1$ and hPAC$_1$ receptor expressing cell lines, with its highest potency (EC_{50}: 0.268 ± 0.006 (4) nM) at the former receptor subtype. In contrast, maxadilan was a highly selective and full hPAC$_1$R agonist (EC_{50}: 0.054 ± 0.009 (3) nM; Table 1.2.2), being equipotent with both PACAPs, whilst eliciting no response at either of the hVPAC receptors. In all three CHO-K1 cell lines expressing the hVPAC$_1$R, hVPAC$_2$R or hPAC$_1$R, the maximal concentrations of $[cAMP]_i$ produced from agonist stimulation were all similar at around 50 nM and were approximately 25x basal levels (Figure 1.2.17), suggesting comparable receptor expression levels.

In short, all agonist potencies generated using the $[cAMP]_i$ assay were similar at hVPAC$_1$R (excluding maxadilan), a trend also observed for hVPAC$_2$R (except [Ala^{11,22,28}]VIP]), albeit with about a 4-fold lower potency at the latter subtype (Table 1.2.2). As a result, agonist ROPs for these two cell lines in the $[cAMP]_i$ assay were as follows: - hVPAC$_1$R: VIP = PACAP-27 = PACAP-38 = [Ala^{11,22,28}]VIP = R3P65, and – hVPAC$_2$R: VIP = PACAP-27 = PACAP-38 = R3P65. In contrast, at hPAC$_1$R, PACAP-27 and PACAP-38 were more potent than at hVPAC$_1$R and hVPAC$_2$R (~ 4 fold) receptors, whereas VIP and R3P65 were more than 100 times less potent compared to hVPAC$_1$R (Table 1.2.2). [Ala^{11,22,28}]VIP, the most potent hVPAC$_1$R agonist, was more than 4 orders of magnitude less potent at hPAC$_1$R (EC_{50} = 1.49 ± 0.208 (3) μM), whereas maxadilan had sub-nanomolar affinity at the latter receptor and even greater selectivity over both hVPAC$_1$R and

hVPAC$_2$R. The resulting ROP for the hPAC$_1$R in the [cAMP]$_i$ assay was therefore: PACAP-27 = PACAP-38 = maxadilan > VIP = R3P65 > [Ala^{11,22,28}]VIP.

1.2.3.2. hVPAC/PACR agonist pharmacology – [Ca^{2+}]$_i$ assay

In the three stable cell lines expressing hVPAC/PACR (Figures 1.2.14b, 1.2.15b and 1.2.16b), the endogenous peptides VIP, PACAP-27 and PACAP-38 all produced a concentration dependent increase in [Ca^{2+}]$_i$. All three peptides had similar potencies to each other at both hVPAC receptors (Table 1.2.2), with EC_{50} values ranging from 14 - 37 nM at the hVPAC$_1$R (VIP = 14.1 ± 0.9 (6) nM, PACAP-27 = 22.6 ± 5.3 (8) nM, PACAP-38 = 37.4 ± 7.9 (10) nM) and 19 - 50 nM at the hVPAC$_2$R (VIP = 49.6 ± 7.9 (10) nM, PACAP-27 = 23.9 ± 2.4 (6) nM, PACAP-38 = 19.4 ± 2.3 (8) nM). In agreement with the [cAMP]$_i$ assay, PACAP-27 and PACAP-38 were potent hPAC$_1$R agonists (EC_{50} values of 5.0 ± 1.1 (9) nM and 4.7 ± 1.2 (6) nM respectively; Table 1.2.2), whereas VIP was considerably less potent at this receptor subtype when compared to the hVPAC receptors (~ 10 fold; EC_{50} = 405 ± 36.3 (5) nM). These three peptides were clearly less potent in the [Ca^{2+}]$_i$ assay than in the [cAMP]$_i$ assay, with EC_{50} values being approximately 100 fold less (Table 1.2.2). [Ala^{11,22,28}]VIP was a potent hVPAC$_1$R agonist in the calcium assay (EC_{50}: 26.8 ± 2.0 (5) nM; Figure 1.2.14), however it had no effect at the hVPAC$_2$R (Figure 1.2.15) or the hPAC$_1$R (Figure 1.2.16). The lack of effect of [Ala^{11,22,28}]VIP at the hPAC$_1$R (EC_{50} = 1.49 ± 0.2.8 (3) μM in the [cAMP]$_i$ studies; Table 1.2.2), may have been due to an insufficient concentration of compound being added. R3P65 was once more not hVPAC$_2$R selective, being slightly more potent at hVPAC$_1$R (EC_{50} values of 108 ± 18.4 (6) nM and 86.1 ± 1.3 (4) nM respectively; Table 1.2.2). R3P65 was a full agonist at the hPAC$_1$R (Figure 1.16b; EC_{50} = 0.59 ± 0.089 (6) μM), although it was 5 fold less potent than at the hVPAC receptors. In agreement with the [cAMP]$_i$ data, maxadilan was equipotent with PACAP-27 and PACAP-38 at the hPAC$_1$R (EC_{50} = 12.6 ± 2.3 (12) nM), whilst being highly receptor selective with no agonist effects in the hVPACR cell lines (Table 1.2.2). The resulting ROPs for each VPAC/PAC receptor in the [Ca^{2+}]$_i$ assay were consistent with those generated from the [cAMP]$_i$ assay, being: - hVPAC$_1$R: VIP = PACAP-27 = PACAP-38 = [Ala^{11,22,28}]VIP ≥ R3P65, - hVPAC$_2$R: VIP = PACAP-27 = PACAP-38 ≥ R3P65 and - hPAC$_1$R: PACAP-27 = PACAP-38 = maxadilan > VIP = R3P65. The calcium dye used in the FlexStation® [Ca^{2+}]$_i$ assay is non-ratiometric and although it was not possible to determine the exact [Ca^{2+}]$_i$, the average maximal response elicited from

the three stable cell lines following exposure to a saturating concentration of agonist produced comparable levels of fluorescence (~ 17,000 RFU), all of which were approximately 7x basal levels (Figure 1.2.17a-c). This is consistent with the equivalent levels of agonist induced $[cAMP]_i$ observed in all three cell lines.

In short, the peptides VIP, PACAP-27, PACAP-38 and R3P65 all had similar potencies in CHO-K1 cells expressing either $hVPAC_1R$ or $hVPAC_2R$. This finding was similar in both the $[cAMP]_i$ and $[Ca^{2+}]_i$ assays, although there was approximately a two order of magnitude difference in the EC_{50} values generated in the two assays (Table 1.2.2). At the $hPAC_1R$, PACAP-27, PACAP-38 and maxadilan were again the most potent agonists, despite the 100-fold reduction in potency (Table 1.2.2). This is clearly illustrated in Figure 1.2.18, which shows a correlation of the agonist potencies from the $[cAMP]_i$ and $[Ca^{2+}]_i$ assays, for all three hVPAC/PACR subtypes. Regression analysis ($r^2 = 0.85$) confirmed that the agonists were approximately 100 fold less potent in the calcium assay.

1.2.3.3. hVPAC/PACR agonists – $[Ca^{2+}]_i$ assay traces

In contrast to the $[cAMP]_i$ assay, which uses an endpoint fluorescence reading, the data generated using the $[Ca^{2+}]_i$ assay is produced in a 'real-time' format, with a reading taken from each well every 1.27 s. In addition to measuring max-min responses, the overall shapes of traces can be analysed, thereby providing an alternative source of information to compare the different cell lines and the effects of compounds. Figure 1.2.19 shows representative sets of fluorescence traces produced by agonist stimulation of the three CHO-hVPAC/PACR cell lines. The traces were produced using a range of agonist concentrations, with fluorescence levels generally monitored for up to 90 s. In general, the agonist induced responses at $hVPAC_1R$ and $hVPAC_2R$ were very similar, consisting of an initial rapid increase, which gradually declined to approximately 40 % of the peak response at the end of the 90 s period (Figure 1.2.19). However, the traces produced for the $hPAC_1R$ were more complex, with the various agonists inducing responses that appeared to decline at a slower rate than those observed from the hVPAC receptors (Figure 1.2.19). To quantitatively compare these observations, the magnitude of the agonist response at the end of the 90 s period was measured for all of the agonist assays performed during the current studies of CHO-hVPAC/PACR pharmacology (Figure 1.2.20), with data presented as the percentage of the peak response for each agonist. As predicted, agonist induced responses at 90 s for both hVPAC receptor cell lines were

(a) CHO-hVPAC$_1$R: [cAMP]$_i$

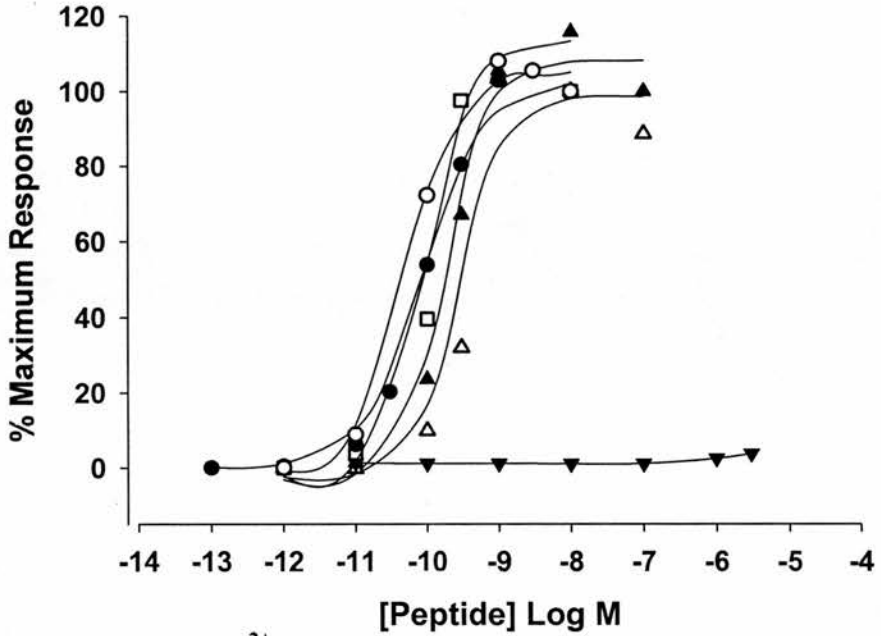

(b) CHO-hVPAC$_1$R: [Ca^{2+}]$_i$

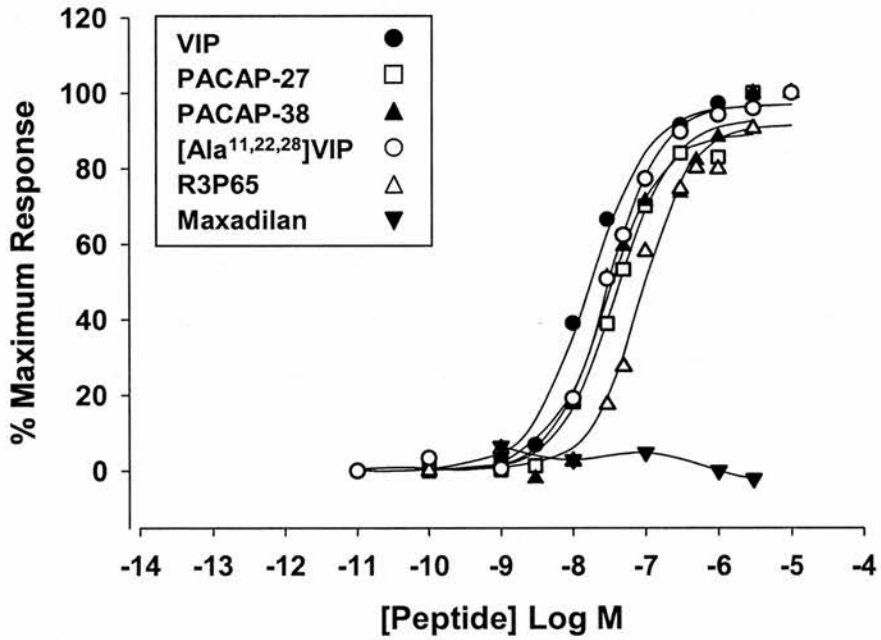

Figure 1.2.14 Characterisation of hVPAC$_1$R using the [cAMP]$_i$ and [Ca^{2+}]$_i$ assays. CHO-hVPAC$_1$R cells (1 x 10^5 per well) were stimulated with a range of VPAC/PACR agonists and [cAMP]$_i$ (**a**) and [Ca^{2+}]$_i$ (**b**) responses measured. The concentration response curves shown are representative, with mean EC_{50} values ± SEM ($n \geq 3$) shown in Table 1.2.2.

(a) CHO-hVPAC$_2$R: [cAMP]$_i$

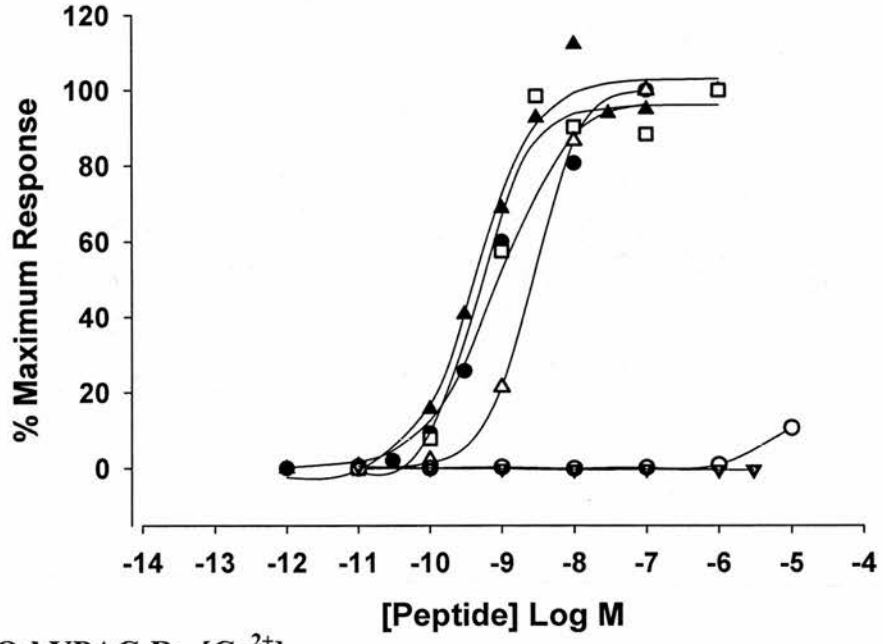

(b) CHO-hVPAC$_2$R: [Ca^{2+}]$_i$

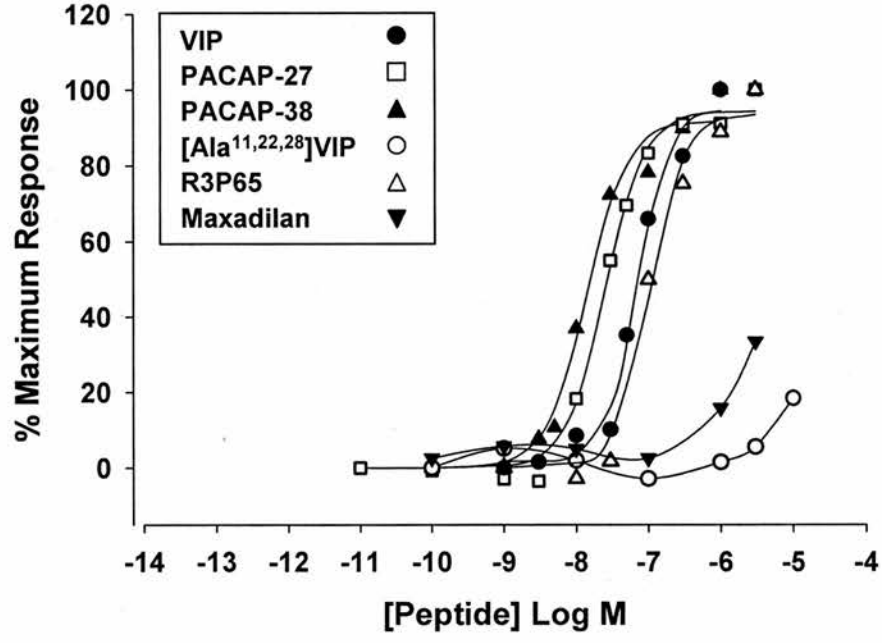

Figure 1.2.15 Characterisation of hVPAC$_2$R using the [cAMP]$_i$ and [Ca^{2+}]$_i$ assays. CHO-hVPAC$_2$R cells (1 x 10^5 per well) were stimulated with a range of VPAC/PACR agonists and [cAMP]$_i$ (**a**) and [Ca^{2+}]$_i$ (**b**) responses measured. The concentration response curves shown are representative, with mean EC_{50} values ± SEM ($n \geq 3$) shown in Table 1.2.2.

(a) CHO-hPAC$_1$R: [cAMP]$_i$

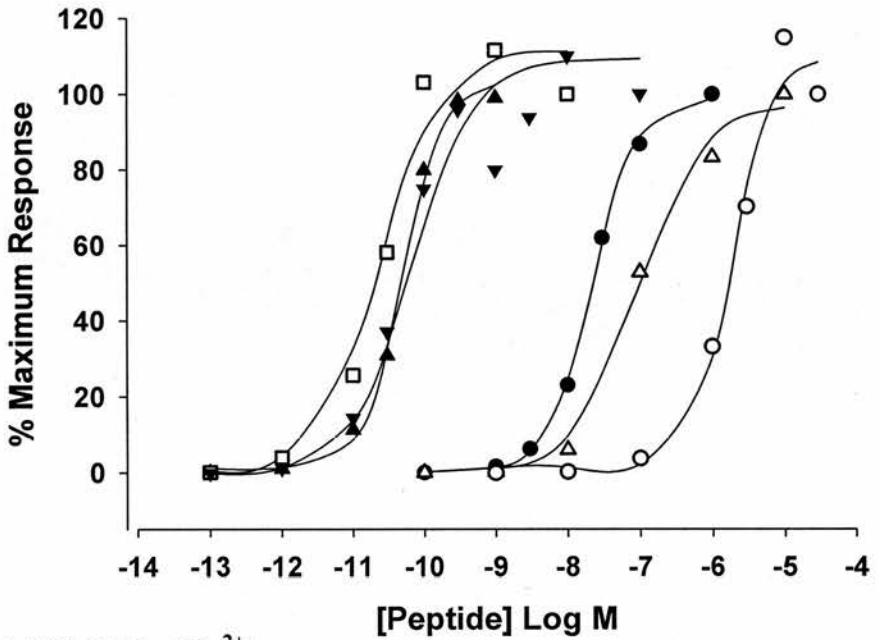

(b) CHO-hPAC$_1$R: [Ca^{2+}]$_i$

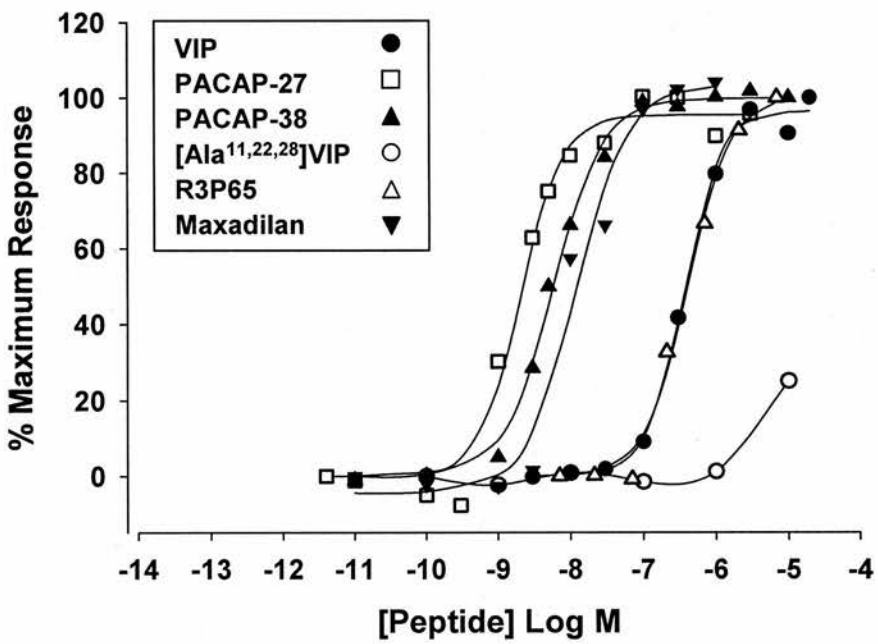

Figure 1.2.16 Characterisation of hPAC$_1$R using the [cAMP]$_i$ and [Ca^{2+}]$_i$ assays. CHO-hPAC$_1$R cells (1 x 10^5 per well) were stimulated with a range of VPAC/PACR agonists and [cAMP]$_i$ (**a**) and [Ca^{2+}]$_i$ (**b**) responses measured. The concentration response curves shown are representative, with mean EC_{50} values ± SEM ($n \geq 3$) shown in Table 1.2.2.

Table 1.2.2 **Comparison of E_{50} values for agonist induced $[cAMP]_i$ and $[Ca^{2+}]_i$ stimulation in CHO-K1 cells stably expressing $hVPAC_1$, $hVPAC_2$ and $hPAC_1$ receptors**

		VIP	PACAP-27	PACAP-38	[Ala^{11,22,28}]VIP	R3P65	Maxadilan
		EC_{50} ± SEM (nM)					
$hVPAC_1R$	$[cAMP]_i$	0.109 ± 0.026 (7)	0.127 ± 0.018 (3)	0.218 ± 0.039 (4)	0.057 ± 0.015 (4)	0.268 ± 0.006 (4)	NE
	$[Ca^{2+}]_i$	14.1 ± 0.9 (6)	22.6 ± 5.3 (8)	37.4 ± 7.9 (10)	26.8 ± 2.0 (5)	86.1 ± 1.3 (4)	NE
$hVPAC_2R$	$[cAMP]_i$	0.628 ± 0.187 (6)	0.383 ± 0.094 (3)	0.528 ± 0.136 (4)	NE	1.75 ± 0.399 (4)	NE
	$[Ca^{2+}]_i$	49.6 ± 7.9 (10)	23.9 ± 2.4 (6)	19.4 ± 2.3 (8)	NE	108 ± 18.4 (6)	NE
$hPAC_1R$	$[cAMP]_i$	15.1 ± 2.76 (4)	0.026 ± 0.003 (7)	0.049 ± 0.011 (3)	1.49 ± 0.208 µM (3)	63.6 ± 19.5 (3)	0.054 ± 0.009 (3)
	$[Ca^{2+}]_i$	405 ± 36.3 (5)	5.0 ± 1.1 (9)	4.7 ± 1.2 (6)	NE	589 ± 88.7 (6)	12.6 ± 2.3 (12)

EC_{50} values are shown as mean ± SEM, with the number of independent experiments given in brackets. NE is no effect at 3 µM.

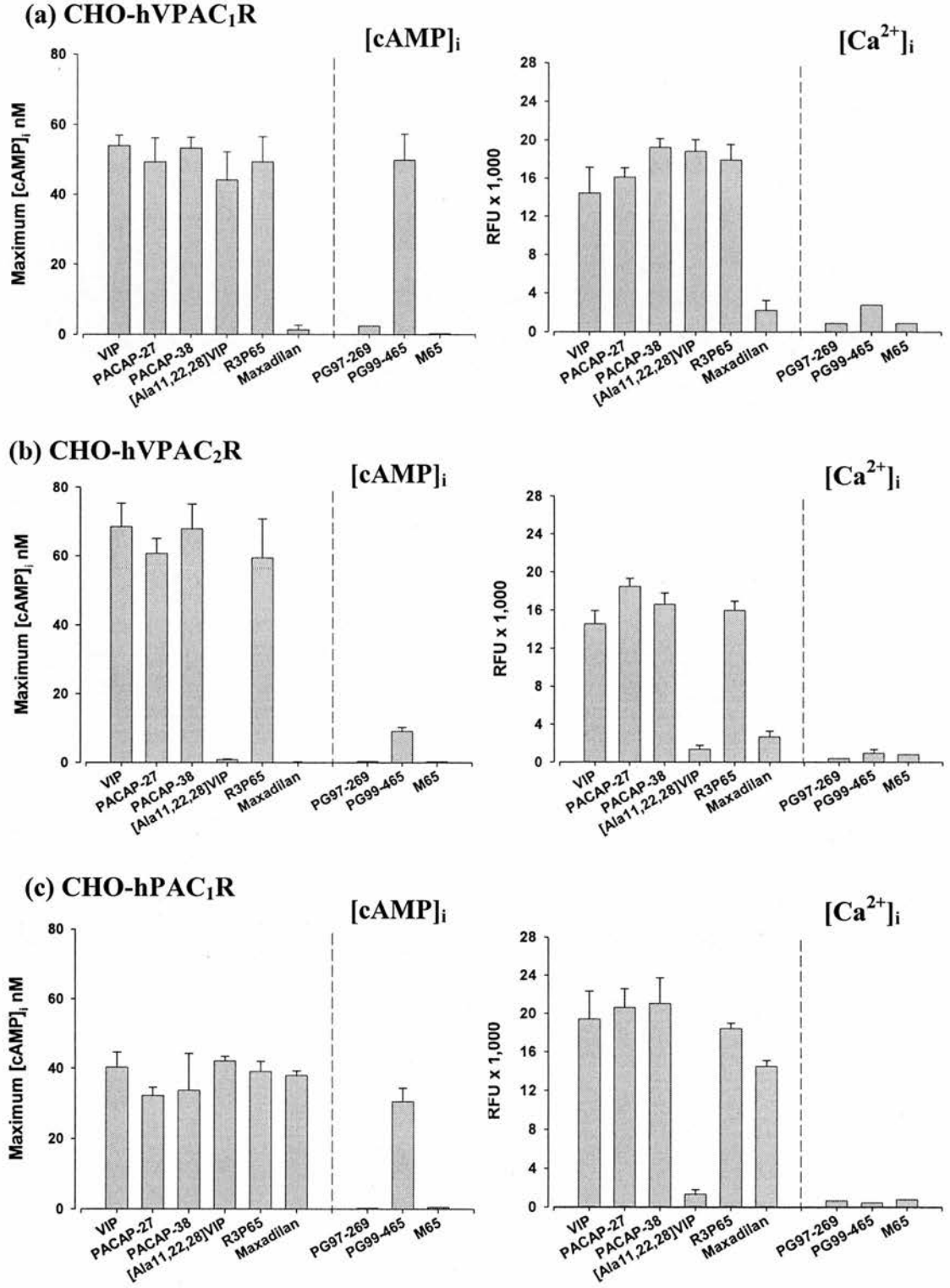

Figure 1.2.17 Maximum peptide induced $[cAMP]_i$ and $[Ca^{2+}]_i$ responses from CHO-hVPAC/PACR cells. Agonist responses shown are the mean maximum responses (± SEM) taken from the top of each concentration response curve which contributes to the EC_{50} values shown in Table 1.2.2. $[cAMP]_i$ and $[Ca^{2+}]_i$ stimulations in response to antagonists were determined with 3 μM of each peptide.

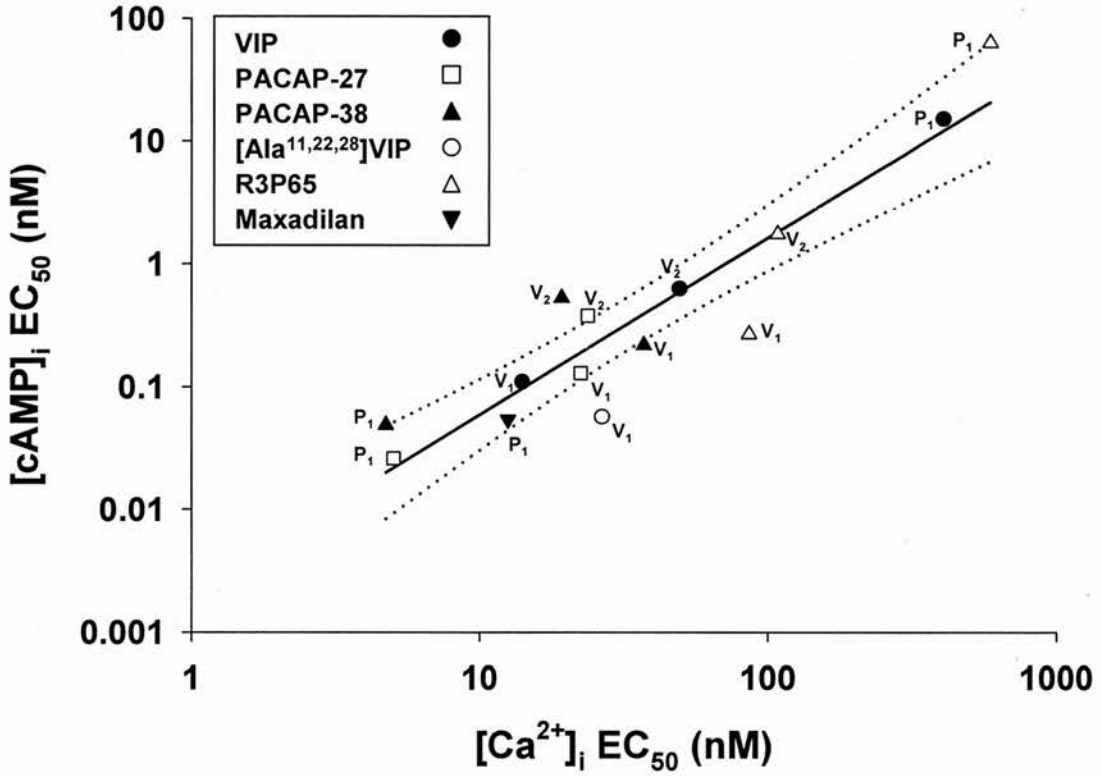

Figure 1.2.18 Correlation of agonist EC_{50} values for stimulation of $[cAMP]_i$ and $[Ca^{2+}]_i$ responses in CHO cells expressing $hVPAC_1$, $hVPAC_2$ and $hPAC_1$ receptors. Mean EC_{50} values for the agonists VIP, PACAP-27, PACAP-38, [Ala[11,22,28]]VIP, R3P65 and maxadilan were taken from Table 1.2.2, generating a correlation coefficient (r^2) of 0.85 using a linear regression analysis (95 % confidence levels are represented by the dashed lines). The receptor subtypes are indicated as follows: $VPAC_1 - V_1$; $VPAC_2 - V_2$; $PAC_1 - P_1$.

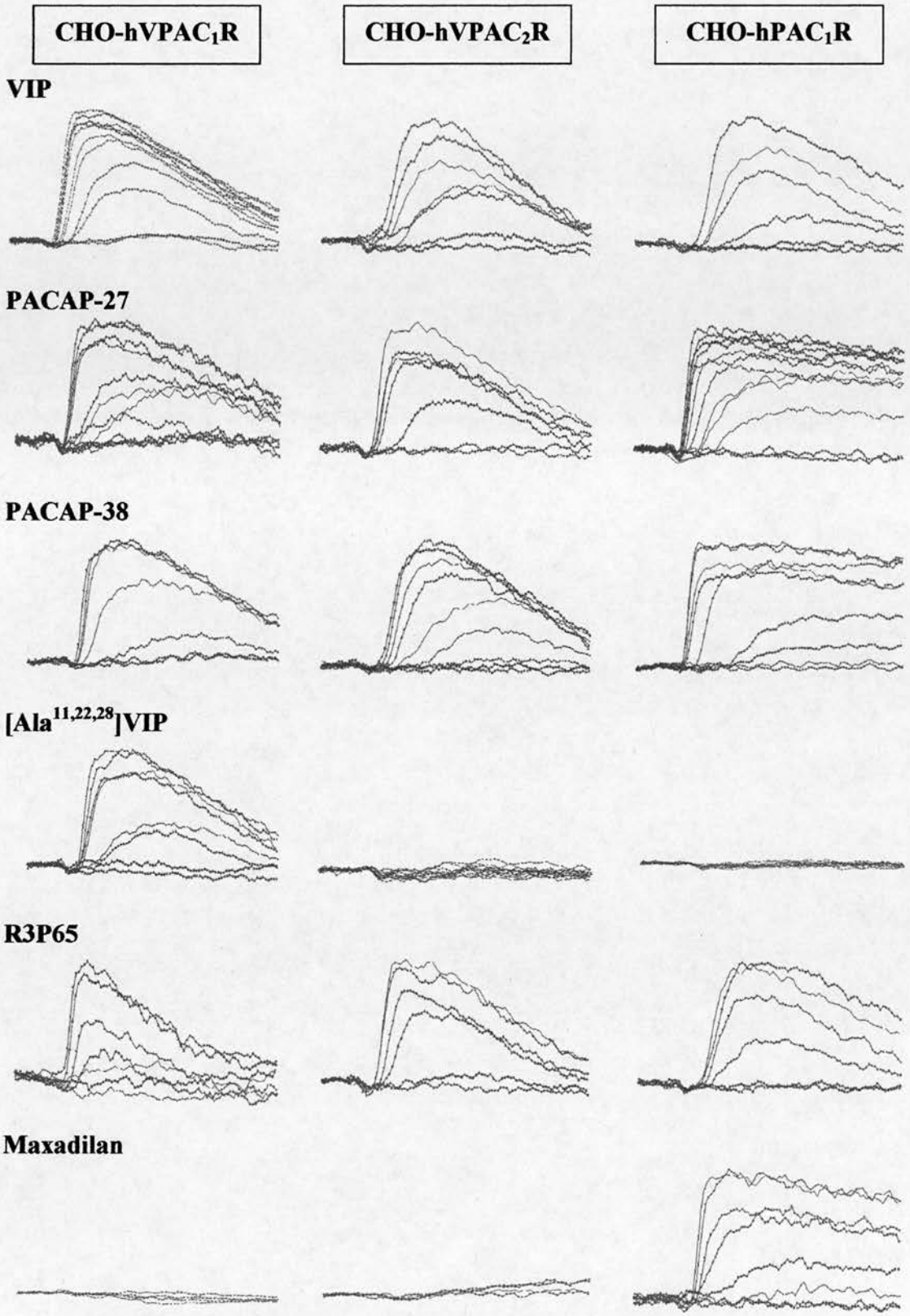

Figure 1.2.19 FlexStation® calcium assay traces from agonist stimulation of CHO-hVPAC/PACR cells. Representative traces shown are from agonist stimulation of the three stable cell lines (1 x 10^5 cells per well; 2 min recording; [agonist] range: 0.01 nM – 3 μM).

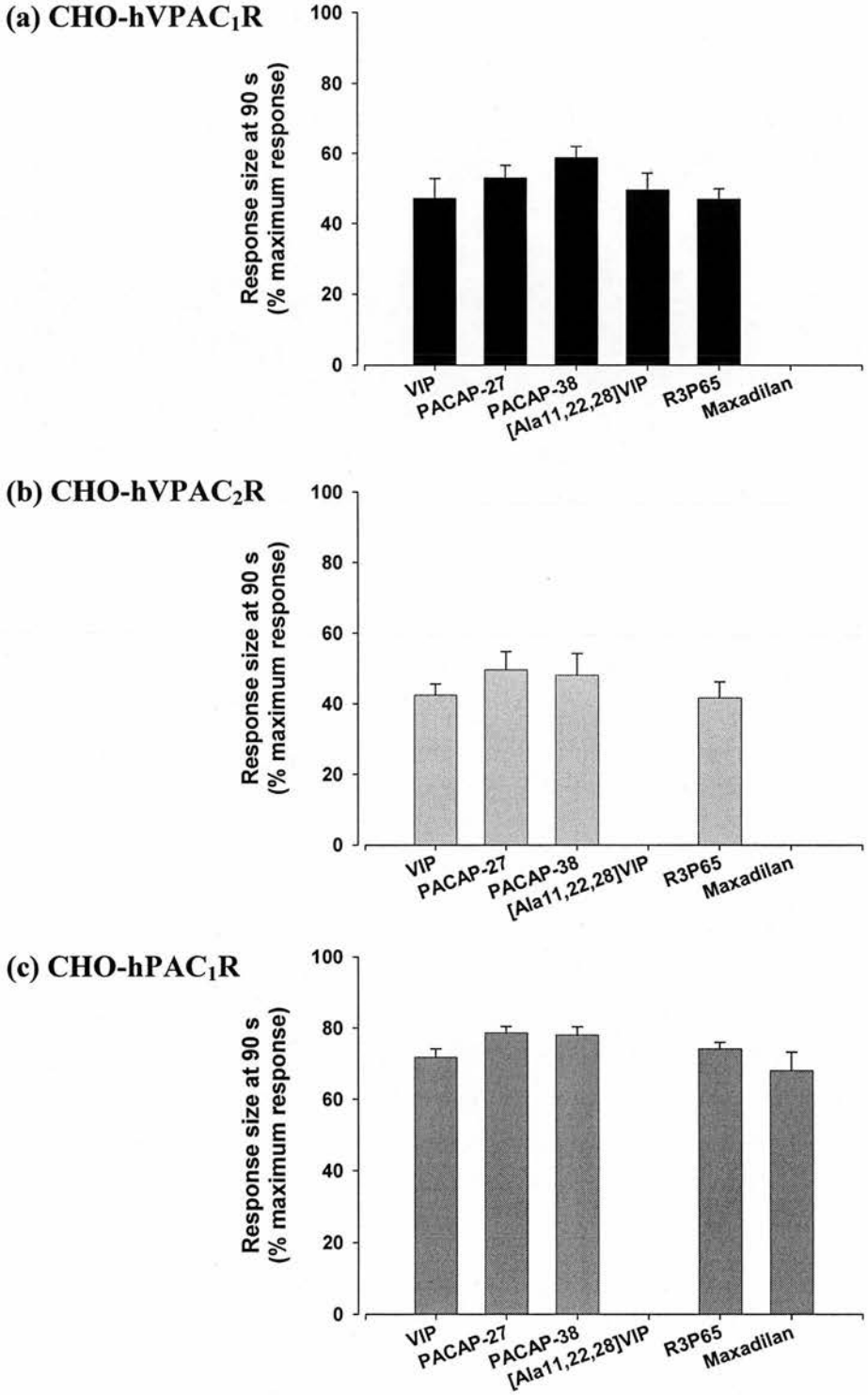

Figure 1.2.20 Magnitude of agonist evoked calcium responses from CHO-hVPAC/PACR cells at 90 s. From each concentration response curve used to generate the data in Table 1.2.2, response sizes at 90 s were measured from fluorescence traces produced from stimulation of CHO-hVPAC$_1$R (**a**), -hVPAC$_2$R (**b**) and -hPAC$_1$R (**c**) cells. The traces selected for analysis were generated from stimulation of the cell lines with agonist concentrations that produced maximal responses (see Figures 1.2.14 - 1.2.16).

(a)

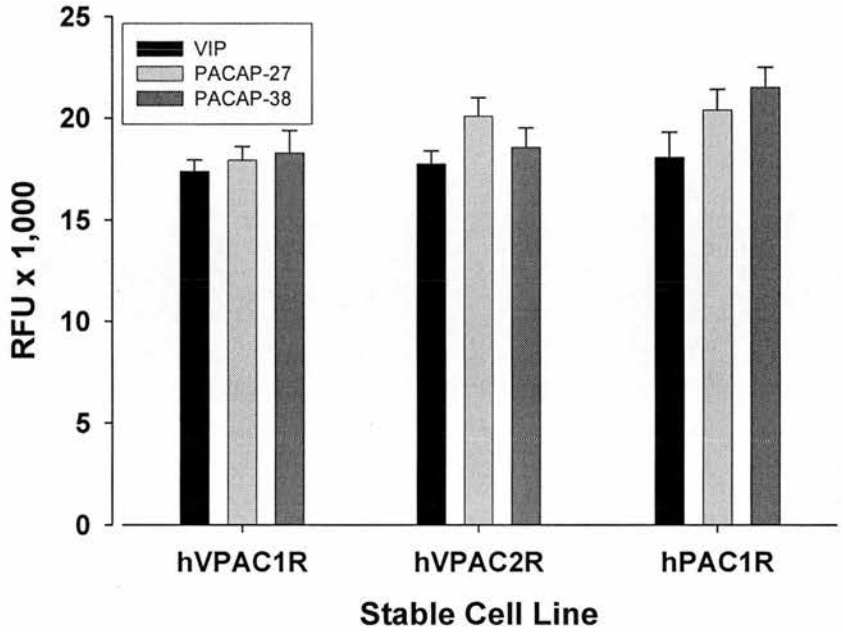

(b)

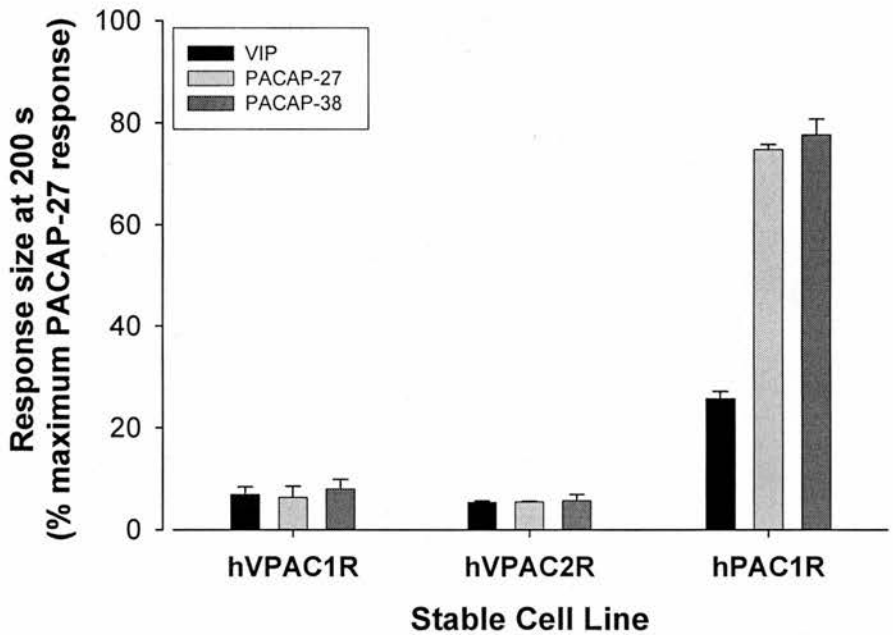

Figure 1.2.21 Magnitude of agonist evoked calcium responses from hVPAC/PACR expressing cell lines at 200 s. The three cell lines were stimulated with VIP, PACAP-27 and PACAP-38 and the maximum responses (**a**) and the responses at 200 s (**b**) were measured from the fluorescence traces. Peptides were tested at 1 μM for the hVPACR cell lines and at 3 μM (VIP) and 0.1 μM (PACAP) for the $hPAC_1R$ cell line.

(a)

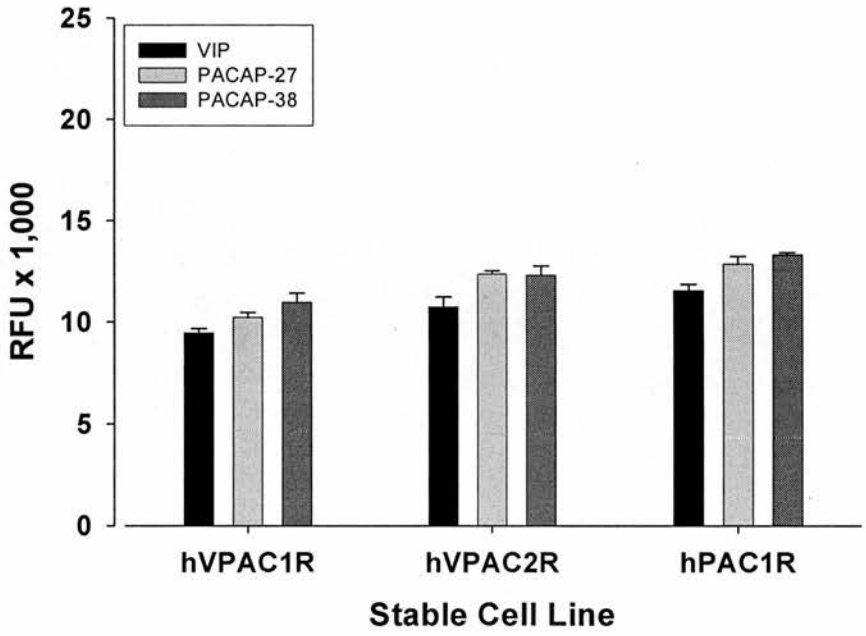

(b)

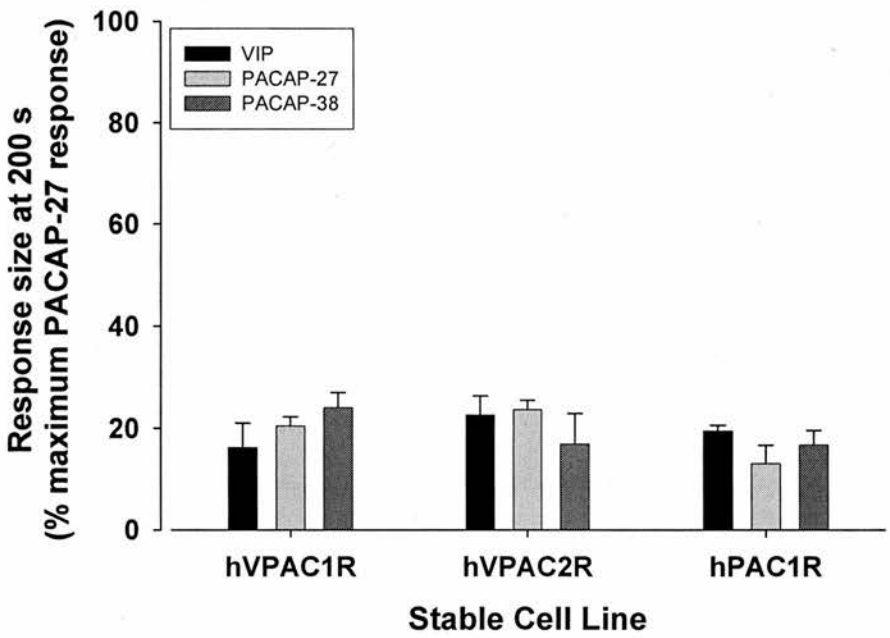

Figure 1.2.22 Magnitude of agonist induced $[Ca^{2+}]_i$ responses from hVPAC/PACR expressing cell lines, using calcium free assay conditions. hVPAC/PACR cells were stimulated with saturating concentrations of agonist and the maximum responses (**a**) and the responses at 200 s (**b**) were measured. Peptides were tested at 1 μM for the hVPACR cell lines and at 3 μM (VIP) and 0.1 μM (PACAP) for the $hPAC_1R$ cell line.

of a similar magnitude, being approximately 40 – 50 % of the peak fluorescence response (Figure 1.2.20). In contrast, at the $hPAC_1R$ fluorescence measurements at 90 s were as large as 70 – 80 % of the peak response. To examine these findings in greater depth, agonist induced responses for all three cell lines were examined at 200 s. With compound stocks limited, only VIP, PACAP-27 and PACAP-38 induced responses were examined. All three agonists were used at a concentration of 1 μM for the hVPACR cell lines, with the concentration of VIP increased (3 μM) and the PACAP peptides decreased (0.1 μM) when examining $hPAC_1R$ responses. The peak fluorescence response produced with the agonists for all three cell lines were, as expected, of a similar magnitude (18,000 – 20,000 RFU; Figure 1.2.21a). After 200 s the response size from the hVPACR cell lines was negligible for all three agonists, being less than 10 % of the peak response. In contrast, the responses from the $hPAC_1R$ cell line remained elevated after 200 s, however the magnitude of this event was ligand dependent (Figure 1.2.21b). VIP induced responses from $hPAC_1R$ were ~ 30 % of the peak response at 200 s, whereas the PACAP-27 and PACAP-38 responses remained high at ~ 80 % of the peak response. To examine the possibility that the enhanced signal sizes observed for the $hPAC_1R$ (at 200 s) with the PACAP peptides were a result of extracellular calcium entry during the assay, a similar experiment was conducted using a 'calcium free' assay, with calcium free buffers used throughout. Once again, the maximal response for each cell line was comparable, although the magnitude was reduced by almost 50 % (9,000 – 13,000 RFU) when compared to previous studies using calcium containing buffers (Figure 1.2.22a). The responses produced by VIP, PACAP-27 and PACAP-38 for all three cell lines were of a similar magnitude at 200 s, being approximately 20 % of the peak 'calcium free' response. This finding suggests that the slower rate of decline of PACAP peptide induced responses at $hPAC_1R$ may be due to an additional component involving extracellular calcium influx.

1.2.3.4. hVPAC/PACR antagonist pharmacology

The pharmacological characteristics of the three putatively receptor selective antagonists PG97-269, PG99-465 and M65 were examined using the hVPAC/PAC stable cell lines. Representative concentration effect curves for each antagonist (in both assays) are shown in Figures 1.2.23 - 1.2.25, with the appropriate quantitative measures (IC_{50}/EC_{50}) summarised in Table 1.2.3.

When tested alone at concentrations up to 3 μM, neither PG97-269 or M65 had any significant effect on $[cAMP]_i$ or $[Ca^{2+}]_i$ in the three hVPAC/PACR stable cell lines (Figures 1.2.23 - 1.2.24, 1.2.17). However, the reportedly $VPAC_1R$ selective antagonist PG97-269 did produce a concentration dependent inhibition of the VIP induced $[cAMP]_i$ and $[Ca^{2+}]_i$ responses in cells expressing $hVPAC_1R$ (IC_{50} values: 80.0 ± 3.2 (3) nM and 9.9 ± 2.1 (7) nM respectively), although with slightly less potency in the former assay (Figure 1.2.23; Table 1.2.3). PG97-269 was selective, having no effect on agonist induced responses at either $hVPAC_2R$ or $hPAC_1R$ in both second messenger assays (Figure 1.2.29). M65 was as receptor selective as PG97-269, inhibiting PACAP-27 induced $[cAMP]_i$ and $[Ca^{2+}]_i$ responses at $hPAC_1R$ with a similar potency (IC_{50} values: 149 ± 13 (3) nM and 282 ± 55 (5) nM respectively), whilst having no effect on agonist activity at hVPAC receptors (Figures 1.2.24, 1.2.29; Table 1.2.3). Typical calcium assay traces showing the reduction of the agonist stimulated responses by PG97-269 (at the $hVPAC_1R$) and M65 (at the $hPAC_1R$) are shown in Figure 1.2.29. In contrast to PG97-269 and M65, the pharmacological activity of PG99-465, the supposedly $hVPAC_2R$ selective

Table 1.2.3 Comparison of IC_{50} (and EC_{50}) values for antagonist inhibition of agonist induced $[cAMP]_i$ and $[Ca^{2+}]_i$ responses in CHO-K1 cells stably expressing $hVPAC_1$, $hVPAC_2$ and $hPAC_1$ receptors

		PG97-269	PG99-465	M65
			IC_{50}/*EC_{50} ± SEM (nM)	
$hVPAC_1R$	$[cAMP]_i$	80.0 ± 3.2 (3)	*8.04 ± 1.9 (5)	NE
	$[Ca^{2+}]_i$	9.90 ± 2.1 (7)	--	NE
$hVPAC_2R$	$[cAMP]_i$	NE	22.9 ± 5.7 (4) *4.9 ± 0.4 (3) partial agonist (10 - 20 % max)	NE
	$[Ca^{2+}]_i$	NE	4.4 ± 0.8 (6)	NE
$hPAC_1R$	$[cAMP]_i$	NE	*71.3 ± 9.6 (6)	149 ± 13 (3)
	$[Ca^{2+}]_i$	NE	--	282 ± 55 (5)

IC_{50}/*EC_{50} values are shown as the mean ± SEM, with the number of independent experiments given in parenthesis. NE is no effect at 3 μM. In the calcium assay, PG99-465 had no clear or reproducible effect on the agonist induced responses from CHO-$hVPAC_1R$ or -$hPAC_1R$ cell lines.

antagonist, was considerably more complex.

At the hVPAC$_2$R, PG99-465 produced a concentration dependent inhibition of the VIP induced $[cAMP]_i$ response (IC_{50}: 22.9 ± 5.7 (4) nM), plateauing at 80 % inhibition (Figure 1.2.25a, Table 1.2.3). This is most likely explained by the observation that when tested alone, this putative VPAC$_2$R antagonist acted as a partial agonist at the hVPAC$_2$R in the $[cAMP]_i$ assay, inducing a response that was 10 - 20 % of the maximum, with an EC_{50} of 4.9 ± 0.4 (3) nM (Figure 1.2.17 and 1.2.25a; Table 1.2.3). However, PG99-465 did produce a complete inhibition of the agonist induced $[Ca^{2+}]_i$ response at the hVPAC$_2$R (see Figure 1.2.29 for illustrative fluorescence traces), having a marginally higher potency (IC_{50}: 4.4 ± 0.8 (6) nM; Figure 1.2.25b), when compared with its EC_{50} value in the $[cAMP]_i$ assay (Table 1.2.3). In the $[cAMP]_i$ assay, PG99-465 acted as a potent, full agonist at hVPAC$_1$R (EC_{50} = 8.04 ± 1.9 (5) nM) and hPAC$_1$R (EC_{50} = 71.3 ± 9.6 (6) nM), with nanomolar potency (Figure 1.2.26; Table 1.2.3*)*. Studies examining PG99-465 inhibition of agonist induced responses at hVPAC$_1$R and hPAC$_1$R in the $[cAMP]_i$ assay were therefore complicated, with the stimulatory effects of PG99-465 appearing to act synergistically with the EC_{50} concentration of agonist (illustrated for the hVPAC$_1$R in Figure 1.2.27). In the $[Ca^{2+}]_i$ assay, PG99-465 did not have any clear or consistent effects on agonist stimulated responses at hVPAC$_1$R and hPAC$_1$R, and when applied alone at concentrations of up to 3 μM, this peptide had no effect in any of the three hVPAC/PACR stable cell lines (Figure 1.2.17). The agonist activity of PG99-465 was specific to the CHO-hVPAC/PACR cells, as this peptide did not stimulate $[cAMP]_i$ or $[Ca^{2+}]_i$ responses in CHO-K1 host cells (Figure 1.2.28). These findings clearly emphasize the complex and variable actions of this peptide at hVPAC/PACR.

In summary, PG97-269 and M65 were found to be selective hVPAC$_1$R and hPAC$_1$R antagonists respectively in both second messenger assays. Whilst the reportedly selective hVPAC$_2$R antagonist PG99-465 did antagonise agonist induced responses at hVPAC$_2$R (both assays), this peptide also displayed agonist activity at all three hVPAC/PACR when applied alone in the $[cAMP]_i$ assay. However, these effects were not observed in the $[Ca^{2+}]_i$ assay.

1.2.4. VPAC/PACR pharmacology in cell lines endogenously expressing the receptors

Having systematically characterized the pharmacology of human VPAC/PACR when stably expressed in CHO-K1 cells, comparative studies were

(a)

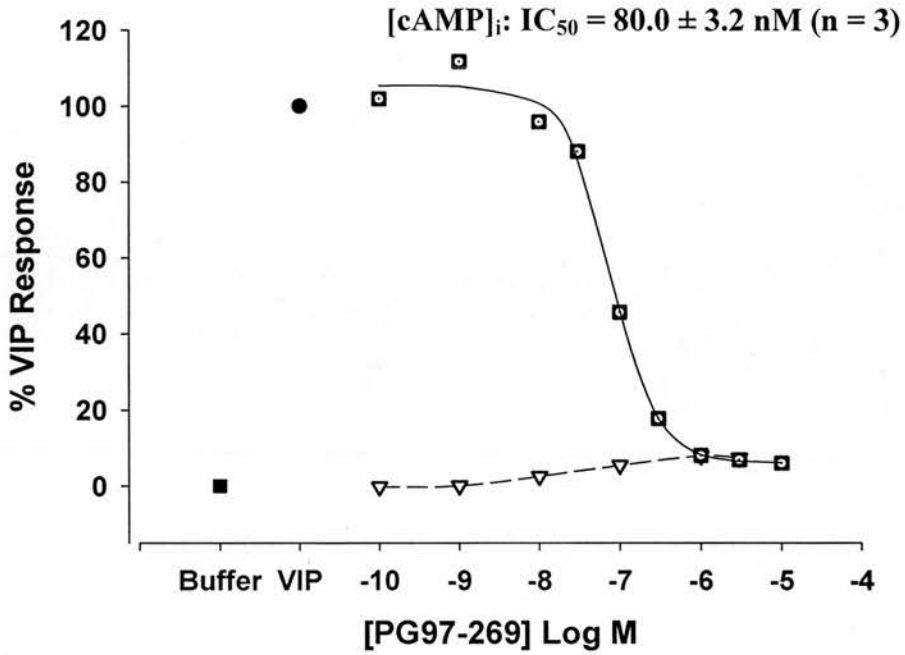

(b)

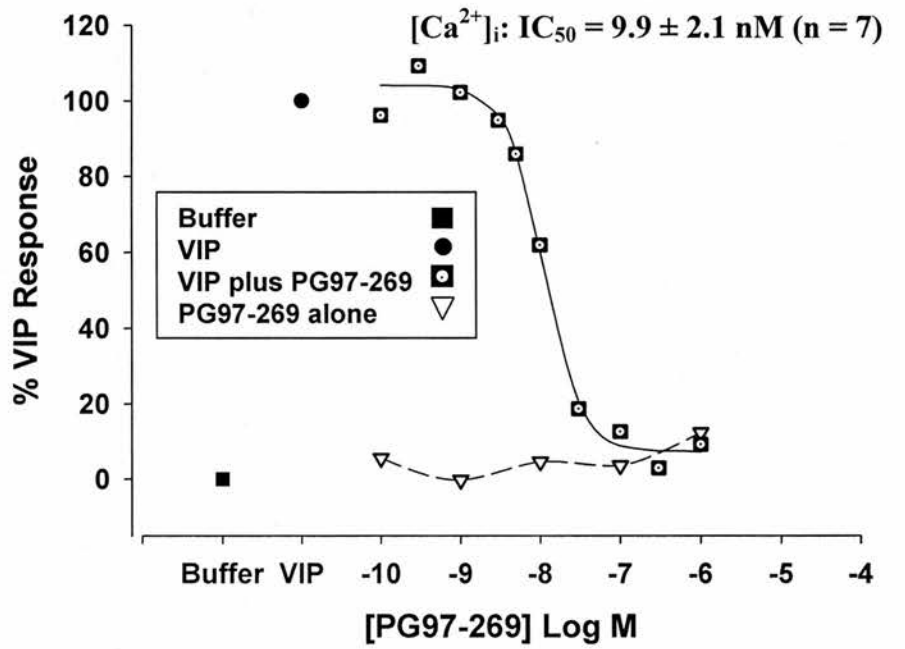

Figure 1.2.23 Inhibition of agonist evoked $[cAMP]_i$ and $[Ca^{2+}]_i$ responses by PG97-269 in CHO-hVPAC$_1$R cells. Representative inhibition curves are shown for both assays ($[cAMP]_i$: **a**; $[Ca^{2+}]_i$: **b**), in which cells (1 x 10^5 per well) were pre-incubated (10 min) with PG97-269, prior to the addition of VIP ($[cAMP]_i$: 0.3 nM; $[Ca^{2+}]_i$: 30 nM). Mean IC_{50} values ± SEM ($n \geq 3$) are shown (see Table 1.2.3).

(a)

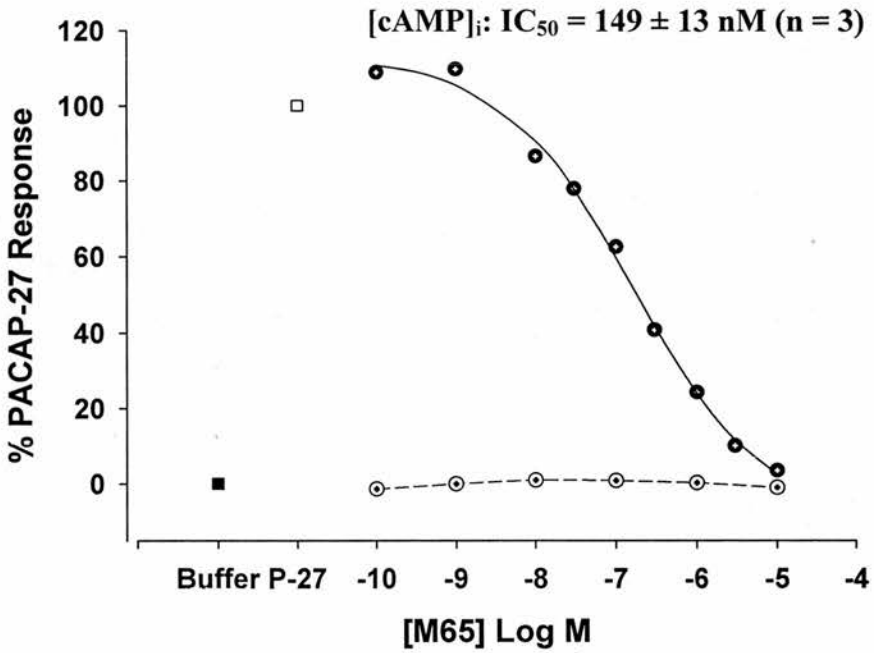

(b)

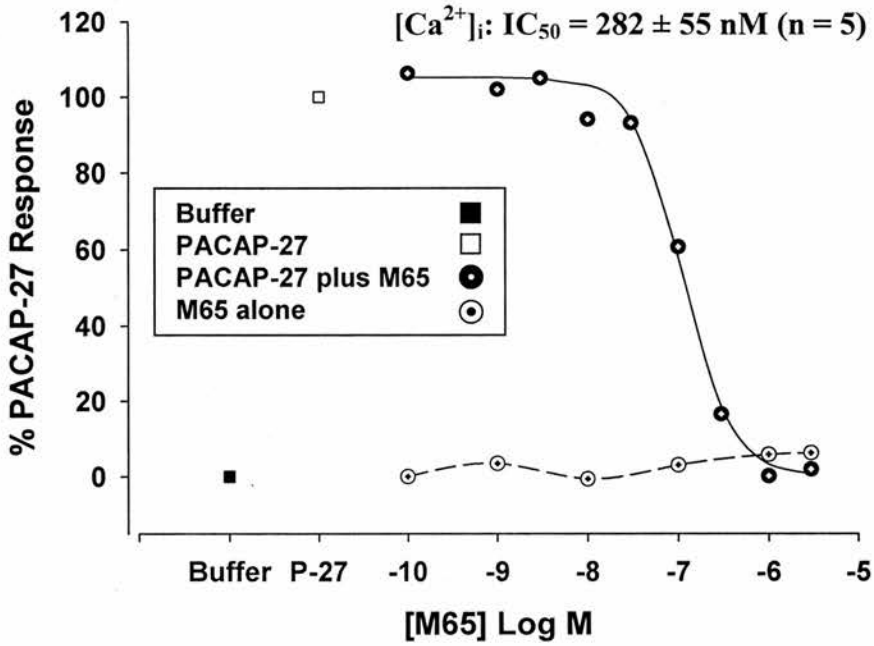

Figure 1.2.24 Inhibition of agonist evoked $[cAMP]_i$ and $[Ca^{2+}]_i$ responses by M65 in CHO-hPAC$_1$R cells. Representative inhibition curves are shown for both assays ($[cAMP]_i$: **a**; $[Ca^{2+}]_i$: **b**), in which cells (1 x 10^5 per well) were pre-incubated (10 min) with M65, prior to the addition of PACAP-27 ($[cAMP]_i$: 0.1 nM; $[Ca^{2+}]_i$: 30 nM). Mean IC_{50} values ± SEM ($n \geq 3$) are shown (see Table 1.2.3).

(a)

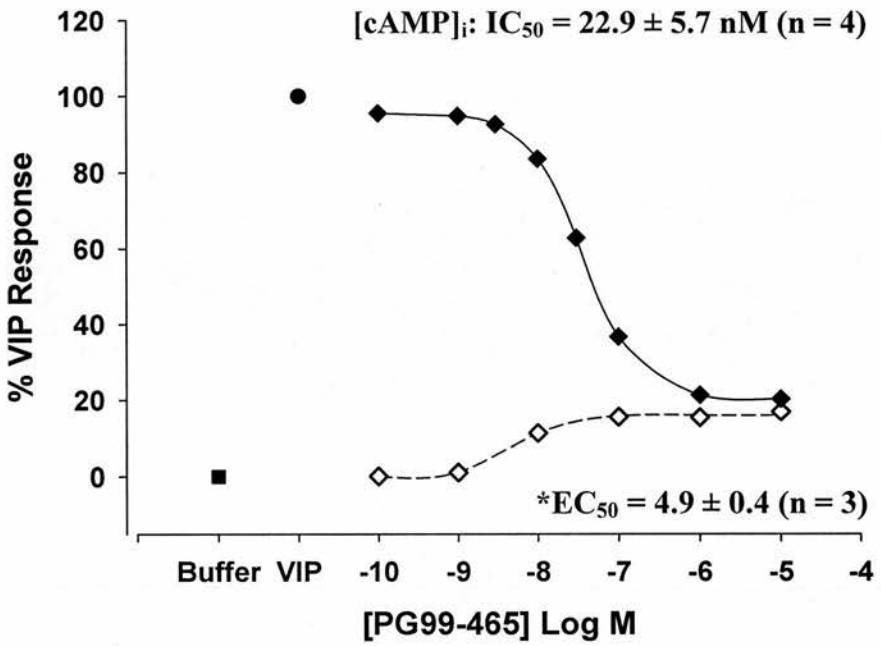

(b)

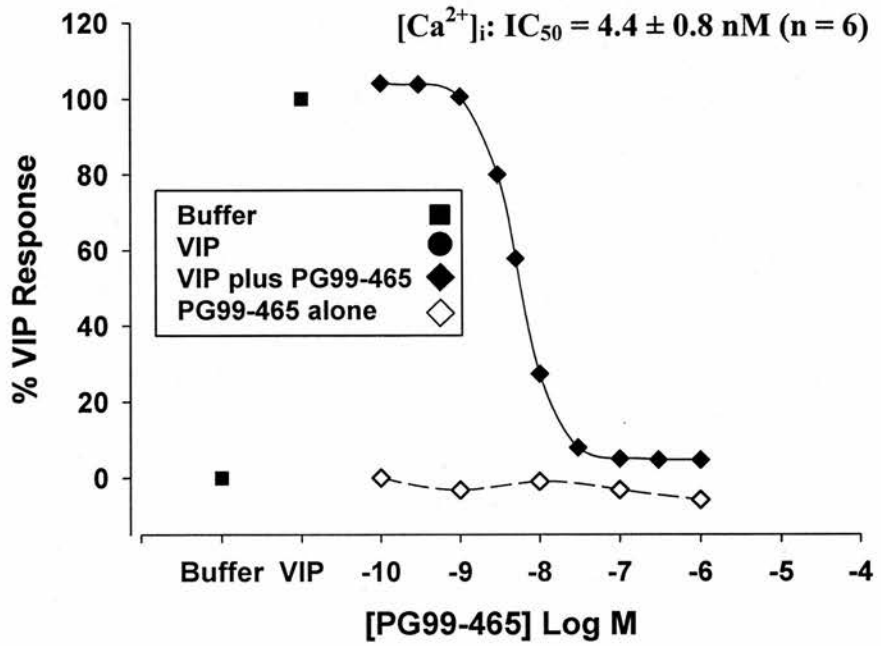

Figure 1.2.25 Inhibition of agonist evoked $[cAMP]_i$ and $[Ca^{2+}]_i$ responses by PG99-465 in CHO-hVPAC$_2$R cells. Representative inhibition curves are shown for both assays ($[cAMP]_i$: **a**; $[Ca^{2+}]_i$: **b**), in which cells (1×10^5 per well) were pre-incubated (10 min) with PG99-465, prior to the addition of VIP ($[cAMP]_i$: 3 nM; $[Ca^{2+}]_i$: 300 nM). Mean IC_{50}/*EC_{50} values ± SEM ($n \geq 3$) are shown (see Table 1.2.3).

(a)

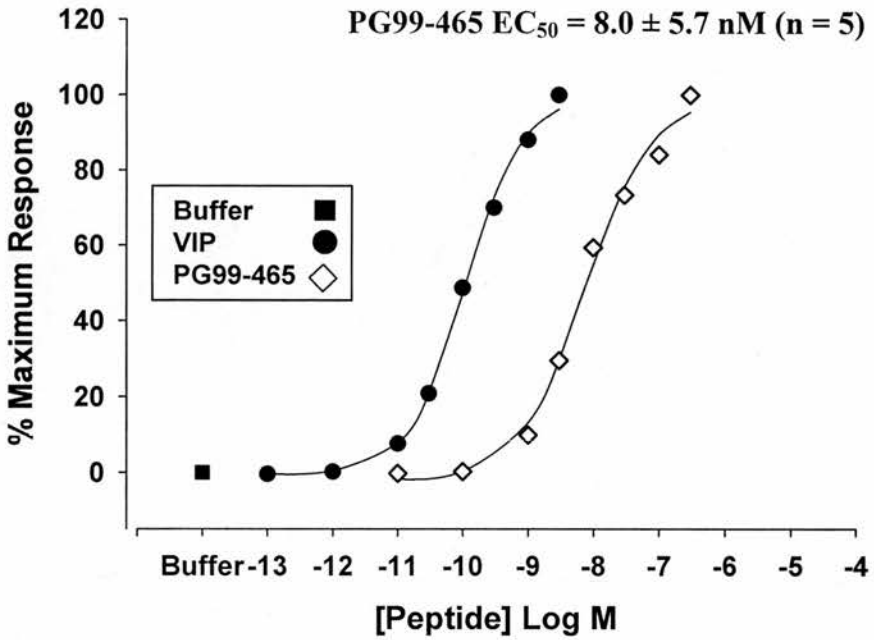

(b)

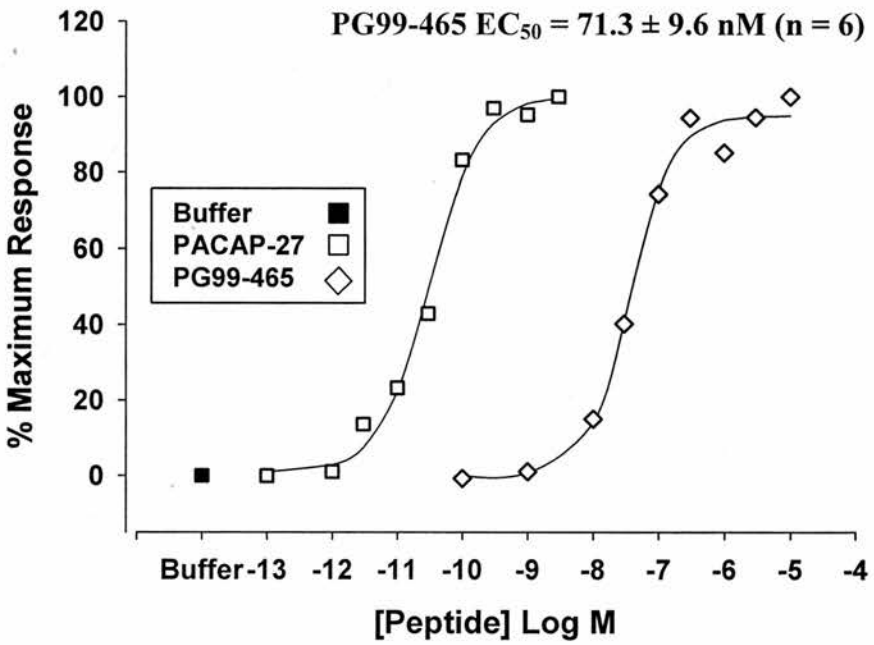

Figure 1.2.26 Concentration response curves showing VIP, PG99-465 or PACAP-27, induced stimulation of $[cAMP]_i$ in $hVPAC_1$ and $hPAC_1$ receptor expressing cell lines. The $hVPAC_1R$ (**a**) and $hPAC_1R$ (**b**) cell lines (1 x 10^5 cells/well) were exposed to the peptides for 15 min before cells were lysed and $[cAMP]_i$ levels determined. Mean EC_{50} values ± SEM ($n \geq 3$) are shown for PG99-465 (see Table 1.2.3).

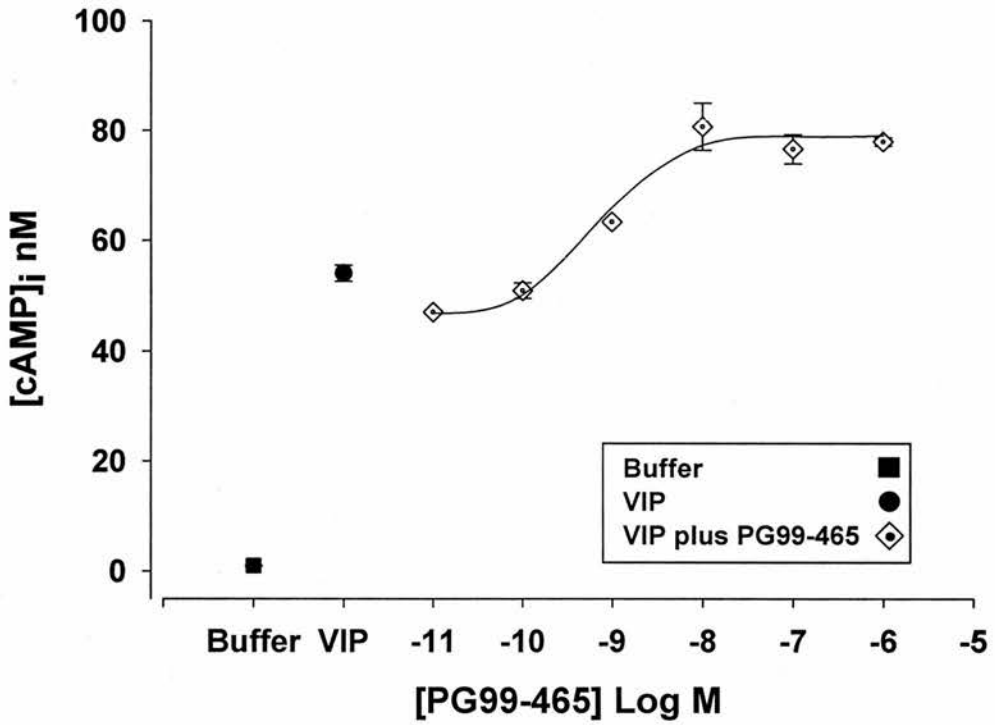

Figure 1.2.27 Synergism of VIP and PG99-465 stimulated $[cAMP]_i$ responses from CHO-hVPAC$_1$R cells. CHO-hVPAC$_1$R cells (1 x 10^5 per well) were pre-incubated (10 min) with increasing concentrations of PG99-465, prior to the addition of VIP (0.3 nM; ~ EC_{50} concentration). The graph shown is representative of four independent experiments in which this effect was observed.

(a)

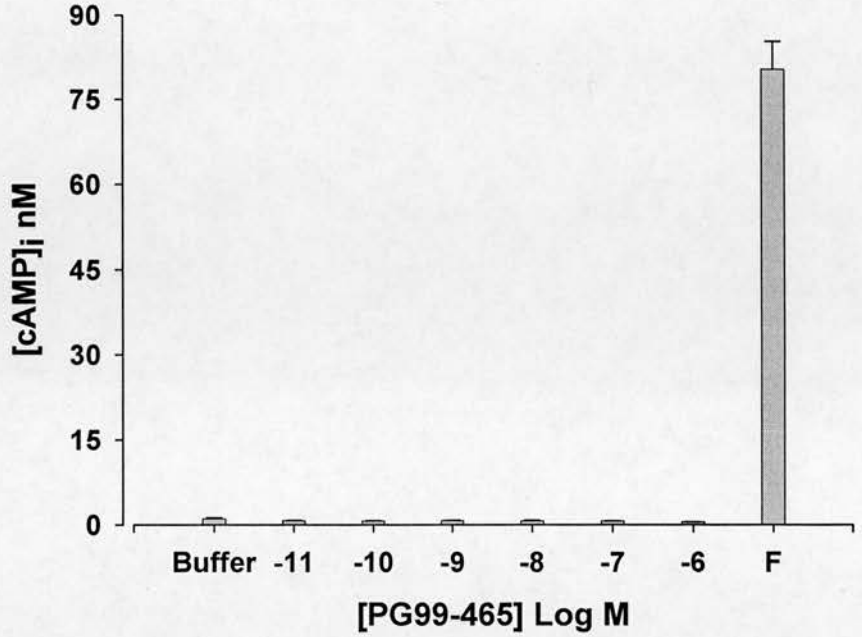

(a)

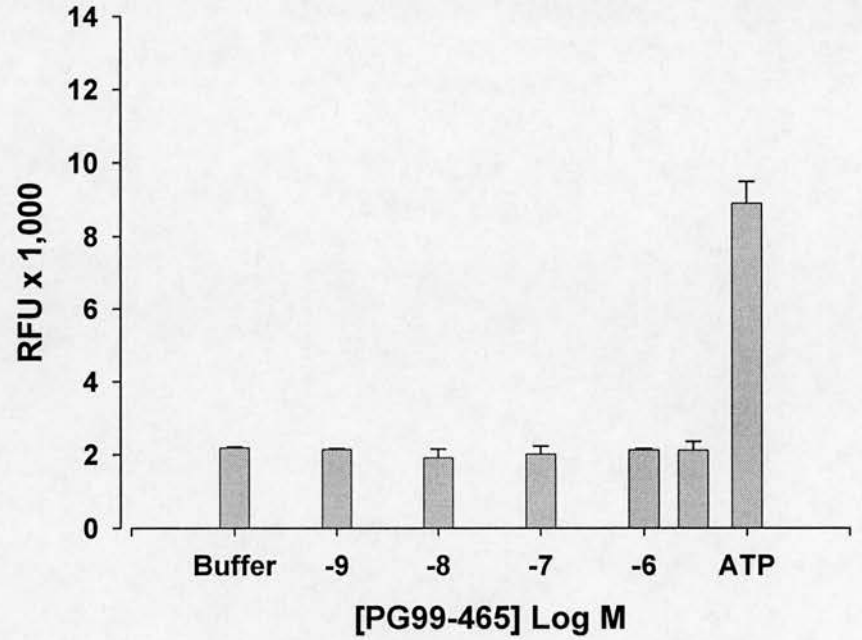

Figure 1.2.28 PG99-465 has no stimulatory effect on $[cAMP]_i$ and $[Ca^{2+}]_i$ levels in CHO-K1 host cells. In both the $[cAMP]_i$ (**a**) and the $[Ca^{2+}]_i$ (**b**) assays, PG99-465 (up to micromolar concentrations) failed to stimulate responses from CHO-K1 host cells (1×10^5 per well; n = 1). The positive controls forskolin (F; 10 μM) and ATP (10 μM) are shown for the $[cAMP]_i$ and $[Ca^{2+}]_i$ assays respectively.

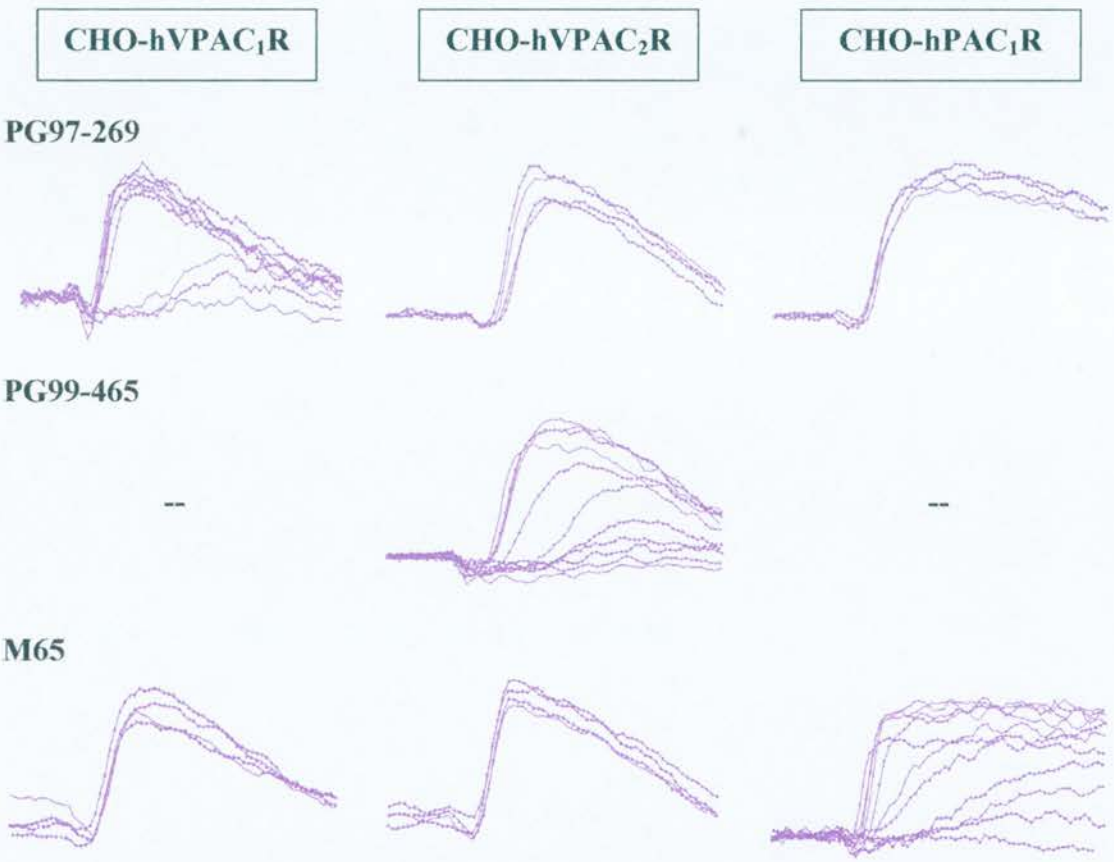

Figure 1.2.29 Traces illustrating the effects of VPAC/PACR antagonists on agonist induced calcium responses from CHO-hVPAC/PACR cells lines. Representative traces are shown for the antagonism of VIP ($hVPAC_1R$; 30 nM, $hVPAC_2R$: 100 nM) and PACAP-27 ($hPAC_1R$: 30 nM) induced responses from the hVPAC/PACR stable cell lines. Antagonists (0.01 nM – 3 μM) were pre-incubated with the cells for 10 min, prior to agonist addition and fluorescence measurement (90 s recording) in the FlexStation®.

then performed using cell lines that endogenously express the receptors to ensure that the observed findings were not a consequence of altered expression levels or G-protein complement as discussed in the introduction to this chapter (p 77). SHSY-5Y cells which natively express PAC_1R were the primary focus of these studies, although the pharmacological characteristics of hVPAC receptors expressed in HT-29 ($hVPAC_1R$) and SUP-T1 ($hVPAC_2R$) cells were also partially characterised.

1.2.4.1. hVPAC/PACR agonist pharmacology in SHSY-5Y cells

For SHSY-5Y cells, the pharmacology of VPAC/PAC receptors was examined using the same six agonists and three antagonists used with the hVPAC/PACR stable cell lines. All of the agonists induced a concentration dependent increase in $[cAMP]_i$, except $[Ala^{11,22,28}]VIP$ although this was probably due to its low micromolar potency (Figure 1.2.30a). PACAP-27 (EC_{50} = 0.13 ± 0.02 (3) nM), PACAP-38 (EC_{50} = 0.56 ± 0.11 (4) nM) and maxadilan (EC_{50} = 0.37 ± 0.05 (3) nM) were highly potent, sub-nanomolar agonists with similar EC_{50} values in the $[cAMP]_i$ assay (Table 1.2.4). The remaining full agonists, VIP (EC_{50} = 26.2 ± 6.6 (5) nM) and R3P65 (EC_{50} = 13.4 ± 0.98 (3) nM), were approximately 60 fold less potent, with $[Ala^{11,22,28}]VIP$ being more than 5,000 fold weaker (Figure 1.2.30a; Table 1.2.4). Therefore, the agonist ROP determined for SHSY-5Y cells in the $[cAMP]_i$ assay was consistent with the CHO-$hPAC_1R$ cells (PACAP-27 = PACAP-38 = maxadilan > VIP = R3P65 > $[Ala^{11,22,28}]VIP$). In the $[Ca^{2+}]_i$ assay, an identical

Table 1.2.4 EC_{50} values for peptide induced $[cAMP]_i$ and $[Ca^{2+}]_i$ stimulation in SHSY-5Y cells

	VIP	PACAP-27	PACAP-38	$[Ala^{11,22,28}]VIP$	R3P65	Maxadilan
			EC_{50} ± SEM (nM)			
$[cAMP]_i$	26.2 ± 6.6 (5)	0.13 ± 0.02 (3)	0.56 ± 0.11 (4)	Agonist from 1 µM	13.4 ± 0.98 (3)	0.37 ± 0.05 (3)
$[Ca^{2+}]_i$	544 ± 57 (7)	12.7 ± 1.6 (14)	9.57 ± 1.3 (9)	NE	1.49 ± 0.28 µM (7)	16.2 ± 2.55 (10)

EC_{50} values are shown as the mean ± SEM, with the number of independent experiments given in parenthesis. NE is no effect at 3 µM.

rank order of potency was observed for the agonists, albeit with a decrease in potency of about 100 fold (Figure 1.2.30b; Table 1.2.4). The increasing fluorescence responses observed with each agonist are illustrated in Figure 1.2.31. Interestingly, both PACAP-27 and PACAP-38 appeared to produce maximum responses in the calcium assay that were almost double the size of those produced by the other agonists (Figure 1.2.30b), therefore further investigation of the maximum agonist induced responses was performed with both assays.

When maximum $[cAMP]_i$ responses were calculated using the data for all the agonist concentration response curves, the levels produced from SHSY-5Y cells proved to be variable. Indeed, separate assays using the same ligand yielded maximum responses that were up to four fold different (for VIP: 2.2 to 8.8 nM). For this reason, a comparison of agonist induced maximal responses in these cells was directly compared, using saturating concentrations of all six agonists on one assay plate (values shown are an average from three independent experiments; Figure 1.2.32a). From this study, all of the agonists (except $[Ala^{11,22,28}]$VIP) induced similar maximal $[cAMP]_i$ responses, ranging from 12.6 to 15.1 nM (4 – 5x basal). Although these values were marginally higher than the average maximal responses from all combined SHSY-5Y experiments (5.1 nM and 10 fold lower that that observed for the stable cell lines), this study confirmed that the ligands used all induced a similar maximal response (Figure 1.2.32a). When tested at concentrations of up to 3 μM, the $hVPAC_1R$ agonist $[Ala^{11,22,28}]$VIP was only capable of stimulating a $[cAMP]_i$ response that was approximately two thirds smaller than that detected with the other five agonists, probably as a consequence of the low potency of this agonist. In similar experiments performed using the $[Ca^{2+}]_i$ assay, $[Ala^{11,22,28}]$VIP did not elicit any calcium response (as expected from the concentration response studies), whereas VIP, R3P65 and maxadilan evoked changes in fluorescence of ~ 3 fold above basal levels and with the overall fluorescent signal being ~ 3 fold less than that observed with the stable cell lines (Figure 1.2.32b). Interestingly, in the same experiments PACAP-27 and PACAP-38 induced a $[Ca^{2+}]_i$ response which was almost double that observed for VIP, R3P65 and maxadilan (Figure 1.2.32b), as had been indicated by the representative concentration response curves in Figure 1.2.30b. In a small number of experiments in which PACAP stimulated calcium responses were examined, there was an indication of agonist activity at two sites (as illustrated by the dashed line in Figure 1.2.33). Attempts were made to investigate this phenomenon, with twice the number of agonist concentrations used in the standard assays. However, the biphasic response was not always evident and as a consequence it was not possible to quantitatively describe the data in terms of a two-site model. In

(a)

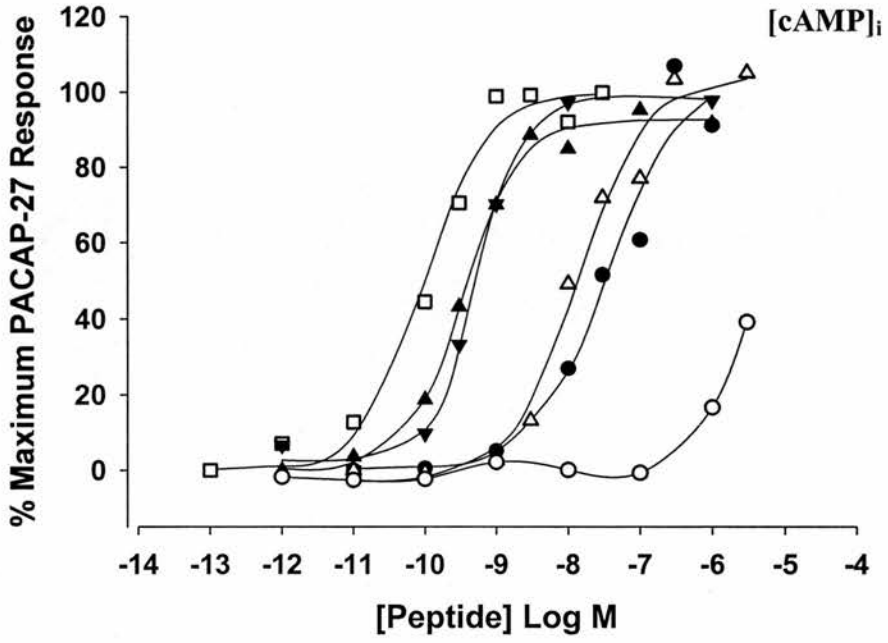

(b)

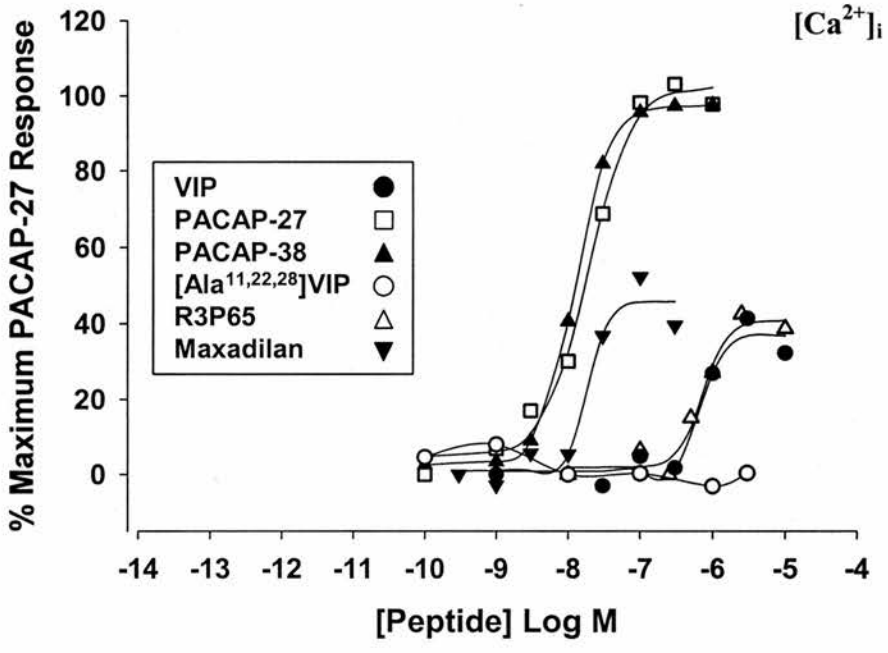

Figure 1.2.30 Characterisation of hVPAC/PACR in the SHSY-5Y cell line using the $[cAMP]_i$ and $[Ca^{2+}]_i$ assays. SHSY-5Y cells (1.25 x 10^5 per well) were stimulated with a range of VPAC/PACR agonists and $[cAMP]_i$ (**a**) and $[Ca^{2+}]_i$ (**b**) responses measured. The concentration response curves shown are representative, with mean EC_{50} values ± SEM ($n \geq 3$) shown in Table 1.2.4.

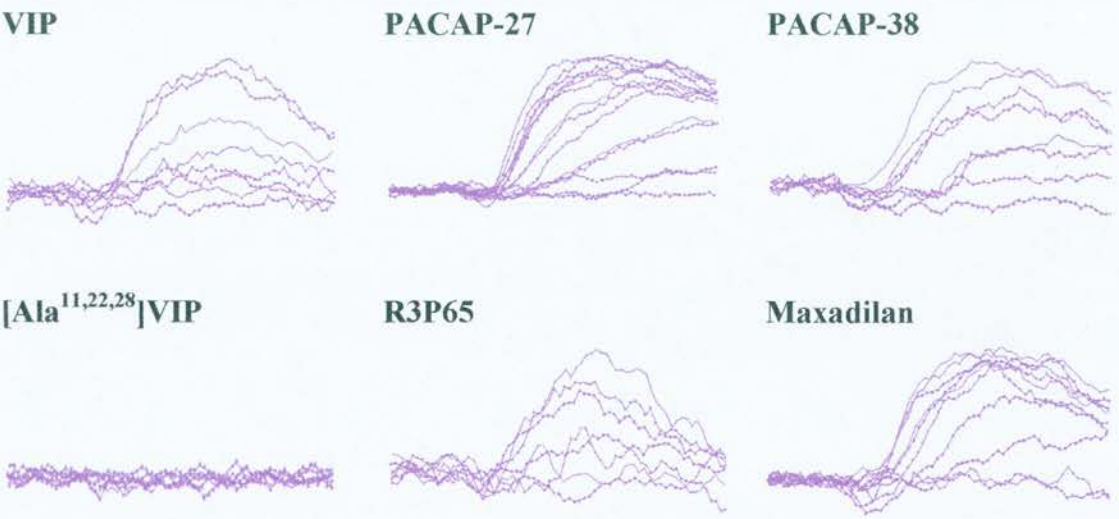

Figure 1.2.31 FlexStation® calcium assay traces produced from VPAC/PACR agonist stimulation of SHSY-5Y cells. Representative traces shown are for agonist stimulation of SHSY-5Y cells (1.25×10^5 cells per well; 90 s recording; [agonist] range: 0.1 nM – 3 μM).

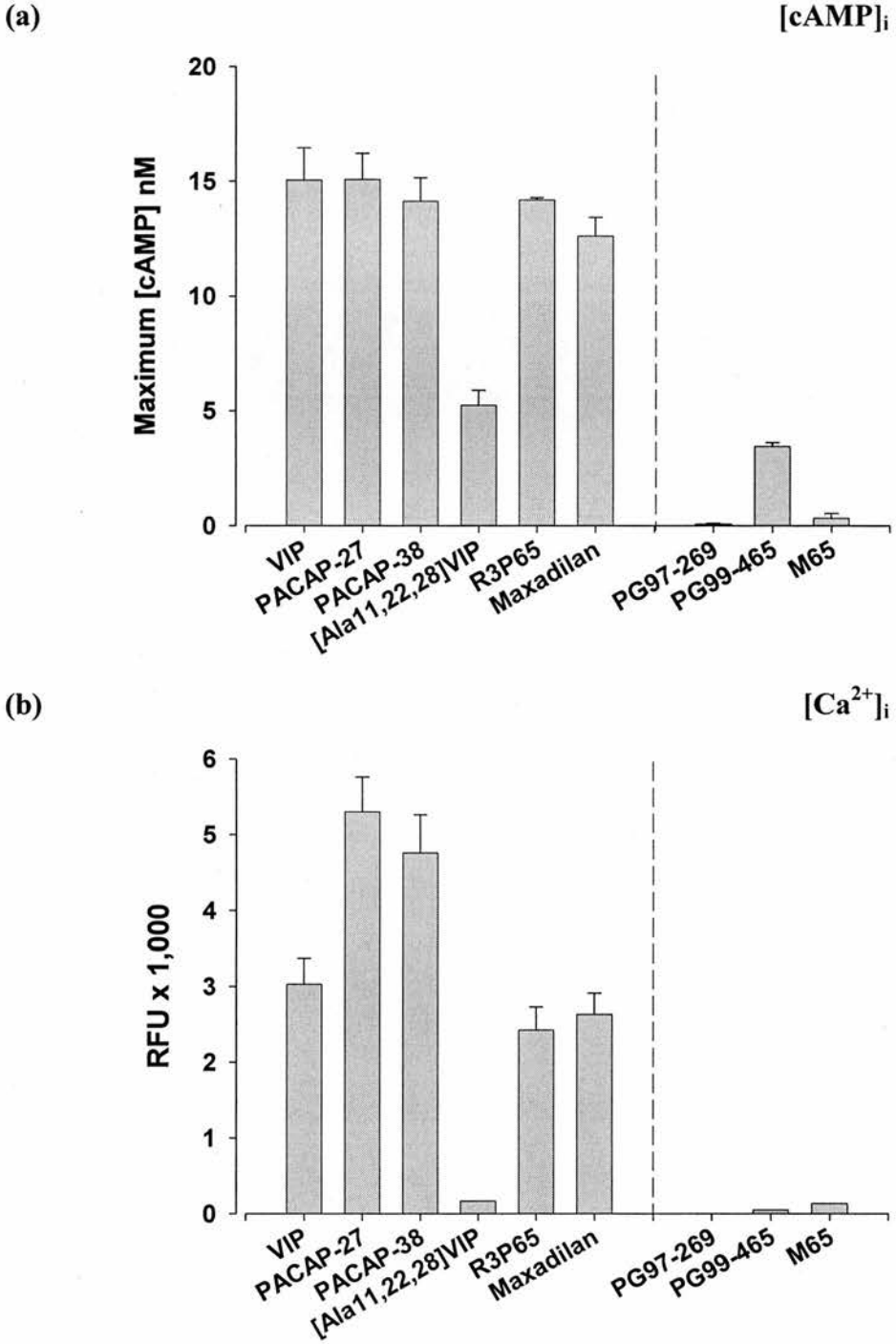

Figure 1.2.32 Maximum peptide induced $[cAMP]_i$ and $[Ca^{2+}]_i$ responses from SHSY-5Y cells. Maximum $[cAMP]_i$ responses (**a**) from SHSY-5Y cells were determined from three independent experiments, in which cells (1.25×10^5 per well) were stimulated with saturating concentrations of peptides (3 μM or 0.3 μM for maxadilan and the PACAP peptides). Mean $[Ca^{2+}]_i$ responses (**b**) were calculated from the upper plateau of the concentration response curves used to calculate the potencies in Table 1.2.4 ($n \geq 3$). In both assays, antagonists were tested at a concentration of 3 μM.

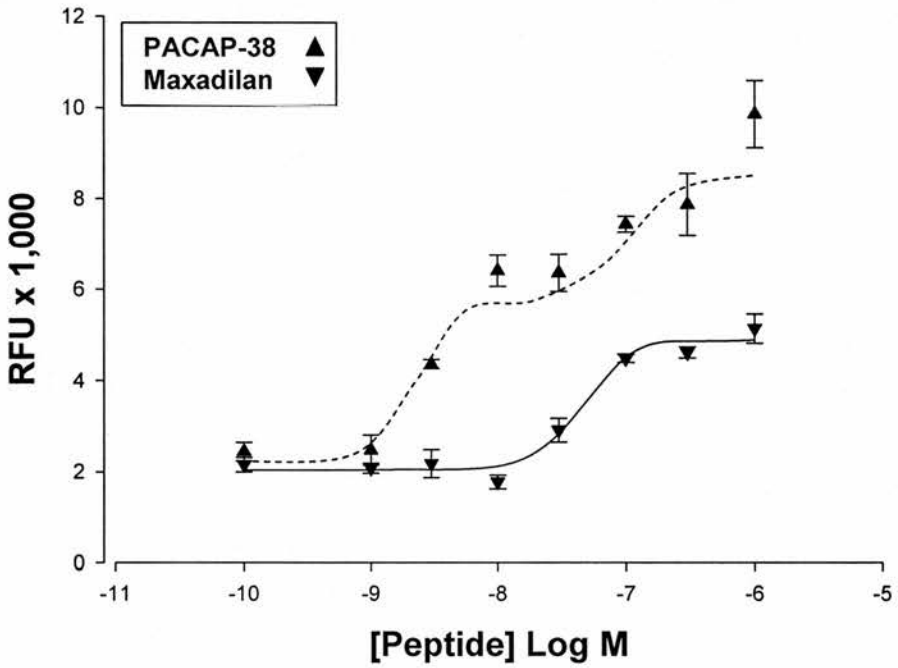

Figure 1.2.33 Biphasic PACAP-38 induced calcium responses in SHSY-5Y cells. On some occasions the PACAP peptides stimulated a biphasic calcium response from SHSY-5Y cells. The figure shows a representative example of this response (dashed line), compared against a typical maxadilan concentration response curve for this cell line. This biphasic nature of the PACAP response was not always evident and consequently could not be quantitatively described.

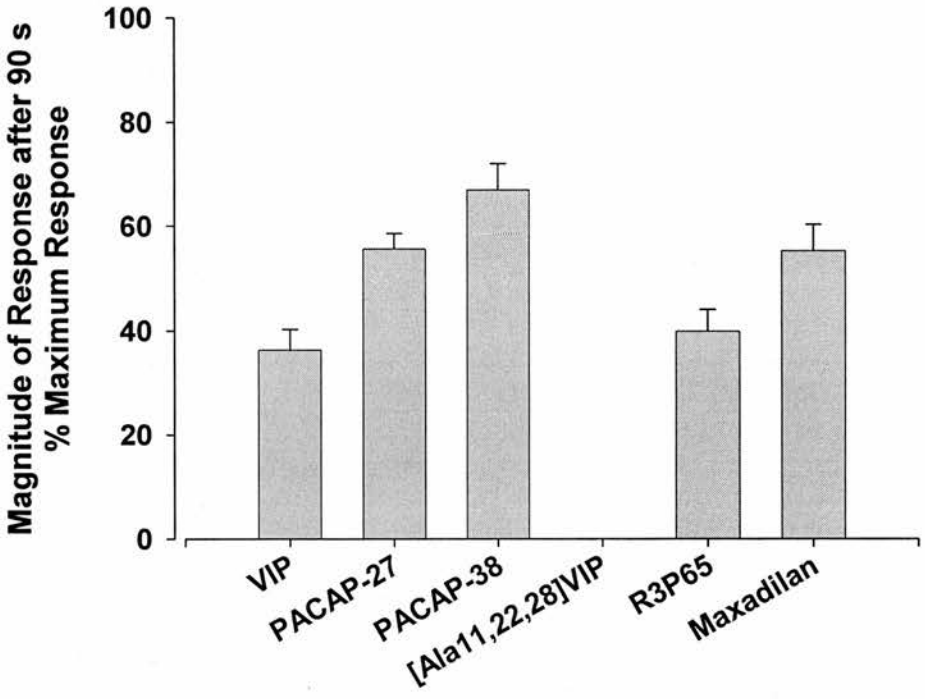

Figure 1.2.34 Magnitude of agonist evoked calcium responses from SHSY-5Y cells at 90 s. From each concentration response curve used to generate the data in Table 1.2.4., response sizes at 90 s were measured from the fluorescence traces produced from stimulation of SHSY-5Y cells. The traces selected for analysis were generated from stimulation of the cells with agonist concentrations that produced maximal responses (see Figures 1.2.30b).

general, the agonist potencies in SHSY-5Y cells for both assays (Table 1.2.4) were very similar (3.3 fold lower) to that observed for the $hPAC_1R$ stable cell line (Table 1.2.2). In addition, and as observed with the $hPAC_1R$ stable cell, agonist potencies were consistently lower in the $[Ca^{2+}]_i$ assay (~ 60 fold), irrespective of the considerably lower levels of $hPAC_1R$ expression (Table 1.2.4).

As the agonist pharmacology indicated that SHSY-5Y cells expressed endogenous $hPAC_1R$ (predominantly), the traces produced following agonist stimulation in the $[Ca^{2+}]_i$ assay were examined in more detail, to investigate whether PACAP induced calcium responses had both an intracellular and extracellular component (as described earlier for the CHO-$hPAC_1R$ cell line, p 117). As before, fluorescence levels at 90 s were expressed as a percentage of the maximum response for each agonist (Figure 1.2.34). From this data, PACAP-27, PACAP-38 and maxadilan stimulated responses (at 90 s) were approximately 60 % of their peak values, whereas VIP and R3P65 induced responses had declined to approximately 40 %. Unfortunately the analysis was not extended to 200 s for SHSY-5Y cells as response sizes became too small and variable. However, the slower rate of decline of the PACAP responses at 90 s is consistent with the effects described (at 200 s) for the agonist traces produced using the $hPAC_1R$ stable cell line (Figure 1.2.21). Moreover, due to limited compound stocks, it was not possible to test maxadilan at 200 s, therefore it remains to be determined whether there is a reduced rate of decline with this peptide.

1.2.4.2. VPAC/PACR antagonist pharmacology in SHSY-5Y cells

The pharmacological properties of the reportedly selective PAC_1R antagonist M65, were examined in the $[cAMP]_i$ and $[Ca^{2+}]_i$ assays using the SHSY-5Y cell line. M65 fully inhibited PACAP-27 (~ EC_{50} concentration) induced responses from SHSY-5Y cells, in a concentration dependent manner, being equipotent in both assays with IC_{50} values of 37.5 ± 5.6 (4) nM ($[cAMP]_i$; Figure 1.2.35a) and 13.6 ± 2.1 (5) nM ($[Ca^{2+}]_i$; Figures 1.2.35b, 1.2.36; Table 1.2.5). As the PACAP induced calcium responses in SHSY-5Y cells were almost double the size of those stimulated by the other agonists (Figures 1.2.30 and 1.2.32), the ability of M65 to fully inhibit the maximum PACAP induced response (in contrast to the standard EC_{50} PACAP-27 induced response) was subsequently evaluated (Figure 1.2.37). M65 fully inhibited the PACAP-27 induced calcium responses from SHSY-5Y cells,

Table 1.2.5 **IC_{50} values for peptide induced $[cAMP]_i$ and $[Ca^{2+}]_i$ stimulation in SHSY-5Y cells**

	PG97-269	PG99-465	M65
		IC_{50} ± SEM (nM)	
$[cAMP]_i$	NE	Agonist from 1 µM Antagonist from 0.1 µM	37.5 ± 5.6 (4)
$[Ca^{2+}]_i$	NE	NE	13.6 ± 2.1 (5)

IC_{50} values are shown as the mean ± SEM, with the number of independent experiments given in parenthesis. NE is no effect at 3 µM.

when the agonist was used at either an EC_{50} (~ 30 nM) or saturating concentration (300 nM), with similar IC_{50} values of 6.7 and 8.4 nM (n = 1).

Although SHSY-5Y cells appear to predominantly express $hPAC_1R$, the hVPACR selective antagonists, PG97-269 and PG99-465, were also examined. PACAP-27 evoked responses in SHSY-5Y cells were completely insensitive to the $hVPAC_1R$ antagonist PG97-269 (up to 3 µM), in both assays (calcium assay traces are presented in Figure 1.2.36; Table 1.2.5). Similarly, PG99-465 had no effect alone or on agonist induced responses in the calcium assay (Figure 1.2.36; Table 1.2.5), however this peptide did exhibit some activity in the $[cAMP]_i$ assay. When applied alone, PG99-465 induced a small, concentration dependent increase in cAMP at concentrations greater than 100 nM (Figure 1.2.38; Table 1.2.5). At the maximum PG99-465 concentration tested (3 µM) the average $[cAMP]_i$ concentration was approximately 3 nM (n = 2; Figure 1.2.38a). A full PG99-465 concentration response curve could not be generated due to compound availability and solubility of the peptide. In preliminary inhibition studies using SHSY-5Y cells, PG99-465 application at concentrations associated with agonist activity in these cells, coincided with a reduction in the PACAP-27 (1 nM) induced response (n = 1; Figure 1.2.38b). This contrasts with the effects observed for $hVPAC_1R$ and $hPAC_1R$ stable cell lines ($[cAMP_i]$ assay), where PG99-465 stimulatory responses appeared to act synergistically with the agonist induced responses (Figure 1.2.27; p 124).

(a)

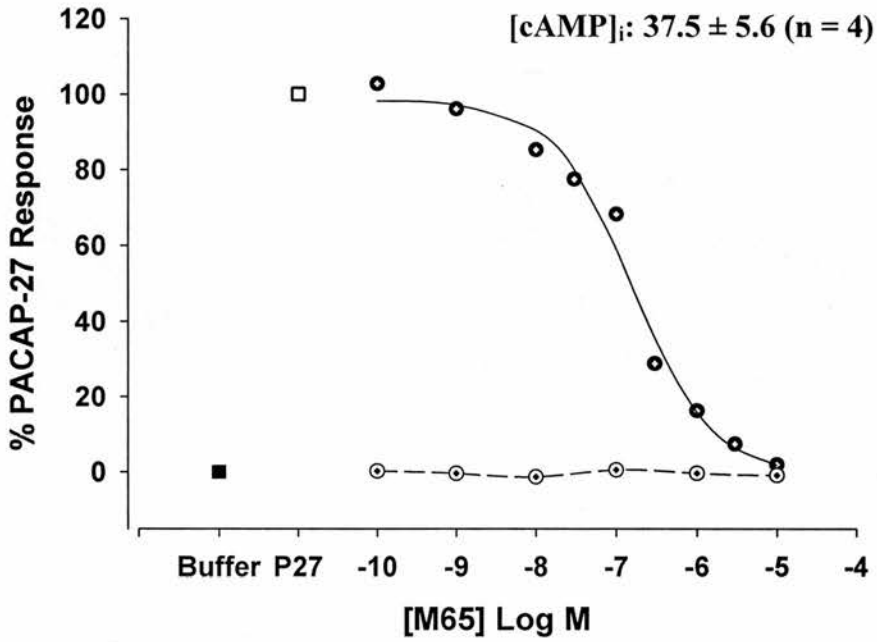

(b)

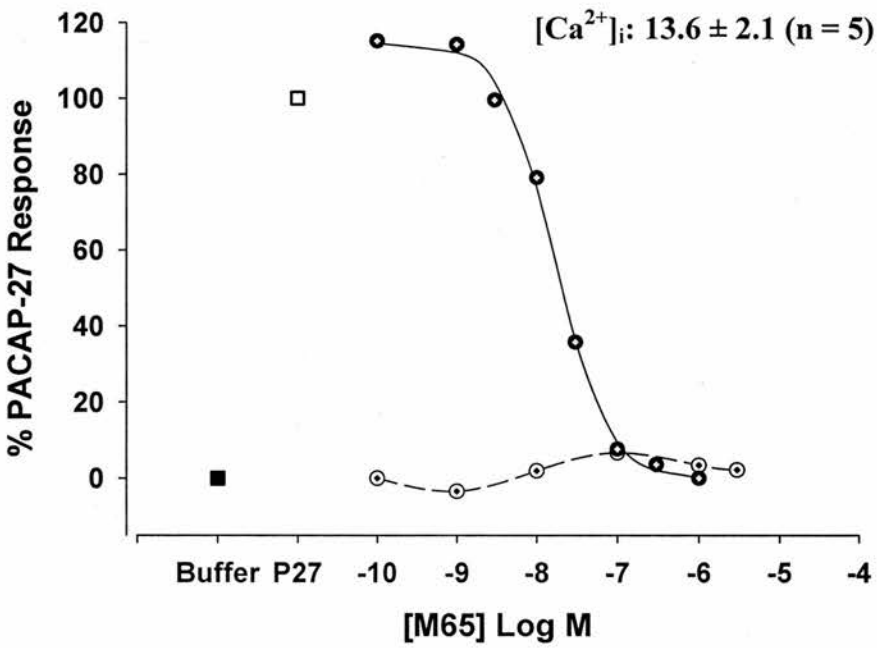

Figure 1.2.35 Inhibition of agonist evoked $[cAMP]_i$ and $[Ca^{2+}]_i$ responses by M65 in SHSY-5Y cells. Representative inhibition curves are shown for both assays ($[cAMP]_i$: **a**; $[Ca^{2+}]_i$: **b**), in which cells (1.25×10^5 per well) were pre-incubated (10 min) with M65, prior to the addition of PACAP-27 ($[cAMP]_i$: 1 nM; $[Ca^{2+}]_i$: 30 nM). Mean IC_{50} values ± SEM ($n \geq 3$) are shown (see Table 1.2.5).

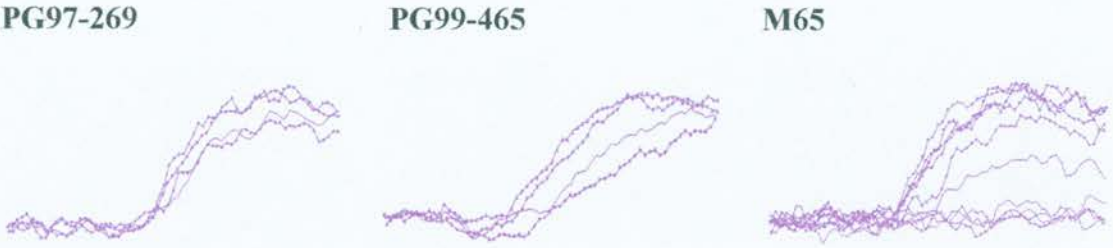

Figure 1.2.36 Traces illustrating the effects of VPAC/PACR antagonists on PACAP-27 stimulated calcium responses in SHSY-5Y cells. Representative traces shown are from SHSY-5Y cells (1.25 x 10^5 cells per well) that have been pre-incubated with antagonist (10 min), prior to PACAP-27 stimulation (90 s recording; [antagonist] range: 0.01 nM – 3 μM).

(a)

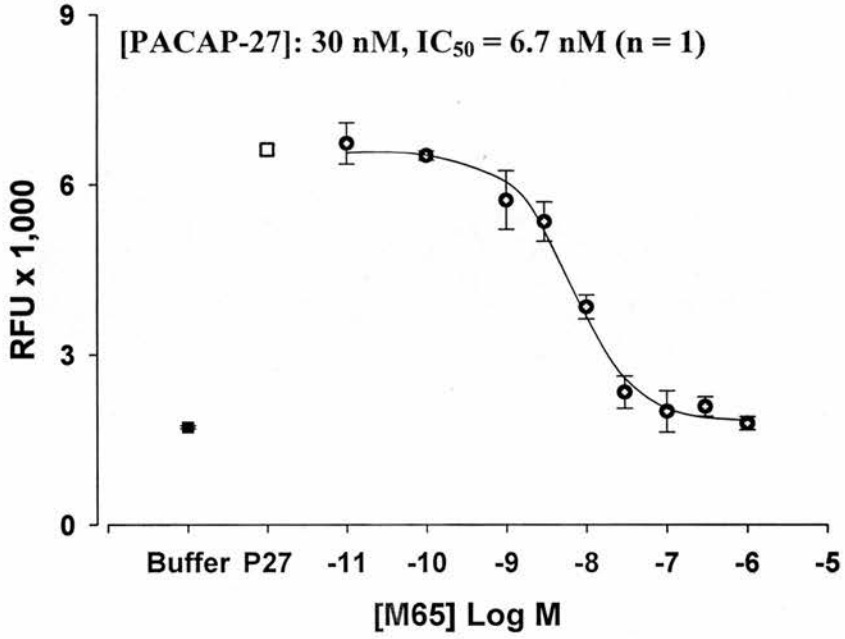

(b)

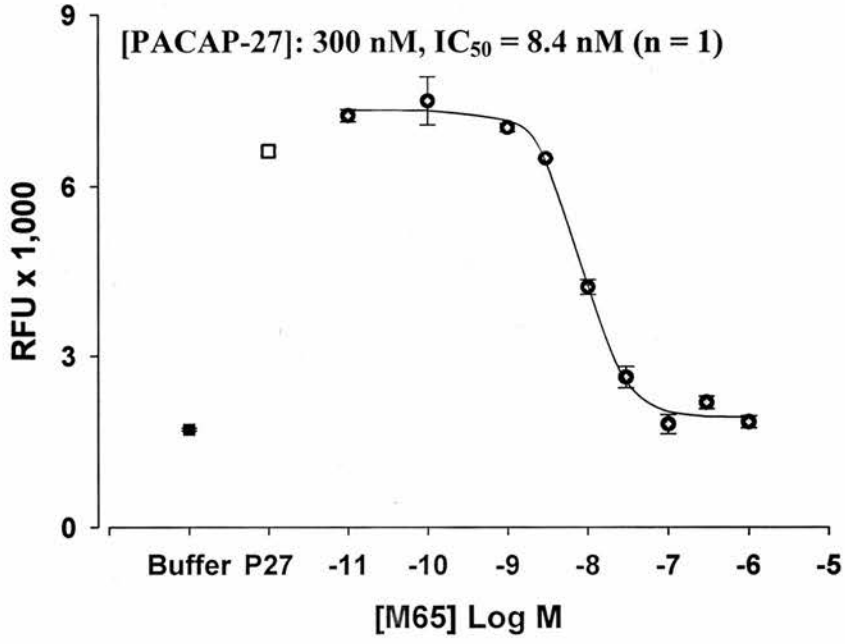

Figure 1.2.37 M65 antagonism of maximal PACAP-27 induced $[Ca^{2+}]_i$ responses in SHSY-5Y cells. Inhibition curves from the same $[Ca^{2+}]_i$ assay plate are shown, in which cells (1.25 x 10^5 per well) were pre-incubated (10 min) with M65, prior to the addition of PACAP-27 at either 30 nM (**a**; ~ EC_{50}) or 300 nM (**b**; ~ EC_{100}).

(a)

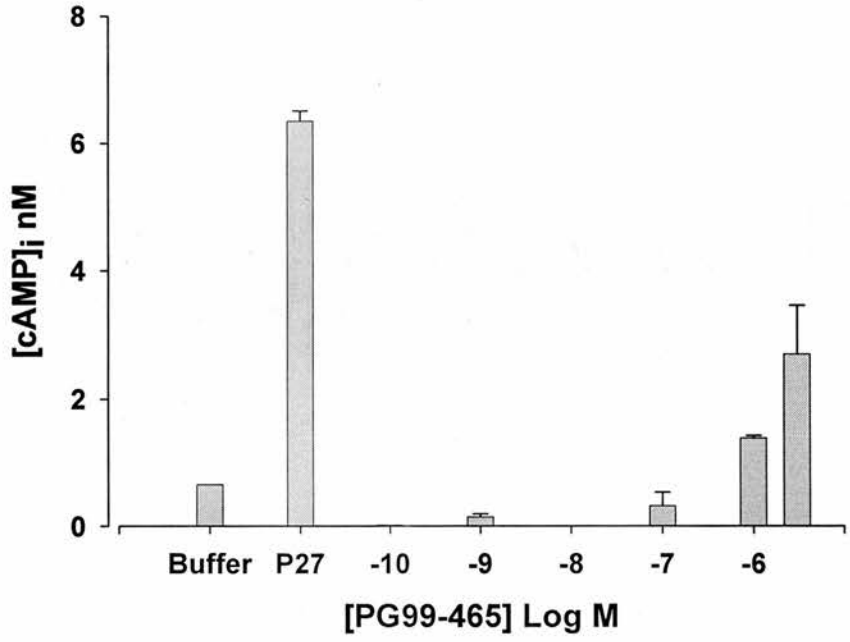

(b)

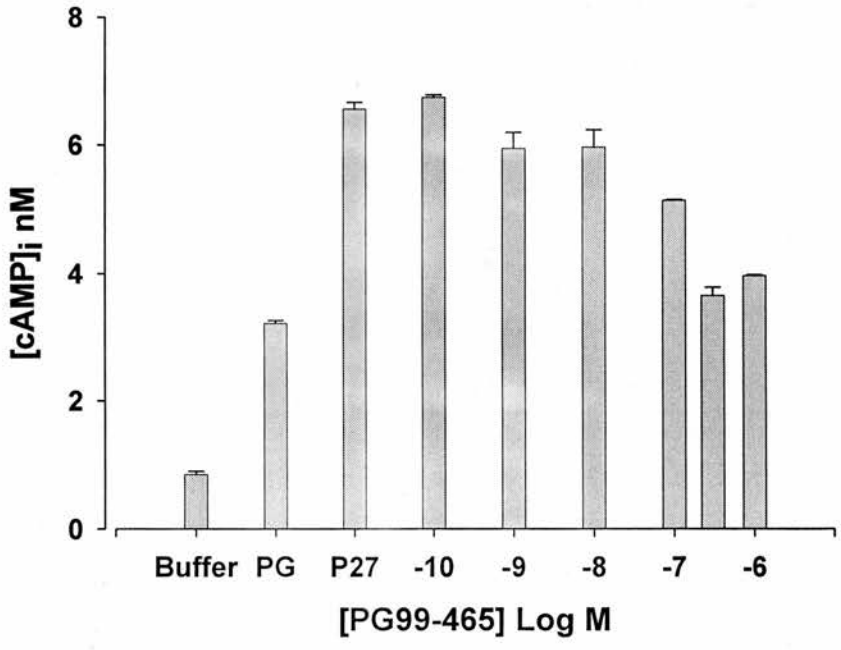

Figure 1.2.38 PG99-465 modulation of $[cAMP]_i$ in SHSY-5Y cells. Alone, PG99-465 increased $[cAMP]_i$ in SHSY-5Y cells (1.25 x 10^5 per well) at micromolar concentrations (**a**; n = 2). The inhibitory action of PG99-465 on agonist induced $[cAMP]_i$ responses was determined in SHSY-5Y cells that had been pre-incubated (10 min) with PG99-465, prior to the addition of 1 nM PACAP-27 (**b**; n = 1).

1.2.4.3. hVPAC/PACR pharmacology in HT-29 and SUP-T1 cells

The pharmacology of VPAC/PACR in the HT-29 and SUP-T1 cell lines was also investigated. From preliminary studies, it was evident that neither cell line was particularly suitable for use in the calcium assay. With HT-29 cells generally growing in clumps (Figure B.3, p 57) and SUP-T1 cells growing in suspension, it proved difficult to obtain the even monolayer of cells on the assay plate that is required for the calcium assay. Several $[Ca^{2+}]_i$ assays were performed with both cell lines, in which the cells were either seeded overnight, or on the day of assay with the cell plate centrifuged as described (B.2.4.1., p 61). However, the responses observed with both seeding procedures, upon agonist addition, were extremely variable and non-reproducible, indicating that these cell lines were not suitable for analysis with this assay. In contrast, the $[cAMP]_i$ assay does not depend upon an even distribution of cells and as result, it was possible to evaluate VPAC/PACR pharmacology in HT-29 and SUP-T1 cells using this assay. As no comparative studies were possible with the calcium assay, these two cell lines were only partially characterised with the $[cAMP]_i$ assay with a limited range of peptides.

In HT-29 cells, VIP, PACAP-27 and PACAP-38 were equipotent agonists, evoking concentration dependent increases in $[cAMP]_i$ (Figure 1.2.39a), with low nanomolar potency (EC_{50} values of 0.13 ± 0.02 (4) nM, 0.12 ± 0.02 (5) nM and 0.17 ± 0.02 (3) nM respectively; Table 1.2.6). These potencies are almost identical to those determined for the CHO-hVPAC$_1$R cell line using this assay (Table 1.2.2, p 110). However, in contrast to the CHO-hVPAC$_1$R data, [Ala^{11,22,28}]VIP and R3P65 were ~ 25 fold less potent than VIP or the PACAP peptides (Figure 1.2.39; Table 1.2.6). The agonist ROP for the HT-29 cell line was therefore: VIP = PACAP-27 =

Table 1.2.6 Comparison of EC_{50} values for agonist stimulation of $[cAMP]_i$ responses in HT-29 cells

	VIP	PACAP-27	PACAP-38	[Ala^{11,22,28}]VIP	R3P65
	EC_{50} ± SEM (nM)				
$[cAMP]_i$	0.13 ± 0.02 (4)	0.12 ± 0.02 (5)	0.17 ± 0.02 (3)	2.88 ± 0.75 (6)	4.15 ± 0.63 (3)

EC_{50} values are shown as the mean ± SEM, with the number of independent experiments given in parenthesis. Maxadilan was not tested with these cells as stocks of this peptide were limited.

(a)

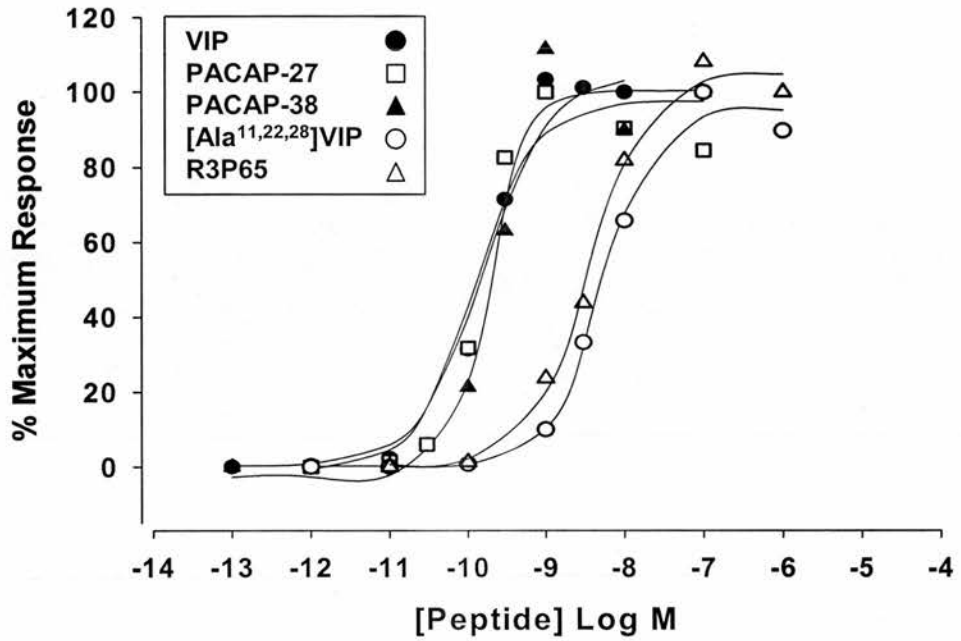

(b)

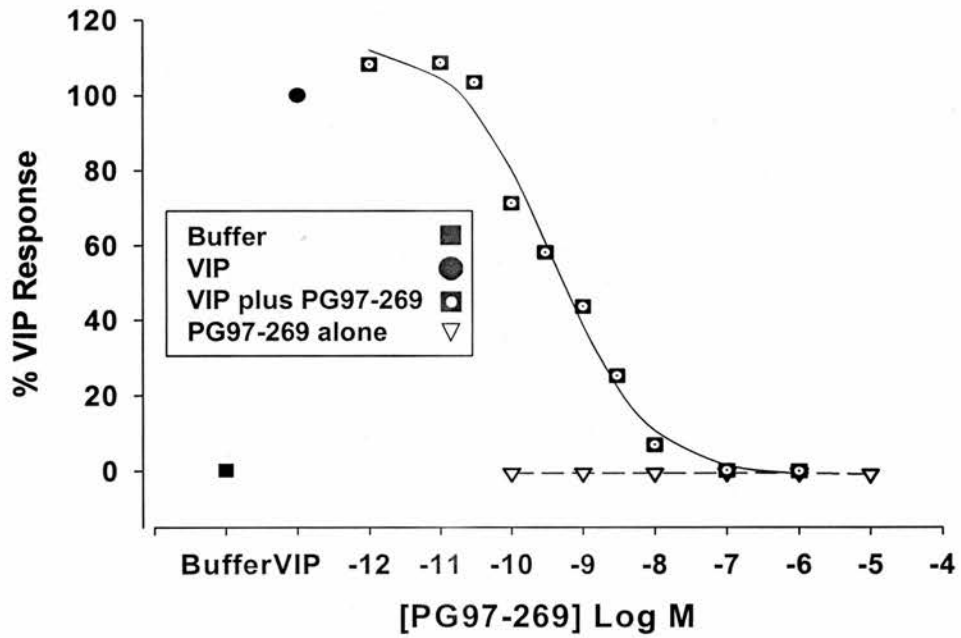

Figure 1.2.39 Characterisation of VPAC/PACR in HT-29 cells. Using the $[cAMP]_i$ assay, HT-29 cells (1×10^5 per well) were stimulated with a range of VPAC/PACR agonists and concentration response curves produced (**a**). The antagonist action of PG97-269 was also determined in the cells (**b**), which were pre-incubated (10 min) with PG97-269, prior to the addition of VIP (0.3 nM). The concentration response curves shown are representative, with mean EC_{50}/IC_{50} values ± SEM ($n \geq 3$) shown in Tables 1.2.6 and 1.2.7.

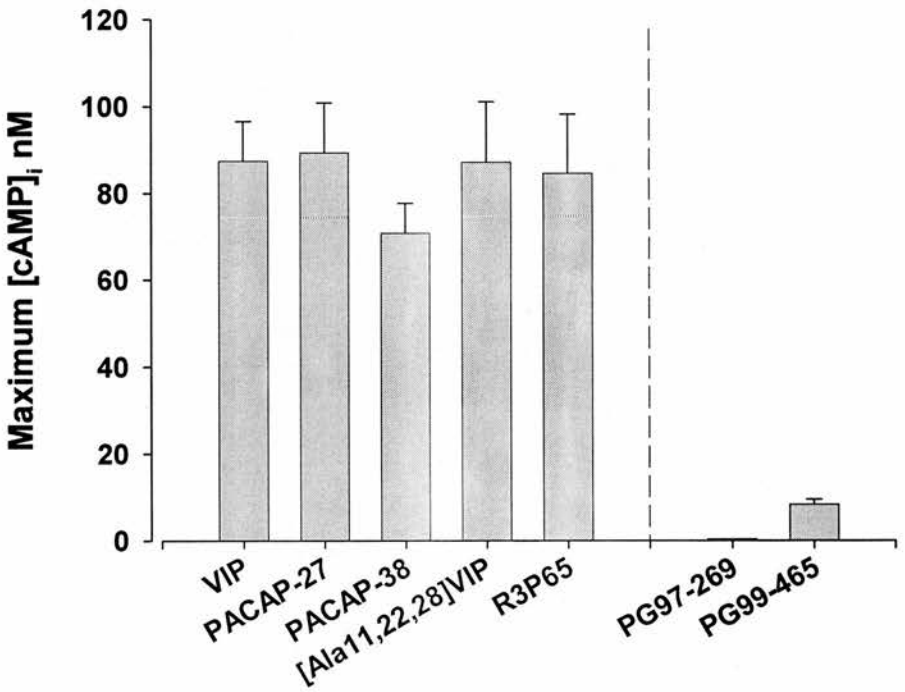

Figure 1.2.40 Maximum peptide induced $[cAMP]_i$ responses from HT-29 cells. Mean $[cAMP]_i$ responses from the HT-29 cell line (1×10^5 per well) were calculated from the upper plateau of the agonist concentration response curves used to calculate the ligands potencies in Table 1.2.6 ($n \geq 3$). Antagonists were tested at a concentration of 3 μM.

Table 1.2.7 Comparison of IC_{50}/*EC_{50} values for antagonist inhibition of VIP induced $[cAMP]_i$ responses in HT-29 cells

	PG97-269	PG99-465
	IC_{50}/*EC_{50} ± SEM (nM)	
$[cAMP]_i$	0.34 ± 0.08 (5)	*53.0 ± 7.65 (4) partial agonist (10 % max)

IC_{50}/*EC_{50} values are shown as the mean ± SEM, with the number of independent experiments given in parenthesis. It was not possible to test M65 with these cells, as stocks of this peptide were limited.

PACAP-38 > [Ala^{11,22,28}]VIP = R3P65. The potency of the $VPAC_1R$ selective antagonist, PG97-269, was also evaluated using the HT-29 cells. PG97-269 inhibited VIP induced $[cAMP]_i$ responses in a concentration dependent manner, with an IC_{50} of 0.34 ± 0.08 (5) nM (Figure 1.2.39b; Table 1.2.7), which is over 200 fold more potent than in the CHO-h$VPAC_1R$ cell line (IC_{50}: 80.0 ± 3.2 (3); Figure 1.2.23, p 120; Table 1.2.3, p 118). In addition, the stimulatory effects of PG99-465, which was shown to be a full agonist in the CHO-h$VPAC_1R$ $[cAMP]_i$ assays, were evaluated. This peptide produced a very small increase in cAMP in HT-29 cells which was equivalent to ~ 10 % of the maximum VPAC/PAC agonist induced responses (EC_{50}: 53.0 ± 7.65 (4) nM; Table 1.2.7). From all of the agonist concentration response curves (Table 1.2.6), maximum responses produced with saturating concentrations of the peptides were evaluated, with all of the agonists evoking a similar peak $[cAMP]_i$ response of approximately 80 nM (Figure 1.2.40). The peak partial agonist response of ~ 10 nM observed from PG99-465 stimulation is also shown.

Table 1.2.8 VPAC/PACR ligand potencies from the partial characterisation of SUP-T1 cells in the $[cAMP]_i$ assay

	VIP	[Ala^{11,22,28}]VIP	PG99-465
	EC_{50} ± SEM (nM)		IC_{50} ± SEM (nM)
$[cAMP]_i$	7.6 ± 1.2 (3)	NE	51.0 (1)

IC_{50}/*EC_{50} values are shown as the mean ± SEM, with the number of independent experiments given in parenthesis. NE is no effect at 3 μM.

(a)

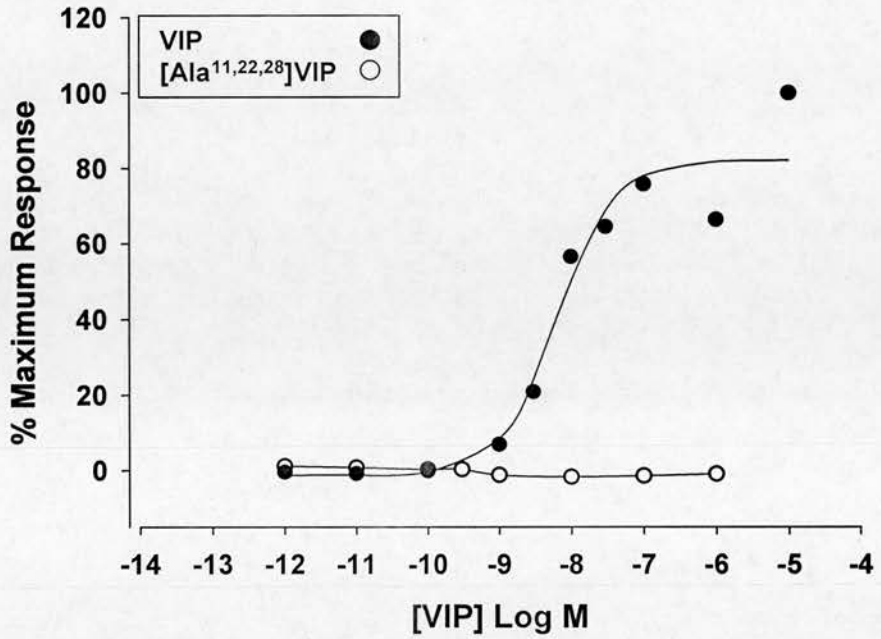

(b)

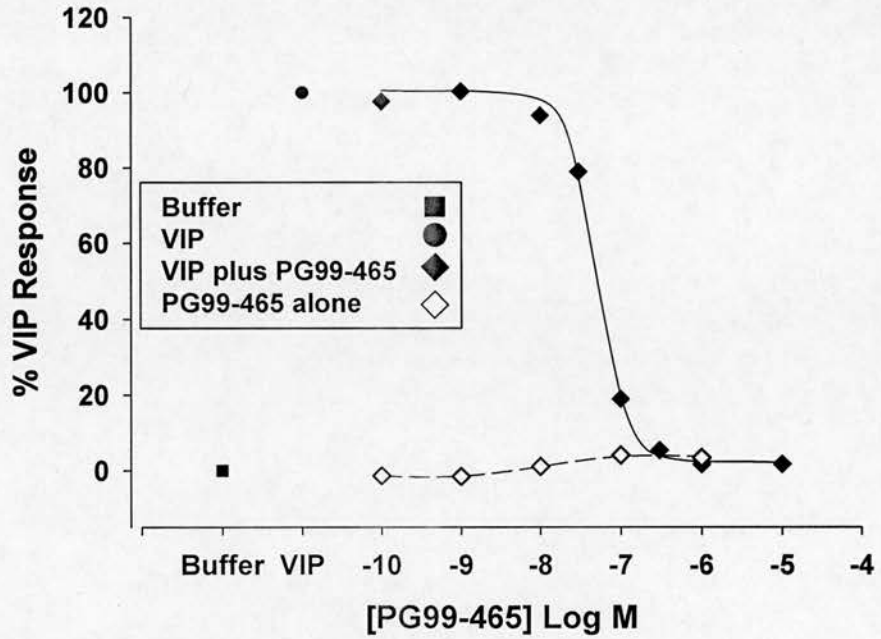

Figure 1.2.41 **Partial characterisation of VPAC/PACR in SUP-T1 cells.** SUP-T1 cells (1 x 10^5 per well) were stimulated with VIP and [Ala^{11,22,28}]VIP for 15 min and $[cAMP]_i$ determined (**a**). In addition, the antagonist action of PG99-465 was determined using the cells, which were pre-incubated (10 min) with the antagonist, prior to the addition of 30 nM VIP (**b**). EC_{50}/IC_{50} values ± SEM ($n \geq 1$) are shown in Tables 1.2.8.

In the $VPAC_2R$ expressing SUP-T1 cell line, VIP induced a concentration dependent increase in cAMP with a maximum response of 21 ± 1.9 (3) nM $[cAMP]_i$ (Figure 1.2.41a). VIP was of nanomolar potency in this cell line with an EC_{50} of 7.6 ± 1.2 (3) nM (Figure 1.2.41a; Table 1.2.8), making it ~ 10 fold more potent than in the CHO-$hVPAC_2R$ cell line (Table 1.2.2, p 110). To confirm that SUP-T1 cells do not express $VPAC_1R$ (Igarashi *et al.*, 2002b), the stimulatory effects of $[Ala^{11,22,28}]VIP$ were evaluated and as expected, this potent $VPAC_1R$ agonist produced no change in $[cAMP]_i$ (Figure 1.2.41a). Finally, PG99-465 was observed to fully inhibit VIP induced $[cAMP]_i$ responses from SUP-T1 cells with an IC_{50} of 51.0 nM (n = 1; Figure 1.2.41b; Table 1.2.8), which is a similar potency to the inhibitory action of this peptide in the CHO-$hVPAC_2R$ cell line (Table 1.2.3).

1.3. Discussion

1.3.1. Functional evaluation of hVPAC/PAC receptor pharmacology

To date, comprehensive studies directly comparing the pharmacology of human VPAC/PAC receptors across multiple functional assays remains limited. In addition, comparison between data from different research groups is complicated by the variation in protocols used (receptor expression system, species of receptor, assay type). To address these limitations, stable cell lines expressing the three human VPAC receptor subtypes ($hVPAC_1R$, $hVPAC_2R$ and $hPAC_1R$) were generated and two simple, non-radioactive, HT-amenable $[cAMP]_i$ and $[Ca^{2+}]_i$ assays were established and characterised. Although VPAC/PAC mediated enhancement of PLD activity has been reported in a limited number of studies (McCulloch *et al.*, 2000; Dejda *et al.*, 2006), there have been no studies to date exploring the physiological relevance of this coupling. Therefore, we sought to characterise hVPAC/PAC receptor pharmacology by comparing the agonist/antagonist modulation of $[cAMP]_i$ and $[Ca^{2+}]_i$ pathways, both of which have been associated with a number of physiological roles (Masmoudi *et al.*, 2003; Perez *et al.*, 2005; Zizzo *et al.*, 2005). These assay platforms were used to evaluate the pharmacology of a selection of agonists and antagonists, including endogenous as well as new and reportedly receptor selective ligands.

For the endogenous peptides VIP, PACAP-27 and PACAP-38, the agonist ROP was identical in both assays for the three human receptor subtypes, although EC_{50} values in the $[Ca^{2+}]_i$ assay were approximately 100 fold less (range: 26 - 174 fold). In the $[cAMP]_i$ studies, the agonists $[Ala^{11,22,28}]VIP$ and maxadilan showed considerable selectivity for $hVPAC_1R$ and $hPAC_1R$ respectively (> 25,000 fold), and whilst R3P65 was not $hVPAC_2R$ selective in our hands, all three peptides were comparably less potent in the $[Ca^{2+}]_i$ assay. With the reduction in agonist potency in the $[Ca^{2+}]_i$ assay also observed in SHSY-5Y cells, which endogenously express $hPAC_1$ receptors, this effect is unlikely to be a consequence of receptor over-expression. In contrast to the agonists, the reportedly selective $VPAC_1R$ (PG97-269) and $VPAC_2R$ (PG99-465) antagonists had slightly lower IC_{50} values and hence greater potency in the $[Ca^{2+}]_i$ assay at their respective receptor subtypes, whereas the $hPAC_1R$ selective antagonist M65 was almost equipotent in both assays. With PG99-465 alone acting as a partial ($hVPAC_2R$) and full ($hVPAC_1R$ and $hPAC_1R$) agonist in the $[cAMP]_i$ assay, this compound is clearly not a selective antagonist. These studies reiterate that there remains a paucity of VPAC/PAC receptor selective drugs, in particular non-peptides, and that functional responses both *in vitro* and *in*

vivo will critically depend upon the range of ligand concentrations tested and the cellular complement of intracellular messengers, as well as other factors outlined in the introduction (p 78).

1.3.2. hPAC$_1$R pharmacology

In the current study, the EC_{50} values of PACAP-27, PACAP-38 and maxadilan at the hPAC$_1$-null receptor (Pisegna & Wank, 1996; equivalent to rat PACAP-R, Spengler *et al.*, 1993) were similar within assays, however a 1 - 200 fold loss in potency was observed on going from the $[cAMP]_i$ to the $[Ca^{2+}]_i$ assay. Although limited, previous studies have shown that the three peptides have a similar affinity/potency in radioligand binding (Moro & Lerner, 1997) and $[cAMP]_i$ assays (Eggenberger *et al.*, 1999), with the former study also demonstrating considerable selectivity for maxadilan at PAC$_1$ receptors, as shown in Table 1.2.2 (p 110). Consistent with our observations, Pisegna and Wank (1996) had reported PACAP-27 and PACAP-38 to be equipotent at the human PAC$_1$-null variant expressed in NIH/3T3 cells using a [^{3}H]cAMP and [^{3}H]IP assay, with both peptides being 60 fold less potent in the latter assay. Moreover, in the human neuroblastoma cell line, NB-OK-1, that endogenously expresses a PAC$_1$ receptor variant, Delporte and colleagues (1993) showed that PACAP-27 and PACAP-38 were considerably less potent in stimulating $[Ca^{2+}]_i$ release when compared to $[cAMP]_i$. Importantly, we confirmed and extended these observations using an alternative human neuroblastoma cell line, SHSY-5Y (Table 1.2.4, p 127), which also endogenously expresses PAC$_1$ receptors (Vertongen *et al.*, 1996). Both $[Ca^{2+}]_i$ and $[cAMP]_i$ were elevated in response to agonists in the SHSY-5Y cells, with identical ROPs and similar potencies to the CHO-hPAC$_1$R cell line (Table 1.2.2 and 1.2.4). More significantly, in our SHSY-5Y studies, there was a clear reduction in agonist potency in the $[Ca^{2+}]_i$ assay, despite $[cAMP]_i$ levels in these cells being 10 fold lower than in the stable cell lines. The recent findings of Lutz and colleagues (2006) support these data, with PACAP-38 and VIP producing a similar fold increase in a [^{3}H]cAMP assay, however no [^{3}H]IP data was presented for SHSY-5Y cells, despite comparing both second messengers for some of the new, individual hPAC$_1$ splice variants. These data support the assertion that the reduction in agonist potency is not a consequence of receptor over-expression (MacKenzie *et al.*, 2001), but could reflect inefficient coupling (Langer *et al.*, 2002b). These observations are not unique to human PAC receptors; in CHO cells expressing rat type I PACAP-R (Delporte *et al.*, 1995) the potency of PACAP-

27 (cAMP, 0.01 nM; $[Ca^{2+}]_i$, 1.1 nM) and the fold difference (110) was almost identical to our human data. Although Spengler et al. (1993) reported a smaller 40-fold reduction in potency for PACAP-38 at the same rat receptor (PACAP-R), these authors showed that PACAP-27 did not stimulate inositol phosphate (IP) production (despite a robust production of cAMP), suggesting species differences in PAC_1 receptor pharmacology and supporting a similar observation in PC12 cells (Deutsch & Sun, 1992).

In our hands, VIP was approximately 300x less potent than PACAP-38 in the CHO-hPAC_1R $[cAMP]_i$ assay, which is consistent with some published data (Spengler *et al.*, 1993). However, Pisegna and Wank (1996) have shown that VIP at concentrations 1000x in excess of the PACAP EC_{50} had no effect on adenylate cyclase. In the present hPAC_1R $[Ca^{2+}]_i$ studies, VIP was only 25x less potent than in the $[cAMP]_i$ assay, resulting in this peptide only being about 75x less potent than the PACAPs (rather than 300x), and possibly why it was possible to determine an EC_{50} value of about 400 nM for VIP (Table 1.2.2, p 110). This is however consistent with the recent data from Lutz and colleagues (2006), with IC_{50} values for VIP of 55 nM ($[^3H]$cAMP) and approximately 1.5 μM ($[^3H]$IP) giving a ratio of 27. The pharmacological properties of R3P65 (Yung *et al.*, 2003) at hPAC_1R were akin to VIP, with only a 10 fold difference in potency in the two assays (Table 1.2.2, p 110). This peptide's sequence differs from VIP by only 4 amino acids (2 within the VIP sequence; Table A.2, p 23), and it is not inconceivable that both peptides induce $[Ca^{2+}]_i$ production more readily than the PACAPs (relative to $[cAMP]_i$) at human PAC_1R, akin to that described for PACAP-38 at rPAC_1 receptors (Spengler *et al.*, 1993).

In the calcium studies with the SHSY-5Y cell line, the PACAP peptides evoked a considerably larger response (~ 30 %) than maxadilan, VIP and R3P65 (Figure 1.2.30, p 129). This larger response was not linked to the potency of the peptides as maxadilan, which was equipotent to the PACAPs, did not produce a similarly enhanced calcium response. This finding extends a preliminary observation made by Eggenberger *et al.* (1999), who showed that peak maxadilan induced calcium responses in SHSY-5Y cells were only ~ 25 % of the size of those induced by PACAP-27 (both peptides tested at 100 nM), despite the cAMP responses to these peptides being similar in magnitude. Furthermore, the tentative suggestion from our data, of a biphasic concentration response relationship for the PACAP induced calcium elevations (Figure 1.2.33, p 132), introduces the possibility that this peptide may act via another group of PACAP sensitive receptors in the SHSY-5Y cell line. The current characterisation of PACAP receptors in the SHSY-5Y cells suggests that

this additional population of receptors would be PACAP sensitive, maxadilan insensitive and M65 sensitive. Although multiple variants of the PAC_1R have been described, a receptor with the specific pharmacological characteristics presented here has not yet been reported. However, Lutz and colleagues (2006) have recently identified up to 14 splice variants of the human PAC_1 receptor, all of which were cloned from the SHSY-5Y cell line. In future studies it would be of interest to examine calcium responses from the individual splice variants cloned from the SHSY-5Y cells, in an attempt to identify the receptor variant responsible for the PACAP (and M65) sensitive, maxadilan insensitive response. Furthermore, it is intriguing to note that these differential agonist responses are specific for the calcium signalling pathway, with the targeting of this specific receptor variant being potentially useful to delineate the functional significance of PAC_1R splice variants.

In the calcium studies using the stable cell lines, there was a clear difference in the kinetics of the responses from the VPACR and PAC_1R expressing cells, with PAC_1R mediated responses appearing to show a prolonged duration of calcium stimulation (Figure 1.2.19, p 113). Upon further examination of PAC_1R mediated calcium responses to the PACAPs and VIP, the prolonged calcium elevation was found to be particularly pronounced in response to PACAP treatment. In contrast to our data, $VPAC_1$ receptor mediated calcium responses have been previously shown to have a sustained phase following the initial peak response (Sreedharan *et al.*, 1994), however these studies also suggested that the kinetics of the response may be dependent on the cell type utilised. As all of the stable cell lines used in the current studies were generated using the same parent cell line, this excludes the possibility that the differences between the VPAC and PAC traces were a result of host cell type. Furthermore, agonist induced responses from the PAC_1R expressing SHSY-5Y cell line also demonstrated differential rates of decline, with responses to the PACAPs and maxadilan appearing to decline at a slower rate than those produced with VIP or R3P65 (Figure 1.2.34, p 133). As only VIP and R3P65 responses declined at a faster rate, these effects do not appear to correlate with the reduced magnitude of response observed for certain agonists in these cells (as discussed in the preceding paragraph), however these effects may be dependent on the potency of the agonist tested. The agonist induced calcium responses mediated by endogenous VPAC and PAC_1R have been shown to be biphasic in nature, with an initial peak response followed by a lower, sustained elevation in calcium (NB-OK-1 cells: Delporte *et al.*, 1993; AR4-2J: Barnhart *et al.*, 1997; polymorphonuclear neutrophils: Harfi & Sariban, 2006; intracardiac neurons: Dehaven & Cuevas, 2004). From these studies the initial peak of the response has been shown to result from mobilisation of

intracellular calcium stores, with the subsequent sustained response attributed to an influx of extracellular calcium, consistent with observations for other GPCR mediated calcium responses (Edelman *et al.*, 1994). Indeed, in the current studies the larger sustained phase of the PACAP induced calcium response through PAC_1R was abolished upon removal of extracellular calcium (Figures 1.2.21 and 1.2.22, p 115 – 116). The precise route of entry for this calcium influx into the cell remains to be determined. A direct comparison of the kinetics of VPAC and PAC receptor mediated calcium responses has not been previously reported, however the apparent receptor and agonist specificity of the sustained phase of the response in the current studies is intriguing. Future studies comparing the kinetics of PAC_1R mediated calcium responses (post 200 s), with all of the agonists described will be useful to determine if the prolonged responses are unique to the PACAPs, given the sustained responses produced by maxadilan and the PACAPs in SHSY-5Y cells. In addition, elucidating the route of calcium influx for the enhanced second phase of the PAC_1R mediated PACAP responses will also prove interesting.

1.3.3. hVPACR pharmacology

In contrast to the data showing that PAC_1 receptor activation is associated with downstream production of both $[cAMP]_i$ and $[Ca^{2+}]_i$, studies fully examining VPAC mediated stimulation of the latter second messenger have been more limited and variable (Dehaven & Cuevas, 2004). The three endogenous peptide ligands, VIP, PACAP-27 and PACAP-38 all exhibited similar, sub-nanomolar potencies in the $[cAMP]_i$ assay in the two cell lines stably expressing either $hVPAC_1$ or $hVPAC_2$ receptors (Table 1.2.2, p110). For the $VPAC_1R$, this pharmacological profile was also observed in the initial $[cAMP]_i$ studies using the HT-29 cell line. In the stable cell lines, the maximal amount of cAMP produced (~ 50 nM) and the fold stimulation above basal levels (~ 25 fold) was the same for all three ligands at both hVPAC receptor subtypes (and $hPAC_1$). Sreedharan *et al.* (1994), reported similar EC_{50} values for VIP at $hVPAC_1$ receptors expressed stably in either HEK-293 or CHO cells, although the same group reported a considerably lower potency (70 fold) for VIP at $hVPAC_2$ in both SUP-T1 and transfected cells (Xia *et al.*, 1996, 1997). In studying cAMP responses at $hVPAC_1R$, Langer and colleagues (2002a) demonstrated that the potencies of VIP (30x) and PACAP-27 (10x), were higher in intact cells when compared to membranes, with the former values (EC_{50}: VIP = 0.1 nM; PACAP-27 = 0.3 nM) similar to those described in these studies (Table 1.2.2, p

110). Similarly, the EC_{50} values of VIP and PACAP-38 for recombinantly expressed rat VPAC/PAC receptors in a whole cell cAMP assay (MacKenzie *et al.*, 2001; McCulloch *et al.*, 2001), were consistent with the present data using human receptors (Table 1.2.2, p 110). Therefore, it is clear that for the endogenous peptide ligands such as VIP and the PACAPs, the use of membrane preparations may result in an underestimate of their potencies, and that the variation in use of whole cell and/or membrane preparations could contribute to the inconsistencies seen in the literature. In the $[Ca^{2+}]_i$ assay, VIP, PACAP-27 and PACAP-38 were again almost equipotent at $hVPAC_1$ and $hVPAC_2$ receptors, although the agonist EC_{50} values were approximately 100x greater than those in the $[cAMP]_i$ studies (Table 1.2.2). The maximal response induced by agonists was about 7x that of basal fluorescence levels for all three VPAC/PAC stable cell lines. Although EC_{50} values were not determined, Sreedharan *et al.* (1994) had shown in an earlier study, that in cells stably (CHO and HEK-293) or endogenously (HT-29) expressing $hVPAC_1R$, VIP could elicit an increase in $[Ca^{2+}]_i$, albeit at higher concentrations than that required for $[cAMP]_i$. Using a luminescence based calcium assay, Langer and colleagues (2001, 2002b) have reported similar EC_{50} values for VIP and PACAP-27 in CHO cells expressing $hVPAC_1R$. In further studies, the same authors have since shown that the enhanced $VPAC_1$ coupling is due to a small number of residues in the third intracellular loop, whilst also suggesting that their absence underlies the inefficient VIP induced $[Ca^{2+}]_i$ response at $VPAC_2$ receptors (Langer *et al.*, 2002b; Langer & Robberecht, 2005).

In human T-lymphoblast cells (SUP-T1) that endogenously express $hVPAC_2$ receptors (Xia *et al.*, 1996), the concentration of VIP (EC_{50} = 30 nM) required to induce $[Ca^{2+}]_i$ production was very similar to the current study (Table 1.2.2, p 110). Xia *et al.* (1997) also reported, but did not fully characterize a $[Ca^{2+}]_i$ response in CHO-cells expressing $hVPAC_2$, although the present data are consistent with that of Langer *et al.* (2002b), who reported a comparable EC_{50} value for VIP at $hVPAC_2R$. In COS7 cells expressing rat $VPAC_2R$, the EC_{50} of PACAP-38 was also similar (37 nM) in an $[^3H]IP$ assay (MacKenzie *et al.*, 2001), however it must be noted that when the same authors expressed either rat $VPAC_1$ or $VPAC_2$ receptors in CHO cells, no stimulation of IP was observed, despite similar data for rat PAC_1 (McCulloch *et al.*, 2000, 2001).

The rightward shift in potency (~ 100 fold) that we observed for VIP, PACAP-27 and PACAP-38 between the cAMP and calcium assays for all three human VPAC/PAC receptors (Figures 1.2.14 – 1.2.16, p 107 - 109), is therefore consistent with the other study using cloned human VPAC/PAC receptors which

compared cell-based assays (Langer *et al.*, 2002a), with lower ratios observed when $[cAMP]_i$ responses were determined in membrane based assays (Langer *et al.*, 2001; Langer & Robberecht, 2005). A similar change in potency between these assay types has also been shown for rat $VPAC_2$ (~ 100 fold) (MacKenzie *et al.*, 2001) and PAC_1 (~ 170 fold) receptors (McCulloch *et al.*, 2001). In contrast, Xia *et al.* (1996) only reported a 2 fold difference in potency for VIP between cAMP and calcium assays, using SUP-T1 cells, perhaps as a consequence of the low potency of VIP in their cAMP assay, as discussed previously (p 150). Although the $[Ca^{2+}]_i/[cAMP]_i$ and phospholipase D/$[cAMP]_i$, ratios were of a comparable magnitude (100 – 300x) for rat PAC_1 (McCulloch *et al.*, 2000, 2001), no $[Ca^{2+}]_i$ response was found for $VPAC_1$ and $VPAC_2$, despite a similar phospholipase D/$[cAMP]_i$ ratio for these two subtypes. It remains unclear whether these variations are due to expression level (Van Rampelbergh *et al.*, 1997; Langer *et al.*, 2002b; Ciccarelli *et al.*, 1995), as MacKenzie *et al.* (2001) clearly showed there was no difference in the $[Ca^{2+}]_i/[cAMP]_i$ potency ratio for PACAP-38 on comparing transfected and endogenously expressed $VPAC_2$ receptors. In contrast, Langer *et al.* (2002b) do show that the magnitude of the cAMP and calcium responses may be dependent upon the level of receptor expression, however they do not discuss what impact this has upon agonist EC_{50} values. However, it is important to stress that the VPAC/PAC induced increase in calcium is of physiological importance (Delgado *et al.*, 2003a; Dehaven & Cuevas, 2004; Zizzo *et al.*, 2005).

1.3.4. Pharmacology of putatively receptor selective ligands

1.3.4.1. $VPAC_1R$ selective peptide ligands

Using a combined approach of alanine scanning and molecular modeling Nicole *et al.* (2000), identified $[Ala^{11,22,28}]VIP$ as the first highly selective human $VPAC_1$ receptor agonist. In agreement with these observations, our $[cAMP]_i$ data also established $[Ala^{11,22,28}]VIP$ to be as potent as VIP at the $hVPAC_1$ receptor, whilst having no demonstrable agonist effect at $hVPAC_2$, at concentrations up to 3 μM. $[Ala^{11,22,28}]VIP$ also induced a concentration dependent increase in $[Ca^{2+}]_i$ in the $hVPAC_1R$ cell line, with an EC_{50} value which was in excess of 2 orders of magnitude greater than that observed for $[cAMP]_i$. To our knowledge this is the first report to show that $[Ala^{11,22,28}]VIP$ stimulates the production of $[cAMP]_i$ in cells expressing $hPAC_1$, albeit at micromolar concentrations, which are approximately 25,000x higher than that required to activate $hVPAC_1R$. The general reduction in

agonist potencies in the $[Ca^{2+}]_i$ assay, meant we were unable to test a sufficient concentration of $[Ala^{11,22,28}]$VIP to evaluate whether this peptide stimulates $[Ca^{2+}]_i$ production at $hPAC_1R$.

Although a range of approaches have resulted in some moderately selective VPAC/PAC agonists, to date there is still a paucity of suitable receptor antagonists (Laburthe & Couvineau, 2002). One notable exception is PG97-269, which was reported to be a $VPAC_1R$ selective antagonist (Gourlet *et al.*, 1997a). Alone, PG-97-269 had no effect on $[Ca^{2+}]_i$ in any of the three human VPAC/PACR cell lines (Table 1.2.3, p 118), however there was a small (up to 5 % of the maximal VIP response), but non-quantifiable, increase in $[cAMP]_i$ in the $hVPAC_1R$ cell line. Although PG97-269 produced a concentration dependent inhibition of both the $[cAMP]_i$ and $[Ca^{2+}]_i$ responses in $hVPAC_1R$ expressing cells, its potency was slightly reduced in the $[cAMP]_i$ assay, perhaps as a consequence of the small agonist-like response. However, the IC_{50} value in the $[Ca^{2+}]_i$ assay is consistent with that observed by Gourlet *et al.* (1997a). Interestingly, this peptide has recently been shown to act as an inverse agonist at the C-terminally truncated form of $VPAC_1R$, which is a constitutively active form of the receptor (Vertongen *et al.*, 2004).

1.3.4.2. $VPAC_2R$ selective peptide ligands

Using an HT-mutagenesis approach, Yung *et al.* (2003) generated a comprehensive range of VIP-related peptides that resulted in a series of putatively receptor selective $VPAC_2$ agonists, including R3P65 (Table A.2, p 23). R3P65 was reported to exhibit at least 80 (radioligand binding) and 500 fold (cAMP) selectivity over human $VPAC_1$ and PAC_1 receptors. Such ligands would be advantageous, as the existing $VPAC_2$ peptide agonists e.g. Ro25-1392 and Ro25-1553 (Moreno *et al.*, 2000), are difficult to synthesize (Yung *et al.*, 2003) and can act as partial agonists at $VPAC_1$ and PAC_1 receptors (Akesson *et al.*, 2005). Although the EC_{50} values of VIP, PACAP-27 and PACAP-38 for $[cAMP]_i$ production, at the three human VPAC/PAC (Table 1.2.2) receptors were very similar to those reported by Yung et *al.* (2003), we could provide no evidence to support their assertion that R3P65 is a selective $hVPAC_2$ agonist. Although our EC_{50} value for R3P65 at $hVPAC_2$ receptors in the $[cAMP]_i$ assay (Table 1.2.2, p 110) was consistent with Yung *et al.* ($EC_{50} \sim 0.4$ nM; 2003), we found this peptide to be slightly more potent at $hVPAC_1$, in addition to acting as a full $hPAC_1$ agonist, albeit with lower potency. In our $[Ca^{2+}]_i$ studies, the pharmacological profile of R3P65 was as observed for $[cAMP]_i$, with the

compound again having a lower potency in the former assay, consistent with the trend observed for the other peptides (Table 1.2.2, p110). These data contrast with the published 80 - 500 fold selectivity for R3P65 over $hVPAC_1$ receptors and with its negligible effect at $hPAC_1R$ (Yung *et al.*, 2003). As both studies used a CHO-based cell line to express human VPAC/PAC receptors, the differences between the two studies are intriguing, although these authors did introduce the promiscuous G-protein $G\alpha_{16}$ into their cell lines (Yung *et al.*, 2003). In both our assays, for all three human VPAC/PAC receptor subtypes, R3P65 was on average 3x less potent than VIP. Compared to the $VPAC_2R$ agonist Ro25-1553, the amino acid sequence of R3P65 is remarkably similar to VIP (Table A.2, p 23), and it is interesting to note that of the four key residues identified by Yung *et al.* (2003), neither V19A (R3P47) or L27K (R3P42) alone, which lie within the VIP sequence, alter selectivity in the binding or functional assays; even the double (R3P49) mutant is only functionally selective (30 fold). Although the further addition of K29 and R30 resulted in R3P65, the authors comment that any reduction in the number of mutations did not produce peptides with comparable selectivity, with no data shown even for the triple mutant without the R30 addition (Yung *et al.*, 2003). It is also interesting to note, that these authors have not published any further studies involving this peptide, instead returning to study BAY 55-9837, a $VPAC_2R$ agonist that was reported by the same group prior to R3P65, in an attempt to improve the poor stability of this compound (Tsutsumi *et al.*, 2002; Pan *et al.*, 2006).

In 2000, Robberecht and colleagues developed PG99-465, which was reported to be the first potent and selective $VPAC_2R$ antagonist (Moreno *et al.*, 2000). In the present investigation, PG99-465 was indeed a potent $hVPAC_2$ receptor antagonist in both the $[cAMP]_i$ and $[Ca^{2+}]_i$ assays, with low nanomolar potency observed (Table 1.2.3, p 118), consistent with the findings of Moreno *et al.* (IC_{50} = 2 nM; 2000). Alone, PG99-465 had no effect on the $hVPAC_2R$ $[Ca^{2+}]_i$ response, however it did display partial agonist activity in the $[cAMP]_i$ assay, perhaps accounting for the 5 fold reduction in potency between assays when added prior to VIP (Table 1.2.3, p 118). This finding contrasts with the original publication which showed that PG99-465 had no effect alone at the $hVPAC_2$ receptor (Moreno *et al.*, 2000), although in two more recent studies there is a suggestion of a small increase in cAMP for both human (Langlet *et al.*, 2004) and rat $VPAC_2$ receptors (Vanneste *et al.*, 2004); with the latter study reporting an EC_{50} similar to that in our present study (30 nM; maximum response ~ 10 % VIP induced response). At both $hVPAC_1$ and $hPAC_1$, PG99-465 was a full agonist in the $[cAMP]_i$ assay (Figure 1.2.26, p 123; Table 1.2.3, p118), with no effect again on the $[Ca^{2+}]_i$ response. Moreno *et al.*

(2000), and more recently Vanneste *et al.* (2004), have reported PG99-465 to be a partial agonist of human and rat $VPAC_1$ receptors respectively, however this is the first description of an agonist effect of PG99-465 at human PAC_1 receptors. As our EC_{50} value for PG99-465 at $hVPAC_1$, was more than 25x lower than that of Moreno *et al.* (2000), the increased sensitivity in the current study may account for the further agonist observations at $hVPAC_2$ and $hPAC_1$ receptors. Furthermore and in agreement with the current observations for PG99-465, Langer and colleagues (2002a), showed that the putative antagonist VIP(4-28) (Ciccarelli *et al.*, 1994) had no detectable effect alone in an adenylate cyclase assay using CHO-$hVPAC_1$ membranes, however it was a full agonist in a whole cell based cAMP assay. These findings suggest that the full agonism observed for PG99-465 may only be detectable in whole cells (rather than membranes) with an appropriate G-protein complement. Indeed in preliminary studies using HT-29 cells, which endogenously express $hVPAC_1$ (Sreedharan *et al.*, 1994), we have continued to examine the properties of PG99-465. Although cAMP concentrations produced were higher in these cells at an equivalent cell density (~ 80 nM), implying at least an equivalent receptor density to our stable cell lines, agonist potencies (VIP, PACAP-27 and PACAP-38) were identical to those seen for the $hVPAC_1$ stable cell line (Figure 1.2.39, p 141; Table 1.2.6, p 140). However, and most importantly, PG99-465 had no agonist effect despite the higher levels of cAMP (Figure 1.2.40, p 142), which would again suggest the agonist effects observed for PG99-465 in the CHO-stable cell lines are a consequence of their particular receptor/G-protein complement and the use of a cell based assay rather than just simply receptor density. These findings do however add further credence to the assertion of Laburthe and Couvineau (2002), who suggest that PG99-465 is not a satisfactory $hVPAC_2$ receptor antagonist, with these observations perhaps complicating the interpretation of some recent *in vitro* studies that use this peptide (Itri & Colwell, 2003; Piggins & Cutler, 2003; Akesson *et al.*, 2005).

1.3.4.3. PAC_1R selective peptide ligands

Maxadilan is a vasodilatory peptide isolated from the salivary glands of sand flies (Lerner *et al.*, 1991). This peptide was reported to be a PAC_1R selective agonist, stimulating receptor mediated cAMP production at low nanomolar concentrations (Moro & Lerner, 1997; Moro *et al.*, 1999). We were able to confirm the high selectivity of this peptide for PAC_1R and report a similar EC_{50} value for maxadilan stimulation of $[cAMP]_i$ to that reported previously (EC_{50} = 0.3 nM; Moro

et al., 1999). Although maxadilan induced calcium responses have been described in the literature using pancreatic β cells (Yamada *et al.*, 2004) and SHSY-5Y cells (Eggenberger *et al.*, 1999), full concentration response curves have never been previously described. In the current studies, we have fully characterised the maxadilan evoked $[Ca^{2+}]_i$ response at hVPAC/PACR, with the compound clearly acting as a full and selective $hPAC_1R$ agonist. As discussed in earlier sections, in the current studies PACAP induced calcium responses in SHSY-5Y cells consisted of a component that was insensitive to maxadilan, yet sensitive to M65 (p 149). Whether the atypical responses to maxadilan and M65 are mediated by a specific PAC_1R splice variant or are not mediated by VPAC/PACR, remains to be determined.

Studies assessing the PAC_1 receptor antagonist M65 (Uchida *et al.*, 1998), are even more limited than those examining the putative VPAC antagonists. M65 alone had no effect in either assay at any of the VPAC/PAC receptors, nor did it exhibit any antagonism of agonist evoked responses at $hVPAC_1$ or $hVPAC_2$. It did however produce a concentration dependent inhibition of agonist evoked responses at the $hPAC_1$ receptor, exhibiting similar potencies (~ 210 nM) in both of the *in vitro* assays. These IC_{50} values (Table 1.2.3, p 118) are lower than those reported in a radioligand binding assay for rat PAC_1, however they are close to the potency of the closely related antagonist max.d.4 (Moro *et al.*, 1999).

1.3.5. Summary

The generation of cell lines stably expressing human VPAC/PAC receptors, combined with the establishment of two simple, non-radioactive, HT-amenable $[cAMP]_i$ and $[Ca^{2+}]_i$ assays, facilitated a systematic characterisation of receptor coupling, clearly demonstrating that all three receptor subtypes can activate more than one downstream messenger in a single cell type. However, with agonist potencies being approximately 100 fold different in the two assays, despite a similar ROP, and with antagonist effects being complex, it is clear that any new compound should be examined in both assays, as the final functional outcome *in vitro*/*in vivo* will be dependent upon the receptor and second messenger complement of the cell or tissue being examined. This may be of considerable physiological importance as a range of VIP/PACAP cAMP-independent effects have been noted (Gressens *et al.*, 1999; Laburthe & Couvineau, 2002; Delgado *et al.*, 2003a; Dehaven & Cuevas, 2004). As VPAC/PAC receptor activation has also been shown to activate the small G-protein ARF and stimulate PLD activity, it would be interesting in future studies

to perform similar receptor characterisation studies using a whole cell, HT-amenable PLD assay. This would allow a comprehensive comparison of VPAC/PAC receptor pharmacology to be made using all three second messengers, which may prove pertinent as the physiological roles, if any, for VPAC/PACR activation of PLD are clarified. Finally, there still remains a distinct lack of truly selective non-peptide agonists and antagonists to examine the functional role of VPAC/PAC receptors both *in vitro* and *in vivo*.

CHAPTER TWO
HT-SCREENING FOR hVPAC$_2$R ANTAGONISTS

2.1. Introduction

2.1.1. VPAC/PAC receptors as drug targets

As discussed in the introduction and chapter one, no truly selective non-peptide antagonists or agonists of the VPAC/PAC receptors have been reported to date. The only selective ligands available are peptides, which are generally modified analogues or chimeric peptides derived from endogenous VPAC/PACR ligands; for example [Ala^{11,22,28}]VIP and PG97-269 (Nicole *et al.*, 2000; Gourlet *et al.*, 1997a). However, even some of the putatively selective peptides, such as R3P65 (Yung *et al.*, 2003) and PG99-465 (Moreno *et al.*, 2000), are not truly specific for the individual VPAC/PACR subtypes, as was clearly demonstrated in the characterisation studies described in chapter one. For example, PG99-465 (the reportedly $VPAC_2R$ antagonist) had a particularly complex pharmacological profile, with different effects at the individual VPAC/PAC receptor subtypes and variable responses between the two functional assays used in the characterisation studies (calcium and cAMP). Therefore, to fully delineate the precise physiological roles and functions of the individual receptors, VPAC/PACR ligands which are truly selective, potent and ideally non-peptide must be found. The need to identify such compounds has been recognised by many researchers in the field (Vaudry *et al.*, 2000; Voice *et al.*, 2001; Laburthe & Couvineau, 2002).

2.1.2. Selection of the $VPAC_2R$ as a target for HT-screening

As VPAC/PAC receptors are thought to be involved in a variety of physiological processes in both normal and disease states, all three subtypes are therefore potentially attractive targets for HT-screening, with the principal aim of identifying potent, non-peptide, selective modulators of receptor function. Within our institute, the $VPAC_2R$ was of particular interest as colleagues in our group had previously been involved in collaborative studies investigating the role of this receptor in the control of circadian activity rhythms using receptor transgenic mice (Shen *et al.*, 2000; Harmar *et al.*, 2002). As described previously (general introduction, p 42), these studies examined running wheel activity of $VPAC_2R$ knock-out mice under various lighting regimes and clearly demonstrated an essential role for this receptor in maintaining normal circadian rhythms of activity (Harmar *et al.*, 2002). In the absence of a strong endogenous circadian rhythm (determined under constant darkness), the activity profiles of these $VPAC_2R$ null mice were

shown to be exquisitely controlled by the lighting schedule. The *in vivo* data identifying a role for the $VPAC_2R$ in circadian rhythm control has been reinforced by *in vitro* electrophysiological brain slice studies, comparing the responses of circadian clock (SCN) neurons from the knock-out and wild-type mice to various $VPAC_2R$ ligands (Reed *et al.*, 2002; Cutler *et al.*, 2003). As indicated from these studies, $VPAC_2R$ selective ligands can modulate the normal activity of SCN neurons. We therefore hypothesised that $VPAC_2R$ selective antagonists, may be of therapeutic value in treating circadian rhythm disorders, such as advanced and delayed sleep phase syndromes, shift work sleep disorder and jet lag. Traditional pharmacological treatments for such disorders include benzodiazepines and melatonin (Turek & Gillette, 2004). The use of benzodiazepines to treat such disorders has proven to be problematic as a consequence of the side effects associated with their long term use, including increased tolerance and dependence (Ebert *et al.*, 2006). Although melatonin treatment has been shown in several studies to help control sleep/wake cycles, the effectiveness of this treatment is often associated with a large degree of variability (Arendt, 1998; Turek & Gillette, 2004). In addition, melatonin modulation of the sleep/wake cycle is usually only observed when it is taken in large doses and its effectiveness appears to be critically dependent on the time of administration in the circadian cycle (Turek & Gillette, 2004; Pandi-Perumal *et al.*, 2005). More recently several new agonists have been developed that selectivity target melatonin receptors, surpassing the potency, selectivity and stability of melatonin itself. Examples of such drugs include the Takeda compound Ramelteon (TAK-375), LY156735 and agomelatine (Turek & Gillette, 2004). Of these drugs, Ramelteon was licensed by the FDA in 2005 and is currently in clinical use. In the absence of a diversity of treatments, investigations into the potential use of $VPAC_2R$ antagonists as treatments for circadian rhythm disorders could provide a novel mechanism that may prove more effective than existing treatments.

2.1.3. Industrial interest in the $VPAC_2R$ as a drug target

The selection of the $VPAC_2R$ as a target for drug discovery is by no means unusual, given that it is a member of the GPCR superfamily (general introduction, p 12) and as such, is part of one of the most 'druggable' target groups in current drug discovery programmes. The pharmaceutical industry's focus on GPCRs has generally proven productive, with approximately one third of all the small molecule drugs available targeting these receptors (Figure 2.1.1). However, upon examination

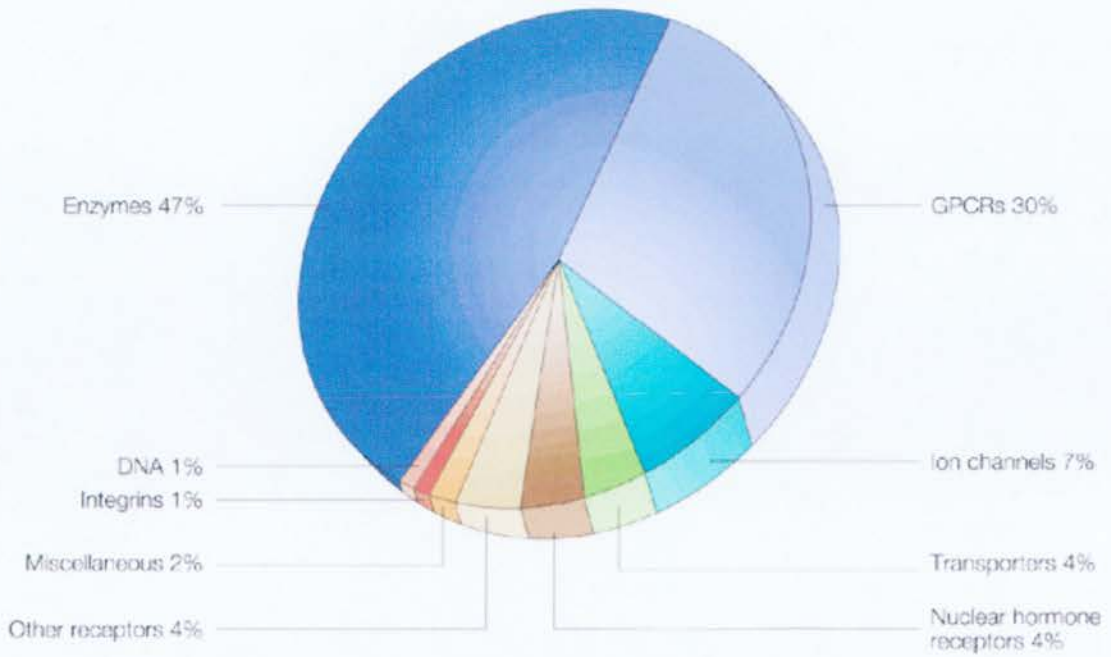

Figure 2.1.1 Pie chart representation of the proportions of marketed small-molecule drug targets by biochemical class (Hopkins & Groom, 2002).

of successful industrial projects that have targeted the Group B GPCRs specifically, novel non-peptide ligands have been developed for only a small proportion of these receptors (Table 2.1.1).

The identification of selective $VPAC_2R$ ligands has proven in recent years to be attractive to some industrial companies, with Hoffman La Roche and more recently Bayer, attempting to develop $VPAC_2R$ selective ligands (Xia *et al.*, 1997; Yung *et al.*, 2003). However, the $VPAC_2R$ ligands identified were all peptides and although potent, showed relatively low selectivity over the other VPAC/PAC receptors, especially when compared to existing ligands such as maxadilan (see chapter one results). From published studies and results presented in this thesis, there is still a clear paucity of truly selective $VPAC_2R$ antagonists, which contrasts with the $VPAC_1$ and PAC_1 receptors, for which PG97-269 and M65 respectively are selective, potent, but peptide antagonists. The only reportedly specific antagonist for the $VPAC_2R$ is the peptide PG99-465 which in our hands was not selective, potentially compromising its value as a tool with which to modulate and study receptor activity and function. Therefore we undertook a collaborative study with Astellas Pharma Inc. (formerly the Fujisawa Pharmaceutical Company), to develop and carry out an HT-screening project in order to identify potential $VPAC_2R$ antagonists from the company's compound libraries.

Drug development status of peptide and nonpeptide ligands targeting Class B G-protein-coupled receptors[a]						
Receptor target	**Indication**	**Agonist or antagonist**	**Name**	**Peptide**	**Company**	**Status**
Peptide ligands						
Calcitonin	Osteoporosis	Agonist	Miacalcin	Salmon calcitonin	Novartis	On market
	Paget's disease	Agonist	Cibacalcin	Human calcitonin	Novartis	On market
	Hypercalcemia	Agonist	Calcimar	Salmon calcitonin	Rhone-Poulenc Rorer and Aventis	On market
PTH	Osteoporosis	Agonist	Forteo	PTH(1–34)	Lilly	On market
			PREOS	PTH(1–84)	NPS	Phase III
GLP-1	Type II diabetes	Agonist	Exenatide	Exendin-4	Amylin and Lilly	Phase III
			Liraglutide	GLP-1 analogue	Novo Nordisk	Phase III
			CJC-1131	GLP-1 analogue	ConjuChem	Phase I and II
Secretin	Autism	Agonist	RG1068	Porcine secretin	RepliGen	Unknown
Nonpeptide ligands						
CGRP	Migraine	Antagonist	BIBN4096BS	NA	Boehringer Ingelheim	Phase II
CRF_1	Depression, anxiety, IBS	Antagonist	Numerous	NA	Numerous	Phase I/II
Glucagon	Type II diabetes	Antagonist	Numerous	NA	Numerous	Unknown

[a]Abbreviations: CGRP, calcitonin gene-related peptide; CRF, corticotropin-releasing factor; GLP, glucagon-like peptide; IBS, irritable bowel syndrome; NA, no PTH, parathyroid hormone

Table 2.1.1 Summary of non-peptide ligands identified for group B GPCRs from the pharmaceutical industry and their stage of progress in the drug discovery pipeline (Hoare, 2005).

2.1.4. HT-screen selection

Following the identification of the $VPAC_2R$ as a target for HT-screening, the normal process would include pharmacological characterisation of the receptor. Clearly, extensive characterisation of this receptor subtype, in addition to the $VPAC_1$ and PAC_1 receptors, had already been performed with a range of peptide agonists and antagonists (chapter one). Additionally, as the characterisation studies had been performed using cell based, 96-well format, functional assays (cAMP and calcium) on the FlexStation®, both assays were amenable to miniaturisation to a 384-well HT format for the FLIPR® workstation. The pharmacological outputs (agonist ROP, antagonist potencies) from both assays were consistent and indicated that monitoring either intracellular messenger would be possible when establishing screening studies for the $VPAC_2R$. From examination of the protocols for both assay types, the calcium assay was selected as the most appropriate screening assay for these studies, due to the simplicity of the procedure, the shorter duration of the assay and the lower cost of this assay. In addition, measurement of intracellular calcium fluxes in FLIPR® assays has a proven track record in successful HT-studies, being described as a 'universal approach to screening small-molecule libraries against GPCRs' (Filmore, 2004).

2.1.5. HT-screening

As will be discussed in this chapter the calcium assay was miniaturised and optimised from the 96-well FlexStation® format to the 384-well format for the FLIPR® workstation of the Astellas laboratories in Tsukuba (Japan). Using the CHO-hVPAC$_2$R cell line characterised in chapter one, HT-screening of a large proportion of the company's compound library (~ 100,000 compounds) was performed and potential VPAC$_2$R antagonists identified. A counter-screening assay for the FLIPR® was also established using the CHO-hVPAC$_1$R cell line. Further evaluation of the potency and selectivity of hit compounds was performed using both the FLIPR® and the FlexStation®.

2.2. Results

2.2.1. HT-screening for hVPAC$_2$R antagonists

From the results presented in chapter one, although a clear shift to lower potency was observed for agonists in the 96-well FlexStation® calcium assay when compared to the cAMP assay, no differences were found in agonist ROPs for any of the VPAC/PAC cell lines. This suggests that measuring either second messenger is potentially appropriate for HT-screening of hVPAC$_2$ receptors. However, for hVPAC$_2$R antagonist screening of the Fujisawa compound libraries, the calcium assay was selected as the most appropriate assay to utilise due to the fact it is a simpler, less time consuming and more cost effective assay to run. HT-screening was performed using the Calcium 3 dye and the FLIPR® workstation. In principle, the FLIPR® calcium assay is identical to its FlexStation® counterpart, however the FLIPR® assay has the added advantage of being ultra HT-compatible, due to the ability of the workstation to simultaneously perform compound additions across an entire 384-well assay plate, whilst reading fluorescence levels in every well.

2.2.2. $[Ca^{2+}]_i$ assay miniaturisation and optimisation for the FLIPR®

2.2.2.1. Cell density

Miniaturisation and optimisation of the hVPAC$_2$R FLIPR® assay involved identifying a suitable cell density, as well as defining the optimal concentrations of calcium dye, agonists and library compounds. Following the standard Fujisawa protocol for calcium assays using transfected CHO cell lines, the CHO-hVPAC/PACR cells were seeded at a density of 1.5 x 10^4 cells per well. Initially, all assay characterisation studies (using VIP and PG99-465) were performed using the recommended dye concentration (1x) and then the optimum concentration was determined. The concentration of the calcium dye can either be increased in an attempt to enhance a small response or, in the case of large fluorescent signals, it can be reduced for economic purposes.

2.2.2.2. Agonist concentration

In the first FLIPR® study CHO-hVPAC$_2$R cells were exposed to increasing concentrations of VIP. The consistency in response size for each VIP concentration

can be seen when the fluorescence traces produced by each concentration are compared; Figure 2.2.1 shows responses to each VIP concentration, tested in 8-well replicates. For each concentration, the responses produced were averaged on the FLIPR® and the resulting composite traces are shown superimposed in Figure 2.2.2a. The average response to each VIP concentration was calculated (max-min reduction) and a concentration response curve produced (EC_{50} = 20.7 nM (n = 1); Figure 2.2.2b). This value was almost identical to the VIP EC_{50} generated in the CHO-h$VPAC_2R$ calcium assay using the FlexStation® (14.1 ± 0.9 nM (n = 6); chapter one, Table 1.2.2, p 110). For screening purposes, the most appropriate agonist concentration should produce a maximal response without saturating the receptor, therefore a VIP concentration between 50 and 100 nM was generally utilised.

2.2.2.3. Antagonist studies

In inhibition studies with PG99-465, the reportedly selective $VPAC_2R$ antagonist (Moreno *et al.*, 2000), two concentrations of VIP (60 and 100 nM) were tested. Using the averaged responses for each set of replicate wells, inhibition curves were generated for PG99-465 antagonism of VIP induced responses from the CHO-h$VPAC_2R$ cell line (Figure 2.2.3). PG99-465 inhibited the VIP stimulated fluorescent responses in a concentration dependent manner, with the higher antagonist concentrations (> 1 μM) producing almost complete inhibition. The IC_{50} values of 116 nM (60 nM VIP) and 150 nM (100 nM VIP) generated from the inhibition curves were very similar for both VIP concentrations. In the FlexStation® calcium assay, PG99-465 had an IC_{50} of 4.4 ± 0.8 nM (n = 6) for the h$VPAC_2R$ (chapter one , Table 1.2.3, p 118), which was approximately 30 times more potent than that observed using the FLIPR® assay. One possible explanation which could have accounted for the change in antagonist potency was the difference in pre-incubation time. Routinely in the FlexStation® assays, antagonists were pre-incubated with cells for 10 min prior to agonist addition, whereas in the FLIPR® assay, this was reduced to 2 min due to constraints associated with the established FLIPR® protocol. To determine if shortening the pre-incubation period contributed to the change in antagonist potency, the effect of changing the pre-incubation time (from 2 - 20 min) on the level of inhibition of the VIP response was investigated. As the duration of the pre-incubation period increased, so did the extent to which PG99-465 (10 nM) inhibited the VIP (100 nM) induced calcium response (Figure 2.2.4a).

Following a 2 min pre-incubation, PG99-465 had reduced the VIP response by 51 %. The level of inhibition increased in a time dependent manner, with the 20 min pre-incubation period completely ablating the VIP response. To further ascertain whether the difference in incubation times between assays was responsible for the change in PG99-465 potency, a full inhibition curve was run on the FlexStation® using a reduced antagonist pre-incubation period of 2 min. The resulting curve had an IC_{50} of 8.9 nM for PG99-465 (Figure 2.2.4b), which was marginally less potent (2 fold) than the IC_{50} generated using the 10 min pre-incubation (4.4 ± 0.8 nM (n = 6) nM; Table 1.2.3, p 118). Therefore, although the shorter pre-incubation appeared to partially contribute to the reduction in PG99-465 potency, it was not fully sufficient to explain the 30 fold shift between the FlexStation® and FLIPR® assays.

2.2.2.4. Calcium dye concentration

For a number of cell lines it is possible to alter the concentration of calcium dye added to the cells in order to maximise the signal. To investigate the effect of calcium dye concentration on agonist response sizes using CHO-hVPAC$_2$R cells, fluorescence responses to VIP (100 nM) were measured for a range (0.75x – 2x) of dye concentrations (Figure 2.2.5a). The magnitude of the VIP response increased with dye concentration, with 2x dye producing a 3 fold larger signal than the recommended dye concentration. In this particular assay, the response to VIP (100 nM) with 1x dye (~ 2,000 RFU) was approximately 5 times smaller than in the previous experiments (Figures 2.2.2 and 2.2.3). As a consequence of this potential variability, the 2x dye concentration was selected for screening, to maximise the signal produced.

2.2.2.5. Concentration of library compounds

The final factor that was assessed before screening commenced was the vehicle in which the library compounds were stored. With the library compounds prepared in 100 % DMSO (0.25 mg/ml), the final concentration of the compounds that could be used was ultimately dependent upon the percentage of DMSO that could be added to the cells without causing any toxic effects. The effect of DMSO concentration on the size of the VIP (100 nM) response from CHO-hVPAC$_2$R cells was examined over a 20 fold range from 0.1 - 2 % (Figure 2.2.5b), which covers the

lower and upper extremes generally used during screening. No major alteration in the VIP induced response was apparent with any of the DMSO concentrations tested (Figure 2.2.5b). As a compromise between DMSO strength and compound concentration, 0.5 % was chosen as the final in-well DMSO concentration to be used during screening. Consequently 4-mix library compounds (0.25 mg/ml per compound in 100 % DMSO) were diluted in inorganic salts buffer (1 in 50) prior to use, generating a 2 % DMSO containing solution which was then diluted during screening (1 in 4 dilution), to give the defined DMSO concentration of 0.5 % and ultimately a compound concentration of 1.25 μg/ml.

In summary, the calcium assay for screening library compounds on the FLIPR® was performed using 384-well clear bottom, black walled plates containing CHO-hVPAC$_2$R cells (1.5 x 10^4 cells per well; 50 μl) seeded on the previous day. The assay was performed as described in the methods (section B.3.2., p 65), with 100 nM VIP selected as the optimal agonist concentration for screening, as the potency of the reference antagonist PG99-465 was unaltered, and the signal size was larger than that obtained with 60 nM VIP. This was expected to facilitate the identification of antagonists during screening of the compound libraries. The calcium dye was used at 2x the recommended concentration (50 μl/well) and library compounds diluted before addition to the cells (20 μl/well), to give a final in-well concentration of 1.25 μg/ml/compound in 0.5 % DMSO. Library compounds were pre-incubated with the CHO-hVPAC$_2$R cells for 2 min before agonist addition, after which fluorescence levels were monitored for a further 3 min.

2.2.3. Screening results

2.2.3.1. Screening data and hit identification

HT-screening for hVPAC$_2$R antagonists was performed using the Fujisawa 'F' and 'M' libraries, which contained a total of 98,240 compounds. The initial screening was performed using library compounds stored in a 4-mix format (4 compounds per well), with compounds tested in duplicate. On each 384-well assay plate, 640 compounds were tested in total, with individual columns designated for VIP alone and vehicle only. For each plate, fluorescence levels were recorded in every well for the entire duration of the 5 min assay. An example of the data generated from a single 384-well assay plate, along with the corresponding fluorescence traces for each well is shown in Figure 2.2.6. Changes in fluorescence from each well (max-min; Figure 2.2.6a) were converted to show the percentage

change from the average VIP response (Figure 2.2.6b) and finally, the percentages from duplicate wells were averaged (Figure 2.2.6c). On the plate shown, fluorescence responses of the CHO-hVPAC$_2$R cells to VIP alone, following pre-incubation with compound buffer (ISB containing 2 % DMSO), were consistent at 6098 ± 234 (mean ± SEM; RFU) and demonstrated a low level of variability of 3.8 % (Figure 2.2.6, column 21). The minimal responses to the VIP buffer (ISB with BSA; 1 mg/ml) following a pre-incubation with compound vehicle, were similarly low between wells (1841 ± 92 RFU), showing 5.0 % variability (Figure 2.2.6, column 22). Prior to screening, it was decided that hit compounds identified from the 4-mix library would be split into 'first' and 'second' priority compounds. 'First priority' compounds were those that demonstrated an average inhibition of the VIP response of more than 60 %, whereas the 'second priority' compounds were those which produced an average inhibition between 50 - 60 %. From the particular assay plate shown in Figure 2.2.6 no hit compounds were identified.

2.2.3.2. Consistency of responses

As the number of plates screened increased, the magnitude of the VIP response varied, as is illustrated in Figure 2.2.7 which shows the fluorescence traces from a CHO-hVPAC$_2$R cell plate treated only with VIP (100 nM). The percent deviations from the average VIP response (for the whole plate (RFU): 7730 ± 78; 1 %) are shown for all wells in Figure 2.2.7b, with negative values indicative of a response below the average. On this particular plate, although the overall variability appeared small (1 %), this masked the fact that the size of the VIP response ranged from 87 % above the average (well D9) to 65 % below (well P18), with the most variable responses produced in the outer wells of the plate. At first, it was proposed that the variability may have arisen from inefficient liquid transfer as a consequence of the re-use of the same FLIPR® tips for 6 - 8 plates. In an attempt to address this issue, the use of new tips with every assay plate was tested (Figure 2.2.8a), as was the use of silicone coated tips (Figure 2.2.8b). However, neither of these measures eliminated the problem and the between-well variability in VIP response size persisted.

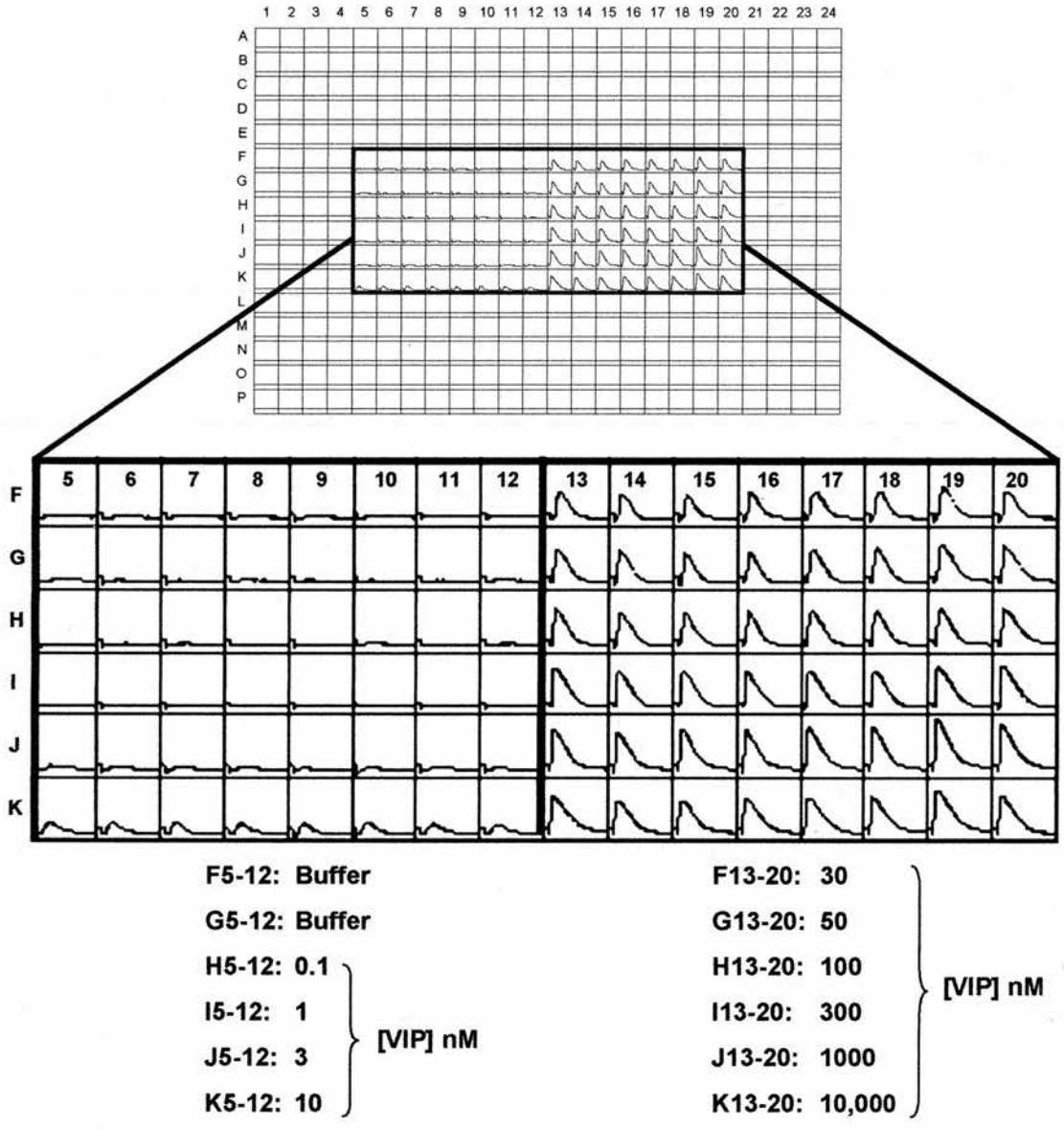

Figure 2.2.1 **Fluorescence traces from the FLIPR® produced following stimulation of CHO-hVPAC$_2$R cells with VIP.** Cells were seeded into 384 well plates (1.5 x 10^4 per well) and left overnight. Following the removal of medium and addition of calcium assay dye (40 µl), cells were stimulated with a range of VIP concentrations (0.1 nM - 10 µM; 20 µl per well; 3 x final assay concentration).

(a)

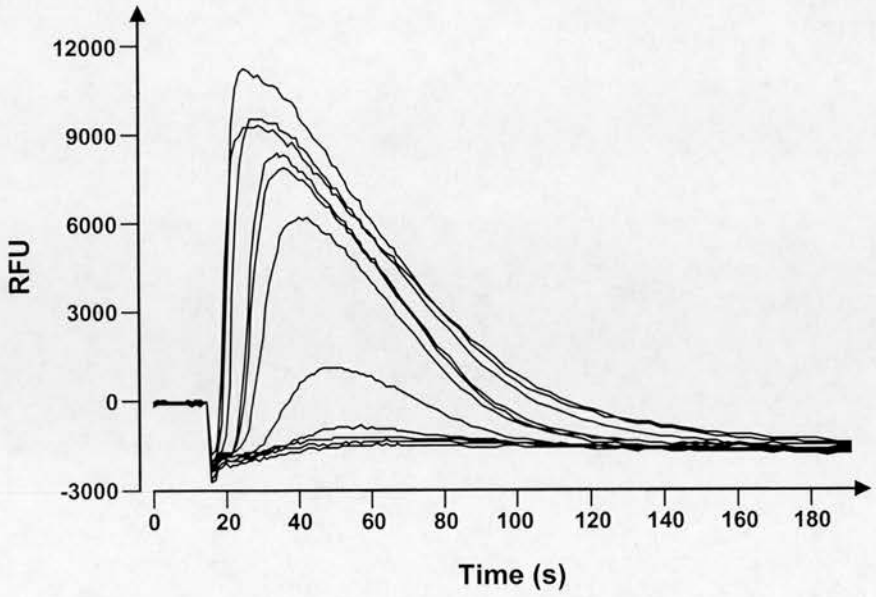

(b)

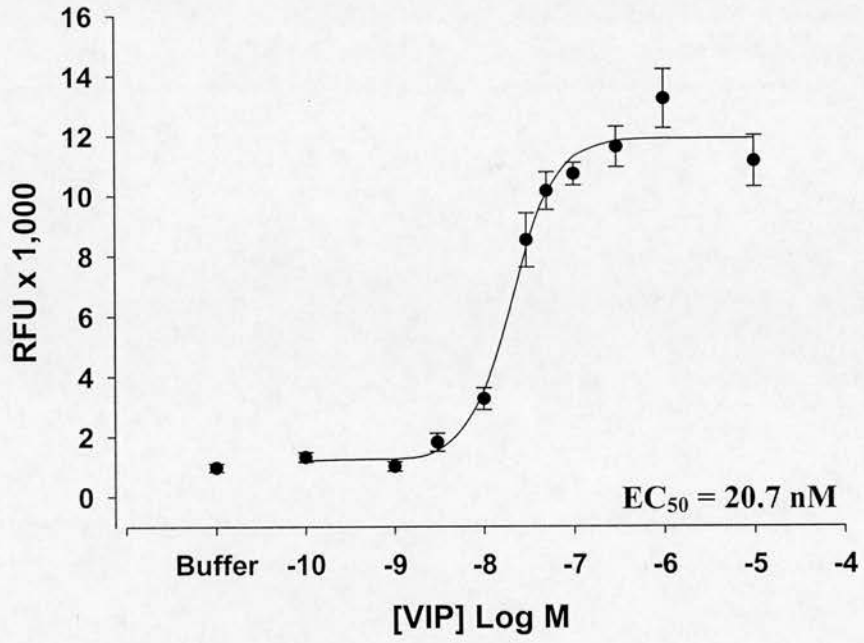

Figure 2.2.2 **VIP produced a concentration dependent increase in fluorescence in CHO-hVPAC$_2$R cells.** VIP solutions were added to CHO-hVPAC$_2$R cells and the resulting fluorescence levels measured by the FLIPR®. From max-min analysis of the data traces shown in (**a**), a concentration response curve for VIP was generated, giving an EC_{50} of 20.7 nM (**b**).

(a)

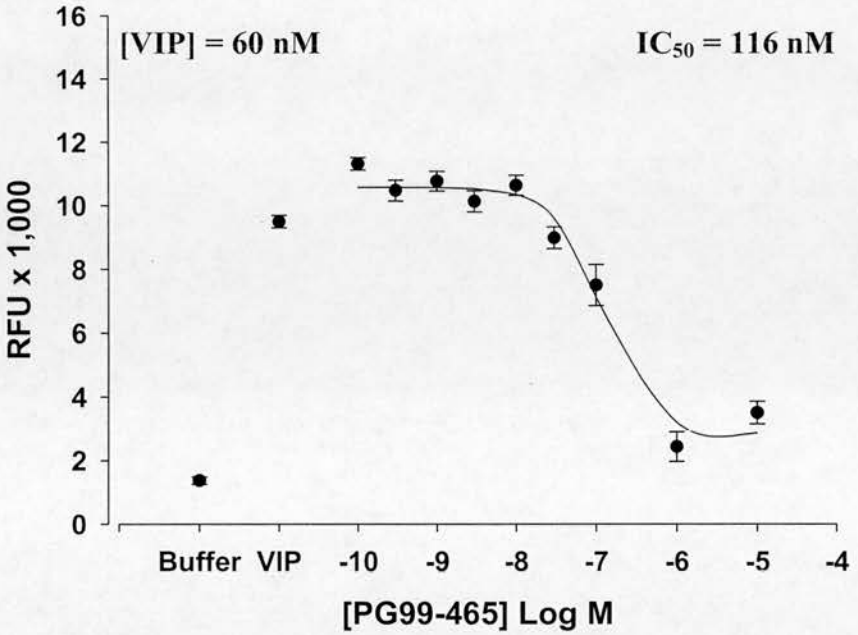

(b)

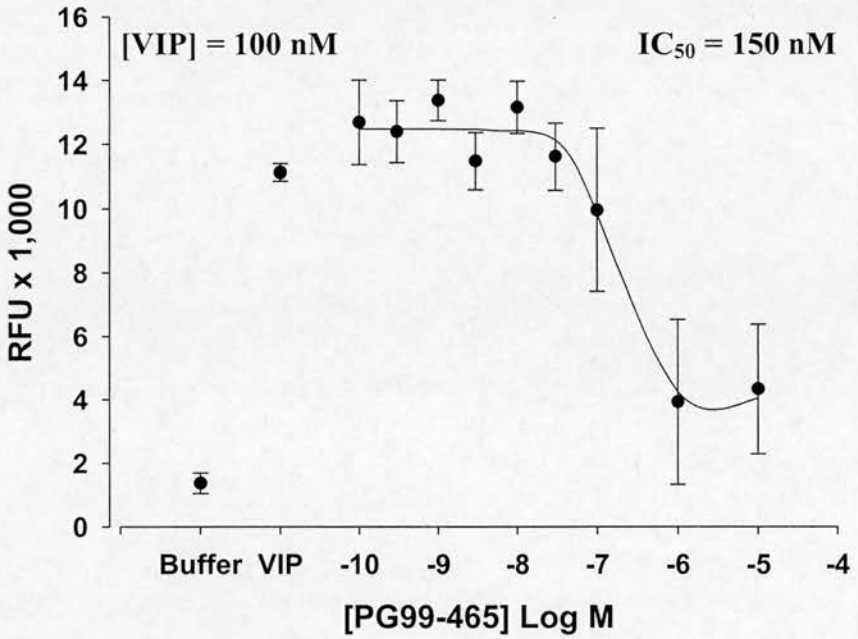

Figure 2.2.3 **Inhibition of VIP induced hVPAC$_2$R mediated calcium responses by PG99-465.** Using the FLIPR® calcium assay, PG99-465 (FAC: 0.1 nM to 10 μM) was added to CHO-hVPAC$_2$R cells (1.5 x 10^4 per well) and pre-incubated for 2 min. VIP was then added to the appropriate wells at a concentration of either 60 nM (**a**) or 100 nM (**b**). Responses (max-min) were averaged for each set of 8 well replicates and inhibition curves were generated.

(a)

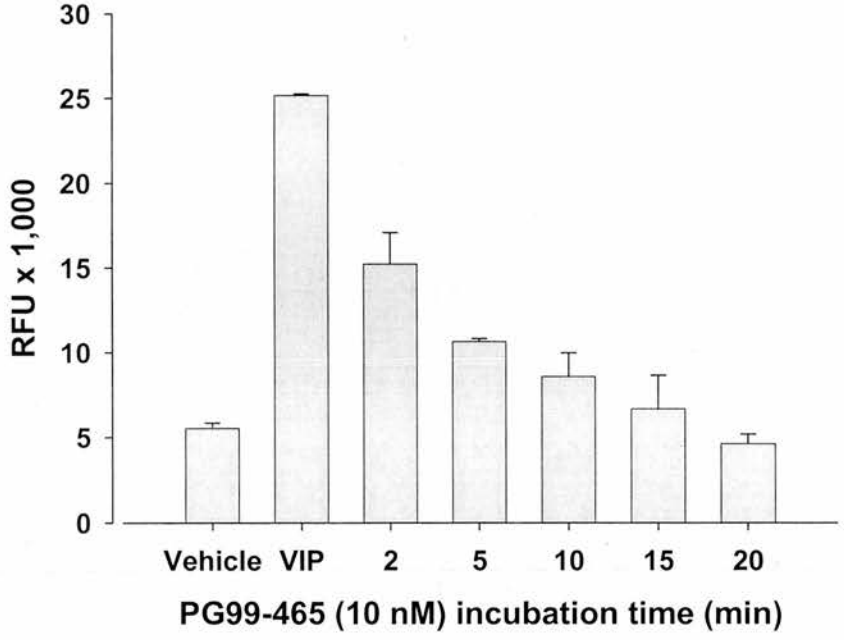

(b)

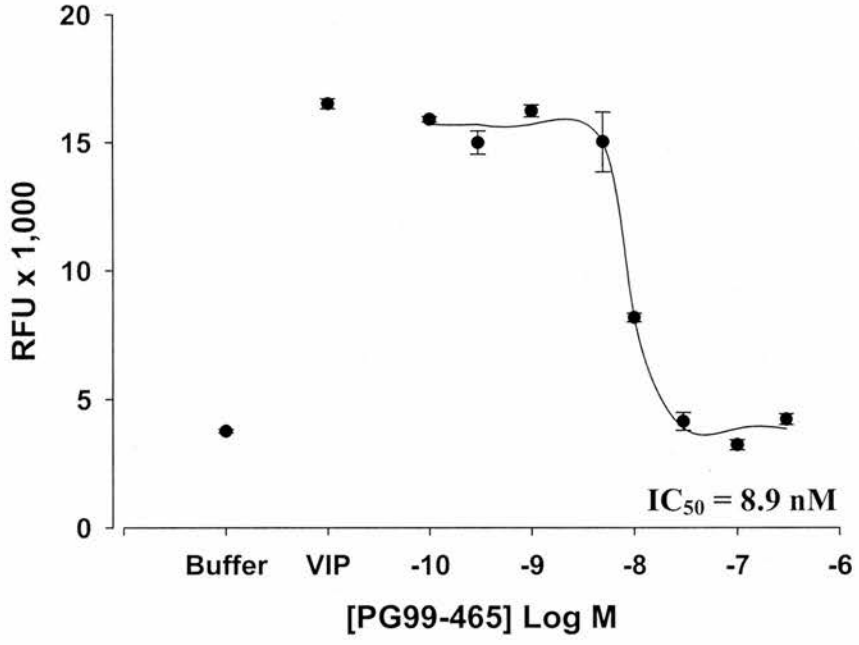

Figure 2.2.4 **Effect of the duration of the PG99-465 pre-incubation period on VIP induced calcium responses in CHO-hVPAC$_2$R cells.** Using the FlexStation® calcium assay, the effect of the length of the pre-incubation period on the potency of PG99-465 (10 nM) to inhibit VIP (100 nM) induced responses (from CHO-hVPAC$_2$R cell) was determined (**a**). PG99-465 (0.1 – 300 nM) was pre-incubated with the cells for 2 min, followed by the addition of VIP (100 nM) and measurement of resulting fluorescent changes (**b**).

(a)

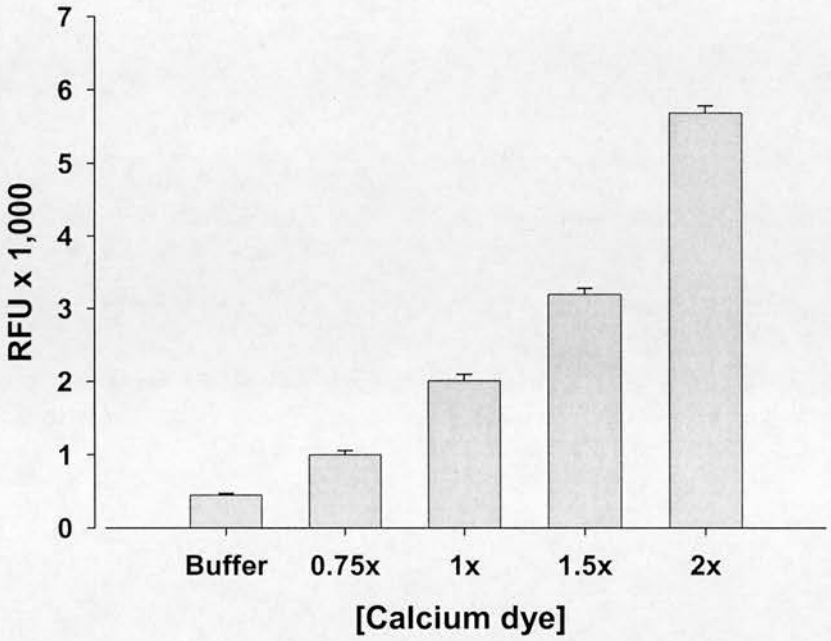

(b)

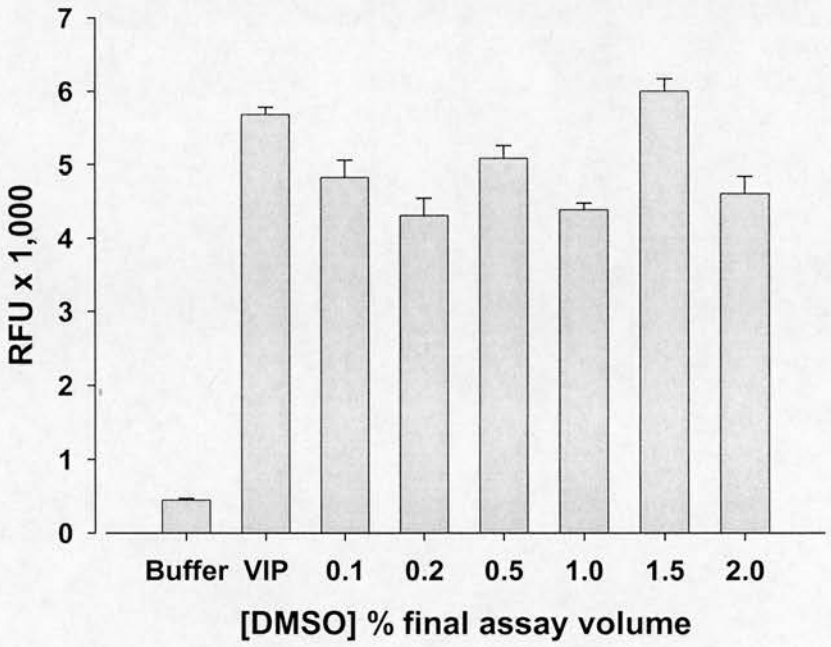

Figure 2.2.5 **Effect of calcium dye and DMSO concentration on the VIP stimulated calcium response in CHO-hVPAC$_2$R cells using the FLIPR®.** Cells were stimulated with VIP (100 nM) in the presence of increasing calcium dye concentrations (**a**). DMSO (0.1 – 2 % final concentration) had no effect on the VIP (100 nM) induced calcium response using CHO-hVPAC$_2$R cells (**b**).

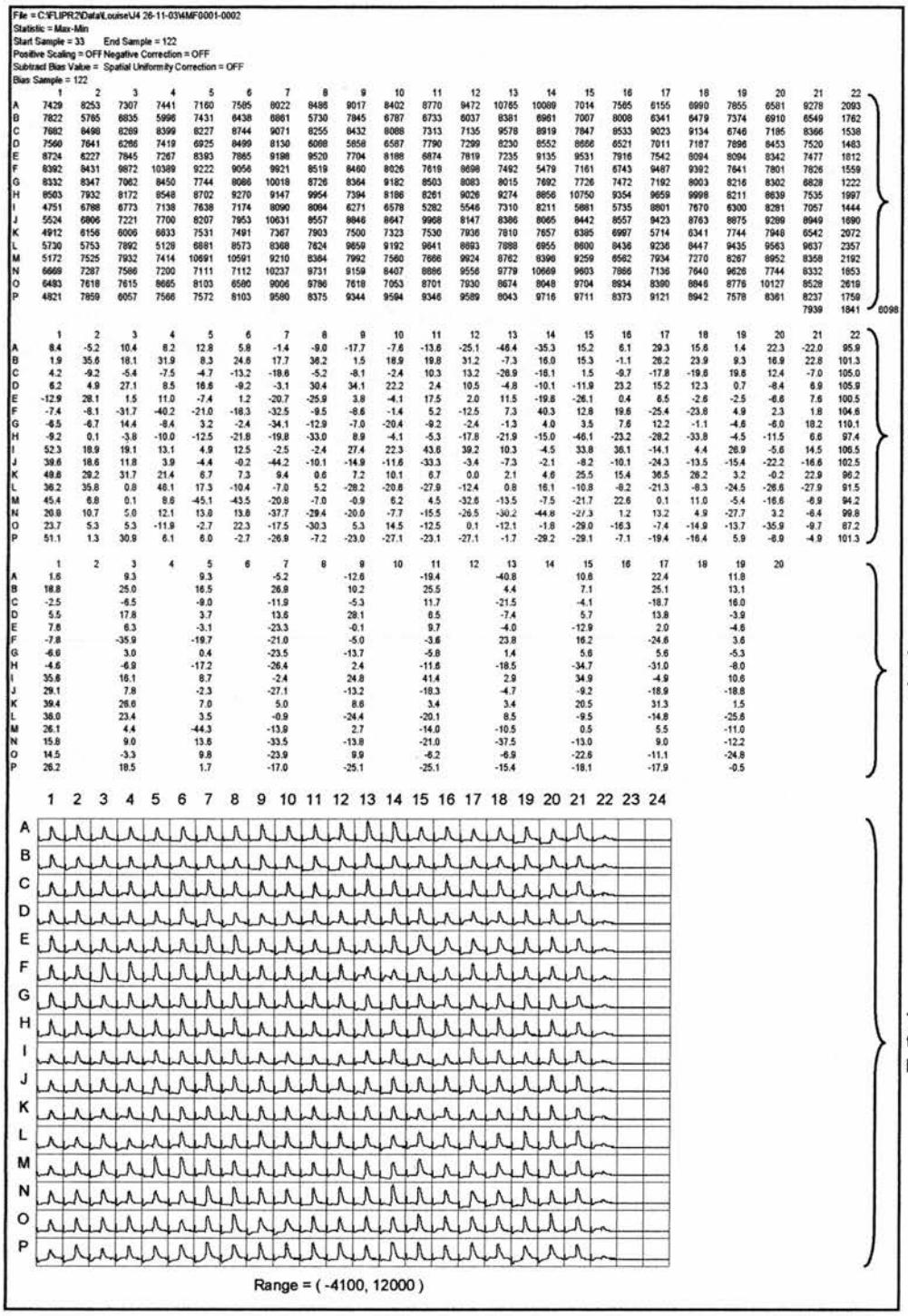

Figure 2.2.6 **An example of 384-well data generated from the screening of an individual compound library plate.** Raw fluorescence counts (from max-min analysis) are shown (**A**), followed by the values expressed as a percentage (**B**) of the VIP alone response (column 21). The average levels of inhibition from duplicate wells were also calculated (**C**). Finally, the traces generated from the individual wells are shown in the lower section (**D**).

(a)

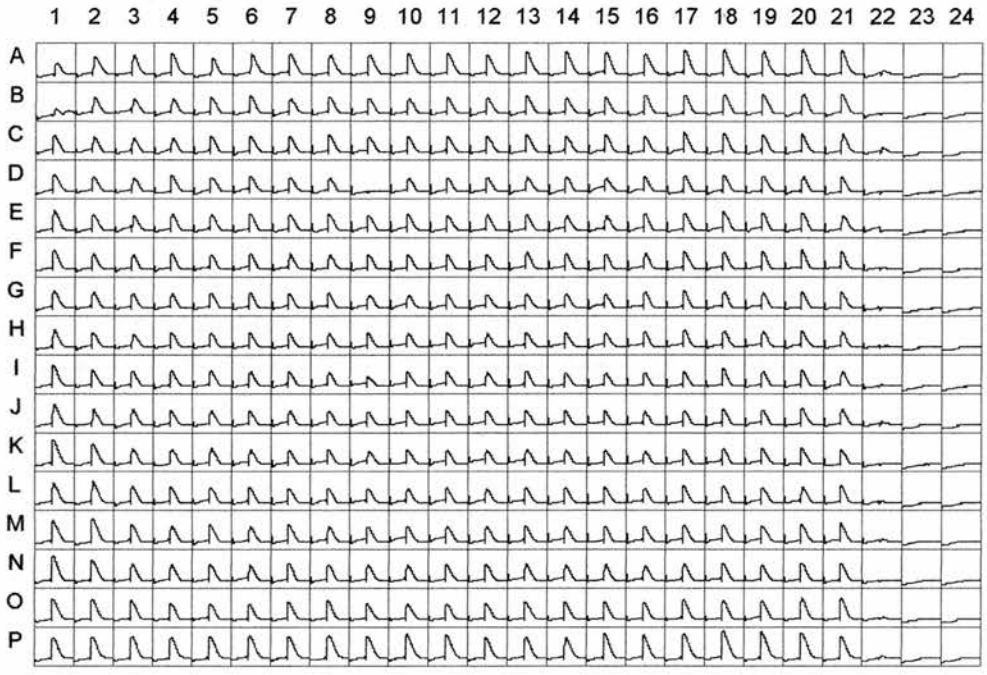

(b)

	1	2	3	4	5	6	7	8	9	10	11	12	13	14	15	16	17	18	19	20	21
A	27	-10	-23	-26	4	-16	-21	-21	-20	-22	-23	-16	-33	-33	-29	-20	-41	-46	-39	-42	-38
B	61	4	19	14	3	1	7	4	8	5	2	4	-7	8	3	-13	-9	-13	-16	-15	-14
C	-9	10	11	15	6	-1	2	-7	4	3	0	-1	-6	2	0	5	-18	-15	-6	-9	-12
D	-4	15	18	6	14	11	15	24	87	23	18	18	19	11	23	17	6	3	11	12	9
E	-23	1	11	2	9	0	3	2	8	4	8	12	8	6	17	1	-3	-11	-5	-4	14
F	-20	1	9	3	14	7	10	11	8	8	6	7	-2	3	10	7	-5	-2	-5	-9	-3
G	-7	4	9	13	11	9	10	10	17	22	16	20	13	15	17	2	-3	4	5	8	6
H	-8	6	19	7	13	11	13	15	8	17	11	21	7	11	19	6	3	1	8	6	8
I	-23	4	8	3	10	11	13	20	41	14	14	19	9	18	23	21	12	-1	11	5	12
J	-26	8	3	10	13	15	18	17	18	15	12	19	12	18	15	22	11	5	12	0	8
K	-44	-21	11	13	6	14	15	14	22	17	17	20	4	20	13	26	7	8	9	7	9
L	-23	-30	-2	3	7	3	9	9	17	14	10	17	8	6	0	13	-2	0	9	9	1
M	-32	-47	-7	2	-6	6	-9	7	7	5	5	8	1	9	7	10	-3	1	0	-6	-9
N	-50	-28	-3	5	-1	8	-12	-1	3	12	-2	1	3	8	5	13	-5	-6	10	-13	-9
O	-33	-25	-15	1	7	3	-8	-16	6	1	4	4	-7	-6	-5	-5	-17	-15	-10	-26	-31
P	-26	-27	-33	-26	-37	-40	-37	-47	-33	-48	-45	-25	-29	-26	-52	-39	-53	-65	-60	-56	-35

Figure 2.2.7 **Variation in response size to VIP stimulation of CHO-hVPAC$_2$R cells.** In an individual 384-well plate, CHO-hVPAC$_2$R cells were stimulated with VIP (100 nM) and the resulting change in fluorescence measured (**a**). The percentage change in response size, compared to the average response for the entire plate, is shown for individual wells (**b**).

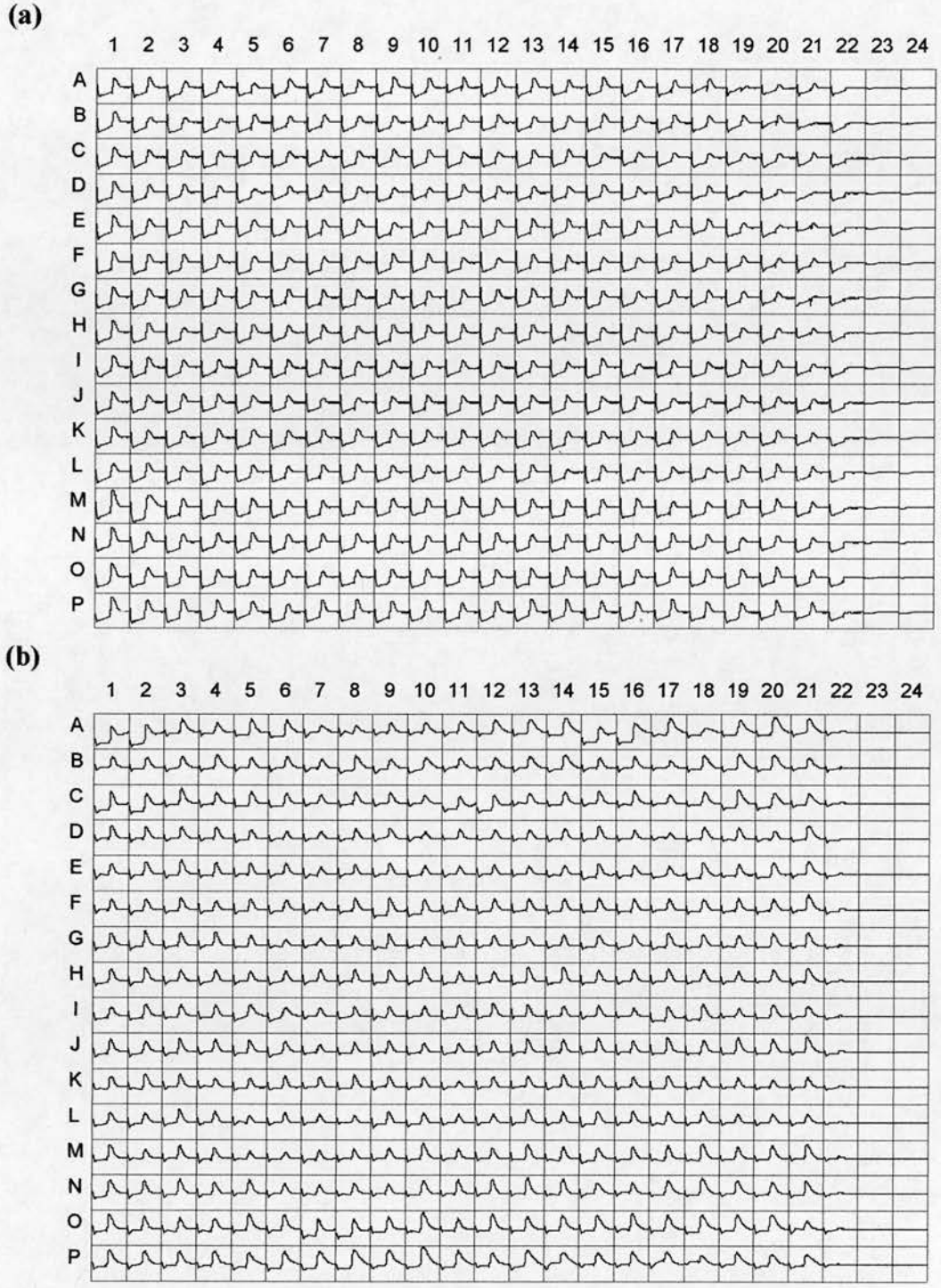

Figure 2.2.8 **Compound plates assayed on the FLIPR® using new tips and silicone-coated tips.** In an attempt to reduce the variation in the VIP response on the assay plate, a new box of tips were utilised (**a**) as were silicone-coated tips (**b**). However, the resulting VIP responses remained small and variable, with the average VIP alone response being 1800 ± 223 (**a**) and 5008 ± 203 (**b**).

2.2.3.3. Reproducibility studies of hit compounds

As a result of variability in the VIP response size, a large number of first and second priority hits compounds were identified from the initial round of library screening (153 assay plates in total). From the 4-mix 'F' library, 69 first priority and 45 second priority hits were identified (from 68 plates). Consequently, a total of 456 'F' library compounds were then re-tested in reproducibility studies to verify the initial hit categorisation. First and second priority hits identified from the 4-mix 'M' library totalled 132 and 136 respectively (from 85 plates). For reproducibility studies, this would mean 1072 individual compounds would need to be tested. The large numbers of 'hits' identified in the 'M' library coincided with the increase in the degree of variability associated with the VIP response elicited from the CHO-hVPAC$_2$R cells. For this reason a number of the 4-mix 'M' plates had to be re-screened, which was ultimately performed at a later stage by colleagues in Japan, so I will focus on the data from the 'F' library alone. As discussed in the materials and methods (section B.3.2.1, p 66), in preparation for reproducibility studies, samples were taken from the 'individual compound' libraries (1 mg/ml; 100 % DMSO) and stored at -20 °C until use (1.5 µl/eppendorf). On the assay day, samples were diluted (1 in 200) with inorganic salts buffer (5 µg/ml; 0.5 % DMSO) and added to 384-well compound plates (5 replicates per sample). Individual compounds were then tested for their ability to inhibit VIP (100 nM) induced responses from CHO-hVPAC$_2$R cells, using the same FLIPR® calcium assay. The majority of the first priority compounds from the 'F' library (276 in total) were then tested in 2 - 3 independent experiments depending on sample availability, with the average percentage inhibition for each compound shown in Table 2.2.1. From these studies, the twelve compounds (highlighted in Table 2.2.1) which produced the strongest and most consistent inhibition of the VIP induced response were characterised more fully in subsequent studies (see below). As can be seen from Table 2.2.1, a number of compounds which produced similar levels of inhibition to the weaker of the twelve highlighted compounds were not selected for further analysis. This was because only a limited number of compounds could be fully evaluated in the following studies due to time restrictions.

Compounds from the second priority group (180 in total) were tested only once, as most of the 'hits' proved to be false positives (Table 2.2.2). Although a small number of the second priority compounds (F0443-C09, F0466-F09 and F0466-G05) produced a reasonably strong inhibition of the VIP induced response, these compounds were not examined further in these studies.

Table 2.2.1 Reproducibility study of first priority hits from the 'F' library

Well no.	% inhibtion	SEM	Well no.	% inhibtion	SEM	Well no.	% inhibtion	SEM	Well no.	% inhibtion	SEM	Well no.	% inhibtion	SEM	Well no.	% inhibtion	SEM	Well no.	% inhibtion	SEM
F0025-C07	8.5	12.6	F0165-B09	25.3	5.0	F0289-A01	18.2	6.4	F0325-B10	20.0	15.1	F0457-G04	-4.2	12.9	F0509-A01	7.1	8.4	F0541-B07	29.7	16.3
F0026-C07	21.4	9.7	F0166-B09	15.9	3.5	F0290-A01	18.7	4.9	F0326-B10	8.0	12.3	F0458-G04	22.4	11.1	F0510-A01	7.6	2.3	F0542-B07	30.5	16.1
F0027-C07	32.3	6.6	F0167-B09	31.9	7.5	F0291-A01	21.4	9.6	F0327-B10	12.1	10.2	F0459-G04	20.1	6.7	F0511-A01	6.8	5.4	F0543-B07	31.4	14.1
F0028-C07	31.8	6.4	F0168-B09	23.6	13.0	F0292-A01	23.0	12.6	F0328-B10	17.7	7.0	F0460-G04	18.6	5.6	F0512-A01	8.8	8.1	F0544-B07	32.4	14.9
F0025-C09	25.6	7.9	F0209-C07	18.3	-	F0301-B10	19.8	9.0	F0345-A02	15.3	32.8	F0457-G09	24.1	2.9	F0537-B04	12.8	3.2	F0541-E05	34.9	10.8
F0026-C09	24.8	14.8	F0210-C07	16.6	-	F0302-B10	18.6	6.9	F0346-A02	9.4	22.1	F0458-G09	15.3	2.1	F0538-B04	16.0	5.0	F0542-E05	36.0	11.5
F0027-C09	10.7	27.2	F0211-C07	2.6	-	F0303-B10	20.8	9.7	F0347-A02	12.9	17.2	F0459-G09	16.6	0.8	F0539-B04	4.7	8.8	F0543-E05	27.4	17.9
F0028-C09	31.6	4.6	F0212-C07	-3.2	-	F0304-B10	22.3	6.5	F0348-A02	9.9	13.9	F0460-G09	12.3	1.5	F0540-B04	9.6	4.5	F0544-E05	17.4	11.2
F0025-F04	33.0	5.2	F0209-E09	18.8	-	F0313-A08	18.4	7.6	F0345-A06	57.7	9.3	F0465-G06	13.7	0.3	F0537-B06	-1.1	5.9	F0541-F10	15.4	25.5
F0026-F04	25.0	11.3	F0210-E09	33.8	-	F0314-A08	17.3	8.3	F0346-A06	15.2	15.3	F0466-G06	16.8	1.1	F0538-B06	-4.0	6.7	F0542-F10	19.5	20.7
F0027-F04	25.7	2.0	F0211-E09	35.0	-	F0315-A08	10.2	8.1	F0347-A06	16.9	7.8	F0467-G06	13.1	8.5	F0539-B06	23.6	11.7	F0543-F10	30.5	15.8
F0028-F04	23.6	10.3	F0212-E09	39.0	-	F0316-A08	11.8	9.3	F0348-A06	15.2	14.7	F0468-G06	11.3	5.0	F0540-B06	1.3	4.6	F0544-F10	41.2	9.0
F0025-G08	15.4	6.7	F0213-A02	35.3	-	F0317-B10	6.7	12.7	F0361-B03	5.7	2.6	F0473-A01	13.6	2.4	F0537-C07	-8.3	2.6	F0541-G03	35.9	10.0
F0026-G08	12.6	10.8	F0214-A02	37.1	-	F0318-B10	9.5	10.0	F0362-B03	13.6	23.4	F0474-A01	9.5	8.2	F0538-C07	0.4	1.3	F0542-G03	44.9	4.0
F0027-G08	13.9	10.0	F0215-A02	36.3	-	F0319-B10	16.9	11.5	F0363-B03	5.4	16.5	F0475-A01	13.8	7.0	F0539-C07	0.4	2.1	F0543-G03	39.0	8.1
F0028-G08	11.4	12.4	F0216-A02	34.7	-	F0320-B10	10.9	11.4	F0364-B03	9.8	10.3	F0476-A01	8.3	0.9	F0540-C07	14.7	2.7	F0544-G03	43.2	1.9
F0037-G08	15.0	8.7	F0213-B05	37.4	-	F0317-C02	25.3	11.6	F0409-A05	4.2	16.7	F0473-A03	-6.7	5.9	F0537-D03	13.2	2.4	F0541-G04	32.5	10.1
F0038-G08	58.9	5.8	F0214-B05	36.1	-	F0318-C02	38.7	6.2	F0410-A05	6.8	27.3	F0474-A03	20.1	11.2	F0538-D03	8.9	7.9	F0542-G04	31.1	13.8
F0039-G08	61.6	4.3	F0215-B05	27.6	-	F0319-C02	40.7	7.0	F0411-A05	19.5	33.5	F0475-A03	22.7	7.8	F0539-D03	5.0	6.4	F0543-G04	28.4	14.1
F0040-G08	30.7	4.8	F0216-B05	33.2	-	F0320-C02	30.9	7.0	F0412-A05	5.1	12.0	F0476-A03	20.8	0.4	F0540-D03	3.8	5.2	F0544-G04	32.0	8.8
F0049-G02	26.2	10.4	F0237-B09	13.4	7.8	F0321-A01	36.9	6.1	F0429-B04	19.4	19.0	F0473-A06	22.6	1.9	F0537-E10	5.5	5.1	F0545-B05	32.5	0.5
F0050-G02	9.8	19.7	F0238-B09	2.5	8.6	F0322-A01	36.2	7.2	F0430-B04	25.8	22.2	F0474-A06	19.3	0.3	F0538-E10	9.5	3.6	F0546-B05	23.3	7.5
F0051-G02	15.8	16.6	F0239-B09	16.1	14.7	F0323-A01	38.9	6.9	F0431-B04	32.2	5.8	F0475-A06	18.4	0.7	F0539-E10	8.4	4.6	F0547-B05	19.3	8.9
F0052-G02	18.6	15.7	F0240-B09	26.9	7.9	F0324-A01	32.8	7.7	F0432-B04	21.9	16.5	F0476-A06	15.2	1.8	F0540-E10	7.7	1.1	F0548-B05	17.0	1.8
F0129-D03	34.8	-	F0237-B10	31.0	14.5	F0321-B01	35.7	5.7	F0441-F10	27.5	29.4	F0473-B01	16.5	1.6	F0537-F07	10.6	5.0	F0545-B06	14.1	23.1
F0130-D03	39.9	-	F0238-B10	19.2	9.2	F0322-B01	28.8	6.4	F0442-F10	16.5	17.6	F0474-B01	9.4	0.6	F0538-F07	2.5	4.1	F0546-B06	18.1	15.0
F0131-D03	32.9	-	F0239-B10	26.8	12.0	F0323-B01	16.8	9.1	F0443-F10	45.4	3.6	F0475-B01	13.5	0.8	F0539-F07	13.1	8.4	F0547-B06	12.2	15.0
F0132-D03	27.9	-	F0240-B10	25.0	9.4	F0324-B01	25.3	6.3	F0444-F10	5.2	16.3	F0476-B01	12.9	4.5	F0540-F07	9.9	9.3	F0548-B06	12.9	13.3
F0145-E08	28.4	8.0	F0277-F02	29.3	10.9	F0321-C10	14.7	14.8	F0441-G01	2.5	21.8	F0477-C02	6.2	1.0	F0537-F08	-5.0	10.5	F0545-B07	17.4	-
F0146-E08	62.3	28.0	F0278-F02	25.4	10.1	F0322-C10	5.8	13.8	F0442-G01	3.7	20.2	F0478-C02	6.4	2.5	F0538-F08	-2.0	8.4	F0546-B07	28.5	-
F0147-E08	16.8	12.7	F0279-F02	15.6	7.7	F0323-C10	8.5	14.0	F0443-G01	41.6	7.0	F0479-C02	8.5	2.1	F0539-F08	-23.1	9.1	F0547-B07	32.9	-
F0148-E08	12.2	15.6	F0280-F02	12.7	5.5	F0324-C10	10.3	16.1	F0444-G01	15.7	26.0	F0480-C02	-0.8	10.4	F0540-F08	-24.5	7.4	F0548-B07	45.2	-
F0157-C10	8.4	15.7	F0281-E06	52.7	5.3	F0321-D02	9.1	17.4	F0457-D04	41.1	3.6	F0501-A10	16.6	18.0	F0537-G02	27.5	13.5	F0545-B08	33.4	-
F0158-C10	14.4	8.0	F0282-E06	11.5	-	F0322-D02	23.1	13.1	F0458-D04	-3.9	6.8	F0502-A10	6.0	12.0	F0538-G02	11.8	33.0	F0546-B08	37.0	-
F0159-C10	8.0	8.5	F0283-E06	10.6	-	F0323-D02	29.3	8.9	F0459-D04	-6.0	4.6	F0503-A10	15.1	11.6	F0539-G02	20.3	20.2	F0547-B08	40.4	19.7
F0160-C10	24.3	21.8	F0284-E06	14.4	-	F0324-D02	27.4	10.4	F0460-D04	5.4	5.1	F0504-A10	5.0	7.9	F0540-G02	29.3	17.6	F0548-B08	32.5	-
F0161-D10	-9.5	10.1	F0285-A10	-3.7	6.5	F0321-G01	15.7	15.0	F0457-G03	8.7	13.1	F0505-B07	-7.4	4.0	F0541-B03	28.6	16.1			
F0162-D10	12.2	4.0	F0286-A10	4.3	2.9	F0322-G01	20.1	11.9	F0458-G03	-3.5	9.9	F0506-B07	15.3	7.0	F0542-B03	30.7	18.6			
F0163-D10	29.9	7.7	F0287-A10	15.0	12.4	F0323-G01	21.8	11.8	F0459-G03	6.0	23.4	F0507-B07	4.7	3.0	F0543-B03	31.5	17.6			
F0164-D10	43.9	8.3	F0288-A10	14.1	7.5	F0324-G01	24.0	10.3	F0460-G03	-11.8	12.6	F0508-B07	7.4	6.2	F0544-B03	36.0	11.7			

First priority hits were defined as those which inhibited the VIP induced response from CHO-hVPAC$_2$R cells by more than 60 %. The majority of compounds were tested at least twice and the average inhibition is shown (mean ± SEM). The compounds selected for further analysis are highlighted in grey.

Table 2.2.2 Reproducibility study of second priority hits from the 'F' library.

Single Well No.	% inhibition	Single Well No.	% inhibition	Single Well No.	% inhibition	Single Well No.	% inhibition	Single Well No.	% inhibition
F0025-D06	14.0	F0213-B06	-0.5	F0385-A03	23.5	F0473-B09	15.1	F0541-A07	-15.9
F0026-D06	20.4	F0214-B06	6.0	F0386-A03	30.1	F0474-B09	14.4	F0542-A07	-1.4
F0027-D06	17.5	F0215-B06	6.5	F0387-A03	25.8	F0475-B09	13.4	F0543-A07	-1.0
F0028-D06	29.7	F0216-B06	-2.2	F0388-A03	35.0	F0476-B09	25.9	F0544-A07	6.8
F0149-D04	21.4	F0225-B04	2.2	F0385-E10	25.0	F0473-D02	3.4	F0541-D06	12.7
F0150-D04	14.1	F0226-B04	5.2	F0386-E10	23.2	F0474-D02	11.7	F0542-D06	1.7
F0151-D04	12.0	F0227-B04	2.9	F0387-E10	25.7	F0475-D02	14.5	F0543-D06	5.0
F0152-D04	11.3	F0228-B04	9.6	F0388-E10	21.9	F0476-D02	17.7	F0544-D06	17.7
F0153-B07	0.5	F0253-B10	21.6	F0409-E02	24.6	F0473-E10	23.7	F0545-B04	9.6
F0154-B07	4.0	F0254-B10	19.2	F0410-E02	32.6	F0474-E10	22.9	F0546-B04	5.1
F0155-B07	7.0	F0255-B10	15.0	F0411-E02	28.4	F0475-E10	32.4	F0547-B04	17.8
F0156-B07	9.6	F0256-B10	20.5	F0412-E02	35.4	F0476-E10	27.7	F0548-B04	19.9
F0185-F07	2.7	F0281-A06	-4.8	F0441-C09	28.1	F0477-B01	32.6	F0545-E09	19.8
F0186-F07	9.3	F0282-A06	16.5	F0442-C09	34.3	F0478-B01	34.2	F0546-E09	28.4
F0187-F07	8.2	F0283-A06	37.1	F0443-C09	57.5	F0479-B01	21.5	F0547-E09	6.8
F0188-F07	4.0	F0284-A06	16.8	F0444-C09	18.1	F0480-B01	19.6	F0548-E09	6.1
F0185-G05	13.4	F0313-D02	9.0	F0441-F08	21.9	F0477-F02	19.5	F0545-F06	13.2
F0186-G05	13.1	F0314-D02	6.1	F0442-F08	26.7	F0478-F02	14.6	F0546-F06	6.2
F0187-G05	10.4	F0315-D02	10.3	F0443-F08	27.7	F0479-F02	5.5	F0547-F06	-6.4
F0188-G05	21.1	F0316-D02	4.0	F0444-F08	12.9	F0480-F02	-1.3	F0548-F06	-0.4
F0205-C10	10.3	F0321-A10	10.5	F0457-A02	29.8	F0497-E05	9.6		
F0206-C10	11.2	F0322-A10	9.1	F0458-A02	15.8	F0498-E05	11.2		
F0207-C10	13.6	F0323-A10	-2.5	F0459-A02	10.2	F0499-E05	-9.9		
F0208-C10	4.6	F0324-A10	29.4	F0460-A02	14.4	F0500-E05	0.9		
F0209-B09	8.5	F0325-C02	34.3	F0461-D03	15.5	F0501-B05	-3.7		
F0210-B09	3.6	F0326-C02	11.4	F0462-D03	23.7	F0502-B05	-5.0		
F0211-B09	3.4	F0327-C02	7.3	F0463-D03	19.9	F0503-B05	18.6		
F0212-B09	9.2	F0328-C02	1.6	F0464-D03	16.9	F0504-B05	4.5		
F0209-D02	2.4	F0325-F03	3.6	F0465-F09	10.4	F0505-H03	-6.4		
F0210-D02	2.0	F0326-F03	-3.0	F0466-F09	45.8	F0506-H03	3.3		
F0211-D02	3.4	F0327-F03	-22.7	F0467-F09	11.1	F0507-H03	8.2		
F0212-D02	0.2	F0328-F03	-3.3	F0468-F09	18.2	F0508-H03	11.8		
F0209-E05	18.0	F0381-B06	33.7	F0465-G05	31.1	F0509-A08	10.3		
F0210-E05	7.4	F0382-B06	29.1	F0466-G05	57.5	F0510-A08	10.7		
F0211-E05	3.1	F0383-B06	32.6	F0467-G05	20.6	F0511-A08	11.4		
F0212-E05	0.0	F0384-B06	20.0	F0468-G05	37.6	F0512-A08	8.5		
F0209-E06	-0.9	F0385-A01	33.0	F0473-B04	29.0	F0537-F10	16.3		
F0210-E06	10.6	F0386-A01	25.6	F0474-B04	34.7	F0538-F10	27.2		
F0211-E06	18.0	F0387-A01	21.9	F0475-B04	31.3	F0539-F10	4.0		
F0212-E06	17.7	F0388-A01	30.4	F0476-B04	27.4	F0540-F10	2.1		

Second priority hits were defined as those which inhibited the VIP induced response from CHO-hVPAC$_2$R cells by 50 - 60 %. As the majority of compounds appeared to be false positive hits they were only tested once in these studies.

2.2.3.4. Hit compound analysis

Following reproducibility studies, twelve compounds which showed consistent $hVPAC_2R$ antagonism were selected for further analysis (FR169879, FR174736, FR228725, FR049554, FR180868, FR134709, FR236314, FR237277, FR237276, FR239478, FR238897 and FR240725). Although one of the twelve compounds was unavailable (FR238897), lyophilised samples of the other eleven were used in FLIPR® assays to generate approximate IC_{50} values. Compound solubility proved to be a problem at high concentrations and as a result, only a limited range of concentrations was examined in these studies (6 concentrations per compound over the range 1×10^{-9} to 1×10^{-3}; 4 replicate wells per concentration). Figure 2.2.9 shows representative FLIPR® traces generated from the inhibition of the VIP response by FR134709, which was one of the more potent compounds identified. Representative inhibition curves for 10 of the compounds (excluding FR044954) are shown in Figure 2.2.10(i) and (ii), with the approximate IC_{50} values for each sample, where calculable, shown in Table 2.2.3. Approximate IC_{50} values ranged from 3 μM for FR169879 to 65 μM for FR228725, with a ROP of FR169879 = FR134709 = FR180868 ≥ FR147436 = FR239478 > FR240725 >> FR228725. Clearly, even some of the hits identified from the reproducibility studies were false positives with FR236314, FR237276 and FR237277 (Figure 2.2.10(ii) f - h) showing no antagonism of the VIP response. As described above, compound solubility proved problematic when trying to prepare sufficiently high compound concentrations, with the presence of a precipitate observed in some of the 0.1 - 1 mM solutions. For FR169879, FR174736 and FR239478 (Figure 2.2.10(i): a, b; 2.2.10(ii): i) this may have contributed to the inability of the compounds to inhibit the VIP response at these higher compound concentrations. The particular responses in which this reversal of inhibitory action was observed, were not included in the data used to determine compound IC_{50} values. Although compound FR044954, appeared to be a potent antagonist in the initial round of screening and in subsequent reproducibility studies (Figure 2.2.11a), the effects of this compound were variable and as a result no consistent inhibition curves could be generated. In further studies when applied alone to CHO-$hVPAC_2R$ cells, this compound appeared to stimulate a large calcium response in the cells, which probably accounts for the subsequent reduction in the VIP response (Figure 2.2.11b). This is supported by the observation that when VIP (100 nM) is added to CHO-$hVPAC_2R$ cells, following a previous addition of VIP, the second response to the agonist is almost totally ablated (Figure 2.2.12).

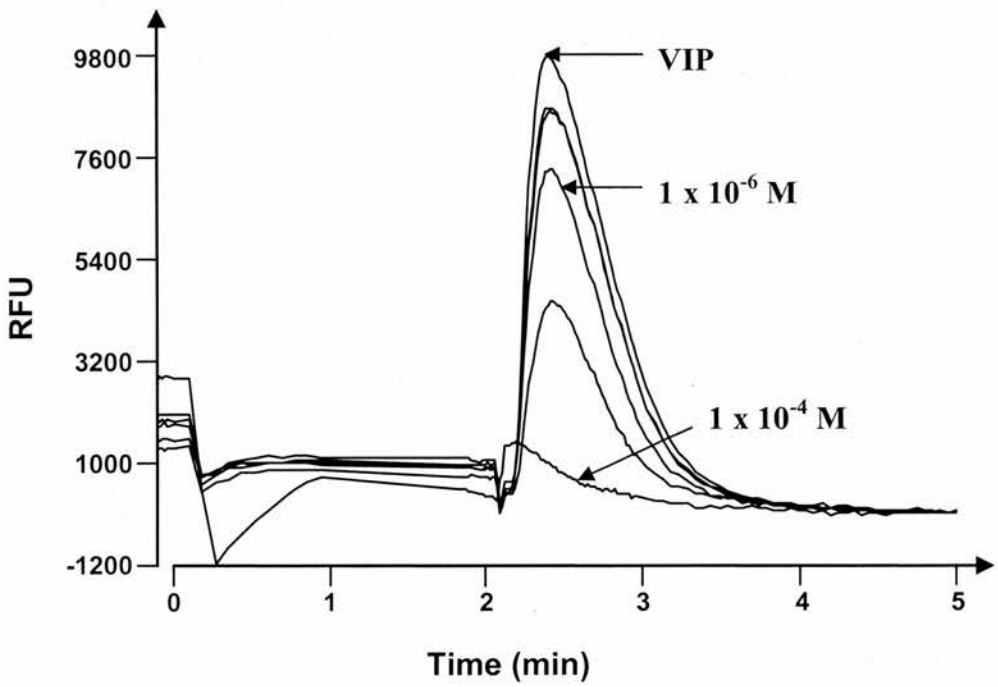

Figure 2.2.9 **FR134709 inhibition of VIP stimulated responses from CHO-hVPAC$_2$R cells.** Using the FLIPR®, FR134709 (1 x 10^{-4} M to 1 x 10^{-9}) inhibited in a concentration dependent manner the VIP (100 nM) induced increase in fluorescence in hVPAC$_2$R cells, with an IC_{50} of approximately 4 μM.

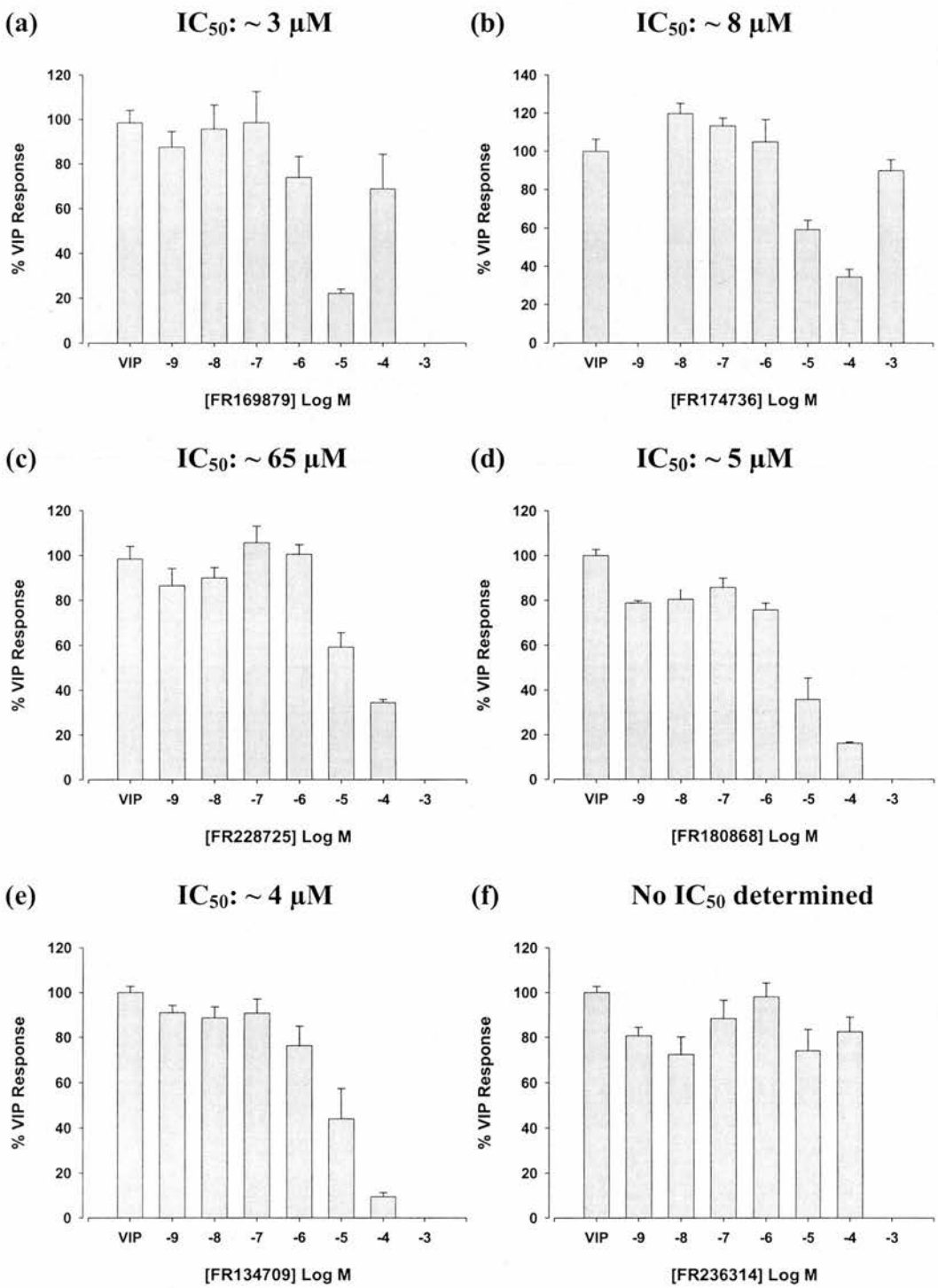

Figure 2.2.10(i) Inhibition of VIP induced calcium responses from CHO-hVPAC$_2$R cells by Fujisawa library compounds. Representative inhibition curves are shown for the following compounds: (**a**) FR169879, (**b**) FR174736, (**c**) FR228725, (**d**) FR180868, (**e**) FR134709 and (**f**) FR236314. The IC_{50} values presented for each compound were determined from two independent FLIPR® experiments, with mean values presented in Table 2.2.3. *Continued in Figure 2.2.10 (ii).*

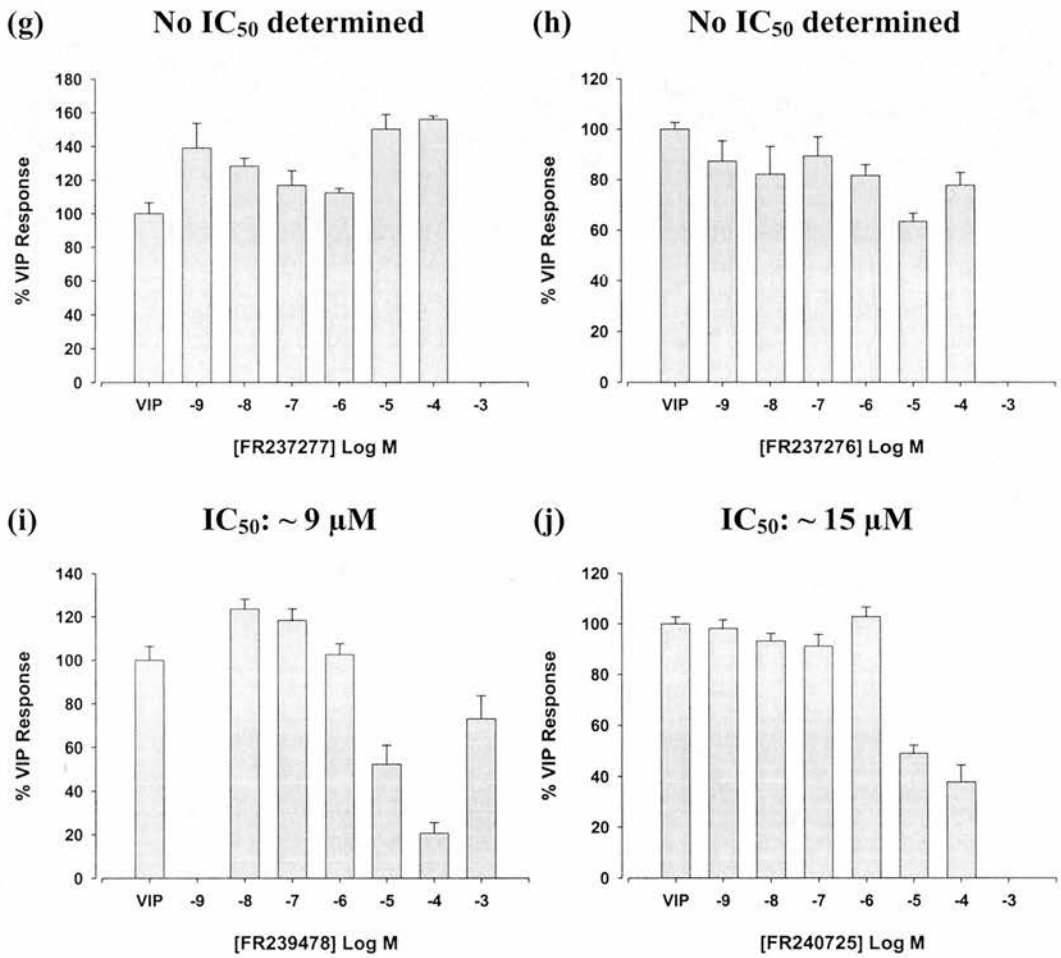

Figure 2.2.10(ii) Inhibition of VIP induced calcium responses from CHO-hVPAC$_2$R cells by Fujisawa library compounds, *continued from Figure 2.2.10(i).* Representative inhibition curves are shown for the compounds: (**g**) FR237277, (**h**) FR237276, (**i**) FR239478 and (**j**) FR240725. The approximate IC_{50} values presented for each compound were again determined from two independent FLIPR® experiments, with mean IC_{50} values shown in Table 2.2.3.

(a)

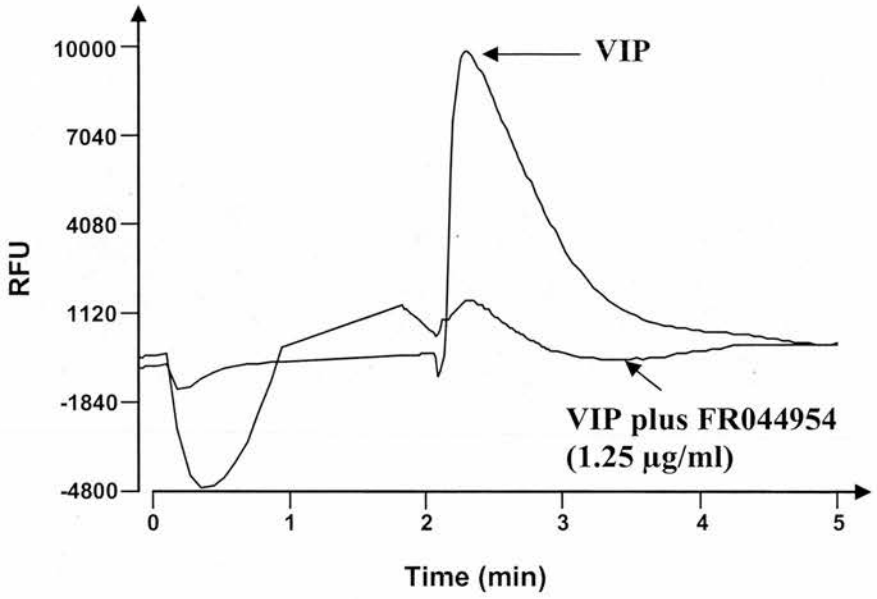

(b)

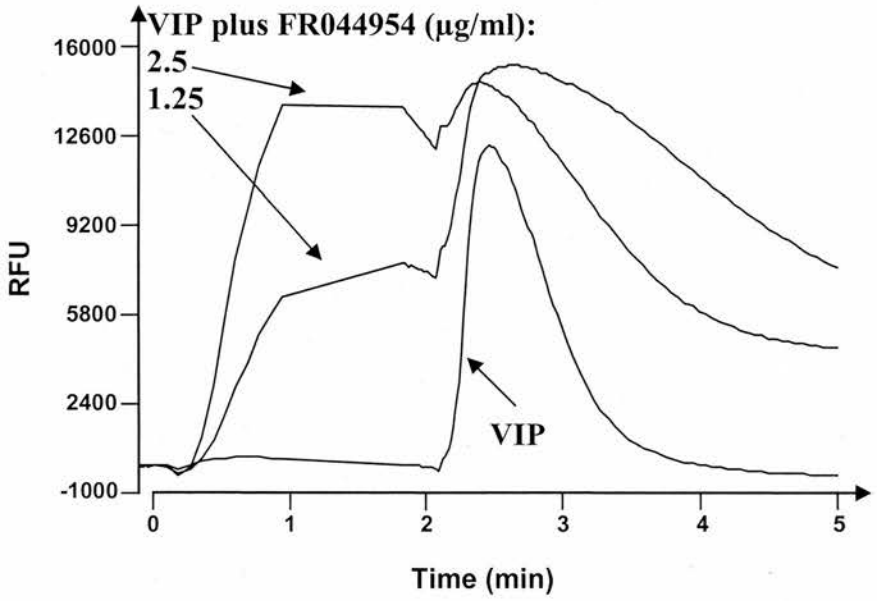

Figure 2.2.11 FR044954 has complex effects on calcium signalling in CHO-hVPAC$_2$R cells. Using the FLIPR®, FR044954 was initially observed to strongly inhibit VIP induced calcium responses mediated by hVPAC$_2$R (**a**). However, upon further examination FR044954 alone induced a large increase in fluorescence in these cells, prior to the addition of agonist (**b**).

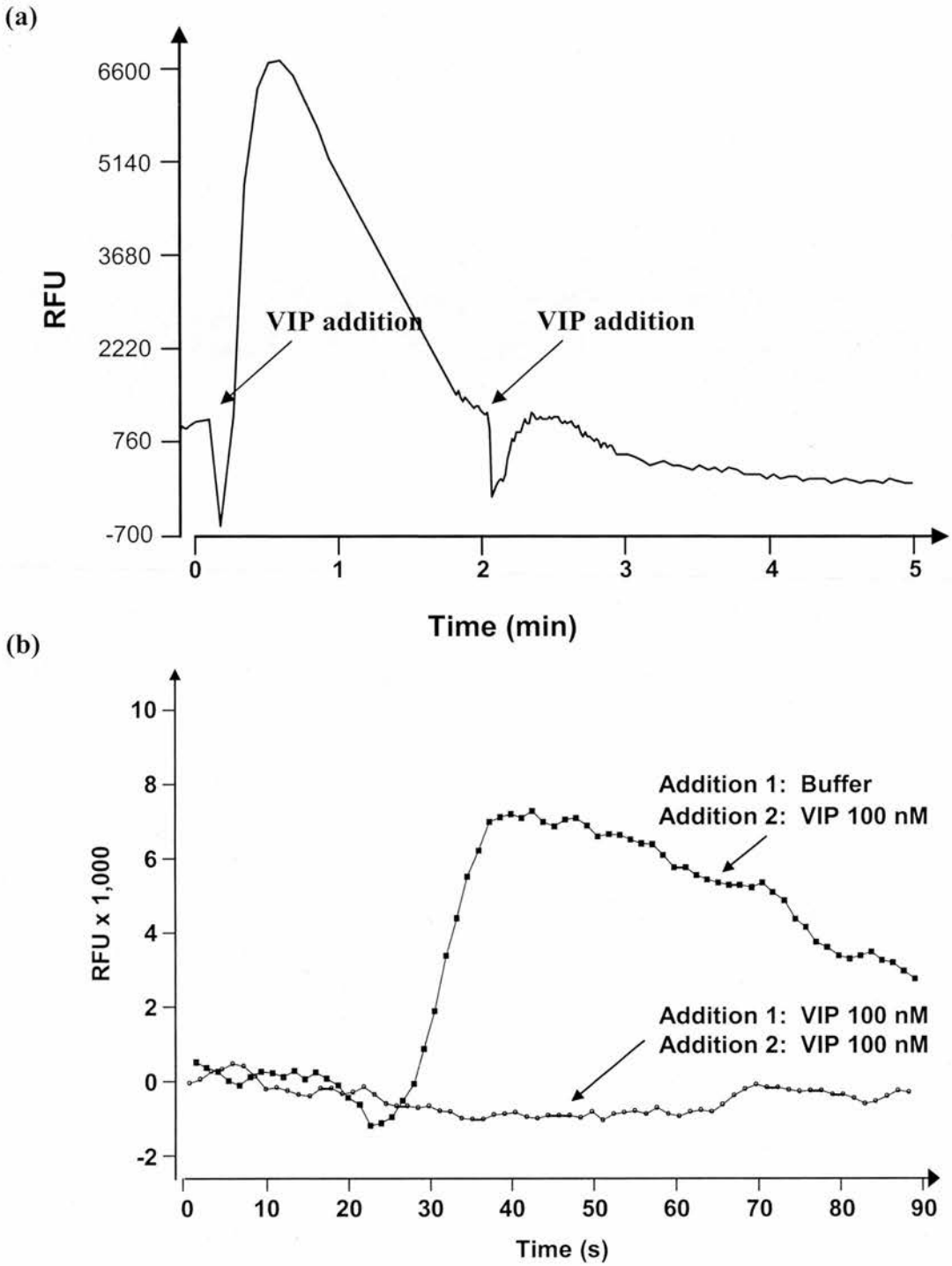

Figure 2.2.12 Multiple additions of VIP to CHO-hVPAC$_2$R cells decreases the evoked calcium response. Using the FLIPR® (**a**) and FlexStation® (**b**), CHO-hVPAC$_2$R cells were stimulated with VIP (100 nM) and after 2 min (FLIPR®) or 10 min (FlexStation®), a second addition of VIP (100 nM) was made. The evoked fluorescence response following the second addition of VIP was dramatically reduced compared to the initial VIP response.

(a)

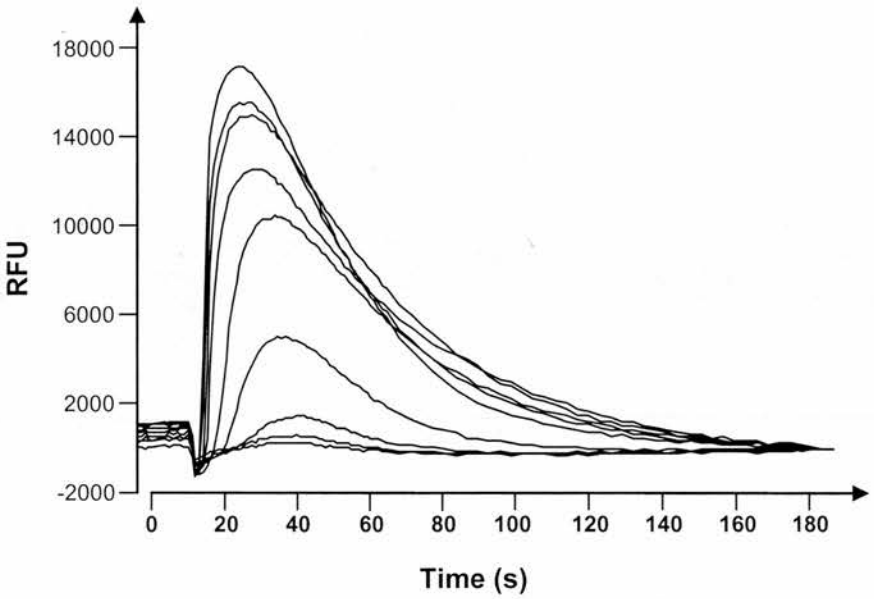

(b)

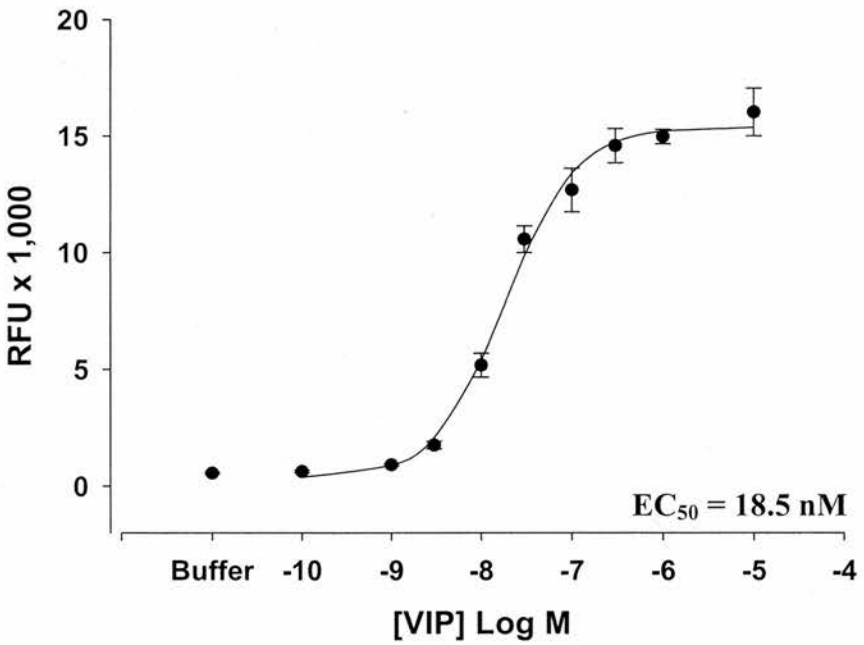

Figure 2.2.13 VIP produced a concentration dependent increase in calcium in CHO cells stably expressing hVPAC$_1$R. In the FLIPR® assay, VIP stimulated an increase in fluorescence from the CHO-hVPAC$_1$R cells in a concentration dependent manner (**a**), with the resulting sigmoidal curve giving an EC_{50} value of 18.5 nM (**b**).

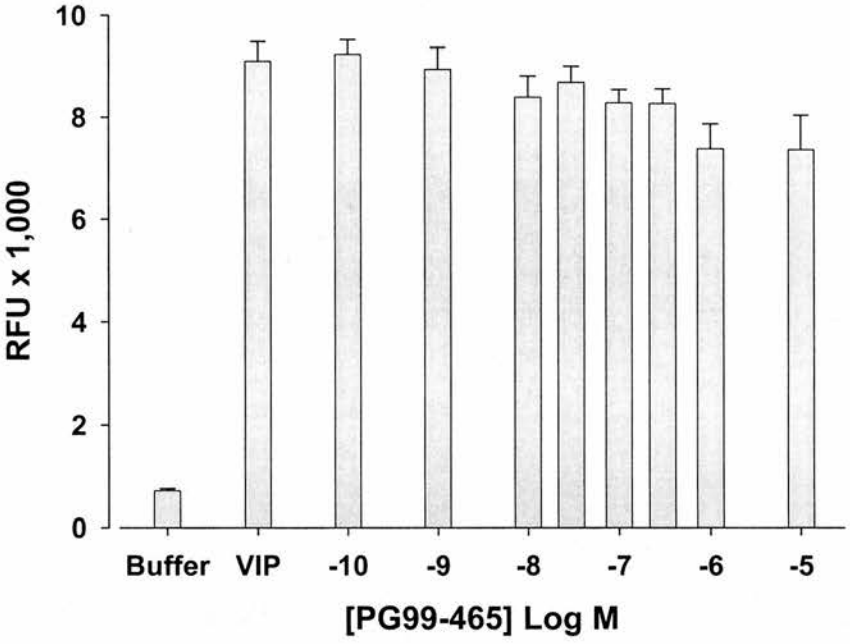

Figure 2.2.14 PG99-465 did not inhibit VIP induced calcium responses from CHO-hVPAC$_1$R cells. PG99-465 was pre-incubated with CHO-hVPAC$_1$R cells for 2 min prior to the addition of VIP (100 nM), with no subsequent reduction in fluorescence levels observed in the FLIPR® assay.

2.2.4. Establishment of the CHO-hVPAC$_1$R counter-screen

In parallel to the CHO-hVPAC$_2$R primary screen, I also established a CHO-hVPAC$_1$R counter-screen in which the selectivity of hit compounds was subsequently evaluated. These assays were performed on the FLIPR® in a similar manner to those for CHO-hVPAC$_2$R cells, with 1.5 x 10^4 cells per well seeded overnight and the 2x calcium dye concentration used. To establish the pharmacology of the hVPAC$_1$R using the FLIPR® assay, a concentration response curve to VIP was generated (0.1 nM to 10 μM; 8 replicates per concentration), which gave an EC_{50} value of 18.8 nM (Figure 2.2.13). This value is consistent with the EC_{50} of 14.1 ± 0.9 nM (n = 6) that was generated for VIP stimulation of CHO-hVPAC$_2$R cells using the FlexStation® calcium assay (Table 1.2.2, p 110). To verify that this was a VPAC$_1$R mediated response, the effect of the VPAC$_2$R antagonist PG99-465 was examined. PG99-465 had no overt effect on the VIP response, perhaps marginally reducing the magnitude of the response at micromolar concentrations (Figure 2.2.14). As the pharmacological data generated for the hVPAC$_1$R receptor using the FLIPR® was consistent with the FlexStation® data (Table 1.2.2, p 110), the counter-screen was deemed ready for use. However, as a consequence of personal time restraints regarding my secondment to Japan, all subsequent hit analysis and counter-screening studies were performed in Edinburgh (see below) using the FlexStation®.

2.2.5. Analysis of hit compound pharmacology using the FlexStation®

On returning to Edinburgh, samples of FR049554, FR169879, FR174736, FR180868 and FR134709 were sent over from the Fujisawa laboratories in Japan for a full pharmacological characterisation, including receptor selectivity studies, using the FlexStation® assay. In addition, the pharmacological properties of FR300771, FR149534 and FR035321 were also characterised, as these compounds had been identified as hits by colleagues in Fujisawa on screening of the 'M' library. The FlexStation® assays were performed as detailed in the materials and methods, with cells seeded overnight (1 x 10^5 cells per well) and the addition of cell buffer and calcium dye solution as previously described (section B.3.1.2., p 64). The effects of each compound alone and on the VIP stimulated response are shown for the three cell lines (a: CHO-hVPAC$_2$R; b: CHO-hVPAC$_1$R; c: CHO-hPAC$_1$R) in Figures 2.2.15 - 2.2.22 (2.2.15: FR169879; 2.2.16: FR174736; 2.2.17: FR180868; 2.2.18: FR134709; 2.2.19: FR300771; 2.2.20: FR149534; 2.2.21: FR035321, 2.2.22:

Table 2.2.3 Summary of the properties of hit compounds identified from screening of Fujisawa compound libraries for $hVPAC_2R$ antagonists

4 mix library compounds		Individual library compounds					FR compounds (lyophilised samples)			
							Approximate IC_{50}/EC_{50}* ± SEM (μM)			
Well number	% inhibition (n = 1)	Well number	FAC (μM)	% inhibition mean ± SEM (n ≥ 2)	FR number	Molecular weight	FLIPR# $hVPAC_2R$ (n = 2)	FlexStation $hVPAC_2R$	FlexStation $hVPAC_1R$	FlexStation $hPAC_1R$
4MF010-G08	62	F038-G08	3.0	59 ± 6	FR169879	418.3	3	2.3 ± 0.8 (3)	> 10 (3)	28.3 ± 5.3 (3)
4MF010-G08	62	F039-G09	3.1	62 ± 4	FR174736	402.3	8	7.6 ± 3.2 (3)	> 30 (3)	35.9 ± 4.4 (3)
4MF010-G08	62	F040-G09	4.0	31 ± 5	FR228725	315.8	65	-	-	-
4MF037-E08	89	F146-E08	4.2	62 ± 28	FR044954	298.8	NA	*4.7 (1)	*3.2 (1)	*2.4 ± 0.5 (2)
4MF071-E06	47	F281-E06	3.3	53 ± 6	FR180868	374.2	5	7.2 ± 1.7 (3)	> 30 (3)	17.2 ± 5.9 (3)
4MF087-A06	66	F345-A06	2.9	58 ± 9	FR134709	427.4	4	3.1 ± 1.3 (3)	35.2 ± 15 (3)	8.9 ± 1.7 (3)
4MF108-B04	74	F431-B04	3.3	32 ± 6	FR236314	382.5	NA	-	-	-
4MF111-F10	60	F443-F10	3.7	46 ± 4	FR237277	341.4	NA	-	-	-
4MF111-G01	64	F443-G01	3.7	42 ± 7	FR237276	365.4	NA	-	-	-
4MF115-D04	54	F457-D04	3.5	41 ± 4	FR239478	352.8	9	-	-	-
4MF136-G03	114	F542-G03	3.8	45 ± 4	FR238897	328.4	Sample unavailable	-	-	-
4MF137-B08	66	F547-B08	3.7	41 ± 20	FR240725	334.4	15	-	-	-
-	-	-	-	-	*FR300771	378.6	-	> 10 (3)	> 10 (3)	> 10 (3)
-	-	-	-	-	*FR149534	326.8	-	22.1 ± 12 (3)	> 30 (3)	> 30 (3)
-	-	-	-	-	*FR035321	337.8	-	> 30 (n = 3)	> 30 (3)	> 30 (3)

The inhibitory actions of samples taken directly from the compound libraries are expressed as percentage change in the VIP response (mean % ± SEM, where appropriate). #IC_{50} values shown for powder samples in the FLIPR® assay are estimated values from limited concentration response studies in which only a small amount of compound was available. For this reason no SEM values were available from these studies. IC_{50} and *EC_{50} values shown from the FlexStation® assays are presented as mean ± SEM, with the number of independent experiments shown in parenthesis. NA indicates samples for which either no inhibition or no consistent inhibition was observed in the FLIPR® assay, and consequently it was not possible determine IC_{50} values.

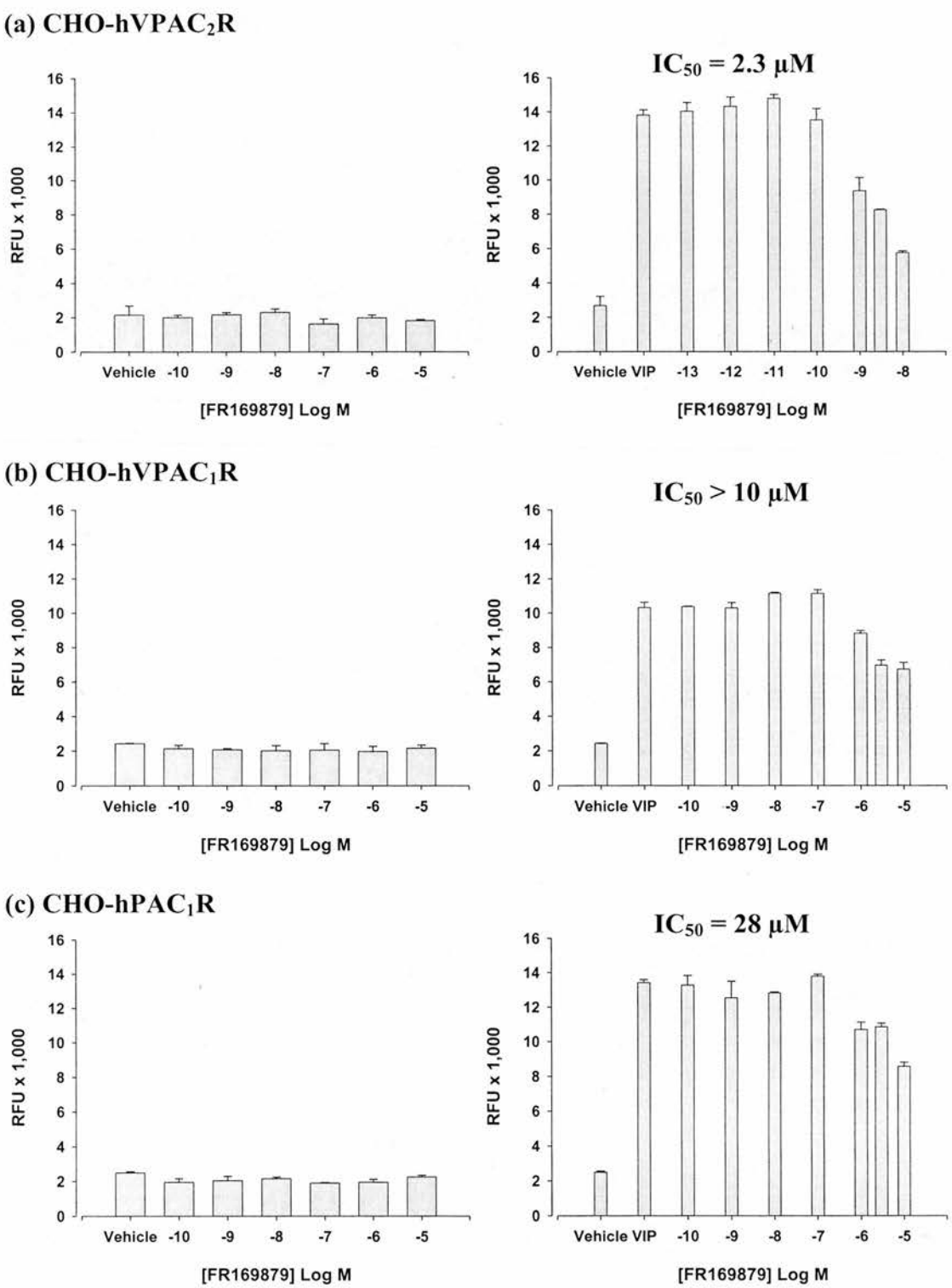

Figure 2.2.15 Potency/selectivity of FR169879 at hVPAC/PAC receptors. Using the FlexStation® calcium assay, the effect of FR169879 alone and on VIP induced responses was determined using CHO-$VPAC_2$ (**a;** VIP = 100 nM), -$VPAC_1$ (**b**; VIP = 30 nM) and -PAC_1 (**c**; VIP = 1000 nM) receptor expressing cells. The graphs shown are representative, with approximate IC_{50} calculated from three independent experiments (data shown in Table 2.2.3).

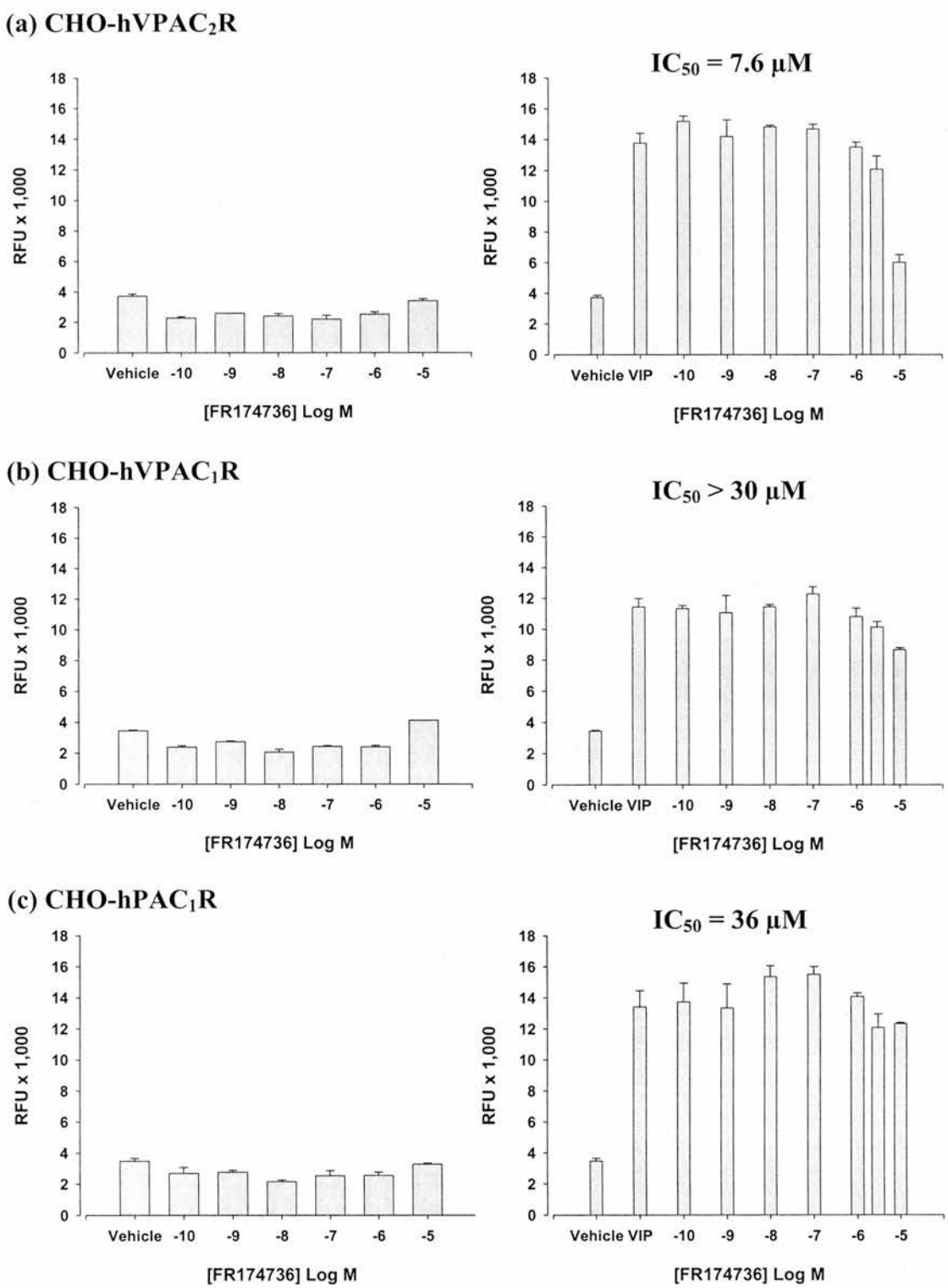

Figure 2.2.16 Potency/selectivity of FR174736 at hVPAC/PAC receptors. Using the FlexStation® calcium assay, the effect of FR174736 alone and on VIP induced responses was determined using CHO-$VPAC_2$ (**a;** VIP = 100 nM), -$VPAC_1$ (**b**; VIP = 30 nM) and -PAC_1 (**c**; VIP = 1000 nM) receptor expressing cells. The graphs shown are representative, with approximate IC_{50} calculated from three independent experiments (data shown in Table 2.2.3).

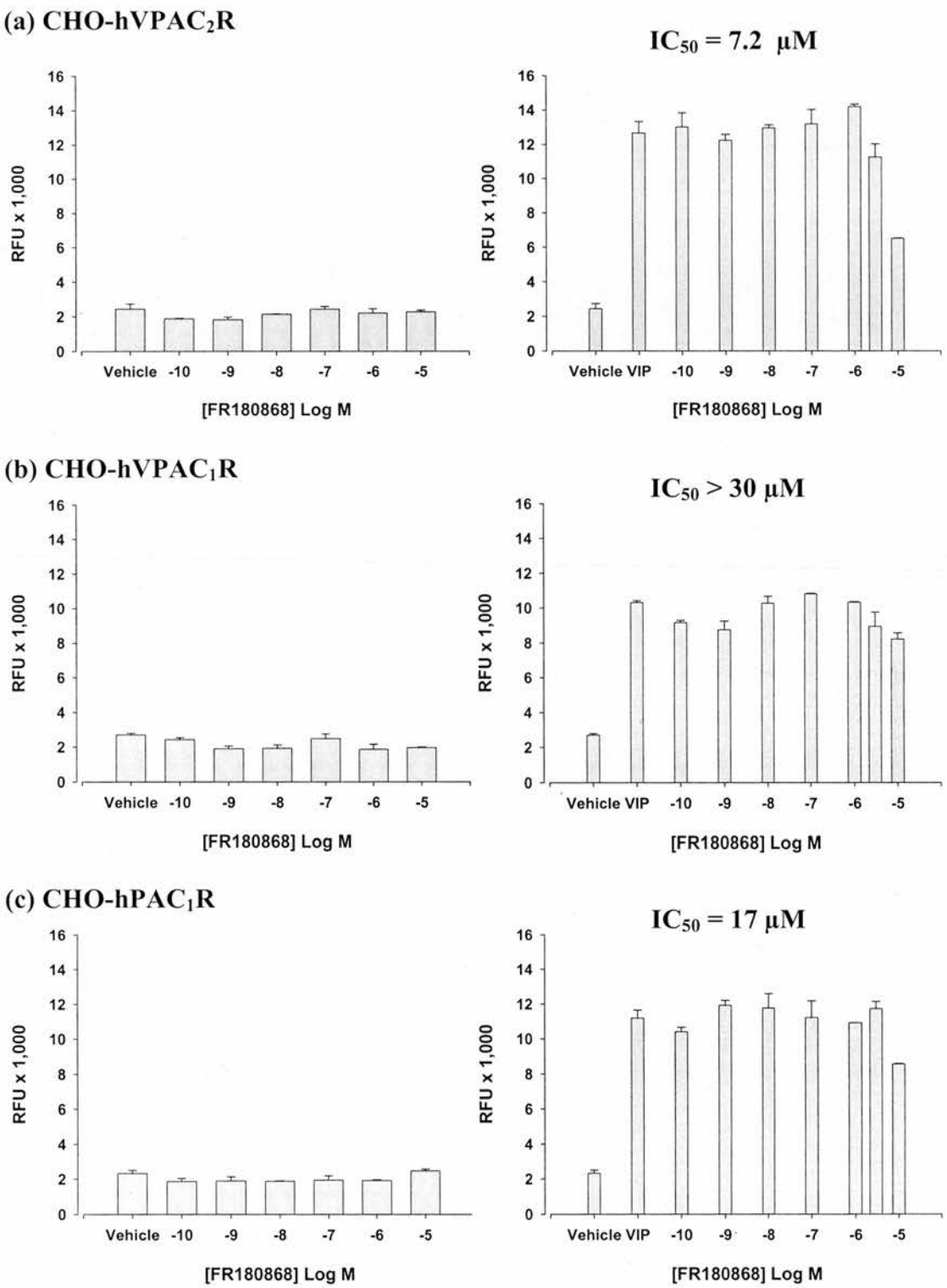

Figure 2.2.17 Potency/selectivity of FR180868 at hVPAC/PAC receptors. Using the FlexStation® calcium assay, the effect of FR180868 alone and on VIP induced responses was determined using CHO-$VPAC_2$ (**a;** VIP = 100 nM), -$VPAC_1$ (**b**; VIP = 30 nM) and -PAC_1 (**c**; VIP = 1000 nM) receptor expressing cells. The graphs shown are representative, with approximate IC_{50} calculated from three independent experiments (data shown in Table 2.2.3).

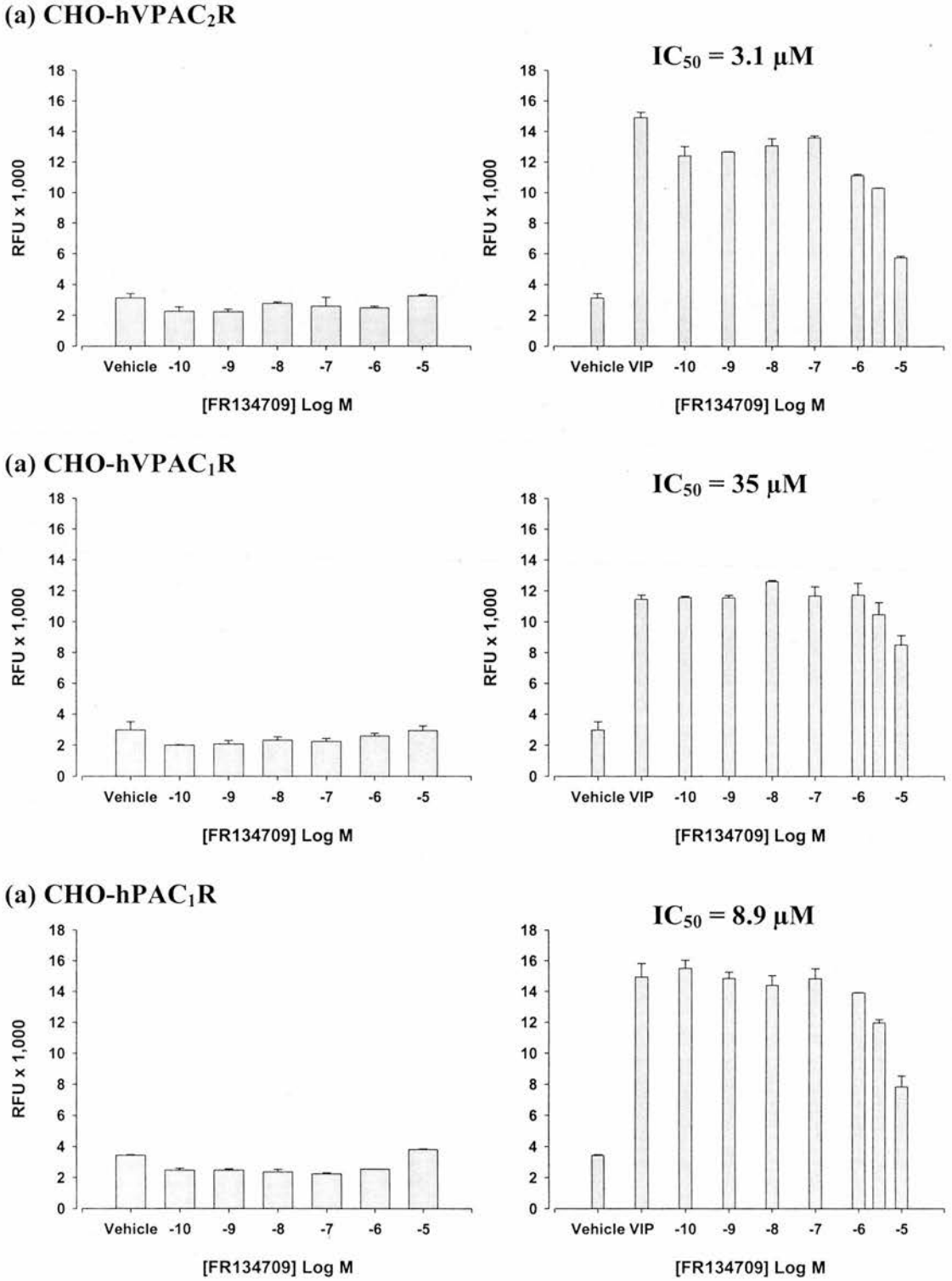

Figure 2.2.18 Potency/selectivity of FR134709 at hVPAC/PAC receptors. Using the FlexStation® calcium assay, the effect of FR134709 alone and on VIP induced responses was determined using CHO-$VPAC_2$ (**a;** VIP = 100 nM), -$VPAC_1$ (**b**; VIP = 30 nM) and -PAC_1 (**c**; VIP = 1000 nM) receptor expressing cells. The graphs shown are representative, with approximate IC_{50} calculated from three independent experiments (data shown in Table 2.2.3).

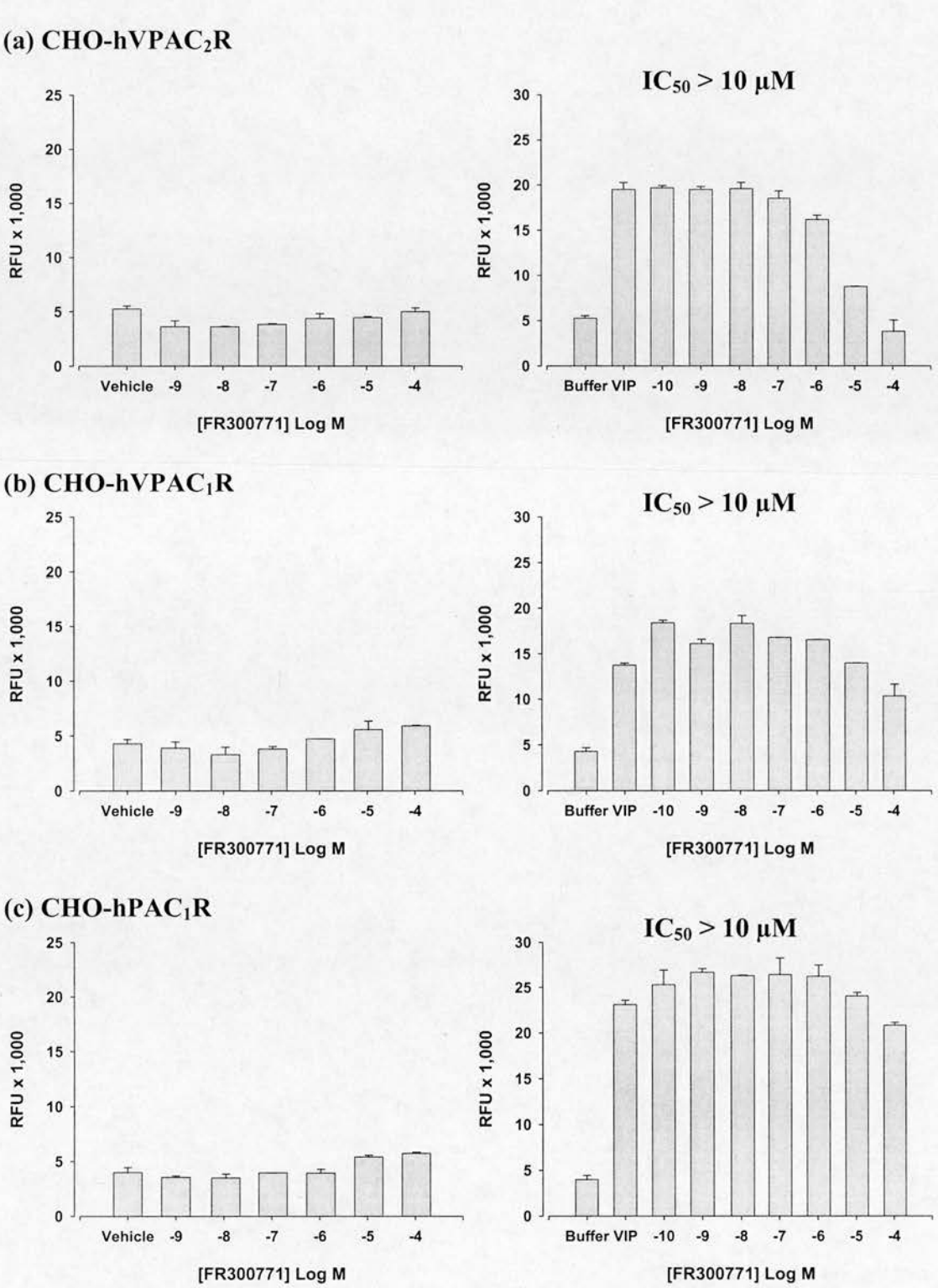

Figure 2.2.19 **Potency/selectivity of FR300771 at hVPAC/PAC receptors.** Using the FlexStation® calcium assay, the effect of FR300771 alone and on VIP induced responses was determined using CHO-$VPAC_2$ (**a;** VIP = 100 nM), -$VPAC_1$ (**b**; VIP = 30 nM) and -PAC_1 (**c**; VIP = 1000 nM) receptor expressing cells. The graphs shown are representative, with approximate IC_{50} calculated from three independent experiments (data shown in Table 2.2.3).

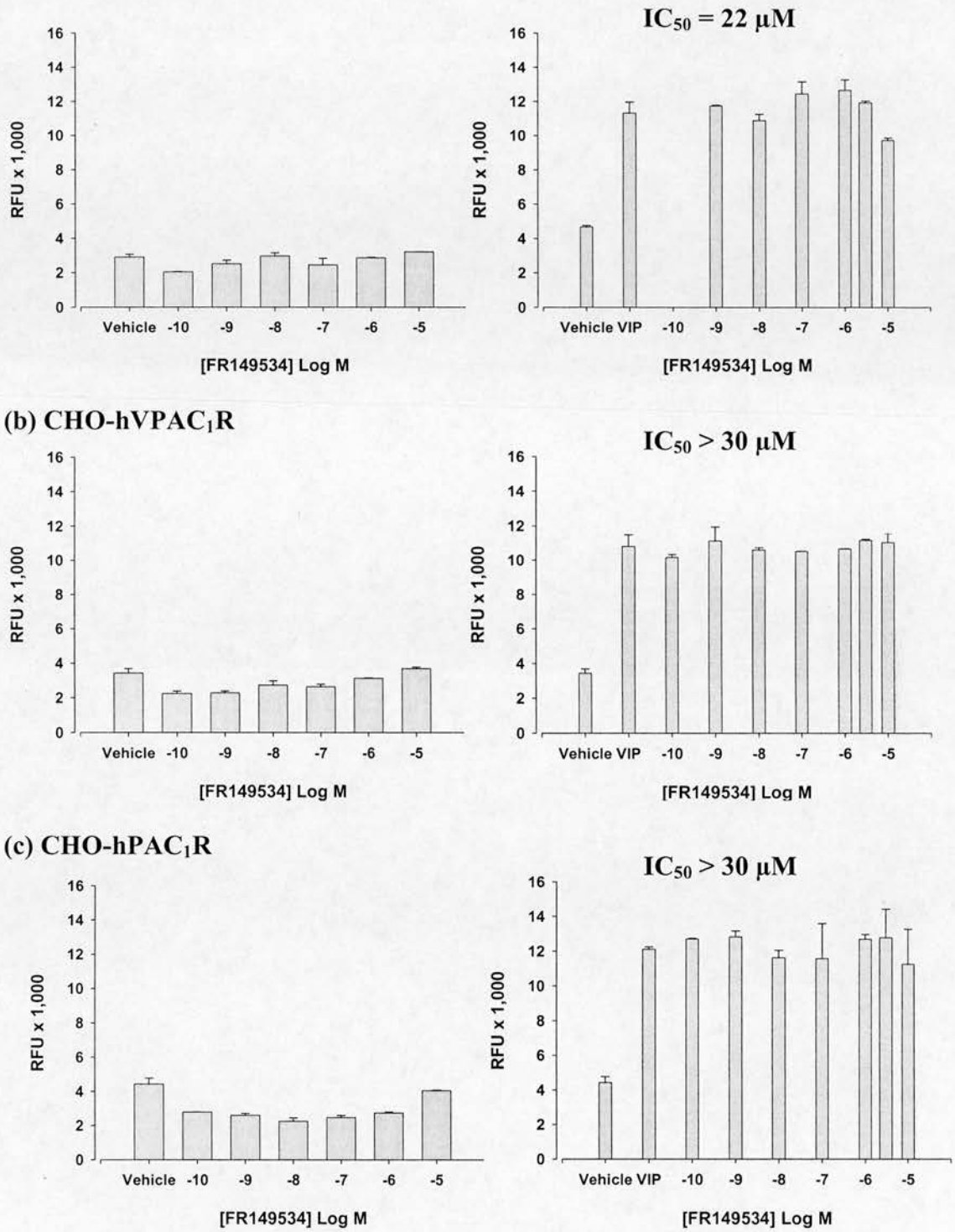

Figure 2.2.20 Potency/selectivity of FR149534 at hVPAC/PAC receptors. Using the FlexStation® calcium assay, the effect of FR149534 alone and on VIP induced responses was determined using CHO-$VPAC_2$ (**a;** VIP = 100 nM), -$VPAC_1$ (**b**; VIP = 30 nM) and -PAC_1 (**c**; VIP = 1000 nM) receptor expressing cells. The graphs shown are representative, with approximate IC_{50} calculated from three independent experiments (data shown in Table 2.2.3).

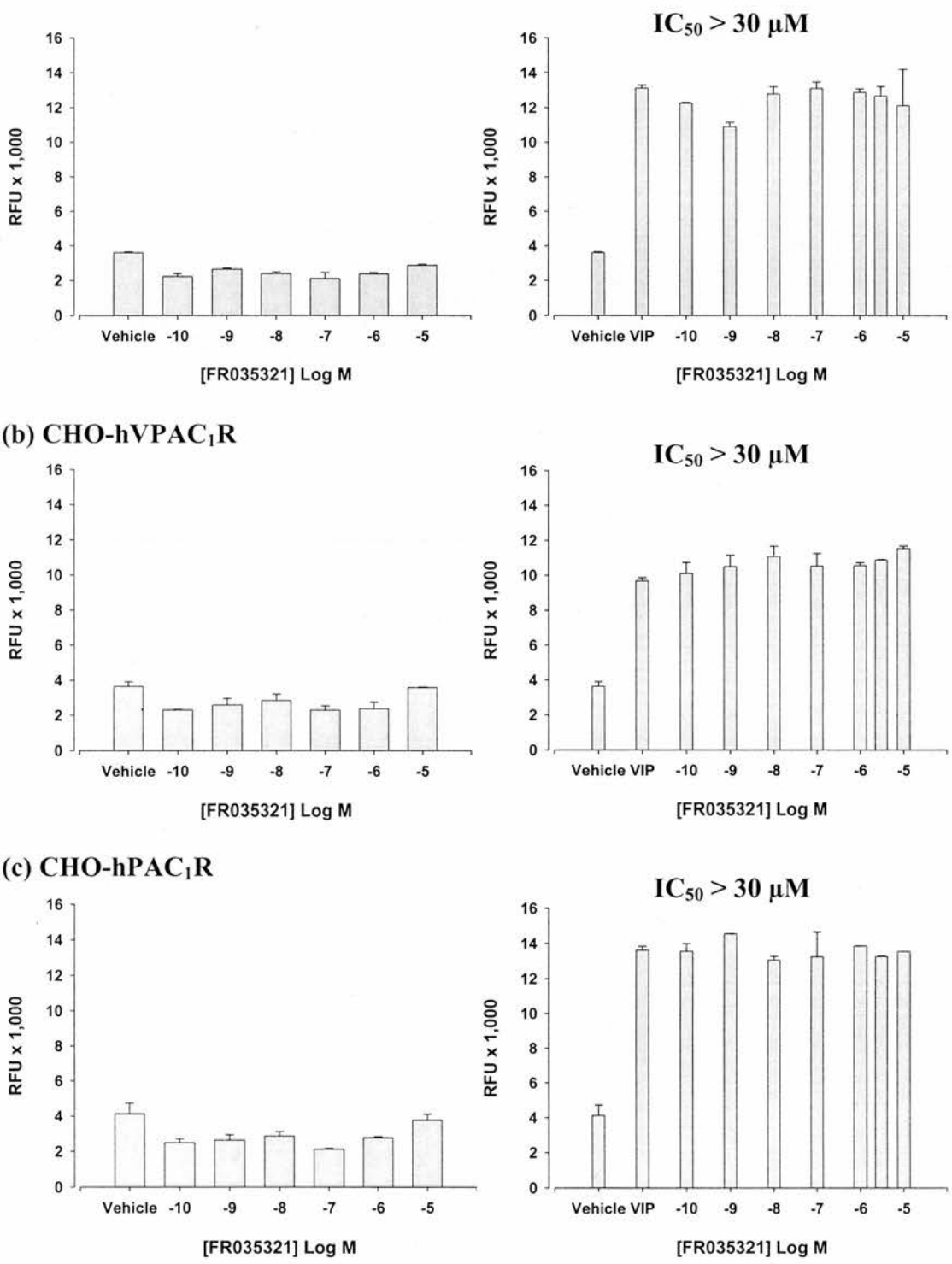

Figure 2.2.21 Potency/selectivity of FR035321 at hVPAC/PAC receptors. Using the FlexStation® calcium assay, the effect of FR035321 alone and on VIP induced responses was determined using CHO-$VPAC_2$ (**a;** VIP = 100 nM), -$VPAC_1$ (**b**; VIP = 30 nM) and -PAC_1 (**c**; VIP = 1000 nM) receptor expressing cells. The graphs shown are representative, with approximate IC_{50} calculated from three independent experiments (data shown in Table 2.2.3).

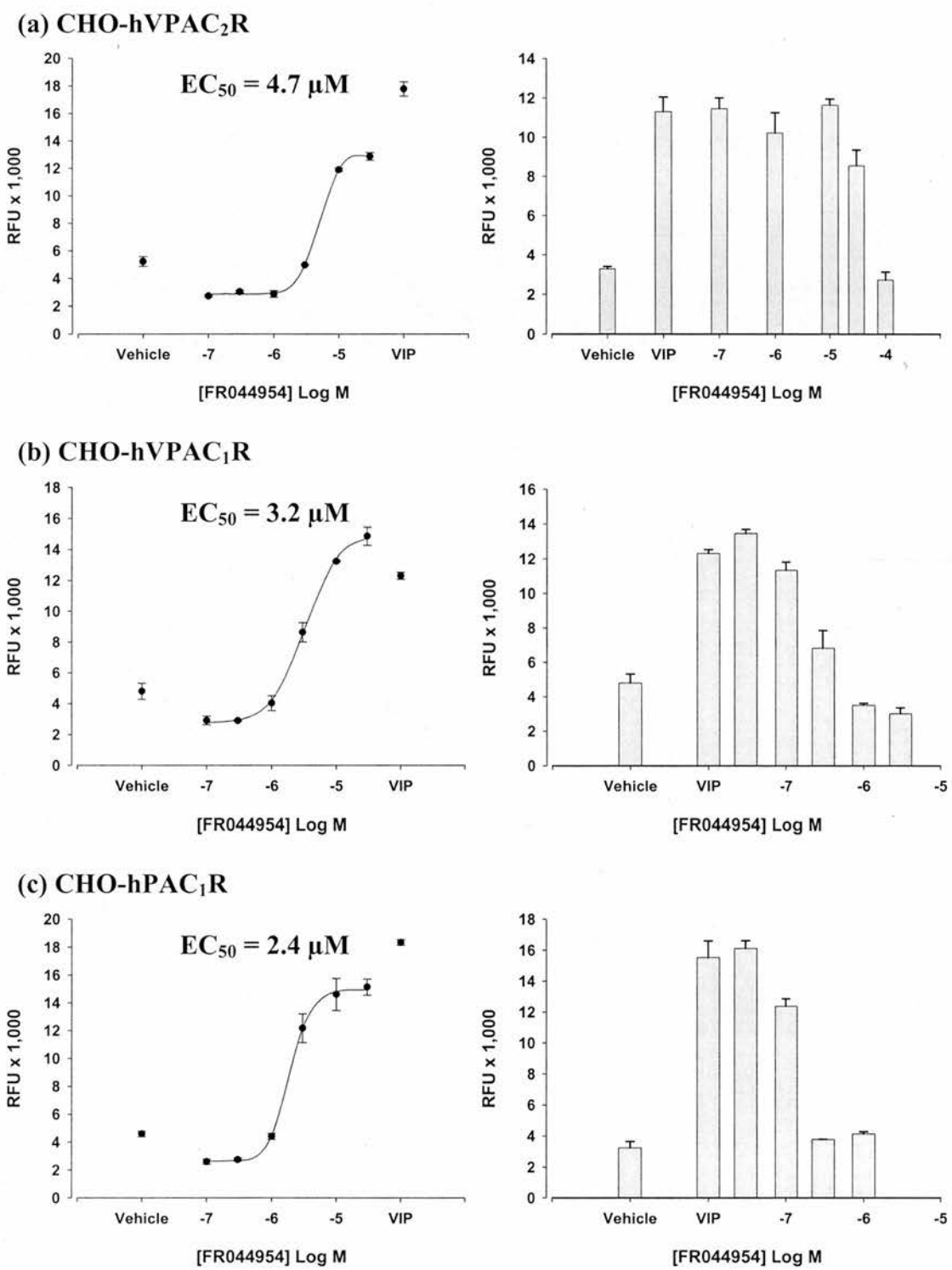

Figure 2.2.22 FR044954 is an agonist in the CHO-hVPAC/PACR cell lines. In all three hVPAC/PACR stable cell lines, FR049554 alone produced a concentration dependent increase in calcium (**a**: $VPAC_1$; **b**: $VPAC_2$; **c**: PAC_1). The EC_{50} values shown here and in Table 2.2.3 are from one or two independent experiments. Pre-incubation (10 min) of FR044954 with the cells prior to VIP addition resulted in reduced responses to the peptide as a result of the initial agonist effect of FR049554.

FR044954). The IC_{50}/EC_{50} values (where applicable) are summarised for each compound in Table 2.2.3. When tested alone at concentrations from 0.1 nM to 10 μM, none of the compounds, excluding FR044954, elicited an obvious effect on basal levels of calcium in any of the three hVPAC/PACR stable cell lines (Figures 2.2.15 - 2.2.22). In contrast, FR044954 demonstrated clear agonist properties when tested alone with all three CHO-hVPAC/PACR cell lines (Figure 2.2.22). FR049554 had EC_{50} values of 4.7 μM (CHO-hVPAC$_2$R), 3.2 μM (CHO-hVPAC$_1$R) and 2.4 μM (CHO-hPAC$_1$R), appearing to be an equipotent, non-selective agonist for these receptor subtypes (Figure 2.2.22). The maximum responses produced by FR049554 in all three cell lines were similar to those produced with the peptide agonists described in chapter one (section 1.2.3.2., p 105). Although FR049554 inhibited the VIP response in each of the three stable cell lines (Figure 2.2.22), this was probably a consequence of its agonist properties as discussed previously (see Figures 2.2.12a and 2.2.12b, from the FLIPR® and FlexStation® respectively). Of the remaining seven compounds, FR169879, FR174736, FR180868, FR134709 and FR149534 all produced a concentration dependent inhibition of agonist evoked calcium signalling at hVPAC$_2$R (Figures 2.2.15-2.2.22), with approximate IC_{50} values ranging from 2.3 to 22.1 μM, which was consistent with data generated using the FLIPR® (Table 2.2.3). The ROP for these compounds was FR169879 = FR134709 > FR174736 = FR180868 > FR149534. FR300771 and FR035321 were less potent than the other compounds and as a result no IC_{50} values could be determined as the concentration range required could not be achieved in these assays; estimated IC_{50} values were expected to be at least greater than 10 - 30 μM. The receptor selectivity of the compounds was also examined using the hVPAC$_1$R and hPAC$_1$R stable cell lines, with the most potent VPAC$_2$R antagonist FR169879, being at least 5 fold less potent at VPAC$_1$R, whilst exhibiting 10-fold selectivity over PAC$_1$R. All of the five non-peptide antagonists that were observed to have micromolar potency at the VPAC$_2$R, exhibited some degree of selectivity over the other receptors (Table 2.2.3), although none of the compounds were as potent or as selective as the peptide antagonist PG99-465 (Table 1.2.3, p 118).

2.3. Discussion

2.3.1. HT-screening to identify $VPAC_2R$ antagonists

The $VPAC_2R$ receptor is critical in the maintenance and control of normal circadian rhythms of activity and consequently, we hypothesised that antagonists of this receptor may be beneficial in treating circadian rhythm disorders in which the sleep/wake cycle is disrupted. In collaboration with Astellas Pharma Inc., I have performed a high-throughput screening study to identify selective, non-peptide $VPAC_2R$ antagonists from the company's compound libraries.

Both of the functional assays (cAMP and calcium assays) performed using the FlexStation® (chapter one) provided sensitive and robust assays with which to characterise the pharmacology of this particular GPCR. However, due its simplicity, increased throughput and cost-effectiveness, the calcium assay was selected for use in the HT-screening process and was miniaturised and optimised accordingly for use in a 384-well format on the FLIPR®. Miniaturisation of the assay involved investigating several factors, including the optimal concentration of calcium dye, agonist and library compounds to use in the assay, in order to maximise the response and facilitate the detection of hit compounds.

2.3.2. Potency and selectivity of hit compounds

Following the successful miniaturisation of the $hVPAC_2R$ assay to the 384-well format, approximately 100,000 compounds, in 4-mix cocktails from the small-compound libraries were evaluated in the initial round of screening. Hit wells were identified and the compounds comprising the appropriate 4-mix cocktails were tested individually and hit compounds identified. From the 'F' library alone, 456 compounds were identified as potential hits and were subsequently re-evaluated to confirm antagonist action. In further studies, the concentration dependence of inhibition was determined for a dozen of the most potent and consistently active compounds, of which five were selected for characterisation in potency and selectivity studies using the FlexStation® assay (FR169879, FR174736, FR044954, FR180868, FR134709). Three additional compounds were selected by colleagues in Astellas for evaluation in these studies (FR300771, FR149534, FR035321). Of these eight compounds, FR169879 was the most potent at the $hVPAC_2R$, inhibiting agonist induced responses with an IC_{50} value of 2.3 ± 0.8 μM (n = 3). However, as also observed for the other less potent compounds, FR169879 was not highly specific for

the $hVPAC_2R$, demonstrating only 5 - 10 fold selectivity over the $hVPAC_1$ and $hPAC_1$ receptors. When compared to the $VPAC_2R$ peptide antagonist PG99-465 (Moreno *et al.*, 2000), which was demonstrated to be both potent (IC_{50} = 4.4 ± 0.8 nM, n = 6) and selective in the calcium assay (Table 1.2.3, p 118), the non-peptide compounds identified during screening were considerably less potent (at least 500 fold), as well as exhibiting little selectivity. As a consequence, these compounds do not exhibit sufficiently good pharmacological properties to allow them to be classified as potent and selective $hVPAC_2R$ antagonists. The structures of several of the hit compounds identified from screening were examined by colleagues in Astellas Pharma Inc. with a view to improving their potency and selectivity for the $hVPAC_2R$, however none were thought to be amenable to chemical modification.

Although FR049554 originally appeared to be an $hVPAC_2R$ antagonist, this effect was subsequently shown to be a result of the agonist activity of this compound. As shown in both the FLIPR® and FlexStation® calcium assays, the fluorescence response induced by an agonist can be almost completely ablated if it follows the pre-incubation of another compound which also behaves as an agonist (Figure 2.2.12). Data generated from the FLIPR® during screening was focussed upon the magnitude of the VIP response and as a result it was not possible to perform detailed retrospective analyses of potential agonist activity of the library compounds, prior to VIP addition. Without the specific evaluation of possible stimulatory effects during the pre-incubation period, such compounds could easily be mistaken for antagonists. FR049554 was found to be an equipotent (EC_{50} = 2.4 – 4.7 μM), non-selective agonist of all three hVPAC/PAC receptor subtypes. Although demonstrating full agonist activity when tested with the three cell lines, FR049554 is clearly much less potent than any of the VPAC/PAC receptor peptide agonists characterised using the calcium assay in chapter one. Therefore, despite being a non-peptide, this compound is again of limited use as a VPAC/PACR agonist given its weak potency. In future studies, this compound would clearly have to be evaluated using VPAC/PACR antagonists and in CHO-K1 host cells to determine if it is truly a selective agonist of receptors in the VPAC/PACR sub-family.

2.3.3. Challenges encountered during screening

As described in the results section, as the screening of library compounds progressed, the fluorescence signals generated in response to VIP using the CHO-$hVPAC_2R$ cell line became increasing variable between wells of individual assay

plates and consequently between assay plates. As a result, a large number of false positive hits were identified during screening, particularly from the 'M' library. In an attempt to rectify this situation, silicone coated FLIPR® tips and a new box of tips for each plate were systematically trialled, but neither resulted in any significant improvement in the consistency of response. The occurrence of this variability meant several compound plates had to be re-screened at a later date.

Although the agonist induced calcium responses from the CHO-hVPAC$_2$R cell line were large enough (in the FlexStation® and initial FLIPR® assays) to justify the use of this assay in HT-screening, the use of the cAMP assay may have proven to be more reliable. When comparing the two assays in the FlexStation®, maximum agonist induced cAMP responses from the stable cell lines were 3 - 4 fold greater than the corresponding calcium responses (~ 25x basal compared to ~ 7x basal; chapter one, p 104 and p 106). Therefore, the use of the cAMP assay during screening may have reduced the impact of the well-to-well variability and decreased the number of false positive hits. A further drawback of the calcium assay became evident in the reproducibility studies, as discussed previously for FR049554. If a particular library compound alone stimulated a calcium response from the hVPAC$_2$R cell line, it would reduce the subsequent response to VIP and appear to be an antagonist, giving a false positive result. This reduction in agonist induced calcium response following an initial stimulation event with agonist has been described for other GPCRs, including VPACR (Porter *et al.*, 2001; Harfi & Sariban, 2006). In our CHO-hVPAC$_2$R studies, this effect may have been a consequence of receptor desensitisation or of a limited availability of calcium in the intracellular stores of the host cell line, as a result of the initial calcium stimulation. In contrast, this effect did not appear to be an issue in the FlexStation® cAMP assay. In preliminary studies using the hVPAC$_1$R and hPAC$_1$R cell lines, in which PG99-465 (which was shown to be a full agonist at these receptors in this assay; chapter one, p 119) was pre-incubated with the cells prior to VIP addition (EC_{50} concentration), the resulting cAMP levels were found to be additive (Figure 1.2.27, p 124). This suggests that when stimulated by these receptors, the $G\alpha_s$-adenylate cyclase pathway in CHO-K1 cells was perhaps less susceptible to desensitisation than the calcium stimulating pathways, or that larger pools of cAMP were available in these cells relative to calcium. As a result, the use of the cAMP assay for screening may again have reduced the number of false positives detected. The possible advantages of the cAMP assay over the calcium assay in our screening studies are speculative at this stage and both assays would need to be compared in a 384-well format on the FLIPR® before this could be verified. Prior to the selection of the screening assay

we intended to perform a pre-screening trial of both assays on the FLIPR®, however as the calcium assay was less time consuming and more cost-effective than the cAMP assay, our colleagues in Astellas Pharma Inc. selected the former assay as the most appropriate to use for this $hVPAC_2R$ screening project. In an industry where the cost of developing one drug from the laboratory into clinical use is estimated to be in the region of $802 million, reducing expenditure during development is of prime importance (Dickson & Gagnon, 2004; O'Connell & Roblin, 2006). The necessity of economical pre-clinical studies is further emphasized when it is considered that only 1 out of every 5 – 10,000 compounds evaluated in pre-clinical testing proceeds to clinical use (Figure 2.3.1; Preziosi, 2004). In addition, the average success rate for CNS targets specifically, has been estimated to be 3 - 5 % (Kola & Landis, 2004; Hurko & Ryan, 2005). The high attrition rates in the drug discovery process are a result of multiple factors, however in most cases (~ 40 %), a lack of efficacy of lead compounds at the clinical trial stage of development is responsible (Preziosi, 2004; Kola & Landis, 2004). Furthermore, there are an emerging number of critics who suggest that the introduction of target based drug discovery and HT-screening is the predominant cause of the declining numbers of new chemical entities (NCE) reaching the clinic (Hilbush *et al.*, 2005; Macarron, 2006).

When multiple assay types are deemed suitable for screening a particular drug target, the logical selection for HT-screening would be the most cost-effective,

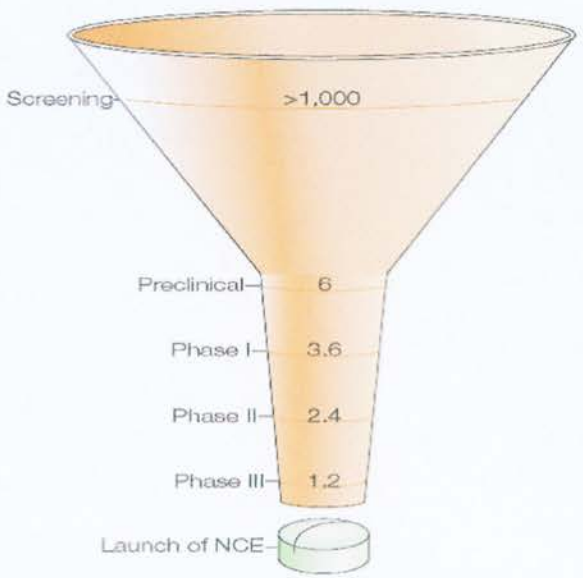

Figure 2.3.1 Estimated proportions of compounds proceeding to various stages in the drug development process. The diagram illustrates hypothetical ratios of compounds that successfully proceed through the stages of drug development. Figure from Preziosi (2004).

high-throughput and simplest assay. However, for GPCRs which activate multiple signalling pathways, selecting a single assay for screening may be limiting. As discussed recently by Gurwtiz & Haring (2003), a more effective strategy may be to utilise multiple assays for a range of second messengers, hence providing a more extensive and thorough (high-content) screening programme. The possible benefits of this approach have been discussed with particular reference to cevimeline (Evoxac), a M_1 receptor agonist that is currently marketed by Daiichi-Sankyo Inc. as a treatment for symptoms associated with Sjögren's Syndrome (Gurwitz & Haring, 2003; Jacoby *et al.*, 2006). This drug has been shown to have remarkably different pharmacological activities at M_1 receptors *in vitro*, depending on the second messenger investigated; being an antagonist in AC assays, a partial agonist in PLC assays and a 'super-agonist' in calcium mobilisation con-focal microscopy studies (Fisher *et al.*, 1996). The use of multiple assays in this case clearly helped identify a therapeutically useful compound, the efficacy of which could otherwise have been overlooked if only AC studies had been utilised to evaluate its pharmacology. Additionally the use of multiplex assays may be an even more attractive alternative to improving the HT-screening process (Jacoby *et al.*, 2006). In these assays the parameters of a single screen are adjusted and modified to facilitate the identification of different types of ligands (agonists, antagonists etc.) from compound libraries, with this approach already implemented into FLIPR® based screening platforms in pharmaceutical companies such as Novartis (Jacoby *et al.*, 2006). Although these approaches produce much more extensive data from screening, they are inevitably of lower throughput and higher cost than the simpler, single assay screens. However there are no advantages to running an ineffective screen, solely for the reason that is fast and economical. A balance between the resources required to run an effective screen and the quality of the data produced should be investigated for each HT-screening study performed.

2.3.4. HT-screening studies of group B GPCR

As discussed in the introduction to this chapter, HT-screening to identify novel ligands for the group B GPCR family has proven challenging for the pharmaceutical industry and consequently, this receptor family is deemed to be a difficult target for drug discovery, with only a few non-peptide antagonists and no potent, non-peptide agonists reported to date (see Table 2.1.1, p 162; Hoare, 2005). Indeed, when the success rates of compounds proceeding from HT-screening to lead

Target class		Success rate: HTS to tractable hit (%)
G-protein-coupled receptors (GPCRs)	Family A	54
	Family B	0
	Family C	0
Ion channels		73
Kinases		7
Nuclear receptors		72
Other enzymes		50
Other targets		33

Table 2.3.1 Success rates of compounds proceeding from HT-screening studies to lead compound (tractable hit) status for a range of drug targets utilised by GSK over a three year period (Macarron, 2006).

compound status are compared between target types utilised in HT-screening at GlaxoSmithKline (GSK; from 2001 to 2004), the group B (and C) GPCR families are clearly lagging behind the group A GPCRs and other classes of target (Table 2.3.1). It has been suggested that structural differences in the transmembrane domains between the group A and B GPCRs may account for the contrasting success rates of HT-screening studies and why it appears to be so difficult to find non-peptide ligands for the group B receptors (Macarron, 2006). The chemical and molecular basis for this hypothesis warrants further consideration as more data becomes available regarding the mechanisms of ligand binding to the group B GPRCs (Hoare, 2005). Such data may facilitate the identification and design of novel non-peptide ligands for this group of receptors in the future, including the VPAC/PAC receptor family. In addition, the poor success rates of group B GPCR screening studies may also be due to a lack of appropriate chemicals in the compound libraries examined. This simple explanation has proven to be pertinent in recent years, as can be clearly seen upon examination of the success rates in lead compound identification from the compound libraries at GSK. Following the merger of GlaxoWellcome and SmithKline Beecham in 2000, the amalgamation of the respective compound libraries led to the identification of lead compounds for almost a third of the targets for which screening studies prior to the merger had proven unsuccessful (Macarron, 2006). Similarly, the merger of the Fujisawa and Yamanouchi Pharmaceutical Companies to form Astellas Pharma Inc., which took place after the current screening studies were performed, has resulted in a much larger and more diverse compound library for the new company. In the future, this could provide a new opportunity to identify novel $VPAC_2R$ specific ligands.

CHAPTER THREE
CENTRAL ROLES FOR VPAC/PAC RECEPTORS

3.1. Introduction

In the final chapter of this thesis I will consider some of the roles of VPAC/PAC receptors in the central nervous system and describe studies investigating such actions, using both *in vitro* and *in vivo* techniques. As discussed in the general introduction, a plethora of potential roles have been described for VIP, PACAP and their cognate receptors, with a large proportion of these studies focusing on glucose homeostasis, neuroprotection, modulation of the immune system and control of circadian function. In this section, I will explore some of the central roles that are potentially mediated via VPAC/PAC receptors, with a primary focus on neuroprotection/immunomodulation and circadian rhythms of activity.

3.1.1. VPAC/PACR in neuroimmunomodulation and neuroprotection

The first descriptions of a neuroprotective action for VIP were published almost twenty years ago by Brenneman and colleagues (Brenneman & Eiden, 1986; Brenneman *et al.*, 1987). In these studies, VIP application to cultures of mouse dorsal root ganglion neurons was reported to increase the survival of the cells (maximal protection observed with nanomolar VIP concentrations) in response to co-treatment with the well established neurotoxin, tetrodotoxin (TTX). In the years following, evidence in support of a neuroprotective role for VIP and PACAP grew considerably, with publications reporting the use of a wide variety of *in vitro* and *in vivo* models, which shall be discussed in depth in the following sections.

3.1.1.1. VIP and PACAP mediated neuroprotection

In agreement with the findings of Brenneman (see above), Kaiser & Lipton (1990) reported that VIP was able to rescue rat retinal ganglion cells from TTX induced cell death, with maximal protection observed with micromolar concentrations of the peptide. Furthermore these authors suggested that the survival promoting effects of VIP involved a cAMP dependent pathway (Kaiser & Lipton, 1990). Using rat cultured cortical neurons, PACAP-38 was subsequently shown to reduce glutamate induced cell death (by approximately 50 %), with the peak of this protective effect observed at considerably lower (picomolar) concentrations (Morio *et al.*, 1996). Comparable protection against glutamate excitotoxicity has also been

demonstrated in rat retinal neurons (with micromolar peptide concentrations) and was reported to occur through a pathway involving cAMP, PKA and MAPK (Shoge *et al.*, 1998, 1999). In rat and murine mixed cortical cultures, the PACAPs have also been shown to protect against neuronal death following an inflammatory insult generated using LPS, which is a major constituent of the cell wall of gram-negative bacteria (Kong *et al.*, 1999; Li *et al.*, 2005). Once again PACAP proved to be neuroprotective even when used at very low (picomolar) concentrations, however its effectiveness appeared to have a biphasic concentration dependence. Furthermore, these studies suggested that the neuroprotective action of PACAP was mediated through PAC_1R and that at least two pathways were involved. One component was reported to involve the stimulation of cAMP (nanomolar peptide concentrations), whereas the second involved stimulation of MAPK (subnanomolar peptide concentrations; Kong *et al.*, 1999; Li *et al.*, 2005). The protective effects of VIP and PACAP are not restricted to neurons and further studies from Brenneman and colleagues demonstrated that in rat cortical astrocytes (RCA), VIP and PACAP-38 could protect against toxicity induced by gp120 derived peptides (glycoprotein envelope of the HIV virus; Brenneman *et al.*, 1999, 2002). As illustrated in Figure 3.1.1, the concentration response relationship for both peptides was biphasic, however the peaks of protective action were different for the individual peptides, indicating different potencies. Vaudry and colleagues have also investigated the neuroprotection of PACAP using rat cerebellar granule cells and have shown that this peptide can protect these cells against ethanol induced apoptosis and cell death from oxidative stress (Vaudry *et al.*, 2002a, 2002b). The authors suggested that the observed neuroprotection was due to the anti-apoptotic effects of the peptide as a

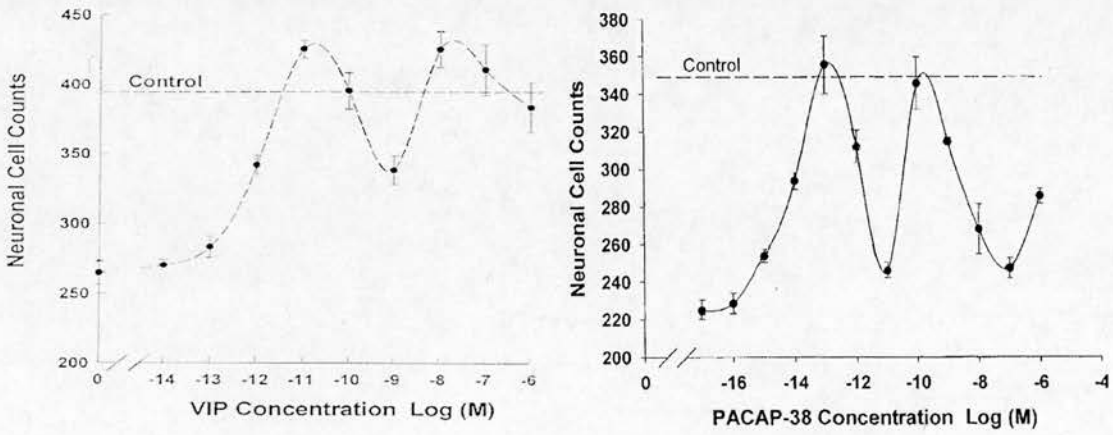

Figure 3.1.1 VIP and PACAP-38 protect rat cortical astrocytes against gp120 induced cell death. These figures are adapted from Brenneman *et al.* (1999, 2002).

consequence of caspase-3 inhibition, which occurred downstream of PAC_1R activation. Consistent with these findings, Onoue and co-workers have used rat PC12 cells (endogenously express PAC_1R) to show that VIP and PACAP-27 were protective against β-amyloid and prion protein induced neurotoxicity, involving a PKA-MAPK pathway, again as a result of caspase-3 inhibition (Onoue *et al.*, 2002a, 2002b). Similar to the effects described for gp120 toxicity (Figure 3.1.1), these studies demonstrated that the peptides had quite different potencies, with significant protection detected with picomolar and nanomolar concentrations of PACAP-27 and VIP respectively. This is consistent with the potency of these peptides at the PAC_1R (chapter one). From the studies described above and others showing VIP/PACAP cellular protection *in vitro*, the protective effects generally appear to be biphasic with regard to their concentration dependence and are partly mediated by pathways involving MAPK and cAMP. In addition, several of the studies described in this section have implied that the PAC_1R mediates the neuroprotective actions of VIP and PACAP. A very recent study exploring the role of specific PAC_1R splice variants demonstrated that the PAC_1-hop2 receptor can protect transfected COS cells from hydrogen peroxide induced oxidative stress (Pilzer & Gozes, 2006b). These authors suggested that cAMP may mediate these effects and also discussed the possible involvement of receptor mediated calcium signals.

Within the last ten years, the neuroprotective properties of VIP and PACAP have been examined in a range of animal models, including models of stroke, Parkinson's disease and traumatic brain injury (TBI). In models of both global and focal ischemia, administration of PACAP-38 (i.c.v. or i.v. injection) has been shown to have remarkable effects on the infarct volume and the integrity of hippocampal neurons (Uchida *et al.*, 1996; Reglodi *et al.*, 2000, 2002). Indeed, even when given 4 h post-insult (transient MCAO) PACAP-38 produced a 50 % reduction in infarct size (Figure 3.1.2; Reglodi *et al.*, 2000). In addition, PACAP was demonstrated to protect hippocampal neurons from ischemic damage even when given up to 24 h post-insult, with these effects suggested to be mediated by astrocytes (Uchida *et al.*, 1996). In further studies these authors suggested that the anti-apoptotic effects involved increased IL-6 release from astrocytes and the modulation of MAPK activity (Shioda *et al.*, 1998). Recent studies using transgenic mice have also confirmed that PACAP can have a number of protective effects. As discussed in the general introduction, PACAP null mice had significantly higher neuronal damage following pCMAO when compared with WT mice (Ohtaki *et al.*, 2006). In addition, these studies also showed that PACAP-38 was not neuroprotective in IL-6 null mice, providing further evidence for a critical role of this cytokine in PACAP induced

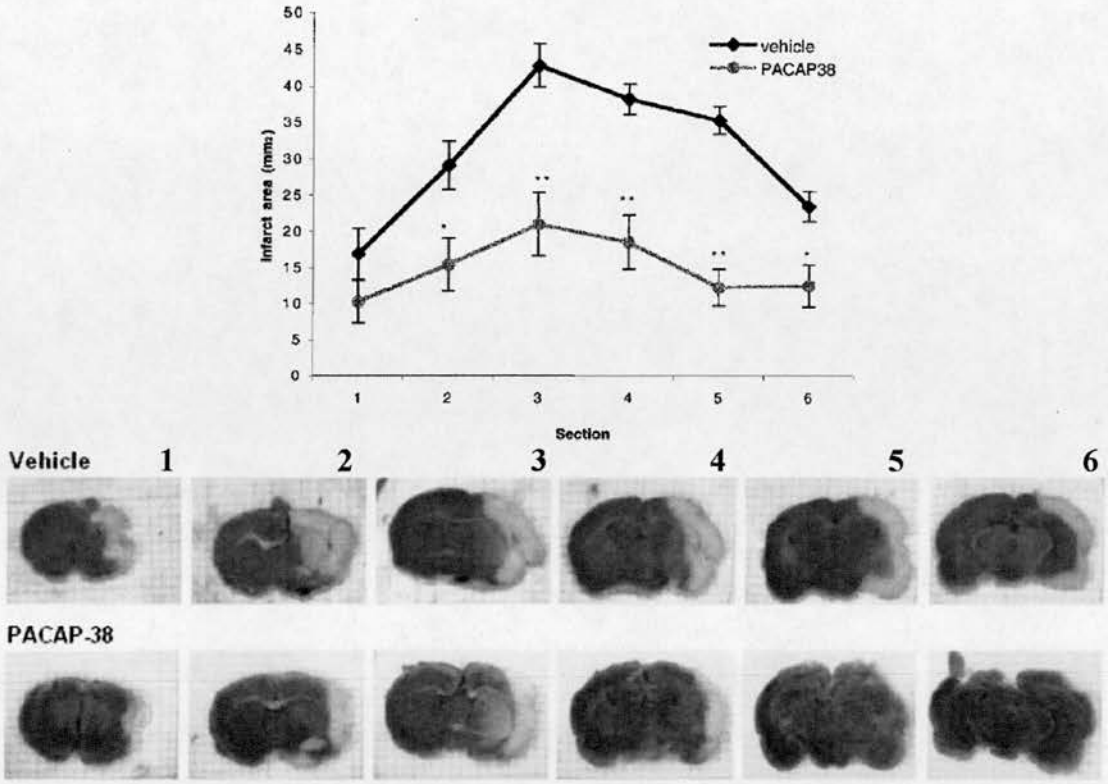

Figure 3.1.2 **Effects of PACAP-38 administration on infarct size following transient MCAO.** MCAO was performed for 2 h and was followed four hours later by the administration of vehicle or PACAP-38 through osmotic mini-pump. The reduction in infarct size with PACAP-38 is evident in both the upper graph and from the representative brain slices. Figures taken from Reglodi *et al.* (2000).

neuroprotection (Ohtaki *et al.*, 2006). In general the doses of peptides that have been shown to be effective *in vivo* are relatively low, in comparison to the doses required to induce a significant increase in cerebral blood flow. This led Reglodi and colleagues to speculate that although the exact mechanism underlying PACAP induced neuroprotection is not clear, the effects may only be partially due to a peptide induced increase in cerebral blood flow (Reglodi *et al.*, 2000). These authors have also used an animal model of Parkinson's disease to examine PACAP induced neuroprotection (Reglodi *et al.*, 2004). In these studies, the neurotoxin 6-hydroxydopamine was used to induce lesions of the substantia nigra in rats and the neuroprotective effects of PACAP-38 pre-treatment were evaluated. PACAP-38 was shown to rescue ~ 50 % of the dopaminergic neurons from death, with a reduction in behavioural deficits. Delgado & Ganea (2003a) have used the MPTP model of Parkinson's disease and reported that VIP administration was also able to reduce neuronal degeneration in the substantia nigra. Again, the mechanism of the VIP

action in this model is not entirely clear, however it was suggested that anti-apoptotic and anti-inflammatory actions of the peptide may be involved. The putative impact of VIP/PACAP and their receptors in TBI has also been explored in a small number of relatively recent studies. In 1999 Skoglösa *et al.*, using the weight drop technique in rats, demonstrated that an insult to the cerebral cortex produced an increase in PACAP mRNA expression in the ipsilateral cortex (for up to 72 h post insult) and hippocampus (peaked at 12 – 48 h post insult; Skoglosa *et al.*, 1999). In contrast, using the stab wound injury model, which induces a much lower inflammatory response, Jaworski and colleagues (2000) found that PACAP mRNA was not up-regulated post insult. However, and perhaps in support of the data from Skoglosa *et al.* (1999), following a TBI insult in rats (weight drop technique), Hang and colleagues (2004) demonstrated that the concentration of VIP in the plasma and gut tissue of the rats was significantly elevated 72 h after the insult. The observed increase in VIP levels was coincident with elevations in other brain-gut peptides, and was suggested to be involved in the gastric dysfunction observed in many patients following TBI (Hang *et al.*, 2004). Furthermore, using the same TBI model Farkas *et al.* (2004) have shown that in contrast to i.v. administration of PACAP pre-insult which was ineffective, i.c.v. administration post-insult reduced the density of damaged neurons, re-iterating the potential therapeutic value of PACAP like peptides. Although much attention has focused on the role of the PAC_1R in mediating these neuroprotective effects, results from a recent study have shown that the $VPAC_2$ receptor may be involved. Using $VPAC_2R$ null mice, Rangon and colleagues (2006) have shown, in contrast to WT mice, that VIP was not protective against ibotenate induced cerebral white matter lesions. In addition, the neuroprotective effect of VIP in the WT mice was shown to be independent of cAMP levels, but dependent on PKC activity (Rangon *et al.*, 2006). From both the *in vitro* and *in vivo* studies discussed, although the exact mechanisms underlying the protective effects of VIP/PACAP remain unclear, anti-apoptotic and anti-inflammatory actions are likely to be involved given the involvement of caspases and cytokines. As shall be discussed in the following section, several factors have now been identified which may mediate the neuroprotective effects of VIP and PACAP.

3.1.1.2. VIP and PACAP secretagogue activity

The neuroprotective effects of VIP and PACAP are suggested to occur through several mechanisms, involving both direct and indirect actions (Dejda *et al.*,

2005). The direct effects are thought to be mediated by the VPAC/PAC receptors expressed on neurons and to involve both cAMP/PKA and PLC/IP_3 signalling pathways leading to modulation of MAPK activity. It is interesting to note that these direct protective effects are not always evident, as the early studies of Brenneman showed that enriched neuronal cultures were not protected by VIP following TTX treatment, in contrast to observations from mixed astrocyte/neuronal cultures (Brenneman *et al.*, 1987). However, this may reflect the different types of neurons that have been examined and the receptor expression levels on those neurons. In addition, some of the indirect protective effects of VIP and PACAP have been attributed in recent years to anti-inflammatory effects mediated by microglia (Delgado *et al.*, 2002). The peptides have been demonstrated to reduce the release of pro-inflammatory cytokines (TNF-α, IL-1β, IL-6) from microglia and hence have been termed 'microglia deactivating factors' (Delgado *et al.*, 2002, 2003b). Much of the research into the protective effects of VIP and PACAP has focused on the indirect effects mediated through VIP/PACAP activity on astrocytes. The role of astrocytes has been well documented since the very first studies of VIP/PACAP neuroprotective effects, in which Brenneman and colleagues (1987) reported that 'a diffusible substance that exhibits neuronal survival-promoting activity is detectable after treatment of non-neuronal cultures with VIP'. Although the exact mechanism underpinning VIP/PACAP neuroprotection via astrocytes is unclear, peptide induced production and release of a number of factors, including cytokines and highly potent neurotrophic factors is involved (Brenneman *et al.*, 1987; Dejda *et al.*, 2005). The secretion of these factors has been demonstrated *in vitro* following stimulation of primary cultures of RCA with VIP and PACAP, and is discussed below.

Much of the research into cytokine release from astrocytes upon VIP/PACAP treatment has come from the Brenneman laboratory, although other groups have also contributed to the existing knowledge (Gottschall *et al.*, 1994; Grimaldi *et al.*, 1994). VIP and PACAP have been shown to stimulate the release of multiple cytokines from RCA including IL-1α, IL-β, IL-3, IL-6, MIP-1α, MIP-1β, RANTES, TNF-α, M-CSF and G-CSF (Brenneman *et al.*, 1995, 1999, 2002, 2003). These studies have shown that the concentration of peptide, and the specific peptide used, will greatly alter the composition of the pool of cytokines released from the RCA (Figure 3.1.3). Furthermore, the involvement of cAMP dependent and cAMP independent mechanisms has been demonstrated in this peptidergic modulation of cytokines (Brenneman *et al.*, 2003). The release of these cytokines is likely to contribute to the neuroprotective effect through modulating the inflammatory process; however their release does not fully account for the VIP/PACAP

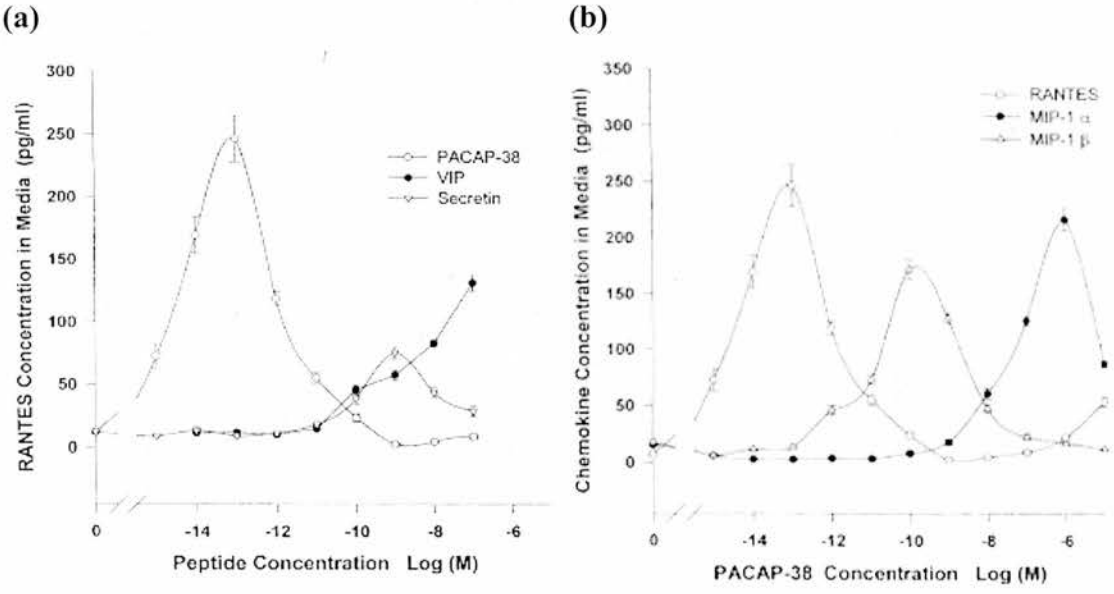

Figure 3.1.3 **VIP and PACAP stimulated release of cytokines from RCA.** The composition of the cytokine pool released from RCA in response to VIP/PACAP is critically dependent on which peptide (**a**) is applied to the cells and at what concentration (**b**). Figures taken from Fukuhara *et al.* (1997) and Brenneman *et al.* (2002).

neuroprotection observed at very low peptide concentrations. These effects have been attributed to a very exciting group of neurotrophic factors, the first of which - 'activity-dependent neurotrophic factor' (ADNF), was purified 10 years ago from rat cortical astrocyte cultures following stimulation with VIP (0.1 nM; Brenneman & Gozes, 1996). These authors reported that ADNF and an active fragment of this factor, ADNF-14 were able to potently reduce neuronal death in cerebral cortical cultures treated with TTX, gp120, NMDA and β-amyloid (Figure 3.1.4), and suggested that these factors may do so by influencing calcium mobilisation. Structure-activity studies of ADNF revealed that a shorter derivative ADNF-9 (9 amino acid residues: SALLRSIPA) was actually even more potent than the parent peptide and was effective over a broader concentration range (Brenneman *et al.*, 1998). In addition the conferred neuroprotection was relatively long lasting, with a 2 h treatment protecting neurons from TTX induced death for 4 days. The potency of this peptide was shown to be increased by ~10,000 fold in mixed neuron/glial cultures compared to neuronal cultures alone, suggesting that in addition to a direct action on neurons, ADNF-9 was able to stimulate the release of additional protective factors from astrocytes. An ADNF-like factor called ADNP (activity-dependent neurotrophic protein) was also identified from a mouse carcinoma cDNA library and was found to contain a short peptide termed NAP (sequence: NAPVSIPQ), which

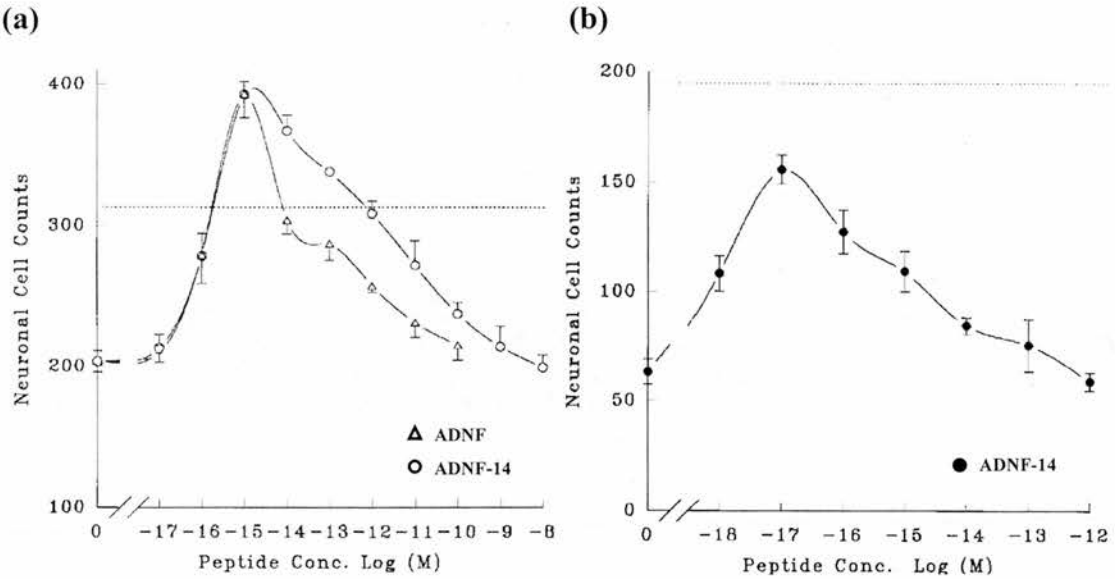

Figure 3.1.4 **ADNF neuroprotection of cerebral cortical cultures.** ADNF derived peptides were shown to potently protect neurons from TTX (**a**) and β-amyloid (**b**) induced cell death. The dashed lines indicate the number of neurons in control cultures. Figures from (Brenneman & Gozes, 1996; Cagampang *et al.*, 1998a)

was subsequently shown to have similar *in vitro* protective properties to the ADNF factors and in some cases, was even more potent (Bassan *et al.*, 1999; Gozes & Brenneman, 2000). The protective actions of NAP have also been demonstrated in several *in vivo* models including stroke, TBI and fetal alcohol syndrome (Beni-Adani *et al.*, 2001; Leker *et al.*, 2002; Vink *et al.*, 2005). These factors are proposed to work in part though cGMP pathways and are thought to target tubulin, a component of the cytoskeleton (Ashur-Fabian *et al.*, 2001; Divinski *et al.*, 2004). The remarkable neuroprotective activity of NAP therefore provides an exciting opportunity for drug development, with the peptide currently entering into phase II clinical trials (Gozes *et al.*, 2005). The mechanisms which link VIP and PACAP to ADNP release from astrocytes, including the exact VPAC/PAC receptors and the downstream signalling pathways involved, remain to be clarified although the $VPAC_2R$ is suggested to be involved (Zusev & Gozes, 2004). The precise mechanisms will depend on the expression levels of VPAC/PAC receptors in the astrocytes, as discussed in the following section.

3.1.1.3. VPAC/PAC receptor expression in RCA

Multiple studies have demonstrated that primary cultures of rat astrocytes (RCA) express several subtypes of VPAC/PAC receptors (Ashur-Fabian *et al.*, 1997; Grimaldi & Cavallaro, 1999; Jaworski, 2000). However, the range of subtypes expressed and their relative expression levels appear to vary considerably between reports. VPAC/PAC receptor expression in astrocytes has been suggested to be developmentally regulated, therefore the expression levels in cultured astrocytes may depend on the age of the animals from which the cells were derived and on the length of time the cells have been maintained in culture (Jaworski, 2000). In general PAC_1R variants have been shown to be the predominant subtype expressed in RCA, with the expression of the null, hop2 and hop1 variants shown (Ashur-Fabian *et al.*, 1997; Grimaldi & Cavallaro, 1999; Jaworski, 2000; Hashimoto *et al.*, 2003). Furthermore, the recently described PAC_1(3a) variant has also been shown to be expressed in rat astrocyte cultures (Pilzer & Gozes, 2006a). The presence of both VPAC receptor subtypes has also been described in these cells, although the expression levels appear to vary, with $VPAC_1R$ expression suggested to be very weak and with $VPAC_2$ levels differing between reports (Ashur-Fabian *et al.*, 1997; Grimaldi & Cavallaro, 1999; Jaworski, 2000; Hashimoto *et al.*, 2003). The complement of receptors expressed in the RCA at any given time will regulate downstream signalling, and the potencies with which they are activated by VPAC/PACR agonists may influence the levels of neuroprotective factors secreted by the cells.

3.1.1.4. VPAC/PAC receptor signalling pathways in RCA

As discussed in chapter one, VPAC/PAC receptors have been demonstrated to couple to G-proteins stimulating intracellular pathways that increase cAMP, calcium and PLD levels. In RCA, the VPAC/PAC receptor modulation of these intracellular messengers is poorly characterised, as is the pharmacology of the receptors present. Further investigation into both of these areas could prove useful to our understanding of the mechanisms linking VPAC/PACR activation to the secretion of neuroprotective factors from astrocytes. The concentration dependent stimulation of cAMP by PACAP in astrocytes has been demonstrated in only a small number of studies (Hashimoto *et al.*, 1993; Grimaldi & Cavallaro, 1999; Masmoudi *et al.*, 2003; Li *et al.*, 2005). The most extensive characterisation was performed by

Hashimoto and colleagues (1993) who compared PACAP-27, PACAP-38 and VIP potencies for cAMP stimulation in RCA, generating an ROP that was consistent with the expression of the PAC_1R. Regarding the other intracellular messengers, only one study has demonstrated a concentration dependent increase of calcium in response to PACAP-38 (Masmoudi *et al.*, 2003), although Dejda and colleagues (2006) have recently reported the characterisation of cAMP, calcium and PLD responses in RCA in response to VIP, PACAP-38 and PHI/PHM. These authors reported that cAMP levels were stimulated by all the agonists examined, with calcium and PLD pathways only sensitive to VIP and PACAP-38. However, no concentration response curves were shown from these studies and no quantification of potency was reported, limiting the interpretation of the results (Dejda *et al.*, 2006).

3.1.1.5. Characterisation of VPAC/PACR pharmacology in RCA and the correlation with cytokine release

Given the highly important roles of astrocyte derived factors in neuroprotection and the poorly characterised VPAC/PACR pharmacology in these cells, we sought to fully investigate the pharmacology of VPAC/PAC receptor mediated intracellular cAMP and calcium responses in primary cultures of rat cortical astrocytes. The characterisation studies were performed using the same FlexStation® assays that were utilised in chapter one. Furthermore, we attempted to determine if any correlation was evident between cAMP and/or calcium signalling and the release of cytokines from the astrocytes upon VPAC/PACR stimulation.

3.1.2. The role of VPAC/PACR in the control of circadian rhythms

As discussed in the general introduction, the generation of mouse lines harbouring transgenes for VIP, PACAP and their receptors, has provided significant insights into the important roles of these peptides and their cognate receptors in circadian function. The basic physiology of circadian rhythm generation and its control shall be discussed here in brief, prior to a more in-depth review of current knowledge regarding VPAC/PACR control of circadian rhythms, with particular reference to the $VPAC_2R$.

3.1.2.1. The mammalian circadian clock

Circadian rhythms are biological cycles of behaviour or physiology which have a period of approximately 24 h. The principal regulator of these cycles in mammals is the suprachiasmatic nucleus (SCN), a small collection of neurons which is located at the base of the brain. The initial identification of this brain area as the circadian pacemaker or clock was reported simultaneously by two groups in 1972 (Moore & Eichler, 1972; Stephan & Zucker, 1972). In these studies, both groups examined circadian rhythms in rats in which the SCN had been lesioned and they found that the rats' activity and drinking rhythms, in addition to rhythms of corticosterone production in the adrenal glands, were severely disrupted. Oscillatory cycles within this nucleus were subsequently demonstrated through evaluation of neuronal activity and glucose utilisation, both of which were demonstrated to be generally high during the day and low during the night (Schwartz & Gainer, 1977; Shibata *et al.*, 1982). Further confirmation of the role of the SCN in the control of circadian cycles was demonstrated through multiple SCN transplant studies (Drucker-Colin *et al.*, 1984; Sawaki *et al.*, 1984; Lehman *et al.*, 1987; Ralph *et al.*, 1990). These studies involved the transplantation of fetal SCN cells into rats/hamsters in which the SCN had been lesioned and which had disrupted circadian cycles. Following surgery, the recipient animals were observed to express normal 24 h cycles of activity. Furthermore, the transplantation of SCN cells from the *tau* hamster mutant which had a short circadian period (~ 22 h), demonstrated that the characteristics of the circadian cycles expressed by recipient animals were governed by those of the donor (Ralph & Menaker, 1988; Ralph *et al.*, 1990).

Since these early studies a wealth of knowledge has been produced to demonstrate how the SCN controls and maintains circadian cycles. The SCN

receives environmental cues principally from the retino hypothalamic tract (RHT), a neural tract which projects from retinal ganglion cells (RGC) to VIP containing neurons in the ventral region of the SCN (Moore & Eichler, 1972; Ibata *et al.*, 1989). The contribution of additional input pathways to the SCN has also been described, for example the geniculo-hypothalamic tract (GHT) which projects from the intergeniculate leaflet, however these pathways appear to have a more minor role compared to the RHT (Piggins & Cutler, 2003). Transmission of photic information from the RHT to the SCN is suggested to principally involve the peptide PACAP and glutamate, the release of which are modulated by retinal signals (Ebling, 1996; Chen *et al.*, 1999; Hannibal, 2002). Within the retina the presence of a photosensitive GPCR termed melanopsin, in a subset of PACAP containing RGC, has been suggested to control the integration of environmental lighting cues into transmitter signals in the RHT (Provencio *et al.*, 2000; Hannibal *et al.*, 2004). Photic information received by the SCN is used to entrain and finely tune the periodicity of the clock, which can then coordinate peripheral oscillators (Hastings *et al.*, 2003). The molecular mechanism of rhythm generation in SCN has cells has been intensively researched in recent years and the generation of rhythmic activity has been shown to involve feedback loops between two pairs of molecules, CLOCK/BMAL1 and CRY/PER (reviewed in detail elsewhere: Albrecht & Eichele, 2003; Ko & Takahashi, 2006).

3.1.2.2. VIP/PACAP and VPAC/PACR expression in the SCN

As discussed above, both VIP and PACAP have been localised to specific areas within the SCN. From both *in situ* hybridisation studies and enzyme immunoassays, expression of VIP and PACAP in their respective areas has been shown to be low during the day and higher at night (Figure 3.1.5; Shinohara *et al.*, 1993, 1999; Ban *et al.*, 1997; Fukuhara *et al.*, 1997). These studies demonstrated that the rhythmic expression of the peptides is not detected under conditions of constant darkness, suggesting that their expression is controlled by light stimulation and thus may be involved in entrainment. Following on from the demonstration of VIP binding sites in the SCN (Besson *et al.*, 1984; Shaffer & Moody, 1986) and the identification of VIP/PACAP receptor subtypes (described in the general introduction), the expression of individual VPAC/PACR in the SCN was investigated. As discussed previously (p 34), the $VPAC_2R$ has been shown to be highly expressed in the SCN and in addition, the density of the receptors changes

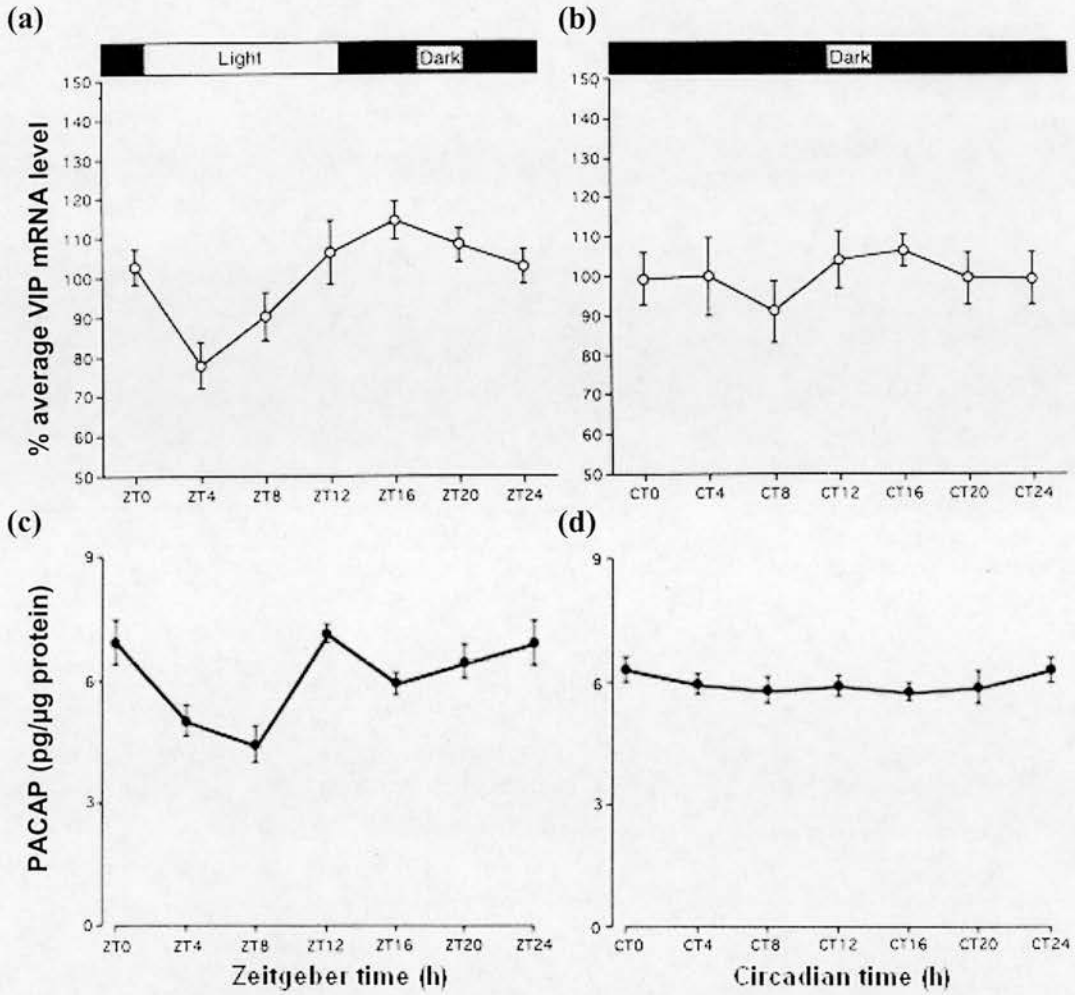

Figure 3.1.5 **Expression of VIP and PACAP mRNA in the rat SCN.** The expression levels of VIP (a/b) and PACAP (c/d) in the SCN under a light/dark cycle (a/c) and constant darkness (b/d) are shown. Figures taken from Ban *et al.* (1997) and Cagampang *et al.* (1998a, 1998b).

throughout the day (Cagampang *et al.*, 1998b). The first examination of the temporal expression of $VPAC_2R$ in the SCN was reported by Cagampang and colleagues (1998b). Using *in situ* hybridisation techniques, these authors showed that daily $VPAC_2R$ expression was biphasic in the SCN, with peak expression levels detected midway through the light cycle (ZT6) and towards the end of the dark cycle (ZT22) (Cagampang *et al.*, 1998b). This rhythm was reported to be sustained in constant darkness with similar peaks of expression (CT10 and CT22; Cagampang *et al.*, 1998b). In contrast, one year later Shinohara *et al.* (1999) used similar techniques and reported that expression of this receptor was generally low during day and high at night. In this study the authors also reported negligible expression of $VPAC_1R$ in the SCN. Finally, PAC_1R expression in the SCN has also been investigated and was reported to peak in the middle of the light and the dark cycles (Cagampang *et al.*,

(a) $VPAC_2R$ mRNA expression **(b) PAC_1R mRNA expression**

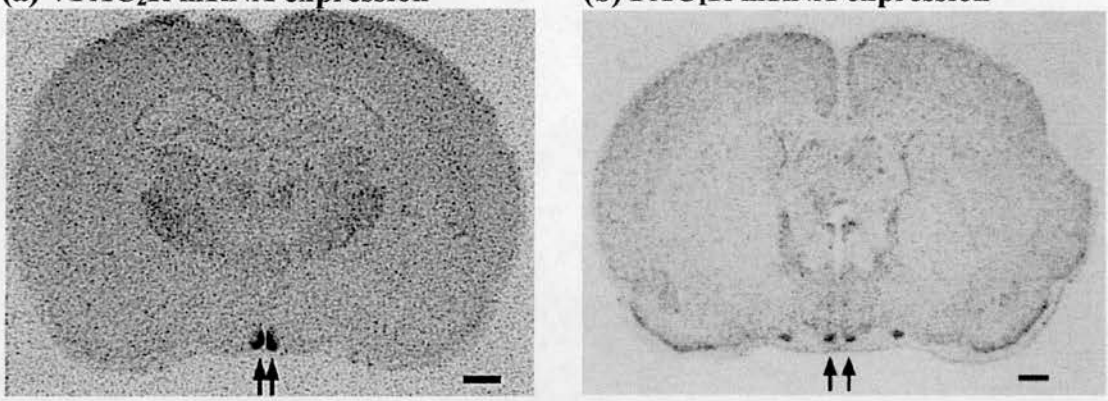

Figure 3.1.6 **$VPAC_2$ and PAC_1R mRNA expression in the rat brain.** The arrows indicate the location of the SCN. Figures taken from Cagampang *et al.* (1998a, 1998b).

1998a). The expression of different splice variants was also reported, with only the null and hop variants being detected in SCN cells (Ajpru *et al.*, 2002).

3.1.2.3. VPAC/PACR modulation of circadian time-keeping

With the combined expression of VIP, PACAP, $VPAC_2R$ and PAC_1R in the SCN, many groups have investigated the effects of modulating VPAC/PACR function on circadian rhythms both *in vitro* and *in vivo*. Hannibal and colleagues (1997, 1998) have reported that the neuronal activity of the rat SCN (brain slice preparations) could be phase advanced by PACAP-38 application in the daytime (CT6), in a concentration dependent manner. These effects were shown to be mediated by PAC_1R, with VIP being 1000 fold less potent in inducing similar phase shifts (Hannibal *et al.*, 1997, 1998). Consistent with the studies of Hannibal (1997, 1998), Harrington and colleagues also reported that PACAP application to hamster brain slices could induce phase shifts when applied during the daytime (Harrington & Hoque, 1997; Harrington *et al.*, 1999). These authors reported that daytime application of PACAP (10 nM to 1 μM) induced phase shifts in SCN neuronal firing rate activity, an effect that was suggested to be cAMP mediated (Harrington *et al.*, 1999). Interestingly, lower doses (~ 1 nM) of the peptide produced phase delays when administered during the night, through glutamate mediated pathways. Furthermore, PACAP has been demonstrated (via a pathway involving PAC_1R and cAMP) to alter the magnitude of the phase shifts produced from nocturnal glutamate application to the SCN *in vitro* (Chen *et al.*, 1999). In contrast to the effects of

PACAP on the SCN which appear to be PAC_1R mediated, the effects of VIP on SCN activity *in vitro* have been reported to depend on $VPAC_2R$ involvement (Reed *et al.*, 2001, 2002). The neuronal firing rhythms of rat SCN cells *in vitro* were shown to be significantly phase advanced by VIP application during the night (ZT19), in a concentration dependant manner (Reed *et al.*, 2001). These effects were very similar to those produced by application of the $VPAC_2R$ agonist Ro25-1553 (100 nM), thus indicating a role for $VPAC_2R$ in the resulting phase advance. The phase shifting effects of PACAP were also examined in these studies and in contrast to the results of Harrington and colleagues (1999), no phase shift was observed. These authors suggested that photic stimuli may stimulate the release of VIP in the SCN, which through the activation of $VPAC_2R$ may then play a role in resetting the clock (Reed *et al.*, 2001). These studies were subsequently extended, with the effects of PG99-465, the reportedly selective $VPAC_2R$ antagonist (Moreno *et al.*, 2000), on VIP activity examined in SCN neurons (Moreno *et al.*, 2000; Reed *et al.*, 2002). When applied alone, PG99-465 (100 nM) had no effect on the neuronal firing rates, however co-application with VIP resulted in a reduced agonist response. Furthermore, the PAC_1R selective agonist maxadilan was shown to modulate neuronal activity in the SCN, which was insensitive to PG99-465. Therefore a number of *in vitro* studies have investigated the phase shifting properties of VIP and PACAP in the SCN and the involvement of the $VPAC_2$ and PAC_1R receptors in mediating these effects.

A small number of studies have also examined the effects of VIP and PACAP on circadian rhythms *in vivo*. The first of these investigations was conducted by Albers and colleagues in 1991, with the effects of SCN microinjected peptides (VIP, PHI, GRP) examined. Individually, none of the peptides were shown to produce any phase shift in activity patterns, however when these peptides were co-injected (at the beginning of activity onset), large progressive phase delays were subsequently observed (Albers *et al.*, 1991). In contrast to these results, Piggins *et al.* (1995) reported that when individual peptides (VIP, PHI and GRP) were microinjected into the SCN of hamsters, they could in fact cause phase shifts in activity patterns. Furthermore no synergism of phase shifting effects was observed when the peptides were co-injected. Analysis of the phase shifting activity of VIP (150 pmol), demonstrated that the peptide induced phase delays at CT12-14 and phase advances at CT20-24 (Piggins *et al.*, 1995).

In summary, these studies show that the effects of VIP and PACAP in the SCN appear complex, with the time of administration and concentration of peptide contributing to the observed outcome in SCN activity. VIP and PACAP clearly have

considerable effects on SCN rhythmicity, highlighting their importance in the normal function of the SCN and the expression of circadian rhythms.

3.1.2.4. Circadian rhythms of VPAC/PACR transgenic mice

The importance of VIP/PACAP and VPAC/PAC receptor activity in the control of circadian rhythms of activity has been further demonstrated through the use of transgenic mice. The behaviours of such mice were extensively discussed in the general introduction (section A.3.1., p 38) and shall be briefly summarised here with reference to circadian activity rhythms.

The generation of VIP and PACAP null mouse lines re-iterated the particularly important role of these peptides in the phase-resetting of circadian activity rhythms, with both types of transgenic mice showing significantly reduced responses to lighting cues that would normally cause phase shifts (Colwell *et al.*, 2003, 2004; Kawaguchi *et al.*, 2003). Furthermore, the VIP null mice had intrinsic activity rhythms that were considerably weaker and more arrhythmic than those of wild-type mice (Colwell *et al.*, 2003). This is in contrast to the PACAP null mice, which demonstrated a similar but slightly shorter free running period than their wild-type littermates (Kawaguchi *et al.*, 2003).

The use of VPAC/PAC receptor transgenic mice has also proven particularly important in contributing to our understanding of their roles in SCN function and circadian rhythm generation. As discussed in the introduction, the behaviours of two $VPAC_2R$ transgenic mouse lines ($hVPAC_2R$ receptor over-expressing and $VPAC_2R$ null) produced by Harmar and colleagues have been crucial in delineating the important role of this receptor in SCN function (Shen *et al.*, 2000; Harmar *et al.*, 2002). The over-expressing mice were observed to have a shorter free running period than wild-type mice and additionally they were also able to adjust more rapidly to an 8 h advance in the light-dark cycle (Shen *et al.*, 2000). Further insights into the role of the $VPAC_2R$ were gained from examination of the behaviour of the null mice. These mice were shown to re-entrain to an 8 h phase advance in the light cycle in about a third of the time taken by wild-type mice (Harmar *et al.*, 2002). When in constant darkness, these mice were shown to have only weakly rhythmic intrinsic cycles of activity and clock gene expression. Furthermore exposure to brief dark bursts during the lights on period resulted in sudden activity bursts from these mice, demonstrating that the major influence on the timing of activity patterns was light. The disruption to normal SCN activity in the null mice was further explored in

subsequent electrophysiological and immunohistochemical studies, which showed a loss of normal rhythmic physiological patterns (Cutler *et al.*, 2003; Hughes *et al.*, 2004).

The role of PAC_1 receptors has also been investigated through the use of transgenic mice (PAC_1R null). These knock-out mice were shown to have a similar activity pattern to wild-type mice under light-dark cycles, however in constant darkness the null mice were observed to have a considerable shorter free running period (Hannibal *et al.*, 2001). The SCN of the null mice appeared to be more sensitive to light stimulation, because upon exposure to brief light pulses in the early stage of the dark cycle, the null mice responded with much larger phase delays than their wild-type littermates. These mice also failed to show increased clock gene expression in response to light stimulated phase shifts (Hannibal *et al.*, 2001).

3.1.2.5. Pharmacological modulation of $VPAC_2R$ *in vivo*

It is now clear that VIP/PACAP and VPAC/PAC receptors play an important role in the normal function of the SCN and thus the control of circadian rhythms. Several studies have highlighted a particularly important role for the $VPAC_2R$ in SCN function, through the use of transgenic mice lines and also via pharmacological modulation of the receptors (*in vivo* and *in vitro*). The data from these studies, as discussed in chapter two, indicates that pharmacological modulation of this receptor may be of therapeutic value in controlling circadian rhythm cycles and increasing re-entrainment rates to phase shifts. Indeed, the use of $VPAC_2R$ selective antagonists may mimic the behavioural characteristics of the $VPAC_2R$ null mice, which could be important therapeutically. In brain slices from wild-type mice, the reportedly $VPAC_2R$ selective antagonist PG99-465 mimicked the electrophysiological characteristics observed in brain slices from the $VPAC_2R$ null mice. However, although the impact of exogenous administration of non-selective VPAC/PACR ligands (agonists) has been investigated *in vivo*, no similar studies have been performed to date using PG99-465. With the current interest in the $VPAC_2R$ as a target for therapeutic intervention in the treatment of circadian rhythm disorders, we therefore sought to evaluate if the use of this $VPAC_2R$ antagonist could indeed mimic the phenotype of the null mice and reduce re-entrainment times to a phase advance.

Prior to PG99-465 studies, a new set of cages and mouse running wheels were established and linked to a computer to monitor running wheel activity.

Consistent with the previous *in vivo* studies examining the effects of VIP/PACAP on circadian rhythms, it was decided that PG99-465 should be injected directly into the brain to maximise the delivery of the peptide to the area surrounding the SCN. This also avoids potential complications regarding the inability of the peptide to cross the blood-brain-barrier. As the fluid filled ventricles within the brain come into close proximity with the SCN, i.c.v. injection was selected as the most appropriate route of administration for PG99-465. The potential effect on mouse circadian activity of the planned surgical procedures was first evaluated. The re-entrainment of the mice to a standard 8 h phase advance was subsequently evaluated as was the ability of the mice to entrain to a shorter 6 h phase advance, which would facilitate future surgical procedures. The effect of PG99-465 on re-entrainment time was then evaluated.

3.2. Results

3.2.1. *In vitro* studies using brain derived astrocytes

3.2.1.1. Purity of rat cortical astrocyte cultures

Rat cortical astrocytes were isolated from a mixed primary cell culture prepared from the cortices of Sprague Dawley rat pups (P1 - P2), as described in the methods section (p 58). In preliminary studies to determine the purity of the astrocyte cultures, samples of the isolated cells were fixed in paraformaldehyde and stained using cell-specific antibodies. Astrocytic cells were stained using a glial fibrillary acidic protein (GFAP) antibody and in the representative field shown (Figure 3.2.1a), astrocytes were clearly the predominant cell type in the cultures. The presence of contaminating microglial cells was assessed with a CD11b antibody (Figure 3.2.1b) and whilst this marker stained a few cells, a similar proportion of cells were identified using the secondary antibody (biotinylated anti-mouse antibody) alone (Figure 3.2.1c). This suggests that the level of microglial contamination of the astrocyte cultures was low and indistinguishable from background levels of non-specific staining. Therefore, as the majority of cells in the isolated cultures appeared to be astrocytic (which is in agreement with previous studies performed in our institute) and as the availability of the cultures was limited, such cultures were used in all of the following studies.

3.2.1.2. Peak agonist induced $[cAMP]_i$ and $[Ca^{2+}]_i$ responses from RCA

In order to compare the peak agonist stimulated $[cAMP]_i$ and $[Ca^{2+}]_i$ responses from RCA, the maximum responses from all agonist concentration response curves included in Table 3.2.1 (p 226) were averaged. The collated peak responses produced with the VPAC/PACR ligands in each assay are presented in Figure 3.2.2 ($[cAMP]_i$: panel a; $[Ca^{2+}]_i$: panel b). Averaged maximal responses for VIP and maxadilan were similar in the $[cAMP]_i$ assay (approximately 50 nM cAMP), whereas PACAP-27, PACAP-38 and R3P65 responses appeared larger (100 – 120 nM cAMP), however no significant differences in response size were detected between the peptides ($p = 0.203$). $[Ala^{11,22,28}]$VIP which was previously shown to be a selective $VPAC_1R$ agonist (section 1.2.3., p 103) had no effect on $[cAMP]_i$ levels in the rat astrocytes (Figure 3.2.2a). In the $[Ca^{2+}]_i$ assay, the PACAPs, VIP and maxadilan were the only agonists that produced full concentration response curves in the astrocytes, with the average maximum PACAP responses being similar, but ~ 30

% larger than the maxadilan and VIP induced fluorescent responses (Figure 3.2.2b). Indeed, from analysis of this data set, VIP responses were significantly smaller than those induced by PACAP-27 ($p = 0.038$). Upon further examination of the average peak responses and the individual assay values, a considerable level of variability between, but not within assays, was evident in the magnitude of responses produced from the astrocytes. The observed variability may have been a result of several potential factors, including the age and health of the pups and the length of time the cells were in culture. To reduce this variability and provide a more relevant comparison, relative peak responses to each agonist were calculated as a percentage of the maximum PACAP-27 response determined on each experimental day (Figure 3.2.3). This method of analysis was applied to all the agonist responses for which complete concentration curves were generated (Figure 3.2.4). When expressed as a percentage of the PACAP-27 response, the maximum responses produced from VIP, PACAP-27, PACAP-38, R3P65 and maxadilan stimulation of RCA in the $[cAMP]_i$ assay, were all similar (90 – 110 % of the PACAP-27 response; Figure 3.2.3a) with no significant differences detected ($p = 0.462$), indicating that these peptides were all full agonists; a finding that was previously masked by the variability when the raw data were compared (Figure 3.2.2). From the raw data for these five agonists, the average maximum $[cAMP]_i$ response was ~ 90 nM (32x basal). Normalised peak agonist responses in the calcium assay were consistent with the profile of response sizes calculated using the raw data (Figures 3.2.2b, 3.2.3b), with PACAP-27 and PACAP-38 inducing similar maximum fluorescence levels (average response: 8650 RFU; 2.1x basal). The PACAP induced responses were significantly larger ($p < 0.001$) than the maxadilan and VIP evoked responses (average response: 6156 RFU; 1.5x basal). As concentration response curves could not be produced for $[Ala^{11,22,28}]$VIP and R3P65 in the $[Ca^{2+}]_i$ assay, it was not possible to include the maximum responses from these agonists in Figure 3.2.3.b.

3.2.1.3. VPAC/PACR agonist pharmacology in RCA

The peptides VIP, R3P65, PACAP-27, PACAP-38 and maxadilan were full agonists in RCA, increasing $[cAMP]_i$ levels in a concentration dependent manner, with a ROP: PACAP-27 = PACAP-38 = maxadilan > VIP = R3P65 (Figure 3.2.4a). The PACAP peptides and maxadilan were of similar nanomolar potency (EC_{50} range: 0.43 – 2.2 nM; Table 3.2.1) and were ~ 150 fold more potent than VIP and R3P65 (EC_{50} values of 179 and 154 nM respectively; Table 3.2.1). This is consistent with

Table 3.2.1 Agonist EC_{50} values for the stimulation of $[cAMP]_i$ and $[Ca^{2+}]_i$ production in primary cultures of rat cortical astrocytes

	VIP	PACAP-27	PACAP-38	$[Ala^{11,22,28}]$VIP	R3P65	Maxadilan
			EC_{50} ± SEM (nM)			
$[cAMP]_i$	179 ± 31.7 (3)	0.68 ± 0.19 (5)	2.2 ± 0.252 (3)	NE	154 ± 32.0 (3)	0.43 ± 0.03 (3)
$[Ca^{2+}]_i$	730 ± 47.9 (4)	6.71 ± 1.08 (8)	3.85 ± 0.62 (8)	NE	Agonist from 1 µM	9.34 ± 1.57 (8)

Agonist EC_{50} values were generated using the standardised $[cAMP]_i$ and $[Ca^{2+}]_i$ assays. Ligand potencies are presented as: EC_{50} (nM) ± SEM, with the number of independent experiments shown in parenthesis. NE is no effect at 3 µM.

data from the CHO-hPAC$_1$R expressing cells and the SHSY-5Y cell line, where the former agonists were also considerably more potent than VIP and R3P65 (sections 1.2.3.1. and 1.2.4.1., p 103 and p 127). $[Ala^{11,22,28}]$VIP had no effect on $[cAMP]_i$ levels in the rat astrocytes, suggesting that VPAC$_1$R were either not expressed or expressed at very low levels in these cells. In the calcium assay, complete concentration response curves were evoked by PACAP-27, PACAP-38, maxadilan and VIP (Figure 3.2.4b). Akin to the $[cAMP]_i$ data, the first three peptides were of similar potency in the $[Ca^{2+}]_i$ assay (EC_{50} range: 3.85 – 9.34 nM; Table 3.2.1), however as indicated by the maximum responses shown in Figure 3.3.3b, the maxadilan concentration response curves were ~ 30 % smaller than either of the PACAP curves. VIP mediated responses were only detected at the upper limit of the peptide concentration range and as a consequence complete concentration response curves for this agonist were not always produced. On the occasions (n = 4) were the upper plateau of the curve was present and a sigmoidal curve fit possible, the maximum VIP induced responses were found to be smaller than those induced by PACAP, which is in agreement with the observation made for maxadilan. This finding was consistent with the differential maximum calcium responses induced by these peptides in the hPAC$_1$R expressing SHSY-5Y cell line (section 1.2.4.1., p 127). In the RCA, VIP was over 100 fold less potent (EC_{50}: 0.7 µM) than the PACAP peptides or maxadilan in the calcium assay, which is consistent with the $[cAMP]_i$ data produced using these cells (Table 3.2.1). Although R3P65 evoked a calcium response in rat astrocytes, this stimulatory effect was only detected at or above micromolar concentrations, and consequently full concentration response curves

could not be generated for this peptide. [Ala^{11,22,28}]VIP had no stimulatory effect on calcium levels in rat astrocytes, which is again consistent with the $[cAMP]_i$ data. As reported for the VPAC/PACR expressing stable cell lines and SHSY-5Y cells (section 1.2.4.1., p 127), agonist potencies determined using the astrocytes were lower in the calcium than the cAMP assay, although the fold shift between assays was less pronounced in these cells when compared with the stable cells lines (RCA: ~ 10 fold, CHO-hPAC$_1$R: ~ 100 fold).

3.2.1.4. Agonist stimulated calcium traces from RCA

Fluorescence traces produced from agonist stimulation of RCA in the calcium assay are illustrated in Figure 3.2.5. On examination of the fluorescence traces in RCA, the responses appeared to remain elevated over the 90 s recording period, akin to that observed in the hPAC$_1$R expressing stable cell line and in SHSY-5Y cells, but in contrast to the CHO-hVPACR expressing cells (sections 1.2.3.3., p 106; 1.2.4.1., p 127). To examine this observation further, the fluorescence levels after 90 s in response to a saturating concentration of peptide were determined and expressed as a percentage of the peak response observed for each peptide (Figure 3.2.6). At 90 s, agonist evoked fluorescence levels from PACAP-27, PACAP-38 and maxadilan stimulation were similar at ~ 75 % of the peak response. In contrast, the VIP response at this time point was significantly lower, at approximately 50 % of the peak response ($p < 0.001$). The differences observed are consistent with hPAC$_1$R mediated responses in SHSY-5Y cells (90 s analysis; Figure 1.2.34, p 133) and with the slower rate of decline reported for PACAP responses in CHO-hPAC$_1$R expressing cells (200 s analysis; Figure 1.2.21, p 115). Further examination of the magnitude of agonist responses at 200 s (as was reported for the CHO-hPAC$_1$R cell line; section 1.2.21., p 115), was not performed with the astrocytes due to the limited amount of primary cultures which could be generated.

3.2.1.5. Antagonism of agonist induced responses in RCA

The ability of M65, the PAC$_1$R antagonist, to inhibit PACAP-27 induced functional responses from RCA was examined. When tested alone in the astrocytes, M65 had no effect in either assay at concentrations up to 3 μM (Figure 3.2.7). M65 fully inhibited PACAP-27 evoked $[cAMP]_i$ and $[Ca^{2+}]_i$ responses from RCA, in a

concentration dependent manner, with equipotent IC_{50} values of 37.3 and 22.0 nM, respectively (Figure 3.2.7; Table 3.2.2). These values are almost identical to the IC_{50} values determined for M65 antagonism of PACAP-27 stimulated responses from the SHSY-5Y cell line ($[cAMP]_i$: 37.5 ± 5.6 nM (4) and $[Ca^{2+}]_i$: 13.6 ± 2.1 nM (5); section 1.2.4.1., p 127), and slightly more potent than the values determined using the CHO-hPAC$_1$R cell line (section 1.2.3.4., p 117).

In a similar set of experiments the effects of the putatively VPAC$_2$R selective antagonist PG99-465 were examined in the $[cAMP]_i$ and $[Ca^{2+}]_i$ assays, using rat astrocytes. In the $[cAMP]_i$ assay, PG99-465 alone (1 – 3 μM) had no effect, however this peptide significantly reduced the PACAP-27 stimulated $[cAMP]_i$ response (50 – 75 %) when pre-incubated with the astrocytes at low micromolar concentrations ($p < 0.001$; Figure 3.2.8a). The concentration dependence of this inhibition was examined, but as can be seen from Figure 3.2.8 although significant effects of PG99-465 were observed in both experiments, the extent of the inhibition varied between assays ($p \leq 0.001$; Figure 3.2.8a, b). Therefore, no true IC_{50} value could be determined for PG99-465 inhibition of $[cAMP]_i$ responses in RCA. In the calcium assay, PG99-465 had no effect when tested at or below 1 μM, however at 3 μM a significant fluorescence response equivalent to ~ 30 % of the maximum PACAP-27 response was observed ($p = 0.017$; Figure 3.2.9a). When PG99-465 was pre-incubated with the astrocytes prior to agonist addition, both at concentrations of 1 and 3 μM, the PACAP-27 induced response was reduced by ~ 50 %, however this

Table 3.2.2 Potency of VPAC/PACR antagonists to inhibit agonist induced $[cAMP]_i$ and $[Ca^{2+}]_i$ responses from RCA

	M65	PG99-465
	IC_{50} ± SEM (nM)	
$[cAMP]_i$	37.3 ± 0.15 (3)	Variable inhibition
$[Ca^{2+}]_i$	22.0 ± 2.16 (4)	Inhibition at micromolar concentrations

Following a 10 min pre-incubation with antagonist, responses to PACAP-27 from RCA were determined in both assays. Potencies are presented as IC_{50} ± SEM, with the number of independent experiments shown in parenthesis. The VPAC$_1$R antagonist PG97-269 was not tested as the presence of these receptors was shown (from the agonist studies) to be negligible in the astrocyte cultures.

reduction was not found to be statistically significant ($p > 0.06$; Figure 3.2.9b). These findings were not extensively pursued, due to the complexities of PG99-465 pharmacology described in chapter one (section 1.2.3.4., p 117) and the limited availability of astrocytes. The fluorescence traces produced in the calcium assay from antagonism of PACAP-27 induced responses with M65 and PG99-465 are shown in Figure 3.2.10. As the use of the selective agonist [$Ala^{11,22,28}$]VIP had indicated that the presence of $VPAC_1R$ in the RCA was negligible (Figure 3.2.4), the effects of the $VPAC_1R$ selective antagonist, PG97-269, on agonist evoked responses were not examined.

3.2.1.6. VPAC/PACR mediated cytokine production from RCA

Preliminary studies were performed to examine the effect of VPAC/PACR stimulation on the secretion of key inflammatory cytokines from primary cultures of rat astrocytes. Briefly, RCA were stimulated with VIP and PACAP-27 for 1 h, the supernatants collected and IL-1β and TNF-α levels determined by ELISA (section B.3.3., p 67). Both VIP and PACAP-27 increased IL-1β secretion from astrocytes in a complex biphasic manner. There were significant peaks in secretion with picomolar and nanomolar concentrations of both peptides ($p \leq 0.001$; Figure 3.2.11). Although the pattern of stimulation observed over the peptide concentration range examined was the same for both peptides, the total amount of IL-1β released was two to three times larger for VIP when compared to PACAP-27. In the TNF-α ELISA, PACAP-27 induced an initial peak in cytokine secretion at picomolar concentrations, in a similar manner to the IL-1β assay (Figure 3.2.12a). The agonist also appeared to induce a secondary stimulation of TNF-α release, with a large increase in TNF-α production at the 100 nM concentration of PACAP-27. However, the peaks in TNF-α secretion were not found to be significantly greater than those detected with buffer alone ($p = 0.16$), perhaps as a consequence of the limited data set available and the level of variation observed. When tested with the same ELISA kit, VIP produced no clear stimulation of TNF-α secretion (Figure 3.2.12b). VPAC/PACR modulation of the cytokines IL-6 and RANTES was also examined, however no consistent responses were obtained (data not shown).

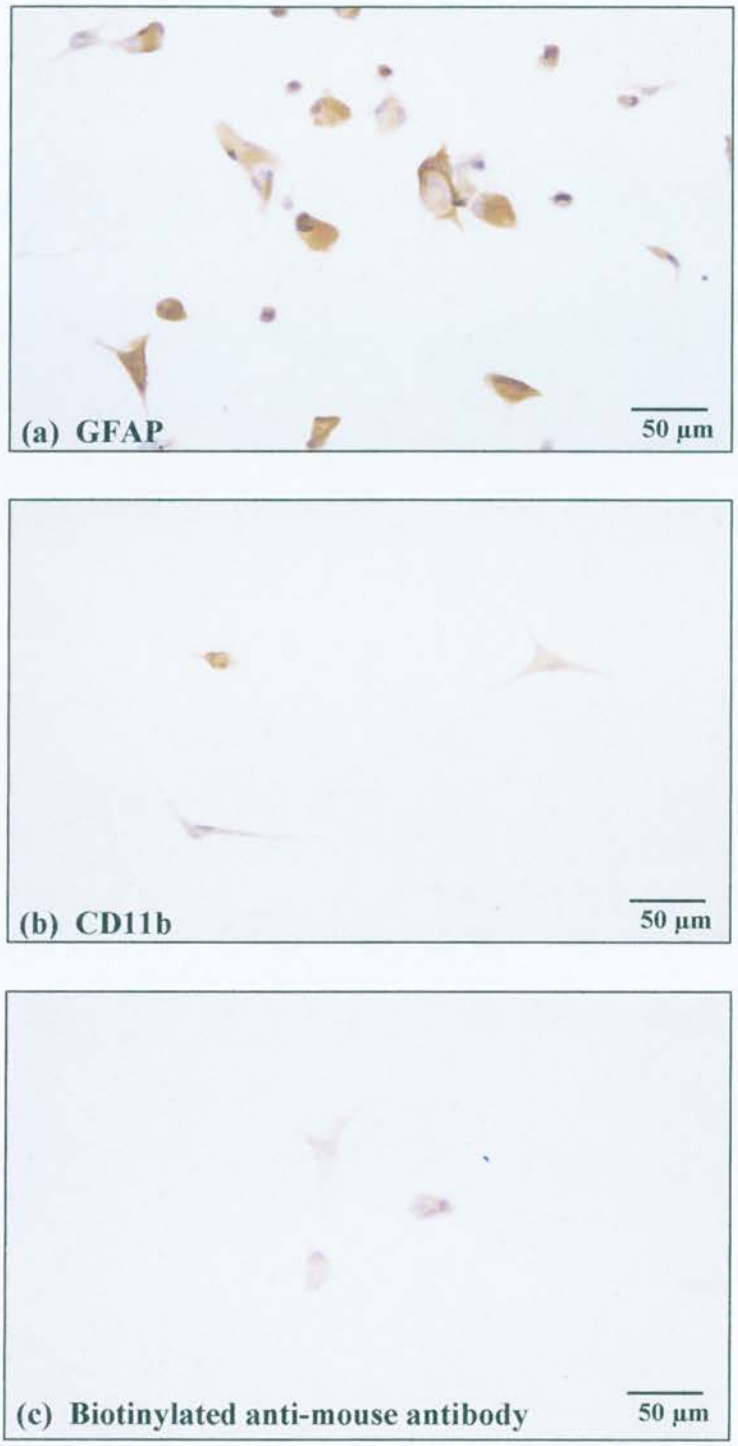

Figure 3.2.1 **Immunohistochemical staining of purified rat cortical astrocyte cultures.** Following isolation of cortical astrocytes, the presence of contaminating microglia was determined. Cell samples were stained with GFAP (**a**) and CD11b (**b**) primary antibodies to detect the presence of astrocytes and microglia respectively. Binding of these primary antibodies was visualised using a biotinylated anti-mouse secondary antibody. Non-specific staining with the secondary antibody alone is also shown (**c**).

(a)

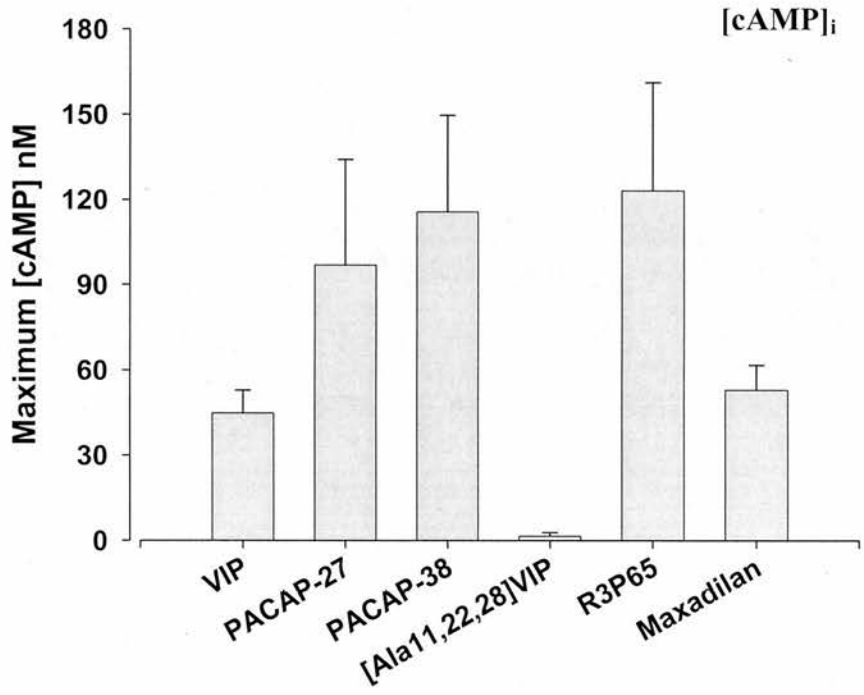

(b)

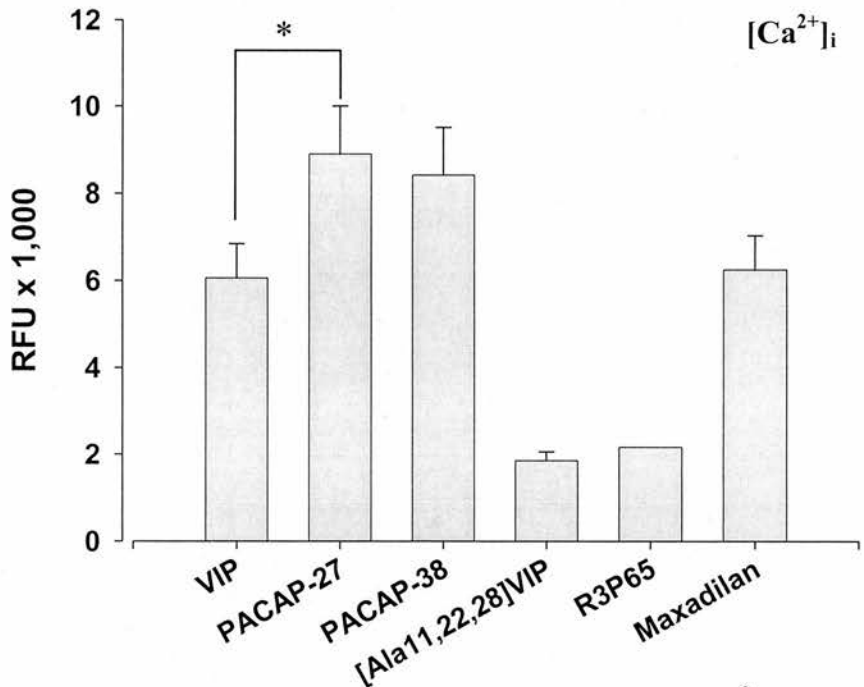

Figure 3.2.2 **Agonist induced maximum $[cAMP]_i$ and $[Ca^{2+}]_i$ responses from RCA.** Peak responses are shown from agonist stimulation of RCA in the $[cAMP]_i$ (**a**) and $[Ca^{2+}]_i$ assays (**b**). Raw data values are shown, averaged from the peaks of the concentration curves detailed in Table 3.2.1 ($n \geq 3$). The relatively large error bars, particularly in the $[cAMP]_i$ assay, indicate the degree of inter-experiment variability observed with these cells. The asterisk indicates relevant comparisons which were significantly different ($p = 0.038$).

(a)

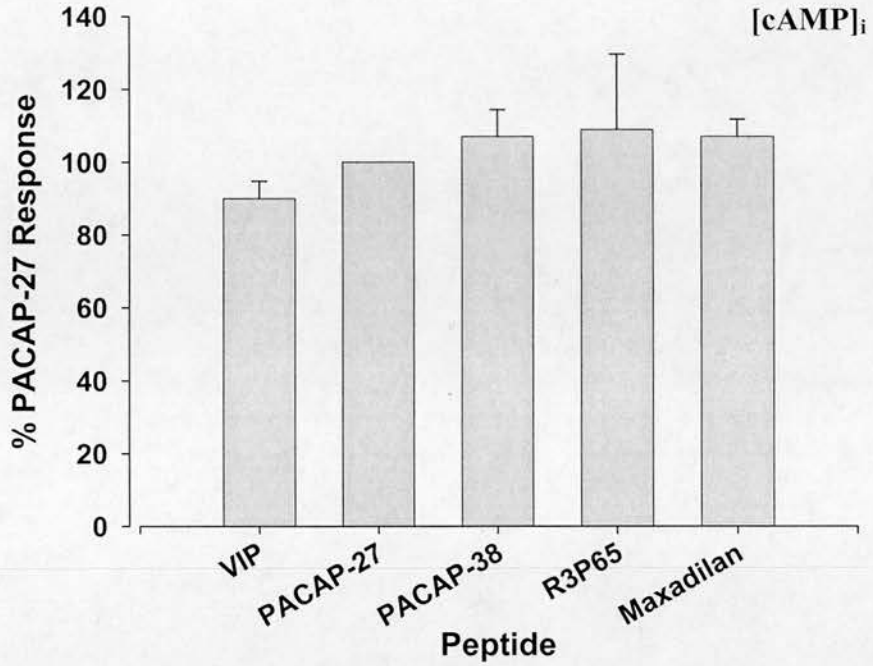

(b)

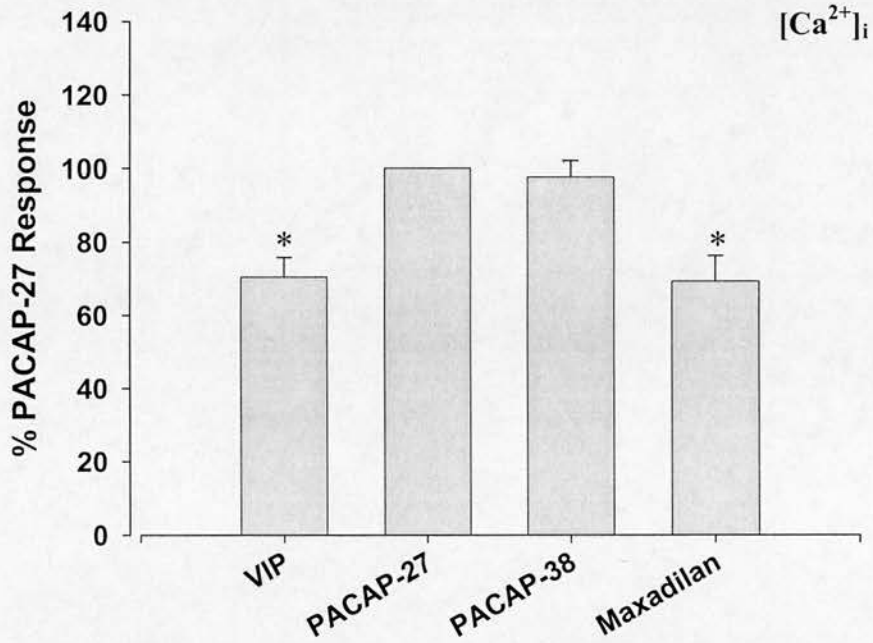

Figure 3.2.3 **Maximum agonist induced $[cAMP]_i$ and $[Ca^{2+}]_i$ responses from RCA, normalised to control PACAP-27 responses.** Peak responses are shown for the agonists for which complete concentration response curves were produced (Figure 3.2.4), following stimulation of RCA in the $[cAMP]_i$ (**a**) and $[Ca^{2+}]_i$ (**b**) assays. Peak responses are expressed as a percentage of the maximum PACAP-27 response on each individual day. The asterisks indicate responses which were significantly smaller than responses to PACAP-27 and PACAP-38 ($p < 0.001$).

(a)

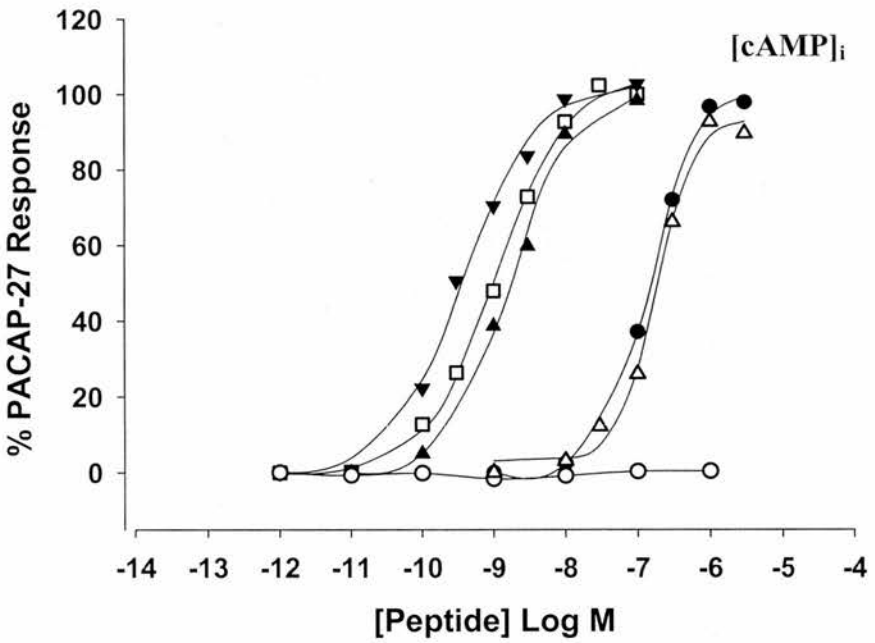

(b)

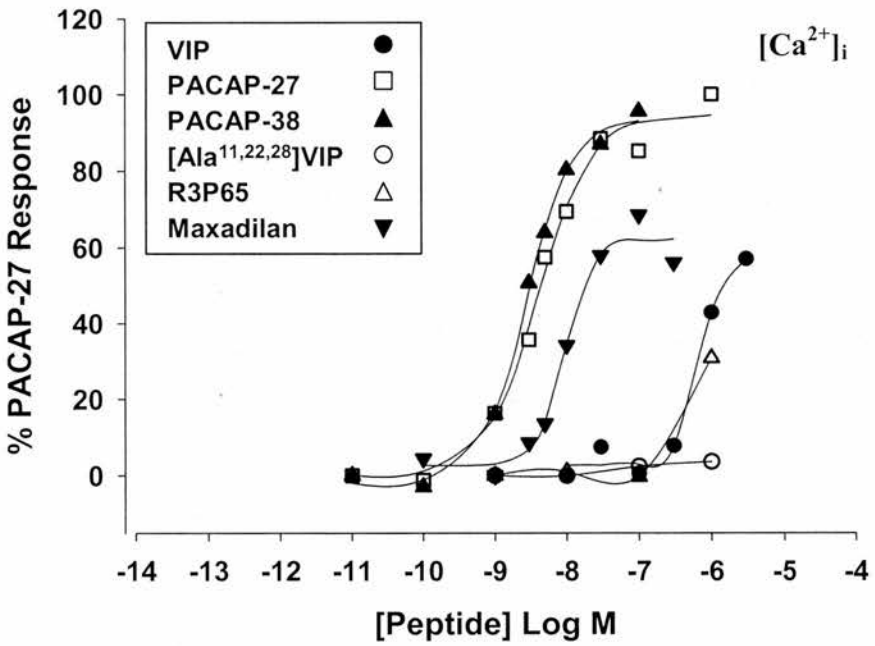

Figure 3.2.4 **VPAC/PACR agonist concentration response curves produced using RCA in the $[cAMP]_i$ and $[Ca^{2+}]_i$ assays.** Using primary cultures of rat astrocytes (1 x 10^5 per well), agonist concentration response curves were produced in the $[cAMP]_i$ (**a**) and $[Ca^{2+}]_i$ (**b**) assays. The graphs shown are representative, with EC_{50} values for each agonist shown in Table 3.2.1 ($EC_{50} \pm$ SEM; $n \geq 3$).

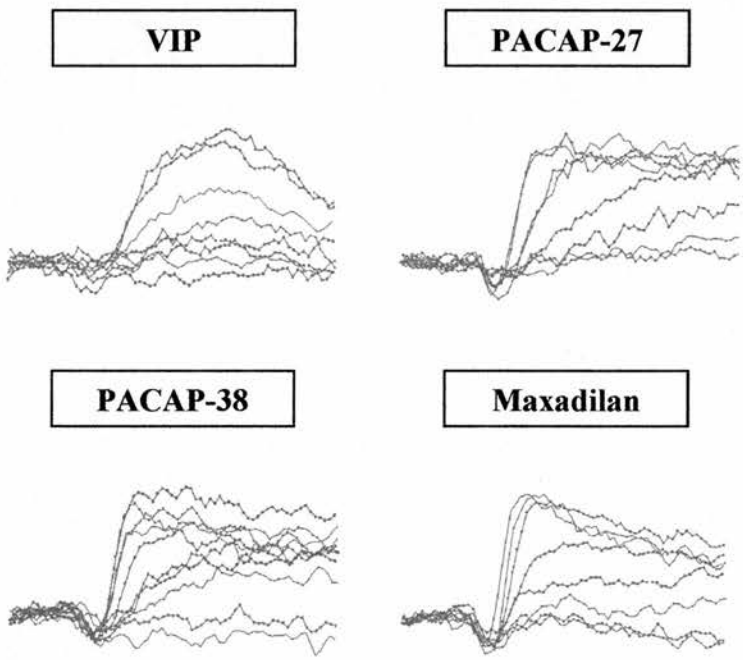

Figure 3.2.5 **Agonist stimulated fluorescence traces from rat cortical astrocytes in the $[Ca^{2+}]_i$ assay.** The representative traces shown are for the stimulation of RCA with the agonists for which complete concentration curves were produced (as shown in Figure 3.2.4b). The traces presented for the individual agonists show the changing fluorescence levels over a 90 s period (with agonist addition at 20 s) and cover the full range of concentrations used to determine agonist potencies (Table 3.2.1). As illustrated by the traces, the magnitude of the fluorescence responses increased with agonist concentration, eventually reaching a maximum response.

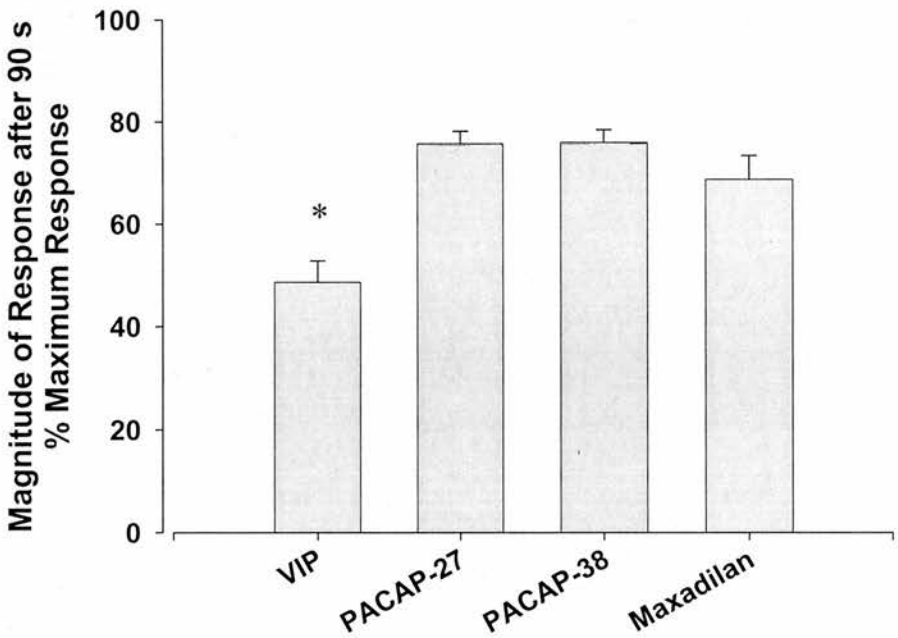

Figure 3.2.6 **Agonist stimulated fluorescence responses from RCA cultures, 90 s after peptide addition.** The fluorescence responses 90 s after peptide addition are expressed as a percentage of the peak response observed for each trace. Each agonist was tested at a concentration which was at the upper limit of the respective concentration response curves from Figure 3.2.4b. The data are shown as the mean ± SEM, calculated using each concentration response curve used to determine the potencies in Table 3.2.1 ($n \geq 3$). The asterisk indicates that the VIP induced response (at 90 s) was significantly smaller than the PACAP-27, PACAP-38 or maxadilan responses ($p < 0.001$).

(a)

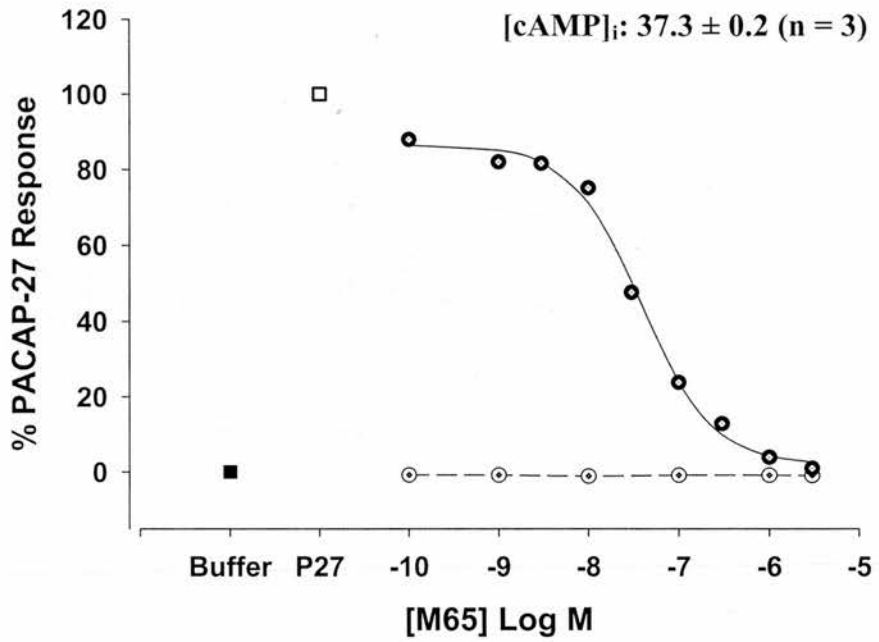

(b)

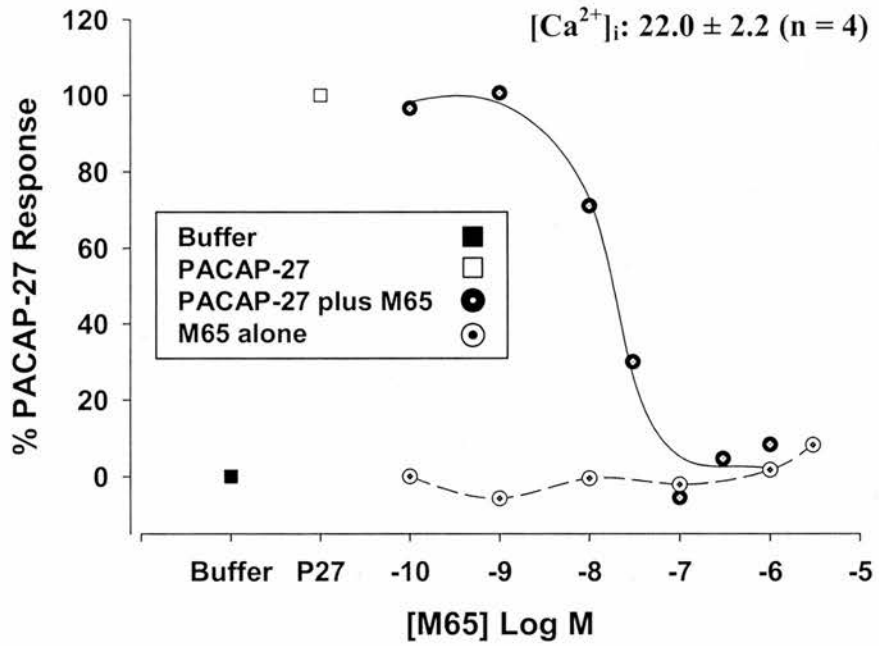

Figure 3.2.7 **M65 inhibition of PACAP-27 induced $[cAMP]_i$ and $[Ca^{2+}]_i$ responses from primary cultures of rat cortical astrocytes.** Astrocytes (1×10^5 per well) were pre-incubated with M65 for 10 min prior to PACAP-27 addition, which was used at approximately EC_{50} concentrations (**a**: $[cAMP]_i$ - 1 nM; **b**: $[Ca^{2+}]_i$ - 10 nM). IC_{50} values ± SEM ($n \geq 3$) are shown (see Table 3.2.2).

(a)

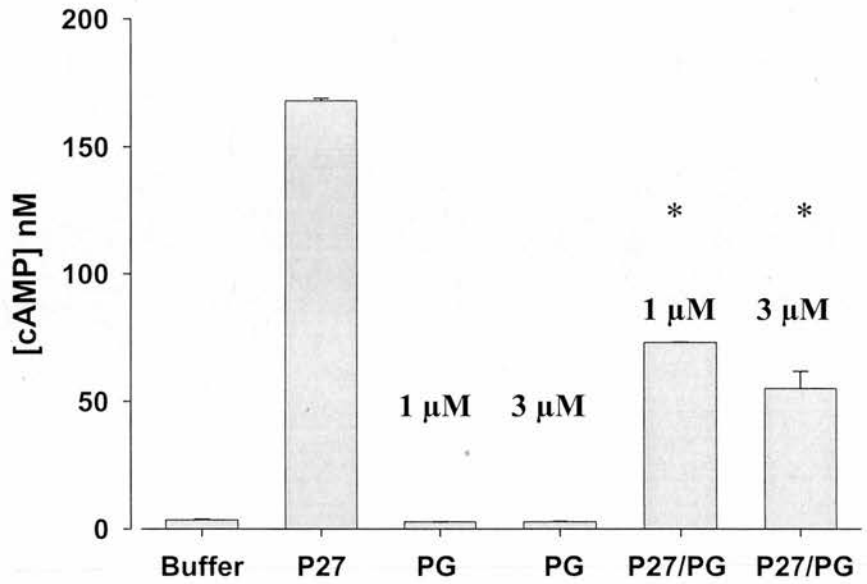

(b)

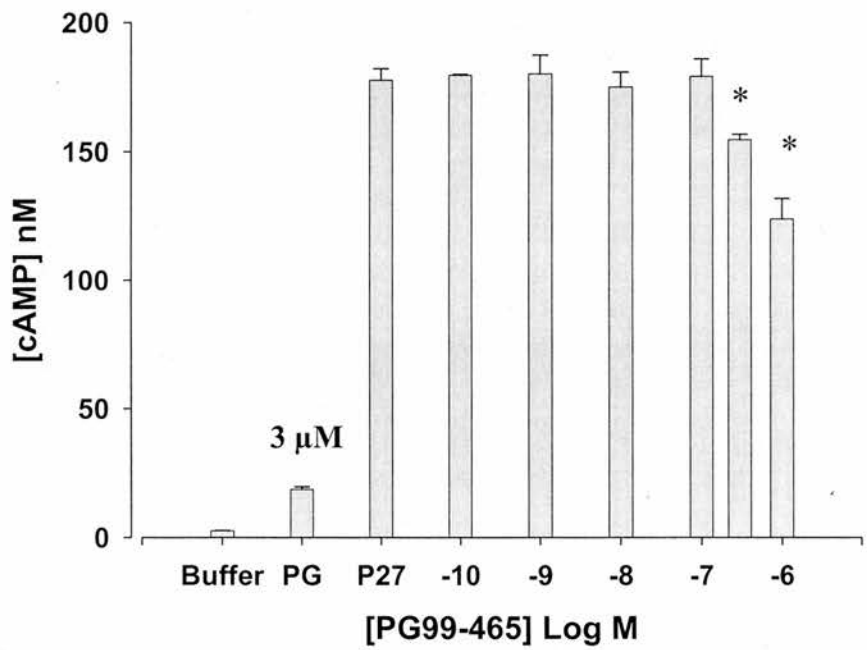

Figure 3.2.8 **Comparison between assays of the inhibitory actions of PG99-465 on agonist induced $[cAMP]_i$ responses in RCA.** PG99-465 activity (at micromolar concentrations) in astrocytes (1 x 10^5 per well) was determined alone and on the PACAP-27 (1 nM) induced response (**a**; n = 1, samples run in duplicate). The concentration dependence of the observed inhibition was subsequently determined, but PG99-465 was less potent in this assay, indicating a degree of inter-experiment variability (**b**; n = 1, samples run in duplicate). In each figure, the asterisks indicate responses which were significantly smaller than the PACAP-27 responses ($p \leq 0.001$).

(a)

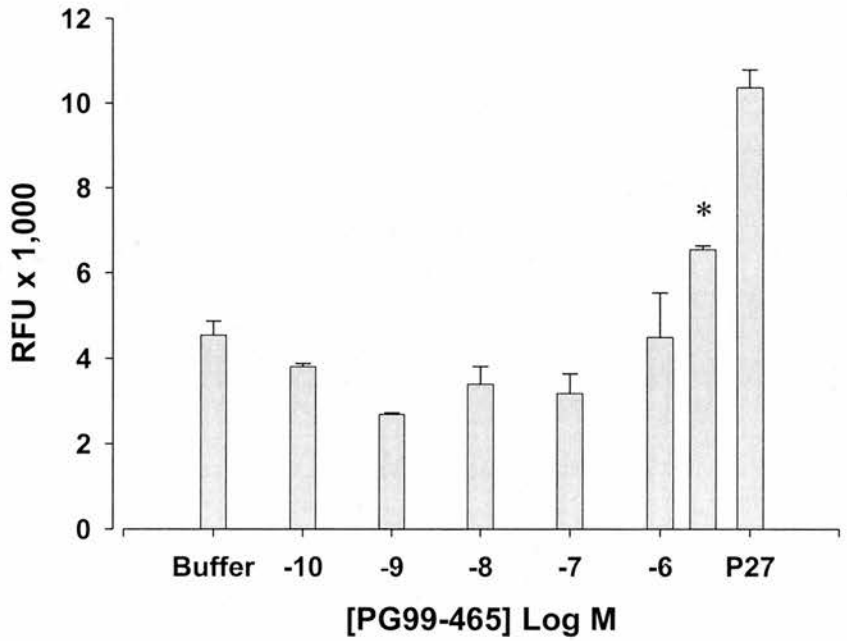

(b)

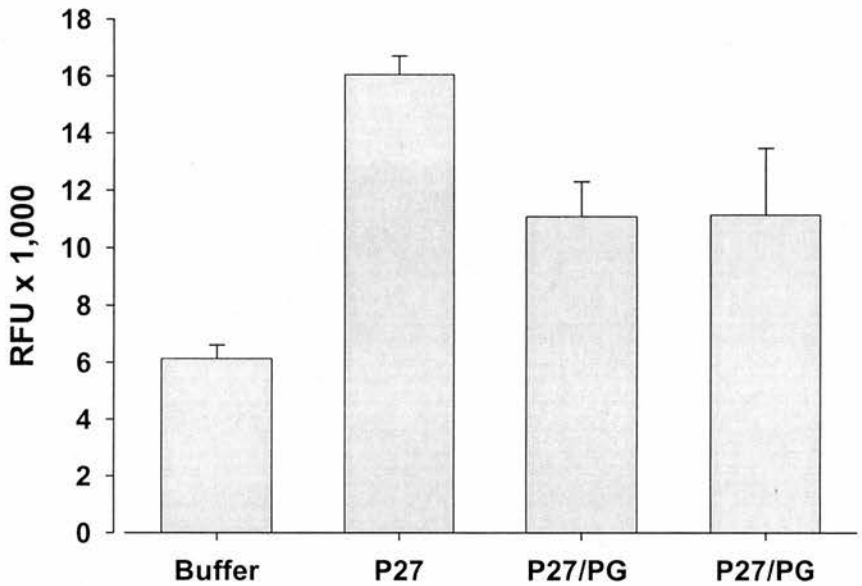

Figure 3.2.9 **PG99-465 modulation of $[Ca^{2+}]_i$ levels in RCA.** The activity of PG99-465 alone in rat astrocytes was examined in the $[Ca^{2+}]_i$ assay (**a**; n = 1, samples run in duplicate). The asterisk indicates significant responses to PG99-465 alone (p = 0.017), relative to buffer. Inhibitory effects of PG99-465 addition were also determined, by pre-incubating the peptide with the astrocytes for 10 min prior to PACAP-27 (10 nM) addition (**b**; n = 1).

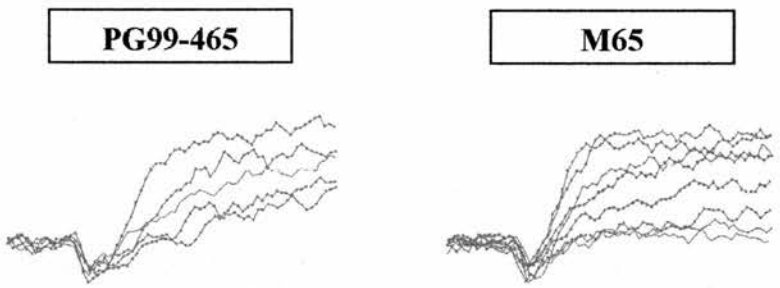

Figure 3.2.10 PG99-465 and M65 inhibition of agonist induced responses in RCA. Representative calcium assay traces are shown for PG99-465 and M65 antagonism of PACAP-27 induced fluorescence responses from rat cortical astrocytes. The cells were pre-incubated with PG99-465 or M65 for 10 min prior to PACAP-27 (10 nM) addition and fluorescence measurement in the FlexStation® (over 90 s). In each panel the largest response illustrates the PACAP-27 response alone, with subsequent decreasing responses produced from pre-incubation with increasing concentrations of antagonist, ranging from 0.1 to 3 μM.

(a)

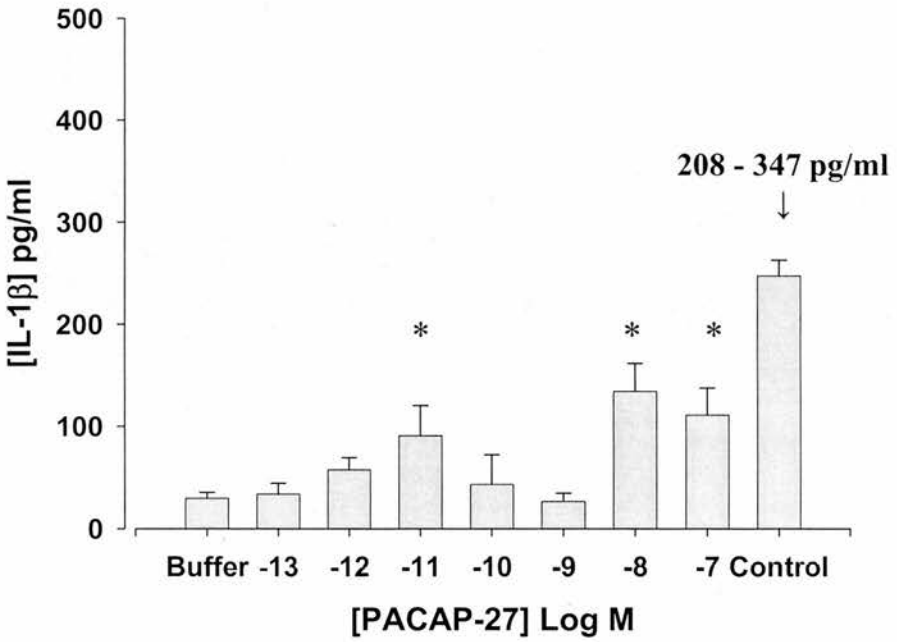

(b)

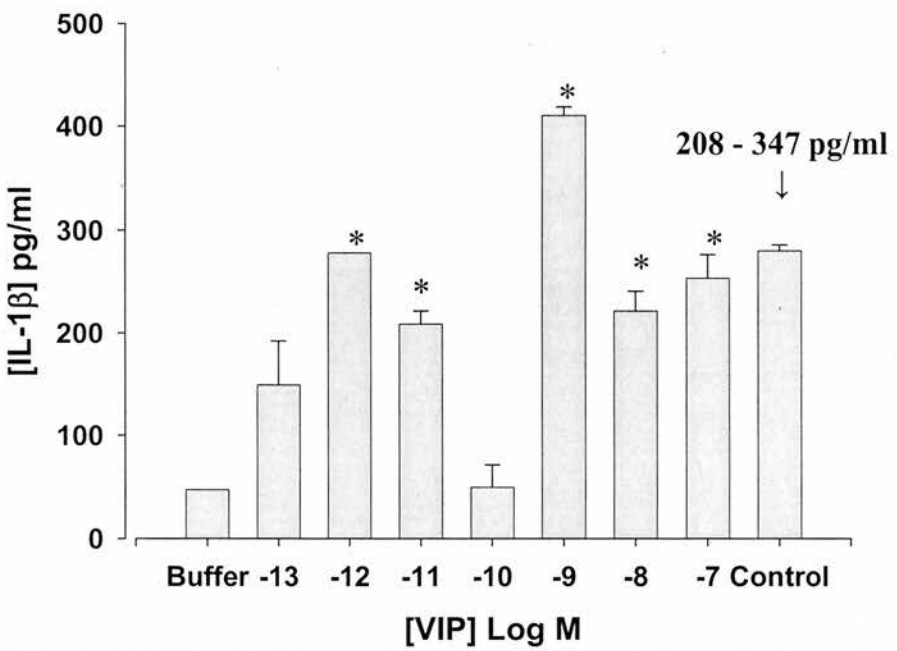

Figure 3.2.11 VPAC/PACR agonist induced stimulation of IL-1β from RCA. RCA cells (5 x 10^5 per well) were incubated with PACAP-27 (**a**) and VIP (**b**) for 1 h, prior to the determination of IL-1β concentrations in the supernatants by ELISA. The data shown is from an individual experiment, with each agonist concentration tested in duplicate wells. The asterisks indicate responses which were significantly larger than those observed with buffer ($p \leq 0.001$).

(a)

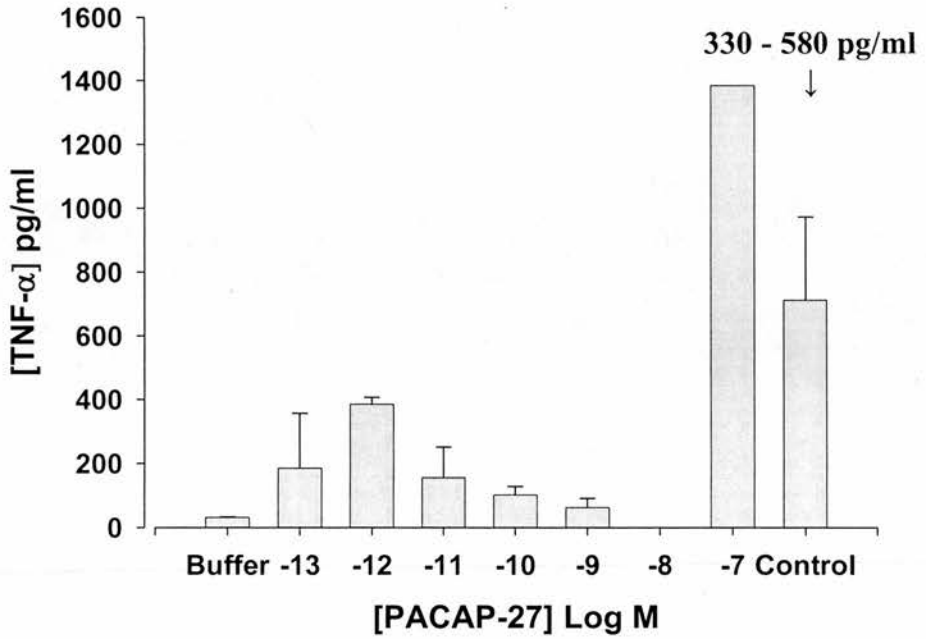

(b)

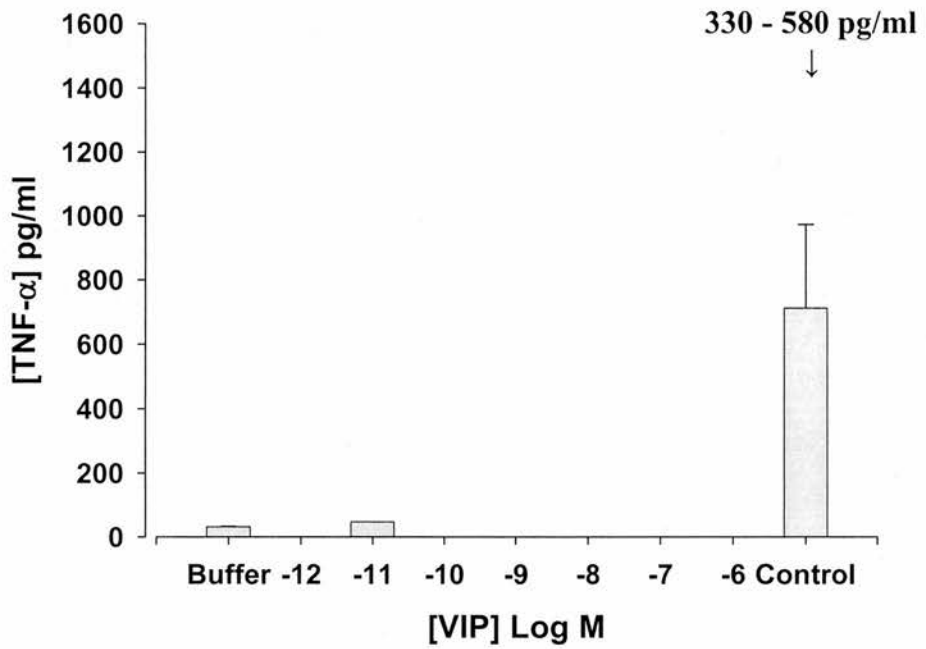

Figure 3.2.12 PACAP-27 and VIP induced TNF-α responses from rat cortical astrocytes. Following a 1 h incubation with PACAP-27 (**a**) or VIP (**b**), supernatants were removed from wells containing RCA (5 x 10^5 per well) and TNF-α levels in the samples determined. The data shown is from a single assay, in which each agonist concentration was tested in duplicate wells.

3.2.2. *In vivo* behavioural studies using C57BL/6J

3.2.2.1. Entrainment of mice to standard 12 h light/dark cycles

To detect and monitor mouse running wheel activity, 16 cages were equipped with new running wheels, each of which was connected to a computer. Rotations produced from activity in the wheels resulted in the transient closure of a relay switch (produced via magnets attached to the wheels), with the number of closures per minute recorded on a computer. As this was a new system, the first task was to establish that the equipment was assembled and connected correctly and that the behaviour of mice using this system was as expected. Mice were initially subjected to a 12 h light/dark cycle, with lights off from 1900 to 0700 h. As expected for nocturnal rodents, the mice were predominantly active during the dark cycle and at rest during the light cycle (Figure 3.2.13). In general, the mice showed intense bursts of activity within the first hour of the dark cycle, the frequency of which gradually declined over the following 6 - 8 hours, as can be seen from the actogram and 24 h activity profile for an individual mouse presented in Figures 3.2.13 and 3.2.14a. In addition, these figures demonstrate that further bursts of activity were generally seen within the last 3 - 4 hours of the dark cycle. This pattern of activity was consistently observed for this mouse, as can be seen from the averaged activity profile over a 7 day period (Figure 3.2.14b). Furthermore, the other mice also displayed a similar and consistent pattern of activity, as clearly presented in Figure 3.2.15, which shows the averaged running wheel counts for all 16 mice over a 7 day period. For these mice, the average activity counts (magnet passes) were 371 ± 54 and 33815 ± 1469, during the light and dark cycles respectively (measured for the 7 day period prior to the study in section 3.2.2.2; Table 3.2.3). Following the stable entrainment of these 16 mice, they were used in the study described below. In all of the following studies, mice were always shown to be stably entrained and expressing consistent activity patterns in an appropriate light/dark cycle prior to treatment or phase alteration.

3.2.2.2. Impact of displacement and surgery on activity patterns

Prior to examining the effect of PG99-465 on circadian cycles of activity, we examined the effects of re-locating the mice and anaesthesia/surgery (for i.c.v. compound administration) on activity levels. Three groups of mice (moved, n = 6; surgery, n = 6; not moved, n = 4), were analysed over a 13 day period under a normal

12 h light/dark cycle, with the challenge on day 7. Representative actograms for the groups are shown in Figure 3.2.16, with all 16 actograms available in appendix I, p 285. Representative activity patterns from each group measured over a 4 day period (days 6 - 9) are shown in Figure 3.2.17, in which the reduction in activity post-treatment can clearly be seen for the moved and surgery groups. The average total activity for each group in the light and dark cycles is illustrated in Figure 3.2.18. As expected, over the 13 day experimentation period the mice were mostly inactive during the daytime, with the exception of the 5th light cycle, in which a relatively small amount of activity (compared to the dark cycle) was observed for all three groups of mice (Figure 3.2.18a). Two-way ANOVA of total light cycle activity demonstrated a significant effect of cycle number ($p < 0.001$), but not of treatment group ($p = 0.285$). The effect of cycle number was exclusively due to a rise in overall activity of the mice, as a consequence of essential animal husbandry procedures on day 5. Analysis of total dark cycle activity (prior to treatment) showed that there was a significant difference in the level of activity between the groups, despite the random allocation of mice to the treatment groups (two-way ANOVA, $p < 0.001$; Figure 3.2.18b). Consequently, data from this study were expressed as proportionate changes from baseline, which was defined as the average activity from the 5 cycles prior to the challenge day (Figure 3.2.19). Two-way ANOVA of proportionate dark cycle activity showed a significant effect of day ($p < 0.001$) and group ($p = 0.003$), with *post-hoc* analysis indicating that activity during the 1st and 2nd dark cycles post procedure was significantly reduced. There was no significant difference ($p = 0.958$) between 'moved' and 'surgical' groups overall, however activity levels from both of these group were shown to be significantly different from the 'not moved' group ($p \leq 0.005$ for both). As group activities during the 3rd dark cycle post procedure were not different from those in any of the cycles prior to treatment, this demonstrated that the disruptive effects of relocation and anaesthesia were absent and group activity levels had returned to normal. No significant interactions were observed between the individual groups and dark cycle number. This challenge demonstrated that movement of mice from their home cages caused a marked decrease in subsequent activity, with full recovery 2 - 3 days later. As no difference was observed in activity between the moved and surgical groups, recovery from anaesthesia does not appear to contribute to the observed reduction in activity, leaving movement alone as the major disruptive factor.

3.2.2.3. Re-entrainment of mice in response to phase advances

Following the successful re-entrainment of a second group of 16 mice to a stable 12 h light/dark cycle, as described before, the responses of the mice to an 8 h phase advance in the cycle were determined, with a representative actogram presented in Figure 3.2.20 and all 16 actograms available in appendix II (p 288). As can be clearly seen from the actograms, the mice gradually entrained to the advance in the light/dark cycle, with a progressively earlier onset time of their activity periods. The leftwards shift in activity onset can also be seen in Figure 3.2.21, where the activity patterns over 24 h are compared during the entrainment period following the phase advance. On average, the mice re-entrained to the new light/dark schedule in 5.9 ± 0.2 full cycles (Table 3.2.3). Analysis of the number of mice that showed activity early in the onset of the new light/dark cycle showed 25 % of mice were active within one hour of the phase shift, which increased to ~ 75 % of mice by the second cycle (Figure 3.2.22a). When only activity was analysed that was greater than or equal to the average activity (per hour) in the 5 dark cycles prior to the phase advance, no mice were active within the first 2 h of the novel lights off period (Figure 3.2.22b).

The same group of 16 mice were then stably entrained to a 12 h light/dark cycle (lights off: 1900 – 0700 h), following which they were subjected to a 6 h phase advance (lights off: 1300 - 0100 h; Figure 3.2.23; appendix III, p 290). A 6 h phase advance was assessed in addition to the standard 8 h advance as it would facilitate the timing of the planned surgical intervention in the subsequent studies. As observed for the 8 h advance, in the days following the 6 h advance there was a

Table 3.2.3 Characteristics of circadian wheel running activity

	Mean	SEM
Wheel running activity – dark cycle (magnet passes)	33815	1469
Wheel running activity – light cycle (magnet passes)	371	54
Re-entrainment to 8 h phase advance (days)	5.9	0.2
Re-entrainment to 6 h phase advance (days)	5.9	0.3
Re-entrainment to 6 h phase advance (days) + saline	7.0	0.5
Re-entrainment to 6 h phase advance (days) + PG99-465	7.9	0.4

The running wheel activity shown for the light and dark cycles is the average activity of the 16 mice used in the study described in section 3.2.2.2., from the 7 days period prior to treatment. For the phase advances, the average number of days taken to re-entrain was estimated from the onset of activity from the actograms (appendices II – IV).

progressive leftwards shift in the onset of activity as can be seen in the representative actogram (Figure 3.2.23) and the 24 h activity patterns following the advance (Figure 3.2.24). On average, the mice re-entrained to the novel cycle in approximately 5.9 ± 0.3 days, which was consistent with that previously reported for the 8 h phase advance (5.9 ± 0.2 days; Table 3.2.3). A number of the mice (n = 6) failed to re-entrain completely to the 6 h advance within a week of the shift and were not included in the calculation of average re-entrainment time. Further inspection of the activity profiles, revealed that half of the mice demonstrated a persistent low level of activity during the first six hours of the dark cycle on the first day of the phase advance (Figure 3.2.25a). As observed in the activity profiles following the 8 h advance, by the second cycle the majority of mice (~ 85 %) were active within the first hour of the novel dark period (Figure 3.2.25a). Excluding activity which was of a lower amplitude to that observed during the 5 dark cycles prior to the phase advance (mean activity per hour), demonstrated that no mice were active within the first two hours of darkness in the novel cycle (Figure 3.2.25b). Following the successful demonstration of a stable entrainment to this 6 h phase advance, the mice were re-entrained to a third light dark cycle (lights on: 0800 - 2000 h), in preparation for surgery and the 6 h phase advance.

3.2.2.4. PG99-465 modulation of responses to phase advances

When the potencies of PG99-465 solutions were examined in the previous *in vitro* studies, BSA was included in the assay to reduce any non-specific interactions of the peptide (B.3.1., p 62 and B.3.2., p 65). However, as injection of BSA into the mouse brain could induce an immunological response (Anisman *et al.*, 2003), BSA had to be removed from the peptide containing solution for the *in vivo* studies. To determine whether BSA removal affected the potency of PG99-465, the ability of the peptide (± BSA) to inhibit VIP induced calcium responses in the CHO-hVPAC$_2$R cell line was examined (Figure 3.2.26). The potencies of PG99-465 were directly compared in an individual experiment and were found to be similar under both conditions (IC_{50} + BSA: 2.8 nM; – BSA: 5.5 nM), and to previous values (IC_{50}: 4.4 ± 0.8 nM (n = 6); chapter one, Table 1.2.3, p 118), therefore BSA was not included in the injected peptide solution.

During surgery (0800 – 1200 h), PG99-465 (1 μM) or vehicle (saline) was administered to the mice through i.c.v. injection (1 μl; injection rate: 0.1 μl/min). Immediately following the injection of PG99-465 *in vivo*, the potency of the solution

was verified in the intracellular calcium assay (Figure 3.2.27). PG99-465 inhibited VIP induced fluorescence responses in the CHO-hVPAC$_2$R cell line in a concentration dependent manner (IC_{50}: 6.5 nM; Figure 3.2.27), with a potency similar to the previously established values (IC_{50}: 4.4 ± 0.8 nM (n = 6); chapter one, Table 1.2.3, p 118) and those described above. Following surgery, the mice were returned to their home cages by 1300 h, to allow a full hour in these cages before the onset of the novel dark cycle (lights off: 1400 - 0200 h) as can be seen in the representative actograms in Figure 3.2.28. The leftwards shift in the onset of dark cycle activity and general activity levels following surgery and the 6 h phase advance are shown in Figure 3.2.29. The activity profiles from both groups of mice were identical, with no wheel running activity observed within the first two hours of the novel dark cycle post treatment (Figures 3.2.30 and 3.2.31). The lack of activity within the first two hours of the novel light/dark cycle was observed whether activity was assessed using all bursts of activity (independent of amplitude; Figures 3.2.30a and 3.2.31a), or just the activity bursts which were of a similar amplitude to the average dark cycle activity (per hour) from the 5 cycles prior to treatment (Figures 3.2.30b and 3.2.31b). By the second dark cycle in the novel lighting regime, the majority of the mice from each group showed some activity within the first hour of the onset of darkness, however this was generally of lower amplitude than the pre-treatment dark cycle activity (Figures 3.2.30 and 3.2.31). One mouse (from the saline treated group) failed to re-entrain within the 9 days post-surgery and was not included in the calculation of re-entrainment time. In summary, the administration of PG99-465 did not accelerate the time to phase advance as had been originally hypothesised.

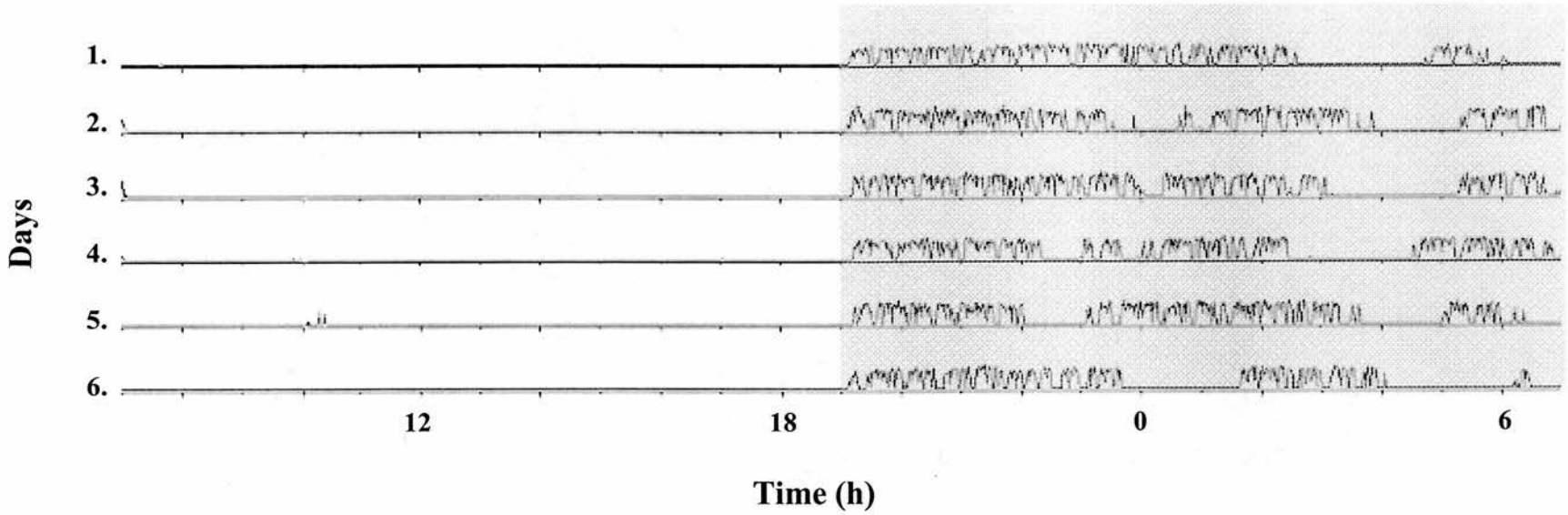

Figure 3.2.13 Stable entrainment of mice to the light/dark cycle. The representative figure shows the running wheel activity of an individual mouse over a 6 day period, in a 12 h light/dark cycle (lights off 1900 –0700 h, as indicated by the grey box). The activity of the mouse correlates well with the onset and duration of darkness, indicating that the animal was stably entrained to the lighting regime.

(a)

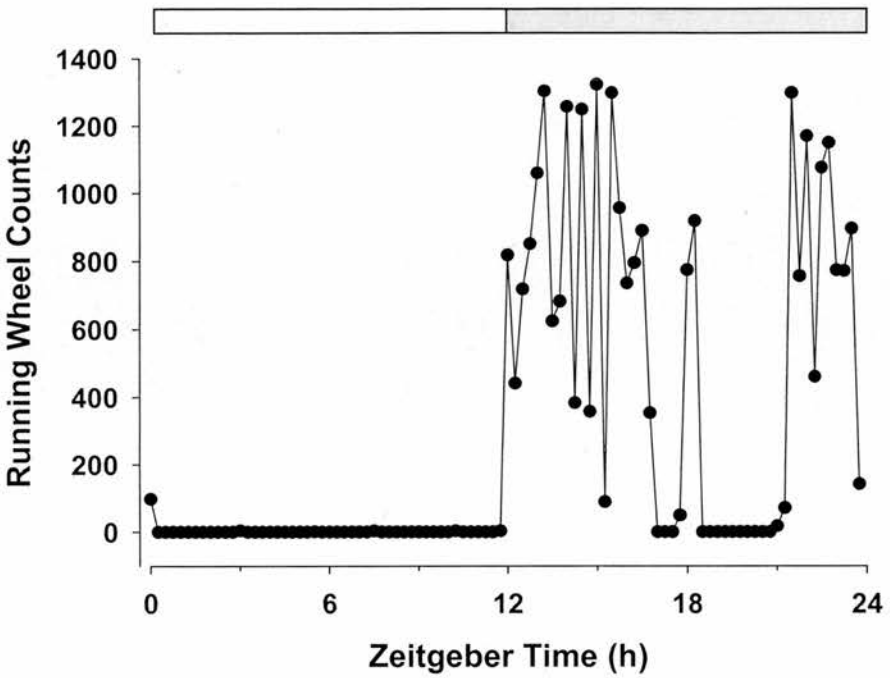

(b)

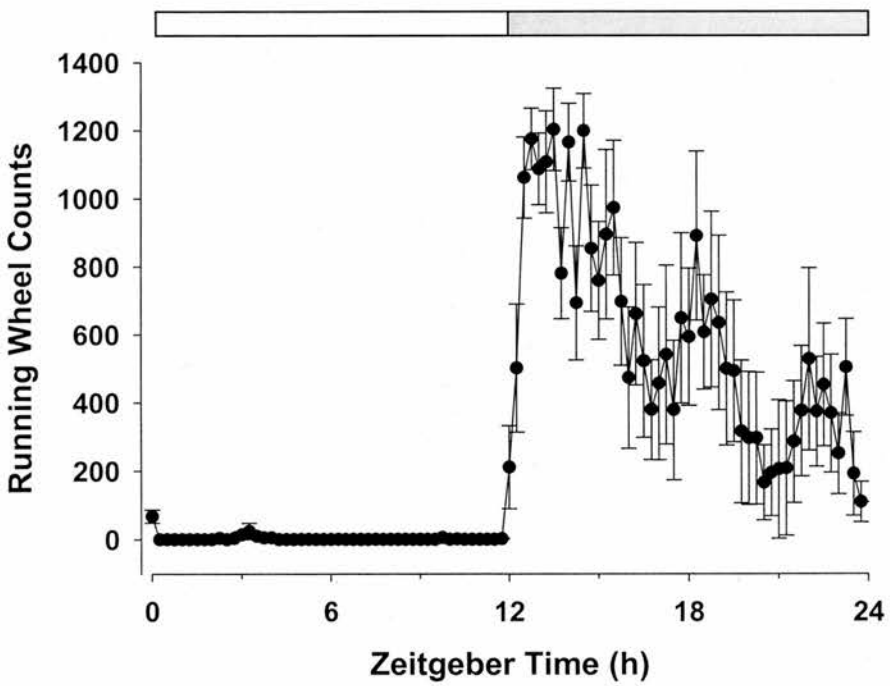

Figure 3.2.14 Intensity of mouse running wheel activity over the 12 h light/dark cycle. The mouse was exposed to a 12 h light/dark cycle as indicated by the bar at the top of each figure (the light phase is shaded in white, darkness shaded in grey). The intensity of running wheel activity (measured in 15 min time bins) is shown for an individual mouse over a 24 h period (**a**). The mean profile of activity (± SEM; in 15 min bins) for the same mouse is shown over a 7 day period prior to treatment in study 1 (**b**).

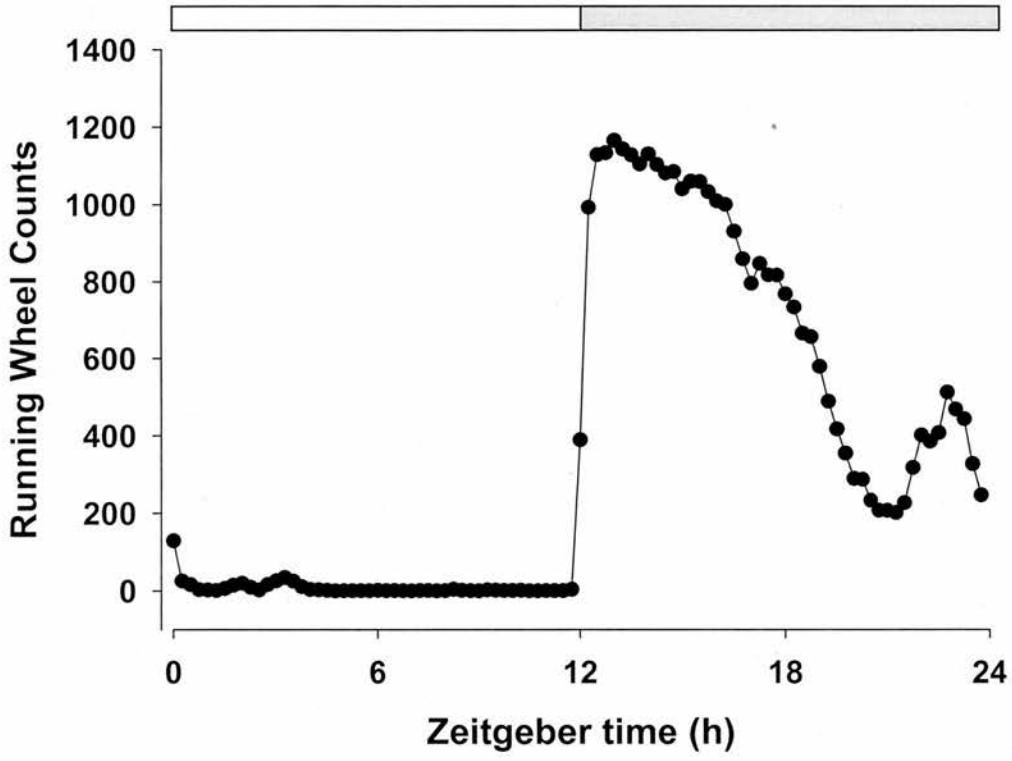

Figure 3.2.15 Intensity of mouse running wheel activity over the 12 h light/dark cycle. The mean intensity of running wheel activity over a 7 day period (measured in 15 min time bins) is shown for all 16 mice used in the study described in section 3.2.2.2., prior to treatment.

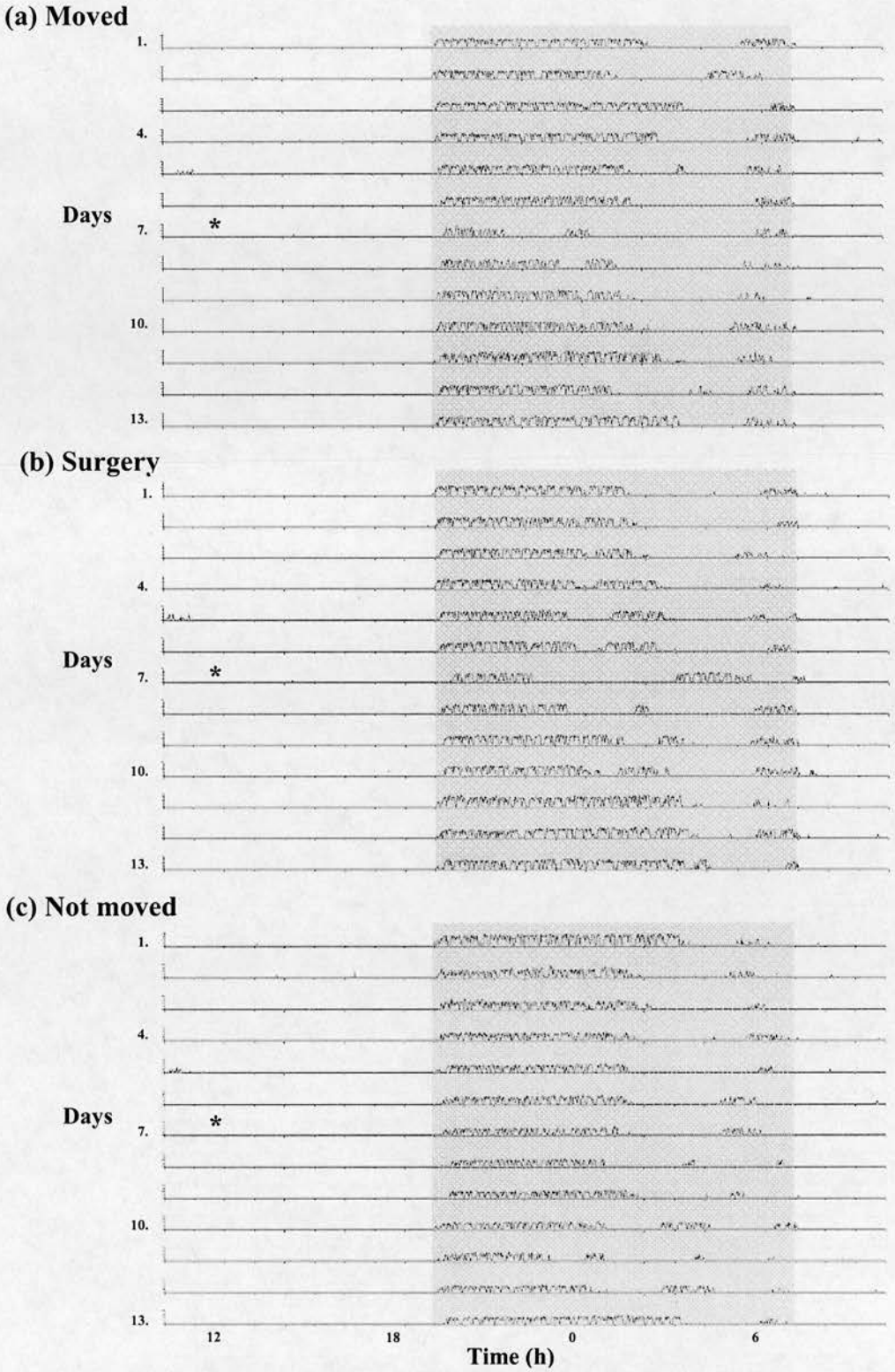

Figure 3.2.16 Activity profiles of mice in the moved, surgery and not moved groups. Representative figures are shown for the individual mice in the moved (**a**), surgery (**b**) and not moved (**c**) groups. The data shows the activity profiles of the mice over a 13 day period (12 h light/dark cycle indicated by the grey box), with the treatment day (and time) indicated by the asterisks.

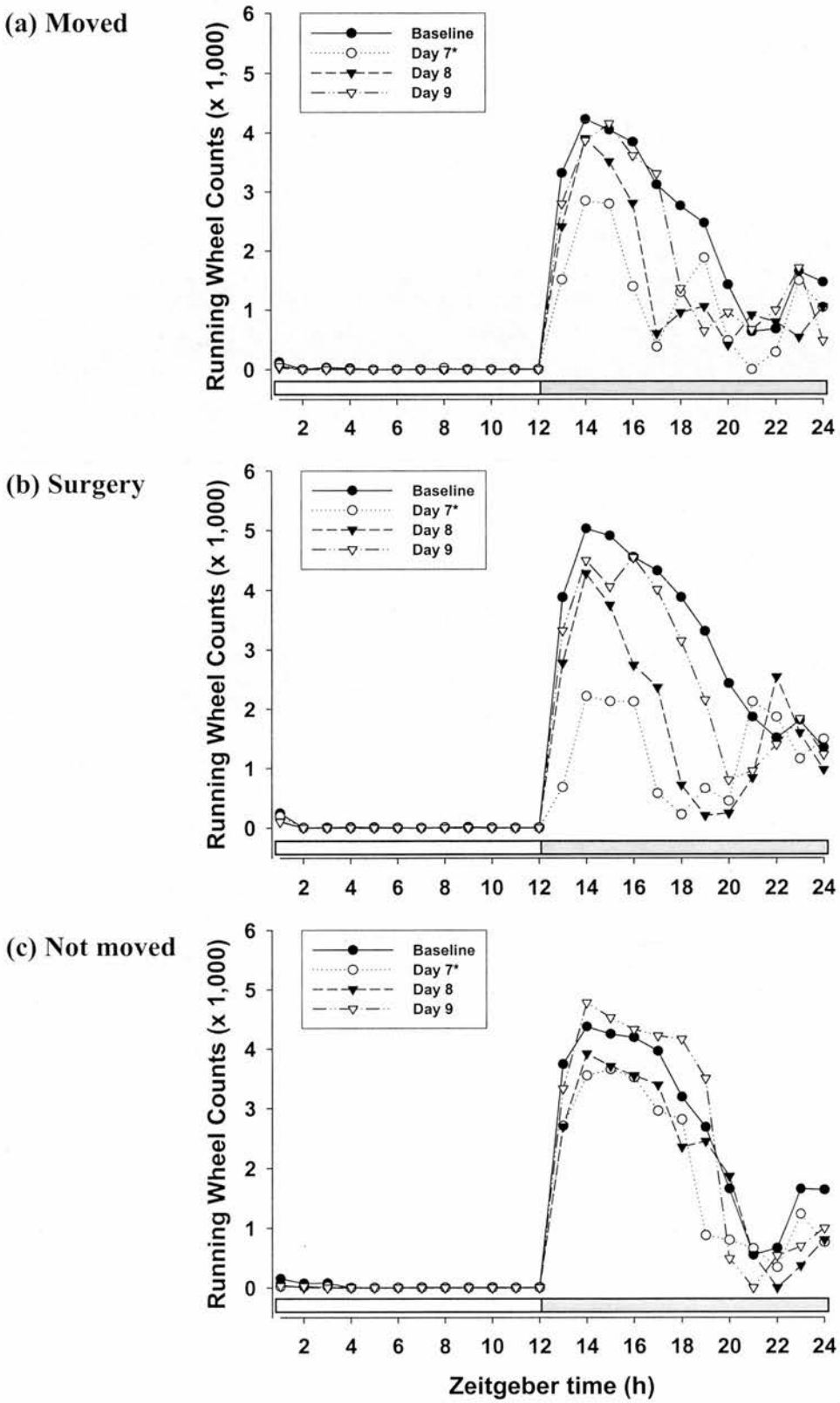

Figure 3.2.17 Activity profiles for mice over a four day period. Average activity profiles for the moved (**a**), surgery (**b**) and not moved (**c**) groups are shown over a 4 day period, with baseline activity calculated from the average of 6 days prior to treatment on day 7*. Running wheel counts are presented in 1 h time bins.

(a)

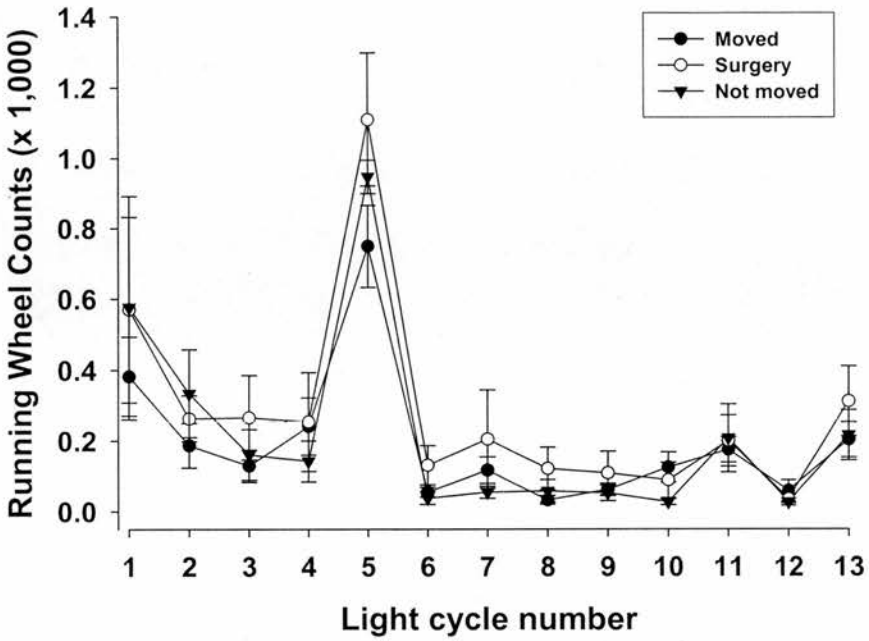

(b)

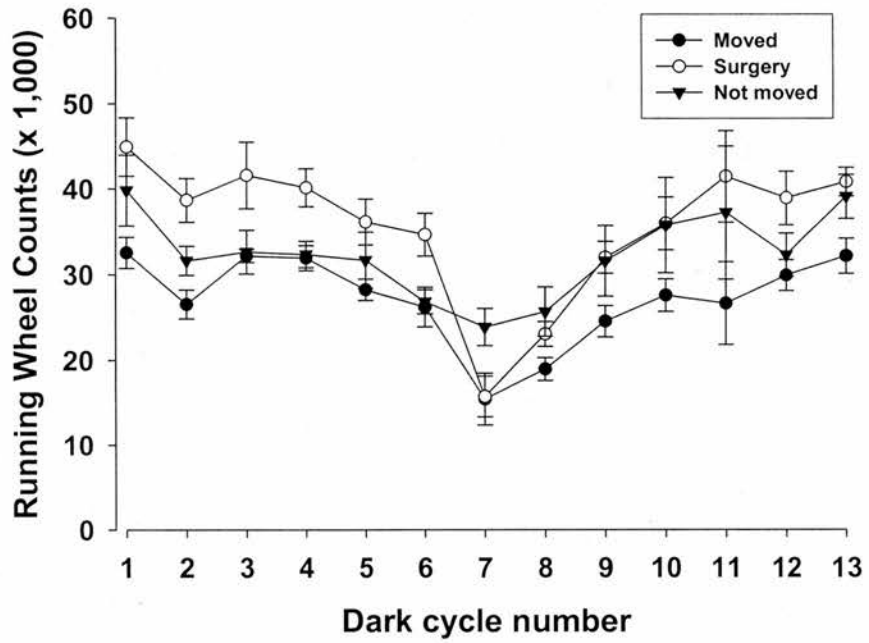

Figure 3.2.18 Light and dark cycle running wheel counts following surgery and movement. The figures show the average total activity (± SEM) counts for the three groups of mice examined in the study described in section 3.2.2.2., measured over the light (**a**) and dark cycles (**b**).

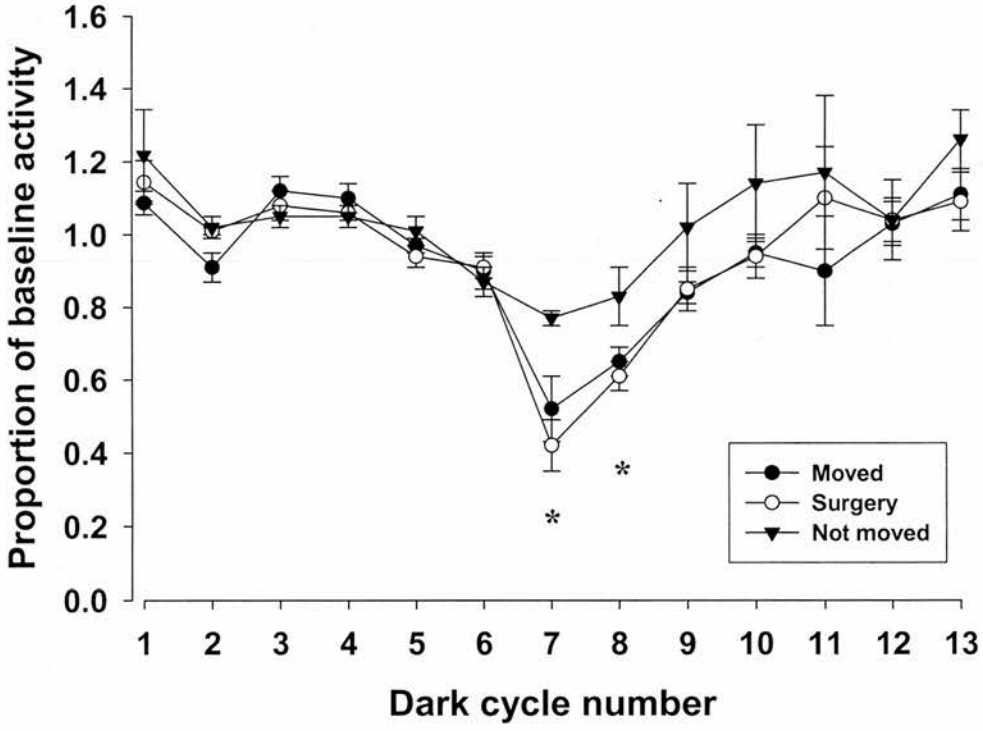

Figure 3.2.19 Movement of mice caused a significant short term drop in total activity within the dark cycle. Total activity within the 12 h of the dark cycle was expressed as a proportion of the average activity (± SEM) over the first five dark cycles for each treatment group. The activities of all groups were significantly different on the 1st and 2nd dark cycles post treatment compared to the rest of the experiment, as indicated by the asterisks.

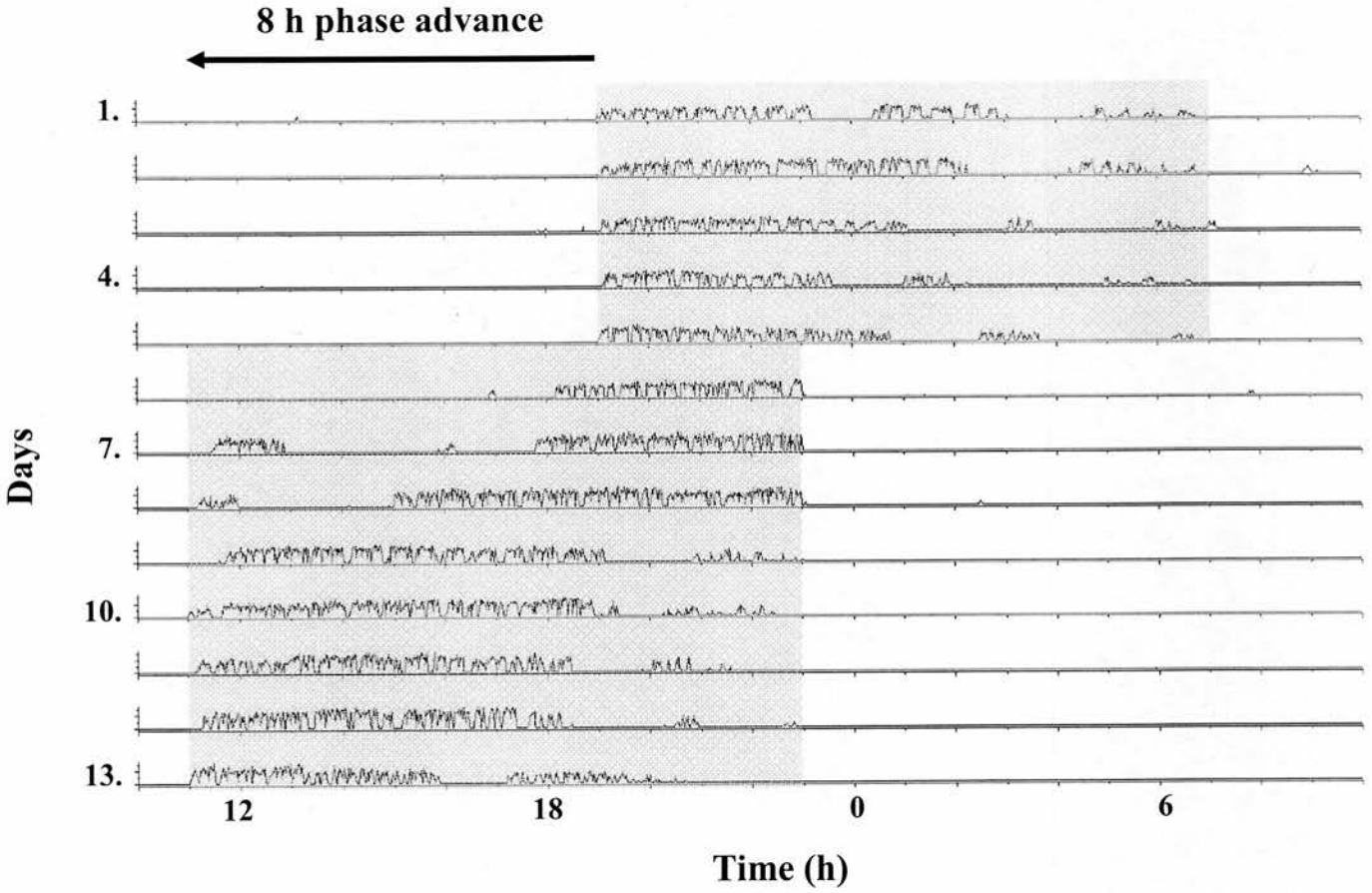

Figure 3.2.20 Stable entrainment of mice to the light/dark cycle and responses to an 8 h phase advance in the cycle. The representative figure shows the stable entrainment of an individual mouse to a 12 h light/dark cycle (lights off 1900 – 0700 h) over a 5 day period. On day 6 of the above actogram, the mouse was subjected to an 8 h advance in the onset of the dark cycle, as indicated by the grey box.

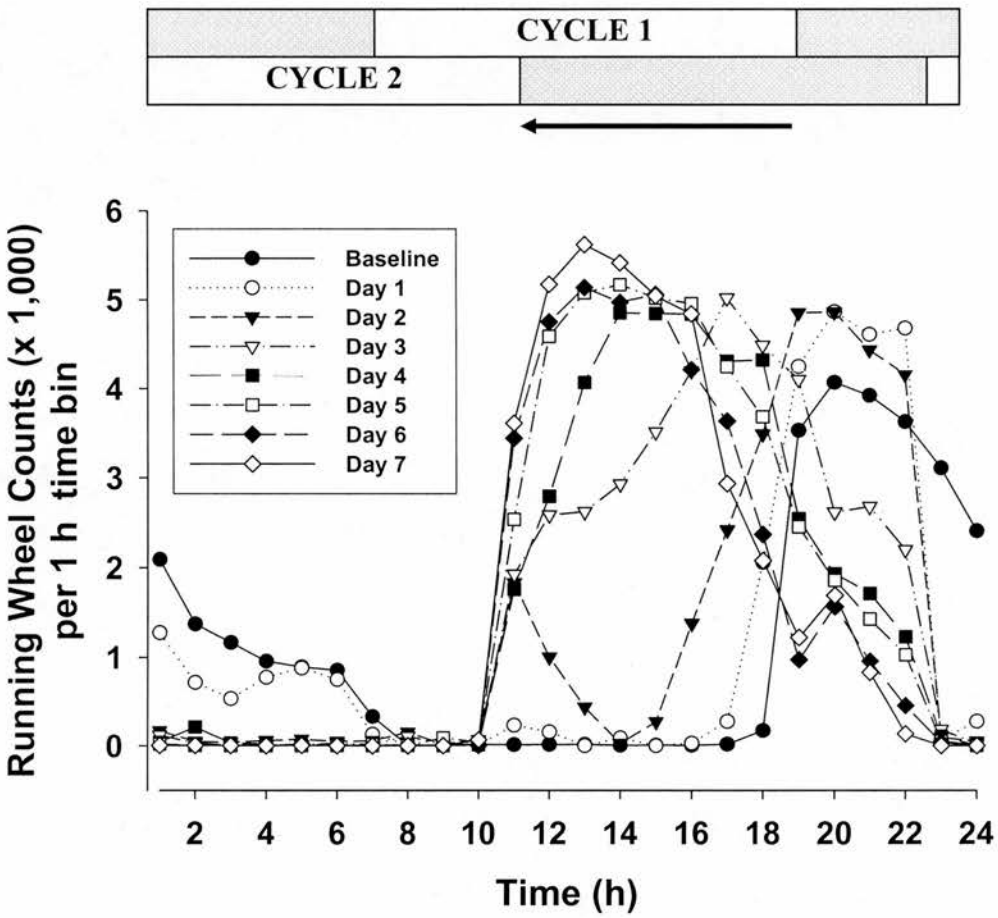

Figure 3.2.21 **Sequential activity profiles following an 8 h phase shift**. Wheel running activity was plotted in 1 h bins, with the baseline calculated from the mean of 5 days stable entrainment on light/dark cycle 1 (lights on: 0700 – 1900 h). An 8 h advance in the dark cycle (cycle 2) was imposed and activity recorded for the next 7 days.

(a)

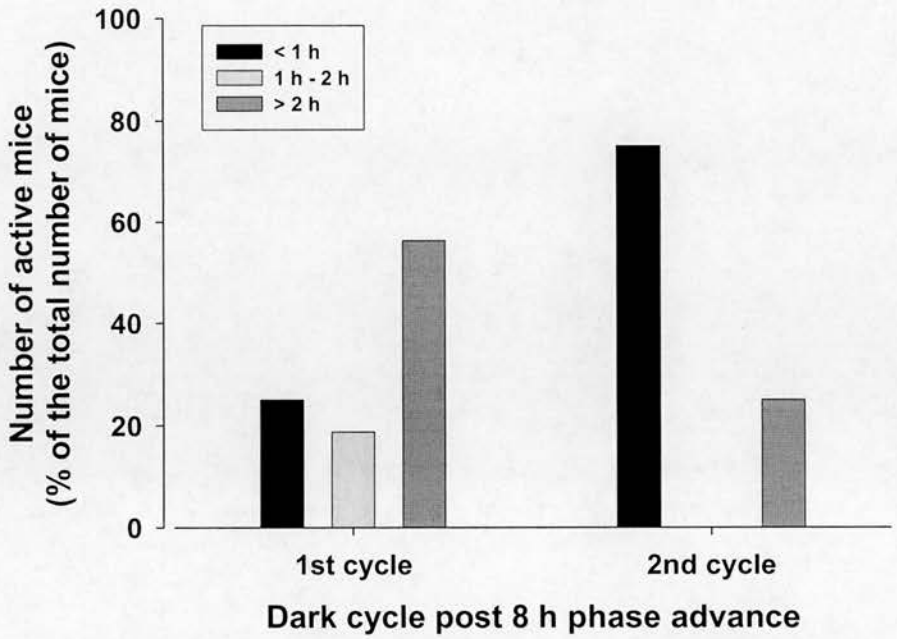

(b)

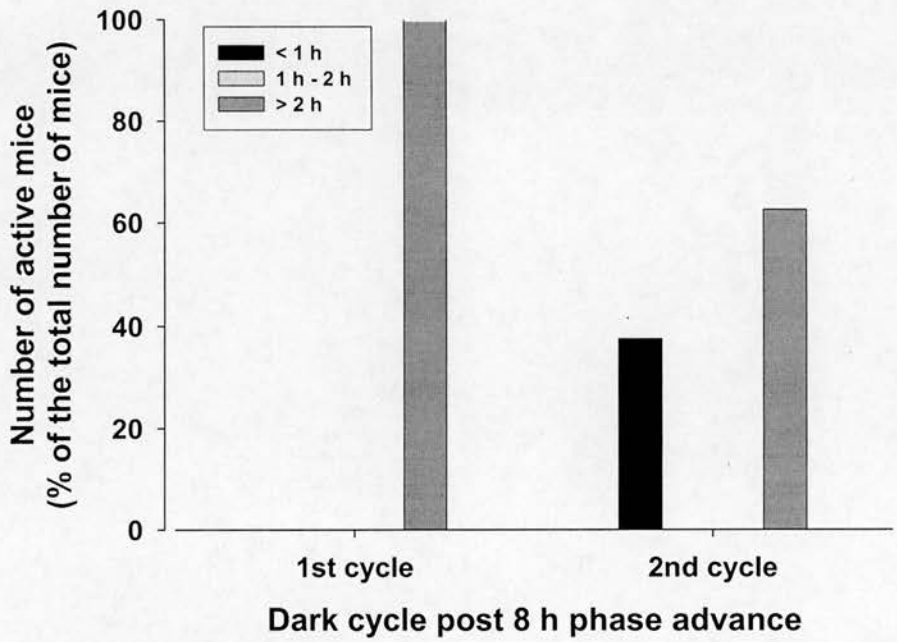

Figure 3.2.22 Timing of activity onset in mice following an 8 h phase advance. The percentage of mice active within either the first hour (< 1 h), the second hour (1 h – 2 h) or more than two hours (> 2 h) after the new onset of the dark cycle was assessed. Data are shown for the first two cycles after the phase advance, initially with all activity recorded (**a**) and latterly, using only activity bursts of comparable amplitude to the average dark cycle activity (per h) from the 5 cycles prior to the phase advance (**b**).

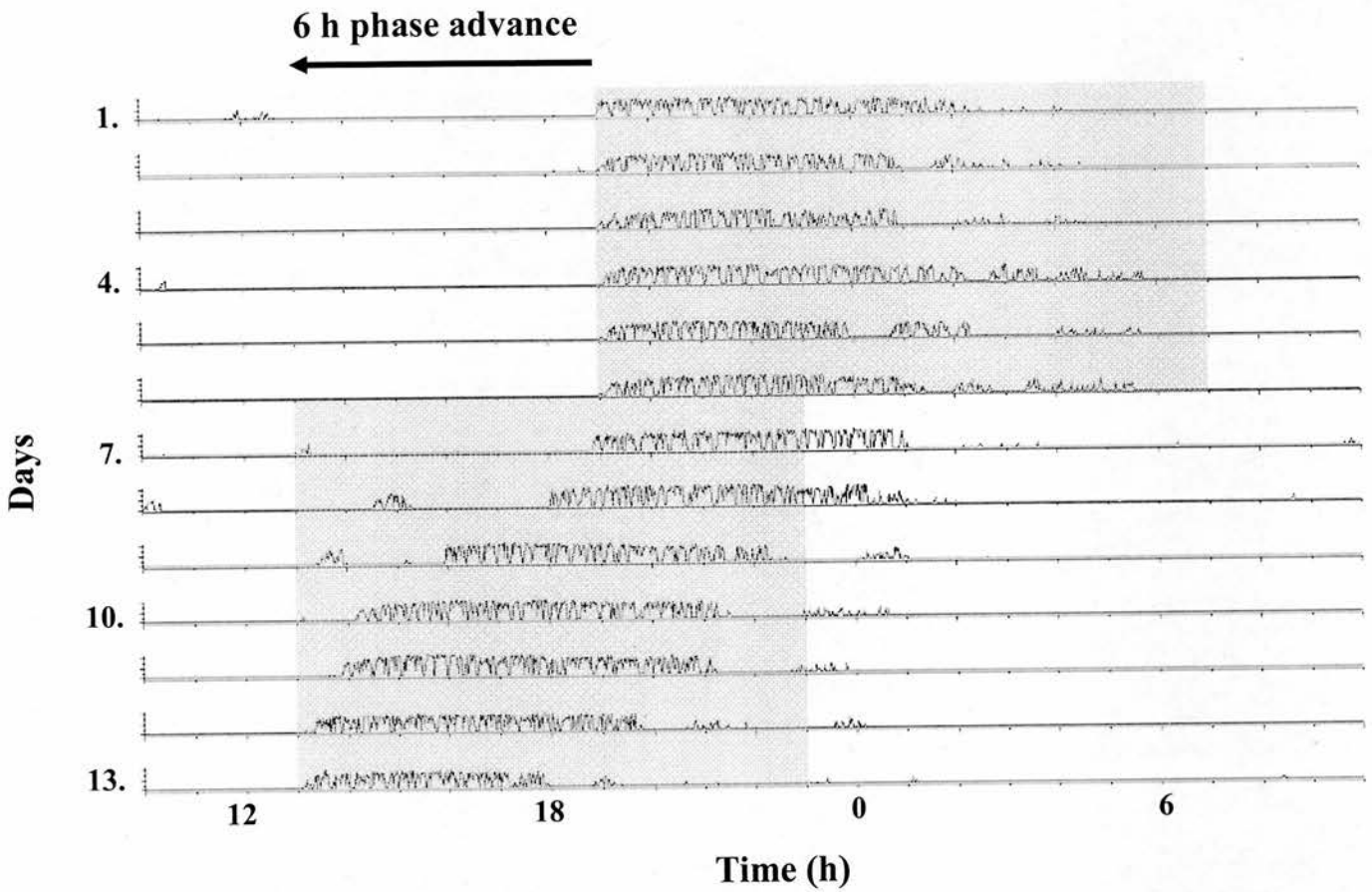

Figure 3.2.23 Stable entrainment of mice to the light/dark cycle and responses to a 6 h phase advance in the cycle. The representative figure shows the stable entrainment of an individual mouse to a 12 h light/dark cycle (lights off 1900 – 0700 h) over a 6 day period. On day 7 of the above actogram, the mouse was subjected to a 6 h advance in the onset of the dark cycle, as indicated by the grey box.

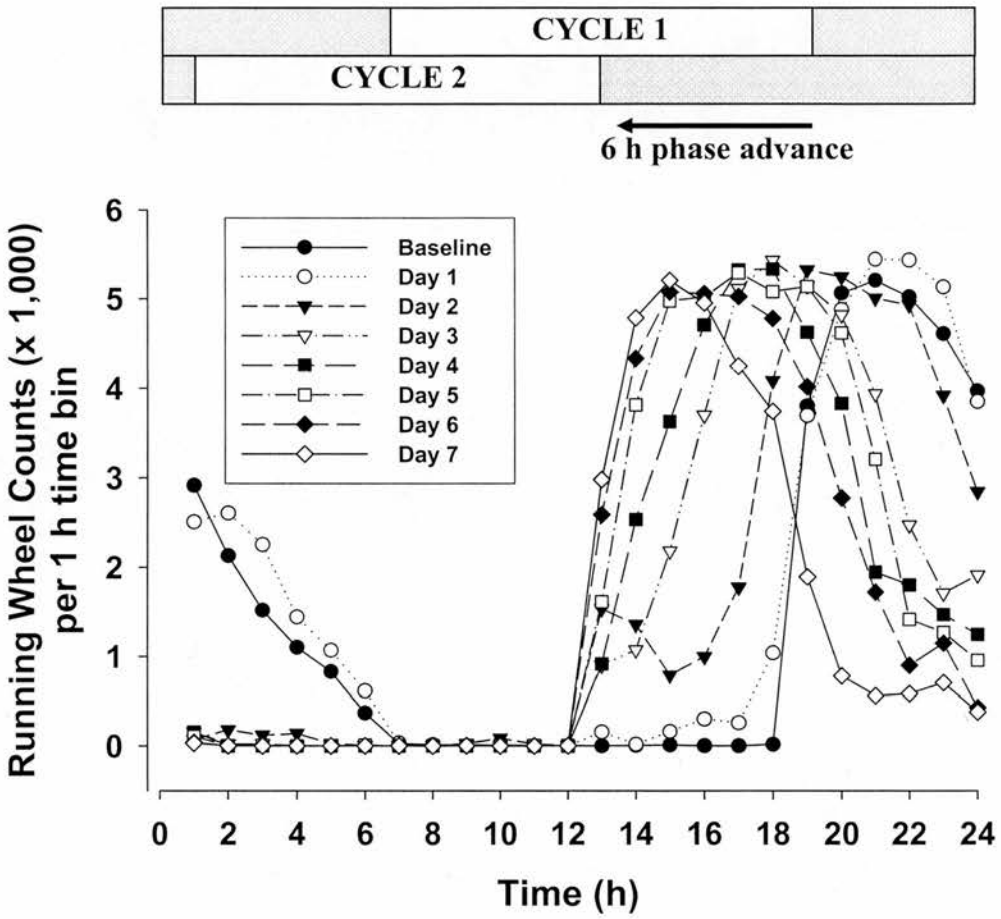

Figure 3.2.24 **Sequential activity profiles following a 6 h phase shift**. Wheel running activity was plotted in 1 h bins, with the baseline calculated from the mean of 5 days stable entrainment on light/dark cycle 1 (lights on 0700 – 1900). A 6 h advance in the dark cycle (cycle 2) was imposed and activity recorded for the next 7 days.

(a)

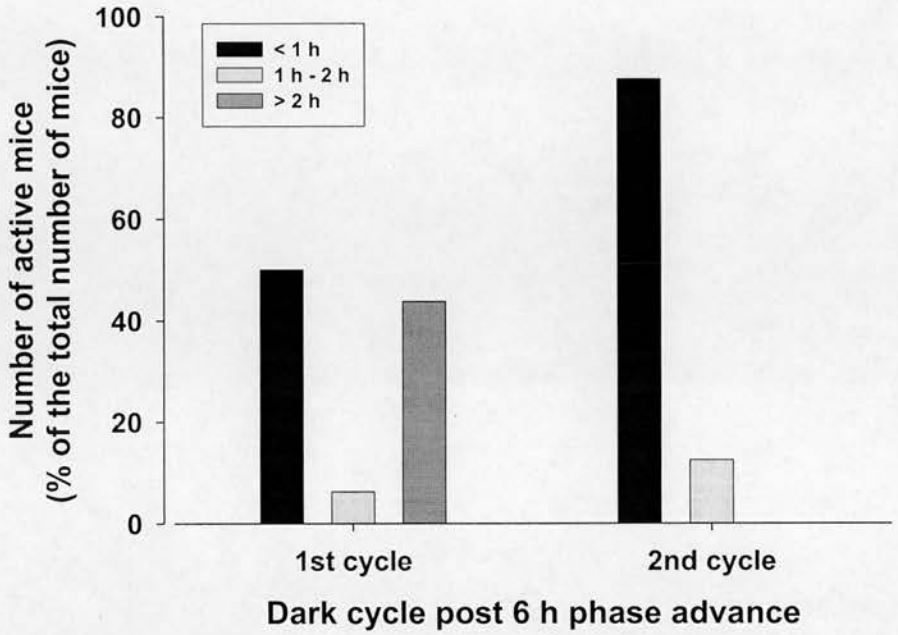

(b)

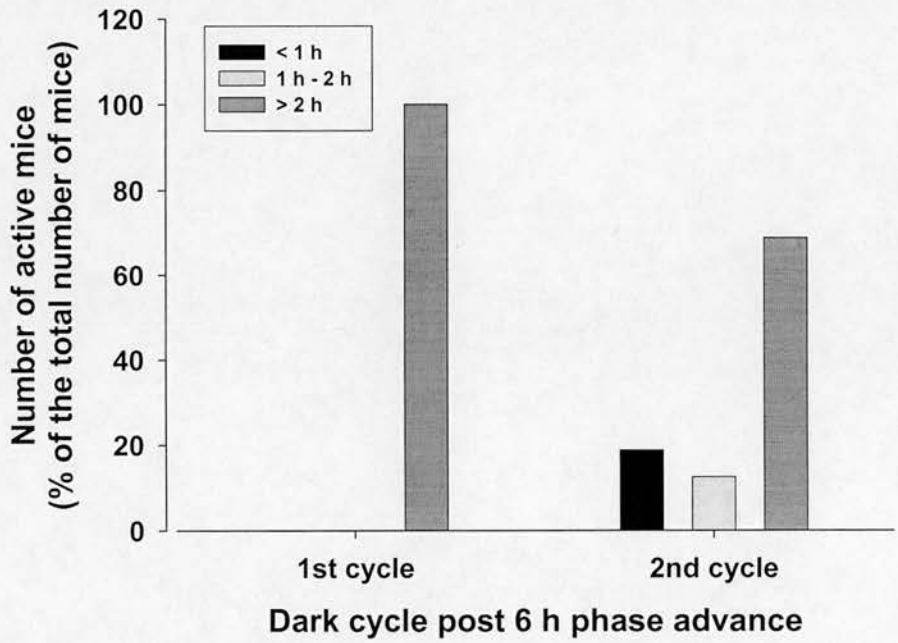

Figure 3.2.25 Timing of activity onset in mice following a 6 h phase advance. Data are shown for the first two cycles following the 6 h phase advance, initially with all activity recorded (**a**) and latterly, using only activity bursts of greater or equal amplitude to the average dark cycle activity (per h), calculated from the 5 cycles prior to the phase advance (**b**). The percentage of mice active within either the first hour (< 1 h), the second hour (1 h – 2 h) or more than two hours (> 2 h) after the new onset of the dark cycle was assessed.

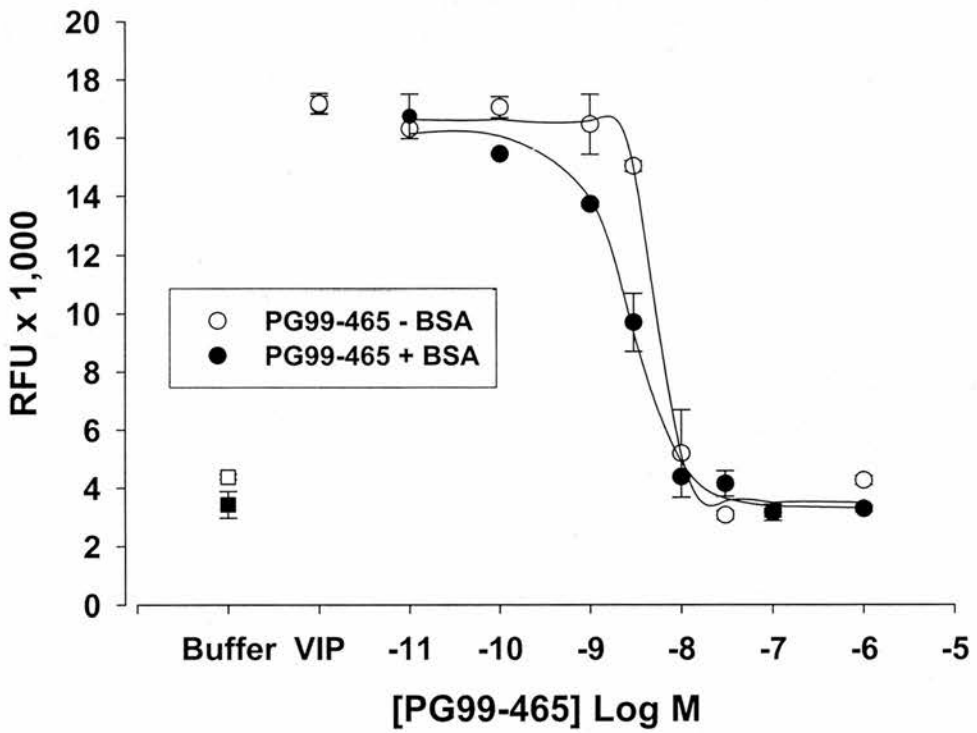

Figure 3.2.26 The potency of PG99-465 is not altered by the removal of BSA. hVPAC$_2$R-expressing cells were seeded overnight in 96-well plates (100,000 cells/well). After loading with calcium dye for 1 h at 37 °C, cells were incubated with PG99-465 (with or without 0.1 mg/ml BSA) for 10 min prior to VIP addition. Fluorescence levels (max-min) were determined using the FlexStation®. IC_{50} values for PG99-465 with and without BSA, were 2.8 and 5.5 nM respectively.

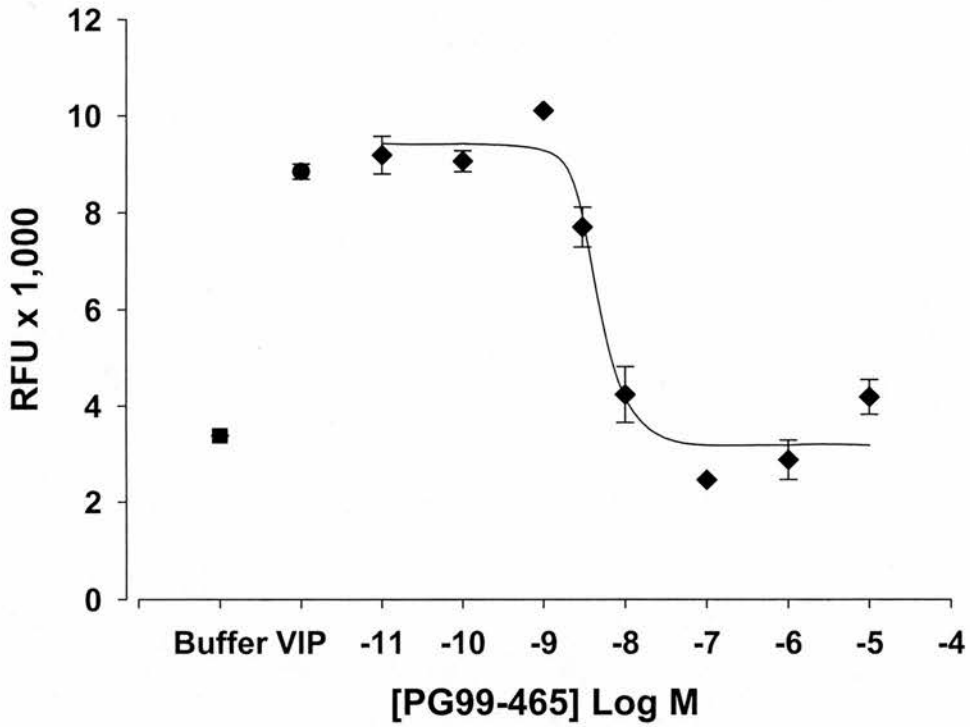

Figure 3.2.27 Confirmation of hVPAC$_2$R antagonism using the *in vivo* PG99-465 solution. PG99-465 was prepared in saline (0.1 mM) and then diluted in assay buffer. Pre-incubation with CHO-hVPAC$_2$R cells for 10 min resulted in a concentration dependent inhibition of the VIP stimulated response (IC_{50} = 6.5 nM).

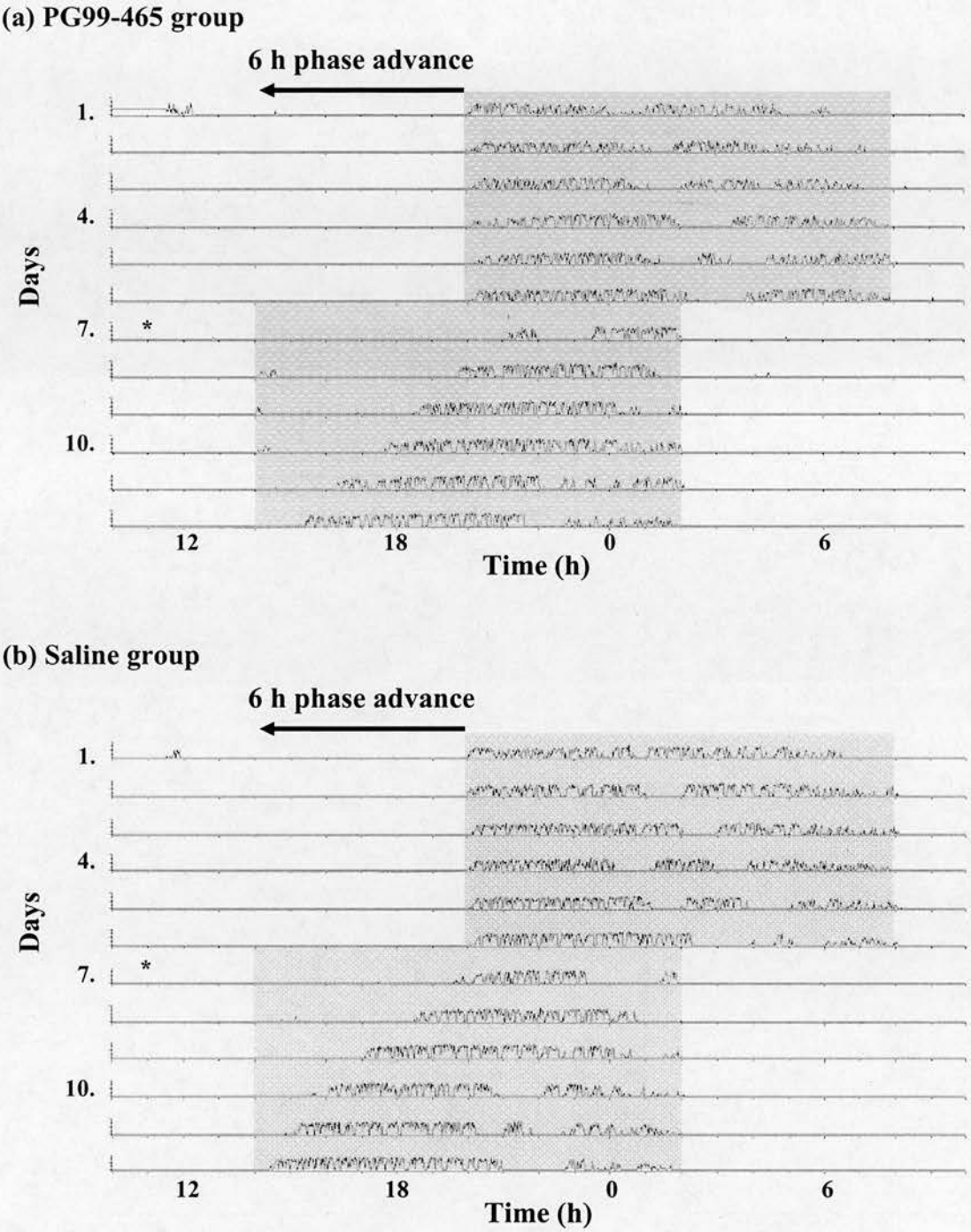

Figure 3.2.28 Activity profiles for PG99-465 and saline treated animals. Representative actograms are shown for the mice treated with either PG99-465 (**a**) or saline (**b**) prior to a 6 h phase advance in the light dark cycle. The time of surgical intervention is indicated (*), with the changing dark cycle shown by the position of the grey box.

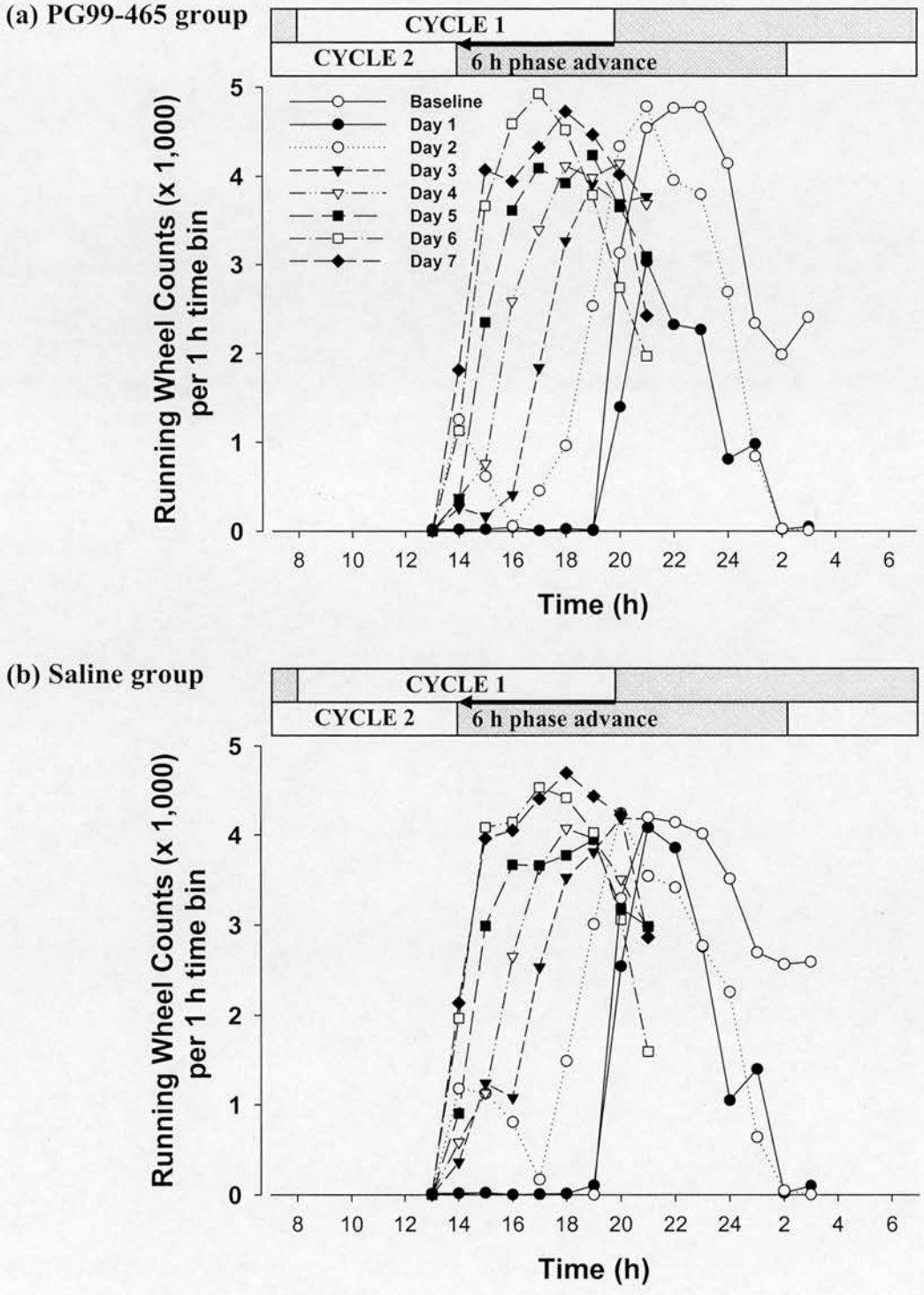

Figure 3.2.29 **Activity profiles following drug treatment and a 6 h phase shift.** Wheel running activity was plotted in 1 h bins, with the mean of 5 days stable entrainment on light/dark cycle 1 (lights on 0700 – 1900) used as a baseline. A 6 h darkness advance (cycle 2) was carried out and activity measured for the next 7 days. Activity is only shown from onset of activity to immediately after peak activity.

(a)

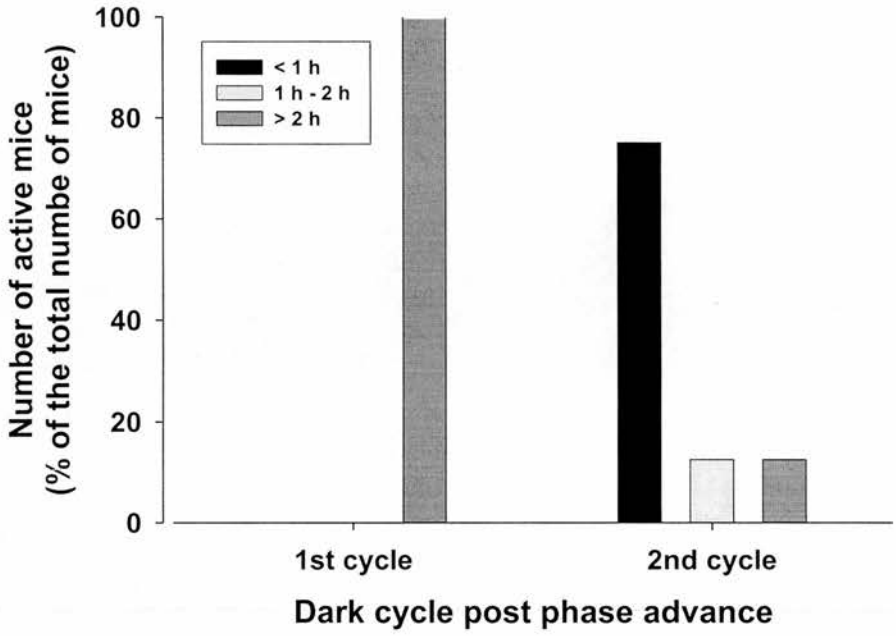

(b)

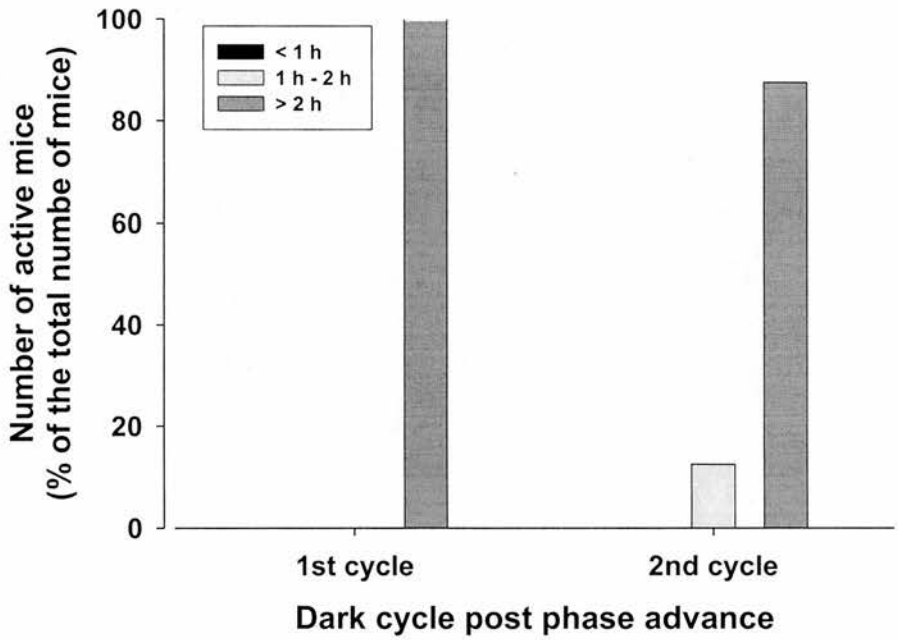

Figure 3.2.30 Timing of activity onset in mice following drug treatment and 6 h phase advance. Data are shown for the first two cycles following the 6 h phase advance for the PG99-465 treated mice, with the percentage of mice active within either the first hour (< 1 h), the second hours (1 h – 2 h) or more than two hours (> 2 h) after the new onset of the dark cycle shown. The data was initially calculated with all activity recorded (**a**) and latterly, using only activity bursts of comparable amplitude to the average dark cycle activity from the 5 cycles prior to treatment (**b**).

(a)

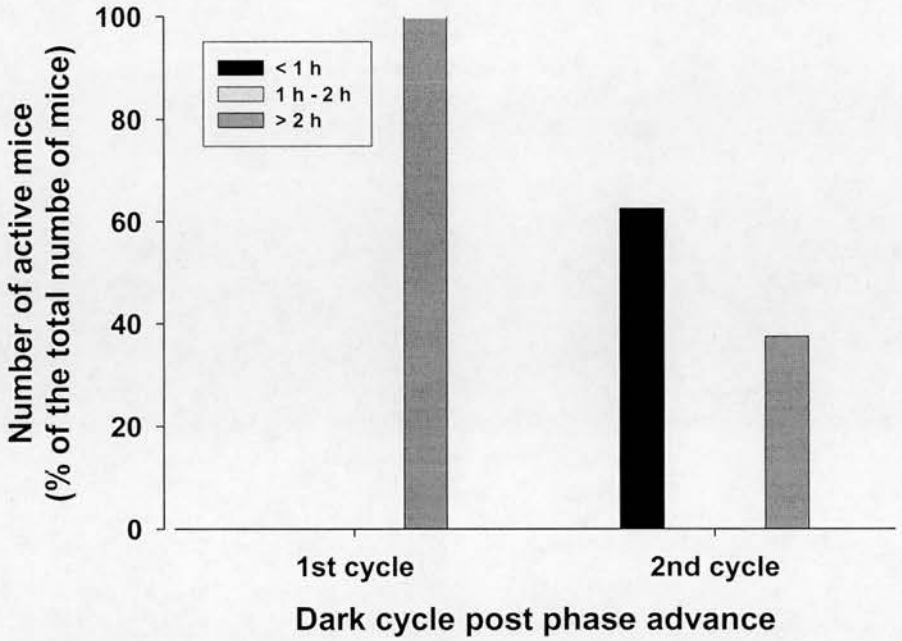

(b)

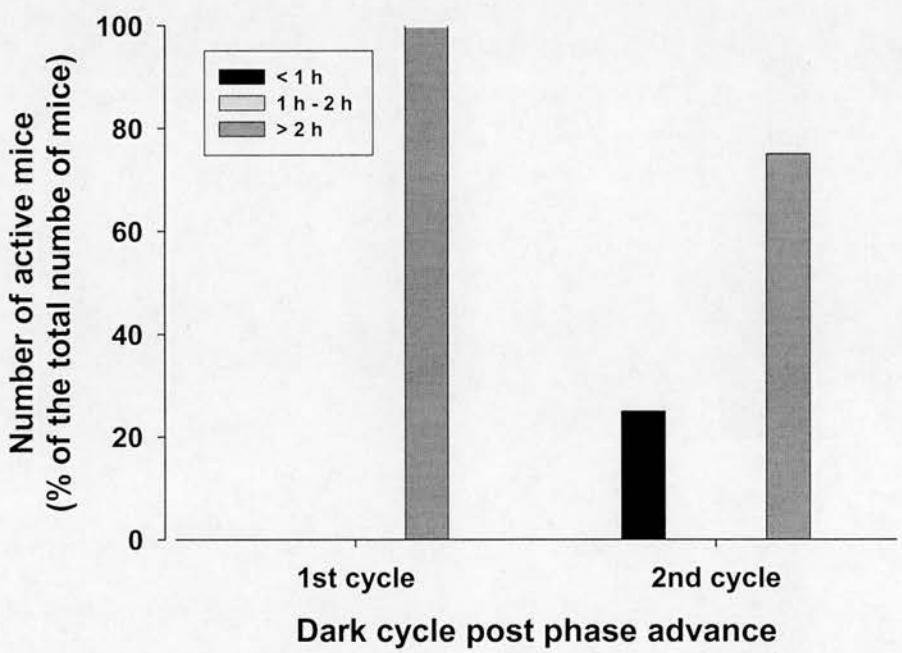

Figure 3.2.31 Timing of activity onset in mice following drug treatment and 6 h phase advance. Data are shown for the first two cycles following the 6 h phase advance for the saline treated mice, with the proportion of mice active within the first hour (< 1 h), the second hour (1 h – 2 h) or more than two hours (> 2 h) after the onset of the novel dark cycle shown. Data were initially calculated with all activity recorded (**a**) and latterly, using only activity bursts of similar amplitude to the average dark cycle activity from the 5 cycles prior to treatment (**b**).

3.3. Discussion

The peptides VIP and PACAP, together with their cognate receptors ($VPAC_1$, $VPAC_2$ and PAC_1) have been implicated in a plethora of physiological processes, as discussed in the general introduction. In this chapter, I have explored the actions of the peptides and receptors and their roles in two distinct central themes; the first being the modulation of astrocyte function with regard to VIP/PACAP mediated neuroprotection and the second, the specific role of $VPAC_2R$ in the control of circadian rhythms of activity.

3.3.1. VIP/PACAP modulation of astrocyte function

Since the initial studies by Brenneman and colleagues (1987), it is now clear that astrocytes play important roles in VIP/PACAP induced neuroprotection. The protective effects of the peptides have been demonstrated in a wide array of *in vitro* and *in vivo* models, as discussed extensively in the introduction. Such studies have led to the isolation of highly potent, neuroprotective factors, which have been shown to be under the control of VIP/PACAP activity (Brenneman *et al.*, 1998; Gozes & Brenneman, 2000). Indeed, these factors have been shown to provide neuroprotection at low concentrations and NAP, an ADNP derivative, is currently progressing through clinical trials as a potential neuroprotective treatment for Alzheimer's disease (Gozes *et al.*, 2005). Despite these exciting developments, the underlying mechanism/receptors responsible for astrocyte mediated VIP/PACAP neuroprotection remain to be fully elucidated, but do currently appear to involve the secretion of a complex balance of both cytokines and neurotrophic factors (Dejda *et al.*, 2005). Furthermore the pharmacology of the VPAC/PAC receptors expressed on astrocytes and their intracellular signalling pathways have been poorly characterised. To try to address these issues, VPAC/PAC receptor pharmacology in primary cultures of rat cortical astrocytes was thoroughly characterised using the HT-amenable $[cAMP]_i$ and $[Ca^{2+}]_i$ assays previously described (methods, B.3.1., p 62).

3.3.1.1. VPAC/PACR pharmacology in rat cortical astrocytes

The current investigation of VPAC/PAC receptor pharmacology in primary cultures of rat cortical astrocytes provides the most comprehensive characterisation

of astrocytic VPAC/PAC receptors to date. Although previous reports have demonstrated VPAC/PACR mediated cAMP elevations, these studies have almost exclusively involved the evaluation of only a single agonist, usually PACAP-38 (Grimaldi & Cavallaro, 1999; Masmoudi *et al.*, 2003; Li *et al.*, 2005). The most extensive study prior to the current investigation was reported by Hashimoto and colleagues over 10 years ago, in which a concentration dependent increase in cAMP was demonstrated in RCA following application of VIP, PACAP-27 and PACAP-38. Furthermore, only a single report to date has fully characterised a VPAC/PACR mediated calcium response in this cell type, and again this involved the evaluation of PACAP-38 alone (Masmoudi *et al.*, 2003). This is in contrast to other investigations of VPAC/PACR mediated calcium signalling in astrocytes, in which no stimulation of calcium was reported (Grimaldi & Cavallaro, 1999; Hashimoto *et al.*, 2003). In the current studies, the six VPAC/PACR agonists evaluated in chapter one were assessed for their ability to stimulate $[cAMP]_i$ and $[Ca^{2+}]_i$ in RCA, with full concentration response curves determined for the majority of agonists in both assays. The agonist ROP was identical between assays for the astrocytes and was also consistent with the CHO-hPAC$_1$R and SHSY-5Y cells characterised in chapter one, indicating a predominantly PAC$_1$R expression. In addition, agonist induced responses (~ EC_{50}) in both assays were fully inhibited by the PAC$_1$R antagonist M65, which again is suggestive of a primarily PAC$_1$R mediated response. Although the expression of VPACR has been reported in RCA, the majority of studies have suggested a predominant PAC$_1$R expression, which is consistent with the ROP produced in the current studies (Grimaldi & Cavallaro, 1999; Hashimoto *et al.*, 1993, 2003). The difference in potency detected between the PACAPs and VIP in our cAMP studies (~ 170 fold) and the corresponding EC_{50} values (VIP = 179 nM, PACAP-27 = 0.68 nM, PACAP-38 = 2.2 nM), are very similar to those reported previously by Hashimoto and colleagues (VIP = ~ 300 nM, PACAP-27 = 1.1 nM, PACAP-38 = 2.4 nM; Hashimoto *et al.*, 1993). In general, the VPAC/PACR agonists stimulated calcium responses from RCA with approximately 10 fold lower potency than agonist induced cAMP responses. Although the magnitude of the potency shift between assays was less pronounced in the astrocyte studies, the reduction in agonist potency in the calcium assay was consistent with the data presented in chapter one, both for the CHO-hPAC$_1$R and SHSY-5Y cells. Furthermore a lower potency in stimulating calcium relative to cAMP in RCA was also found for PACAP-38 in the study by Masmoudi and colleagues (2003), although again the fold shift (~ 60 fold) was larger than that detected in the current studies.

3.3.1.2. Maximum agonist induced responses from RCA

In agreement with data generated for the VPAC/PAC receptor expressing cell lines in chapter one (p 104), maximum agonist induced $[cAMP]_i$ responses from RCA were similar within assays. However, the peak responses observed between assays were considerably more variable, perhaps reflecting the heterogeneous nature of primary cell cultures. In the calcium assay, a differential profile of peak responses was observed with the agonists, with concentration curves for the PACAP peptides being approximately one third larger than the other agonists. This profile is identical to that determined for the $hPAC_1R$ expressing SHSY-5Y cell line in chapter one (p 128), in which concentration response curves for the PACAPs were again larger than the other agonists in the calcium assay, despite no differences in the maximum cAMP responses from that cell line. In recent studies reported by Dejda and colleagues (2006), although no EC_{50} values or concentration response curves were shown, PACAP-38 and VIP were demonstrated to stimulate IP_3 accumulation in RCA with apparently different maximum responses. It is not clear from the data presented in that report whether the maximum IP_3 responses for each peptide were achieved, particularly for PACAP-38. However, at micromolar peptide concentrations VIP responses appeared to be maximal, which would be consistent with the findings presented from the current studies, and in addition were approximately 30 % lower than the corresponding PACAP-38 response (at 5 μM). Akin to the SHSY-5Y cells, RCA have been shown to express multiple PAC_1R splice variants, comprising the null, hop1, hop2 variants, as well as the more recently identified PAC_1(3a) variant (Ashur-Fabian *et al.*, 1997; Hashimoto *et al.*, 2003; Pilzer & Gozes, 2006a). It is possible that the combined presence of multiple PAC_1R splice variants, in both of these cell types, may contribute to the differential calcium responses observed. Furthermore, the expression of VPACR in RCA may also contribute to the observed profile of responses. The expression of $VPAC_1R$ in RCA appears to be minimal both from prior studies and the current investigations, in which the selective $VPAC_1R$ agonist, $[Ala^{11,22,28}]VIP$ was without effect in the $[cAMP]_i$ and $[Ca^{2+}]_i$ assays (Ashur-Fabian *et al.*, 1997). However, as expression of the $VPAC_2R$ in RCA has been reported in several studies, we attempted to evaluate the contribution of this receptor to agonist induced responses by examining the effect of PG99-465 (Ashur-Fabian *et al.*, 1997; Grimaldi & Cavallaro, 1999; Moreno *et al.*, 2000). In preliminary studies, a small inhibition of PACAP-27 induced cAMP responses was observed at micromolar PG99-465 concentrations, however the degree of inhibition appeared to be variable. Similarly, in the calcium assay, a small degree

of inhibition was observed with higher PG99-465 concentrations, however the independence of this inhibition from a small agonist effect when tested alone, could not be confirmed in these studies. Due to the limited availability of astrocyte cultures, it was not possible to extensively investigate these responses, however it would be of interest to do so in future studies to try and identify the cause of the intriguing differential responses observed in the calcium assay.

3.2.1.3. RCA agonist responses – $[Ca^{2+}]_i$ assay traces

In the characterisation studies of PAC_1R mediated calcium responses in chapter one (CHO-hPAC_1R and SHSY-5Y cells), it was observed that the fluorescence traces produced by different agonists had distinct shapes with regard to the duration of the agonist induced response. Similarly, agonist stimulated fluorescence responses from RCA were also distinct, with PACAP and maxadilan responses after 90 s being ~ 80 % of the peak signal. This is in contrast to VIP, for which responses were ~ 50 % of the peak signal at this time-point. This profile was very similar to that reported for the SHSY-5Y cell line (at 90 s; Figure 1.2.34, p 133). In addition, the difference between the duration of the PACAP and VIP responses is also consistent with data produced using the CHO-hPAC_1R cell line (at 200 s; Figure 1.2.21, p 115). Unfortunately the availability of astrocyte cultures was limited and as a result it was not possible to extend the comparison of agonist induced calcium responses to 200 s, as was presented for the CHO-hPAC_1R in chapter one, however it would be interesting to compare these responses in future studies. VPAC/PACR stimulated calcium responses have previously been reported in rat cortical neurons and were shown to consist of two phases, an initial calcium release from intracellular stores which subsequently triggered a sustained influx of extracellular calcium across the plasma membrane (Grimaldi & Cavallaro, 1999). With the demonstration of relatively robust VPAC/PACR mediated calcium responses from cortical astrocytes in the present studies, future investigations could determine if such a pattern of calcium release is also observed in these cells. Furthermore, if a similar pattern was observed, the possibility of differential modulation of the extracellular influx by the agonists would be interesting to determine, as described in chapter one for the CHO-PAC_1R cell line. Clearly RCA predominantly express PAC_1R variants and further investigation of the signalling pathways and pharmacology of the individual PAC_1R splice variants in these cells, as

described in this section, may help to delineate the function of VIP/PACAP in these cells.

3.3.1.4. VPAC/PACR mediated cytokine production from RCA

Given the important contribution of VPAC/PACR activation in astrocyte mediated neuroprotective effects, the role of the receptors in stimulating cytokine production from the RCA was explored in preliminary studies. Elevated levels of both IL-1β (VIP and PACAP-27) and TNF-α (PACAP-27) were secreted from the astrocytes in response to VPAC/PACR activation, confirming earlier reports by Brenneman *et al.* (1995, 2003). In agreement with these previous studies, a peak in cytokine secretion was detected with nanomolar concentrations of peptide in the current investigation (Brenneman *et al.*, 2003). Although the pattern of cytokine release presented by Brenneman and colleagues (2003) appeared to be vaguely biphasic, the peaks of cytokine release at picomolar peptide concentrations were considerably more pronounced in the current studies. These differences in cytokine expression may simply reflect the distinct assay procedures used and the condition of astrocyte cultures used in both studies. In parallel studies, the modulation of other cytokines (RANTES, IL-6) was also examined, however no clear responses were produced in these preliminary assays. As the availability of astrocyte cultures was limiting, it was not possible to perform more extensive investigations into the modulation of cytokine release by VPAC/PACR ligands. However in future studies it would be interesting to examine the pharmacology of the IL-1β and TNF-α responses. Optimising the assay procedure through time-course and cell densities studies would perhaps produce clearer results and allow for a full characterisation of the cytokines (and neurotrophic factors) released form RCA upon VPAC/PACR stimulation. Furthermore it would be pertinent to explore the pharmacology of the agonist induced cytokine and neurotrophic factor release using receptor selective ligands such as maxadilan and M65, in an attempt to delineate the contribution of individual VPAC/PACR subtypes as this has not previously been evaluated. In the longer term, it would also have been very interesting to further explore the putative impact of VIP/PACAP and their receptors in TBI, a model in which their neuroprotective role has not been extensively studied. Only a handful of relatively recent studies have been described in which VIP/PACAP and/or their cognate receptors have been studied in models of TBI, as discussed in the introduction (p 210). In addition, some of these studies have produced conflicting data regarding the

involvement of the peptides and receptors in the aftermath of TBI (Skoglosa *et al.*, 1999; Jaworski, 2000). However, the use of different injury models may underlie these conflicting results (stab wound injury versus weight drop technique), especially when it is considered that the stab wound injury induces a much smaller inflammatory response than the weight drop injury. Given the finding that exogenous administration of VIP/PACAP in models of TBI can reduce the extent of neurodegeneration, it would be valuable to further explore the putative protective effects conferred by endogenous VIP and PACAP (Delgado & Ganea, 2003; Farkas *et al.*, 2004). If time had permitted, I had planned to use the lateral fluid percussion model of TBI in rats, to further investigate the expression and possible neuroprotective effects of VIP/PACAP and their receptors following brain trauma.

3.3.1.5. Summary

In summary, these studies have clearly characterised VPAC/PACR pharmacology in rat cortical astrocytes. Robust $[cAMP]_i$ and $[Ca^{2+}]_i$ responses were detected with a range of agonists, the ROP of which indicated a predominant expression of PAC_1R, although the contribution of $VPAC_2R$ mediated responses could not be excluded. The considerable production of intracellular calcium with a range of ligands has not been previously reported in RCA and should be further investigated for its functional significance and possible contribution to VPAC/PACR mediated neuroprotection. The link between second messenger production, the increase in IL-1β, TNF-α and other cytokines, and their roles in neuroprotection remains to be evaluated in future studies.

3.3.2. Pharmacological modulation of $VPAC_2R$ *in vivo*

The mammalian circadian clock is located in the suprachiasmatic nucleus and is essential for the normal expression of circadian rhythms (Weaver, 1998; Hastings *et al.*, 2003). The peptides VIP and PACAP, together with the $VPAC_2$ and PAC_1 receptors have been shown to have important modulatory roles in the normal function of the SCN. The PAC_1R has been shown to be important in mediating phase shifts in response to light stimulation during the dark cycle and is suggested to control the sensitivity of the SCN to light (Hannibal *et al.*, 2001). Importantly, the expression of the $VPAC_2R$ in the SCN has been shown to be critical in the normal expression of circadian activity rhythms and in the re-entrainment of the SCN to novel light/dark cycles. Studies delineating the role of $VPAC_2R$ in circadian rhythm generation have focussed on the characterisation of circadian activity rhythms of transgenic mice and on the *in vitro* electrophysiological properties of SCN cells in brain slices (from wild-type and transgenic mice) treated with VPAC/PACR ligands (Shen *et al.*, 2000; Harmar *et al.*, 2002; Cutler *et al.*, 2003). More recently, real-time imaging of clock gene expression (*Per*) in SCN cells from the $VPAC_2R$ null mice has further elucidated the precise role of this receptor in the circadian cycle (Maywood *et al.*, 2006). However, the *in vivo* pharmacological modulation of the $VPAC_2R$ and corresponding effects on circadian activity patterns has not been reported. With the potential benefits $VPAC_2R$ modulation could have as a therapeutic route with which to treat circadian rhythm disorders, the evaluation of receptor modulating drugs is extremely pertinent. In the studies of $VPAC_2R$ null mice, the activity cycles of the mice were demonstrated to be almost exclusively governed by the timing of the light/dark cycle, with these mice displaying only weakly rhythmic intrinsic circadian cycles (Harmar *et al.*, 2002). The pharmacological blockade of $VPAC_2R$ function *in vivo*, through the use of receptor selective antagonists would be expected to mimic such behaviours. Therefore, we hypothesised that administration of PG99-465, the only reportedly selective $VPAC_2R$ antagonist described to date, may induce a more rapid entrainment to phase advances in the light/dark cycle.

3.3.2.1. Evaluation of PG99-465 administration on re-entrainment

As PG99-465 has not previously been evaluated *in vivo*, the selected route of drug administration was through i.c.v. injection, in order to avoid the potentially

problematic transport of the peptide across the blood-brain–barrier. As the process of injection into the SCN has been shown previously to cause small phase shifts (Piggins *et al.*, 1995), the impact of i.c.v. surgery on activity levels was assessed prior to the drug study. Following the stable entrainment of the mice to a 12 hour light/dark cycle, the effects on activity of simply moving the mice, as well as anaesthesia and i.c.v. surgery were assessed. In the first two dark cycles post treatment, both the 'surgery' group and the 'moved' group displayed considerable reductions in dark cycle activity, indicating that the movement of the mice was as disruptive to their activity patterns as undergoing anaesthesia and surgery. Previous studies have shown that manual drug/vehicle administration can have considerable phase effects on activity and with the combined effects of anaesthesia, a drop in activity following surgery was not unexpected (Hastings *et al.*, 1992). However the impact on activity of moving the mice was surprising, considering the mice were only handled very briefly during the transfer to and from an incubator. The effects of such brief episodes of handling have not previously been reported to disrupt activity cycles. However, similar protocols (10 s period of handling) have been show to produce significantly elevated serum levels of various factors (IL-1β, ACTH, β-endorphin) which may be involved in stress responses (Ottaviani & Franceschi, 1996; Hale *et al.*, 2003). Previous behavioural studies of $VPAC_2R$ transgenic mice, in addition to other circadian cycle studies, have utilised phase shifts of 8 h to evaluate and compare re-entrainment times (Shen *et al.*, 2000; Harmar *et al.*, 2002; Satoh *et al.*, 2006). To facilitate the planned surgical procedures a 6 h phase advance was more desirable, thus the ability of mice to adapt to this magnitude of shift was compared to that of an 8 h shift. The mice stably entrained to the shorter phase shift as readily as the standard 8 h protocol, with the re-entrainment time in both cases being ~ 6 days. The time to re-entrain was consistent with those of the previous $VPAC_2R$ transgenic studies, in which groups of wild-type mice were shown to re-entrain to an 8 h phase advance in ~ 6 days (Shen *et al.*, 2000; Harmar *et al.*, 2002). Although 6 h phase shifts have not been routinely used in circadian biology studies of $VPAC_2R$ transgenic mice, several reports have described the use of this shorter phase advance in the examination of other mouse lines and in drug studies (Moriya *et al.*, 2000; Sollars *et al.*, 2002; Horikawa & Shibata, 2004). In these studies, re-entrainment of C57BL/6J mice appeared to take slightly longer than that observed with the 8 h advance, with average re-entrainment times reported to be ~ 8 days. However differences in experimental protocols and testing methods could account for the small difference between this and our 6 day re-entrainment period.

Subsequent to the demonstration of successful re-entrainment to a 6 h phase advance, the mice were entrained to a 12 h light/dark cycle in preparation for the PG99-465 study. During the light cycle, PG99-465 (1 μM) or vehicle was injected into the lateral ventricles and following a full hour of recovery, the mice were subjected to a 6 h advance in the dark cycle and their activity monitored continuously. In previous studies, $VPAC_2R$ null mice were exposed to unexpected and brief (2 h) periods of darkness during the light cycle (Harmar *et al.*, 2002). During these periods the transgenic mice showed strong bursts of activity in response to these unexpected dark periods, whereas wild-type mice showed minimal responsiveness to the lighting change. As it was hypothesised that PG99-465 antagonism of the $VPAC_2$ receptor *in vivo* might produce a similar effect, the activity of the PG99-465 and vehicle groups in the initial 2 h period of darkness following the phase shift was assessed. The disruptive effect of surgery reported earlier was not expected to interfere with the identification of potential PG99-465 effects as only the amplitude and not the onset of activity was affected following surgery. Indeed, following drug treatment there was a small reduction in total dark cycle activity, however the onset of activity was not altered. These effects were independent of treatment group and were completely consistent with the previously determined effect of surgery upon activity levels. Administration of PG99-465 did not increase responsiveness to the novel light/dark cycle in this study, with no alterations in response time to the phase advance detected when compared to vehicle.

3.3.2.2. Stability of PG99-465 *in vivo*

PG99-465 is an analogue of VIP, in which a fatty acid (myristoyl group) was attached to the amino terminal of the peptide (Moreno *et al.*, 2000). Although fatty acid modification of peptides has been suggested to improve the stability of peptides *in vivo*, including VIP derivates, no data regarding the stability of PG99-465 has been reported (Gozes *et al.*, 1996; Dasgupta *et al.*, 1999). Therefore it is uncertain whether this compound remains active once delivered into the brain. *In vitro*, brief administration (10 min) of PG99-465 alone to SCN slice preparations did not affect overall firing rhythms, however it did attenuate responses induced from exogenous VIP application, in both mouse and rat tissues (Reed *et al.*, 2002; Cutler *et al.*, 2003). Interestingly, Cutler and colleagues (2003) reported that chronic application (7 h) of PG99-465 prevented normal electrical firing rhythms in mouse SCN slices during the light cycle. Furthermore, studies have shown that a single i.v.

bolus injection of PACAP-38 had no protective effects following a forebrain ischemic episode, in contrast to i.c.v. infusion of the peptide (over a period of 7 days) which produced a significant increase in the number of viable hippocampal cells (Somogyvari-Vigh *et al.*, 1998). These studies may imply that prolonged application of PG99-465 may be necessary to observe inhibition of endogenous VIP induced responses through the $VPAC_2R$. In addition, the complex pharmacology of PG99-465 presented in chapter one may also have contributed to the lack of effect seen on re-entrainment rates. $VPAC_1$ receptors are unlikely to be involved in SCN responses to PG99-465, as the expression of these receptors in the SCN is negligible (Shinohara *et al.*, 1999). However, given the expression of PAC_1R in the SCN and the agonist effects reported in chapter one for PG99-465 at this receptor, an interaction with these receptors is plausible (Cagampang *et al.*, 1998a). Although the use of lower peptide concentrations may have reduced potential interactions with PAC_1R, this may also have precluded the detection of $VPAC_2R$ antagonist effects *in vivo*.

3.3.2.2. Future studies using PG99-465 *in vivo*

In future studies the putative effects of PG99-465 on re-entrainment times in response to phase advances could be studied with the use of mini-pumps, allowing a longer term infusion of the peptide. Ideally, such *in vivo* evaluation of receptor function would be performed using non-peptide antagonists, with a greater selectivity for the $VPAC_2R$ than PG99-465. However, given the paucity of such compounds for the $VPAC_2R$ (and $VPAC_1R$ and PAC_1R), the use of PG99-465 is the only pharmacological means to currently inhibit $VPAC_2R$ function.

3.3.3. SCN astrocyte function and circadian rhythms

Although the two areas explored in this final chapter appear quite distinct, there are some intriguing links between VPAC/PACR activity in astrocytes and circadian rhythms. To begin with, the SCN as well as containing neurons also contains a high density of astrocytes, with the astrocyte/neuron ratio estimated to be 1:3 (Morin *et al.*, 1971; Guldner, 1983). The density of astrocytes in the SCN has been suggested to be temporally regulated, however there are some conflicting data regarding this diurnal expression (Gerhold & Wise, 2006; Leone *et al.*, 2006). It has

recently been shown that cortical astrocytes in culture express clock genes, such as *per1* and *per2*, in a rhythmic manner (for up to 7 days) with peak expression around midday (Prolo *et al.*, 2005). In addition, these studies also demonstrated that the expression of *Per* genes in these cells could be phase shifted in response to light cues. These authors suggest a possible role for glia as modulators of neuronal rhythms. Further support for an astroglial role in SCN clock function has been provided from studies in which gap junction blockers have been shown to disrupt SCN function. More specifically, these studies suggested that the application of gap junction blockers to SCN slices may desynchronise the phase relationship between VIP and AVP expression (Shinohara *et al.*, 1995, 2000). Furthermore, it was recently proposed that SCN astrocytes may be involved in the modulation of SCN activity through possible inflammatory/immune based mechanisms involving cytokines such as IL-1β, TNF-α and NF-κB (Leone *et al.*, 2006). These authors also suggested that light mediated glutamate release might activate the transcription factor NF-κB in astrocytes. Further support for the role of cytokines in the SCN comes from studies demonstrating IL-1β and TNF-α involvement in the regulation of sleep cycles (Cearley *et al.*, 2003; Opp, 2006). Although VPAC/PACR expression in cortical astrocytes has been previously investigated, the specific expression of these receptors in astrocytes of the SCN has not been reported to date. Given the VPAC/PACR modulation of cytokines in cortical astrocytes that has been discussed in this chapter and the suggested link between cytokines and SCN function, it may be interesting in future studies to explore the potential links between VPAC/PAC receptors in SCN astrocytes and circadian function.

GENERAL DISCUSSION

4. General discussion

In the past 20 – 30 years, since the isolation of the endogenous peptides VIP, PACAP-27 and PACAP-38, a wealth of knowledge has been generated with respect to the distribution of these peptides in the body, the receptors which they activate and the plethora of physiological functions that they are involved in regulating. Both the peptides and their established cognate receptors ($VPAC_1$, $VPAC_2$ and PAC_1) have been shown to be widely distributed throughout the body, with specific localisations reported in a multitude of cell types, tissues and organs. This widespread distribution correlates with the many functional roles that have been reported for these peptides and receptors. In recent years, much of the research effort in this field has focused on roles for these peptides and receptors in the modulation of circadian cycles, neuroprotection, glucose homeostasis and immunomodulation.

Many of the physiological effects of VIP and PACAP are known to be mediated through cAMP, produced via coupling of the VPAC/PAC receptors to $G\alpha_s$. In addition, several reports have also documented the modulation of intracellular calcium levels upon receptor activation as well as the stimulation of PLD activity. However, the link between each receptor and the different pathways appears to depend on the cell/tissue being studied, with the receptor expression level, G-protein complement and species of receptor potentially contributing to the differences reported. In order to attempt to clearly delineate the physiological functions mediated by individual VPAC/PAC receptors, it is crucial to understand their pharmacology and the intracellular signalling cascades which they activate. However, for the VPAC/PAC receptor family although the general characteristics are established, it is sometimes difficult to gain a clear and consistent description of their pharmacology/signalling characteristics from reports in the literature, perhaps as a consequence of the inevitable variation which exists in the assay platforms and expression systems utilised between different research groups. The relatively small size of the VPAC/PACR family, makes the full characterisation and comparison of the receptors in functional assays a manageable task, even more so considering the relatively small pool of peptide ligands with which they are normally evaluated. However, reports of systematic comparisons between multiple signalling pathways for VPAC/PAC receptors are limited, often examining only a very small number of ligands which reduces the pharmacological value of some of these studies. Therefore, in this thesis, I performed a thorough and systematic pharmacological characterisation of all three human VPAC/PAC receptor subtypes using two standardised, whole-cell based, HT-amenable, non-radioactive functional assays to

measure intracellular cAMP and calcium. To provide a full pharmacological evaluation of human VPAC/PACR pharmacology, a number of peptide ligands were utilised in addition to VIP and PACAP. From the limited number of putatively receptor selective ligands reported in the literature, an agonist and antagonist for each receptor were examined ($VPAC_1$: [$Ala^{11,22,28}$]VIP (Nicole *et al.*, 2000), PG97-269 (Gourlet *et al.*, 1997a); $VPAC_2$: R3P65 (Yung *et al.*, 2003), PG99-465 (Moreno *et al.*, 2000); PAC_1: maxadilan (Lerner *et al.*, 1991), M65 (Uchida *et al.*, 1998)). Using receptor expressing stable cell lines, the agonist ROP was demonstrated to be consistent between assays, although an approximately 100 fold reduction in agonist potency was observed in the calcium assay. This shift to lower agonist potency in stimulating calcium was confirmed using the SHSY-5Y cell line which endogenously expresses PAC_1, and is also in agreement with a range of more limited studies (Pisegna & Wank, 1993; Delporte *et al.*, 1995; McCulloch *et al.*, 2000; Langer *et al.*, 2001). Such consistent observations between all three human receptor subtypes with an extensive range of ligands have not previously been described in a single study. Furthermore, a number of new findings arose from these studies, including the observation of full agonism for [$Ala^{11,22,28}$]VIP at the PAC_1R and the lack of selectivity of R3P65 for the $VPAC_2R$. In addition, the reportedly selective $VPAC_2R$ antagonist PG99-465 was demonstrated to have a complicated pharmacological profile, with agonist effects at all three VPAC/PACR when tested alone in the $[cAMP]_i$ assay. Being the only $VPAC_2R$ antagonist described to date, PG99-465 has been used in several *in vitro* investigations of $VPAC_2R$ function, however the findings presented here suggest that the results from such studies could potentially be complicated by cross receptor activity. Further examination of VPAC/PACR pharmacology in SHSY-5Y cells and rat cortical astrocytes revealed differential peak calcium responses for the agonists tested, with the identification of a PACAP response that was sensitive to M65 (a PAC_1R antagonist), but insensitive to maxadilan (a PAC_1R agonist). This is the first report of such a response and its occurrence was hypothesised to result from the presence of multiple PAC_1R splice variants. Further examination of the receptors mediating these responses could potentially help to identify the functional properties of PAC_1R splice variants. A large proportion of the findings from the current studies have been recently published in two peer reviewed manuscripts and it is hoped that this will prove useful for other researchers in the field and facilitate further investigation into VPAC/PACR pharmacology and function (Dickson *et al.*, 2006a; Dickson *et al.*, 2006b). In addition these studies also highlight the lack of selective ligands, particularly non-peptides which are currently available for this receptor family and emphasize that the

opportunity still exists to identify and develop novel, non-peptide ligands. These studies also re-iterate the importance of evaluating novel VPAC/PACR ligands in multiple functional assays in order to fully understand their downstream signalling characteristics.

In an attempt to identify novel, non-peptide ligands for VPAC/PACR, an HT-screening study of part of the Astellas Pharma Inc. (formerly the Fujisawa Pharmaceutical Company) compound library was performed. The screening studies were designed to identify potential non-peptide $VPAC_2R$ antagonists, as it was hypothesised that such compounds may be of therapeutic value in treating circadian rhythm disorders, based on studies using transgenic mouse lines (Shen *et al.*, 2000; Harmar *et al.*, 2002). Following the establishment and optimisation of the calcium assay for HT-screening, a total of 100,000 compounds were examined for $VPAC_2R$ antagonist activity. A number of potential $VPAC_2R$ ligands were identified from these studies and were fully examined in further potency and selectivity studies. The compounds identified, although non-peptides, were less potent and selective than the only currently available peptide antagonist, PG99-465 (Moreno *et al.*, 2000). Due to a lack of success in hit compound identification/development, the group B GPCR family, which includes the VPAC/PAC receptors, has been deemed to be a difficult target in the drug discovery process (Hoare, 2005). As further knowledge is published examining ligand-receptor interactions for the VPAC/PACR family, it may help identify the molecular characteristics that non-peptide antagonists are likely to harbour and so facilitating the optimisation of future screening studies and the selection of compounds to be screened. Indeed, the possibility that screening studies to date have simply not tested the most appropriate type of chemical structures remains a possibility (Macarron, 2006). Astellas Pharma Inc. maintain a general interest in the VPAC/PAC receptor family, in addition to other neuropeptide receptors and with the recent formation of the company following a merger, the expanded compound libraries may provide future opportunities to identify novel ligands for the individual receptor subtypes.

As discussed throughout this thesis, VPAC/PAC receptors are associated with numerous interesting physiological roles and in the final section of the current studies, I have explored two of the aspects that the receptors are involved with in the CNS. The two areas investigated were VPAC/PACR induced astrocyte-mediated neuroprotection and VPAC/PACR control of circadian rhythm expression. Both areas have been the focus of a considerable amount of research in recent years, perhaps underlying the requirement for developing novel therapeutics in associated disease states. VIP and PACAP have been known for some time to stimulate the

release of a number of cytokines and neurotrophic factors from cortical astrocytes, with the secretion of such molecules shown to confer a degree of neuroprotection to compromised neurons in a variety of experimental models (Brenneman & Eiden, 1986; Brenneman *et al.*, 1998; Dejda *et al.*, 2005). However, the individual VPAC/PACR subtypes responsible for mediating the release of these factors remain to be fully clarified. In addition, the signalling pathways downstream of VPAC/PACR activation which contribute to such neuroprotective responses have not been well described. As a consequence, I initially characterised the pharmacology of VPAC/PACR in primary cultures of rat cortical astrocytes, using the cAMP and calcium assays described previously. The agonist ROPs obtained for the astrocytes were consistent between assays and had a predominantly PAC_1R mediated profile, which is in agreement with limited published studies (Hashimoto *et al.*, 1993; Ashur-Fabian *et al.*, 1997). The full characterisation of VPAC/PACR stimulated calcium responses in rat cortical astrocytes has not been previously described and the robust coupling of the receptors to this pathway highlights the potential contribution calcium signalling could make in the secretion of neuroprotective factors. To try to correlate the stimulation of the cAMP and calcium pathways with cytokine secretion, the VPAC/PACR mediated secretion of several cytokines from rat cortical astrocytes was examined. Biphasic secretion of IL-1β and TNF-α was observed upon VIP and PACAP simulation, with peak responses detected using picomolar and nanomolar peptide concentrations. Future studies further examining the pharmacology of cytokine secretion with receptor selective ligands would be useful in order to delineate the precise receptor subtypes and transduction pathways involved in VPAC/PACR induced neuroprotection through astrocytes.

The important role of $VPAC_2R$ in the control and maintenance of circadian activity cycles was also explored. Recent studies from Harmar and colleagues using receptor transgenic mice have highlighted crucial roles for the $VPAC_2R$ in the expression of circadian cycles (Shen *et al.*, 2000; Harmar *et al.*, 2002). These studies suggested that the modulation of this receptor with pharmacological agents may be a novel way to therapeutically treat circadian rhythm disorders. Therefore, the $VPAC_2R$ antagonist PG99-465 was evaluated *in vivo* and its effects on the timing of activity cycles determined. Following the establishment of a new system of cages and running wheels, mice were stably entrained to a light/dark cycle and the effects of movement and surgery on activity levels were determined, prior to drug administration studies. Interestingly, it was found that simply moving the animals from their home cages to an incubator was as disruptive to their activity cycles as exposure to anaesthesia and surgery. This finding has implications for all studies of

this nature and emphasises that the degree of disruption from surgical procedures should be fully evaluated prior to any drug treatments. Following i.c.v. injection of PG99-465 and a 6 h phase advance in the light/dark cycle, no alteration in re-entrainment rates were observed when compared to the saline treated group. PG99-465 may have been ineffective in this study for a number of reasons. To my knowledge, this was the first report of the use of PG99-465 *in vivo*, and unfortunately no information is available regarding the *in vivo* stability or duration of action of this peptide. Therefore breakdown of the peptide or an inability of the compound to reach the target area (the SCN) may have also contributed to the ineffectiveness observed in these studies. Furthermore, the complex pharmacology of this peptide highlighted in this thesis may have compromised the detection of a $VPAC_2R$ antagonist effect. Future studies examining the chronic administration of this peptide may prove beneficial in further validating the role of $VPAC_2R$ in the control of circadian rhythms.

Although in some respects, the field of VIP/PACAP and VPAC/PAC receptor biology is relatively small, the research which has been undertaken to date and the impact of the published results are considerable and widespread, having relevance to many physiological functions. As research continues in this area, the actions of these peptides and their cognate receptors will become clearer and provide insights into the significance of VIP/PACAP action in normal physiology and the potential roles for VPAC/PACR in the treatment or prevention of disease. Finally, clear opportunities still exist to develop non-peptide selective ligands, whose identification will be pivotal to understanding the roles that these peptides and receptors play and will ultimately determine whether they have therapeutic value in the clinic.

APPENDICES

5. Appendices

5.1. Appendix I: This appendix contains actograms from section 3.2.2.2 in chapter three (p 242), showing the activity profiles of the 16 mice used in the study, with the timing of the imposed 12 h dark cycle (1900 to 0700 h) represented by the grey box. In these and all other actograms presented, each horizontal line represents a 24 h period with subsequent days continuing directly underneath. Treatments were administered on 'day 7' of the figures shown. Actogram sets A, B and C correspond to the mice from the 'moved' (A1 – A6), 'surgery' (B1 - B6) and 'not moved' (C1 – C4) groups respectively.

5.2. Appendix II: Actograms in this appendix are from 16 mice (D1 – D16), whose activity patterns were monitored in response to an 8 h phase advance in the light/dark cycle (section 3.2.2.3., chapter three; p 244). Following a period of entrainment (lights off: 1900 – 0700 h) the mice were subjected to the phase advance (lights off: 1100 – 2300 h), indicated by the changing position of the grey box (lights off period) on 'day 6' of the actograms.

5.3. Appendix III: In this appendix, the actograms presented are from 16 mice (E1 – 16) that were exposed to a 6 h phase advance in the light/dark cycle (section 3.2.2.3., chapter three; p 244). Initially the mice were entrained to a 12 h light/dark cycle (lights off: 1900 to 0700 h). On 'day 9' of the actograms the 12 h lights off period was advanced, beginning at 1300 h, as shown by the position of the grey box.

5.4. Appendix IV: Actograms from the PG99-465 (F1 – F8) and saline (G1 - G8) treated mice are shown, with dark cycles represented by the grey box. Mice were entrained to a light/dark cycle (lights off: 2000 to 0800 h), followed by surgery and drug administration on either 'day 6' or 'day 8' of the actograms. The mice were treated in two separate groups due to time restraints of the surgical procedures. Surgery was performed during the light cycle, in the few hours prior to the onset of a novel dark phase resulting from a 6 h phase advance (lights off: 1300 – 0100 h).

5.5. Appendix V: List of abbreviations.

5.1. Appendix I

Actograms from section 3.2.2.2. for the 'moved' group (A1 - A6).

A1

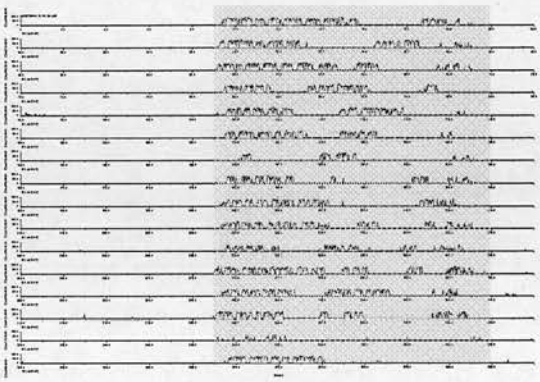

A4

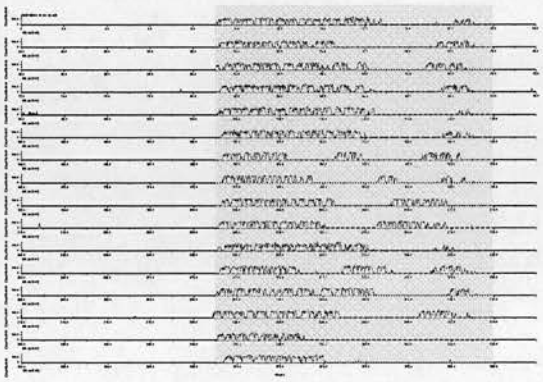

A2

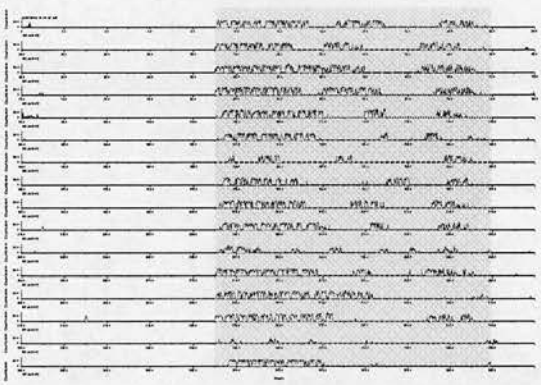

A5

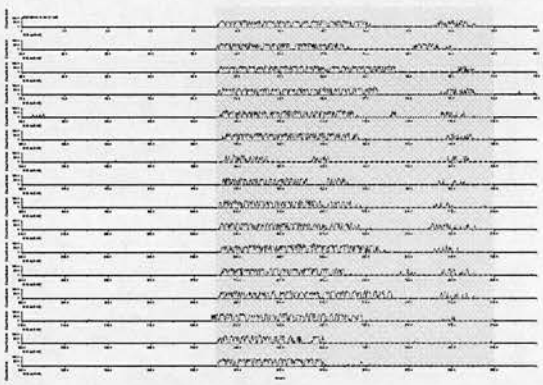

A3

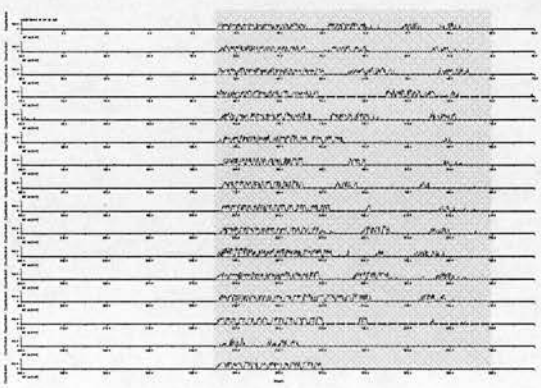

A6

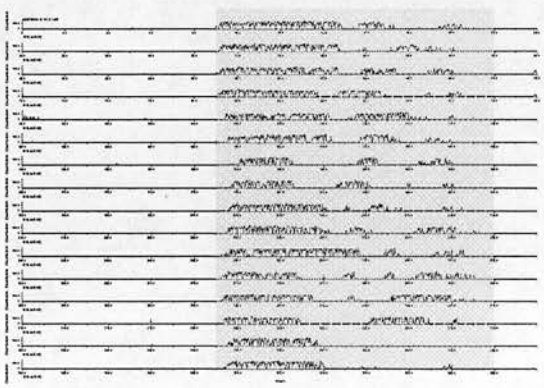

5.1. Appendix I

Actograms from section 3.2.2.2. for the 'surgery' group (B1 - B6).

B1

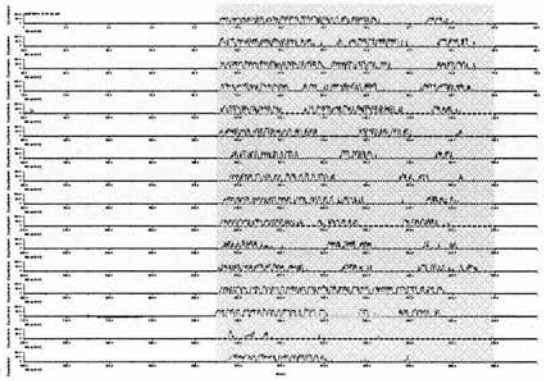

B4

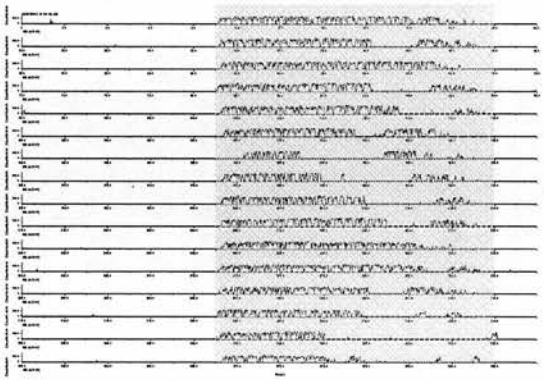

B2

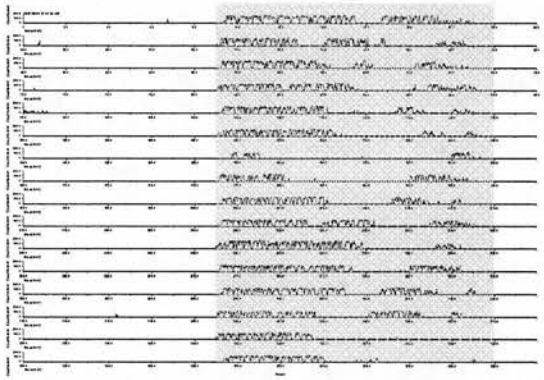

B5

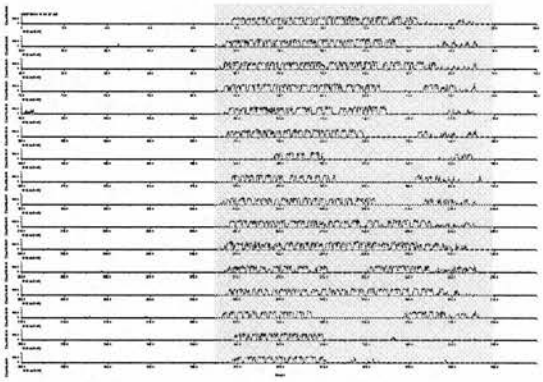

B3

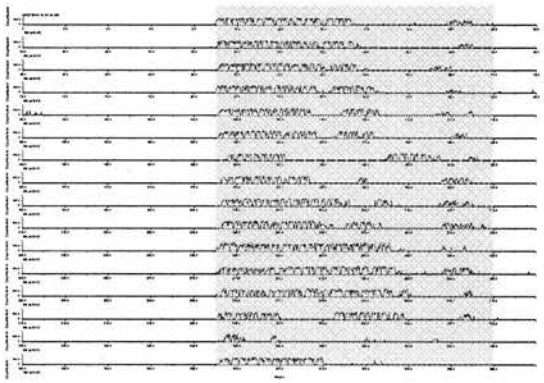

B6

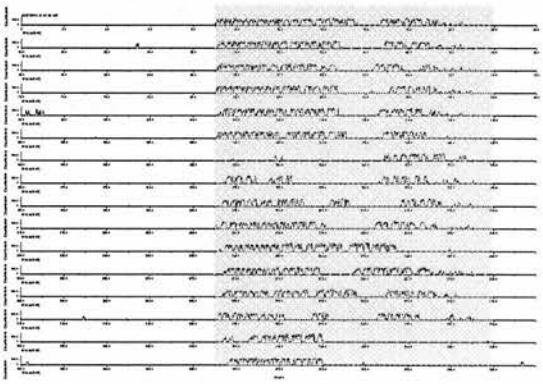

5.1. Appendix I

Actograms from section 3.2.2.2. for the 'not moved' group (C1 – C4).

C1

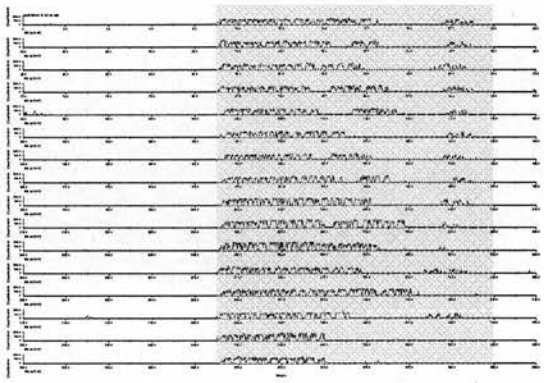

C3

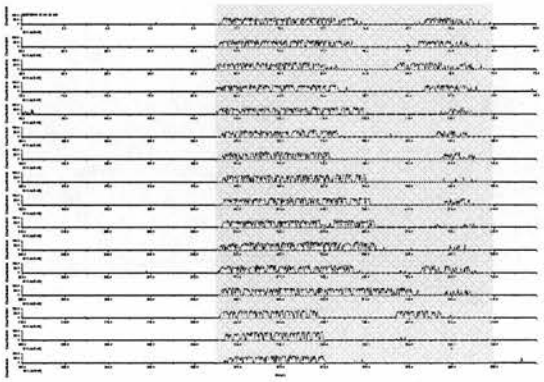

C2

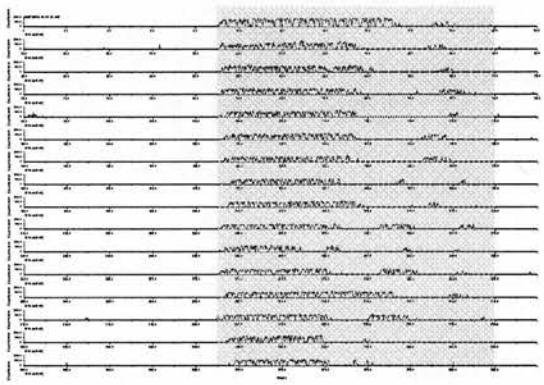

C4

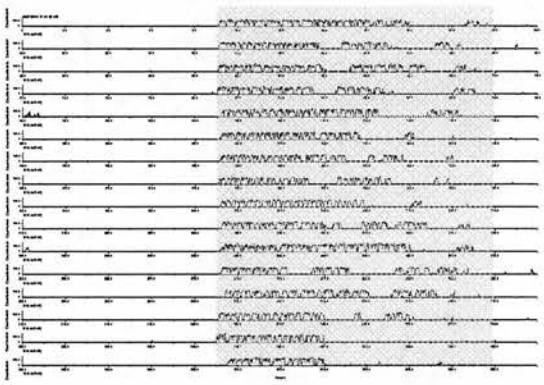

5.2. Appendix II

Actograms from section 3.2.2.3. for the 8 h phase advance (D1 – D8).

D1

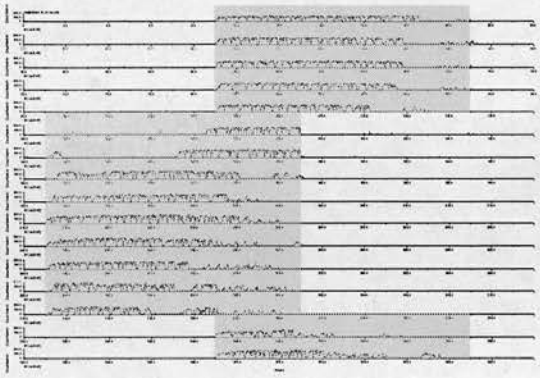

D5

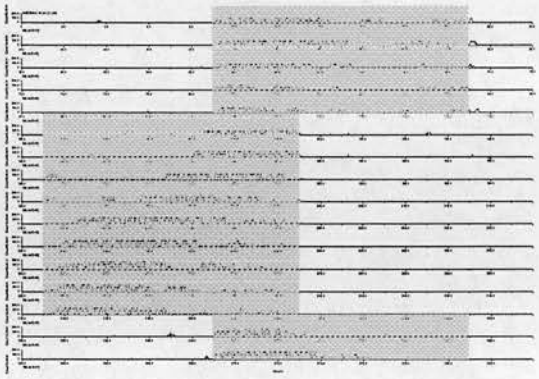

D2

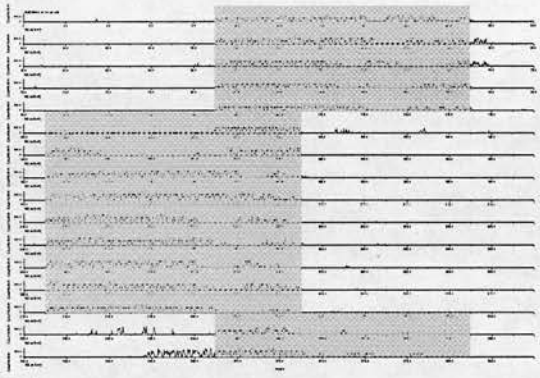

D6

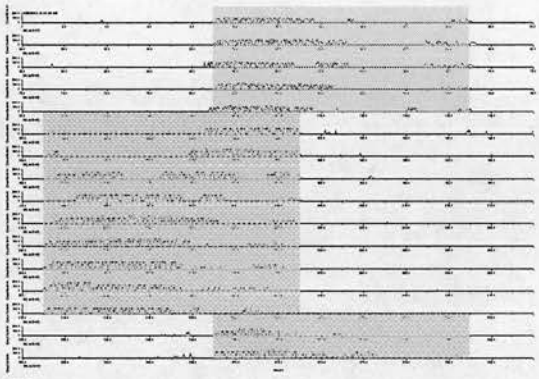

D3

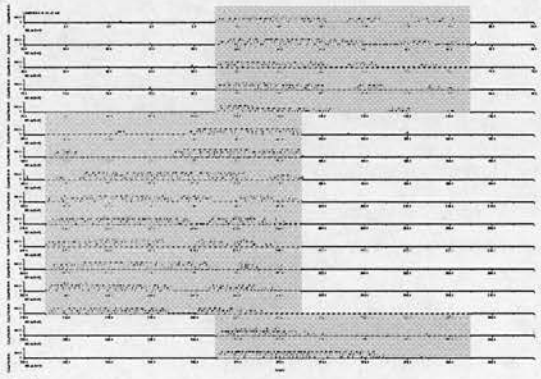

D7

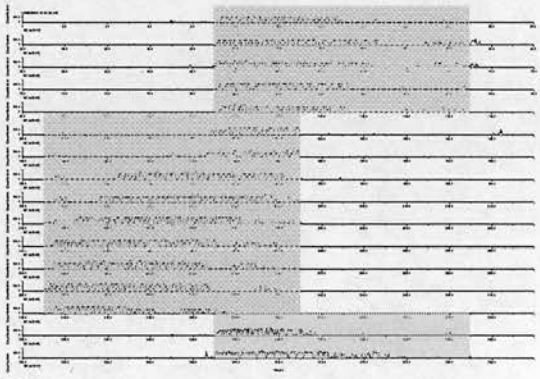

D4

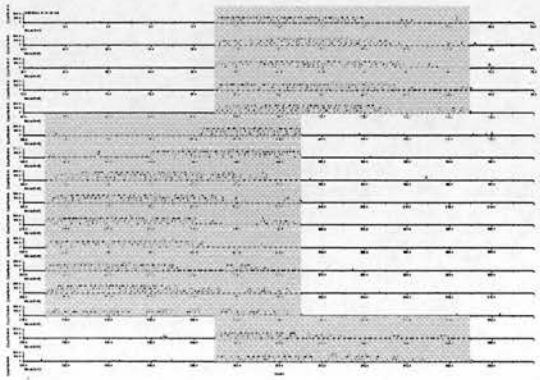

D8

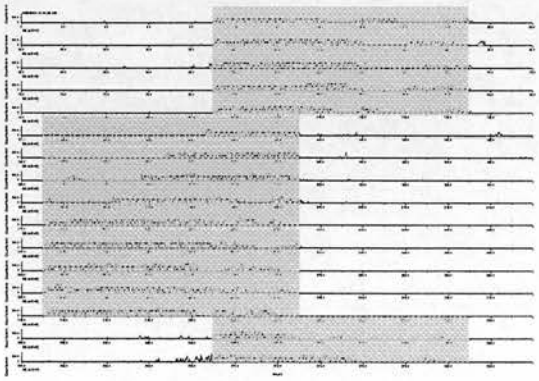

5.2. Appendix II

Actograms from section 3.2.2.3. for the 8 h phase advance (D9 - D16).

D9

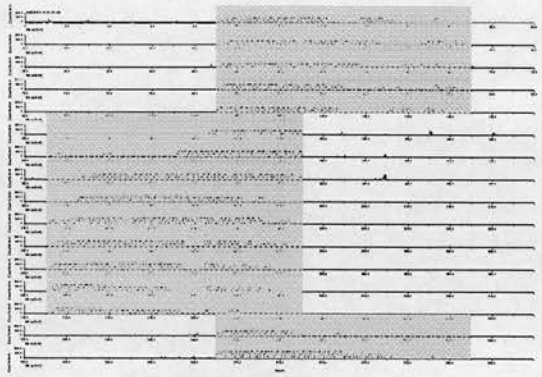

D13

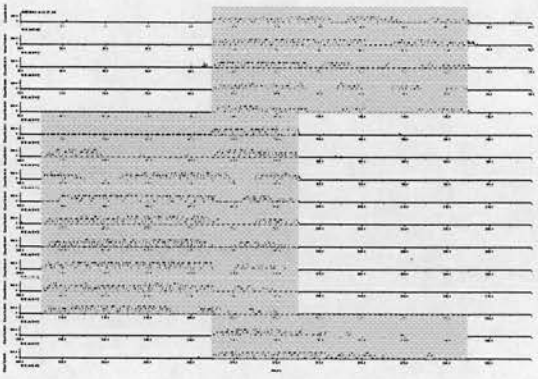

D10

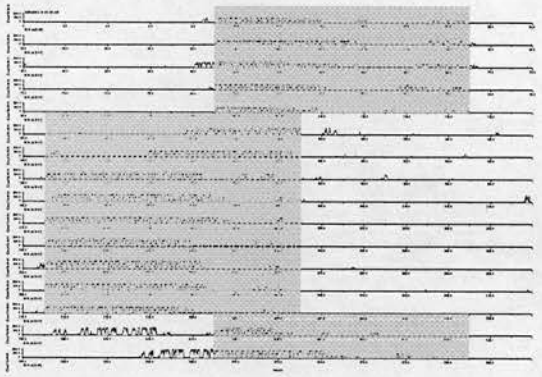

D14

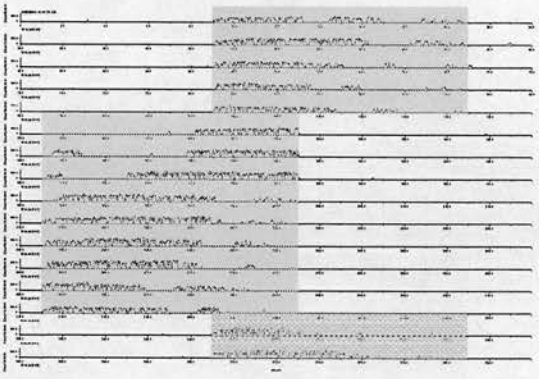

D11

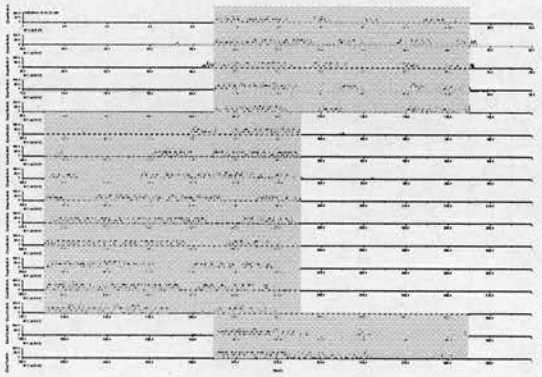

D15

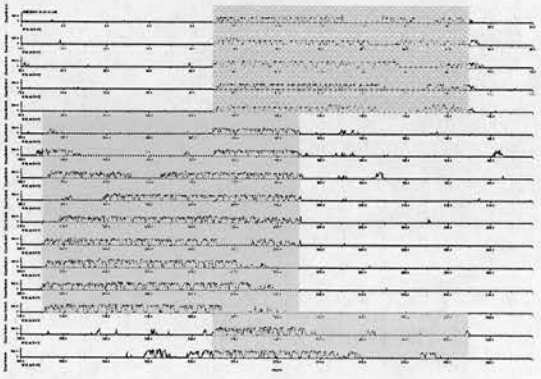

D12

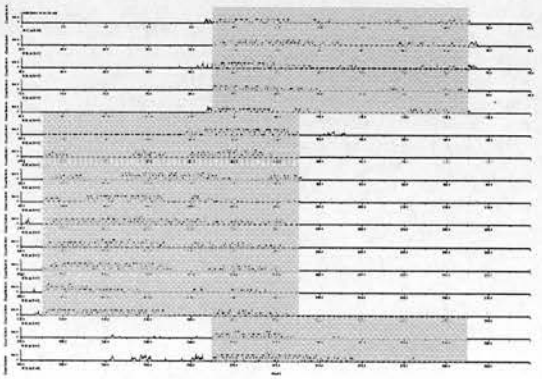

D16

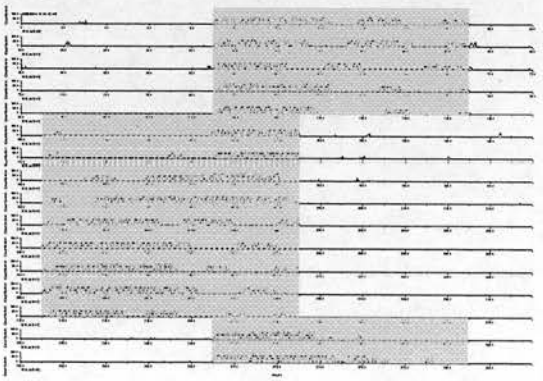

5.3. Appendix III

Actograms from section 3.2.2.3. for the 6 h phase advance (E1 – E8).

E1

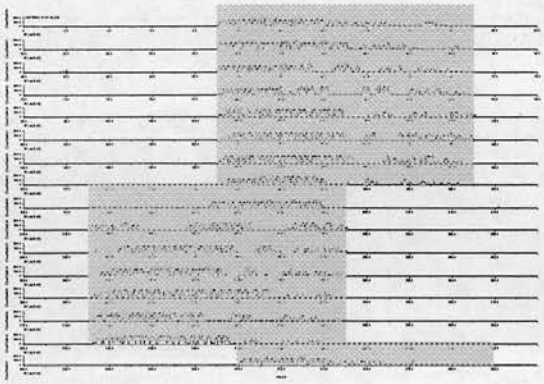

E5

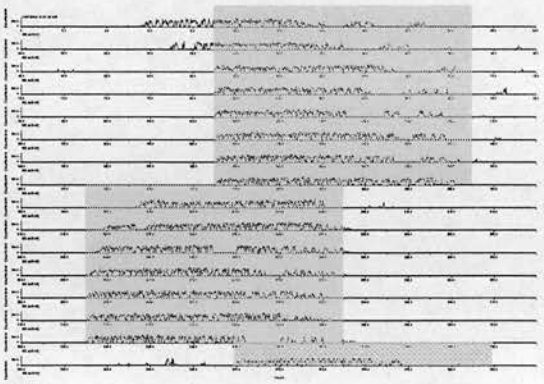

E2

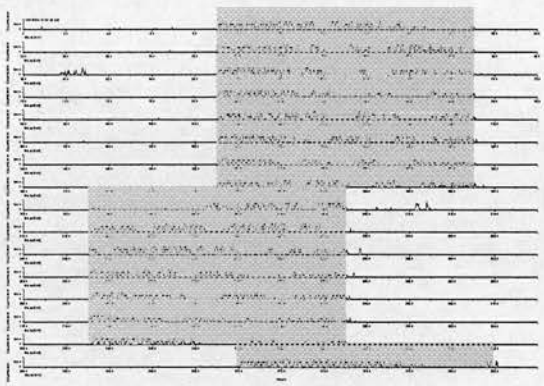

E6

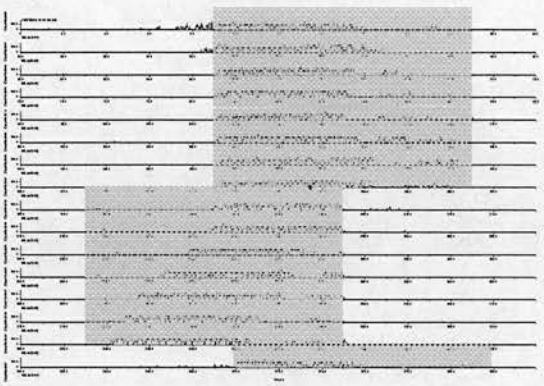

E3

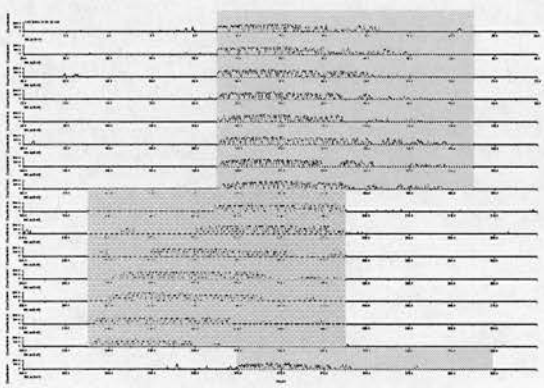

E7

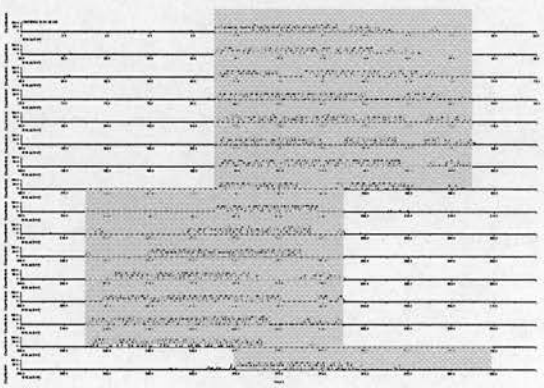

E3

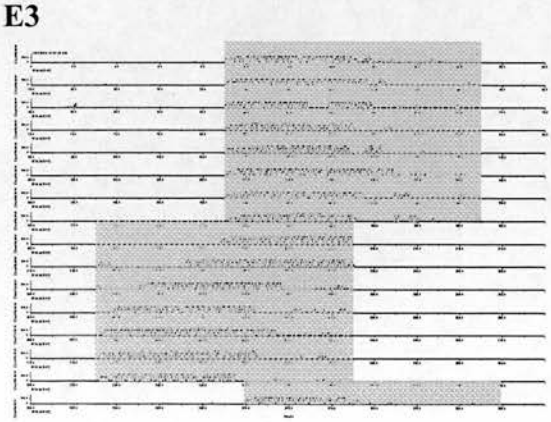

E8

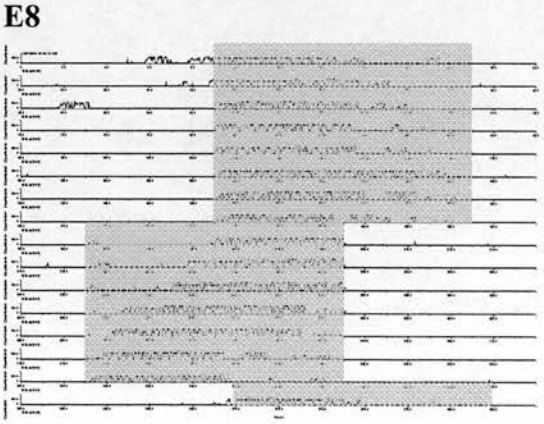

5.3. Appendix III

Actograms from section 3.2.2.3. for the 6 h phase advance (E9 – E16).

E9

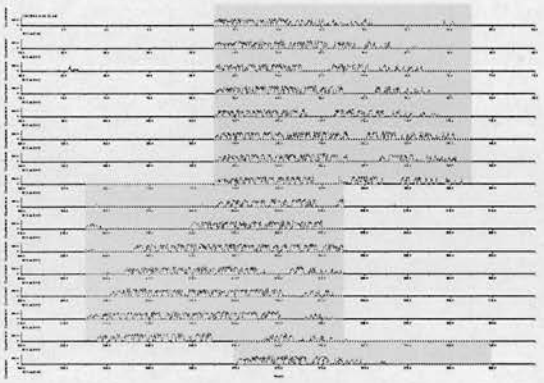

E13

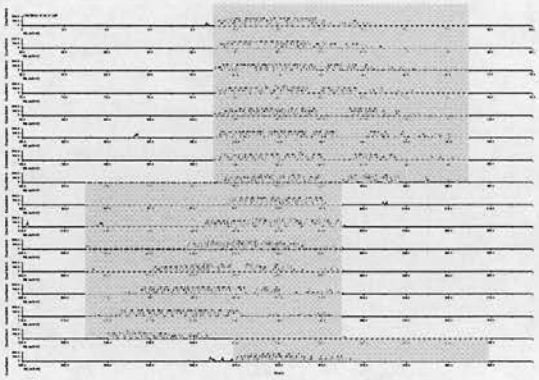

E10

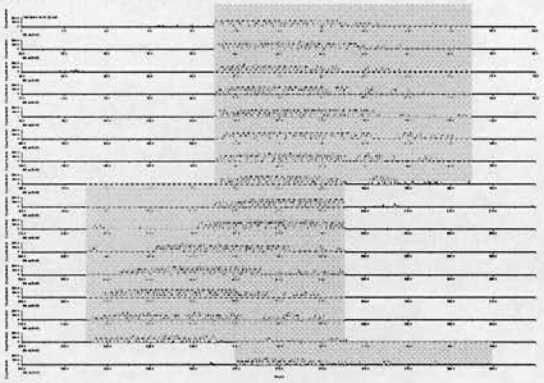

E14

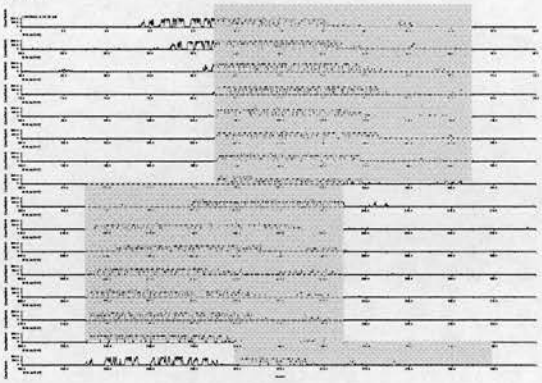

E11

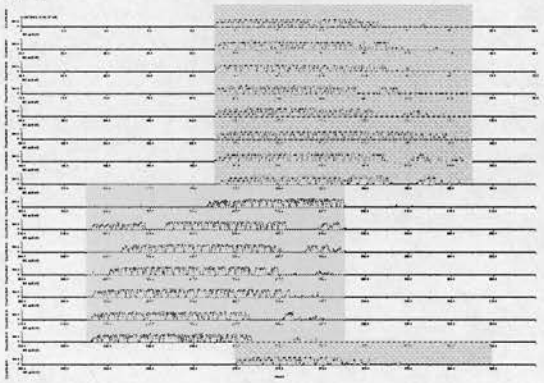

E15

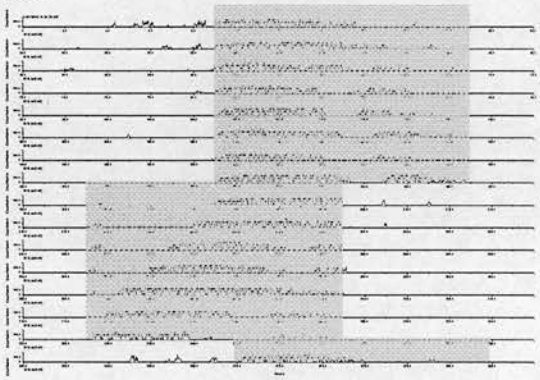

E12

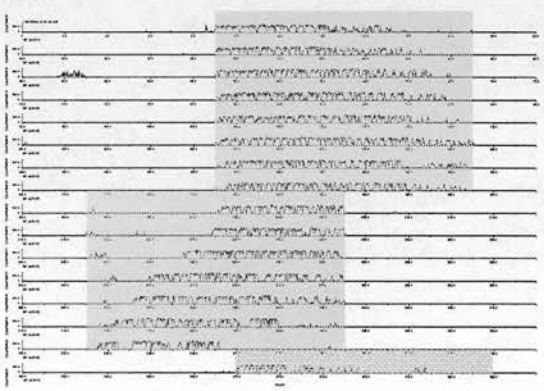

E16

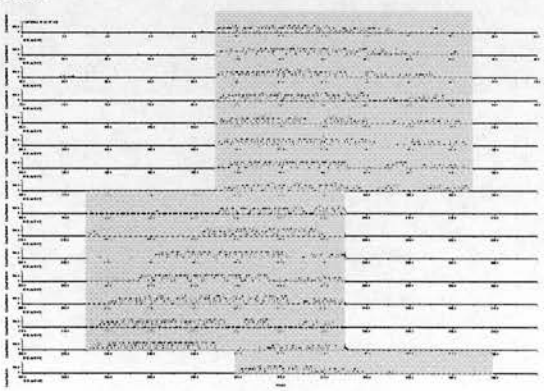

5.4. Appendix IV

Actograms from section 3.2.2.4. for the PG99-465 treated group (F1 - F8).

F1

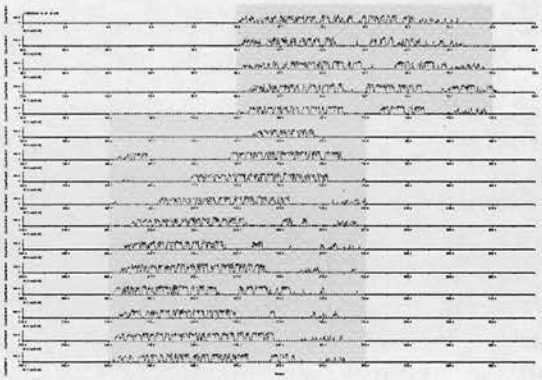

F5

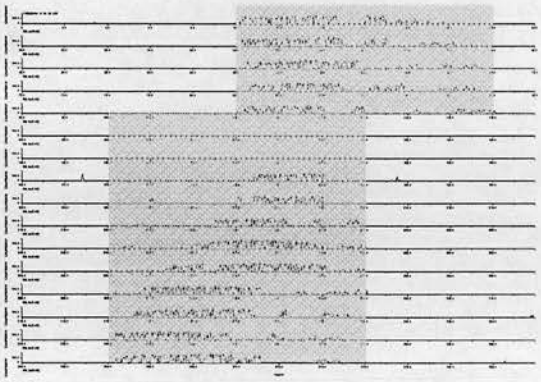

F2

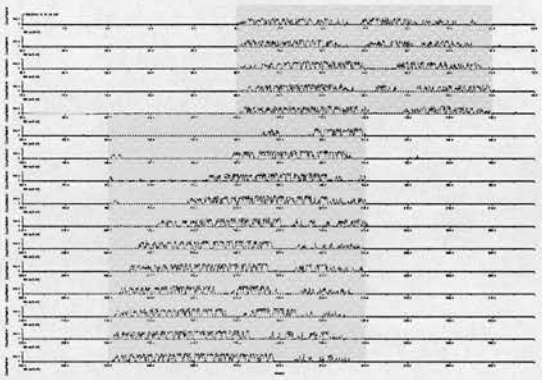

F6

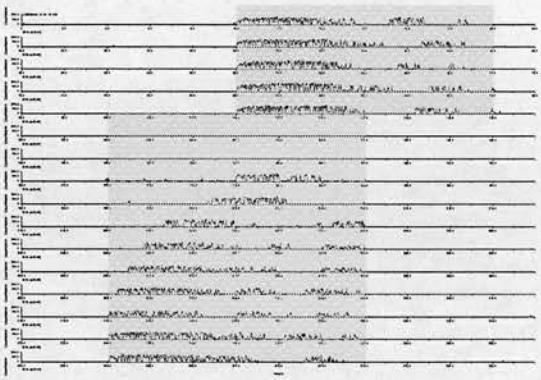

F3

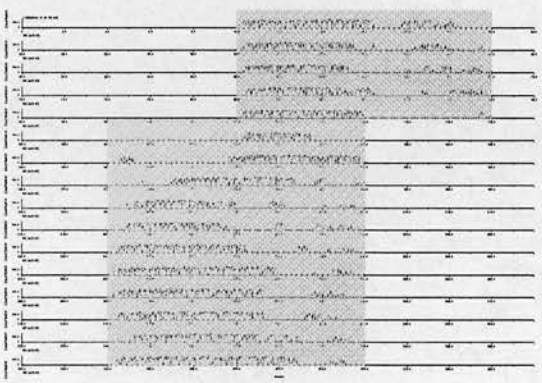

F7

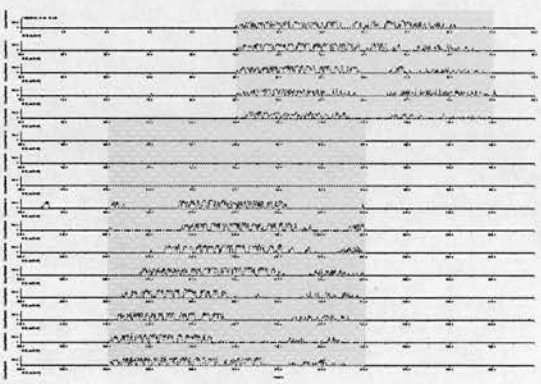

F4

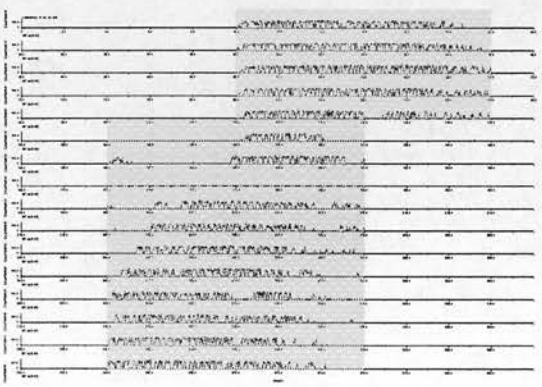

F8

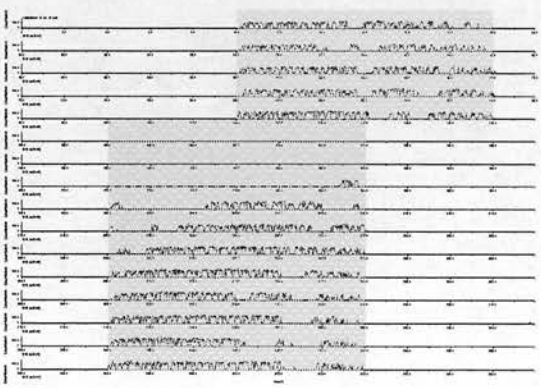

5.4. Appendix IV

Actograms from section 3.2.2.4. for the saline treated group (G1 - G8).

G1

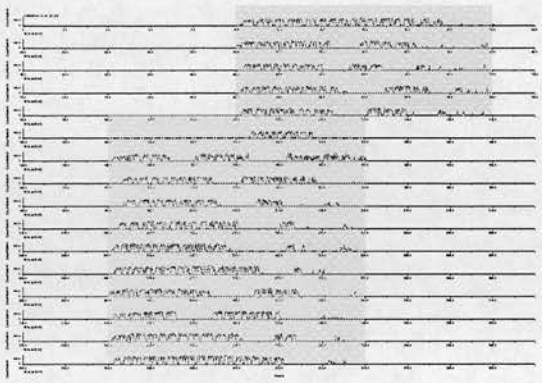

G5

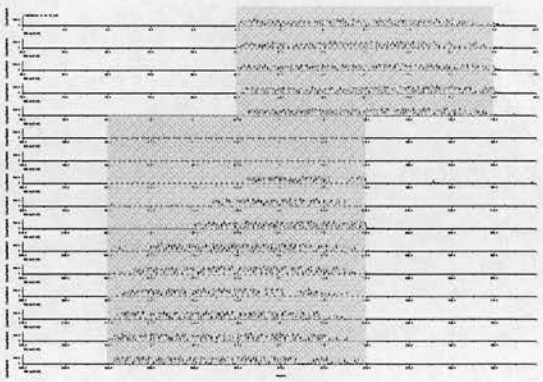

G2

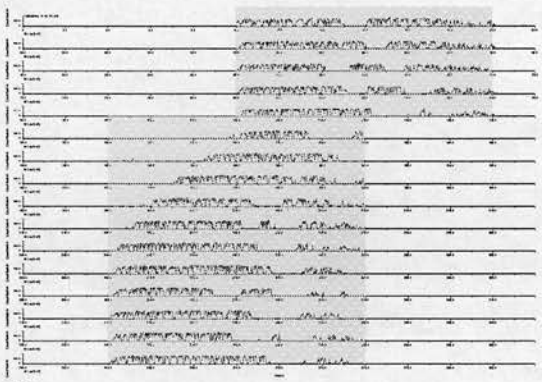

G6

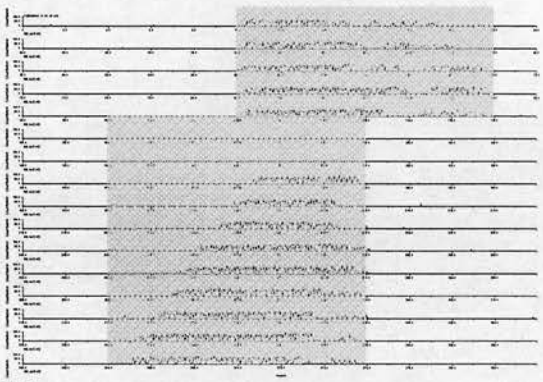

G3

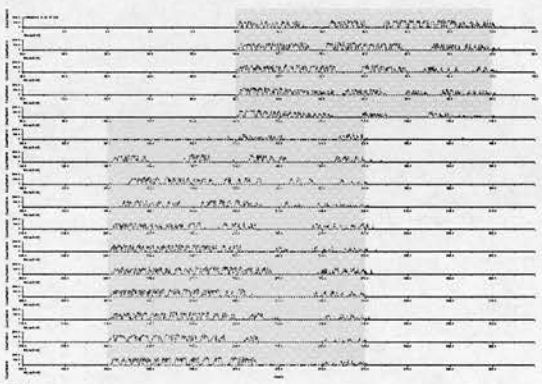

G7

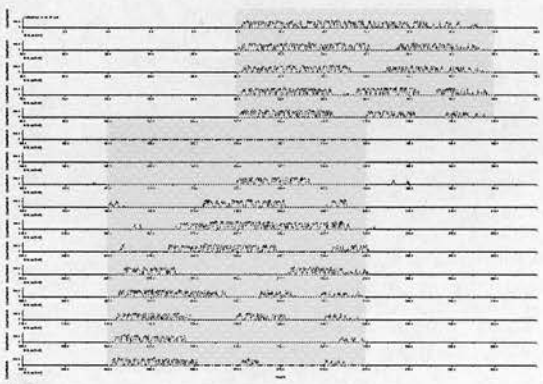

G4

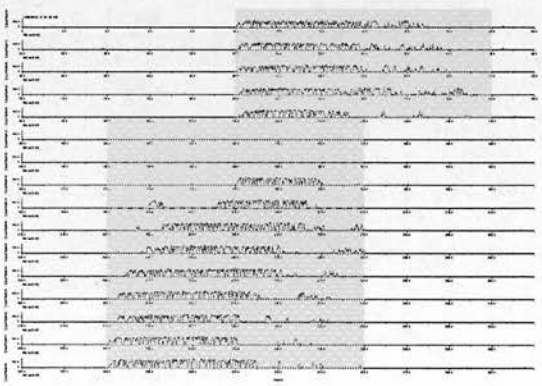

G8

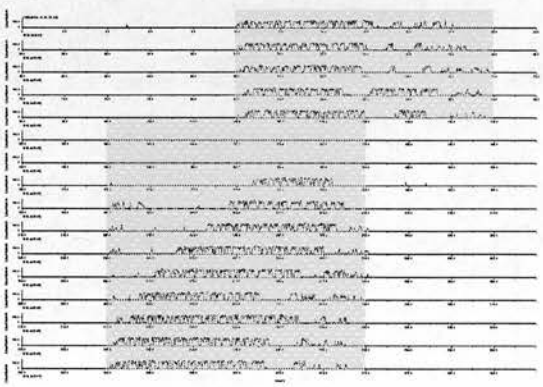

5.5. Appendix V

List of Abbreviations:

AC	adenylate cyclase
ADNF	activity dependent neurotrophic factor
ADNP	activity dependent neurotrophic protein
ADP	adenosine diphosphate
ARF	ADP-ribosylation factor
AUC	area under the curve
BSA	bovine serum albumin
Ca^{2+}	calcium
cAMP	cyclic adenosine monophosphate
cGMP	cyclic guanosine monophosphate
CGRP	calcitonin gene related peptide
CHO	Chinese hamster ovary
CNS	central nervous system
CRE	cAMP response element
CSF	cerebrospinal fluid
CT	circadian time
DMEM	Dulbecco's modified minimal essential medium
DMSO	dimethyl sulfoxide
DNA	deoxyribonucleic acid
EC	extracellular
EDTA	ethylenediaminetetraacetic acid
EGF	epidermal growth factor
ELISA	enzyme-linked immunoabsorbent assay
FAC	final assay concentration
FBS	fetal bovine serum
FLIPR	fluorometric imaging plate reader
HBSS	Hanks' balanced salt solution
G-CSF	granulocyte-colony-stimulating factor
GDP	guanine diphosphate
GFAP	glial fibrillary acidic protein
GHRH	growth hormone-releasing hormone
GHT	geniculo-hypothalamic tract
GPCR	G-protein coupled receptor

GTP	guanine triphosphate
h	human
HEK	human embryonic kidney
HIV	human immunodeficiency virus
HT	high throughput
IBMX	3-isobutyl-1-methylxanthine
IC	intracellular
i.c.v.	intracerebroventricular
IL	interleukin
IP	inositol phosphate
ISB	inorganic salts buffer
IUPHAR	International Union of Pharmacology
i.v.	intravenous
KO	knock-out
KRBG	Krebs-Ringer bicarbonate buffer with glucose
LB	Luria Bertani
LPS	lipopolysaccharide
LTP	long term potentiation
MAPK	mitogen activated protein kinase
M-CSF	macrophage-colony-stimulating factor
MD	Molecular Devices
MEM	minimal essential medium
MIP	macrophage inflammatory protein
NCE	new chemical entity
NMR	nuclear magnetic resonance
OE	over-expressing
OD	optical density
ORF	open reading frame
PACAP	pituitary adenylate cyclase activating polypeptide
PBS	phosphate buffered saline
PCR	polymerase chain reaction
PHI	peptide histidine-isoleucine
PHM	peptide histidine-methionine
PHV	peptide histidine-valine
PKC	protein kinase C
PLC	phospholipase C
PLD	phospholipase D

pMCAO	permanent middle cerebral artery occlusion
PNS	peripheral nervous system
PRP	PACAP-related peptide
r	rat
RAMP	receptor activity-modifying protein
RANTES	regulated upon activation, normal T-cell expressed and secreted factor
RBL	rat basophilic leukaemia
RCA	rat cortical astrocytes
RGC	retinal ganglion cells
RHT	retino-hypothalamic tract
RME	Basal medium Eagle
ROP	rank order of potency
RT	room temperature
SCG	superior cervical ganglion
SCN	suprachiasmatic nucleus
SDS	sodium dodecyl sulfate
TAE	Tris-acetate-EDTA buffer
TBI	traumatic brain injury
TM	transmembrane
TNF	tumour necrosis factor
Tris-HCl	Tris hydrochloride
TTX	tetrodotoxin
VIP	vasoactive intestinal peptide
WT	wild type
ZT	zeitgeiber time

REFERENCES

6. References

Abad, C., Martinez, C., Leceta, J., Juarranz, M. G., Delgado, M., & Gomariz, R. P. (2002). Pituitary adenylate-cyclase-activating polypeptide expression in the immune system. *Neuroimmunomodulation* **10**, 177-186.

Adler, E. M. & Fink, J. S. (1993). Calcium regulation of vasoactive intestinal polypeptide mRNA abundance in SH-SY5Y human neuroblastoma cells. *J. Neurochem.* **61**, 727-737.

Aiyar, N., Disa, J., Stadel, J. M., & Lysko, P. G. (1999). Calcitonin gene-related peptide receptor independently stimulates 3',5'-cyclic adenosine monophosphate and Ca^{2+} signaling pathways. *Mol.Cell Biochem.* **197**, 179-185.

Ajpru, S., McArthur, A. J., Piggins, H. D., & Sugden, D. (2002). Identification of PAC1 receptor isoform mRNAs by real-time PCR in rat suprachiasmatic nucleus. *Brain Res. Mol. Brain Res.* **105**, 29-37.

Akesson, L., Ahren, B., Edgren, G., & Degerman, E. (2005). VPAC2-R mediates the lipolytic effects of pituitary adenylate cyclase-activating polypeptide/vasoactive intestinal polypeptide in primary rat adipocytes. *Endocrinology* **146**, 744-750.

Albers, H. E., Liou, S. Y., Stopa, E. G., & Zoeller, R. T. (1991). Interaction of colocalized neuropeptides: functional significance in the circadian timing system. *J. Neurosci.* **11**, 846-851.

Albrecht, U. & Eichele, G. (2003). The mammalian circadian clock. *Curr. Opin. Genet. Dev.* **13**, 271-277.

Alm, P., Alumets, J., Hakanson, R., Owman, O., Sjoberg, N. O., Sundler, F., & Walles, B. (1980). Origin and distribution of VIP (vasoactive intestinal polypeptide)-nerves in the genito-urinary tract. *Cell Tissue Res.* **205**, 337-347.

Amiranoff, B., Vauclin-Jacques, N., Boige, N., Rouyer-Fessard, C., & Laburthe, M. (1983). Interaction of Gila monster venom with VIP receptors in intestinal epithelium of human. A comparison with rat. *FEBS Lett.* **164**, 299-302.

Anisman, H., Turrin, N. P., Merali, Z., & Hayley, S. (2003). Neurochemical sensitization associated with systemic administration of tumor necrosis factor-alpha: adjuvant action in combination with bovine serum albumin. *J. Neuroimmunol.* **145**, 91-102.

Aramori, I. & Nakanishi, S. (1992). Coupling of two endothelin receptor subtypes to differing signal transduction in transfected Chinese hamster ovary cells. *J. Biol. Chem.* **267**, 12468-12474.

Aramori, I., Zenkoh, J., Morikawa, N., O'Donnell, N., Asano, M., Nakamura, K., Iwami, M., Kojo, H., & Notsu, Y. (1997). Novel subtype-selective nonpeptide

bradykinin receptor antagonists FR167344 and FR173657. *Mol. Pharmacol.* **51**, 171-176.

Arendt, J. (1998). Melatonin and the pineal gland: influence on mammalian seasonal and circadian physiology. *Rev. Reprod.* **3**, 13-22.

Arimura, A. (1998). Perspectives on pituitary adenylate cyclase activating polypeptide (PACAP) in the neuroendocrine, endocrine, and nervous systems. *Jpn. J. Physiol.* **48**, 301-331.

Arimura, A., Somogyvari-Vigh, A., Miyata, A., Mizuno, K., Coy, D. H., & Kitada, C. (1991). Tissue distribution of PACAP as determined by RIA: highly abundant in the rat brain and testes. *Endocrinology* **129**, 2787-2789.

Ashur-Fabian, O., Giladi, E., Brenneman, D. E., & Gozes, I. (1997). Identification of VIP/PACAP receptors on rat astrocytes using antisense oligodeoxynucleotides. *J. Mol. Neurosci.* **9**, 211-222.

Ashur-Fabian, O., Giladi, E., Furman, S., Steingart, R. A., Wollman, Y., Fridkin, M., Brenneman, D. E., & Gozes, I. (2001). Vasoactive intestinal peptide and related molecules induce nitrite accumulation in the extracellular milieu of rat cerebral cortical cultures. *Neurosci. Lett.* **307**, 167-170.

Asnicar, M. A., Koster, A., Heiman, M. L., Tinsley, F., Smith, D. P., Galbreath, E., Fox, N., Ma, Y. L., Blum, W. F., & Hsiung, H. M. (2002). Vasoactive intestinal polypeptide/pituitary adenylate cyclase-activating peptide receptor 2 deficiency in mice results in growth retardation and increased basal metabolic rate. *Endocrinology* **143**, 3994-4006.

Audigier, S., Barberis, C., & Jard, S. (1986). Vasoactive intestinal polypeptide increases inositol phospholipid breakdown in the rat superior cervical ganglion. *Brain Res.* **376**, 363-367.

Ban, Y., Shigeyoshi, Y., & Okamura, H. (1997). Development of vasoactive intestinal peptide mRNA rhythm in the rat suprachiasmatic nucleus. *J. Neurosci.* **17**, 3920-3931.

Barbezat, G. O. & Grossman, M. I. (1971). Intestinal secretion: stimulation by peptides. *Science* **174**, 422-424.

Barnes, M. R., Duckworth, D. M., & Beeley, L. J. (1998). Frizzled proteins constitute a novel family of G protein-coupled receptors, most closely related to the secretin family. *Trends Pharmacol. Sci.* **19**, 399-400.

Barnhart, D. C., Sarosi, G. A., Jr., & Mulholland, M. W. (1997). PACAP-38 causes phospholipase C-dependent calcium signaling in rat acinar cell line. *Surgery* **122**, 465-474.

Bassan, M., Zamostiano, R., Davidson, A., Pinhasov, A., Giladi, E., Perl, O., Bassan, H., Blat, C., Gibney, G., Glazner, G., Brenneman, D. E., & Gozes, I. (1999). Complete sequence of a novel protein containing a femtomolar-activity-dependent neuroprotective peptide. *J. Neurochem.* **72**, 1283-1293.

Bayliss, W. M. & Starling, E. H. (1902). The mechanism of pancreatic secretion. *J. Physiol.* **28**, 325-353.

Beed, E. A., O'Dorisio, M. S., O'Dorisio, T. M., & Gaginella, T. S. (1983). Demonstration of a functional receptor for vasoactive intestinal polypeptide on Molt 4b T lymphoblasts. *Regul. Pept.* **6**, 1-12.

Beni-Adani, L., Gozes, I., Cohen, Y., Assaf, Y., Steingart, R. A., Brenneman, D. E., Eizenberg, O., Trembolver, V., & Shohami, E. (2001). A peptide derived from activity-dependent neuroprotective protein (ADNP) ameliorates injury response in closed head injury in mice. *J. Pharmacol. Exp. Ther.* **296**, 57-63.

Besson, J., Dussaillant, M., Marie, J. C., Rostene, W., & Rosselin, G. (1984). *In vitro* autoradiographic localization of vasoactive intestinal peptide (VIP) binding sites in the rat central nervous system. *Peptides* **5**, 339-340.

Besson, J., Rotsztejn, W., Laburthe, M., Epelbaum, J., Beaudet, A., Kordon, C., & Rosselin, G. (1979). Vasoactive intestinal peptide (VIP): brain distribution, subcellular localization and effect of deafferentation of the hypothalamus in male rats. *Brain Res.* **165**, 79-85.

Blank, M. A., Brown, J. R., Hunter, J. C., Bloom, S. R., & Tyers, M. B. (1986). Effects of VIP and related peptides and Gila monster venom on genitourinary smooth muscle. *Eur. J. Pharmacol.* **132**, 155-161.

Bloom, S. R., Polak, J. M., & Pearse, A. G. (1973). Vasoactive intestinal peptide and watery-diarrhoea syndrome. *Lancet* **2**, 14-16.

Bodner, M., Fridkin, M., & Gozes, I. (1985). Coding sequences for vasoactive intestinal peptide and PHM-27 peptide are located on two adjacent exons in the human genome. *Proc. Natl. Acad. Sci. U.S.A.* **82**, 3548-3551.

Bokaei, P. B., Ma, X. Z., Byczynski, B., Keller, J., Sakac, D., Fahim, S., & Branch, D. R. (2006). Identification and characterization of five-transmembrane isoforms of human vasoactive intestinal peptide and pituitary adenylate cyclase-activating polypeptide receptors. *Genomics* **88,** 791-800.

Bolin, D. R., Michalewsky, J., Wasserman, M. A., & O'Donnell, M. (1995). Design and development of a vasoactive intestinal peptide analog as a novel therapeutic for bronchial asthma. *Biopolymers* **37**, 57-66.

Braas, K. M. & May, V. (1999). Pituitary adenylate cyclase-activating polypeptides directly stimulate sympathetic neuron neuropeptide Y release through PAC(1)

receptor isoform activation of specific intracellular signaling pathways. *J. Biol. Chem.* **274**, 27702-27710.

Brenneman, D. E. & Eiden, L. E. (1986). Vasoactive intestinal peptide and electrical activity influence neuronal survival. *Proc. Natl. Acad. Sci. U.S.A.* **83**, 1159-1162.

Brenneman, D. E. & Gozes, I. (1996). A femtomolar-acting neuroprotective peptide. *J. Clin. Invest.* **97**, 2299-2307.

Brenneman, D. E., Hauser, J., Neale, E., Rubinraut, S., Fridkin, M., Davidson, A., & Gozes, I. (1998). Activity-dependent neurotrophic factor: structure-activity relationships of femtomolar-acting peptides. *J. Pharmacol. Exp. Ther.* **285**, 619-627.

Brenneman, D. E., Hauser, J., Spong, C. Y., Phillips, T. M., Pert, C. B., & Ruff, M. (1999). VIP and D-ala-peptide T-amide release chemokines which prevent HIV-1 GP120-induced neuronal death. *Brain Res.* **838**, 27-36.

Brenneman, D. E., Hauser, J. M., Spong, C., & Phillips, T. M. (2002). Chemokine release is associated with the protective action of PACAP-38 against HIV envelope protein neurotoxicity. *Neuropeptides* **36**, 271-280.

Brenneman, D. E., Hill, J. M., Glazner, G. W., Gozes, I., & Phillips, T. W. (1995). Interleukin-1 alpha and vasoactive intestinal peptide: enigmatic regulation of neuronal survival. *Int. J. Dev. Neurosci.* **13**, 187-200.

Brenneman, D. E., Neale, E. A., Foster, G. A., d'Autremont, S. W., & Westbrook, G. L. (1987). Nonneuronal cells mediate neurotrophic action of vasoactive intestinal peptide. *J. Cell Biol.* **104**, 1603-1610.

Brenneman, D. E., Phillips, T. M., Hauser, J., Hill, J. M., Spong, C. Y., & Gozes, I. (2003). Complex array of cytokines released by vasoactive intestinal peptide. *Neuropeptides* **37**, 111-119.

Broyart, J. P., Dupont, C., Laburthe, M., & Rosselin, G. (1981). Characterization of vasoactive intestinal peptide receptors in human colonic epithelial cells. *J. Clin. Endocrinol. Metab.* **52**, 715-721.

Bryant, M. G., Polak, M. M., Modlin, I., Bloom, S. R., Albuquerque, R. H., & Pearse, A. G. (1976). Possible dual role for vasoactive intestinal peptide as gastrointestinal hormone and neurotransmitter substance. *Lancet* **1**, 991-993.

Bunnett, N. W., Reeve, J. R., Jr., Dimaline, R., Shively, J. E., Hawke, D., & Walsh, J. H. (1984). The isolation and sequence analysis of vasoactive intestinal peptide from a ganglioneuroblastoma. *J. Clin. Endocrinol. Metab.* **59**, 1133-1137.

Buscail, L., Gourlet, P., Cauvin, A., De Neef, P., Gossen, D., Arimura, A., Miyata, A., Coy, D. H., Robberecht, P., & Christophe, J. (1990). Presence of highly selective

receptors for PACAP (pituitary adenylate cyclase activating peptide) in membranes from the rat pancreatic acinar cell line AR 4-2J. *FEBS Lett.* **262**, 77-81.

Busto, R., Prieto, J. C., Bodega, G., Zapatero, J., Fogue, L., & Carrero, I. (2003). VIP and PACAP receptors coupled to adenylyl cyclase in human lung cancer: a study in biopsy specimens. *Peptides* **24**, 429-436.

Cagampang, F. R., Piggins, H. D., Sheward, W. J., Harmar, A. J., & Coen, C. W. (1998a). Circadian changes in PACAP type 1 (PAC1) receptor mRNA in the rat suprachiasmatic and supraoptic nuclei. *Brain Res.* **813**, 218-222.

Cagampang, F. R., Sheward, W. J., Harmar, A. J., Piggins, H. D., & Coen, C. W. (1998b). Circadian changes in the expression of vasoactive intestinal peptide 2 receptor mRNA in the rat suprachiasmatic nuclei. *Brain Res. Mol. Brain Res.* **54**, 108-112.

Cai, Y., Xin, X., Yamada, T., Muramatsu, Y., Szpirer, C., & Matsumoto, K. (1995). Assignments of the genes for rat pituitary adenylate cyclase activating polypeptide (Adcyap1) and its receptor subtypes (Adcyap1r1, Adcyap1r2, and Adcyap1r3). *Cytogenet. Cell Genet.* **71**, 193-196.

Canny, B. J., Rawlings, S. R., & Leong, D. A. (1992). Pituitary adenylate cyclase-activating polypeptide specifically increases cytosolic calcium ion concentration in rat gonadotropes and somatotropes. *Endocrinology* **130**, 211-215.

Card, J. P., Brecha, N., Karten, H. J., & Moore, R. Y. (1981). Immunocytochemical localization of vasoactive intestinal polypeptide-containing cells and processes in the suprachiasmatic nucleus of the rat: light and electron microscopic analysis. *J. Neurosci.* **1**, 1289-1303.

Carlquist, M., Mutt, V., & Jornvall, H. (1979). Isolation and characterization of bovine vasoactive intestinal peptide (VIP). *FEBS Lett.* **108**, 457-460.

Carmena, M. J. & Prieto, J. C. (1985). VIP binding to epithelial cell membranes of rat ventral prostate: effect of guanine nucleotides. *Gen. Pharmacol.* **16**, 495-500.

Carstairs, J. R. & Barnes, P. J. (1986). Visualization of vasoactive intestinal peptide receptors in human and guinea pig lung. *J. Pharmacol. Exp. Ther.* **239**, 249-255.

Cauvin, A., Buscail, L., Gourlet, P., De Neef, P., Gossen, D., Arimura, A., Miyata, A., Coy, D. H., Robberecht, P., & Christophe, J. (1990a). The novel VIP-like hypothalamic polypeptide PACAP interacts with high affinity receptors in the human neuroblastoma cell line NB-OK. *Peptides* **11**, 773-777.

Cauvin, A., Vandermeers-Piret, M. C., Vandermeers, A., Coussaert, E., De Neef, P., Robberecht, P., & Christophe, J. (1990b). Rat PHI, PHI-GLY and PHV (1-42) stimulate adenylate cyclase in six rat tissue and cell membranes. *Peptides* **11**, 1009-1014.

Cearley, C., Churchill, L., & Krueger, J. M. (2003). Time of day differences in IL1beta and TNFalpha mRNA levels in specific regions of the rat brain. *Neurosci. Lett.* **352**, 61-63.

Chartrel, N., Tonon, M. C., Vaudry, H., & Conlon, J. M. (1991). Primary structure of frog pituitary adenylate cyclase-activating polypeptide (PACAP) and effects of ovine PACAP on frog pituitary. *Endocrinology* **129**, 3367-3371.

Chatterjee, T. K., Sharma, R. V., & Fisher, R. A. (1996). Molecular cloning of a novel variant of the pituitary adenylate cyclase-activating polypeptide (PACAP) receptor that stimulates calcium influx by activation of L-type calcium channels. *J. Biol. Chem.* **271**, 32226-32232.

Chedeville, A., Mirossay, L., Chastre, E., Hurbain-Kosmath, I., Lopez, M., & Gespach, C. (1993). Interaction of VIP, PACAP and related peptides in normal and leukemic human monocytes and macrophages. *FEBS Lett.* **319**, 171-176.

Chen, D., Buchanan, G. F., Ding, J. M., Hannibal, J., & Gillette, M. U. (1999). Pituitary adenylyl cyclase-activating peptide: a pivotal modulator of glutamatergic regulation of the suprachiasmatic circadian clock. *Proc. Natl. Acad. Sci. U.S.A.* **96**, 13468-13473.

Christophe, J. P., Conlon, T. P., & Gardner, J. D. (1976). Interaction of porcine vasoactive intestinal peptide with dispersed pancreatic acinar cells from the guinea pig. Binding of radioiodinated peptide. *J. Biol. Chem.* **251**, 4629-4634.

Christopoulos, A., Christopoulos, G., Morfis, M., Udawela, M., Laburthe, M., Couvineau, A., Kuwasako, K., Tilakaratne, N., & Sexton, P. M. (2003). Novel receptor partners and function of receptor activity-modifying proteins. *J. Biol. Chem.* **278**, 3293-3297.

Ciccarelli, E., Svoboda, M., De Neef, P., Di Paolo, E., Bollen, A., Dubeaux, C., Vilardaga, J. P., Waelbroeck, M., & Robberecht, P. (1995). Pharmacological properties of two recombinant splice variants of the PACAP type I receptor, transfected and stably expressed in CHO cells. *Eur. J. Pharmacol.* **288**, 259-267.

Ciccarelli, E., Vilardaga, J. P., De Neef, P., Di Paolo, E., Waelbroeck, M., Bollen, A., & Robberecht, P. (1994). Properties of the VIP-PACAP type II receptor stably expressed in CHO cells. *Regul. Pept.* **54**, 397-407.

Clore, G. M., Martin, S. R., & Gronenborn, A. M. (1986). Solution structure of human growth hormone releasing factor. Combined use of circular dichroism and nuclear magnetic resonance spectroscopy. *J. Mol. Biol.* **191**, 553-561.

Colwell, C. S., Michel, S., Itri, J., Rodriguez, W., Tam, J., Lelievre, V., Hu, Z., Liu, X., & Waschek, J. A. (2003). Disrupted circadian rhythms in VIP- and PHI-deficient mice. *Am. J. Physiol. Regul. Integr. Comp. Physiol.* **285**, R939-R949.

Colwell, C. S., Michel, S., Itri, J., Rodriguez, W., Tam, J., Lelievre, V., Hu, Z., & Waschek, J. A. (2004). Selective deficits in the circadian light response in mice lacking PACAP. *Am. J. Physiol. Regul. Integr. Comp. Physiol.* **287**, R1194-R1201.

Couvineau, A., Amiranoff, B., & Laburthe, M. (1986). Solubilization of the liver vasoactive intestinal peptide receptor. Hydrodynamic characterization and evidence for an association with a functional GTP regulatory protein. *J. Biol. Chem.* **261**, 14482-14489.

Cutler, D. J., Haraura, M., Reed, H. E., Shen, S., Sheward, W. J., Morrison, C. F., Marston, H. M., Harmar, A. J., & Piggins, H. D. (2003). The mouse VPAC2 receptor confers suprachiasmatic nuclei cellular rhythmicity and responsiveness to vasoactive intestinal polypeptide in vitro. *Eur. J. Neurosci.* **17**, 197-204.

Daniel, P. B., Kieffer, T. J., Leech, C. A., & Habener, J. F. (2001). Novel alternatively spliced exon in the extracellular ligand-binding domain of the pituitary adenylate cyclase-activating polypeptide (PACAP) type 1 receptor (PAC1R) selectively increases ligand affinity and alters signal transduction coupling during spermatogenesis. *J. Biol. Chem.* **276**, 12938-12944.

Dasgupta, P., Singh, A. T., & Mukherjee, R. (1999). Lipophilization of somatostatin analog RC-160 improves its bioactivity and stability. *Pharm. Res.* **16**, 1047-1053.

Dautzenberg, F. M., Mevenkamp, G., Wille, S., & Hauger, R. L. (1999). N-terminal splice variants of the type I PACAP receptor: isolation, characterization and ligand binding/selectivity determinants. *J. Neuroendocrinol.* **11**, 941-949.

Dehaven, W. I. & Cuevas, J. (2004). VPAC receptor modulation of neuroexcitability in intracardiac neurons: dependence on intracellular calcium mobilization and synergistic enhancement by PAC1 receptor activation. *J. Biol. Chem.* **279**, 40609-40621.

Dejda, A., Jozwiak-Bebenista, M., & Nowak, J. Z. (2006). PACAP, VIP, and PHI: effects on AC-, PLC-, and PLD-driven signaling systems in the primary glial cell cultures. *Ann. N.Y. Acad. Sci.* **1070**, 220-225.

Dejda, A., Sokolowska, P., & Nowak, J. Z. (2005). Neuroprotective potential of three neuropeptides PACAP, VIP and PHI. *Pharmacol. Rep.* **57**, 307-320.

Delgado, M., Abad, C., Martinez, C., Juarranz, M. G., Leceta, J., Ganea, D., & Gomariz, R. P. (2003a). PACAP in immunity and inflammation. *Ann. N.Y. Acad. Sci.* **992**, 141-157.

Delgado, M. & Ganea, D. (2003a). Neuroprotective effect of vasoactive intestinal peptide (VIP) in a mouse model of Parkinson's disease by blocking microglial activation. *FASEB J.* **17**, 944-946.

Delgado, M. & Ganea, D. (2003b). Vasoactive intestinal peptide prevents activated microglia-induced neurodegeneration under inflammatory conditions: potential therapeutic role in brain trauma. *FASEB J.* **17**, 1922-1924.

Delgado, M., Jonakait, G. M., & Ganea, D. (2002). Vasoactive intestinal peptide and pituitary adenylate cyclase-activating polypeptide inhibit chemokine production in activated microglia. *Glia* **39**, 148-161.

Delgado, M., Leceta, J., & Ganea, D. (2003b). Vasoactive intestinal peptide and pituitary adenylate cyclase-activating polypeptide inhibit the production of inflammatory mediators by activated microglia. *J. Leukoc. Biol.* **73**, 155-164.

Delgado, M., Martinez, C., Johnson, M. C., Gomariz, R. P., & Ganea, D. (1996a). Differential expression of vasoactive intestinal peptide receptors 1 and 2 (VIP-R1 and VIP-R2) mRNA in murine lymphocytes. *J. Neuroimmunol.* **68**, 27-38.

Delgado, M., Martinez, C., Leceta, J., Garrido, E., & Gomariz, R. P. (1996b). Differential VIP and VIP1 receptor gene expression in rat thymocyte subsets. *Peptides* **17**, 803-807.

Delgado, M., Pozo, D., Martinez, C., Garrido, E., Leceta, J., Calvo, J. R., & Gomariz, R. P. (1996c). Characterization of gene expression of VIP and VIP1-receptor in rat peritoneal lymphocytes and macrophages. *Regul. Pept.* **62**, 161-166.

Delporte, C., Poloczek, P., De Neef, P., Vertongen, P., Ciccarelli, E., Svoboda, M., Herchuelz, A., Winand, J., & Robberecht, P. (1995). Pituitary adenylate cyclase activating polypeptide (PACAP) and vasoactive intestinal peptide stimulate two signaling pathways in CHO cells stably transfected with the selective type I PACAP receptor. *Mol. Cell. Endocrinol.* **107**, 71-76.

Delporte, C., Van Praet, A., Herchuelz, A., Winand, J., & Christophe, J. (1993). Contrasting effects of PACAP and carbachol on $[Ca^{2+}]_i$ and inositol phosphates in human neuroblastoma NB-OK-1 cells. *Peptides* **14**, 1111-1118.

Desbuguois, B., Laudat, M. H., & Laudat, P. (1973). Vasoactive intestinal polypeptide and glucagon: stimulation of adenylate cyclase activity via distinct receptors in liver and fat cell membranes. *Biochem. Biophys. Res. Commun.* **53**, 1187-1194.

Deutsch, P. J. & Sun, Y. (1992). The 38-amino acid form of pituitary adenylate cyclase-activating polypeptide stimulates dual signaling cascades in PC12 cells and promotes neurite outgrowth. *J. Biol. Chem.* **267**, 5108-5113.

Dickinson, T. & Fleetwood-Walker, S. M. (1999). VIP and PACAP: very important in pain? *Trends Pharmacol. Sci.* **20**, 324-329.

Dickson, L., Aramori, I., McCulloch, J., Sharkey, J., & Finlayson, K. (2006a). A systematic comparison of intracellular cyclic AMP and calcium signalling highlights

complexities in human VPAC/PAC receptor pharmacology. *Neuropharmacology* **51**, 1086-1098.

Dickson, L., Aramori, I., Sharkey, J., & Finlayson, K. (2006b). VIP and PACAP receptor pharmacology: a comparison of intracellular signaling pathways. *Ann. N.Y. Acad. Sci.* **1070**, 239-242.

Dickson, M. & Gagnon, J. P. (2004). Key factors in the rising cost of new drug discovery and development. *Nat. Rev. Drug Discov.* **3**, 417-429.

Dimaline, R., Reeve, J. R., Jr., Shively, J. E., & Hawke, D. (1984). Isolation and characterization of rat vasoactive intestinal peptide. *Peptides* **5**, 183-187.

Divinski, I., Mittelman, L., & Gozes, I. (2004). A femtomolar acting octapeptide interacts with tubulin and protects astrocytes against zinc intoxication. *J. Biol. Chem.* **279**, 28531-28538.

Dong, M., Pinon, D. I., Asmann, Y. W., & Miller, L. J. (2006). Possible endogenous agonist mechanism for the activation of secretin family G protein-coupled receptors. *Mol. Pharmacol.* **70**, 206-213.

Drews, J. (2000). Drug discovery: a historical perspective. *Science* **287**, 1960-1964.

Drucker-Colin, R., Aguilar-Roblero, R., Garcia-Hernandez, F., Fernandez-Cancino, F., & Bermudez, R. F. (1984). Fetal suprachiasmatic nucleus transplants: diurnal rhythm recovery of lesioned rats. *Brain Res.* **311**, 353-357.

Du, B. H., Eng, J., Hulmes, J. D., Chang, M., Pan, Y. C., & Yalow, R. S. (1985). Guinea pig has a unique mammalian VIP. *Biochem. Biophys. Res. Commun.* **128**, 1093-1098.

Duckles, S. P. & Said, S. I. (1982). Vasoactive intestinal peptide as a neurotransmitter in the cerebral circulation. *Eur. J. Pharmacol.* **78**, 371-374.

Dupont, C., Broyart, J. P., Broer, Y., Chenut, B., Laburthe, M., & Rosselin, G. (1981). Importance of the vasoactive intestinal peptide receptor in the stimulation of cyclic adenosine 3',5'-monophosphate in gallbladder epithelial cells of man. Comparison with the guinea pig. *J. Clin. Invest.* **67**, 742-752.

Ebert, B., Wafford, K. A., & Deacon, S. (2006). Treating insomnia: Current and investigational pharmacological approaches. *Pharmacol. Ther.* **112**, 612-629.

Ebling, F. J. (1996). The role of glutamate in the photic regulation of the suprachiasmatic nucleus. *Prog. Neurobiol.* **50**, 109-132.

Edelman, J. L., Kajimura, M., Woldemussie, E., & Sachs, G. (1994). Differential effects of carbachol on calcium entry and release in CHO cells expressing the m3 muscarinic receptor. *Cell Calcium* **16**, 181-193.

Edvinsson, L. & Ekman, R. (1984). Distribution and dilatory effect of vasoactive intestinal polypeptide (VIP) in human cerebral arteries. *Peptides* **5**, 329-331.

Eggenberger, M., Born, W., Zimmermann, U., Lerner, E. A., Fischer, J. A., & Muff, R. (1999). Maxadilan interacts with receptors for pituitary adenylyl cyclase activating peptide in human SH-SY5Y and SK-N-MC neuroblastoma cells. *Neuropeptides* **33**, 107-114.

Ekblad, E., Jongsma, H., Brabet, P., Bockaert, J., & Sundler, F. (2000). Characterization of intestinal receptors for VIP and PACAP in rat and in PAC1 receptor knockout mouse. *Ann. N.Y. Acad. Sci.* **921**, 137-147.

Ekblad, E. & Sundler, F. (1997). Distinct receptors mediate pituitary adenylate cyclase-activating peptide and vasoactive intestinal peptide-induced relaxation of rat ileal longitudinal muscle. *Eur. J. Pharmacol.* **334**, 61-66.

Eng, J., Du, B. H., Raufman, J. P., & Yalow, R. S. (1986). Purification and amino acid sequences of dog, goat and guinea pig VIPs. *Peptides* **7 Suppl 1**, 17-20.

Estival, A., Mounielou, P., Trocheris, V., Scemama, J. L., Clemente, F., Hollande, E., & Ribet, A. (1983). Presence of VIP receptors in a human pancreatic adenocarcinoma cell line. Modulation of the cAMP response during cell proliferation. *Biochem. Biophys. Res. Commun.* **111**, 958-963.

Fahrenkrug, J. & Hannibal, J. (2004). Neurotransmitters co-existing with VIP or PACAP. *Peptides* **25**, 393-401.

Farkas, O., Tamas, A., Zsombok, A., Reglodi, D., Pal, J., Buki, A., Lengvari, I., Povlishock, J. T., & Doczi, T. (2004). Effects of pituitary adenylate cyclase activating polypeptide in a rat model of traumatic brain injury. *Regul. Pept.* **123**, 69-75.

Farmery, S. M., Owen, F., Poulter, M., & Crow, T. J. (1984). Characterisation and distribution of vasoactive intestinal polypeptide binding sites in human brain. *Neuropharmacology* **23**, 101-104.

Filmore, D. (2004). It's a GPCR world. *Modern Drug Discovery* **7**, 24-28.

Fisher, A., Heldman, E., Gurwitz, D., Haring, R., Karton, Y., Meshulam, H., Pittel, Z., Marciano, D., Brandeis, R., Sadot, E., Barg, Y., Pinkas-Kramarski, R., Vogel, Z., Ginzburg, I., Treves, T. A., Verchovsky, R., Klimowsky, S., & Korczyn, A. D. (1996). M1 agonists for the treatment of Alzheimer's disease. Novel properties and clinical update. *Ann. N.Y. Acad. Sci.* **777**, 189-196.

Foord, S. M., Bonner, T. I., Neubig, R. R., Rosser, E. M., Pin, J. P., Davenport, A. P., Spedding, M., & Harmar, A. J. (2005). International Union of Pharmacology. XLVI. G protein-coupled receptor list. *Pharmacol. Rev.* **57**, 279-288.

Foord, S. M., Jupe, S., & Holbrook, J. (2002). Bioinformatics and type II G-protein-coupled receptors. *Biochem. Soc. Trans.* **30**, 473-479.

Fredriksson, R., Gloriam, D. E., Hoglund, P. J., Lagerstrom, M. C., & Schioth, H. B. (2003a). There exist at least 30 human G-protein-coupled receptors with long Ser/Thr-rich N-termini. *Biochem. Biophys. Res. Commun.* **301**, 725-734.

Fredriksson, R., Lagerstrom, M. C., Lundin, L. G., & Schioth, H. B. (2003b). The G-protein-coupled receptors in the human genome form five main families. Phylogenetic analysis, paralogon groups, and fingerprints. *Mol. Pharmacol.* **63**, 1256-1272.

Fukuhara, C., Suzuki, N., Matsumoto, Y., Nakayama, Y., Aoki, K., Tsujimoto, G., Inouye, S. I., & Masuo, Y. (1997). Day-night variation of pituitary adenylate cyclase-activating polypeptide (PACAP) level in the rat suprachiasmatic nucleus. *Neurosci. Lett.* **229**, 49-52.

Gaytan, F., Martinez-Fuentes, A. J., Garcia-Navarro, F., Vaudry, H., & Aguilar, E. (1994). Pituitary adenylate cyclase-activating peptide (PACAP) immunolocalization in lymphoid tissues of the rat. *Cell Tissue Res.* **276**, 223-227.

Gentles, A. J. & Karlin, S. (1999). Why are human G-protein-coupled receptors predominantly intronless? *Trends Genet.* **15**, 47-49.

Georg, B. & Fahrenkrug, J. (2000). Pituitary adelylate cyclase-activating peptide is an activator of vasoactive intestinal polypeptide gene transcription in human neuroblastoma cells. *Brain Res. Mol. Brain Res.* **79**, 67-76.

Gerhold, L. M. & Wise, P. M. (2006). Vasoactive intestinal polypeptide regulates dynamic changes in astrocyte morphometry: impact on gonadotropin-releasing hormone neurons. *Endocrinology* **147**, 2197-2202.

Gespach, C., Bawab, W., de Cremoux, P., & Calvo, F. (1988). Pharmacology, molecular identification and functional characteristics of vasoactive intestinal peptide receptors in human breast cancer cells. *Cancer Res.* **48**, 5079-5083.

Gether, U. (2000). Uncovering molecular mechanisms involved in activation of G protein-coupled receptors. *Endocr. Rev.* **21**, 90-113.

Ghatei, M. A., Takahashi, K., Suzuki, Y., Gardiner, J., Jones, P. M., & Bloom, S. R. (1993). Distribution, molecular characterization of pituitary adenylate cyclase-activating polypeptide and its precursor encoding messenger RNA in human and rat tissues. *J. Endocrinol.* **136**, 159-166.

Goetzl, E. J., Voice, J. K., Shen, S., Dorsam, G., Kong, Y., West, K. M., Morrison, C. F., & Harmar, A. J. (2001). Enhanced delayed-type hypersensitivity and diminished immediate-type hypersensitivity in mice lacking the inducible VPAC(2)

receptor for vasoactive intestinal peptide. *Proc. Natl. Acad. Sci. U.S.A.* **98**, 13854-13859.

Gomariz, R. P., Martinez, C., Abad, C., Leceta, J., & Delgado, M. (2001). Immunology of VIP: a review and therapeutical perspectives. *Curr. Pharm. Des.* **7**, 89-111.

Gossen, D., Buscail, L., Cauvin, A., Gourlet, P., De Neef, P., Rathe, J., Robberecht, P., Vandermeers-Piret, M. C., Vandermeers, A., & Christophe, J. (1990). Amino acid sequence of VIP, PHI and secretin from the rabbit small intestine. *Peptides* **11**, 123-128.

Gottschall, P. E., Tatsuno, I., & Arimura, A. (1994). Regulation of interleukin-6 (IL-6) secretion in primary cultured rat astrocytes: synergism of interleukin-1 (IL-1) and pituitary adenylate cyclase activating polypeptide (PACAP). *Brain Res.* **637**, 197-203.

Gourlet, P., De Neef, P., Cnudde, J., Waelbroeck, M., & Robberecht, P. (1997a). *In vitro* properties of a high affinity selective antagonist of the VIP1 receptor. *Peptides* **18**, 1555-1560.

Gourlet, P., De Neef, P., Woussen-Colle, M. C., Vandermeers, A., Vandermeers-Piret, M. C., Robberecht, P., & Christophe, J. (1991). The activation of adenylate cyclase by pituitary adenylate cyclase activating polypeptide (PACAP) via helodermin-preferring VIP receptors in human SUP-T1 lymphoblastic membranes. *Biochim. Biophys. Acta* **1066**, 245-251.

Gourlet, P., Vandermeers, A., Van Rampelbergh, J., De Neef, P., Cnudde, J., Waelbroeck, M., & Robberecht, P. (1998). Analogues of VIP, helodermin, and PACAP discriminate between rat and human VIP1 and VIP2 receptors. *Ann. N.Y. Acad. Sci.* **865**, 247-252.

Gourlet, P., Vertongen, P., Vandermeers, A., Vandermeers-Piret, M. C., Rathe, J., De Neef, P., Waelbroeck, M., & Robberecht, P. (1997b). The long-acting vasoactive intestinal polypeptide agonist RO 25-1553 is highly selective of the VIP2 receptor subclass. *Peptides* **18**, 403-408.

Gozes, I., Avidor, R., Yahav, Y., Katznelson, D., Croce, C. M., & Huebner, K. (1987). The gene encoding vasoactive intestinal peptide is located on human chromosome 6p21----6qter. *Hum. Genet.* **75**, 41-44.

Gozes, I., Bardea, A., Reshef, A., Zamostiano, R., Zhukovsky, S., Rubinraut, S., Fridkin, M., & Brenneman, D. E. (1996). Neuroprotective strategy for Alzheimer disease: intranasal administration of a fatty neuropeptide. *Proc. Natl. Acad. Sci. U.S.A.* **93**, 427-432.

Gozes, I. & Brenneman, D. E. (2000). A new concept in the pharmacology of neuroprotection. *J. Mol. Neurosci.* **14**, 61-68.

Gozes, I., Glowa, J., Brenneman, D. E., McCune, S. K., Lee, E., & Westphal, H. (1993). Learning and sexual deficiencies in transgenic mice carrying a chimeric vasoactive intestinal peptide gene. *J. Mol. Neurosci.* **4**, 185-193.

Gozes, I., Morimoto, B. H., Tiong, J., Fox, A., Sutherland, K., Dangoor, D., Holser-Cochav, M., Vered, K., Newton, P., Aisen, P. S., Matsuoka, Y., van Dyck, C. H., & Thal, L. (2005). NAP: research and development of a peptide derived from activity-dependent neuroprotective protein (ADNP). *CNS Drug Rev.* **11**, 353-368.

Gray, S. L., Cummings, K. J., Jirik, F. R., & Sherwood, N. M. (2001). Targeted disruption of the pituitary adenylate cyclase-activating polypeptide gene results in early postnatal death associated with dysfunction of lipid and carbohydrate metabolism. *Mol. Endocrinol.* **15**, 1739-1747.

Gressens, P., Besse, L., Robberecht, P., Gozes, I., Fridkin, M., & Evrard, P. (1999). Neuroprotection of the developing brain by systemic administration of vasoactive intestinal peptide derivatives. *J. Pharmacol. Exp. Ther.* **288**, 1207-1213.

Grimaldi, M. & Cavallaro, S. (1999). Functional and molecular diversity of PACAP/VIP receptors in cortical neurons and type I astrocytes. *Eur. J. Neurosci.* **11**, 2767-2772.

Grimaldi, M., Pozzoli, G., Navarra, P., Preziosi, P., & Schettini, G. (1994). Vasoactive intestinal peptide and forskolin stimulate interleukin 6 production by rat cortical astrocytes in culture via a cyclic AMP-dependent, prostaglandin-independent mechanism. *J. Neurochem.* **63**, 344-350.

Grinninger, C., Wang, W., Oskoui, K. B., Voice, J. K., & Goetzl, E. J. (2004). A natural variant type II G protein-coupled receptor for vasoactive intestinal peptide with altered function. *J. Biol. Chem.* **279**, 40259-40262.

Gronenborn, A. M., Bovermann, G., & Clore, G. M. (1987). A 1H-NMR study of the solution conformation of secretin. Resonance assignment and secondary structure. *FEBS Lett.* **215**, 88-94.

Guerrero, J. M., Prieto, J. C., Elorza, F. L., Ramirez, R., & Goberna, R. (1981a). Interaction of vasoactive intestinal peptide with human blood mononuclear cells. *Mol. Cell. Endocrinol.* **21**, 151-160.

Guerrero, J. M., Prieto, J. C., Ramirez-Cardenas, R., Calvo, J. R., & Goberna, R. (1981b). Properties of vasoactive intestinal peptide-receptor interaction in rat liver membranes. *Rev. Esp. Fisiol.* **37**, 1-8.

Guldner, F. H. (1983). Numbers of neurons and astroglial cells in the suprachiasmatic nucleus of male and female rats. *Exp. Brain Res.* **50**, 373-376.

Gurwitz, D. & Haring, R. (2003). Ligand-selective signaling and high-content screening for GPCR drugs. *Drug Discov. Today* **8**, 1108-1109.

Hahm, S. H. & Eiden, L. E. (1996). Tissue-specific expression of the vasoactive intestinal peptide gene requires both an upstream tissue specifier element and the 5' proximal cyclic AMP-responsive element. *J. Neurochem.* **67**, 1872-1881.

Hale, K. D., Weigent, D. A., Gauthier, D. K., Hiramoto, R. N., & Ghanta, V. K. (2003). Cytokine and hormone profiles in mice subjected to handling combined with rectal temperature measurement stress and handling only stress. *Life Sci.* **72**, 1495-1508.

Hamelink, C., Tjurmina, O., Damadzic, R., Young, W. S., Weihe, E., Lee, H. W., & Eiden, L. E. (2002). Pituitary adenylate cyclase-activating polypeptide is a sympathoadrenal neurotransmitter involved in catecholamine regulation and glucohomeostasis. *Proc. Natl. Acad. Sci. U.S.A.* **99**, 461-466.

Hamidi, S. A., Szema, A. M., Lyubsky, S., Dickman, K. G., Degene, A., Mathew, S. M., Waschek, J. A., & Said, S. I. (2006). Clues to VIP Function from Knockout Mice. *Ann. N.Y. Acad. Sci.* **1070**, 5-9.

Hang, C. H., Shi, J. X., Li, J. S., Wu, W., Li, W. Q., & Yin, H. X. (2004). Levels of vasoactive intestinal peptide, cholecystokinin and calcitonin gene-related peptide in plasma and jejunum of rats following traumatic brain injury and underlying significance in gastrointestinal dysfunction. *World J. Gastroenterol.* **10**, 875-880.

Hannibal, J. (2002). Neurotransmitters of the retino-hypothalamic tract. *Cell Tissue Res.* **309**, 73-88.

Hannibal, J., Ding, J. M., Chen, D., Fahrenkrug, J., Larsen, P. J., Gillette, M. U., & Mikkelsen, J. D. (1997). Pituitary adenylate cyclase-activating peptide (PACAP) in the retinohypothalamic tract: a potential daytime regulator of the biological clock. *J. Neurosci.* **17**, 2637-2644.

Hannibal, J., Ding, J. M., Chen, D., Fahrenkrug, J., Larsen, P. J., Gillette, M. U., & Mikkelsen, J. D. (1998). Pituitary adenylate cyclase activating peptide (PACAP) in the retinohypothalamic tract: a daytime regulator of the biological clock. *Ann. N.Y. Acad. Sci.* **865**, 197-206.

Hannibal, J., Hindersson, P., Ostergaard, J., Georg, B., Heegaard, S., Larsen, P. J., & Fahrenkrug, J. (2004). Melanopsin is expressed in PACAP-containing retinal ganglion cells of the human retinohypothalamic tract. *Invest. Ophthalmol. Vis. Sci.* **45**, 4202-4209.

Hannibal, J., Jamen, F., Nielsen, H. S., Journot, L., Brabet, P., & Fahrenkrug, J. (2001). Dissociation between light-induced phase shift of the circadian rhythm and clock gene expression in mice lacking the pituitary adenylate cyclase activating polypeptide type 1 receptor. *J. Neurosci.* **21**, 4883-4890.

Harfi, I. & Sariban, E. (2006). Mechanisms and modulation of pituitary adenylate cyclase-activating protein-induced calcium mobilization in human neutrophils. *Ann. N.Y. Acad. Sci.* **1070**, 322-329.

Harmar, A. J. (2001). Family-B G-protein-coupled receptors. *Genome Biol.* **2**, 3013.1-3013.10.

Harmar, A. J., Arimura, A., Gozes, I., Journot, L., Laburthe, M., Pisegna, J. R., Rawlings, S. R., Robberecht, P., Said, S. I., Sreedharan, S. P., Wank, S. A., & Waschek, J. A. (1998). International Union of Pharmacology. XVIII. Nomenclature of receptors for vasoactive intestinal peptide and pituitary adenylate cyclase-activating polypeptide. *Pharmacol. Rev.* **50**, 265-270.

Harmar, A. J., Marston, H. M., Shen, S., Spratt, C., West, K. M., Sheward, W. J., Morrison, C. F., Dorin, J. R., Piggins, H. D., Reubi, J. C., Kelly, J. S., Maywood, E. S., & Hastings, M. H. (2002). The VPAC(2) receptor is essential for circadian function in the mouse suprachiasmatic nuclei. *Cell* **109**, 497-508.

Harmar, A. J., Sheward, W. J., Morrison, C. F., Waser, B., Gugger, M., & Reubi, J. C. (2004). Distribution of the VPAC2 receptor in peripheral tissues of the mouse. *Endocrinology* **145**, 1203-1210.

Harrington, M. E. & Hoque, S. (1997). NPY opposes PACAP phase shifts via receptors different from those involved in NPY phase shifts. *Neuroreport* **8**, 2677-2680.

Harrington, M. E., Hoque, S., Hall, A., Golombek, D., & Biello, S. (1999). Pituitary adenylate cyclase activating peptide phase shifts circadian rhythms in a manner similar to light. *J. Neurosci.* **19**, 6637-6642.

Hashimoto, H., Ishihara, T., Shigemoto, R., Mori, K., & Nagata, S. (1993). Molecular cloning and tissue distribution of a receptor for pituitary adenylate cyclase-activating polypeptide. *Neuron* **11**, 333-342.

Hashimoto, H., Kunugi, A., Arakawa, N., Shintani, N., Fujita, T., Kasai, A., Kawaguchi, C., Morita, Y., Hirose, M., Sakai, Y., & Baba, A. (2003). Possible involvement of a cyclic AMP-dependent mechanism in PACAP-induced proliferation and ERK activation in astrocytes. *Biochem. Biophys. Res. Commun.* **311**, 337-343.

Hashimoto, H., Nogi, H., Mori, K., Ohishi, H., Shigemoto, R., Yamamoto, K., Matsuda, T., Mizuno, N., Nagata, S., & Baba, A. (1996a). Distribution of the mRNA for a pituitary adenylate cyclase-activating polypeptide receptor in the rat brain: an in situ hybridization study. *J. Comp. Neurol.* **371**, 567-577.

Hashimoto, H., Shintani, N., Tanaka, K., Mori, W., Hirose, M., Matsuda, T., Sakaue, M., Miyazaki, J., Niwa, H., Tashiro, F., Yamamoto, K., Koga, K., Tomimoto, S.,

Kunugi, A., Suetake, S., & Baba, A. (2001). Altered psychomotor behaviors in mice lacking pituitary adenylate cyclase-activating polypeptide (PACAP). *Proc. Natl. Acad. Sci. U.S.A.* **98**, 13355-13360.

Hashimoto, H., Yamamoto, K., Hagigara, N., Ogawa, N., Nishino, A., Aino, H., Nogi, H., Imanishi, K., Matsuda, T., & Baba, A. (1996b). cDNA cloning of a mouse pituitary adenylate cyclase-activating polypeptide receptor. *Biochim. Biophys. Acta* **1281**, 129-133.

Hastings, M. H., Mead, S. M., Vindlacheruvu, R. R., Ebling, F. J., Maywood, E. S., & Grosse, J. (1992). Non-photic phase shifting of the circadian activity rhythm of Syrian hamsters: the relative potency of arousal and melatonin. *Brain Res.* **591**, 20-26.

Hastings, M. H., Reddy, A. B., & Maywood, E. S. (2003). A clockwork web: circadian timing in brain and periphery, in health and disease. *Nat. Rev. Neurosci.* **4**, 649-661.

Hay, D. L., Poyner, D. R., & Sexton, P. M. (2006). GPCR modulation by RAMPs. *Pharmacol. Ther.* **109**, 173-197.

Hayakawa, Y., Obata, K., Itoh, N., Yanaihara, N., & Okamoto, H. (1984). Cyclic AMP regulation of pro-vasoactive intestinal polypeptide/PHM-27 synthesis in human neuroblastoma cells. *J. Biol. Chem.* **259**, 9207-9211.

Hilbush, B. S., Morrison, J. H., Young, W. G., Sutcliffe, J. G., & Bloom, F. E. (2005). New prospects and strategies for drug target discovery in neurodegenerative disorders. *NeuroRx.* **2**, 627-637.

Hoare, S. R. (2005). Mechanisms of peptide and nonpeptide ligand binding to Class B G-protein-coupled receptors. *Drug Discov. Today* **10**, 417-427.

Hopkins, A. L. & Groom, C. R. (2002). The druggable genome. *Nat. Rev. Drug Discov.* **1**, 727-730.

Horikawa, K. & Shibata, S. (2004). Phase-resetting response to (+)8-OH-DPAT, a serotonin 1A/7 receptor agonist, in the mouse in vivo. *Neurosci. Lett.* **368**, 130-134.

Horn, F., Bywater, R., Krause, G., Kuipers, W., Oliveira, L., Paiva, A. C., Sander, C., & Vriend, G. (1998). The interaction of class B G protein-coupled receptors with their hormones. *Receptors Channels* **5**, 305-314.

Hosoya, M., Kimura, C., Ogi, K., Ohkubo, S., Miyamoto, Y., Kugoh, H., Shimizu, M., Onda, H., Oshimura, M., Arimura, A., & . (1992). Structure of the human pituitary adenylate cyclase activating polypeptide (PACAP) gene. *Biochim. Biophys. Acta* **1129**, 199-206.

Hosoya, M., Onda, H., Ogi, K., Masuda, Y., Miyamoto, Y., Ohtaki, T., Okazaki, H., Arimura, A., & Fujino, M. (1993). Molecular cloning and functional expression of rat cDNAs encoding the receptor for pituitary adenylate cyclase activating polypeptide (PACAP). *Biochem. Biophys. Res. Commun.* **194**, 133-143.

Huang, M. C., Miller, A. L., Wang, W., Kong, Y., Paul, S., & Goetzl, E. J. (2006). Differential signaling of T cell generation of IL-4 by wild-type and short-deletion variant of type 2 G protein-coupled receptor for vasoactive intestinal peptide (VPAC2). *J. Immunol.* **176**, 6640-6646.

Hughes, A. T., Fahey, B., Cutler, D. J., Coogan, A. N., & Piggins, H. D. (2004). Aberrant gating of photic input to the suprachiasmatic circadian pacemaker of mice lacking the VPAC2 receptor. *J. Neurosci.* **24**, 3522-3526.

Hurko, O. & Ryan, J. L. (2005). Translational research in central nervous system drug discovery. *NeuroRx.* **2**, 671-682.

Ibata, Y., Takahashi, Y., Okamura, H., Kawakami, F., Terubayashi, H., Kubo, T., & Yanaihara, N. (1989). Vasoactive intestinal peptide (VIP)-like immunoreactive neurons located in the rat suprachiasmatic nucleus receive a direct retinal projection. *Neurosci. Lett.* **97**, 1-5.

Igarashi, H., Ito, T., Hou, W., Mantey, S. A., Pradhan, T. K., Ulrich, C. D., Hocart, S. J., Coy, D. H., & Jensen, R. T. (2002a). Elucidation of vasoactive intestinal peptide pharmacophore for VPAC(1) receptors in human, rat, and guinea pig. *J. Pharmacol. Exp. Ther.* **301**, 37-50.

Igarashi, H., Ito, T., Pradhan, T. K., Mantey, S. A., Hou, W., Coy, D. H., & Jensen, R. T. (2002b). Elucidation of the vasoactive intestinal peptide pharmacophore for VPAC(2) receptors in human and rat and comparison to the pharmacophore for VPAC(1) receptors. *J. Pharmacol. Exp. Ther.* **303**, 445-460.

Inagaki, N., Yoshida, H., Mizuta, M., Mizuno, N., Fujii, Y., Gonoi, T., Miyazaki, J., & Seino, S. (1994). Cloning and functional characterization of a third pituitary adenylate cyclase-activating polypeptide receptor subtype expressed in insulin-secreting cells. *Proc. Natl. Acad. Sci. U.S.A.* **91**, 2679-2683.

Inooka, H., Ohtaki, T., Kitahara, O., Ikegami, T., Endo, S., Kitada, C., Ogi, K., Onda, H., Fujino, M., & Shirakawa, M. (2001). Conformation of a peptide ligand bound to its G-protein coupled receptor. *Nat. Struct. Biol.* **8**, 161-165.

International Human Genome Sequencing Consortium (2004). Finishing the euchromatic sequence of the human genome. *Nature* **431**, 931-945.

Ishihara, T., Nakamura, S., Kaziro, Y., Takahashi, T., Takahashi, K., & Nagata, S. (1991). Molecular cloning and expression of a cDNA encoding the secretin receptor. *EMBO J.* **10**, 1635-1641.

Ishihara, T., Shigemoto, R., Mori, K., Takahashi, K., & Nagata, S. (1992). Functional expression and tissue distribution of a novel receptor for vasoactive intestinal polypeptide. *Neuron* **8**, 811-819.

Isobe, K., Kaneko, M., Kaneko, S., Nissato, S., Nanmoku, T., Takekoshi, K., Okuda, Y., & Kawakami, Y. (2004). Expression of mRNAs for PACAP and its receptor in human neuroblastomas and their relationship to catecholamine synthesis. *Regul. Pept.* **123**, 29-32.

Itoh, N., Obata, K., Yanaihara, N., & Okamoto, H. (1983). Human preprovasoactive intestinal polypeptide contains a novel PHI-27-like peptide, PHM-27. *Nature* **304**, 547-549.

Itri, J. & Colwell, C. S. (2003). Regulation of inhibitory synaptic transmission by vasoactive intestinal peptide (VIP) in the mouse suprachiasmatic nucleus. *J. Neurophysiol.* **90**, 1589-1597.

Jacoby, E., Bouhelal, R., Gerspacher, M., & Seuwen, K. (2006). The 7 TM G-protein-coupled receptor target family. *ChemMedChem.* **1**, 761-782.

Jamen, F., Persson, K., Bertrand, G., Rodriguez-Henche, N., Puech, R., Bockaert, J., Ahren, B., & Brabet, P. (2000). PAC1 receptor-deficient mice display impaired insulinotropic response to glucose and reduced glucose tolerance. *J. Clin. Invest.* **105**, 1307-1315.

Jaworski, D. M. (2000). Expression of pituitary adenylate cyclase-activating polypeptide (PACAP) and the PACAP-selective receptor in cultured rat astrocytes, human brain tumors, and in response to acute intracranial injury. *Cell Tissue Res.* **300**, 219-230.

Johnson, M. C., McCormack, R. J., Delgado, M., Martinez, C., & Ganea, D. (1996). Murine T-lymphocytes express vasoactive intestinal peptide receptor 1 (VIP-R1) mRNA. *J. Neuroimmunol.* **68**, 109-119.

Joo, K. M., Chung, Y. H., Kim, M. K., Nam, R. H., Lee, B. L., Lee, K. H., & Cha, C. I. (2004). Distribution of vasoactive intestinal peptide and pituitary adenylate cyclase-activating polypeptide receptors (VPAC1, VPAC2, and PAC1 receptor) in the rat brain. *J. Comp. Neurol.* **476**, 388-413.

Journot, L., Waeber, C., Pantaloni, C., Holsboer, F., Seeburg, P. H., Bockaert, J., & Spengler, D. (1995). Differential signal transduction by six splice variants of the pituitary adenylate cyclase-activating peptide (PACAP) receptor. *Biochem. Soc. Trans.* **23**, 133-137.

Juarranz, M. G., Van Rampelbergh, J., Gourlet, P., De Neef, P., Cnudde, J., Robberecht, P., & Waelbroeck, M. (1999). Vasoactive intestinal polypeptide VPAC1 and VPAC2 receptor chimeras identify domains responsible for the specificity of ligand binding and activation. *Eur. J. Biochem.* **265**, 449-456.

Kaiser, P. K. & Lipton, S. A. (1990). VIP-mediated increase in cAMP prevents tetrodotoxin-induced retinal ganglion cell death in vitro. *Neuron* **5**, 373-381.

Kalamatianos, T., Kallo, I., Piggins, H. D., & Coen, C. W. (2004). Expression of VIP and/or PACAP receptor mRNA in peptide synthesizing cells within the suprachiasmatic nucleus of the rat and in its efferent target sites. *J. Comp. Neurol.* **475**, 19-35.

Kato, I., Suzuki, Y., Akabane, A., Yonekura, H., Tanaka, O., Kondo, H., Takasawa, S., Yoshimoto, T., & Okamoto, H. (1994). Transgenic mice overexpressing human vasoactive intestinal peptide (VIP) gene in pancreatic beta cells. Evidence for improved glucose tolerance and enhanced insulin secretion by VIP and PHM-27 in vivo. *J. Biol. Chem.* **269**, 21223-21228.

Kawaguchi, C., Tanaka, K., Isojima, Y., Shintani, N., Hashimoto, H., Baba, A., & Nagai, K. (2003). Changes in light-induced phase shift of circadian rhythm in mice lacking PACAP. *Biochem. Biophys. Res. Commun.* **310**, 169-175.

Kermode, J. C., DeLuca, A. W., Zilberman, A., Valliere, J., & Shreeve, S. M. (1992). Evidence for the formation of a functional complex between vasoactive intestinal peptide, its receptor, and Gs in lung membranes. *J. Biol. Chem.* **267**, 3382-3388.

Kilpatrick, G. J., Dautzenberg, F. M., Martin, G. R., & Eglen, R. M. (1999). 7TM receptors: the splicing on the cake. *Trends Pharmacol. Sci.* **20**, 294-301.

Kim, W. K., Kan, Y., Ganea, D., Hart, R. P., Gozes, I., & Jonakait, G. M. (2000). Vasoactive intestinal peptide and pituitary adenylyl cyclase-activating polypeptide inhibit tumor necrosis factor-alpha production in injured spinal cord and in activated microglia via a cAMP-dependent pathway. *J. Neurosci.* **20**, 3622-3630.

Kimura, C., Ohkubo, S., Ogi, K., Hosoya, M., Itoh, Y., Onda, H., Miyata, A., Jiang, L., Dahl, R. R., Stibbs, H. H., & . (1990). A novel peptide which stimulates adenylate cyclase: molecular cloning and characterization of the ovine and human cDNAs. *Biochem. Biophys. Res. Commun.* **166**, 81-89.

Ko, C. H. & Takahashi, J. S. (2006). Molecular components of the mammalian circadian clock. *Hum. Mol. Genet.* **15 Spec No 2**, R271-R277.

Kola, I. & Landis, J. (2004). Can the pharmaceutical industry reduce attrition rates? *Nat. Rev. Drug Discov.* **3**, 711-715.

Kong, L. Y., Maderdrut, J. L., Jeohn, G. H., & Hong, J. S. (1999). Reduction of lipopolysaccharide-induced neurotoxicity in mixed cortical neuron/glia cultures by femtomolar concentrations of pituitary adenylate cyclase-activating polypeptide. *Neuroscience* **91**, 493-500.

Koshiyama, H., Kato, Y., Inoue, T., Christophe, J., Yanaihara, N., & Imura, H. (1987). Helodermin stimulates prolactin secretion in the rat. *Eur. J. Pharmacol.* **141**, 319-321.

Kristensen, B., Georg, B., & Fahrenkrug, J. (1997). Cholinergic regulation of VIP gene expression in human neuroblastoma cells. *Brain Res.* **775**, 99-106.

Kristiansen, K. (2004). Molecular mechanisms of ligand binding, signaling, and regulation within the superfamily of G-protein-coupled receptors: molecular modeling and mutagenesis approaches to receptor structure and function. *Pharmacol. Ther.* **103**, 21-80.

Kuhlow, C. J., Krady, J. K., Basu, A., & Levison, S. W. (2003). Astrocytic ceruloplasmin expression, which is induced by IL-1beta and by traumatic brain injury, increases in the absence of the IL-1 type 1 receptor. *Glia* **44**, 76-84.

Kwakkenbos, M. J., Kop, E. N., Stacey, M., Matmati, M., Gordon, S., Lin, H. H., & Hamann, J. (2004). The EGF-TM7 family: a postgenomic view. *Immunogenetics* **55**, 655-666.

Laburthe, M., Amiranoff, B., Boige, N., Rouyer-Fessard, C., Tatemoto, K., & Moroder, L. (1983). Interaction of GRF with VIP receptors and stimulation of adenylate cyclase in rat and human intestinal epithelial membranes. Comparison with PHI and secretin. *FEBS Lett.* **159**, 89-92.

Laburthe, M., Boissard, C., Chevalier, G., Zweibaum, A., & Rosselin, G. (1981). Peptide receptors in human lung tumor cells in culture: vasoactive intestinal peptide (VIP) and secretin interaction with the Calu-1 and SW-900 cell lines. *Regul. Pept.* **2**, 219-230.

Laburthe, M. & Couvineau, A. (2002). Molecular pharmacology and structure of VPAC Receptors for VIP and PACAP. *Regul. Pept.* **108**, 165-173.

Laburthe, M., Rousset, M., Boissard, C., Chevalier, G., Zweibaum, A., & Rosselin, G. (1978). Vasoactive intestinal peptide: a potent stimulator of adenosine 3':5'-cyclic monophosphate accumulation in gut carcinoma cell lines in culture. *Proc. Natl. Acad. Sci. U.S.A.* **75**, 2772-2775.

Laburthe, M., Rousset, M., Chevalier, G., Boissard, C., Dupont, C., Zweibaum, A., & Rosselin, G. (1980). Vasoactive intestinal peptide control of cyclic adenosine 3':5'-monophosphate levels in seven human colorectal adenocarcinoma cell lines in culture. *Cancer Res.* **40**, 2529-2533.

Lam, H. C., Takahashi, K., Ghatei, M. A., Kanse, S. M., Polak, J. M., & Bloom, S. R. (1990). Binding sites of a novel neuropeptide pituitary-adenylate-cyclase-activating polypeptide in the rat brain and lung. *Eur. J. Biochem.* **193**, 725-729.

Lamperti, E. D., Rosen, K. M., & Villa-Komaroff, L. (1991). Characterization of the gene and messages for vasoactive intestinal polypeptide (VIP) in rat and mouse. *Brain Res. Mol. Brain Res.* **9**, 217-231.

Lang, B., Song, B., Davidson, W., MacKenzie, A., Smith, N., McCaig, C. D., Harmar, A. J., & Shen, S. (2006). Expression of the human PAC1 receptor leads to dose-dependent hydrocephalus-related abnormalities in mice. *J. Clin. Invest.* **116**, 1924-1934.

Langer, I., Perret, J., Vertongen, P., Waelbroeck, M., & Robberecht, P. (2001). Vasoactive intestinal peptide (VIP) stimulates $[Ca^{2+}]_i$ and cyclic AMP in CHO cells expressing Galpha16. *Cell Calcium* **30**, 229-234.

Langer, I. & Robberecht, P. (2005). Mutations in the carboxy-terminus of the third intracellular loop of the human recombinant VPAC1 receptor impair VIP-stimulated $[Ca^{2+}]_i$ increase but not adenylate cyclase stimulation. *Cell Signal.* **17**, 17-24.

Langer, I., Vertongen, P., Perret, J., Cnudde, J., Gregoire, F., De Neef, P., Robberecht, P., & Waelbroeck, M. (2002a). VPAC(1) receptors have different agonist efficacy profiles on membrane and intact cells. *Cell Signal.* **14**, 689-694.

Langer, I., Vertongen, P., Perret, J., Waelbroeck, M., & Robberecht, P. (2002b). A small sequence in the third intracellular loop of the VPAC(1) receptor is responsible for its efficient coupling to the calcium effector. *Mol. Endocrinol.* **16**, 1089-1096.

Langer, I., Vertongen, P., Perret, J., Waelbroeck, M., & Robberecht, P. (2003). Lysine 195 and aspartate 196 in the first extracellular loop of the VPAC1 receptor are essential for high affinity binding of agonists but not of antagonists. *Neuropharmacology* **44**, 125-131.

Langlet, C., Gaspard, N., Nachtergael, I., Robberecht, P., & Langer, I. (2004). Comparative efficacy of VIP and analogs on activation and internalization of the recombinant VPAC2 receptor expressed in CHO cells. *Peptides* **25**, 2079-2086.

Lara-Marquez, M. L., O'Dorisio, M. S., & Karacay, B. (2000). Vasoactive intestinal peptide (VIP) receptor type 2 (VPAC2) is the predominant receptor expressed in human thymocytes. *Ann. N.Y. Acad. Sci.* **921**, 45-54.

Larsson, L. I., Edvinsson, L., Fahrenkrug, J., Hakanson, R., Owman, C., Schaffalitzky, d. M., & Sundler, F. (1976a). Immunohistochemical localization of a vasodilatory polypeptide (VIP) in cerebrovascular nerves. *Brain Res.* **113**, 400-404.

Larsson, L. I., Fahrenkrug, J., Schaffalitzky, d. M., Sundler, F., Hakanson, R., & Rehfeld, J. R. (1976b). Localization of vasoactive intestinal polypeptide (VIP) to central and peripheral neurons. *Proc. Natl. Acad. Sci. U.S.A.* **73**, 3197-3200.

Leceta, J., Martinez, M. C., Delgado, M., Garrido, E., & Gomariz, R. P. (1994). Lymphoid cell subpopulations containing vasoactive intestinal peptide in the rat. *Peptides* **15**, 791-797.

Lehman, M. N., Silver, R., Gladstone, W. R., Kahn, R. M., Gibson, M., & Bittman, E. L. (1987). Circadian rhythmicity restored by neural transplant. Immunocytochemical characterization of the graft and its integration with the host brain. *J. Neurosci.* **7**, 1626-1638.

Leker, R. R., Teichner, A., Grigoriadis, N., Ovadia, H., Brenneman, D. E., Fridkin, M., Giladi, E., Romano, J., & Gozes, I. (2002). NAP, a femtomolar-acting peptide, protects the brain against ischemic injury by reducing apoptotic death. *Stroke* **33**, 1085-1092.

Lelianova, V. G., Davletov, B. A., Sterling, A., Rahman, M. A., Grishin, E. V., Totty, N. F., & Ushkaryov, Y. A. (1997). Alpha-latrotoxin receptor, latrophilin, is a novel member of the secretin family of G protein-coupled receptors. *J. Biol. Chem.* **272**, 21504-21508.

Lelievre, V., Meunier, A. C., Caigneaux, E., Falcon, J., & Muller, J. M. (1998). Differential expression and function of PACAP and VIP receptors in four human colonic adenocarcinoma cell lines. *Cell Signal.* **10**, 13-26.

Leone, M. J., Marpegan, L., Bekinschtein, T. A., Costas, M. A., & Golombek, D. A. (2006). Suprachiasmatic astrocytes as an interface for immune-circadian signalling. *J. Neurosci. Res.* **84**, 1521-1527.

Lerner, E. A., Ribeiro, J. M., Nelson, R. J., & Lerner, M. R. (1991). Isolation of maxadilan, a potent vasodilatory peptide from the salivary glands of the sand fly Lutzomyia longipalpis. *J. Biol. Chem.* **266**, 11234-11236.

Leroux, P., Vaudry, H., Fournier, A., St Pierre, S., & Pelletier, G. (1984). Characterization and localization of vasoactive intestinal peptide receptors in the rat lung. *Endocrinology* **114**, 1506-1512.

Li, M., David, C., Kikuta, T., Somogyvari-Vigh, A., & Arimura, A. (2005). Signaling cascades involved in neuroprotection by subpicomolar pituitary adenylate cyclase-activating polypeptide 38. *J. Mol. Neurosci.* **27**, 91-105.

Lieu, S. N., Oh, D. S., Pisegna, J. R., & Germano, P. M. (2006). Neuroendocrine tumors express PAC1 receptors. *Ann. N.Y. Acad. Sci.* **1070**, 399-404.

Lin, Y. J., Seroude, L., & Benzer, S. (1998). Extended life-span and stress resistance in the Drosophila mutant methuselah. *Science* **282**, 943-946.

Lins, L., Couvineau, A., Rouyer-Fessard, C., Nicole, P., Maoret, J. J., Benhamed, M., Brasseur, R., Thomas, A., & Laburthe, M. (2001). The human VPAC1 receptor:

three-dimensional model and mutagenesis of the N-terminal domain. *J. Biol. Chem.* **276**, 10153-10160.

Lutz, E. M., Ronaldson, E., Shaw, P., Johnson, M. S., Holland, P. J., & Mitchell, R. (2006). Characterization of novel splice variants of the PAC1 receptor in human neuroblastoma cells: consequences for signaling by VIP and PACAP. *Mol. Cell Neurosci.* **31**, 193-209.

Lutz, E. M., Sheward, W. J., West, K. M., Morrow, J. A., Fink, G., & Harmar, A. J. (1993). The VIP2 receptor: molecular characterisation of a cDNA encoding a novel receptor for vasoactive intestinal peptide. *FEBS Lett.* **334**, 3-8.

Mabuchi, T., Shintani, N., Matsumura, S., Okuda-Ashitaka, E., Hashimoto, H., Muratani, T., Minami, T., Baba, A., & Ito, S. (2004). Pituitary adenylate cyclase-activating polypeptide is required for the development of spinal sensitization and induction of neuropathic pain. *J. Neurosci.* **24**, 7283-7291.

Macarron, R. (2006). Critical review of the role of HTS in drug discovery. *Drug Discov. Today* **11**, 277-279.

MacKenzie, C. J., Lutz, E. M., Johnson, M. S., Robertson, D. N., Holland, P. J., & Mitchell, R. (2001). Mechanisms of phospholipase C activation by the vasoactive intestinal polypeptide/pituitary adenylate cyclase-activating polypeptide type 2 receptor. *Endocrinology* **142**, 1209-1217.

MacKenzie, C. J., Lutz, E. M., McCulloch, D. A., Mitchell, R., & Harmar, A. J. (1996). Phospholipase C activation by VIP1 and VIP2 receptors expressed in COS 7 cells involves a pertussis toxin-sensitive mechanism. *Ann. N.Y. Acad. Sci.* **805**, 579-584.

Magistretti, P. J., Manthorpe, M., Bloom, F. E., & Varon, S. (1983). Functional receptors for vasoactive intestinal polypeptide in cultured astroglia from neonatal rat brain. *Regul. Pept.* **6**, 71-80.

Malhotra, R. K., Wakade, T. D., & Wakade, A. R. (1988). Vasoactive intestinal polypeptide and muscarine mobilize intracellular Ca2+ through breakdown of phosphoinositides to induce catecholamine secretion. Role of IP3 in exocytosis. *J. Biol. Chem.* **263**, 2123-2126.

Mammi, C., Frajese, G. V., Vespasiani, G., Mariani, S., Gnessi, L., Farini, D., Fabbri, A., Frajese, G., & Moretti, C. (2006). PAC1-R null isoform expression in human prostate cancer tissue. *Prostate* **66**, 514-521.

Mangeat, P., Marvaldi, J., Ahmed, O. A., & Marchis-Mouren, G. (1981). Parallel activation of cyclic AMP phosphodiesterase and cyclic AMP-dependent protein kinase in two human gut adenocarcinoma cells (HT 29 and HRT 18) in culture, by vasoactive intestinal peptide (VIP) and other effectors activating the cyclic AMP system. *Regul. Pept.* **1**, 397-414.

Masmoudi, O., Gandolfo, P., Leprince, J., Vaudry, D., Fournier, A., Patte-Mensah, C., Vaudry, H., & Tonon, M. C. (2003). Pituitary adenylate cyclase-activating polypeptide (PACAP) stimulates endozepine release from cultured rat astrocytes via a PKA-dependent mechanism. *FASEB J.* **17**, 17-27.

Masuo, Y., Suzuki, N., Matsumoto, H., Tokito, F., Matsumoto, Y., Tsuda, M., & Fujino, M. (1993). Regional distribution of pituitary adenylate cyclase activating polypeptide (PACAP) in the rat central nervous system as determined by sandwich-enzyme immunoassay. *Brain Res.* **602**, 57-63.

Maywood, E. S., Reddy, A. B., Wong, G. K., O'Neill, J. S., O'Brien, J. A., McMahon, D. G., Harmar, A. J., Okamura, H., & Hastings, M. H. (2006). Synchronization and maintenance of timekeeping in suprachiasmatic circadian clock cells by neuropeptidergic signaling. *Curr. Biol.* **16**, 599-605.

McCarthy, K. D. & de Vellis, J. (1980). Preparation of separate astroglial and oligodendroglial cell cultures from rat cerebral tissue. *J. Cell Biol.* **85**, 890-902.

McCulloch, D. A., Lutz, E. M., Johnson, M. S., MacKenzie, C. J., & Mitchell, R. (2000). Differential activation of phospholipase D by VPAC and PAC1 receptors. *Ann. N.Y. Acad. Sci.* **921**, 175-185.

McCulloch, D. A., Lutz, E. M., Johnson, M. S., Robertson, D. N., MacKenzie, C. J., Holland, P. J., & Mitchell, R. (2001). ADP-ribosylation factor-dependent phospholipase D activation by VPAC receptors and a PAC(1) receptor splice variant. *Mol. Pharmacol.* **59**, 1523-1532.

McCulloch, D. A., MacKenzie, C. J., Johnson, M. S., Robertson, D. N., Holland, P. J., Ronaldson, E., Lutz, E. M., & Mitchell, R. (2002). Additional signals from VPAC/PAC family receptors. *Biochem. Soc. Trans.* **30**, 441-446.

McCulloch, J. & Edvinsson, L. (1980). Cerebral circulatory and metabolic effects of vasoactive intestinal polypeptide. *Am. J. Physiol.* **238**, H449-H456.

McFarlin, D. R., Lehn, D. A., Moran, S. M., MacDonald, M. J., & Epstein, M. L. (1995). Sequence of a cDNA encoding chicken vasoactive intestinal peptide (VIP). *Gene* **154**, 211-213.

McKnight, A. J. & Gordon, S. (1998). The EGF-TM7 family: unusual structures at the leukocyte surface. *J. Leukoc. Biol.* **63**, 271-280.

McRory, J. & Sherwood, N. M. (1997). Two protochordate genes encode pituitary adenylate cyclase-activating polypeptide and related family members. *Endocrinology* **138**, 2380-2390.

McRory, J. E., Parker, R. L., & Sherwood, N. M. (1997). Expression and alternative processing of a chicken gene encoding both growth hormone-releasing hormone and pituitary adenylate cyclase-activating polypeptide. *DNA Cell Biol.* **16**, 95-102.

Miller, A. L., Verma, D., Grinninger, C., Huang, M. C., & Goetzl, E. J. (2006). Functional Splice Variants of the Type II G Protein-Coupled Receptor (VPAC2) for Vasoactive Intestinal Peptide in Mouse and Human Lymphocytes. *Ann. N.Y. Acad. Sci.* **1070**, 422-426.

Miyata, A., Arimura, A., Dahl, R. R., Minamino, N., Uehara, A., Jiang, L., Culler, M. D., & Coy, D. H. (1989). Isolation of a novel 38 residue-hypothalamic polypeptide which stimulates adenylate cyclase in pituitary cells. *Biochem. Biophys. Res. Commun.* **164**, 567-574.

Miyata, A., Jiang, L., Dahl, R. D., Kitada, C., Kubo, K., Fujino, M., Minamino, N., & Arimura, A. (1990). Isolation of a neuropeptide corresponding to the N-terminal 27 residues of the pituitary adenylate cyclase activating polypeptide with 38 residues (PACAP38). *Biochem. Biophys. Res. Commun.* **170**, 643-648.

Moody, T. W. & Jensen, R. T. (2006). Breast cancer VPAC1 receptors. *Ann. N.Y. Acad. Sci.* **1070**, 436-439.

Moore, R. Y. & Eichler, V. B. (1972). Loss of a circadian adrenal corticosterone rhythm following suprachiasmatic lesions in the rat. *Brain Res.* **42**, 201-206.

Moreno, D., Gourlet, P., De Neef, P., Cnudde, J., Waelbroeck, M., & Robberecht, P. (2000). Development of selective agonists and antagonists for the human vasoactive intestinal polypeptide VPAC(2) receptor. *Peptides* **21**, 1543-1549.

Morin, L. P., Johnson, R. F., & Moore, R. Y. (1989). Two brain nuclei controlling circadian rhythms are identified by GFAP immunoreactivity in hamsters and rats. *Neurosci. Lett.* **99**, 55-60.

Morio, H., Tatsuno, I., Hirai, A., Tamura, Y., & Saito, Y. (1996). Pituitary adenylate cyclase-activating polypeptide protects rat-cultured cortical neurons from glutamate-induced cytotoxicity. *Brain Res.* **741**, 82-88.

Morisset, J., Douziech, N., Rydzewska, G., Buscail, L., & Rivard, N. (1995). Cell signalling pathway involved in PACAP-induced AR4-2J cell proliferation. *Cell Signal.* **7**, 195-205.

Moriya, T., Takahashi, S., Ikeda, M., Suzuki-Yamashita, K., Asai, M., Kadotani, H., Okamura, H., Yoshioka, T., & Shibata, S. (2000). N-methyl-D-aspartate receptor subtype 2C is not involved in circadian oscillation or photoic entrainment of the biological clock in mice. *J. Neurosci. Res.* **61**, 663-673.

Moro, O. & Lerner, E. A. (1997). Maxadilan, the vasodilator from sand flies, is a specific pituitary adenylate cyclase activating peptide type I receptor agonist. *J. Biol. Chem.* **272**, 966-970.

Moro, O., Wakita, K., Ohnuma, M., Denda, S., Lerner, E. A., & Tajima, M. (1999). Functional characterization of structural alterations in the sequence of the vasodilatory peptide maxadilan yields a pituitary adenylate cyclase-activating peptide type 1 receptor-specific antagonist. *J. Biol. Chem.* **274**, 23103-23110.

Morrow, J. A., Lutz, E. M., West, K. M., Fink, G., & Harmar, A. J. (1993). Molecular cloning and expression of a cDNA encoding a receptor for pituitary adenylate cyclase activating polypeptide (PACAP). *FEBS Lett.* **329**, 99-105.

Muller, J. M., Philippe, M., Chevrier, L., Heraud, C., Alleaume, C., & Chadeneau, C. (2006). The VIP-receptor system in neuroblastoma cells. *Regul. Pept.* **137**, 34-41.

Mumby, S. M., Kahn, R. A., Manning, D. R., & Gilman, A. G. (1986). Antisera of designed specificity for subunits of guanine nucleotide-binding regulatory proteins. *Proc. Natl. Acad. Sci. U.S.A.* **83**, 265-269.

Mutt, V. & Said, S. I. (1974). Structure of the porcine vasoactive intestinal octacosapeptide. The amino-acid sequence. Use of kallikrein in its determination. *Eur. J. Biochem.* **42**, 581-589.

Nachtergael, I., Vertongen, P., Langer, I., Perret, J., Robberecht, P., & Waelbroeck, M. (2003). Evidence for a direct interaction between the Thr11 residue of vasoactive intestinal polypeptide and Tyr184 located in the first extracellular loop of the VPAC2 receptor. *Biochem. J.* **370**, 1003-1009.

Nakata, M., Kohno, D., Shintani, N., Nemoto, Y., Hashimoto, H., Baba, A., & Yada, T. (2004). PACAP deficient mice display reduced carbohydrate intake and PACAP activates NPY-containing neurons in the rat hypothalamic arcuate nucleus. *Neurosci. Lett.* **370**, 252-256.

Naruse, S., Yasui, A., Kishida, S., Kadowaki, M., Hoshino, M., Ozaki, T., Robberecht, P., Christophe, J., Yanaihara, C., & Yanaihara, N. (1986). Helodermin has a VIP-like effect upon canine blood flow. *Peptides* **7 Suppl 1**, 237-240.

Nicole, P., Lins, L., Rouyer-Fessard, C., Drouot, C., Fulcrand, P., Thomas, A., Couvineau, A., Martinez, J., Brasseur, R., & Laburthe, M. (2000). Identification of key residues for interaction of vasoactive intestinal peptide with human VPAC1 and VPAC2 receptors and development of a highly selective VPAC1 receptor agonist. Alanine scanning and molecular modeling of the peptide. *J. Biol. Chem.* **275**, 24003-24012.

O'Connell, D. & Roblin, D. (2006). Translational research in the pharmaceutical industry: from bench to bedside. *Drug Discov. Today* **11**, 833-838.

O'Donnell, M., Garippa, R. J., Rinaldi, N., Selig, W. M., Simko, B., Renzetti, L., Tannu, S. A., Wasserman, M. A., Welton, A., & Bolin, D. R. (1994). Ro 25-1553: a novel, long-acting vasoactive intestinal peptide agonist. Part I: In vitro and in vivo bronchodilator studies. *J. Pharmacol. Exp. Ther.* **270**, 1282-1288.

O'Dorisio, M. S., Hermina, N. S., O'Dorisio, T. M., & Balcerzak, S. P. (1981). Vasoactive intestinal polypeptide modulation of lymphocyte adenylate cyclase. *J. Immunol.* **127**, 2551-2554.

Oettling, G., Bruchelt, G., Lohmann, F., Teufel, M., Niethammer, D., Treuner, J., & Drews, U. (1990). Vasoactive intestinal polypeptide (VIP) induces calcium mobilization in the human neuroblastoma cell line SK-N-SH. *Cancer Lett.* **50**, 203-207.

Ogi, K., Kimura, C., Onda, H., Arimura, A., & Fujino, M. (1990). Molecular cloning and characterization of cDNA for the precursor of rat pituitary adenylate cyclase activating polypeptide (PACAP). *Biochem. Biophys. Res. Commun.* **173**, 1271-1279.

Ogi, K., Miyamoto, Y., Masuda, Y., Habata, Y., Hosoya, M., Ohtaki, T., Masuo, Y., Onda, H., & Fujino, M. (1993). Molecular cloning and functional expression of a cDNA encoding a human pituitary adenylate cyclase activating polypeptide receptor. *Biochem. Biophys. Res. Commun.* **196**, 1511-1521.

Ohsawa, K., Hayakawa, Y., Nishizawa, M., Yamagami, T., Yamamoto, H., Yanaihara, N., & Okamoto, H. (1985). Synergistic stimulation of VIP/PHM-27 gene expression by cyclic AMP and phorbol esters in human neuroblastoma cells. *Biochem. Biophys. Res. Commun.* **132**, 885-891.

Ohtaki, H., Nakamachi, T., Dohi, K., Aizawa, Y., Takaki, A., Hodoyama, K., Yofu, S., Hashimoto, H., Shintani, N., Baba, A., Kopf, M., Iwakura, Y., Matsuda, K., Arimura, A., & Shioda, S. (2006). Pituitary adenylate cyclase-activating polypeptide (PACAP) decreases ischemic neuronal cell death in association with IL-6. *Proc. Natl. Acad. Sci. U.S.A.* **103**, 7488-7493.

Ohtaki, T., Watanabe, T., Ishibashi, Y., Kitada, C., Tsuda, M., Gottschall, P. E., Arimura, A., & Fujino, M. (1990). Molecular identification of receptor for pituitary adenylate cyclase activating polypeptide. *Biochem. Biophys. Res. Commun.* **171**, 838-844.

Okazaki, K., Itoh, Y., Ogi, K., Ohkubo, S., & Onda, H. (1995). Characterization of murine PACAP mRNA. *Peptides* **16**, 1295-1299.

Okazaki, K., Kimura, C., Kosaka, T., Watanabe, T., Ohkubo, S., Ogi, K., Kitada, C., Onda, H., & Fujino, M. (1992). Expression of human pituitary adenylate cyclase activating polypeptide (PACAP) cDNA in CHO cells and characterization of the products. *FEBS Lett.* **298**, 49-56.

Onoue, S., Endo, K., Ohshima, K., Yajima, T., & Kashimoto, K. (2002a). The neuropeptide PACAP attenuates beta-amyloid (1-42)-induced toxicity in PC12 cells. *Peptides* **23**, 1471-1478.

Onoue, S., Matsumoto, A., Nagano, Y., Ohshima, K., Ohmori, Y., Yamada, S., Kimura, R., Yajima, T., & Kashimoto, K. (2004). Alpha-helical structure in the C-terminus of vasoactive intestinal peptide: functional and structural consequences. *Eur. J. Pharmacol.* **485**, 307-316.

Onoue, S., Ohshima, K., Endo, K., Yajima, T., & Kashimoto, K. (2002b). PACAP protects neuronal PC12 cells from the cytotoxicity of human prion protein fragment 106-126. *FEBS Lett.* **522**, 65-70.

Onoue, S., Waki, Y., Nagano, Y., Satoh, S., & Kashimoto, K. (2001). The neuromodulatory effects of VIP/PACAP on PC-12 cells are associated with their N-terminal structures. *Peptides* **22**, 867-872.

Opp, M. R. (2006). Sleep and psychoneuroimmunology. *Neurol. Clin.* **24**, 493-506.

Ottaviani, E. & Franceschi, C. (1996). The neuroimmunology of stress from invertebrates to man. *Prog. Neurobiol.* **48**, 421-440.

Otto, C., Hein, L., Brede, M., Jahns, R., Engelhardt, S., Grone, H. J., & Schutz, G. (2004). Pulmonary hypertension and right heart failure in pituitary adenylate cyclase-activating polypeptide type I receptor-deficient mice. *Circulation* **110**, 3245-3251.

Otto, C., Kovalchuk, Y., Wolfer, D. P., Gass, P., Martin, M., Zuschratter, W., Grone, H. J., Kellendonk, C., Tronche, F., Maldonado, R., Lipp, H. P., Konnerth, A., & Schutz, G. (2001). Impairment of mossy fiber long-term potentiation and associative learning in pituitary adenylate cyclase activating polypeptide type I receptor-deficient mice. *J. Neurosci.* **21**, 5520-5527.

Pan, C. Q., Li, F., Tom, I., Wang, W., Dumas, M., Froland, W., Yung, S. L., Li, Y., Roczniak, S., Claus, T. H., Wang, J. Y., & Whelan, J. P. (2006). Engineering Novel VPAC2 Selective Agonists with Improved Stability and Glucose Lowering Activity In Vivo. *J. Pharmacol. Exp. Ther.* DOI:10.1124/jpet.106.112276

Pandi-Perumal, S. R., Zisapel, N., Srinivasan, V., & Cardinali, D. P. (2005). Melatonin and sleep in aging population. *Exp. Gerontol.* **40**, 911-925.

Pandol, S. J., Dharmsathaphorn, K., Schoeffield, M. S., Vale, W., & Rivier, J. (1986). Vasoactive intestinal peptide receptor antagonist [4Cl-D-Phe6, Leu17] VIP. *Am. J. Physiol.* **250**, G553-G557.

Pantaloni, C., Brabet, P., Bilanges, B., Dumuis, A., Houssami, S., Spengler, D., Bockaert, J., & Journot, L. (1996). Alternative splicing in the N-terminal extracellular domain of the pituitary adenylate cyclase-activating polypeptide

(PACAP) receptor modulates receptor selectivity and relative potencies of PACAP-27 and PACAP-38 in phospholipase C activation. *J. Biol. Chem.* **271**, 22146-22151.

Paxinos & Franklin (2001). The Mouse Brain in Stereotaxic Coordinates (2nd edition), Academic Press, London.

Perez, V., Bouschet, T., Fernandez, C., Bockaert, J., & Journot, L. (2005). Dynamic reorganization of the astrocyte actin cytoskeleton elicited by cAMP and PACAP: a role for phosphatidylInositol 3-kinase inhibition. *Eur. J. Neurosci.* **21**, 26-32.

Pierce, K. L., Premont, R. T., & Lefkowitz, R. J. (2002). Seven-transmembrane receptors. *Nat. Rev. Mol. Cell. Biol.* **3**, 639-650.

Piggins, H. D., Antle, M. C., & Rusak, B. (1995). Neuropeptides phase shift the mammalian circadian pacemaker. *J. Neurosci.* **15**, 5612-5622.

Piggins, H. D. & Cutler, D. J. (2003). The roles of vasoactive intestinal polypeptide in the mammalian circadian clock. *J. Endocrinol.* **177**, 7-15.

Pilzer, I. & Gozes, I. (2006a). A splice variant to PACAP receptor that is involved in spermatogenesis is expressed in astrocytes. *Ann. N.Y. Acad. Sci.* **1070**, 484-490.

Pilzer, I. & Gozes, I. (2006b). VIP provides cellular protection through a specific splice variant of the PACAP receptor: a new neuroprotection target. *Peptides* **27**, 2867-2876.

Piper, P. J., Said, S. I., & Vane, J. R. (1970). Effects on smooth muscle preparations of unidentified vasoactiv peptides from intestine and lung. *Nature* **225**, 1144-1146.

Pisegna, J. R., Moody, T. W., & Wank, S. A. (1996). Differential signaling and immediate-early gene activation by four splice variants of the human pituitary adenylate cyclase-activating polypeptide receptor (hPACAP-R). *Ann. N.Y. Acad. Sci.* **805**, 54-64.

Pisegna, J. R. & Wank, S. A. (1993). Molecular cloning and functional expression of the pituitary adenylate cyclase-activating polypeptide type I receptor. *Proc. Natl. Acad. Sci. U.S.A.* **90**, 6345-6349.

Pisegna, J. R. & Wank, S. A. (1996). Cloning and characterization of the signal transduction of four splice variants of the human pituitary adenylate cyclase activating polypeptide receptor. Evidence for dual coupling to adenylate cyclase and phospholipase C. *J. Biol. Chem.* **271**, 17267-17274.

Porter, R. H., Malcolm, C. S., Allen, N. H., Lamb, H., Revell, D. F., & Sheardown, M. J. (2001). Agonist-induced functional desensitization of recombinant human 5-HT2 receptors expressed in CHO-K1 cells. *Biochem. Pharmacol.* **62**, 431-438.

Power, R. F., Bishop, A. E., Wharton, J., Inyama, C. O., Jackson, R. H., Bloom, S. R., & Polak, J. M. (1988). Anatomical distribution of vasoactive intestinal peptide binding sites in peripheral tissues investigated by in vitro autoradiography. *Ann. N.Y. Acad. Sci.* **527**, 314-325.

Pozo, D. & Delgado, M. (2004). The many faces of VIP in neuroimmunology: a cytokine rather a neuropeptide? *FASEB J.* **18**, 1325-1334.

Pozo, D., Delgado, M., Martinez, C., Gomariz, R. P., Guerrero, J. M., & Calvo, J. R. (1997). Functional characterization and mRNA expression of pituitary adenylate cyclase activating polypeptide (PACAP) type I receptors in rat peritoneal macrophages. *Biochim. Biophys. Acta* **1359**, 250-262.

Preziosi, P. (2004). Science, pharmacoeconomics and ethics in drug R&D: a sustainable future scenario? *Nat. Rev. Drug Discov.* **3**, 521-526.

Prieto, J. C., Guerrero, J. M., De Miguel, C., & Goberna, R. (1981). Interaction of vasoactive intestinal peptide with a cell line (HeLa) derived from human carcinoma of the cervix: binding to specific sites and stimulation of adenylate cyclase. *Mol. Cell Biochem.* **37**, 167-176.

Prolo, L. M., Takahashi, J. S., & Herzog, E. D. (2005). Circadian rhythm generation and entrainment in astrocytes. *J. Neurosci.* **25**, 404-408.

Provencio, I., Rodriguez, I. R., Jiang, G., Hayes, W. P., Moreira, E. F., & Rollag, M. D. (2000). A novel human opsin in the inner retina. *J. Neurosci.* **20**, 600-605.

Ralph, M. R., Foster, R. G., Davis, F. C., & Menaker, M. (1990). Transplanted suprachiasmatic nucleus determines circadian period. *Science* **247**, 975-978.

Ralph, M. R. & Menaker, M. (1988). A mutation of the circadian system in golden hamsters. *Science* **241**, 1225-1227.

Ramirez-Cardenas, R., Prieto, J. C., Guerrero, J. M., & Goberna, R. (1981). Guanyl nucleotide regulation of vasoactive intestinal peptide interaction with rat liver membranes. *Rev. Esp. Fisiol.* **37**, 9-16.

Rangon, C. M., Dicou, E., Goursaud, S., Mounien, L., Jegou, S., Janet, T., Muller, J. M., Lelievre, V., & Gressens, P. (2006). Mechanisms of VIP-induced neuroprotection against neonatal excitotoxicity. *Ann. N.Y. Acad. Sci.* **1070**, 512-517.

Raufman, J. P., Jensen, R. T., Sutliff, V. E., Pisano, J. J., & Gardner, J. D. (1982). Actions of Gila monster venom on dispersed acini from guinea pig pancreas. *Am. J. Physiol.* **242**, G470-G474.

Reddy, V. B., Iuga, A. O., Kounga, K., & Lerner, E. A. (2006). Functional analysis of recombinant mutants of maxadilan with a PAC1 receptor-expressing melanophore cell line. *J. Biol. Chem.* **281**, 16197-16201.

Reed, H. E., Cutler, D. J., Brown, T. M., Brown, J., Coen, C. W., & Piggins, H. D. (2002). Effects of vasoactive intestinal polypeptide on neurones of the rat suprachiasmatic nuclei in vitro. *J. Neuroendocrinol.* **14**, 639-646.

Reed, H. E., Meyer-Spasche, A., Cutler, D. J., Coen, C. W., & Piggins, H. D. (2001). Vasoactive intestinal polypeptide (VIP) phase-shifts the rat suprachiasmatic nucleus clock in vitro. *Eur. J. Neurosci.* **13**, 839-843.

Reglodi, D., Lubics, A., Tamas, A., Szalontay, L., & Lengvari, I. (2004). Pituitary adenylate cyclase activating polypeptide protects dopaminergic neurons and improves behavioral deficits in a rat model of Parkinson's disease. *Behav. Brain Res.* **151**, 303-312.

Reglodi, D., Somogyvari-Vigh, A., Vigh, S., Kozicz, T., & Arimura, A. (2000). Delayed systemic administration of PACAP38 is neuroprotective in transient middle cerebral artery occlusion in the rat. *Stroke* **31**, 1411-1417.

Reglodi, D., Tamas, A., Somogyvari-Vigh, A., Szanto, Z., Kertes, E., Lenard, L., Arimura, A., & Lengvari, I. (2002). Effects of pretreatment with PACAP on the infarct size and functional outcome in rat permanent focal cerebral ischemia. *Peptides* **23**, 2227-2234.

Reubi, J. C. (2000). In vitro evaluation of VIP/PACAP receptors in healthy and diseased human tissues. Clinical implications. *Ann. N.Y. Acad. Sci.* **921**, 1-25.

Reubi, J. C., Laderach, U., Waser, B., Gebbers, J. O., Robberecht, P., & Laissue, J. A. (2000). Vasoactive intestinal peptide/pituitary adenylate cyclase-activating peptide receptor subtypes in human tumors and their tissues of origin. *Cancer Res.* **60**, 3105-3112.

Robberecht, P., Conlon, T. P., & Gardner, J. D. (1976). Interaction of porcine vasoactive intestinal peptide with dispersed pancreatic acinar cells from the guinea pig. Structural requirements for effects of vasoactive intestinal peptide and secretin on cellular adenosine 3':5'-monophosphate. *J. Biol. Chem.* **251**, 4635-4639.

Robberecht, P., De Neef, P., Gourlet, P., Cauvin, A., Coy, D. H., & Christophe, J. (1989). Pharmacological characterization of the novel helodermin/VIP receptor present in human SUP-T1 lymphoma cell membranes. *Regul. Pept.* **26**, 117-126.

Robberecht, P., Gourlet, P., De Neef, P., Woussen-Colle, M. C., Vandermeers-Piret, M. C., Vandermeers, A., & Christophe, J. (1992). Structural requirements for the occupancy of pituitary adenylate-cyclase-activating-peptide (PACAP) receptors and adenylate cyclase activation in human neuroblastoma NB-OK-1 cell membranes. Discovery of PACAP(6-38) as a potent antagonist. *Eur. J. Biochem.* **207**, 239-246.

Robberecht, P., Waelbroeck, M., De Neef, P., Tastenoy, M., Gourlet, P., Cogniaux, J., & Christophe, J. (1988). A new type of functional VIP receptor has an affinity for helodermin in human SUP-T1 lymphoblasts. *FEBS Lett.* **228**, 351-355.

Robberecht, P., Waelbroeck, M., Dehaye, J. P., Winand, J., Vandermeers, A., Vandermeers-Piret, M. C., & Christophe, J. (1984). Evidence that helodermin, a newly extracted peptide from Gila monster venom, is a member of the secretin/VIP/PHI family of peptides with an original pattern of biological properties. *FEBS Lett.* **166**, 277-282.

Robberecht, P., Woussen-Colle, M. C., De Neef, P., Gourlet, P., Buscail, L., Vandermeers, A., Vandermeers-Piret, M. C., & Christophe, J. (1991). The two forms of the pituitary adenylate cyclase activating polypeptide (PACAP (1-27) and PACAP (1-38)) interact with distinct receptors on rat pancreatic AR 4-2J cell membranes. *FEBS Lett.* **286**, 133-136.

Roberts, G. W., Woodhams, P. L., Bryant, M. G., Crow, T. J., Bloom, S. R., & Polak, J. M. (1980). VIP in the rat brain: evidence for a major pathway linking the amygdala and hypothalamus via the stria terminalis. *Histochemistry* **65**, 103-119.

Said, S. I. (1984). Vasoactive intestinal polypeptide (VIP): current status. *Peptides* **5**, 143-150.

Said, S. I. & Faloona, G. R. (1975). Elevated plasma and tissue levels of vasoactive intestinal polypeptide in the watery-diarrhea syndrome due to pancreatic, bronchogenic and other tumors. *N. Engl. J. Med.* **293**, 155-160.

Said, S. I. & Mutt, V. (1970). Polypeptide with broad biological activity: isolation from small intestine. *Science* **169**, 1217-1218.

Salomon, R., Couvineau, A., Rouyer-Fessard, C., Voisin, T., Lavallee, D., Blais, A., Darmoul, D., & Laburthe, M. (1993). Characterization of a common VIP-PACAP receptor in human small intestinal epithelium. *Am. J. Physiol.* **264**, E294-E300.

Satoh, Y., Kawai, H., Kudo, N., Kawashima, Y., & Mitsumoto, A. (2006). Temperature rhythm reentrains faster than locomotor rhythm after a light phase shift. *Physiol. Behav.* **88**, 404-410.

Sauvage, M., Brabet, P., Holsboer, F., Bockaert, J., & Steckler, T. (2000). Mild deficits in mice lacking pituitary adenylate cyclase-activating polypeptide receptor type 1 (PAC1) performing on memory tasks. *Brain Res. Mol. Brain Res.* **84**, 79-89.

Sawaki, Y., Nihonmatsu, I., & Kawamura, H. (1984). Transplantation of the neonatal suprachiasmatic nuclei into rats with complete bilateral suprachiasmatic lesions. *Neurosci. Res.* **1**, 67-72.

Schwartz, C. J., Kimberg, D. V., Sheerin, H. E., Field, M., & Said, S. I. (1974). Vasoactive intestinal peptide stimulation of adenylate cyclase and active electrolyte secretion in intestinal mucosa. *J. Clin. Invest.* **54**, 536-544.

Schwartz, W. J. & Gainer, H. (1977). Suprachiasmatic nucleus: use of 14C-labeled deoxyglucose uptake as a functional marker. *Science* **197**, 1089-1091.

Sexton, P. M., Morfis, M., Tilakaratne, N., Hay, D. L., Udawela, M., Christopoulos, G., & Christopoulos, A. (2006). Complexing receptor pharmacology: modulation of family B G protein-coupled receptor function by RAMPs. *Ann. N.Y. Acad. Sci.* **1070**, 90-104.

Shaffer, M. M. & Moody, T. W. (1986). Autoradiographic visualization of CNS receptors for vasoactive intestinal peptide. *Peptides* **7**, 283-288.

Shen, S., Spratt, C., Sheward, W. J., Kallo, I., West, K., Morrison, C. F., Coen, C. W., Marston, H. M., & Harmar, A. J. (2000). Overexpression of the human VPAC2 receptor in the suprachiasmatic nucleus alters the circadian phenotype of mice. *Proc. Natl. Acad. Sci. U.S.A.* **97**, 11575-11580.

Sherwood, N. M., Krueckl, S. L., & McRory, J. E. (2000). The origin and function of the pituitary adenylate cyclase-activating polypeptide (PACAP)/glucagon superfamily. *Endocr. Rev.* **21**, 619-670.

Sheward, W. J., Lutz, E. M., & Harmar, A. J. (1995). The distribution of vasoactive intestinal peptide2 receptor messenger RNA in the rat brain and pituitary gland as assessed by in situ hybridization. *Neuroscience* **67**, 409-418.

Shibata, S., Oomura, Y., Kita, H., & Hattori, K. (1982). Circadian rhythmic changes of neuronal activity in the suprachiasmatic nucleus of the rat hypothalamic slice. *Brain Res.* **247**, 154-158.

Shinohara, K., Funabashi, T., & Kimura, F. (1999). Temporal profiles of vasoactive intestinal polypeptide precursor mRNA and its receptor mRNA in the rat suprachiasmatic nucleus. *Brain Res. Mol. Brain Res.* **63**, 262-267.

Shinohara, K., Funabashi, T., Mitushima, D., & Kimura, F. (2000). Effects of gap junction blocker on vasopressin and vasoactive intestinal polypeptide rhythms in the rat suprachiasmatic nucleus in vitro. *Neurosci. Res.* **38**, 43-47.

Shinohara, K., Honma, S., Katsuno, Y., Abe, H., & Honma, K. (1995). Two distinct oscillators in the rat suprachiasmatic nucleus in vitro. *Proc. Natl. Acad. Sci. U.S.A.* **92**, 7396-7400.

Shinohara, K., Tominaga, K., Isobe, Y., & Inouye, S. T. (1993). Photic regulation of peptides located in the ventrolateral subdivision of the suprachiasmatic nucleus of the rat: daily variations of vasoactive intestinal polypeptide, gastrin-releasing peptide, and neuropeptide Y. *J. Neurosci.* **13**, 793-800.

Shintani, N., Mori, W., Hashimoto, H., Imai, M., Tanaka, K., Tomimoto, S., Hirose, M., Kawaguchi, C., & Baba, A. (2002). Defects in reproductive functions in PACAP-deficient female mice. *Regul. Pept.* **109**, 45-48.

Shioda, S., Ozawa, H., Dohi, K., Mizushima, H., Matsumoto, K., Nakajo, S., Takaki, A., Zhou, C. J., Nakai, Y., & Arimura, A. (1998). PACAP protects hippocampal neurons against apoptosis: involvement of JNK/SAPK signaling pathway. *Ann. N.Y. Acad. Sci.* **865**, 111-117.

Shivers, B. D., Gorcs, T. J., Gottschall, P. E., & Arimura, A. (1991). Two high affinity binding sites for pituitary adenylate cyclase-activating polypeptide have different tissue distributions. *Endocrinology* **128**, 3055-3065.

Shoge, K., Mishima, H. K., Saitoh, T., Ishihara, K., Tamura, Y., Shiomi, H., & Sasa, M. (1998). Protective effects of vasoactive intestinal peptide against delayed glutamate neurotoxicity in cultured retina. *Brain Res.* **809**, 127-136.

Shoge, K., Mishima, H. K., Saitoh, T., Ishihara, K., Tamura, Y., Shiomi, H., & Sasa, M. (1999). Attenuation by PACAP of glutamate-induced neurotoxicity in cultured retinal neurons. *Brain Res.* **839**, 66-73.

Shreeve, S. M., Sreedharan, S. P., Hacker, M. P., Gannon, D. E., & Morgan, M. J. (2000). VIP activates G(s) and G(i3) in rat alveolar macrophages and G(s) in HEK293 cells transfected with the human VPAC(1) receptor. *Biochem. Biophys. Res. Commun.* **272**, 922-928.

Skoglosa, Y., Lewen, A., Takei, N., Hillered, L., & Lindholm, D. (1999). Regulation of pituitary adenylate cyclase activating polypeptide and its receptor type 1 after traumatic brain injury: comparison with brain-derived neurotrophic factor and the induction of neuronal cell death. *Neuroscience* **90**, 235-247.

Sollars, P. J., Ogilvie, M. D., Rea, M. A., & Pickard, G. E. (2002). 5-HT1B receptor knockout mice exhibit an enhanced response to constant light. *J. Biol. Rhythms* **17**, 428-437.

Somogyvari-Vigh, A., Svoboda-Teet, J., Vigh, S., & Arimura, A. (1998). Is an intravenous bolus injection required prior to initiating slow intravenous infusion of PACAP38 for prevention of neuronal death induced by global ischemia? The possible presence of a binding protein for PACAP38 in blood. *Ann. N.Y. Acad. Sci.* **865**, 595-600.

Spengler, D., Waeber, C., Pantaloni, C., Holsboer, F., Bockaert, J., Seeburg, P. H., & Journot, L. (1993). Differential signal transduction by five splice variants of the PACAP receptor. *Nature* **365**, 170-175.

Sreedharan, S. P., Patel, D. R., Huang, J. X., & Goetzl, E. J. (1993). Cloning and functional expression of a human neuroendocrine vasoactive intestinal peptide receptor. *Biochem. Biophys. Res. Commun.* **193**, 546-553.

Sreedharan, S. P., Patel, D. R., Xia, M., Ichikawa, S., & Goetzl, E. J. (1994). Human vasoactive intestinal peptide 1 receptors expressed by stable transfectants couple to two distinct signaling pathways. *Biochem. Biophys. Res. Commun.* **203**, 141-148.

Stacey, M., Lin, H. H., Gordon, S., & McKnight, A. J. (2000). LNB-TM7, a group of seven-transmembrane proteins related to family-B G-protein-coupled receptors. *Trends Biochem. Sci.* **25**, 284-289.

Staun-Olsen, P., Ottesen, B., Gammeltoft, S., & Fahrenkrug, J. (1985). The regional distribution of receptors for vasoactive intestinal polypeptide (VIP) in the rat central nervous system. *Brain Res.* **330**, 317-321.

Stephan, F. K. & Zucker, I. (1972). Circadian rhythms in drinking behavior and locomotor activity of rats are eliminated by hypothalamic lesions. *Proc. Natl. Acad. Sci. U.S.A.* **69**, 1583-1586.

Summers, M. A., O'Dorisio, M. S., Cox, M. O., Lara-Marquez, M., & Goetzl, E. J. (2003). A lymphocyte-generated fragment of vasoactive intestinal peptide with VPAC1 agonist activity and VPAC2 antagonist effects. *J. Pharmacol. Exp. Ther.* **306**, 638-645.

Suzuki, N., Harada, M., Hosoya, M., & Fujino, M. (1994). Enhanced production of pituitary adenylate-cyclase-activating polypeptide by 1, N6-dibutyryladenosine 3',5'-monophosphate, phorbol 12-myristate 13-acetate and by the polypeptide itself in human neuroblastoma cells, IMR-32. *Eur. J. Biochem.* **223**, 147-153.

Svoboda, M., De Neef, P., Tastenoy, M., & Christophe, J. (1988). Molecular characteristics and evidence for internalization of vasoactive-intestinal-peptide (VIP) receptors in the tumoral rat-pancreatic acinar cell line AR 4-2 J. *Eur. J. Biochem.* **176**, 707-713.

Svoboda, M., Tastenoy, M., Ciccarelli, E., Stievenart, M., & Christophe, J. (1993). Cloning of a splice variant of the pituitary adenylate cyclase-activating polypeptide (PACAP) type I receptor. *Biochem. Biophys. Res. Commun.* **195**, 881-888.

Svoboda, M., Tastenoy, M., Van Rampelbergh, J., Goossens, J. F., De Neef, P., Waelbroeck, M., & Robberecht, P. (1994). Molecular cloning and functional characterization of a human VIP receptor from SUP-T1 lymphoblasts. Biochem. *Biophys. Res. Commun.* **205**, 1617-1624.

Swift, P. G., Bloom, S. R., & Harris, F. (1975). Watery diarrhoea and ganglioneuroma with secretion of vasoactive intestinal peptide. *Arch. Dis. Child* **50**, 896-899.

Symes, A., Lewis, S., Corpus, L., Rajan, P., Hyman, S. E., & Fink, J. S. (1994). STAT proteins participate in the regulation of the vasoactive intestinal peptide gene by the ciliary neurotrophic factor family of cytokines. *Mol. Endocrinol.* **8**, 1750-1763.

Takahashi, K., Tsuchida, K., Tanabe, Y., Masu, M., & Nakanishi, S. (1993). Role of the large extracellular domain of metabotropic glutamate receptors in agonist selectivity determination. *J. Biol. Chem.* **268**, 19341-19345.

Takeda, S., Kadowaki, S., Haga, T., Takaesu, H., & Mitaku, S. (2002). Identification of G protein-coupled receptor genes from the human genome sequence. *FEBS Lett.* **520**, 97-101.

Tan, Y. V., Couvineau, A., Murail, S., Ceraudo, E., Neumann, J. M., Lacapere, J. J., & Laburthe, M. (2006). Peptide agonist docking in the N-terminal ectodomain of a class II G protein-coupled receptor, the VPAC1 receptor. Photoaffinity, NMR, and molecular modeling. *J. Biol. Chem.* **281**, 12792-12798.

Tatemoto, K. & Mutt, V. (1981). Isolation and characterization of the intestinal peptide porcine PHI (PHI-27), a new member of the glucagon--secretin family. *Proc. Natl. Acad. Sci. U.S.A.* **78**, 6603-6607.

Tatsuno, I., Gottschall, P. E., Koves, K., & Arimura, A. (1990). Demonstration of specific binding sites for pituitary adenylate cyclase activating polypeptide (PACAP) in rat astrocytes. *Biochem. Biophys. Res. Commun.* **168**, 1027-1033.

Tatsuno, I., Uchida, D., Tanaka, T., Saeki, N., Hirai, A., Saito, Y., Moro, O., & Tajima, M. (2001). Maxadilan specifically interacts with PAC1 receptor, which is a dominant form of PACAP/VIP family receptors in cultured rat cortical neurons. *Brain Res.* **889**, 138-148.

Tatsuno, I., Yada, T., Vigh, S., Hidaka, H., & Arimura, A. (1992). Pituitary adenylate cyclase activating polypeptide and vasoactive intestinal peptide increase cytosolic free calcium concentration in cultured rat hippocampal neurons. *Endocrinology* **131**, 73-81.

Taylor, D. P. & Pert, C. B. (1979). Vasoactive intestinal polypeptide: specific binding to rat brain membranes. *Proc. Natl. Acad. Sci. U.S.A.* **76**, 660-664.

Teng, B. Q., Grider, J. R., & Murthy, K. S. (2001). Identification of a VIP-specific receptor in guinea pig tenia coli. *Am. J. Physiol. Gastrointest. Liver Physiol.* **281**, G718-G725.

Theriault, Y., Boulanger, Y., & St Pierre, S. (1991). Structural determination of the vasoactive intestinal peptide by two-dimensional H-NMR spectroscopy. *Biopolymers* **31**, 459-464.

Tsukada, T., Fink, J. S., Mandel, G., & Goodman, R. H. (1987). Identification of a region in the human vasoactive intestinal polypeptide gene responsible for regulation by cyclic AMP. *J. Biol. Chem.* **262**, 8743-8747.

Tsukada, T., Horovitch, S. J., Montminy, M. R., Mandel, G., & Goodman, R. H. (1985). Structure of the human vasoactive intestinal polypeptide gene. *DNA* **4**, 293-300.

Tsutsumi, M., Claus, T. H., Liang, Y., Li, Y., Yang, L., Zhu, J., Dela, C. F., Peng, X., Chen, H., Yung, S. L., Hamren, S., Livingston, J. N., & Pan, C. Q. (2002). A potent and highly selective VPAC2 agonist enhances glucose-induced insulin release and glucose disposal: a potential therapy for type 2 diabetes. *Diabetes* **51**, 1453-1460.

Turek, F. W. & Gillette, M. U. (2004). Melatonin, sleep, and circadian rhythms: rationale for development of specific melatonin agonists. *Sleep Med.* **5**, 523-532.

Turner, J. T., Jones, S. B., & Bylund, D. B. (1986). A fragment of vasoactive intestinal peptide, VIP(10-28), is an antagonist of VIP in the colon carcinoma cell line, HT29. *Peptides* **7**, 849-854.

Uchida, D., Arimura, A., Somogyvari-Vigh, A., Shioda, S., & Banks, W. A. (1996). Prevention of ischemia-induced death of hippocampal neurons by pituitary adenylate cyclase activating polypeptide. *Brain Res.* **736**, 280-286.

Uchida, D., Tatsuno, I., Tanaka, T., Hirai, A., Saito, Y., Moro, O., & Tajima, M. (1998). Maxadilan is a specific agonist and its deleted peptide (M65) is a specific antagonist for PACAP type 1 receptor. *Ann. N.Y. Acad. Sci.* **865**, 253-258.

Uddman, R., Goadsby, P. J., Jansen, I., & Edvinsson, L. (1993). PACAP, a VIP-like peptide: immunohistochemical localization and effect upon cat pial arteries and cerebral blood flow. *J. Cereb. Blood Flow Metab.* **13**, 291-297.

Unson, C. G. (2002). Molecular determinants of glucagon receptor signaling. *Biopolymers* **66**, 218-235.

Usdin, T. B., Bonner, T. I., & Mezey, E. (1994). Two receptors for vasoactive intestinal polypeptide with similar specificity and complementary distributions. *Endocrinology* **135**, 2662-2680.

Van Geldre, L. A. & Lefebvre, R. A. (2004). Interaction of NO and VIP in gastrointestinal smooth muscle relaxation. *Curr. Pharm. Des.* **10**, 2483-2497.

Van Rampelbergh, J., Poloczek, P., Francoys, I., Delporte, C., Winand, J., Robberecht, P., & Waelbroeck, M. (1997). The pituitary adenylate cyclase activating polypeptide (PACAP I) and VIP (PACAP II VIP1) receptors stimulate inositol phosphate synthesis in transfected CHO cells through interaction with different G proteins. *Biochim. Biophys. Acta* **1357**, 249-255.

Vandermeers, A., Vandermeers-Piret, M. C., Robberecht, P., Waelbroeck, M., Dehaye, J. P., Winand, J., & Christophe, J. (1984). Purification of a novel pancreatic secretory factor (PSF) and a novel peptide with VIP- and secretin-like properties (helodermin) from Gila monster venom. *FEBS Lett.* **166**, 273-276.

Vanneste, G., Robberecht, P., & Lefebvre, R. A. (2004). Inhibitory pathways in the circular muscle of rat jejunum. *Br. J. Pharmacol.* **143**, 107-118.

Vaudry, D., Gonzalez, B. J., Basille, M., Yon, L., Fournier, A., & Vaudry, H. (2000). Pituitary adenylate cyclase-activating polypeptide and its receptors: from structure to functions. *Pharmacol. Rev.* **52**, 269-324.

Vaudry, D., Pamantung, T. F., Basille, M., Rousselle, C., Fournier, A., Vaudry, H., Beauvillain, J. C., & Gonzalez, B. J. (2002a). PACAP protects cerebellar granule neurons against oxidative stress-induced apoptosis. *Eur. J. Neurosci.* **15**, 1451-1460.

Vaudry, D., Rousselle, C., Basille, M., Falluel-Morel, A., Pamantung, T. F., Fontaine, M., Fournier, A., Vaudry, H., & Gonzalez, B. J. (2002b). Pituitary adenylate cyclase-activating polypeptide protects rat cerebellar granule neurons against ethanol-induced apoptotic cell death. *Proc. Natl. Acad. Sci. U.S.A.* **99**, 6398-6403.

Vertongen, P., Devalck, C., Sariban, E., De Laet, M. H., Martelli, H., Paraf, F., Helardot, P., & Robberecht, P. (1996). Pituitary adenylate cyclase activating peptide and its receptors are expressed in human neuroblastomas. *J. Cell. Physiol.* **167**, 36-46.

Vertongen, P., Langlet, C., Langer, I., Gaspard, N., & Robberecht, P. (2004). Ac His1 [D-Phe2, K15, R16, L27] VIP (3-7)/GRF (8-27)--a VPAC1 receptor antagonist--is an inverse agonist on two constitutively active truncated VPAC1 receptors. *Peptides* **25**, 1943-1949.

Vertongen, P., Schiffmann, S. N., Gourlet, P., & Robberecht, P. (1998). Autoradiographic visualization of the receptor subclasses for vasoactive intestinal polypeptide (VIP) in rat brain. *Ann. N.Y. Acad. Sci.* **865**, 412-415.

Vertongen, P., Solano, R. M., Juarranz, M. G., Perret, J., Waelbroeck, M., & Robberecht, P. (2001). Proline residue 280 in the second extracellular loop (EC2) of the VPAC2 receptor is essential for the receptor structure. *Peptides* **22**, 1363-1370.

Vink, J., Auth, J., Abebe, D. T., Brenneman, D. E., & Spong, C. Y. (2005). Novel peptides prevent alcohol-induced spatial learning deficits and proinflammatory cytokine release in a mouse model of fetal alcohol syndrome. *Am. J. Obstet. Gynecol.* **193**, 825-829.

Voice, J. K., Dorsam, G., Lee, H., Kong, Y., & Goetzl, E. J. (2001). Allergic diathesis in transgenic mice with constitutive T cell expression of inducible vasoactive intestinal peptide receptor. *FASEB J.* **15**, 2489-2496.

Waelbroeck, M., Robberecht, P., Coy, D. H., Camus, J. C., De Neef, P., & Christophe, J. (1985). Interaction of growth hormone-releasing factor (GRF) and 14 GRF analogs with vasoactive intestinal peptide (VIP) receptors of rat pancreas. Discovery of (N-Ac-Tyr1,D-Phe2)-GRF(1-29)-NH2 as a VIP antagonist. *Endocrinology* **116**, 2643-2649.

Wang, S. C., Du, B. H., Eng, J., Chang, M., Hulmes, J. D., Pan, Y. C., & Yalow, R. S. (1985). Purification of dog VIP from a single animal. *Life Sci.* **37**, 979-983.

Weaver, D. R. (1998). The suprachiasmatic nucleus: a 25-year retrospective. *J. Biol. Rhythms* **13**, 100-112.

Wietfeld, D., Heinrich, N., Furkert, J., Fechner, K., Beyermann, M., Bienert, M., & Berger, H. (2004). Regulation of the coupling to different G proteins of rat corticotropin-releasing factor receptor type 1 in human embryonic kidney 293 cells. *J. Biol. Chem.* **279**, 38386-38394.

Wray, V., Nokihara, K., & Naruse, S. (1998). Solution structure comparison of the VIP/PACAP family of peptides by NMR spectroscopy. *Ann. N.Y. Acad. Sci.* **865**, 37-44.

Xia, M., Sreedharan, S. P., Bolin, D. R., Gaufo, G. O., & Goetzl, E. J. (1997). Novel cyclic peptide agonist of high potency and selectivity for the type II vasoactive intestinal peptide receptor. *J. Pharmacol. Exp. Ther.* **281**, 629-633.

Xia, M., Sreedharan, S. P., & Goetzl, E. J. (1996). Predominant expression of type II vasoactive intestinal peptide receptors by human T lymphoblastoma cells: transduction of both Ca2+ and cyclic AMP signals. *J. Clin. Immunol.* **16**, 21-30.

Xiao, R. P., Avdonin, P., Zhou, Y. Y., Cheng, H., Akhter, S. A., Eschenhagen, T., Lefkowitz, R. J., Koch, W. J., & Lakatta, E. G. (1999). Coupling of beta2-adrenoceptor to Gi proteins and its physiological relevance in murine cardiac myocytes. *Circ. Res.* **84**, 43-52.

Yamada, H., Watanabe, M., & Yada, T. (2004). Cytosolic Ca^{2+} responses to sub-picomolar and nanomolar PACAP in pancreatic beta-cells are mediated by VPAC2 and PAC1 receptors. *Regul. Pept.* **123**, 147-153.

Yamamoto, K., Hashimoto, H., Hagihara, N., Nishino, A., Fujita, T., Matsuda, T., & Baba, A. (1998). Cloning and characterization of the mouse pituitary adenylate cyclase-activating polypeptide (PACAP) gene. *Gene* **211**, 63-69.

Yamamoto, K., Hashimoto, H., Tomimoto, S., Shintani, N., Miyazaki, J., Tashiro, F., Aihara, H., Nammo, T., Li, M., Yamagata, K., Miyagawa, J., Matsuzawa, Y., Kawabata, Y., Fukuyama, Y., Koga, K., Mori, W., Tanaka, K., Matsuda, T., & Baba, A. (2003). Overexpression of PACAP in transgenic mouse pancreatic beta-cells

enhances insulin secretion and ameliorates streptozotocin-induced diabetes. *Diabetes* **52**, 1155-1162.

Yiangou, Y., Requejo, F., Polak, J. M., & Bloom, S. R. (1986). Characterization of a novel prepro VIP derived peptide. *Biochem. Biophys. Res. Commun.* **139**, 1142-1149.

Yu, D., Seitz, P. K., Selvanayagam, P., Rajaraman, S., Townsend, C. M., Jr., & Cooper, C. W. (1992). Effects of vasoactive intestinal peptide on adenosine 3',5'-monophosphate, ornithine decarboxylase, and cell growth in a human colon cell line. *Endocrinology* **131**, 1188-1194.

Yung, S. L., Dela, C. F., Hamren, S., Zhu, J., Tsutsumi, M., Bloom, J. W., Caudle, M., Roczniak, S., Todd, T., Lemoine, L., MacDougall, M., Shanafelt, A. B., & Pan, C. Q. (2003). Generation of highly selective VPAC2 receptor agonists by high throughput mutagenesis of vasoactive intestinal peptide and pituitary adenylate cyclase-activating peptide. *J. Biol. Chem.* **278**, 10273-10281.

Zendman, A. J., Cornelissen, I. M., Weidle, U. H., Ruiter, D. J., & van Muijen, G. N. (1999). TM7XN1, a novel human EGF-TM7-like cDNA, detected with mRNA differential display using human melanoma cell lines with different metastatic potential. *FEBS Lett.* **446**, 292-298.

Zhou, C. J., Kikuyama, S., Shibanuma, M., Hirabayashi, T., Nakajo, S., Arimura, A., & Shioda, S. (2000). Cellular distribution of the splice variants of the receptor for pituitary adenylate cyclase-activating polypeptide (PAC(1)-R) in the rat brain by in situ RT-PCR. *Brain Res. Mol. Brain Res.* **75**, 150-158.

Zhou, H., Huang, J., & Murthy, K. S. (2006). Molecular cloning and functional expression of a VIP-specific receptor. *Am. J. Physiol. Gastrointest. Liver Physiol.* **291**, G728-G734.

Zhu, X., Gilbert, S., Birnbaumer, M., & Birnbaumer, L. (1994). Dual signaling potential is common among Gs-coupled receptors and dependent on receptor density. *Mol. Pharmacol.* **46**, 460-469.

Zizzo, M. G., Mule, F., & Serio, R. (2005). Mechanisms underlying the inhibitory effects induced by pituitary adenylate cyclase-activating peptide in mouse ileum. *Eur. J. Pharmacol.* **521**, 133-138.

Zusev, M. & Gozes, I. (2004). Differential regulation of activity-dependent neuroprotective protein in rat astrocytes by VIP and PACAP. *Regul. Pept.* **123**, 33-41.

Websites cited in this thesis:

American Type Culture Collection http://www.lgcpromochem.com/atcc
Human Genome Browser http://ensembl.lcb.uu.se:8080/Homo_sapiens

IUPHAR Receptor Database	http://www.iuphar-db.org
Molecular Devices	http://moleculardevices.com
National Centre for Biotechnology Information	http://www.ncbi.nlm.nih.gov
Qiagen Bench Guide	http://www.qiagen.com
The Mouse Brain Library:	http://www.mbl.org